

OCTOBER 2025

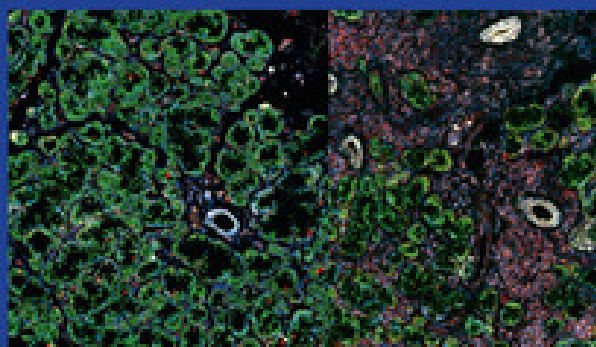
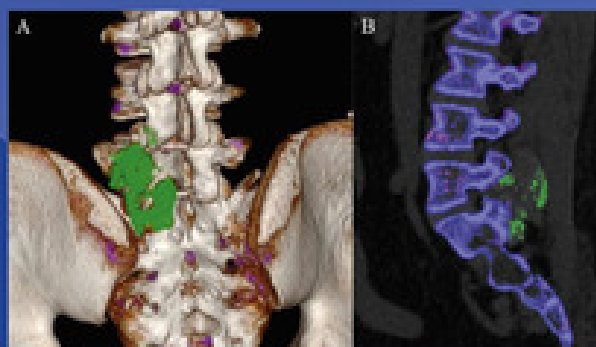
VOLUME 84

ISSUE

10

# ANNALS OF THE **RHEUMATIC DISEASES**

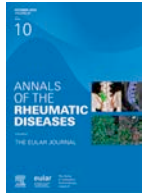
THE EULAR JOURNAL



eular

EUROPEAN ALLIANCE  
OF ASSOCIATIONS  
FOR RHEUMATOLOGY

The home  
of innovative  
rheumatology  
research



## Editorial

## Annals of the rheumatic diseases collection on genetic studies of rheumatic diseases

### INTRODUCTION

Rheumatic diseases include rare congenital genetic disorders, but most are multifactorial disorders involving multiple genetic and environmental factors. While hereditary diseases have traditionally been analysed using methods such as familial linkage analysis, identifying the genetic factors responsible for multifactorial common diseases has been challenging. Following the completion of human genome sequencing in 2003, genome-wide association studies (GWAS) emerged in their current form in 2007, leading to their widespread application across various multifactorial diseases. Rheumatic diseases have been extensively studied using GWAS, revealing genetic factors for many conditions. However, due to the block structure of our chromosomes, the genomic regions identified by GWAS represent chromosomal areas containing genetic variants (primarily tested with single-nucleotide polymorphisms [SNPs]) that occur at different frequencies, mainly between healthy individuals and patients with specific diseases. These regions can span from several to hundreds of kilobases and contain numerous genetic variants and multiple genes.

While GWAS clearly identify chromosomal regions containing disease-related genetic variants, determining which specific variant is responsible and understanding how it contributes to disease development remains challenging. The field of functional genetics, which investigates these relationships, is still developing. Importantly, many causal genetic variants are located in noncoding regions, making their interpretations particularly difficult.

The genetic factors identified through these studies provide valuable information for disease diagnosis, distinguishing disease subgroups, understanding gene-environment interactions, identifying causal intermediate traits, and discovering new drug targets. Advancing functional genetics is therefore crucial for further progress in understanding rheumatic diseases. This article reviews genome analysis studies published in the Annals of the Rheumatic Diseases from 2021 to mid-2025, highlighting key trends in this rapidly evolving field.

### LARGE-SCALE GWAS

A single GWAS examines frequency differences in 500,000 to 1 million genetic variants between groups, requiring statistical correction for multiple testing. Consequently, these studies use a

significance threshold of  $P < 5 \times 10^{-8}$ , which is substantially more stringent than the conventional  $P$  value of .05 usually used. Many rheumatic diseases have relatively low prevalence, making it difficult to recruit large sample sizes. Early GWAS, which included only hundreds of samples, detected a few significant genetic associations. As sample sizes increase,  $P$  values tend to decrease, enabling the detection of more subtle genetic effects. To address sample size limitations, researchers have been collaborating to increase patient numbers within the same population or combining samples from different populations. Recent studies demonstrate that larger sample sizes significantly expand our scope of detectable genetic associations. One of the examples is a paper titled 'Multi-ancestry genome-wide association analyses identify novel genetic mechanisms in rheumatoid arthritis' in Nature Genetics [1].

Saevarsdottir et al [2] analysed 31,313 rheumatoid arthritis (RA) patients (68% seropositive) and 1 million controls from Northwestern Europe, identifying 37 variants across 34 non-HLA (human leukocyte antigen) loci with significant disease associations. This represented one of the largest RA GWAS as of 2022, examining both overall RA and its seropositive and seronegative subtypes. By integrating messenger RNA (mRNA) expression data from various tissues and plasma proteome data from patients positive for rheumatoid factor or anticitrullinated protein antibodies (ACPA), they found that many variants are associated with mRNAs and proteins in interferon  $\alpha/\beta$  and interleukin (IL)-12/23 signalling networks mediated by the JAK/STAT pathway. This connects genetic findings with biological mechanisms and current treatment approaches. However, for example, a randomised phase 2 study of ustekinumab (anti-IL-12/23 p40) and guselkumab (anti-IL-23 p19) did not significantly reduce the signs and symptoms of RA [3], despite the clear benefit of ustekinumab in psoriatic arthritis (PsA) [4]. Thus, more investigations are needed to understand the roles of these pathways in RA.

Bossini-Castillo et al [5] validated the performance of a genetic risk score (GRS) in predicting systemic sclerosis (SSc) risk using the largest dataset from a GWAS comprising 9095 European SSc patients and 17,584 healthy controls. They demonstrated that GRS could potentially support early and differential diagnosis of SSc [5]. Acosta-Herrera et al [6] used the same dataset to study genes in the MHC region using a method called imputation, which involves a broad analysis of the major histocompatibility complex (MHC) region to evaluate SNPs, classical HLA alleles, and their polymorphic amino acid positions. They identified new associations between HLA class I genes and SSc, suggesting new pathways for disease onset, such as the involvement of cytotoxic T cells [6]. They also reported disease subtypes and that the targets of autoantibodies are associated with different HLA class II subtypes.

Yin et al [7] conducted the largest genome-wide meta-analysis of systemic lupus erythematosus (SLE) in East Asian populations (10,029 SLE cases and 180,167 controls). They identified new SLE-associated genetic loci and applied Bayesian statistical approaches to identify causal variants. Linkage disequilibrium score regression detected genetic correlations of SLE with albumin/globulin ratio and nonalbumin protein. This study highlights the importance of conducting genetic studies in diverse populations, as genetic risk factors can vary significantly across different ancestry groups [7]. Che et al [8] conducted a family-based study using national medical registry data from Sweden on idiopathic inflammatory myopathies (IIMs). They matched IIM patients (1620 cases) with non-IIM patients (7797 cases) and then tracked down 7615 first-degree relatives of IIM patients and 37,309 first-degree relatives of non-IIM patients to examine the presence or absence of IIM. The results revealed that IIM has a familial component, with an increased risk in first-degree relatives and a heritability of approximately 20% [8]. This study suggests the importance of a high-quality nationwide registry and family history in a clinical setting. Further studies are needed to obtain more precise genetic contributions. Juvenile idiopathic arthritis (JIA) is the most common juvenile rheumatic disease, but due to the small number of patients and clinical heterogeneity, understanding its genetic risk factors is limited. López-Isac et al [9] conducted a GWAS involving 3305 patients and 9196 healthy controls using Bayesian model selection to systematically investigate the specificity and shared genetic loci across clinical subtypes of JIA. As a result, they identified 5 new risk loci and examined the potential functions of JIA-associated variants [9].

Shirai et al [10] aimed to clarify the differences and common elements in the genetic backgrounds of autoimmune and allergic diseases. They integrated data from BioBank Japan and the UK Biobank and analysed 105,721 cases and 433,663 controls. The results revealed that genetic backgrounds not only classified diseases into mutually exclusive categories but also exhibited multiple positive genetic correlations across classifications [10].

## SUBTYPES OF RHEUMATIC DISEASES

An established rheumatic disease often has different clinical forms, and these subtypes may have unique genetic backgrounds. However, it is more difficult to study subtypes than the overall disease because each subgroup includes fewer patients. Currently, approximately 150 RA-associated genetic loci have been identified, but most relate to disease susceptibility rather than specific disease features. Fewer studies have identified genetic factors associated with disease activity, joint damage severity, or treatment response. This gap exists partly because collecting sufficient numbers of patients with specific subtypes is difficult, and confounding factors, such as medication use (which changes over time), can complicate analyses.

Osteoarthritis (OA) encompasses multiple subtypes with different clinical and genetic characteristics. Erosive hand OA (EHOA) represents a severe form of OA. Stykarsdottir et al [11] conducted a meta-analysis of EHOA involving 1484 cases and 550,680 controls from 5 populations, identifying 3 causal genetic variants. Their findings suggest that EHOA represents a severe form of finger OA and may differ from OA in larger joints [11]. On the other hand, Henkel et al [12] investigated genetic associations with knee and hip OA. This study suggested that

the genetic associations differ between individuals who progress to joint replacement and those who do not [12].

Kronzer et al [13] found that respiratory diseases were associated with an increased risk of RA. Six out of 11 non-*HLA* RA risk alleles interacted strongly with specific respiratory diseases for RA risk. Although replication studies are needed, this work suggests several genetic-respiratory disease interactions drive RA onset [13]. Palomäki et al [14] estimated the lifetime risk of RA interstitial lung disease (ILD) up to age 80 with respect to the strongest known risk factor for pulmonary fibrosis, the *MUC5B* promoter variants. The data were from FinnGen, which integrates genetic data from a nationwide registry in Finland with up to 50 years of follow-up. Among RA patients, lifetime risks of ILD were 16.8% in those with the variant compared with 6.1% in noncarriers, with the risk difference emerging at age 65 and being higher in men [14].

## GENE EXPRESSION STUDIES

Recent advances in gene expression analysis, particularly single-cell techniques, have provided new insights into disease mechanisms. While not directly examining chromosomal DNA, these studies are often included in genomic research partly because many disease-associated genetic variants influence gene expression through expression quantitative trait loci (eQTLs). eQTLs are also detected in single-cell analyses [15,16].

Goldmann et al [17] performed eQTL analyses using RNA sequencing (RNA-seq) of synovial biopsies (n = 85) and blood samples (n = 51) from untreated RA patients. They identified 898 eQTL genes in synovial tissue, with 232 overlapping with blood samples, indicating a high proportion of synovial-specific eQTLs. Regarding the HLA region, they found that the SNP rs3128921 enhances *HLA-DPB2* expression in synovial tissue, and both this SNP and *HLA-DPB2* expression correlate with clinical disease severity. This provides a mechanistic link between genetic variation, gene expression, and clinical outcome [17].

Wilkinson et al [18] performed RNA-seq on CD4+, CD8+, CD14+, and CD19+ cells selected from peripheral blood mononuclear cells (PBMCs) of patients with juvenile dermatomyositis (JDM) before and during treatment. They also measured mitochondrial morphology and cellular metabolism. Their findings revealed a novel pathway in which mitochondrial changes in JDM CD14+ monocytes lead to oxidised mitochondrial DNA production, stimulating interferon-stimulated gene expression [18]. This work illustrates how integrating gene expression data with functional cellular studies can uncover disease mechanisms.

Skaug et al [19] obtained 339 forearm skin biopsies, including healthy controls, to clarify the relationship between clinical disease characteristics of SSc and temporal changes in skin gene expression. In SSc, skin thickness was associated with greater gene expression in dysregulated immune cells and fibroblasts compared with nonaffected skin. In early diffuse SSc, skin gene expression changed over time and tended to normalise. Immunohistochemical staining also revealed that T cells and macrophages were abundant in the early stages and decreased over time [19].

Alaswad et al [20] performed single-cell RNA-seq using PBMCs to elucidate the precise role of CD14 monocytes in the initiation of the inflammatory response in gout. New insights were gained into the role of CD14 monocytes in gout onset, particularly as a major regulatory factor of IL-1 $\beta$  production,

involving hypoxia-related pathways, including *HIF1A*, and the contribution of inflammatory and metabolic pathways through the high expression of S100A monocytes [20]. The S100A family proteins are well-characterised inflammatory proteins, and the S100A<sup>high</sup> monocyte subset is reported to be involved in neutrophil-mediated immunity.

## RARE PHENOTYPES

Rare phenotypes are often considered genetic disorders caused by single mutations. However, patients with identical mutations can exhibit different clinical manifestations, indicating that genetic background and environmental factors may modify mutation effects.

Kozycki et al [21] investigated whether ROSAH syndrome (retinal dystrophy, optic nerve oedema, splenomegaly, anhidrosis, and headache), caused by a dominant mutation in the *ALPK1* gene, represents an autoinflammatory disease. Prior to their work, inflammation was not considered relevant to this condition. They found that nearly all 27 patients studied showed at least 1 inflammatory feature, including recurrent fever, headaches with meningeal enhancement, premature basal ganglia/brainstem calcification, deforming arthritis, or amyloidosis with serum amyloid A (AA amyloidosis). Anti-tumor necrosis factor (TNF) and anti-IL-1 therapies suppressed systemic inflammation and improved quality of life, but only anti-IL-6 therapy (tocilizumab) improved intraocular inflammation. This research demonstrates how genetic insights can lead to targeted therapeutic approaches [21].

Drug reaction with eosinophilia and systemic symptoms (DRESS) is a severe delayed-type hypersensitivity reaction characterised by eosinophilia and systemic symptoms. Saper et al [22] investigated a group of Still's disease patients with atypical pulmonary disease plus DRESS (66 cases) in response to IL-1 or IL-6 inhibitors and compared them with a control group of drug-tolerant Still's disease patients (65 cases). Characteristics of Still's-DRESS included eosinophilia (89%), elevated aspartate aminotransferase and alanine aminotransferase (AST-ALT) (75%), and nonevanescent rash (95%; 88% involving the face). Macrophage activation syndrome was frequently observed in Still's-DRESS (64%) compared with drug-tolerant Still's disease (3%;  $P = 1.2 \times 10^{-14}$ ). DRESS-like reactions occurred in patients treated with IL-1/IL-6 inhibitors and were strongly associated with the common HLA-DRB1\*15 haplotype [22].

JIA is the most common form of arthritis in children, as described above. However, Meng et al [23] investigated the contribution of rare coding variants to JIA. They established a rare variant calling/filtering pipeline and performed rare coding variant and gene-based association analyses on 3 RNA-seq datasets comprising 228 JIA patients registered in the Gene Expression Omnibus. They further validated their findings using whole-exome sequencing (WES) data from 56 JIA patients. The results revealed that 2 genetic variants previously reported in the literature as causative mutations for JIA were identified in the RNA-seq data, along with 63 rare coding variants unique to JIA patients [23]. This suggests that common and rare variants may be involved in autoimmune diseases.

## SOMATIC GENE MUTATIONS

Somatic gene mutations (those occurring after conception and not inherited) are increasingly recognised in autoimmune diseases. These mutations may affect immune cell function or

responses, although direct causal relationships are not always clear.

VEXAS (vacuoles, E1-enzyme, X-linked, autoinflammatory, and somatic) syndrome is an adult-onset autoinflammatory disease associated with somatic variants in the *UBA1* gene that encodes ubiquitin-like modifier activating enzyme, catalysing the first step in ubiquitin conjugation. Mascaro et al [24] detected *UBA1* mosaicism outside haematopoietic tissues for the first time, challenging the conventional understanding that mosaicism in this condition is limited to bone marrow. This finding has important implications for understanding disease mechanisms and developing therapeutic approaches [24]. Tsuchida et al [25] identified somatic mutations in the *UBA1* gene in 13 cases of relapsing polychondritis (RP), affecting 8 of 11 males and 1 of 2 females. They recommended that genetic screening for pathogenic *UBA1* mutations should be considered in RP patients, particularly males with skin lesions [25]. This work demonstrates how genetic findings in one rare disease (VEXAS syndrome) can inform the understanding of other conditions with overlapping clinical features.

Zeng et al [26] reported a case of early-onset SLE characterised by multiple systemic manifestations, including acute immune thrombocytopenia, recurrent fever, pneumonia, myocardial dysfunction, thyroid dysfunction, lymphadenopathy, hepatosplenomegaly, and intracranial calcification. Using WES and targeted sequencing, they identified somatic mutations in the *TLR7* gene. The TLR7 F506S mutation induced excessive inflammatory signalling in the patient's PBMCs, contributing to disease onset [26]. This case illustrates how genetic analysis can provide insights into unusual disease presentations.

Mosaic chromosomal changes (mCA) are acquired changes that increase with age. Uchiyama et al [27] reported that mosaic loss of Y (mLOY) was significantly increased in late-onset RA (LORA) and interacted with the polygenic risk score of RA, but no such interaction was observed in young-onset RA (YORA) [27].

## FUNCTIONAL GENETICS

Noncoding variants are extremely important in understanding the genetic basis of diseases. Taking advantage of recent advances in massively parallel reporter assays (MPRA), Jajodia et al [28] focused on variants in enhancers and performed MPRA on primary activated T helper cells to functionally fine-map RA-associated variants. They also utilised promoter capture Hi-C, a 3-dimensional genomic structure, and eQTL data to identify target genes of enhancers showing allelic differences in activity. Using a clustered regularly interspaced short palindromic repeat-CRISPR associated protein 9 (CRISPR-Cas9) knockout method on primary T cells, they confirmed the interaction between enhancer activity and target genes [28]. Functional validation of RA-associated variants brings us one step closer to identifying causal variants and providing target genes that could serve as therapeutic targets. In fact, there are several different approaches, such as a colocalisation analysis of GWAS risk variants and eQTL [29], ReapTEC, a novel enhancer detection method [30], CRISPR interference/activation [31], and others. Further progress is desired.

## CONCLUSION

Rheumatic diseases show a wide range of symptoms, severities, and treatment responses. If each of these differences has its own genetic basis, then many more GWAS will be needed. In



addition, different genetic factors may apply to different ancestry groups. To move forward, it is essential to carefully define patient subgroups and collect enough samples for analysis.

Beyond GWAS, we need studies that identify specific disease-causing variants, explore how these variants work, and guide new drug development. In recent *Annals of the Rheumatic Diseases*, papers on these directions have been published [23]. Genomic research is rapidly evolving, and future discoveries will deepen our understanding of rheumatic diseases and improve patient care.

## Competing interests

The author declares no competing interests.

## Funding

This article was funded by an AMED grant JP223fa627010.

## Patient consent for publication

Not applicable.

## Ethics approval


Not applicable.

## Provenance and peer review

Not commissioned; externally peer reviewed.

## Orcid

Kazuhiko Yamamoto: <http://orcid.org/0000-0001-9037-3625>

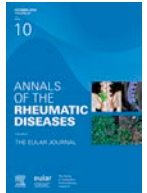
Kazuhiko Yamamoto   
RIKEN Center for Integrative Medical Sciences,  
Yokohama, Japan

\*Correspondence to Dr. Kazuhiko Yamamoto.  
E-mail address: [kazuhiko.yamamoto@riken.jp](mailto:kazuhiko.yamamoto@riken.jp)

## REFERENCES

- [1] Ishigaki K, Sakaue S, Terao C, Luo Y, Sonehara K, Yamaguchi K, et al. Multi-ancestry genome-wide association analyses identify novel genetic mechanisms in rheumatoid arthritis. *Nat Genet* 2022;54(11):1640–51.
- [2] Saevarsdottir S, Stefansdottir L, Sulem P, Thorleifsson G, Ferkingstad E, Rutsdottir G, et al. Multiomics analysis of rheumatoid arthritis yields sequence variants that have large effects on risk of the seropositive subset. *Ann Rheum Dis* 2022;81(8):1085–95.
- [3] Smolen JS, Agarwal SK, Ilivanova E, Xu XL, Miao Y, Zhuang Y, et al. A randomised phase II study evaluating the efficacy and safety of subcutaneously administered ustekinumab and guselkumab in patients with active rheumatoid arthritis despite treatment with methotrexate. *Ann Rheum Dis* 2017;76(5):831–9.
- [4] Smolen JS, Siebert S, Korotaeva TV, Selmi C, Bergmans P, Gremese E, et al. Effectiveness of IL-12/23 inhibition (ustekinumab) versus tumour necrosis factor inhibition in psoriatic arthritis: observational PsABio study results. *Ann Rheum Dis* 2021;80(11):1419–28.
- [5] Bossini-Castillo L, Villanueva-Martin G, Kerick M, Acosta-Herrera M, López-Isac E, Simeón CP, et al. Genomic risk score impact on susceptibility to systemic sclerosis. *Ann Rheum Dis* 2021;80(1):118–27.
- [6] Acosta-Herrera M, Kerick M, López-Isac E, Assassi S, Beretta L, Simeón-Aznar CP, et al. Comprehensive analysis of the major histocompatibility complex in systemic sclerosis identifies differential HLA associations by clinical and serological subtypes. *Ann Rheum Dis* 2021;80(8):1040–7.
- [7] Yin X, Kim K, Suetsugu H, Bang SY, Wen L, Koido M, et al. Meta-analysis of 208370 East Asians identifies 113 susceptibility loci for systemic lupus erythematosus. *Ann Rheum Dis* 2021;80(5):632–40.
- [8] Che WI, Westerlind H, Lundberg IE, Hellgren K, Kuja-Halkola R, Holmqvist M. Familial aggregation and heritability: a nationwide family-based study of idiopathic inflammatory myopathies. *Ann Rheum Dis* 2021;80(11):1461–6.
- [9] López-Isac E, Smith SL, Marion MC, Wood A, Sudman M, Yarwood A, et al. Combined genetic analysis of juvenile idiopathic arthritis clinical subtypes identifies novel risk loci, target genes and key regulatory mechanisms. *Ann Rheum Dis* 2021;80(3):321–8.
- [10] Shirai Y, Nakanishi Y, Suzuki A, Konaka H, Nishikawa R, Sonehara K, et al. Multi-trait and cross-population genome-wide association studies across autoimmune and allergic diseases identify shared and distinct genetic component. *Ann Rheum Dis* 2022;81(9):1301–12.
- [11] Styrkarsdottir U, Stefansdottir L, Thorleifsson G, Stefansson OA, Saevarsdottir S, Lund SH, et al. Meta-analysis of erosive hand osteoarthritis identifies four common variants that associate with relatively large effect. *Ann Rheum Dis* 2023;82(6):873–80.
- [12] Henkel C, Styrkarsdottir U, Thorleifsson G, Stefansdottir L, Björnsdottir G, Banasik K, et al. Genome-wide association meta-analysis of knee and hip osteoarthritis uncovers genetic differences between patients treated with joint replacement and patients without joint replacement. *Ann Rheum Dis* 2023;82(3):384–92.
- [13] Kronzer VL, Williamson KA, Hayashi K, Atkinson EJ, Crowson CS, Wang X, et al. Uncovering specific genetic-respiratory disease endotypes for rheumatoid arthritis risk. *Ann Rheum Dis* 2025;84(2):221–31.
- [14] Palomäki A, FinnGen Rheumatology Clinical Expert Group, Palotie A, Koskela J, Eklund KK, Pirinen M, et al. Lifetime risk of rheumatoid arthritis-associated interstitial lung disease in *MUC5B* mutation carriers. *Ann Rheum Dis* 2021;80(12):1530–6.
- [15] Yazari S, Alquicira-Hernandez J, Wing K, Senabouth A, Gordon MG, Andersen S, et al. Single-cell eQTL mapping identifies cell type-specific genetic control of autoimmune disease. *Science* 2022;376(6589):eabf3041.
- [16] Soskic B, Cano-Gamez E, Smyth DJ, Ambridge K, Ke Z, Matte JC, et al. Immune disease risk variants regulate gene expression dynamics during CD4<sup>+</sup> T cell activation. *Nat Genet* 2022;54(6):817–26.
- [17] Goldmann K, Spiliopoulou A, Iakovliev A, Plant D, Nair N, Cubuk C, et al. Expression quantitative trait loci analysis in rheumatoid arthritis identifies tissue specific variants associated with severity and outcome. *Ann Rheum Dis* 2024;83(3):288–99.
- [18] Wilkinson MGL, Moulding D, McDonnell TCR, Orford M, Wincup C, Ting JYJ, et al. Role of CD14<sup>+</sup> monocyte-derived oxidised mitochondrial DNA in the inflammatory interferon type 1 signature in juvenile dermatomyositis. *Ann Rheum Dis* 2023;82(5):658–69.
- [19] Skaug B, Lyons MA, Swindell WR, Salazar GA, Wu M, Tran TM, et al. Large-scale analysis of longitudinal skin gene expression in systemic sclerosis reveals relationships of immune cell and fibroblast activity with skin thickness and a trend towards normalisation over time. *Ann Rheum Dis* 2022;81(4):516–23.
- [20] Alaswad A, Cabau G, Crişan TO, Zhou L, Zoodma M, Botey-Bataller J, et al. Integrative analysis reveals the multilateral inflammatory mechanisms of CD14 monocytes in gout. *Ann Rheum Dis* 2025;84(7):1253–63.
- [21] Kozycki CT, Kodati S, Huryn L, Wang H, Warner BM, Jani P, et al. Gain-of-function mutations in *ALPK1* cause an NF-κB-mediated autoinflammatory disease: functional assessment, clinical phenotyping and disease course of patients with ROSA syndrome. *Ann Rheum Dis* 2022;81(10):1453–64.
- [22] Saper VE, Ombrello MJ, Tremoulet AH, Montero-Martin G, Prahalad S, Canna S, et al. Severe delayed hypersensitivity reactions to IL-1 and IL-6 inhibitors link to common HLA-DRB1\*15 alleles. *Ann Rheum Dis* 2022;81(3):406–15.
- [23] Meng X, Hou X, Wang P, Glessner JT, Qu HQ, March ME, et al. Association of novel rare coding variants with juvenile idiopathic arthritis. *Ann Rheum Dis* 2021;80(5):626–31.
- [24] Mascaro JM, Rodriguez-Pinto I, Poza G, Mensa-Vilaro A, Fernandez-Martin J, Caminal-Montero L, et al. Spanish cohort of VEXAS syndrome: clinical manifestations, outcome of treatments and novel evidences about *UBA1* mosaicism. *Ann Rheum Dis* 2023;82(12):1594–605.
- [25] Tsuchida N, Kunishita Y, Uchiyama Y, Kirino Y, Enaka M, Yamaguchi Y, et al. Pathogenic *UBA1* variants associated with VEXAS syndrome in Japanese patients with relapsing polychondritis. *Ann Rheum Dis* 2021;80(8):1057–61.

- [26] Zeng Y, Tao P, Wang J, Li T, Du Y, Wang X, et al. Somatic gain-of-function mutation in *TLR7* causes early-onset systemic lupus erythematosus. *Ann Rheum Dis* 2025;84(3):442–50.
- [27] Uchiyama S, Ishikawa Y, Ikari K, Honda S, Hikino K, Tanaka E, et al. Mosaic loss of chromosome Y characterises late-onset rheumatoid arthritis and contrasting associations of polygenic risk score based on age at onset. *Ann Rheum Dis* 2025;84(8):1313–23.
- [28] Jajodia A, Mishra A, Doni Jayavelu N, Lambert K, Moss N, Yang Z, et al. Functional dissection of noncoding variants associated with rheumatoid arthritis. *Ann Rheum Dis* 2025;84(7):1117–29.
- [29] Pan S, Kang H, Liu X, Li S, Yang P, Wu M, et al. COLOCdb: a comprehensive resource for multi-model colocalization of complex traits. *Nucleic Acids Res* 2024;52(D1):D871–81.
- [30] Oguchi A, Suzuki A, Komatsu S, Yoshitomi H, Bhagat S, Son R, et al. An atlas of transcribed enhancers across helper T cell diversity for decoding human diseases. *Science* 2024;385(6704):eadd8394.
- [31] Schmidt R, Steinhart Z, Layeghi M, Freimer JW, Bueno R, Nguyen VQ, et al. CRISPR activation and interference screens decode stimulation responses in primary human T cells. *Science* 2022;375(6580):eabj4008.



## Review

# How does Elie Metchnikoff relate to the investigator of today?

Charlotte R. Edwards<sup>1,2,\*</sup>, Peter E. Lipsky<sup>1,2</sup>

<sup>1</sup> AMPEL BioSolutions, LLC, Charlottesville, VA, USA

<sup>2</sup> RILITE Research Institute, Charlottesville, VA, USA

## ARTICLE INFO

## Article history:

Received 31 March 2025

Received in revised form 23 June 2025

Accepted 30 June 2025

## ABSTRACT

Elie Metchnikoff (Ilya Ilyich Mechnikov, 1845–1916) was a Russian-born (born in Kharkiv, current Ukraine) zoologist who shared the Nobel Prize with Paul Ehrlich in 1908 “in recognition of their work on the theory of immunity.” This description hardly gives credit to the important observations of Metchnikoff and how they served as the basis of modern thinking in immunology. In 1882, while in Messina, Sicily, Metchnikoff observed that the introduction of a rose thorn induced the influx of phagocytic cells in starfish larvae. The “phagocytosis theory” resulting from this simple experiment along with Metchnikoff’s genius served not only as the eventual basis of the discipline of innate immunity, but also the entire field of immunology, in which a system of cells and their products is considered to play an active role in host defence by recognising and destroying pathogenic microorganisms. Metchnikoff was clearly a flawed genius who led a rich and complex life, including insightful experimentation, scientific debate, the evolution of ideas, personal change, loss and growth, and a willingness to explore new ideas. As such, his personal characteristics are relevant to today’s scientists, students, and scholars.

## TENACITY

When Metchnikoff made his seminal discoveries, as in [Figure 1](#), humoral theories of host defence were established and dominant. Pasteur, van Behring, Ehrlich, and others had demonstrated that serologic factors, subsequently shown to be antibodies and complement, were the major elements of host defence, especially against toxins produced by bacteria [1]. Notably, even proponents of the humoral theory did not think of serologic factors as actively killing invading microorganisms, but rather that serologic factors might limit the availability of nutrients, causing bacteria to die of starvation [2]. Metchnikoff’s ideas not only challenged the dominance of the humoral theory but also the very mechanism of acquired host resistance to microorganisms. The debate between the humoral and cellular camps was intense, often personal and quite public. The public debate between humoral and cellular theories of immunity was highlighted in the play by Shaw [3], “The Doctor’s Dilemma,”

in 1902, in which one character declares “Nature has provided the white corpuscles as you call them, the phagocytes as we call them, a natural means of devouring and destroying all disease germs. There is at bottom only one genuinely scientific treatment for all diseases, and that is to stimulate the phagocytes, drugs are a delusion.” The humoralists countered this by citing the success of serum transfer in preventing certain complications of infection.

Scientifically based resolution of this debate would require many years of experimentation until it became clear that both humoral factors and cells were important in host defence. However, until that convergence of thinking, the debate was intense –so intense that Metchnikoff declined to attend the Nobel Prize Award Ceremony, even though many believe that the 1908 Nobel Prize was awarded as a kind of truce, identifying roles for both phagocytes and serum factors in host defence. As Metchnikoff himself pointed out in his delayed Nobel Prize oration, “The theory of phagocytosis has come under fire from all sides”

\*Correspondence to Ms. Charlotte R. Edwards, RILITE Foundation, Charlottesville, VA, USA.

E-mail address: [charlotte.edwards@ampelbiosolutions.com](mailto:charlotte.edwards@ampelbiosolutions.com) (C.R. Edwards).

Handling editor Josef S. Smolen.

### WHAT IS ALREADY KNOWN ON THIS TOPIC

- The life of Elie Metchnikoff has been chronicled by multiple biographers
- Metchnikoff's phagocytosis experiments served as the basis of the field of innate immunology

### WHAT THIS STUDY ADDS

This review provides evidence of the importance of Metchnikoff's traits to modern investigators:

- Metchnikoff's **tenacity** in the face of established theories allowed him to shift immunological thinking towards an understanding of the active role of innate immunity in host defence.
- Metchnikoff's **curiosity** across disciplines allowed him to use existing tools and ideas creatively and to keep an open mind to new results.
- Metchnikoff's **perseverance** allowed him to continue through personal and career adversity before he found his successes.
- Metchnikoff's **collegiality** with both rivals and friends protected his career and personal happiness.
- Metchnikoff's **mentorship** carried his legacy beyond his lifetime.
- Metchnikoff's **purpose** of benefitting mankind sustained him through adversity and allowed him to find his niche within existing work.
- Metchnikoff's self-**reinventions** ensured his work remained relevant as he addressed new scientific ideas.

### HOW THIS STUDY MIGHT AFFECT RESEARCH, PRACTICE OR POLICY

- Through character investigation of a great and complex scientist, this review encourages modern investigators to work through issues to achieve personal and professional success

[4]. He commented, “The controversy over phagocytosis could have killed me, or permanently weakened me” [5]. Despite the controversy, he continued to support his ideas with a series of masterful experiments, demonstrating that in many *in vivo* models, phagocytes mediated host defence by ingesting live and dead microorganisms, that macrophages could destroy ingested

microorganisms by virtue of “cytases” and acidification of endolysosomes, and elucidated many of the steps in inflammation, including chemotaxis and diapedesis. Metchnikoff also demonstrated the role of macrophages in disposing of dead or senescent host cells. Based on this vast array of emerging data, he felt comfortable persistently advocating for his ideas. As Thomas Kuhn pointed out, shared assumptions guide the scientific community and paradigm shifts are resisted [6]. Both excellent scientific support and tenacity, as exhibited by Metchnikoff, are required to change scientific thinking and direction.

### CURIOSITY

Great science is motivated by persistent curiosity about the world, whereas the scientific method provides the tools to focus that inquisitiveness into meaningful insights. From an early age, Metchnikoff was passionate about exploring natural phenomena and became a creative experimentalist. As an embryologist, he examined the wandering cells of the mesoderm and their ability to take up particles, which he presumed served a nutritive function [2]. Being well-versed in the theories of Darwin, he believed that he could learn about more complex organisms from simple invertebrates, whose anatomy allowed for *in vivo* examination with the instruments available at that time.

A major advance was the introduction of a noxious rather than innocuous stimulus (a rose thorn vs a harmless particle) and the study of cellular aggregation rather than digestion. This resulted in the evolution of this thinking from phagocytosis as a part of cellular nutrition to playing a role in host defence. Similarly, by first following curiosity rather than previous assumptions or even perceived feasibility, modern investigators perform truly new science and translate their curiosity into creativity to circumvent contemporary barriers to further investigation. During both Metchnikoff's experiments and modern investigations, results are produced that do not fit expectations. It is tempting to dismiss or reject these results. But investigators who prioritise curiosity over expectations, face nonconforming results with an open mind, test the validity of new findings, and

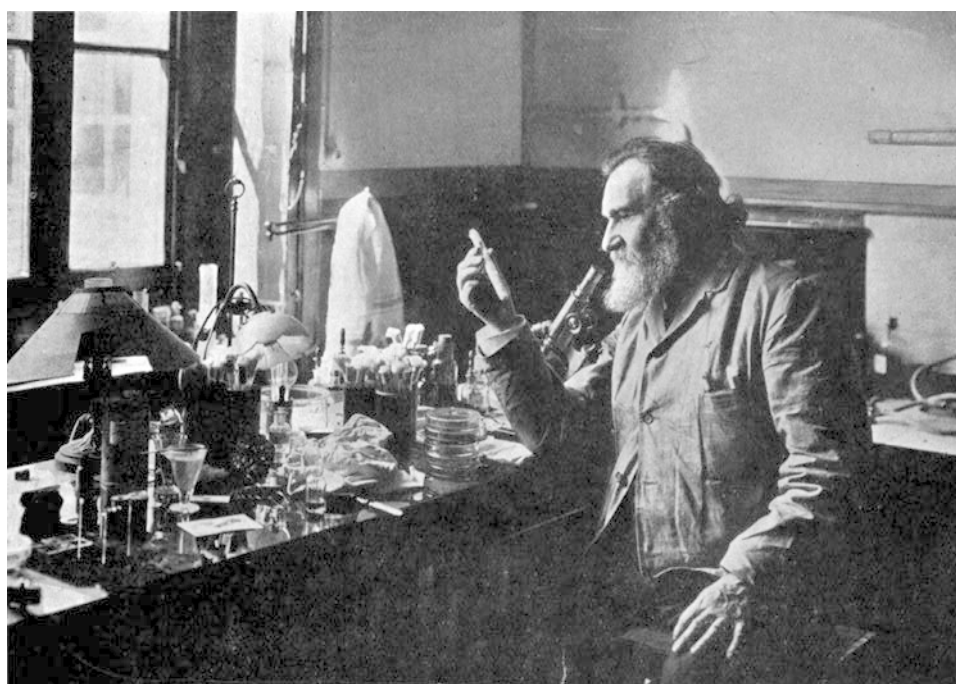


Figure 1. Elie Metchnikoff in his laboratory [7].



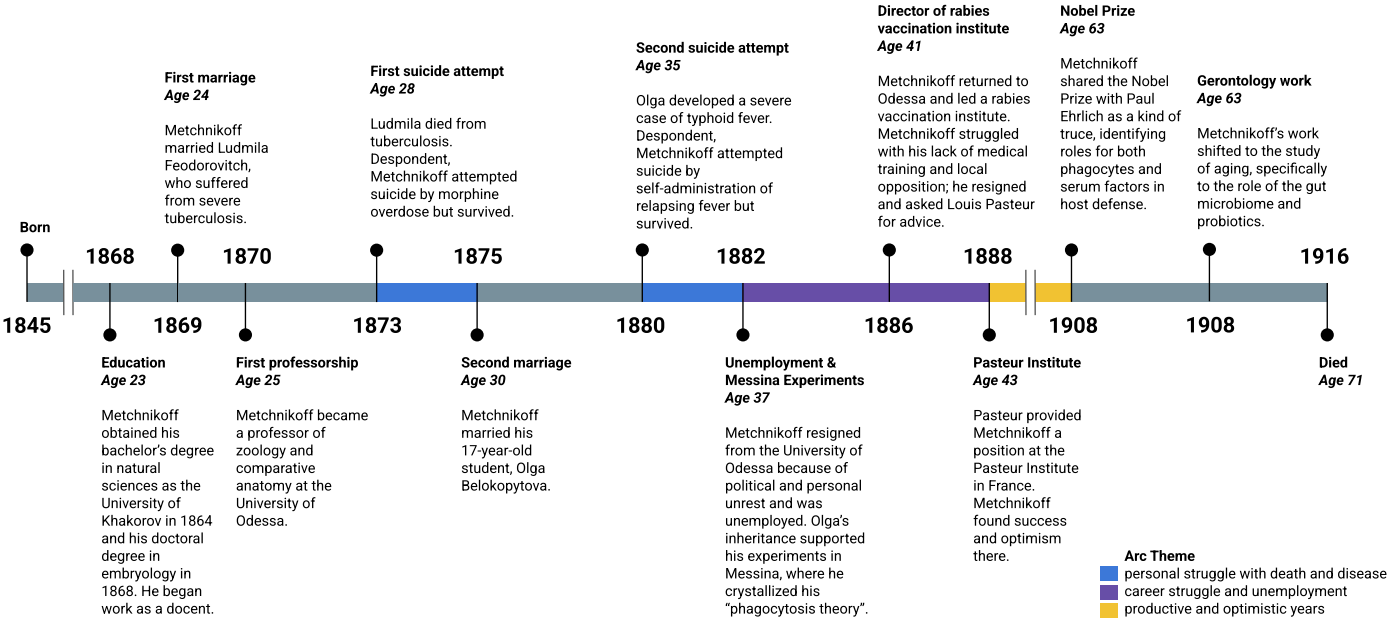


Figure 2. The arc of Metchnikoff's life.

defend and explain their new theories with tenacity, contribute great advances in knowledge.

PERSEVERANCE THROUGH ADVERSITY

Metchnikoff's early career was thwarted by adversity and pessimism. For various reasons, including political and academic unrest, Metchnikoff's early career was characterised by a considerable lack of success. Indeed, his major discovery of phagocytic cells in Messina in 1882 occurred while he was unemployed [7]. Fortunately, his second wife, Olga, whom he married when she was a 16-year-old student of his (a relationship that would be unacceptable today but resulted in a life-long marriage of mutual love, respect, and support), had recently come into an inheritance that supported Metchnikoff's experiments in Messina. Even after his remarkable Messina experiments, Metchnikoff experienced additional failure as the director of an institute in Odessa focused on generating vaccines. While unemployed again and travelling through Europe, Louis Pasteur offered him a position at the Institut Pasteur in Paris, where he worked productively for the rest of his life.

Despite much early failure, considerable frustration and depression, 2 (fortunately) unsuccessful suicide attempts (both triggered by illnesses of his wives), and considerable downtime, Metchnikoff found both supportive personal and collegial professional environments and great success. This perseverance through adversity to achieve success is illustrated in Figure 2. Not every decision is inspired, not every position is ideal, and sometimes life seems overwhelming. But the combination of a vision, persistence, and a strong support system fosters eventual success. Despite his lack of medical training, Metchnikoff was able to utilise his specific knowledge to make Nobel Prize-worthy contributions to the field of medicine. A lack of a typical background does not preclude modern investigators from contributing to their field of interest, but allows them to contribute knowledge informed by their training background and learn through experimentation, targeted study, and collaboration. Through overcoming personal challenges, investigators build a unique perspective and skill set—a valuable blend that they alone can lend to their colleagues and work. Additionally, like Metchnikoff, successful modern investigators allow themselves

to continue through failures before success. An investigator succeeds by learning from their failures, discovering what does not work before finding what does work.

COLLEGIALITY

Metchnikoff's phagocytic theory was met with extreme rejection by the established humoralists, as many new ideas do [4,5]. Despite the ongoing conflict, especially with the group of Robert Koch in Berlin, exacerbated by the lingering hostilities over the recently concluded Franco-Prussian War (1870-1871), Metchnikoff maintained cordial relationships with many of his antagonists, including Ehrlich and Koch. Moreover, he became extremely familiar with the work of his rivals, often reinterpreting their results and incorporating them into his theories. Today, science is very competitive, and Metchnikoff's embrace of collegiality in dealing with adversaries is a good example of a long, productive career. By working across differences and forgiving hostilities, and not begrudging others' successes, he built a strong support system that contributed to more meaningful scientific contributions. Additionally, it was Metchnikoff's collegial connection with Pasteur that assisted Metchnikoff in securing a job at the Institut Pasteur. After this point, he continued to find success, even describing himself as a newfound optimist [8]. Collegiality protected not only an investigative career but also contributed to personal happiness.

MENTORSHIP

During his 28 years at the Institut Pasteur, Metchnikoff mentored nearly 100 students, including Jules Bordet, who was awarded the Nobel Prize in 1919 for his studies on "Alexine" (now known to be complement components). Metchnikoff took great pride in his trainees and their success [9]. It is notable that many of his trainees came from outside France and, as a result, were exposed to considerable discrimination. Metchnikoff, however, remained very supportive, devoting a great deal of his time to personal mentoring. With his trainees, he was able to extend his findings beyond the description of macrophages and microphages (neutrophils), identifying alveolar macrophages,

microglia (neuronophages), chemotaxis, efferocytosis, and netosis, among many other discoveries.

On the occasion of his 70th birthday, Emile Roux, Institut Pasteur director, noted, “The Institut Pasteur owes much to you, you brought the prestige of your reputation, and your work and that of your students have greatly contributed to its glory” [8]. As Metchnikoff’s work at the Institut Pasteur exemplifies, mentoring relationships between investigators and less experienced scientists benefit not only the mentee but also the mentors, drawing new talent to the field to carry on their years of work. Future investigators will face unforeseen challenges. Mentorship by experienced investigators with great scientific minds ensures that modern and future investigators will learn how to think scientifically and adapt to new questions.

## PURPOSE

Metchnikoff was motivated by a desire to benefit mankind through basic research [8]. Every modern investigator has their own purpose. By discovering and centering this purpose in their work, modern investigators, like Metchnikoff, provide themselves with motivation that sustains them through remarkable adversity to ultimately achieve their goals. Cognisance of their purpose allows modern investigators not only to get through adversity but also to find a way to benefit from it, translating their adverse experiences into tenacity and other skills to further their work. While working towards his purpose, Metchnikoff was also masterful in incorporating the data from other investigators into his ideas, eventually earning acceptance of his phagocytic theory. Modern investigators who understand how their work fits into current social, scientific, and economic models, as well as prior work, are able to hone their purpose to make the most needed and useful impact.

## REINVENTION

Metchnikoff was trained as an embryologist. His understanding of the behaviour of the mesoderm prepared him to understand his observations in Messina. Phagocytosis had been described years before, but his background allowed him to understand the ramifications of his findings, namely that a noxious stimulus induced the entry of large phagocytic cells or macrophages in the absence of a nervous or vascular system, and these phagocytic cells were involved in defending the host from injury. Metchnikoff himself noted that these findings served to convert him from a zoologist to a pathologist [7]. These initial results were supported by many subsequent findings made by Metchnikoff and his students, serving as the basis for the emerging discipline of cellular immunology, a field that required more than 75 years before technology was available to rigorously test some of its major hypotheses.

In the meantime, Metchnikoff had moved on to explore the role of noxious stimuli in the process of ageing, and since there was no established discipline, he named the field gerontology [10]. It was his work that stimulated an interest in the role of gut bacteria in the process of ageing, eventually leading to the study of the gut microbiome and also the development of the commercial yogurt industry as a means to combat dysbiosis.

The lesson for modern scientists is that Metchnikoff followed an important question and was not governed by the available technology. He avoided a condition described by Joseph Goldstein, the corecipient of the 1985 Nobel Prize in Physiology or Medicine, as Paralyzed Academic Investigator Disease Syndrome [11]. This is characterised by an investigator who learns a technique during training and thinks it can be applied repeatedly

throughout their career. But science changes rapidly, and such an investigator is soon obsolete. Metchnikoff recognised this and evolved throughout his career by reinventing himself to address new questions. Review of his Nobel Prize oration indicates the many novel experimental designs employed throughout his career to delineate and support the theory of phagocytosis [4]. Indeed, his subsequent application of the theory of phagocytosis and the role of intestinal bacteria provided the first scientific basis for the study of ageing and longevity, and survives today, with a focus on the microbiome and probiotic-containing diets as a possible means to promote health [10,12]. Metchnikoff’s scientific and personal evolution provides evidence of the need for reinvention of a successful scientific career, and as such, he is a timeless example for modern scientists a century later.

## CONCLUSIONS

Elie Metchnikoff was the principal founder of cellular immunology and even immunology itself. His career exemplifies many inspirational aspects of his creative spirit, scientific curiosity, tenacity, and perseverance. Like many current investigators, his career did not follow a straight-line course, and at many points he needed a lifeline. Recognising his successes in the context of his challenges provides a model that remains relevant for modern-day investigators. When adversity arises, intrinsic tenacity and collegial and personal networks guide investigators back to working towards their purpose. In good times, scientific curiosity and mentorship, which are investments in the future of an investigator’s work, flourish. Through both hardship and success, commitment to their purpose allows modern investigators to make the most of their unique traits to do great science, as Elie Metchnikoff did.

## Competing interests

CRE reports financial support was provided by Re-Imagine Lupus Investigation, Treatment and Education (RILITE) Foundation. PEL reports financial support was provided by RILITE Foundation.

## CRedit authorship contribution statement

**Charlotte R. Edwards:** Writing – review & editing. **Peter E. Lipsky:** Writing – original draft.

## Funding

This research did not receive any specific grant from funding agencies in the public, commercial, or not-for-profit sectors.

## Patient consent for publication

Not applicable.

## Ethics approval

Not applicable.

## Provenance and peer review

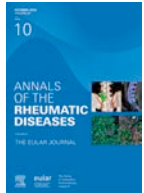
Not commissioned; externally peer reviewed.

## Orcid

Charlotte R. Edwards: <http://orcid.org/0009-0000-3883-4180>

## REFERENCES

- [1] Chernyak L, Tauber AI. The birth of immunology: Metchnikoff, the embryologist. *Cell Immunol* 1988;117(1):218–33.
- [2] Teti G, Biondo C, Beninati C. The phagocyte, Metchnikoff, and the foundation of immunology. *Microbiol Spectr* 2016;4(2).
- [3] Shaw GB. *The Doctor's Dilemma*. Baltimore: Penguin Books; 1913.
- [4] Metchnikoff I. On the present state of the question of immunity in infectious disease. Nobel Prize lecture 1908.
- [5] Cavaillon JM. The historical milestones in the understanding of leukocyte biology initiated by Elie Metchnikoff. *J Leuk Biol* 2011;90(3):413–24.
- [6] Kuhn TS. *The structure of scientific revolutions*. Chicago: University of Chicago Press; 1970.
- [7] Metchnikoff O. *The life of Elie Metchnikoff, 1845-1916*. Lankester ER, translator. London: Constable; 1924.
- [8] Gordon S. Elie Metchnikoff, the man and the myth. *J Innate Immun* 2016;8(3):223–7.
- [9] Cavaillon JM, Duclaux Legout S, Chamberland Roux. Grancher and Metchnikoff: the five musketeers of Louis Pasteur. *Microbes Infect* 2019;21(5-6):192–201.
- [10] Stambler IS. Elie Metchnikoff—the founder of longevity science and a founder of modern medicine: in honor of the 170th anniversary. *Adv Gerontol* 2015;28(2):207–17.
- [11] Goldstein JL. On the origin and prevention of PAIDS (Paralyzed Academic Investigator's Disease Syndrome). *J Clin Invest* 1986;78(3):848–54.
- [12] Metchnikov II. *Etudes on the nature of man*. Moscow: Akad Nauk SSSR; 1903.



## Recommendations

# EULAR recommendations for a core dataset to support clinical care and translational and observational research in systemic lupus erythematosus

Johanna Mucke<sup>1,2,\*</sup>, George Bertsias<sup>3</sup>, Martin Aringer<sup>4,5</sup>, Laurent Arnaud<sup>6</sup>, Carina Boström<sup>7</sup>, Ricard Cervera<sup>8,9</sup>, Gamal Chehab<sup>2,10</sup>, László Czirják<sup>11</sup>, Lene Wohlfahrt Dreyer<sup>12</sup>, Luís Inês<sup>13</sup>, Søren Jacobsen<sup>14</sup>, Charite Kjaerside Nielsen<sup>15</sup>, Emiliano Marasco<sup>16</sup>, Marta Mosca<sup>17</sup>, Kirsi Myllys<sup>15</sup>, Cristina Pamfil<sup>18</sup>, Jose M. Pego-Reigosa<sup>19</sup>, Jutta G. Richter<sup>2,20</sup>, Savino Sciascia<sup>21</sup>, Farah Tamirou<sup>22</sup>, Michel Tsang-A-Sjoe<sup>23</sup>, Edward M. Vital<sup>24</sup>, Ronald Van Vollenhoven<sup>23</sup>, Chris Wincup<sup>25</sup>, Matthias Schneider<sup>2,20</sup>, on behalf of Taskforce for development of EULAR recommendations for a core dataset to support clinical care and translational and observational research in systemic lupus erythematosus

<sup>1</sup> Ruhr-Universität Bochum, Germany; Rheumazentrum Ruhrgebiet, Herne, Germany

<sup>2</sup> Department of Rheumatology, Heinrich-Heine University, Duesseldorf, Germany

<sup>3</sup> Department of Rheumatology, Clinical Immunology and Allergy, University of Crete, Medical School, Heraklion, Greece

<sup>4</sup> Division of Rheumatology, Department of Medicine III, University Medical Center and Faculty of Medicine at the TU Dresden, Dresden, Germany

<sup>5</sup> Interdisciplinary University Center for Autoimmune and Rheumatic Entities (UCARE), University Medical Center and Faculty of Medicine at the TU Dresden, Dresden, Germany

<sup>6</sup> Department of Rheumatology & National Reference Center for Autoimmune Diseases (CRMR RESO), Hôpital de Hautepierre, Strasbourg, France

<sup>7</sup> Department of Neurobiology, Karolinska Institute, Care Sciences and Society, Stockholm, Sweden

<sup>8</sup> Department of Autoimmune Diseases, University of Barcelona, Hospital Clínic, Institut d'Investigacions Biomèdiques August Pi i Sunyer, Barcelona, Spain

<sup>9</sup> IRIDIS (Investigation in Rheumatology and Immune-Mediated Diseases)-VIGO Group, Galicia Sur Health Research Institute, Vigo, Spain

<sup>10</sup> Department of Rheumatology and Clinical Immunology, Evangelisches Krankenhaus Kliniken Essen-Mitte, Essen, Germany

<sup>11</sup> Department of Rheumatology and Immunology, University of Pecs, Medical School, Pecs, Hungary

<sup>12</sup> Department of Rheumatology, Center of Rheumatic Research Aalborg (CERRA), Aalborg University Hospital, Aalborg University, Aalborg, Denmark

<sup>13</sup> Rheumatology Department, Centro Hospitalar Universitário de Coimbra, Coimbra, Portugal

<sup>14</sup> Copenhagen Research Center for Autoimmune Connective Tissue Diseases (COPEACT), Center for Rheumatology and Spine Diseases, Rigshospitalet, University of Copenhagen, Copenhagen, Denmark

<sup>15</sup> Lupus Europe, Rue d'Egmont 11, 1000 Bruxelles, Belgium

<sup>16</sup> Division of Rheumatology, Bambino Gesù Children's Hospital, Rome, Italy

<sup>17</sup> Department of Clinical and Experimental Medicine, University of Pisa, Pisa, Italy

<sup>18</sup> Department of Rheumatology, Iuliu Hatieganu University of Medicine and Pharmacy, Cluj-Napoca, Romania

\*Correspondence to Dr. Johanna Mucke, Rheumazentrum Ruhrgebiet, Herne, Germany.

E-mail address: [johanna.mucke@med.uni-duesseldorf.de](mailto:johanna.mucke@med.uni-duesseldorf.de) (J. Mucke).

Handling editor Josef S. Smolen.



<sup>19</sup> Rheumatology Department, University Hospital of Vigo, Vigo, Spain

<sup>20</sup> Hiller Research Center for Rheumatology, Heinrich-Heine University, Duesseldorf, Germany

<sup>21</sup> Department of Clinical and Biological Sciences, University Center of Excellence on Nephrology, Rheumatology and Rare Diseases, ASL Città Di Torino and University of Turin, Turin, Italy

<sup>22</sup> Department of Rheumatology, Cliniques Universitaires Saint-Luc, UCLouvain, Brussels, Belgium

<sup>23</sup> Department of Rheumatology and Clinical Immunology, Amsterdam Rheumatology and Immunology Center, Amsterdam, the Netherlands

<sup>24</sup> Leeds Institute of Rheumatic and Musculoskeletal Medicine, University of Leeds, Leeds, UK

<sup>25</sup> Department of Clinical and Academic Rheumatology, King's College Hospital, London, UK

## ARTICLE INFO

### Article history:

Received 13 February 2025

Received in revised form 26 June 2025

Accepted 1 July 2025

## ABSTRACT

**Objectives:** To enhance clinical and multicentre research outcomes in systemic lupus erythematosus (SLE), standardised documentation of patient- and disease-related features is important. The aim of this European Alliance of Associations for Rheumatology (EULAR) taskforce was to define a core set of essential items for the comprehensive care of SLE patients in clinical practice, with an extension for vital elements required for translational and observational research.

**Methods:** A multidisciplinary EULAR task force group engaged in a multistep approach including a 4-round Delphi survey and a face-to-face meeting.

**Results:** Twenty-five stakeholders from 14 different countries participated. During the process, the initial list of 99 items was reduced to 73 items for inclusion in the clinical core dataset and 8 additional items for research extension. The items were grouped in the domains ‘general’, ‘disease activity’, ‘disease history’, ‘disease damage’, ‘comorbidities’, ‘patient reported outcomes’, ‘laboratory markers’, ‘outcomes’, and ‘treatment’, with suggested frequencies of assessment.

**Conclusions:** The presented clinical core dataset and its research extension are designed to improve SLE patient care and facilitate collaborative research by ensuring the comparability of datasets and cohort descriptions. This initiative lays the foundation for the establishment of a global SLE data space and has the potential to expedite the implementation of personalised medicine in SLE care.

### What is already known on this topic?

- Standardized datasets are crucial for analyzing big data to identify disease patterns and patient subgroups for targeted clinical trials, but such standards have been lacking in systemic lupus erythematosus.
- Numerous national and international SLE registries exist, but their potential for collaboration is limited by a lack of interoperable documentation standards.
- Previously, EULAR recommendations for monitoring SLE patients were formulated, but they were not developed through a consensus-based process.

### What this study adds

- This study provides a consensus-based core data set of 73 essential items for the clinical care of adult SLE patients, plus an 8-item extension for research purposes.
- It establishes a standardized framework for documenting patient and disease-related information, aiming to improve the comparability of datasets and cohort descriptions across different countries.
- The data set does not endorse specific assessment instruments, instead focusing on the systematic assessment of organ systems to allow for flexibility while ensuring comprehensive data collection.

### How this study might affect research, practice, or policy

- The core data set is intended to improve patient care by ensuring all crucial elements for managing SLE are documented.
- It aims to facilitate collaborative translational and observational research by creating a foundation for harmonized data collection across international registries.

- This standardization can enable clinical benchmarking, which promotes best practices and enhances interoperable patient care.
- The study lays the groundwork for establishing a global SLE data space and could accelerate the move towards personalized medicine in SLE care.

## INTRODUCTION

Systemic lupus erythematosus (SLE) is a complex and potentially life-threatening autoimmune disease, with marked heterogeneity in manifestations, course, and treatment response. In the past 3 decades, optimised use of older drugs, availability of newer drugs, improved diagnostic methods that help detect milder cases, and the implementation of evidence-based recommendations have collectively improved outcomes for individuals with SLE [1–5]. However, this positive trend has slowed in recent times [6]; mortality rates of patients with SLE remain significantly higher compared to the general population [7].

The endeavour in managing SLE is to optimise patient care and improve outcomes by shifting from a ‘trial and error’ approach to personalised medicine. This involves anticipating each patient’s individual trajectory and reducing the use of ineffective drugs. However, such efforts are hampered by a variety of factors, including the complexity and heterogeneity of the disease.

Coupled with the stagnation of improvements in patient outcomes in terms of mortality, organ damage, and health related quality of life, this underscores the need for comprehensive

analysis of big data to identify distinct disease patterns and states. Such analyses can then guide the identification of patient subgroups suitable for targeted clinical trials, a pressing need defined in the RheumaMap 2019 report [8]. However, achieving meaningful insights from such analyses depends on the availability of standardised datasets, which have not yet been available due to, among other reasons, the unsystematic utilisation of assessment instruments [9,10].

In the same context, a number of international and national SLE registers have been initiated over the past years across many European countries (Belgium, Denmark, Germany, Greece, Italy, the Netherlands, Portugal, Spain, and the United Kingdom) [11]. Smaller scale registries for individual hospitals, research centres, or regions have also emerged [11]. However, the potential for collaborative efforts among these groups to generate larger, more representative datasets is hampered by the absence of interoperable documentation standards. This deficit is particularly problematic for research focusing on challenging, less frequent disease manifestations, where collaboration is crucial [12].

Standardised documentation serves as the bedrock of all scientific collaborations that seek to ensure data integrity and comparability. While core datasets and standardised approaches have been established for other diseases, these cannot be seamlessly applied to SLE; due to the inherent variability of the disease and highly heterogeneous manifestations, a variety of different instruments are required to capture the full clinical spectrum of the disease. Moreover, the lack of standardised definitions of treatment targets was relieved only recently with definitions such as the Definition of Remission in SLE (DORIS) remission and Lupus Low Disease Activity State [13,14].

It was our aim to propose a SLE-specific dataset reaching out for standardising documentation not limited to outcomes, to improve patient care, enable comparisons of patient cohorts across different countries, and establish the groundwork for international registries. Data collected for research should meet principles of Findability, Accessibility, Interoperability, and Reusability (FAIR) [15].

Our objective was to define a comprehensive core dataset that includes all essential elements necessary to ensure complete clinical care and facilitate scientific research for the benefit of SLE patients. As for feasibility, we aimed to keep the number of items minimal while avoiding the need for additional items in clinical or scientific practice. This approach aligns with the definition provided by Ehlers et al [16] in their core dataset for giant cell arteritis.

## METHODS

The task force comprised a convenor (MS), a methodologist (GB), a fellow (JM), 16 members (MA, LA, RC, GC, LC, LWD, LI, SJ, MM, CP, JMP-R, SS, JGR, FT, MT-A-S, EMV, RVV), 2 EMEUNET members (EM, CW), 2 patient research partners (CKN, KM), and an associate professor for rehabilitation medicine and physiotherapist (CB), from a total of 14 different European countries.

### Generation of items

A stepwise process according to the European Alliance of Associations for Rheumatology (EULAR) standardised operating procedures (SOPs) [17] was applied. These SOPs were developed for the generation of treatment recommendations, whereas no SOPs exist for the generation of core datasets. The SOPs

were thus adapted where necessary. The flow chart illustrates the consensus process for the project (Fig 1). First, a hierarchical literature review was conducted in PubMed to identify items proposed by previous core datasets on SLE published from international societies (hierarchy level 1), previously published EULAR recommendations for monitoring SLE [18] and core datasets [16,19,20] as well as points to consider when reporting comorbidities [21] (hierarchy level 2), and relevant domains and items as well as instruments used in existing SLE registers and clinical cohorts and the frequency with which these items and instruments are collected (hierarchy level 3). The literature search for hierarchy level 1 retrieved zero results. The search for level 2 revealed 22 results, of which 6 publications were included. The search for relevant publications in hierarchy level 3 resulted in a total of 115 publications of 35 cohorts and registries that matched the inclusion criteria. A manual search was conducted to identify the primary methodological publications of domains and items collected in the respective cohorts. Five cohorts were not identified in the search process but were added manually. The literature review is described in detail in Supplementary Material. In addition, items identified as SLE-specific during the process of development of the American College of Rheumatology (ACR)/EULAR classification criteria were integrated into the collection [22]. The list was reviewed for missing elements of the International Classification of Functioning, Disability and Health (ICF) categories with implications for the functioning of SLE patients [23]. However, all relevant components of the ICF had been encompassed in the original list, although some were phrased in a less specific manner. Furthermore, the Core Outcome Set-Standards for Development recommendations were followed [24]. The primary collection was completed by the task force members, who were asked to add any missing items or instruments.

### Consensus process

In an anonymous online survey, the expert panel rated the perceived importance of each item and instrument to be included in a core dataset, using a numerical rating scale (NRS) from 1 (not important) to 10 (very important). The focus in this survey was on their clinical importance rather than their feasibility, which was discussed separately during a following physical meeting. Here, it became apparent that it would not be feasible to obtain a single dataset for both clinical care and research since this would result in an extensive list of items that might be challenging for practitioners to uniformly collect. Consequently, we decided to divide the dataset into 2 distinct components: a core dataset for clinical care and an extension dataset of additional items essential only for observational and translational research.

Further, the group agreed not to include any specific instruments for item collection, given the multitude and varied use of the established instruments.

The task force also ranked the identified items and instruments in small groups and assigned them to 1 of the 3 following categories: (1) essential items, (2) items of questionable necessity, and (3) items that need not be included. Each item was also assigned to (A) clinical care, (B) research, or (C) both care and research. The results from these subgroup discussions were then presented to the entire group and further discussed in plenary, focusing on both importance and feasibility.

After the meeting, the results were summarised and circulated among the task force to be commented on. Further, the assessment frequency of each item was discussed. After

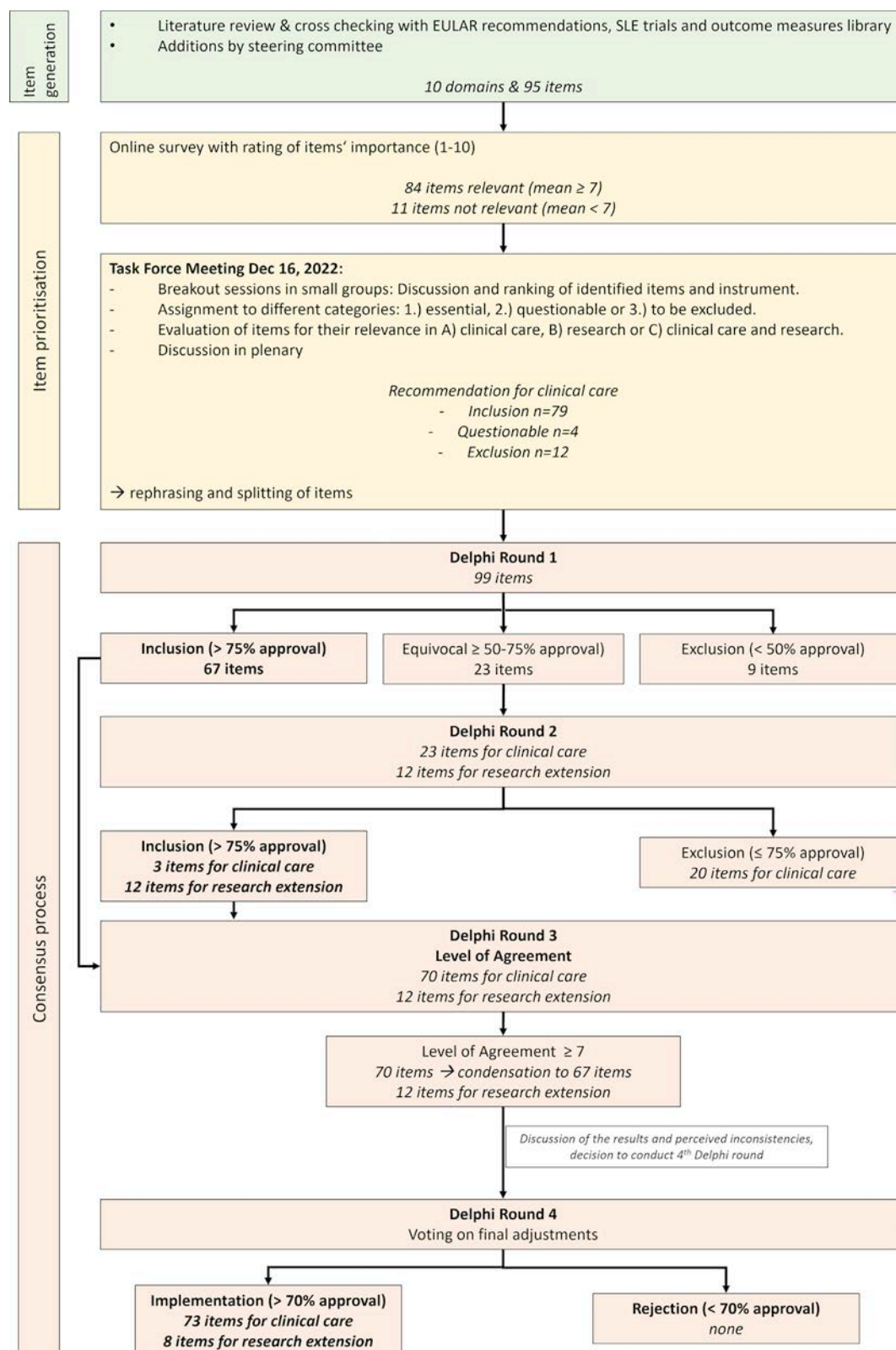


**Figure 1.** Flow chart of the development and consensus process. EULAR, European Alliance of Associations for Rheumatology; SLE, systemic lupus erythematosus.

harmonisation of feedback, a preliminary core set of parameters for clinical care and a research extension were generated.

A 3-round online Delphi survey was initiated. In the first round, the task force members were asked to evaluate each item for their relevance to be included in (A) a core dataset for clinical care and (B) an extension for translational and observational research, allowing only 'yes' or 'no' answers. According to the EULAR-approved voting procedures, consensus for inclusion

was defined as >75% in favour of the respective item. Items with <50% favourable votes were excluded. If between 50% and 75% of the votes were in favour, items were rediscussed and modified, and the task force members were asked to reconsider these items in the second Delphi round. With focus on item reduction, items were accepted if >75% voted in favour in the second Delphi round. All items with  $\leq 75\%$  in favour were excluded. As the clinical core dataset creates the framework for

observational research, items included in the clinical core dataset were excluded from consideration during the research extension voting process.

After achieving consensus on all items, a third voting step assessed the level of agreement (LoA) for the items included. LoA was rated on a NRS from 0 (indicating no agreement) to 10 (reflecting absolute agreement). Only items that gathered a minimum agreement rating of 7 were incorporated into the final set. The final round also comprised voting on the assessment frequency of each item, and the participants could express their agreement or disagreement with the proposed frequency.

After the third Delphi round, the group evaluated the results and identified remaining inconsistencies. Some items were included only in the research extension, even though they play an important role in clinical care. Additionally, important items needed for complete assessment of organ damage were missing. After intensive discussion, it was agreed to conduct a fourth Delphi round to address these inconsistencies. All proposed changes with more than 70% approval were implemented.

After voting on each item individually, items were placed in categories (of no formal impact), which resulted from consensus discussions without formal voting.

RESULTS

Item generation and prioritisation

The list of items generated after the hierarchical literature review and additions by the task force members resulted in a list of 10 domains with 95 items. Of the 95 items, 84 were voted relevant,

and 11 irrelevant in the online survey. Discussion of all items during the face-to-face meeting resulted in the informal inclusion of 76 items and exclusion of another 12 items and 4 debatable items for a clinical core dataset. Rephrasing and splitting resulted in a final list of 99 items to be voted on in the Delphi process.

Consensus process

After the first Delphi round, 9 items were excluded, and 23 had to be re-evaluated in the second Delphi round. Of the 23 items, 3 were included after the second round, and the remaining 20 items were excluded from the dataset holding 93 items at this time (Fig 2). Of the 29 items excluded from the clinical core dataset, 12 items reached consensus after the second round to be included in an extension dataset for translational and observational research.

To increase feasibility, items were merged where possible, as for example grouping lupus anticoagulant, anticardiolipin antibodies and anti-beta-2-glycoprotein-I antibodies as antiphospholipid antibodies and merging drug toxicity and intolerance. Many additional items could be grouped in specific domains, such as disease activity, damage, history, or comorbidities, and were further reorganised. These processes resulted in a clinical core dataset of 9 domains with 67 items with different assessment frequencies. The domains general, disease history, and serology (20 items) are to be assessed only at first visit. The domains comorbidities and damage are to be assessed (26 items) annually, whereas the domains laboratory parameters, outcomes, treatment, patient-reported outcomes (PROs) and disease activity (21 items) are to be assessed at each visit (Table 1).

Items excluded during the first voting process	
Items excluded during second voting process	<div>General</div> <div>Fulfilment of classification criteria</div> <div>Laboratory</div> <div>Immunoglobulin levels</div> <div>Treatment</div> <div>Drug adherence</div> <div>Other medication</div> <div>UV protection</div> <div>Disease activity</div> <div>Peripheral vascular manifestations</div> <div>Gastrointestinal manifestations</div> <div>Outcomes</div> <div>Low disease activity</div> <div>History</div> <div>Constitutional manifestations</div> <div>Gastrointestinal manifestations</div> <div>Ophthalmic manifestations</div>
	<div>Core items</div> <div>See table 3</div> <div>Damage</div> <div>Gastrointestinal</div> <div>Comorbidities</div> <div>Chronic liver disease</div> <div>Peptic ulcer disease</div> <div>Premature gonadal failure</div> <div>Vaccination</div> <div>Patient reported outcomes</div> <div>Health related quality of life</div> <div>Functionality</div>
Items excluded during the first voting process	
<div>General</div> <div>Family history of autoimmune diseases</div> <div>Dietary issues</div> <div>Treatment</div> <div>Non-pharmacologic treatment</div> <div>History</div> <div>Pain</div> <div>Comorbidities</div> <div>Osteoarthritis</div> <div>Patient reported outcomes</div> <div>Work productivity/status</div> <div>Physical activity</div> <div>Anxiety</div> <div>Stress</div>	

Figure 2. Excluded items considered for inclusion in the core dataset to support clinical care.



**Table 1**  
**Core dataset for clinical care**

First visit & on demand			Yearly			Regularly		
Domain/item	LoA <sup>a</sup> for item inclusion	Agreement with assessment frequency	Domain/item	LoA <sup>a</sup>	Agreement with assessment frequency	Domain/item	LoA <sup>a</sup>	Agreement with assessment frequency
<b>General</b>			<b>Comorbidities</b>			<b>Laboratory</b>		
Date of first symptoms (y)	8.28 ± 3.00 (80%)	96%	Diabetes mellitus	7.83 ± 2.81 (67%)	88%	Routine (electrolytes, CBC, WBC diff, creatinine, liver enzymes, urinalysis)	9.13 ± 1.51 (88%)	96%
Date of SLE diagnosis (y)	9.76 ± 0.59 (100%)	96%	Hypertension	8.42 ± 2.31 (75%)	83%	Complement levels (C3, C4)	9.29 ± 1.27 (92%)	88%
Date of birth	9.76 ± 0.71 (96%)	100%	Hypercholesterolemia	7.29 ± 2.91 (54%)	75%	Anti-dsDNA antibodies	9.54 ± 0.82 (100%)	88%
Sex	9.92 ± 0.39 (100%)	96%	Chronic kidney disease	8.42 ± 2.83 (79%)	83%			
Race/ethnicity	8.88 ± 2.41 (84%)	96%	Chronic pulmonary disease	7.79 ± 2.83 (67%)	67%	<b>Outcomes</b>		
Date of death	8.88 ± 2.89 (88%)	54%	Psychiatric disease	6.92 ± 2.97 (42%)	58%	Hospitalisation incl. reason	8.21 ± 2.74 (71%)	79%
Height	7.68 ± 2.78 (68%)	71%	Depression	7.46 ± 2.86 (54%)	63%	Flares	9.25 ± 1.39 (88%)	92%
Weight	7.80 ± 2.81 (72%)	54%	Osteoporosis	7.79 ± 2.50 (58%)	75%	Physician Global Assessment	8.71 ± 1.57 (79%)	83%
Pregnancy morbidity history/ pregnancy losses	8.48 ± 2.30 (80%)	54%	Fibromyalgia	6.79 ± 3.56 (50%)	54%	Remission	9.21 ± 2.02 (96%)	83%
			Cardiovascular events	8.38 ± 2.78 (79%)	75%	<b>Treatment</b>		
			Stroke	8.42 ± 2.77 (83%)	83%	Lupus specific	9.71 ± 0.68 (100%)	96%
			Cancer	8.00 ± 2.78 (67%)	79%	Antiplatelet drugs & anticoagulants	8.83 ± 2.21 (92%)	75%
			Thromboembolic event	8.33 ± 2.81 (79%)	79%	Drug toxicity & intolerance	8.17 ± 2.70 (71%)	75%
			Infections	7.38 ± 2.98 (63%)	71%			
			Sjögren's Disease	7.38 ± 2.83 (58%)	63%	<b>Patient-reported outcomes</b>		
			Other rheumatic diseases	7.75 ± 2.40 (67%)	63%	Fatigue	8.25 ± 2.28 (75%)	75%
			Other autoimmune diseases <sup>b</sup>	7.92 ± 2.45 (67%)	63%	Current pain	8.25 ± 2.13 (75%)	75%
<b>Disease history</b>			<b>Damage</b>			<b>Disease activity</b>		
Mucocutaneous	8.79 ± 2.22 (75%)	92%	Mucocutaneous	9.36 ± 1.26 (92%)	88%	Mucocutaneous	9.72 ± 0.66 (100%)	92%
Renal	9.29 ± 1.34 (88%)	92%	Renal	9.52 ± 1.20 (92%)	88%	Renal	9.80 ± 0.57 (100%)	92%
Cardiovascular	8.38 ± 2.75 (75%)	92%	Cardiovascular	9.28 ± 1.40 (88%)	88%	Cardiovascular	9.40 ± 1.17 (92%)	83%
Respiratory	8.33 ± 2.76 (71%)	92%	Respiratory	9.40 ± 1.23 (92%)	79%	Respiratory	9.44 ± 1.10 (92%)	79%
Neuropsychiatric	8.99 ± 2.15 (79%)	92%	Neuropsychiatric	9.44 ± 1.24 (92%)	83%	Neuropsychiatric	9.48 ± 0.98 (96%)	83%
Peripheral vascular	7.71 ± 3.17 (63%)	88%	Peripheral vascular	8.84 ± 2.20 (88%)	79%	Constitutional	9.04 ± 1.59 (84%)	83%
Haematology	8.88 ± 2.15 (79%)	92%				Haematology	9.68 ± 0.79 (96%)	92%
Musculoskeletal	8.79 ± 2.22 (75%)	92%	Musculoskeletal	9.40 ± 1.30 (88%)	88%	Musculoskeletal	9.68 ± 0.79 (96%)	92%
Secondary APS	9.25 ± 1.42 (88%)	92%	Ophthalmic	8.60 ± 2.38 (76%)	88%	Ophthalmic	8.72 ± 1.73 (80%)	58%
		Agreement 4th Delphi round			Agreement 4th Delphi round			Agreement 4th Delphi round
Gastrointestinal <sup>c</sup>	na	77%	Gastrointestinal <sup>d</sup>	8.21 ± 2.63 (71%)	69%	Gastrointestinal <sup>d</sup>	8.04 ± 2.47 (67%)	83%
Ophthalmic <sup>c</sup>	na	73%	Premature gonadal failure <sup>d</sup>	8.63 ± 2.29 (79%)	100%	Peripheral vascular <sup>d</sup>	8.46 ± 2.50 (75%)	83%
Constitutional <sup>d</sup>	8.04 ± 2.51 (63%)	82%	Diabetes <sup>c</sup>	na	77%			
			Cancer <sup>c</sup>	na	77%			
<b>Serology</b>		<b>Agreement with assessment frequency</b>						
ANA + ENA profile	9.38 ± 1.11 (88%)	96%						
Antiphospholipid antibodies (LA, aCL, a/β2-GP I)	9.46 ± 0.96 (96%)	79%						

a/β2-GP I, anti-beta2 glycoprotein I; aCL, anticardiolipin; ANA, antinuclear antibody; APS, antiphospholipid syndrome; CBC, complete blood count; ENA, extractable nuclear antigen; LA, lupus anticoagulant; LoA, level of agreement; na, not applicable; SLE, systemic lupus erythematosus; WBC diff, white blood cell differential.

<sup>a</sup> LoA in mean ± SD (proportion of taskforce members with an agreement ≥7 on the 1-10 scale, expressed in percent).

<sup>b</sup> Including Sjögren's Disease (LoA<sup>a</sup> 7.38 ± 2.83 [58%]) and other rheumatic diseases (LoA<sup>a</sup> 7.75 ± 2.40 [67%]).

<sup>c</sup> Inclusion as result of the 4th Delphi round.

<sup>d</sup> Transfer from research extension as result of 4th Delphi round.

Table 2  
Research extension

Domain/item	LoA <sup>a</sup>
General	
Fulfilment of classification criteria at diagnosis	9.58 ± 1.11 (96%)
Damage	
Haematology <sup>b</sup>	8.84 ± 2.31 (84%)
Comorbidities	
Vaccinations	8.04 ± 2.15 (67%)
Outcomes	
Low disease activity	8.38 ± 2.45 (75%)
Treatment	
Drug adherence	8.25 ± 2.20 (71%)
Other medication	7.96 ± 2.75 (71%)
Patient-reported outcomes	
Health related quality of life	9.00 ± 1.44 (83%)
Work productivity/status	7.92 ± 1.85 (63%)

LoA, level of agreement.

<sup>a</sup> LoA in mean ± SD (proportion of taskforce members with an agreement >7 in percent).

<sup>b</sup> Transfer from clinical core set with 91% agreement as result of 4th Delphi round.

In the third Delphi round, all items included in the clinical core dataset reached a LoA of 7 or higher (Table 1). Likewise, all 12 items included in the research extension reached LoA of ≥7 and were therefore included (Table 2). Most participants agreed with the proposed frequency of item assessment, although less agreement was seen for those items that had already lower average LoA regarding their inclusion (Table 1).

Following the discussion of the consensus results, all the following proposed changes were agreed on in a fourth Delphi round:

1. Transferring ‘peripheral vascular’ and ‘gastrointestinal’ disease activity to the clinical core dataset, to enable a complete evaluation of disease activity.
2. Moving ‘haematological’ damage to the research extension since it is not standardised as a damage item.
3. Shifting ‘gastrointestinal’ and ‘premature gonadal failure’ from the research extension to the clinical core dataset to complete the assessment of organ damage.
4. Adding ‘diabetes’ and ‘cancer’ to disease damage, as these items are defined as such only if starting after the diagnosis of SLE, while they are captured under the comorbidities field regardless of the time of onset.
5. Combining the comorbidities ‘other rheumatic diseases’ and ‘Sjögren Disease’ under ‘other autoimmune diseases.’
6. Including ‘ophthalmic’ and ‘gastrointestinal’ disease history in the clinical core dataset and transferring ‘constitutional’ disease history from the research extension to the clinical core dataset, based on the rationale that disease history represents previous activity, and all disease activity items should be included in the disease history domain within the clinical core dataset.

This resulted in a final core dataset for clinical care of 9 domains with 73 items and a research extension of 8 items (Table 3).

The documentation of both lupus-specific and nonspecific medications sparked discussion within the taskforce. Much of the debate centred on the precise documentation of glucocorticoids and the question whether it was necessary to assess non-specific drugs, particularly those needed to treat comorbidities of patients with SLE. Additionally, there were challenges in

distinguishing between SLE-specific and nonspecific drugs. No consensus regarding nonspecific drugs was reached. Therefore, these were not included into the final dataset.

The inclusion of PROs elicited mixed responses within the taskforce. Members recognised that a considerable amount of information about a patient’s well-being is gathered through effective communication between clinicians and patients during visits, which might not be fully captured by specific items. However, there was a consensus that, at a minimum, the impact of the disease on the patient’s life should be assessed. Consequently, fatigue and current pain achieved consensus for inclusion in the clinical core dataset, whereas aspects like health related quality of life and work productivity or work status were designated part of the research extension. Nonetheless, patient-centred aspects such as quality of life and depression were deemed important and should be addressed during the clinical visits, given their impact on patients’ lives and their significance as patient outcomes.

We debated whether the assessment of disease activity should focus only on the most common features or include all manifestations, including rare features such as ophthalmic involvement. We noted that in cases where less common features are present, they would be crucial to clinical decision making and should already be captured in routine medical records. To date, no validated instrument exists for the assessment of disease flares outside the context of randomised controlled studies. It was therefore decided to include the raw data to capture flares such as disease activity and treatment changes instead of including a specific instrument.

Regarding comorbidities, it was discussed to refer to the EULAR initiative on points to consider for reporting, screening for and preventing selected comorbidities in chronic inflammatory rheumatic diseases in daily practice [21] as well as the EULAR recommendations for cardiovascular risk management in rheumatic and musculoskeletal diseases, including SLE and antiphospholipid syndrome [25]. However, from the point of view of this panel, the recommended comorbidities were not depicted in a sufficiently comprehensive way. Thus, a separate list was developed and subjected to the voting process. Assessment of comorbidities should be performed at baseline and then be rechecked at least yearly for changes. Although validated scoring systems could be utilised, it was recognised that these scores might not cover all the comorbidities included in the assessment, underlining the need for comprehensive evaluation.

Use of instruments

There is a variety of competing validated instruments, particularly for assessing disease activity. Each of these disease activity instruments, including SLE disease activity index (SLEDAI) [26], SLE disease activity score (SLE-DAS) [27], and British Isles Lupus Assessment Group (BILAG) 2004 index [28], has advantages and disadvantages. There is also an ongoing revision of the SLE inception cohort (SLICC)/ACR damage index [29,30] as well as a disease activity response measure for trials [31]. Therefore, the taskforce decided to focus on systematic assessment of organ systems within the core dataset, instead of recommending specific instruments for data collection. However, there was strong emphasis on the importance of using validated instruments for assessment of disease activity and disease damage, as recommended in the current 2023 update of the EULAR recommendations for the management of SLE [5]. The choice of which instrument to use was left to the discretion of the practitioner, provided that it encompasses all the items outlined in the core

Table 3

Core dataset for SLE to support clinical care and research extension for observational and translational research (research extension in red)

	First visit & on demand		Regularly		Yearly	
	Demographics	Date of birth	Treatment	Lupus specific		
		Sex		Antiplatelet & anticoagulants		
		Race/ethnicity		Drug toxicities & intolerance		
		Height		Adherence		
		Weight		Other medication		
	Date of death					
	Disease onset	Year of first SLE symptom	Lab	Routine lab		
		Year of diagnosis		C3, C4		
		Fulfillment of classification criteria at diagnosis	dsDNA antibodies			
Basic lab	ANA & ENA profile	Outcomes	Hospitalization			
	aPL antibodies		Flares			
			PGA			
			Remission			
			LDA			
		PRO	Fatigue			
			Pain			
			HRQoL			
			Work productivity			
	Disease history		Disease activity		Damage	Comorbidities
Skin/ mucocutaneous	X		X		X	
Renal	X		X		X	X
Cardiovascular	X		X		X	X
Respiratory	X		X		X	X
Neuropsychiatric	X		X		X	X
Peripheral vascular	X		X		X	X
Hematology	X		X		X	
Musculoskeletal	X		X		X	
Ophthalmic	X		X		X	
Constitutional	X		X			
Gastrointestinal	X		X		X	X
Sec. Aps	X					
History of pregnancy morbidity	X					
Premature gonadal failure					X	
Diabetes					X	X
Cancer					X	X
Hypertension						X
Vaccinations						X
Other autoimmune diseases						X

ANA, antinuclear antibody; aPL, antiphospholipid; APS, antiphospholipid syndrome; C3/C4, complement 3/4; dsDNA, double-stranded DNA; ENA, extractable nuclear antigen; HRQoL, health related quality of life; LDA, low disease activity; PRO, patient-reported outcome; SLE, systemic lupus erythematosus.

dataset. This approach was thought to allow for flexibility, while ensuring comprehensive data collection and maintaining the highest standards of patient care and research. In addition, this should also guarantee that FAIR data can be made available.

## DISCUSSION

The aim of the taskforce was to develop a EULAR-endorsed core set of items to support clinical care and observational and translational research in SLE patients that also enables FAIR data. Given the inherent diversity of the disease, compounded by the use of various assessment tools, achieving standardisation in SLE care is complex.

However, standardisation will be essential for ensuring high-quality care aiming to optimise the patients' outcome and to facilitate collaborative research. This standardisation would also enable both the comparison of patient cohorts and clinical

benchmarking, ultimately promoting best practice and the enhancement of interoperable patient care over time.

As a consequence, the taskforce embarked on a systematic approach to develop this core dataset, encompassing all the essential elements required for managing SLE patients in clinical practice and for performing observational and translational research. The taskforce applied a stepwise methodological process, which resulted in a clinical core dataset of 73 items and additional 8 items for research purposes.

The initial list of 99 items was reduced during the voting process. Moreover, many of the items could be grouped into broader domains, such as disease activity or comorbidity. However, the taskforce made a deliberate decision to still include all items individually. Listing these items separately aimed to emphasise their individual importance in the evaluation of SLE patients, ensuring that no critical details were overlooked during the assessment process.

In 2010, Mosca et al [18] formulated EULAR recommendations for monitoring SLE patients in clinical practice and observational studies. These guidelines encompass an inherent core set for disease, but were not developed in a consensus-based process [18]. Since this dataset served as a foundation for the initial item list generation, a substantial portion of the items proposed by Mosca et al [18] constitutes the core dataset presented here. Diverging from those recommendations, each item underwent thorough discussions regarding its significance and practical application, culminating in a consensus-based voting process.

We made the deliberate choice not to endorse specific instruments and, as a result, have also intentionally refrained from including definitions of specific items. When assessing disease activity and damage, the definitions provided within the validated instruments should be used. As a consequence, merging core data from different sources may need some adaptation to ensure interoperability. Furthermore, depending on the favoured instruments, some instrument-specific items must be documented in addition to the core set to capture disease activity and damage. It is the physician's responsibility to ensure that applied instruments are collected comprehensively.

This core dataset may partly overlap with the continuous Outcome Measures in Rheumatology (OMERACT) international consensus efforts on identifying definitions for clinical domains and outcomes [32–34]. The OMERACT core domain is to define domains to be used in randomised controlled trials and longitudinal observational studies, and may well lead to new instruments, if none of sufficient quality are available.

In some contrast, our work aimed at the development of a SLE-specific dataset reaching out for standardising documentation not limited to outcomes, to improve patient care, enable comparisons of patient cohorts across different countries, and establish the groundwork for international registries.

Developing this dataset that is both comprehensive and feasible for clinical assessment proved challenging. Given the complexity of SLE, we anticipated the resulting dataset to be more extensive than previously proposed EULAR-endorsed core datasets. However, we believe that the 73 items remain feasible for assessment in clinical care, particularly considering that many of these items do not require regular assessment but rather periodic, eg, yearly, or only one-time evaluation. Nevertheless, it is important to recognise that this dataset represents a compromise between extensive data collection and the essential minimum needed to support clinical care effectively. In the context of digital application, future endeavours will involve extracting a common general assessment applicable to all inflammatory rheumatic diseases and employing standardised nomenclature (eg, Systematized Nomenclature or Medicine and Clinical Terms [SNOMED CT [35]]) alongside a common data dictionary (including metadata and machine-resolvable persistent identifiers as required by the FAIR principles) to facilitate interaction, interoperability, FAIR data, and successful collaboration.

Despite their parallels, childhood-onset and adult SLE differs significantly in many aspects. Therefore, this dataset is aimed at adult SLE patients, only. A comprehensive core dataset for childhood-onset SLE has recently been published and should be applied in these children and adolescents with SLE.

The implementation of the core dataset is a vital step towards ensuring its successful development. With the taskforce consisting of experts from 14 countries, they will actively support integrating the dataset into future national and international SLE registries, such as a potential European Reference Network (ERN) ReCONNET registry. Additionally, existing cohorts and

registries will be checked to ensure that they contain all recommended items.

Three years after the publication of this core dataset, we aim to evaluate its implementation by surveying its citation in published observational and translational studies and assessing whether these studies have incorporated the recommended items.

This work was performed to support the work of ongoing and future taskforces in the field of SLE by providing a core set of items to be collected in clinical care and observational and translational research. A uniform collection of these items will homogenise datasets and facilitate research that will then inform future taskforces.

## CONCLUSION

We developed a comprehensive core dataset that encompasses all the crucial elements required for the effective management of SLE patients in clinical care. This standardised dataset further serves as the fundamental framework for collaborative translational and observational research by enabling comparability of datasets and patient cohorts. This comparability facilitates clinical benchmarking, leading to advancements in our understanding and treatment of SLE. Ultimately, in this way, we aim at improving the care and quality of life for individuals living with SLE.

## Competing interests

Johanna Mucke reports financial support, administrative support, and travel were provided by EULAR. Johanna Mucke reports a relationship with AbbVie Inc, AstraZeneca, BMS, GSK, Janssen-Cilag, Lilly, Novartis that includes: consulting or advisory and speaking and lecture fees. Chris Wincup reports a relationship with AbbVie, AstraZeneca, Bristol Myers Squibb, Kyverna, Otsuka, UCB that includes: speaking and lecture fees. Chris Wincup reports a relationship with Biogen Inc that includes: board membership. Edward M Vital reports a relationship with Roche, GSK, AstraZeneca, UCB, Otsuka, BMS, Pfizer, AbbVie, Alpine, Alumis, Merck, BMS, Aurinia Pharmaceuticals that includes: consulting or advisory. Edward M Vital reports a relationship with AstraZeneca, Sandoz that includes: funding grants. George Bertias reports a relationship with AbbVie, Pfizer, GSK, AstraZeneca, Lilly, Otsuka, Novartis that includes: funding grants and speaking and lecture fees. Gamal Chehab reports a relationship with GSK, AstraZeneca, Otsuka, Alexion that includes: consulting or advisory and speaking and lecture fees. Jose M Pego-Reigosa reports a relationship with GSK, Pfizer that includes: funding grants. Jose M Pego-Reigosa reports a relationship with GSK, AstraZeneca, Lilly that includes: speaking and lecture fees. Jose M Pego-Reigosa reports a relationship with GSK, AstraZeneca that includes: travel reimbursement. Jose M Pego-Reigosa reports a relationship with GSK, Otsuka, Gebro, AstraZeneca, Boehringer Ingelheim, MSD that includes: consulting or advisory. Laurent Arnaud reports a relationship with Alexion, Amgen, AstraZeneca, AbbVie, Alpine, Biogen, BMS, Boehringer Ingelheim, Chugai, GSK, Grifols, Janssen-Cilag, Kezar, LFB, Lilly, Medac, Novartis, Pfizer, Roche, UCB that includes: consulting or advisory, funding grants, and speaking and lecture fees. László Czirkjak reports a relationship with AbbVie, AstraZeneca, Boehringer Ingelheim, GSK, Lilly, MSD, Novartis, Pfizer that includes: consulting or advisory and speaking and lecture fees. Luís Ines reports a relationship with GSK, AstraZeneca that includes: consulting or advisory. Lene



Wohlfahrt Dreyer reports a relationship with BMS, AbbVie that includes: funding grants. Martin Aringer reports a relationship with AbbVie, AstraZeneca, Boehringer Ingelheim, GSK, Lilly, Novartis, Otsuka Pharma, Pfizer, Roche, UCB that includes: consulting or advisory and funding grants. Marta Mosca reports a relationship with AstraZeneca, GSK, AbbVie, UCB, Jansse, BMS, Otsuka, Alpine, Pfizer, Novartis that includes: consulting or advisory and speaking and lecture fees. Matthias Schneider reports a relationship with GSK, AstraZeneca, Otsuka that includes: consulting or advisory and speaking and lecture fees. Matthias Schneider reports a relationship with GSK, AstraZeneca that includes: funding grants. Michel W P Tsang-A-Sjoe reports a relationship with AstraZeneca, GSK that includes: consulting or advisory and speaking and lecture fees. Ricard Cervera reports a relationship with GSK, AstraZeneca, Celgene, Janssen, Eli Lilly, Pfizer, UCB, Rubió, Werfen, ThermoFisher that includes: consulting or advisory. Ronald Van Vollenhoven reports a relationship with BMS, Alfasigma, AstraZeneca, Galapagos, MSD, Novartis, Pfizer, Roche, Sanofi, UCB that includes: funding grants. Ronald Van Vollenhoven reports a relationship with AbbVie, AstraZeneca, Biogen, BMS, Galapagos, GSK, Janssen, Pfizer, RemeGen, UCB that includes: consulting or advisory and speaking and lecture fees. The other authors declare they have no competing interests.

## CRediT authorship contribution statement

**Johanna Mucke:** Writing – original draft, Project administration, Methodology, Funding acquisition, Formal analysis, Data curation, Conceptualization. **George Bertsias:** Writing – review & editing, Methodology, Data curation, Conceptualization. **Martin Aringer:** Writing – review & editing, Data curation. **Laurent Arnaud:** Writing – review & editing, Data curation. **Carina Boström:** Writing – review & editing, Data curation. **Ricard Cervera:** Writing – review & editing, Data curation. **Gamal Chehab:** Writing – review & editing, Data curation, Conceptualization. **László Cziráj:** Writing – review & editing, Data curation. **Lene Wohlfahrt Dreyer:** Writing – review & editing, Data curation. **Luís Inês:** Writing – review & editing, Data curation. **Søren Jacobsen:** Writing – review & editing, Data curation. **Charite Kjaerside Nielsen:** Writing – review & editing, Data curation. **Emiliano Marasco:** Writing – review & editing, Data curation. **Marta Mosca:** Writing – review & editing, Data curation. **Kirsi Myllys:** Writing – review & editing, Data curation. **Cristina Pamfil:** Writing – review & editing, Data curation. **Jose M. Pego-Reigosa:** Writing – review & editing, Data curation. **Jutta G. Richter:** Writing – review & editing, Data curation. **Savino Sciascia:** Writing – review & editing, Data curation. **Farah Tamirou:** Writing – review & editing, Data curation. **Michel Tsang-A-Sjoe:** Writing – review & editing, Data curation. **Edward M. Vital:** Writing – review & editing, Data curation. **Ronald Van Vollenhoven:** Writing – review & editing, Data curation. **Chris Wincup:** Writing – review & editing, Data curation. **Matthias Schneider:** Writing – original draft, Project administration, Methodology, Funding acquisition, Data curation, Conceptualization.

## Funding

This work was funded by a EULAR grant (QoC 007).

## Patient consent for publication

Not required.

## Ethics approval

Full information about the study was given when inviting potential participants via email as well as during the face-to-face meeting and in preparation of the Delphi survey. This study was reviewed and approved by all task force members prior to submission.

## Provenance and peer review

Not commissioned; externally peer reviewed.

## Data availability statement

The data that support the findings of this study are available from the corresponding author (JM) upon reasonable request.

## Patient and public involvement

Patients were involved in the design, conduct, reporting, and dissemination plans of this research. Refer to the Methods section for further details.

## Supplementary materials

Supplementary material associated with this article can be found in the online version at [doi:10.1016/j.ard.2025.07.001](https://doi.org/10.1016/j.ard.2025.07.001).

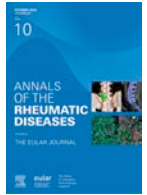
## Orcid

Johanna Mucke: <http://orcid.org/0000-0001-8915-7837>  
 George Bertsias: <http://orcid.org/0000-0001-5299-1406>  
 Martin Aringer: <http://orcid.org/0000-0003-4471-8375>  
 Carina Boström: <http://orcid.org/0000-0002-2506-687X>  
 Gamal Chehab: <http://orcid.org/0000-0001-7309-2370>  
 Luís Inês: <http://orcid.org/0000-0003-3172-3570>  
 Søren Jacobsen: <http://orcid.org/0000-0002-5654-4993>  
 Jutta G. Richter: <http://orcid.org/0000-0001-8194-3243>  
 Michel Tsang-A-Sjoe: <http://orcid.org/0000-0002-4982-3505>  
 Chris Wincup: <http://orcid.org/0000-0002-8742-8311>  
 Matthias Schneider: <http://orcid.org/0009-0007-2106-9196>

## REFERENCES

- [1] Doria A, Iaccarino L, Ghirardello A, Zampieri S, Arienti S, Sarzi-Puttini P, et al. Long-term prognosis and causes of death in systemic lupus erythematosus. *Am J Med* 2006;119(8):700–6.
- [2] Bertsias G, Ioannidis JPA, Boletis J, Bombardieri S, Cervera R, Dostal C, et al. EULAR recommendations for the management of systemic lupus erythematosus. Report of a task force of the EULAR Standing Committee for International Clinical Studies Including Therapeutics. *Ann Rheum Dis* 2008;67(2):195–205. doi: [10.1136/ard.2007.070367](https://doi.org/10.1136/ard.2007.070367).
- [3] Fanouriakis A, Kostopoulou M, Alunno A, Aringer M, Bajema I, Boletis JN, et al. 2019 update of the EULAR recommendations for the management of systemic lupus erythematosus. *Ann Rheum Dis* 2019;78(6):736–45.
- [4] Fanouriakis A, Kostopoulou M, Cheema K, Anders HJ, Aringer M, Bajema I, et al. 2019 Update of the Joint European League Against Rheumatism and European Renal Association-European Dialysis and Transplant Association (EULAR/ERA-EDTA) recommendations for the management of lupus nephritis. *Ann Rheum Dis* 2020;79(6):713–23. doi: [10.1136/annrheumdis-2020-216924](https://doi.org/10.1136/annrheumdis-2020-216924).
- [5] Fanouriakis A, Kostopoulou M, Andersen J, Aringer M, Arnaud L, Bae SC, et al. EULAR recommendations for the management of systemic lupus erythematosus: 2023 update. *Ann Rheum Dis* 2024;83:15–29. doi: [10.1136/ard-2023-224762](https://doi.org/10.1136/ard-2023-224762).

- [6] Ruiz E, Ramalle-Gómara E, Á Elena, Quiñones C, Alonso V, Posada M, et al. Trends in systemic lupus erythematosus mortality in Spain from 1981 to 2010. *Lupus* 2014;23(4):431–5.
- [7] Lee YH, Choi SJ, Ji JD, Song GG. Overall and cause-specific mortality in systemic lupus erythematosus: an updated meta-analysis. *Lupus* 2016;25(7):727–34.
- [8] European Alliance of Associations for Rheumatology. RheumaMap-Research Roadmap to transform the lives of people with rheumatic and musculoskeletal diseases 2019. [ cited 2024 Nov 23 ] <https://www.eular.org/web/static/lib/pdfs/web/viewer.html?file=https://www.eular.org/document/download/184/9ad4d185-1db2-4018-b343-7668837ffdab/188>.
- [9] Askanase AD, Merrill JT. Measuring disease activity in SLE is an ongoing struggle. *Nat Rev Rheumatol* 2019;15(4):194–5.
- [10] Petri M. Disease activity assessment in SLE: do we have the right instruments? *Ann Rheum Dis* 2007;66(Suppl 3):iii61–4 Suppl 3.
- [11] Bandeira M, Di Cianni F, Marinello D, Arnaud L, Cannizzo S, Carta C, et al. An overlook on the current registries for rare and complex connective tissue diseases and the future scenario of TogethERN ReCONNET. *Front Med (Lausanne)* 2022;9:889997. doi: 10.3389/fmed.2022.889997.
- [12] Le Sueur H, Bruce IN, Geifman N, MASTERPLANS Consortium. The challenges in data integration - heterogeneity and complexity in clinical trials and patient registries of systemic lupus erythematosus. *BMC Med Res Methodol* 2020;20(1):164.
- [13] van Vollenhoven RF, Bertsias G, Doria A, Isenberg D, Morand E, Petri MA, et al. 2021 DORIS definition of remission in SLE: final recommendations from an international task force. *Lupus Sci Med* 2021;8(1):e000538.
- [14] Franklyn K, Lau CS, Navarra SV, Louthrenoo W, Lateef A, Hamijoyo L, et al. Definition and initial validation of a lupus low disease activity state (LLDAS). *Ann Rheum Dis* 2016;75(9):1615–21.
- [15] Wilkinson MD, Dumontier M, Aalbersberg IJJ, Appleton G, Axton M, Baak A, et al. The FAIR guiding principles for scientific data management and stewardship. *Sci Data* 2016;3:160018. doi: 10.1038/sdata.2016.18.
- [16] Ehlers L, Askling J, Bijlsma HW, Cid MC, Cutolo M, Dasgupta B, et al. 2018 EULAR recommendations for a core data set to support observational research and clinical care in giant cell arteritis. *Ann Rheum Dis* 2019;78(9):1160–6.
- [17] van der Heijde D, Aletaha D, Carmona L, Edwards CJ, Kvien TK, Kouloumas M, et al. 2014 Update of the EULAR standardised operating procedures for EULAR-endorsed recommendations. *Ann Rheum Dis* 2015;74(1):8–13.
- [18] Mosca M, Tani C, Aringer M, Bombardieri S, Boumpas D, Brey R, et al. European League Against Rheumatism recommendations for monitoring patients with systemic lupus erythematosus in clinical practice and in observational studies. *Ann Rheum Dis* 2010;69(7):1269–74.
- [19] Meissner Y, Fischer-Betz R, Andreoli L, Costedoat-Chalumeau N, De Cock D, Dolhain RJEM, et al. EULAR recommendations for a core data set for pregnancy registries in rheumatology. *Ann Rheum Dis* 2021;80:49–56.
- [20] Radner H, Chatzidionysiou K, Nikiphorou E, Gossec L, Hyrich KL, Zabalán C. 2017 EULAR recommendations for a core data set to support observational research and clinical care in rheumatoid arthritis. *Ann Rheum Dis* 2018;77(4):476–9. doi: 10.1136/annrheumdis-2017-212256.
- [21] Baillet A, Gossec L, Carmona L, Md Wit, van Eijk-Hustings Y, Bertheussen H, et al. Points to consider for reporting, screening for and preventing selected comorbidities in chronic inflammatory rheumatic diseases in daily practice: a EULAR initiative. *Ann Rheum Dis* 2016;75(6):965–73.
- [22] Aringer M, Costenbader K, Daikh D, Brinks R, Mosca M, Ramsey-Goldman R, et al. 2019 European League Against Rheumatism/American College of Rheumatology classification criteria for systemic lupus erythematosus. *Ann Rheum Dis* 2019;78(9):1151–9.
- [23] Leuchten N, Bauernfeind B, Kuttner J, Stamm T, Smolen JS, Pisetsky DS, et al. Relevant concepts of functioning for patients with systemic lupus erythematosus identified in a Delphi exercise of experts and a literature review. *Arthritis Care Res (Hoboken)* 2014;66(12):1895–904.
- [24] Kirkham JJ, Davis K, Altman DG, Blazeby JM, Clarke M, Tunis S, et al. Core Outcome Set-STAndards for Development: the COS-STAD recommendations. *PLoS Med* 2017;14(11):e1002447.
- [25] Drosos GC, Vedder D, Houben E, Boekel L, Atzeni F, Badreh S, et al. EULAR recommendations for cardiovascular risk management in rheumatic and musculoskeletal diseases, including systemic lupus erythematosus and antiphospholipid syndrome. *Ann Rheum Dis* 2022;81(6):768–79. doi: 10.1136/annrheumdis-2021-221733.
- [26] Gladman DD, Ibañez D, Urowitz MB. Systemic lupus erythematosus disease activity index 2000. *J Rheumatol* 2002;29(2):288–91.
- [27] Jesus D, Matos A, Henriques C, Zen M, Larosa M, Iaccarino L, et al. Derivation and validation of the SLE Disease Activity Score (SLE-DAS): a new SLE continuous measure with high sensitivity for changes in disease activity. *Ann Rheum Dis* 2019;78(3):365–71.
- [28] Isenberg DA, Rahman A, Allen E, Farewell V, Akil M, Bruce IN, et al. BILAG 2004. Development and initial validation of an updated version of the British Isles Lupus Assessment Group's disease activity index for patients with systemic lupus erythematosus. *Rheumatology (Oxford)* 2005;44(7):902–6. doi: 10.1093/rheumatology/keh624.
- [29] Gladman DD, Ginzler E, Goldsmith C, Fortin P, Liang M, Urowitz M, et al. The development and initial validation of the systemic lupus international collaborating clinics/American College of Rheumatology damage index for systemic lupus erythematosus. *Arthritis Rheum* 1996;39(3):363–9.
- [30] Johnson SR, Gladman DD, Brunner HI, Isenberg D, Clarke AE, Barber MRW, et al. Evaluating the construct of damage in systemic lupus erythematosus. *Arthritis Care Res (Hoboken)* 2023;75(5):998–1006. doi: 10.1002/acr.24849.
- [31] Connelly K, Eades LE, Koelmeyer R, Ayton D, Golder V, Kandane-Rathnayake R, et al. Towards a novel clinical outcome assessment for systemic lupus erythematosus: first outcomes of an international taskforce. *Nat Rev Rheumatol* 2023;19(9):592–602. doi: 10.1038/s41584-023-00993-7.
- [32] Nielsen W, Kharouf F, Grajales CM, Thayaparan A, Anderson M, Strand V, et al. Scoping literature review to identify candidate domains for the OMER-ACT systemic lupus erythematosus core outcome set. *Semin Arthritis Rheum* 2025;72:152684. doi: 10.1016/j.semarthrit.2025.
- [33] Nielsen W, Strand V, Simon L, Pinsker E, Bonilla D, Morand E, et al. OMER-ACT systemic lupus erythematosus domain survey. *Semin Arthritis Rheum* 2024;68:152520. doi: 10.1016/j.semarthrit.2024.152520.
- [34] Smolen JS, Strand V, Cardiel M, Edworthy S, Furst D, Gladman D, et al. Randomized clinical trials and longitudinal observational studies in systemic lupus erythematosus: consensus on a preliminary core set of outcome domains. *J Rheumatol* 1999;26(2):504–7.
- [35] SNOMED International. SNOMED CT 2024 [cited 2024 Mar 21]. Available from: <https://www.snomed.org/>



## Rheumatoid arthritis

## Global recruitment patterns and placebo responses in clinical trials of rheumatoid arthritis

Andreas Kerschbaumer<sup>1</sup>, Marlene Steiner<sup>1</sup>, Pascale Pruckner<sup>1</sup>,  
Brigitte Wildner<sup>2</sup>, Magdalena Maad<sup>3</sup>, Josef S. Smolen<sup>1</sup>, Daniel Aletaha<sup>1,\*</sup>

<sup>1</sup> Department of Medicine III, Division of Rheumatology, Medical University of Vienna, Spitalgasse 23, 1090 Vienna, Austria

<sup>2</sup> University Library, Medical University of Vienna, Währinger Gürtel 18-20, 1090 Vienna, Austria

<sup>3</sup> Vienna University of Economics and Business, Welthandelsplatz 1, 1020 Vienna, Austria

## ARTICLE INFO

## Article history:

Received 19 February 2025

Received in revised form 2 July 2025

Accepted 9 July 2025

## ABSTRACT

**Objectives:** Placebo effects pose significant challenges in clinical trials for rheumatoid arthritis (RA). Understanding how socioeconomic factors of recruiting countries influence placebo responses is crucial for improving clinical trial design and outcomes. Here, we investigated the impact of global recruitment patterns on placebo responses in randomised controlled trials of RA.

**Methods:** We analysed 124 trials (14 272 patients) investigating targeted therapeutics in RA and assessed how global recruitment patterns are related to placebo response rates using the per-capita gross national income (GNI; weighted by recruiting centres/country) as proxy for socioeconomic status in linear mixed models. Primary outcome was the American College of Rheumatology 20% response placebo response rate. Other socioeconomic metrics utilised were the Human Development Index and out-of-pocket health expenditures. Findings were validated using patient-level data from one global in randomised controlled trial.

**Results:** We identified a negative association of GNI and placebo response rates across all trials ( $\beta = -3.7\%$  placebo response per 10 000 international dollars; 95% CI:  $-5.61$  to  $-1.80$ ;  $P < .001$ ). Results were confirmed using alternative metrics as well as using geographic data on individual patient level. Importantly, we could demonstrate a meaningful difference of this association when compared to active treatment responses.

**Conclusions:** Our findings indicate that recruiting patients from lower-income countries is associated with higher placebo response rates, whereas active treatment responses remain stable. This may be driven by incentives to recruit patients into trials, such as limited access to therapies in less affluent countries. Addressing these factors is critical for improving trial design and ensuring accurate efficacy assessments.

## INTRODUCTION

Double-blind randomised placebo-controlled trials continue to be the mainstay of drug approval in inflammatory rheumatic diseases [1]. Over the last decades, a decreasing number of patients have been found eligible for rheumatoid arthritis (RA)

clinical trials in high-income countries, where studies were typically recruiting. In these countries, new and effective drugs are easily accessible, RA is typically well controlled, and enrolling patients with active disease for inclusion in clinical trials has therefore become a challenge [2,3]. Independently, over the last 2 decades many new drugs have progressed to evaluation in RA

\*Correspondence to Dr Daniel Aletaha, MD, MSc, Department of Medicine III, Division of Rheumatology, Medical University of Vienna, Spitalgasse 23, 1090 Vienna, Austria.

E-mail address: [daniel.aletaha@meduniwien.ac.at](mailto:daniel.aletaha@meduniwien.ac.at) (D. Aletaha).

Handling editor David S. Pisetsky.

<https://doi.org/10.1016/j.ard.2025.07.010>

### WHAT IS ALREADY KNOWN ON THIS TOPIC

- Placebo responses have posed significant challenges in clinical trials, particularly in rheumatoid arthritis. Previous research highlighted increasing placebo response rates over the last 2 decades, with some trials showing rates up to 60%.
- Global clinical trial recruitment, with a particular expansion towards lower-income regions, has been hypothesised as a potential contributor to this, although the underlying reasons remain poorly understood.

### WHAT THIS STUDY ADDS

- Our study is the first comprehensive analysis to quantitatively assess the association between global recruitment patterns and placebo rates of rheumatoid arthritis clinical trials.
- By integrating several socioeconomic indicators such as the gross national income, the United Nations Human Development Index and the World Health Organization's out-of-pocket health expenditures, we provide robust evidence of a negative association between socioeconomic wellbeing and placebo response rates.
- We could validate these findings using patient-level data from a multi-national randomised controlled trial.
- A meaningful difference comparing placebo response rates to the respective active treatment responses in trials investigating tumour necrosis factor alpha inhibitors was identified.

### HOW THIS STUDY MIGHT AFFECT RESEARCH, PRACTICE OR POLICY

- The findings of our study suggest that the global trend in clinical trial recruitment towards less affluent countries could inadvertently increase placebo responses in rheumatoid arthritis clinical trials. This has significant implications for clinical trial design, as higher placebo rates may obscure the true efficacy of investigational therapies, necessitating larger sample sizes and therefore potentially compromising ethical considerations of subjecting more patients to placebo treatments.
- Future trials should consider incorporating socioeconomic factors into trial design and analysis, educate patients and investigators, and consider statistical adjustments when analysing multi-national trials. This could enhance the accuracy of efficacy assessments, improve the reliability of efficacy outcomes, and ultimately inform better regulatory and health care decisions on a global scale.

clinical trials, also increasing recruitment pressure on sponsors and investigators. At the same time, major political changes and improvements in care for patients have allowed for moving clinical trials into regions and countries that had previously not been the focus of such activities. All these reasons have led to a progressive global expansion of clinical study recruitment when compared with the previously predominant inclusion of patients from North America and Western Europe [4–8].

However, in parallel to the broadening of the clinical study arena, placebo rates in RA trials have increased over the last 2 decades, meanwhile ranging up to 60% [9–11]. These high placebo rates have imposed a challenge to the design of clinical trials, as they demand larger sample sizes to differentiate signal from noise and, consequently, may impose ethical problems, since larger numbers of patients have then to be exposed to placebo. With lower access of RA patients to biological (b) and conventional synthetic (cs) disease-modifying antirheumatic drugs (DMARD) therapies in low-income countries [12,13], a greater interest of patients and their treating rheumatologists in study participation can be hypothesised. This shift of recruitment to less affluent regions of the world may therefore have a

consequence on placebo responses by creating a regression to the mean phenomenon in trials and, therefore, increases in placebo rates. However, within an individual country or region of recruitment, considerable differences between placebo response rates of study centres, centre experience, and patients' socioeconomic status might exist, although factors like access to health care services and out-of-pocket health expenditures are shared factors within most countries [14]. Additionally, significant differences in response rates were observed in placebo treated patients with continued, previously instituted methotrexate therapy compared to placebo responses of patients without any background therapy, highlighting potentially inadequate csDMARD adherence before enrolment into a clinical trial [15]. Here, we set out to investigate if and to what extent the well-known increase in placebo rates in large-scale trials [16,17] may be related to the mechanism of expansion to less affluent countries as a compensation for recruitment problems in RA clinical trials in high-income regions.

## METHODS

### Patient populations

To explore placebo responses, we analysed placebo arms in all double-blind studies investigating biologic or targeted synthetic DMARDs in rheumatoid arthritis. Trials had to be conducted at multiple centres and report the number of recruiting sites per country. Studies were stratified into those investigating patients with an inadequate response (IR) to csDMARDs and bDMARD. Stable concomitant therapies (such as low-dose glucocorticoids, csDMARDs) were generally allowed. A table on the precise study selection criteria is provided in the supplement (Table S1). Patients and the public were not involved in the design, conduct, reporting, or dissemination plans of this research.

### Database search

Medline, EMBASE, and CENTRAL (Cochrane Central Register of Controlled Trials) were searched by a database expert (BW) from 1995 until 2024. Search results were screened in duplicates by two researchers (PP and AK). Details on data sources, data extraction, imputation, and quality control are described in the Supplement (Table S2).

### Study outcomes

We chose to analyse the most commonly used primary endpoint, the American College of Rheumatology (ACR) 20% response criteria (at week 12  $\pm$  4). In sensitivity analyses we assessed more stringent American College of Rheumatology response criteria (50% and 70%) at a later timepoint (week 24  $\pm$  4), as these are not sensitive at earlier timepoints [18].

### Estimates of socioeconomic status

To assess geographic recruiting patterns, we used the number of recruiting centres per country as a suitable and widely available estimate because it is common practice to report the countries of recruiting study centres in clinical trials and these data are readily available in clinical trial registries. Before performing these analyses, we investigated if numbers of recruited patients per country were associated with the number of recruiting centres in trials which reported both metrics. Furthermore,



for one of the trials, we had data on the country origins of individual patient available [19], allowing us to validate this approach.

We used the per-capita gross national income (GNI) in international dollars, the broadest and most widely used indicator of a nation's economic activity in 1 year, to assess economic wellbeing. Since GNI itself has a strong longitudinal trend, which can confound analyses spanning decades of trial conduction [20], we normalised the weighted GNI by the mean GNI of the included countries (nGNI; Table S3; Fig S1, Panel A). For example, both the GNI of Poland and that of the United States increased significantly between 2003 and 2023. However, in 2023, Poland's GNI was similar to the GNI of the United States in 2003. This means that a mono-national study conducted in Poland in 2023 would yield a weighted GNI similar to that of a study conducted in the United States in 2003. Adjusting the data accordingly, ie, normalising by the mean GNI of all included countries controls for the general secular increase in economic welfare and allows for a more accurate analysis of the data. To validate the data obtained using the nGNI, we employed another metric of socioeconomic status, the United Nations Human Development Index (HDI) [21]. Furthermore, as access to innovative medicines is mainly restricted by costs of medication, we utilised the World Health Organization's out-of-pocket (OOP) health expenditures (Table S3). The World Health Organization defines the OOP health expenditures as part of the System of Health Accounts Framework [20]. It includes expenses for consultations, medicines, hospital care, and diagnostic tests, but does not include any insurance premiums, tax-based health services, or employer contributions. The unit of measurement is reported in % of all current health spending in a country that comes from household OOP payments [20]. The HDI and OOP were likewise normalised as described for the GNI (nHDI and nOOP, respectively; Figure S1, Panels B, C).

To link each study with each of these estimates of socioeconomic status, we first extracted numbers of recruiting centres per country (from the original articles or study locations provided on clinicaltrials.gov), as well as study start date from the respective original articles. We then calculated weighted GNI, HDI and OOP (separately) for each study (Equations 1 and 2, Table S3).

**Equation 1. Weighted gross national income per study.** The weighted GNI per study is calculated by the sum of the gross national income per capita for each centre divided by the total number of centres in the study.

$$GNI_{\text{weighted}} = \frac{\sum_{i=1}^c (n_i \times GNI_i)}{\sum_{i=1}^c n_i}$$

Here,  $c$  is the number of participated countries,

$n_i$  is the number of centres for country  $i$ , and

$GNI_i$  is the gross national income per capita in international dollars of country  $i$  (at the study start year).

**Equation 2. Normalised gross national income per study.** This formula calculates the normalised GNI per study, which adjusts the weighted GNI by the ratio of the mean GNI of included countries of all years to the mean GNI of all included countries of the study start year to adjust for changes in GNI over time.

$$GNI_{\text{normalized}} = GNI_{\text{weighted}} * \left( \frac{\text{mean}(GNI_{\text{all years}})}{\text{mean}(GNI_{\text{study start year}})} \right)$$

Further details on these metrics are provided in Table S3.

## Validation analysis using patient-level data of a single randomised controlled trial

The analytic approach was validated using patient-level data of a randomised controlled trial [19] by performing linear regression analysis to examine ACR20 placebo response rates and the GNI of each country at the study start year (2005), stratifying patients by recruiting country. We investigated the intention-to-treat population utilising nonresponder imputation for missing data and patients rescued to active therapy at week 16.

## Comparison of placebo to active treatment responses

Finally, we compared the magnitude of the association to response rates of active treatment arms by assessing studies investigating tumor necrosis factor (TNF) inhibitors (utilising the licensed dosing) and the respective difference (per study) to placebo. We chose to only utilise TNF inhibitor treatments as they show comparable efficacy and allow to assess the effect of continuous globalisation of recruitment because trials investigating TNF inhibitors were conducted across the full period of the era of targeted therapies, allowing to investigate differences of recruiting patterns in these trials.

## Statistical analysis

We performed linear mixed model regressions with a random effect on study level (to control for study heterogeneity) and weighted each placebo arm by the number of patients, utilising a mixed linear regression approach [22]. Throughout the analysis, 2-sided  $P$  values  $< .05$  were considered as statistically significant. Statistics were conducted using R (version 4.4.1) [23].

## RESULTS

We identified all studies with a placebo arm in each indication investigating targeted therapies (Table S2, Figure S2), resulting in a total of 124 randomised controlled trials with available primary outcome data in rheumatoid arthritis. In 6 trials, the numbers of recruited patients per country were reported in addition to the number of centres. In line with our hypothesis, we found a strong correlation between the number of patients recruited per country and the number of recruiting centres per country ( $R^2 = 0.84$ ;  $P < .001$ ). A summary of study characteristics is shown in Table.

## Trends of recruitment patterns in clinical trials over time

Among the included trials, the year of study start date ranged from 1994 to 2021. Visual inspection on a world map of global recruiting patterns of rheumatoid arthritis trials over time (Figure 1, Figure S3) revealed that study regions have expanded from initially covering only North America and Western Europe to an increasing global recruitment over time. Studies conducted in the 1990s until the early 2000s comprised only of centres in Western Europe and North America. After approval of the first targeted therapies in the late 1990s and their widespread use in the early 2000s in these regions, a trend towards multiregional recruiting, with continuously increasing numbers of study centres from Eastern Europe, the Asia-Pacific region, and Latin America could be seen, especially from 2005 onwards, with a mean nGNI of  $30.136 \pm 9.870$  international dollars.

Linear regression analysis showed a significant and clearly negative association of the nGNI per study (Formulas 1 and 2) with the year of study conduction (Figure 1, Panel B): more

Table  
Baseline characteristics of included placebo arms

Baseline Characteristics	csDMARD-IR	bdMARD-IR
Number of trials (n)	97	27
Total number of patients (n)	11,060	3,212
Mean number of participants per arm (n)	114 ± 119.3	119 ± 80
Study start year (year) <sup>a</sup>	2010 (1994–2019)	2012 (2003–2021)
Number of recruiting centres (n)	75 ± 65	112 ± 62
Female (%)	82 ± 5.7	81 ± 6.4
Age (years)	53 ± 2.6	55 ± 2.4
Disease duration (years)	7 ± 1.9	10 ± 2.2
Patients with concomitant systemic DMARD/immunosuppressive therapy (%)	80 ± 22.1	89 ± 8.5
Swollen joint count 66 (0–66)	15 ± 2.6	17 ± 2.7
Tender joint count 68 (0–68)	22 ± 4.9	27 ± 4.2
Patient global assessment (mm)	61 ± 6.7	67 ± 3.1
Evaluator Global Assessment (mm)	61 ± 5.6	65 ± 3.1
C-reactive protein (mg/dL)	1.8 ± 0.7	2.0 ± 0.9

Note: Values are shown as means (standard deviation) of all studies unless indicated otherwise.  
bdMARD, biologic disease-modifying antirheumatic drug; csDMARD, conventional synthetic disease-modifying antirheumatic drug; DMARD, disease-modifying antirheumatic drug; iR, inadequate response.  
<sup>a</sup> Shown as median (range).

recent studies showed lower nGNI, as more centres were located in less affluent countries ( $-1027 \pm 149$  international dollars per study year;  $P < .001$ ).

Secular trend of placebo response rates over time

Mixed model analyses (Fig S4) showed a significant positive association of placebo response rates with the study start year ( $\beta = 0.9 \pm 0.2\%$ ;  $P < .001$ ), accounting for a mean total increase of placebo response rates in the observed study time period (1994–2021) of 25%.

Placebo response rates and societal wellbeing

We identified a strong and significant association with placebo response rates of the ACR20 at week 12 (the most

commonly utilised primary endpoint) and poor socioeconomic status, such as captured by the gross national income ( $\beta = -3.7\%$  placebo response per 10 000 international dollars; 95% confidence interval [CI]:  $-5.6$  to  $-1.8$ ;  $P < .001$ ). When stratified by population (Fig 3, Panel A) [19], we found similar results observed in the csDMARD-iR ( $\beta = -2.85\%$ ; 95% CI:  $-5.11$  to  $-0.59$ ;  $P = .013$ ) and the bdMARD-IR population ( $\beta = -4.58\%$ ; 95% CI:  $-8.49$  to  $-0.67$ ;  $P = .022$ ). In other words, the higher the GNI the lower the placebo response rates (and vice versa). Similar results were shown using other socioeconomic measures: the HDI ( $\beta = -61.2$ ; 95% CI:  $-97.7$  to  $-24.6$ ;  $P = .001$ ; Fig 2, Panel B) and OOP health expenditures ( $\beta = 0.26$ ; 95% CI:  $0.001$  to  $0.52$ ;  $P = .049$ ; Fig 2, Panel C). Detailed statistical model results are shown in Tables S5 and S6.

Validation analysis

Our findings were confirmed in the analysis of patient-level data from a single global placebo-controlled trial investigating RA patients [19]. After stratification of response rates by country of patient recruitment, we found higher ACR20 placebo responses in low-income countries than in more affluent regions ( $n = 119$ ; GNI:  $\beta = -9.6 \pm 3.8\%$ ; 95% CI:  $-18.1$  to  $-1.1$ ;  $P = .031$ ; Fig 3).

Sensitivity analyses on clinical outcomes

We also assessed more stringent endpoints in trials with available data ( $n = 57$ ) at week 24. Here, our analyses were in line with our primary analyses, irrespective of the outcome measure. Details of these analyses are shown in Table S4 and Figure S5.

Active treatment responses, treatment differences, and consequences for sample size calculations

Figure 4 visualises the differences of placebo and active treatment response rates. TNFi responses are shown in Figure 4 (left panel, red), next to the respective placebo rates (left panel, blue). The estimates for treatment differences between TNFi and placebo were 1.6% per 10 000 international dollars (right panel).

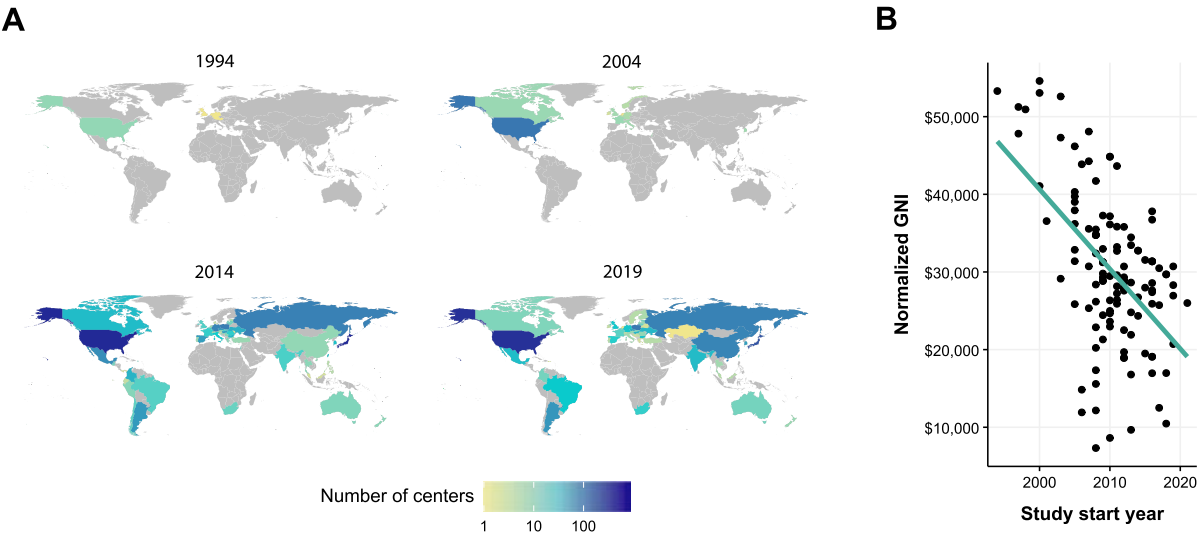
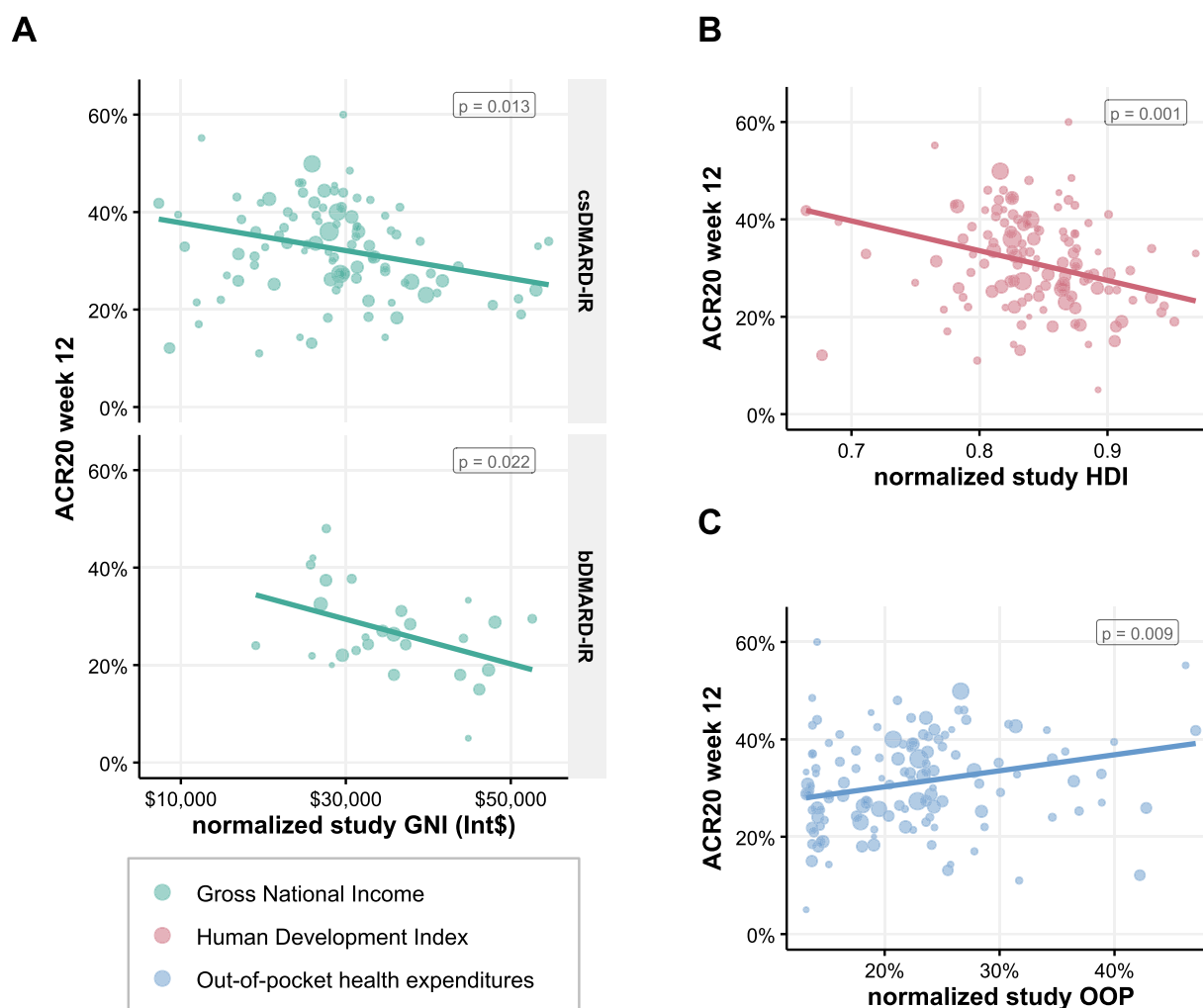


Figure 1. (A) Patterns of recruiting centres (per country) for the years 1994, 2004, 2014, and 2019 in rheumatoid arthritis clinical trials. (B) Time trend of normalised per-capita gross national income (international dollar) of placebo-controlled studies from 1994 to 2021. Each dot represents the weighted, normalised gross national income of an individual study.



**Figure 2.** Association of placebo response rates with the weighted gross national income (GNI) per study (A), the United Nations Human Development Index (HDI) (B), and the World Health Organization's out-of-pocket (OOP) health expenditures (C). (A) Stratified results by study population (csDMARD/bDMARD: conventional synthetic and biologic disease modifying antirheumatic drug) inadequate responder (iR). (B, C) show the overall study population. Linear regression lines show associations of the primary outcome with the normalised GNI, HDI, and OOP, separately; respective *P* values are shown in the top right corner. Average slopes are weighted by the number of studies. Each bubble represents the placebo response rate of one individual study. The size of the bubbles represents the number of patients analysed in the respective placebo arm. The y-axis corresponds to the respective outcome analysed. bDMARD, biologic disease-modifying antirheumatic drug; csDMARD, conventional synthetic disease-modifying antirheumatic drug; DMARD, disease-modifying antirheumatic drug; GNI, gross national income; HDI, Human Development Index; iR, inadequate response; OOP, out-of-pocket (health expenditures); WHO, World Health Organization.

These findings lead to considerable consequences for sample size calculations: considering a scenario with a fixed power of 80%, our results suggest a required sample size of 116 patients for a randomised controlled trial in RA patients with a mean study GNI of 25 000 international dollars compared to 76 patients in a study in a region with a mean GNI of 50 000 international dollars.

## DISCUSSION

Our analyses demonstrate that global geographic expansion of study recruitment with its increasing inclusion of centres from less affluent countries is associated with higher placebo response rates in randomised controlled trials in RA. This was clearly seen in trials of both, csDMARD-IR and bDMARD-IR patient populations. This link may be an important contributor to the rising placebo response rates that have been documented over the years [16,17]. Importantly, higher placebo response rates in less affluent areas are also accompanied by somewhat higher active treatment response rates. However, the effect on

placebo response rates is stronger, leading to smaller differences between active therapy and control with consequences for sample size calculations. Of note, we found similar significant associations in plaque psoriasis and psoriatic arthritis trials [24].

The reason for the link between socioeconomic variables and placebo response rates is currently unclear, but one can attempt to develop hypotheses that may explain such an association. First, where there is limited access to health care (or coverage of medication costs), recruitment into a clinical trial may constitute an attractive option to receive medical care and medicines at no cost, leading to a high motivation to enrol at trial screening [12,25]. Once enrolment is achieved, however, subsequent assessments of patients are performed without that pressure and the readout more accurately reflects clinical reality, leading to a phenomenon known as 'regression to the mean'. Indeed, in our analysis, higher placebo response rates were associated with higher weighted OOP expenditures for medications, reflecting that in studies recruiting in countries with higher drug costs for patients, placebo responses are higher. This might relate to a limited access to medication and consequently to an insufficient

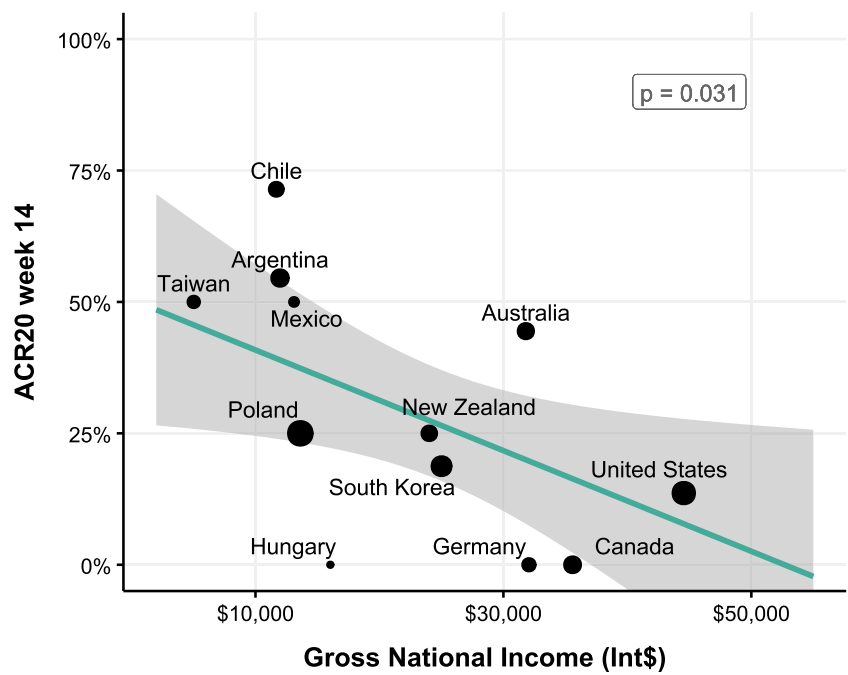


**Figure 3.** Association of placebo response rates with the weighted gross national income (GNI) at individual patient level from a randomized controlled trial [19], stratified by country of recruitment. The regression line demonstrates the association of American College of Rheumatology 20 placebo response rates at week 24 with the GNI of the respective countries at the study start year (2005). The band represents 95% confidence intervals. Each bubble represents the mean placebo response rate of patients recruited in the respective countries. The size of bubbles represents the number of patients recruited per country. GNI, gross national income.

adherence to background drug therapy before inclusion into a trial [15]. The higher levels of disease activity at baseline in RA patients from regions with lower income and thus lower bDMARD affordability and usage may be a reflection of both, the high motivation to fulfil inclusion criteria at screening and poorer access to biological therapies, ultimately leading to the perceived benefit of enrolment into, as well as an incentive for patients to remain in the trial [13,26]. Finally, a higher incentive to recruit patients into a trial may also come from investigators, eg, through the lack of alternative treatment options for their patients outside clinical trials or appealing compensation for patient enrolment. It remains an open question which disease activity measures (subjective, objective, patient/evaluator

reported) drive these effects, but for an ACR20 or ACR70 response the patients have to experience at least the respective reduction in swollen joint counts. Thus, the placebo response cannot only be due to improvement of presumed subjective variables.

Our analysis has several limitations. First, due to nonreporting of the number of recruited patients per country, we analysed the number of recruiting centres of individual clinical trials as a surrogate. While we did not have patient-level data of each study site available to assess the distribution of responses of different centres recruiting in an individual country, the patient-level data available in one of the trials fully validated the respective country level data. Also, we found clear evidence that the

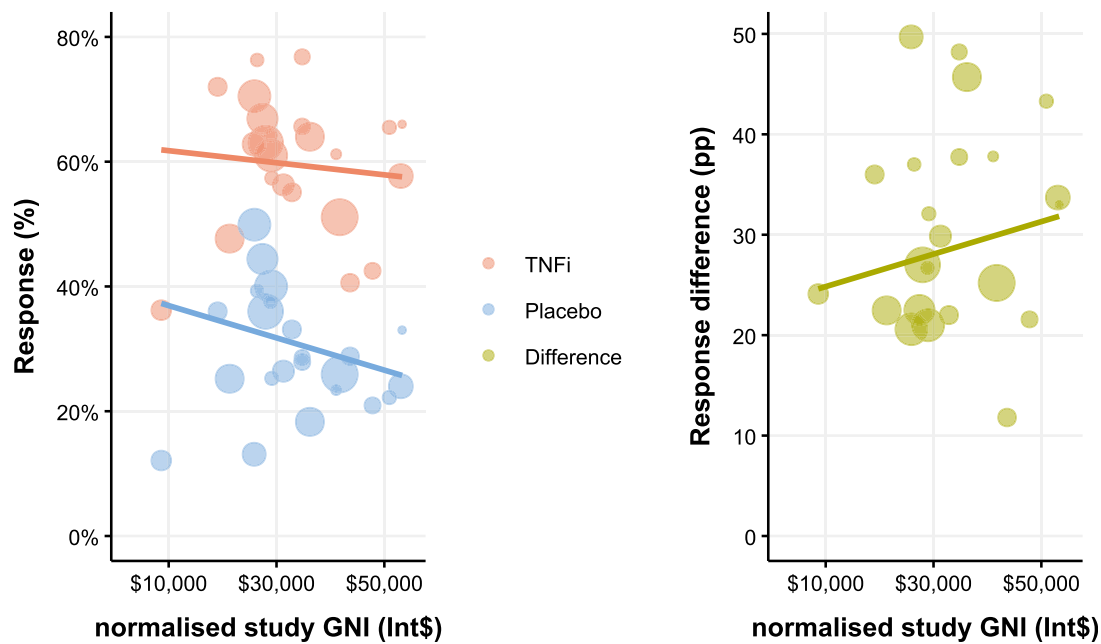


**Figure 4.** Comparison of active treatment and placebo response rates in trials investigating tumour necrosis factor alpha inhibitors (TNFis) with the weighted gross national income (GNI) per study. The left panel shows TNFi treatment arms in red and placebo responses in blue. Response differences (green) between active and placebo response rates are shown in the right panel. The size of the bubbles represents the number of patients analysed. The y-axis corresponds to the American College of Rheumatology 20% response. GNI, gross national income; TNFi, tumour necrosis factor alpha inhibitor.



number of centres has a strong association with the number of recruited patients per country. We also validated this approach using detailed geographic information on individual patients available for analysis in one of the trials. Second, our data rely on comparing socioeconomic measures on country level, with data of placebo responses on study site level being unavailable. In this context, it must be noted that placebo response rates may vary between sites within a country or a specific geographic region, as certain centres in high-income countries might have high placebo response rates. In contrast, some centres in low affluent countries might show low placebo response rates. However, we could not fully confirm the country differences using patient-level data that were available in one of the studies, and also patient-level data from trials in plaque psoriasis and psoriatic arthritis are fully in line with the current observation [24]. Third, we had to rely on ACR response rates throughout the analyses, as the ACR response was the only consistently reported outcome measure across almost all clinical trials since the advent of biological therapies and other instruments (like the Clinical Disease Activity Index and Simplified Disease Activity Index) were employed much later in time, which would have excluded many of the early trials from the analysis. With respect to more stringent outcomes, the ACR70 response rates showed a similar association with socioeconomic variables as the ACR20 responses. Fourth, despite being aware of the ‘Beyond gross domestic product’ (and GNI) debate highlighting the inability of the gross domestic product to enable wellbeing comparison between countries, we chose the GNI, as GNI data are available from 1990 onwards over a large group of countries and a common understanding of this measure exists also within disciplines outside of the economic field [27]. However, to validate and support our findings, we also analysed additional metrics of socioeconomic status and access to health care, and could validate our findings using the United Nations’ HDI and the World Health Organization’s OOP health expenditures [28,29].

Beyond socioeconomic differences as important driver for placebo responses, other factors might contribute to the increase of placebo response rates over the past decades, eg, increased recruitment pressure with subsequent increased utilisation of inexperienced study sites. Although limited access to modern therapies is evident also in some high-income countries [30,31], this problem is still much larger in countries with low economic wealth.

The results of our study suggest that managing patient expectations and training for investigators on these potential issues, especially adequate assessment of background therapy adherence before trial enrolment is critical. Patients as well as physicians should be educated in how assessments during the trial are conducted and how they might be confounded. Further, and even more importantly, clinical trials sponsors should not attempt to address recruitment challenges solely through expansion of recruitment areas but consider the potential cost to data quality and its implications for an even higher sample size required. Sponsors and investigators should publish response rates stratified by geographic region and incorporate socioeconomic assessments in the trial design as well as in the reporting of clinical trials, thus improving the reliability of trial outcomes, regulatory decisions, and ultimately enhance patient care globally. Conversely, taking these insights into practice could reduce the size of clinical trials in the future and consequently reduce the number of patients subjected to placebo. Sponsors need to assess the investigators (in every region) more carefully to only select investigators with rich clinical trial experience who report quality results whether positive or negative and not just rely on

the number of individuals they enrol in a trial. Potential strategies for this would be measuring methotrexate polyglutamate levels at screening and baseline in trials recruiting patients with IR to methotrexate [32], establishing a run-in phase at the beginning of a trial [15], or limiting the number of patients that can be recruited per individual centre or country to reduce the impact from a single centre (or country). In addition, appropriate endpoints and outcomes instruments and their use at appropriate time points should be applied [18,33].

In summary, considering socioeconomic disparities when designing and conducting drug trials in RA appears critical for sponsors, investigators, health care providers, and political stakeholders. Implementation of physician as well as patient education, assessment of treatment adherence before trial enrolment, and quality control measures are key to ensure accurate efficacy outcome assessment and a more ethical conduction of clinical trials, ultimately bringing benefit to all patients in clinical trials and rheumatology in general.

## Competing interests

AK has received honoraria from the speakers bureaus of Lilly, Galapagos, JNJ, MSD, Novartis, Pfizer, and Stada; has served as a consultant for AbbVie, Lilly, JNJ, and UCB; and has received travel support from Boehringer-Ingelheim, Lilly, and UCB. MS, PP, BW, and MM have nothing to declare. JSS reports grants to their institution from AbbVie, AstraZeneca, Lilly, and Galapagos; royalties from Elsevier for a textbook; consulting fees from AbbVie, UCB, BMS, Samsung, Chugai, R-Pharma, Ananda, Immunovant, and Celltrion; has participated in speakers bureaus for Novartis-Sandoz, Lilly, Chugai, and R-Pharma; and served on a Data Safety Monitoring Board or Advisory Board for AstraZeneca.

DA reports grants to their institution from Lilly and Galapagos; consulting fees from AbbVie, Gilead, JNJ, Lilly, MSD, Novartis, and Sandoz; and has participated in speakers bureaus for AbbVie, Gilead, JNJ, Lilly, MSD, Novartis, and Sandoz.

## Acknowledgements

The authors thank Bruno Bierbaumer, MSc for his assistance in developing the underlying database for this project. We also thank Centocor/Janssen for providing a 90% data cut of the GO-FORWARD trial.

## Contributors

AK was responsible for the study design; literature search; data collection; data analysis and methodology; validation; visualisation; original manuscript drafting, critical review, and editing; and provided supervision and coordination throughout the project. MS contributed to data curation, methodology, statistical analysis, data validation, visualization, writing (manuscript drafting, critical review, and editing), figure creation, and data collection. PP and BW were involved in the literature search, data collection, and writing (critical review and editing). MM contributed to methodology, formal analysis, data collection, manuscript (critical review and editing), and data analysis. JSS and DA were involved in the study design; manuscript drafting, critical review, and editing; resources; and provided supervision and coordination.

All authors had full access to all the data in the study and take responsibility for the integrity of the data and the accuracy of

the analysis. All authors reviewed and approved the final version of the manuscript before submission.

## Funding

This research did not receive any specific grant from funding agencies in the public, commercial, or not-for-profit sectors.

## Ethics approval

This study involved the analysis of data from previously conducted clinical trials, each of which had obtained independent ethics approval from the respective institutional review boards or ethics committees at the time of their original conduct. As this analysis did not involve new data collection or direct patient contact, additional ethics approval was not required for this study.

## Patient and public involvement statement

Patients and the public were not involved in the design, conduct, reporting, or dissemination plans of this research.

## Patient consent for publication

Not applicable.

## Provenance and peer review

Not commissioned; externally peer reviewed.

## Data availability statement

The data used in this study were accessed from publicly available clinical trial registries and original publications. Detailed information on data extraction and processing is provided in the supplementary materials. The data supporting the findings of this study is available online via GitHub. The full URL to access the supporting data can be found in the [Supplementary Appendix \(Table S2\)](#). Data of the GO-FORWARD study were provided by the study sponsor and are not publicly available.

## Supplementary materials

Supplementary material associated with this article can be found in the online version at [doi:10.1016/j.ard.2025.07.010](https://doi.org/10.1016/j.ard.2025.07.010).

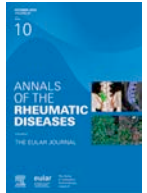
## Orcid

Marlene Steiner: <http://orcid.org/0009-0007-3056-7664>  
Brigitte Wildner: <http://orcid.org/0000-0002-0683-0801>

## REFERENCES

- [1] Smolen JS, Landewé RBM, Bergstra SA, Kerschbaumer A, Sepriano A, Aletaha D, et al. EULAR recommendations for the management of rheumatoid arthritis with synthetic and biological disease-modifying anti-rheumatic drugs: 2022 update. *Ann Rheum Dis* 2023;82:3–18. doi: [10.1136/ard-2022-223356](https://doi.org/10.1136/ard-2022-223356).
- [2] Zink A, Strangfeld A, Schneider M, Herzer P, Hierse F, Stoyanova-Scholz M, et al. Effectiveness of tumor necrosis factor inhibitors in rheumatoid arthritis in an observational cohort study: comparison of patients according to their eligibility for major randomized clinical trials. *Arthritis Rheum* 2006;54:3399–407. doi: [10.1002/art.22193](https://doi.org/10.1002/art.22193).
- [3] Vashisht P, Sayles H, Cannella AC, Mikuls TR, Michaud K. Generalizability of patients with rheumatoid arthritis in biologic agent clinical trials. *Arthritis Care Res (Hoboken)* 2016;68:1478–88. doi: [10.1002/acr.22860](https://doi.org/10.1002/acr.22860).
- [4] Elliott MJ, Maini RN, Feldmann M, Kalden JR, Antoni C, Smolen JS, et al. Randomised double-blind comparison of chimeric monoclonal antibody to tumour necrosis factor alpha (cA2) versus placebo in rheumatoid arthritis. *Lancet* 1994;344:1105–10. doi: [10.1016/s0140-6736\(94\)90628-9](https://doi.org/10.1016/s0140-6736(94)90628-9).
- [5] Genovese MC, Kalunian K, Gottenberg J-E, Mozaffarian N, Bartok B, Matzkies F, et al. Effect of filgotinib vs placebo on clinical response in patients with moderate to severe rheumatoid arthritis refractory to disease-modifying anti-rheumatic drug therapy: the FINCH 2 randomized clinical trial. *JAMA* 2019;322:315–25. doi: [10.1001/jama.2019.9055](https://doi.org/10.1001/jama.2019.9055).
- [6] Fleischmann R, Kremer J, Cush J, Schulze-Koops H, Connell CA, Bradley JD, et al. Placebo-controlled trial of tofacitinib monotherapy in rheumatoid arthritis. *N Engl J Med* 2012;367:495–507. doi: [10.1056/NEJMoa1109071](https://doi.org/10.1056/NEJMoa1109071).
- [7] Burmester GR, Kremer JM, Van den Bosch F, Kivitz A, Bessette L, Li Y, et al. Safety and efficacy of upadacitinib in patients with rheumatoid arthritis and inadequate response to conventional synthetic disease-modifying anti-rheumatic drugs (SELECT-NEXT): a randomised, double-blind, placebo-controlled phase 3 trial. *Lancet* 2018;391:2503–12. doi: [10.1016/s0140-6736\(18\)31115-2](https://doi.org/10.1016/s0140-6736(18)31115-2).
- [8] Maini R, St Clair EW, Breedveld F, Furst D, Kalden J, Weisman M, et al. Infliximab (chimeric anti-tumour necrosis factor alpha monoclonal antibody) versus placebo in rheumatoid arthritis patients receiving concomitant methotrexate: a randomised phase III trial. ATTRACT Study Group. *Lancet* 1999;354:1932–9. doi: [10.1016/s0140-6736\(99\)05246-0](https://doi.org/10.1016/s0140-6736(99)05246-0).
- [9] Combe B, Kivitz A, Tanaka Y, van der Heijde D, Simon JA, Baraf HSB, et al. Filgotinib versus placebo or adalimumab in patients with rheumatoid arthritis and inadequate response to methotrexate: a phase III randomised clinical trial. *Ann Rheum Dis* 2021;80:848–58. doi: [10.1136/annrheumdis-2020-219214](https://doi.org/10.1136/annrheumdis-2020-219214).
- [10] Taylor PC, Weinblatt ME, McInnes IB, Atsumi T, Strand V, Takeuchi T, et al. Anti-GM-CSF otilimab versus sarilumab or placebo in patients with rheumatoid arthritis and inadequate response to targeted therapies: a phase III randomised trial (contRAst 3). *Ann Rheum Dis* 2023;82:1527–37. doi: [10.1136/ard-2023-224449](https://doi.org/10.1136/ard-2023-224449).
- [11] Smolen JS, Feist E, Fatenejad S, Grishin SA, Korneva EV, Nasonov EL, et al. Olokizumab versus placebo or adalimumab in rheumatoid arthritis. *N Engl J Med* 2022;387:715–26. doi: [10.1056/NEJMoa2201302](https://doi.org/10.1056/NEJMoa2201302).
- [12] Putrik P, Ramiro S, Kvien TK, Sokka T, Pavlova M, Uhlig T, et al. Inequities in access to biologic and synthetic DMARDs across 46 European countries. *Ann Rheum Dis* 2014;73:198–206. doi: [10.1136/annrheumdis-2012-202603](https://doi.org/10.1136/annrheumdis-2012-202603).
- [13] Bergstra SA, Branco JC, Vega-Morales D, Salomon-Escoto K, Govind N, Allaart CF, et al. Inequity in access to bDMARD care and how it influences disease outcomes across countries worldwide: results from the METEOR-registry. *Ann Rheum Dis* 2018;77:1413–20. doi: [10.1136/annrheumdis-2018-213289](https://doi.org/10.1136/annrheumdis-2018-213289).
- [14] de Loop M, LaFortune G. Measuring disparities in health status and in access and use of health care in OECD countries. *OECD Health Working Papers*; 2009. doi: [10.1787/225748084267](https://doi.org/10.1787/225748084267).
- [15] Kerschbaumer A, Rivai ZI, Smolen JS, Aletaha D. Impact of pre-existing background therapy on placebo responses in randomised controlled clinical trials of rheumatoid arthritis. *Ann Rheum Dis* 2022;81:1374–8. doi: [10.1136/annrheumdis-2021-221807](https://doi.org/10.1136/annrheumdis-2021-221807).
- [16] Bechman K, Yates M, Norton S, Cope AP, Galloway JB. Placebo response in rheumatoid arthritis clinical trials. *J Rheumatol* 2020;47:28–34. doi: [10.3899/jrheum.190008](https://doi.org/10.3899/jrheum.190008).
- [17] Nagai K, Matsubayashi K, Ide K, Seto K, Kawasaki Y, Kawakami K. Factors influencing placebo responses in rheumatoid arthritis clinical trials: a meta-analysis of randomized, double-blind, placebo-controlled studies. *Clin Drug Investig* 2020;40:197–209. doi: [10.1007/s40261-020-00887-6](https://doi.org/10.1007/s40261-020-00887-6).
- [18] Konzett V, Kerschbaumer A, Smolen JS, Aletaha D. Determination of the most appropriate ACR response definition for contemporary drug approval trials in rheumatoid arthritis. *Ann Rheum Dis* 2024;83:58–64. doi: [10.1136/ard-2023-224477](https://doi.org/10.1136/ard-2023-224477).
- [19] Keystone EC, Genovese MC, Klareskog L, Hsia EC, Hall ST, Miranda PC, et al. Golimumab, a human antibody to tumour necrosis factor {alpha} given by monthly subcutaneous injections, in active rheumatoid arthritis despite methotrexate therapy: the GO-FORWARD Study. *Ann Rheum Dis* 2009;68:789–96. doi: [10.1136/ard.2008.099010](https://doi.org/10.1136/ard.2008.099010).
- [20] Organisation for Economic Co-operation and Development (OECD). National Accounts of OECD Countries, 2022. Paris: OECD Publishing; 2023. doi: [10.1787/3e073951-en](https://doi.org/10.1787/3e073951-en).
- [21] UNDP, Human Development Report 1990 (New York: Oxford University Press), 1990.
- [22] Viechtbauer W. Conducting Meta-Analyses in R with the metafor Package. *J Stat Softw* 2010;36. doi: [10.18637/jss.v036.i03](https://doi.org/10.18637/jss.v036.i03).

- [23] R Core Team. R: A Language and Environment for Statistical Computing. Vienna, Austria: R Foundation for Statistical Computing; 2024. <https://www.R-project.org/>.
- [24] Kerschbaumer A, Steiner M, Khalili S, Shehab A, Jordanov A, Wildner B, et al. Global recruiting patterns affect placebo response rates in clinical trials of psoriatic arthritis and plaque psoriasis. *Arthritis Rheumatol* 2025 Jun 30. doi: [10.1002/art.43302](https://doi.org/10.1002/art.43302).
- [25] Putrik P, Ramiro S, Kvien TK, Sokka T, Uhlig T, Boonen A, et al. Variations in criteria regulating treatment with reimbursed biologic DMARDs across European countries. Are differences related to country's wealth? *Ann Rheum Dis* 2014;73:2010–21. doi: [10.1136/annrheumdis-2013-203819](https://doi.org/10.1136/annrheumdis-2013-203819).
- [26] Sokka T, Kautiainen H, Pincus T, Toloza S, da Rocha Castelar Pinheiro G, Lazovskis J, et al. Disparities in rheumatoid arthritis disease activity according to gross domestic product in 25 countries in the QUEST-RA database. *Ann Rheum Dis* 2009;68:1666–72. doi: [10.1136/ard.2009.109983](https://doi.org/10.1136/ard.2009.109983).
- [27] Jean-Paul F, Martine D. *Beyond GDP measuring what counts for economic and social performance*. OECD Publishing 2018.
- [28] UNDP (United Nations Development Programme). Human Development Report 2021-22: Uncertain Times, Unsettled Lives: Shaping our Future in a Transforming World. New York: UNDP (United Nations Development Programme); 2022. <https://hdr.undp.org/content/human-development-report-2021-22>.
- [29] WHO. Out-of-pocket expenditure as percentage of current health expenditure (CHE) (%). Accessed 6 March 2024. <https://www.who.int/data/gho/data/indicators/indicator-details/GHO/out-of-pocket-expenditure-as-percentage-of-current-health-expenditure-che>(-)
- [30] Wright GC, Zueger PM, Copley-Merriman C, Khan S, Costello J, Krumbach A, et al. Health disparities in rheumatology in the United States. *Open Access Rheumatol* 2025;17:1–12. doi: [10.2147/OARRR.S493457](https://doi.org/10.2147/OARRR.S493457).
- [31] Taylor PC, Woods M, Rycroft C, Patel P, Blanthorn-Hazell S, Kent T, et al. Targeted literature review of current treatments and unmet need in moderate rheumatoid arthritis in the United Kingdom. *Rheumatology (Oxford)* 2021;60:4972–81. doi: [10.1093/rheumatology/keab464](https://doi.org/10.1093/rheumatology/keab464).
- [32] Goodman S. Measuring methotrexate polyglutamates. *Clin Exp Rheumatol* 2010;28:S24–6.
- [33] Studenic P, Aletaha D, de Wit M, Stamm TA, Alasti F, Lacaille D, et al. American College of Rheumatology/EULAR remission criteria for rheumatoid arthritis: 2022 revision. *Ann Rheum Dis* 2023;82:74–80. doi: [10.1136/ard-2022-223413](https://doi.org/10.1136/ard-2022-223413).



## Rheumatoid arthritis

## Development of bispecific antibodies that drive selective targeted local complement inhibition on rheumatoid arthritis-related antigens

Haiyu Wang<sup>1</sup>, Saskia Nugteren<sup>1</sup>, Rick J. Groenland<sup>1</sup>,  
 Stef van der Meulen<sup>1</sup>, Hanneke Kapsenberg<sup>1</sup>, Christoph Gstöttner<sup>2</sup>,  
 Elena Domínguez-Vega<sup>2</sup>, Jan Piet van Hamburg<sup>3,4</sup>, Sander W. Tas<sup>3,4</sup>,  
 Rene E.M. Toes<sup>5</sup>, Paul W.H.I. Parren<sup>1,6</sup>, Leendert A. Trouw<sup>1,\*</sup>

<sup>1</sup> Department of Immunology, Leiden University Medical Center, Leiden, Netherlands

<sup>2</sup> Center for Proteomics and Metabolomics, Leiden University Medical Center, Leiden, Netherlands

<sup>3</sup> Department of Rheumatology and Clinical Immunology, Amsterdam Rheumatology and Immunology Center, Amsterdam University Medical Center, University of Amsterdam, Amsterdam, Netherlands

<sup>4</sup> Department of Experimental Immunology, Amsterdam University Medical Center, University of Amsterdam, Amsterdam, Netherlands

<sup>5</sup> Department of Rheumatology, Leiden University Medical Center, Leiden, Netherlands

<sup>6</sup> Gyes BV, Utrecht, Netherlands

## ARTICLE INFO

## Article history:

Received 30 December 2024

Received in revised form 30 May 2025

Accepted 18 June 2025

## ABSTRACT

**Objectives:** In rheumatoid arthritis (RA) autoantibodies can trigger complement activation in the joint, contributing to tissue damage. Complement inhibitory drugs have shown important benefit in other clinical conditions. However, their use is limited because these drugs act systemically, not only requiring high doses but also rendering patients more susceptible to infections. Therefore, we designed a strategy to only inhibit complement locally, while leaving the systemic complement system intact to fight infections.

**Methods:** We designed bispecific antibodies (bsAbs) using controlled Fab-arm exchange. In these bsAbs, one antibody arm binds to a specific disease-relevant antigen, like carbamylated proteins, while the other arm recruits endogenous complement regulators, like factor H (FH) or C4b-binding protein (C4BP). These bsAbs were subsequently evaluated for their specificity and complement regulator recruiting capacity.

**Results:** We generated anti-carbamylated protein antibody (anti-CarP)-based bsAbs and confirmed specificity for carbamylated proteins. The bsAbs efficiently recruited FH or C4BP to surfaces containing carbamylated proteins. The bsAbs inhibited complement activation induced by immunoglobulin G immune complexes and more importantly, the bsAbs were able to inhibit complement activation triggered by anti-CarP antibodies from RA patients to background levels.

**Conclusions:** This study shows that bsAbs that bind carbamylated proteins and FH or C4BP can specifically recruit the endogenous complement regulatory proteins from plasma to achieve selective local targeted complement inhibition, providing a new therapeutic approach for the local treatment of autoimmune diseases.

\*Correspondence to Dr. Leendert A. Trouw, Department of Immunology, Leiden University Medical Center, Leiden, Netherlands.

E-mail address: [L.A.Trouw@LUMC.nl](mailto:L.A.Trouw@LUMC.nl) (L.A. Trouw).

Handling editor Josef S. Smolen.

<https://doi.org/10.1016/j.ard.2025.06.2130>



**WHAT IS ALREADY KNOWN ON THIS TOPIC**

- Autoantibodies are present in rheumatoid arthritis, including anti-citrullinated protein antibodies (ACPA) and anti-carbamylated protein antibodies (anti-CarP).
- Antibody driven complement activation is taking place in the inflamed joint.
- Complement inhibition is employed in other clinical conditions but the costs and infectious risks associated with these systemically acting complement inhibitors may limit its use in rheumatic diseases.
- Systemic complement inhibition is associated with the risk for infections.

**WHAT THIS STUDY ADDS**

- We have generated anti-CarP-based bispecific antibodies that can bind to carbamylated proteins and recruit endogenous complement inhibitory proteins to achieve local targeted complement inhibition.

**HOW THIS STUDY MIGHT AFFECT RESEARCH, PRACTICE OR POLICY**

- As most complement driven (autoimmune) diseases occur locally, targeted local complement inhibition may be a promising approach to protect tissues against complement mediated damage while maintaining the protective effects of complement against infections.

**INTRODUCTION**

Rheumatoid arthritis (RA) is a chronic inflammatory autoimmune disease characterised by synovial inflammation, cartilage degradation, and bone erosion [1,2]. In addition, RA is characterised by the presence of autoantibodies, including rheumatoid factor (RF) [3] and anti-modified protein antibodies (AMPAs) such as anti-citrullinated protein antibodies (ACPA) [4] and anti-carbamylated protein antibodies (anti-CarP) [5]. Both of these antibodies are detectable prior to disease onset [6,7], are present in the inflamed joint, and are associated with the severity of joint destruction [5]. These antibodies are thought to contribute to tissue damage by activating cellular Fc receptors [8] and by activating the complement system locally in the inflamed joint [9]. As part of the innate immune system, complement contributes effectively against infections. However, it can also contribute to the immunopathology induced by autoantibodies [10].

Currently, there is increasing evidence indicating that complement activation is a driver of inflammation in RA [11], as increased amounts of complement activation products were detected in RA patients' synovial fluid, including C3d, C4d, and soluble C5b-9 [12,13], confirming that complement activation occurred in the joints. There are several complement inhibitory drugs currently on the market. However, these drugs may not be particularly well suited for treatment in the context of RA as they all act systemically, not only requiring high dosages and high costs, but especially leaving patients more vulnerable to infection [14]. Therefore, inhibiting complement activation locally at the site where autoantibodies like AMPA deposit, as opposed to systemic inhibition, may be more effective and is, conceivably, safer. This notion represents a novel, innovative avenue for achieving effective therapeutic intervention while preserving the systemic complement pool untouched to combat infections. We recently generated such locally acting complement inhibitory antibodies focused on model antigens like dinitrophenyl and biotin [15]. We set out to achieve local, targeted

complement inhibition by generating a comprehensive set of bispecific antibodies recognising carbamylated proteins. We now show that complement activation mediated by anti-CarP antibodies or ACPA in sera of RA patients is inhibited by bispecific antibodies (bsAbs) that target carbamylated proteins with one binding arm while recruiting endogenous complement inhibitors with the other.

**METHODS***Generation of anti-CarP antibody 4A10*

The anti-CarP monoclonal antibody (mAb) 4A10 was used to target carbamylated proteins. This antibody was generated by immunising C57BL/6 mice with carbamylated mouse albumin using standard protocols. Using traditional hybridoma technology, we obtained a panel of carbamylated protein-specific mAbs that were sequenced and produced recombinantly as chimeric human immunoglobulin G1s (IgG1s) containing the mouse VH and VL in combination with the human IgG1 and kappa light chain constant regions. The Fc domain included clinically validated mutations including the K409R mutation to allow for controlled Fab-arm exchange with F405L-containing IgG1s and the L234A-L235A-P329G mutations to silence immune effector functions.

*Complement activation/inhibition enzyme-linked immunosorbent assay*

The inhibitory function of bsAbs was tested using a plate-bound enzyme-linked immunosorbent assay (ELISA). A mix was prepared of 10 µg/mL IgG (intravenous immunoglobulin [IVIG], Privigen) and 10 µg/mL carbamylated fetal calf serum (CarP-FCS, produced in-house) in coating buffer (0.1 M Na<sub>2</sub>CO<sub>3</sub>/NaHCO<sub>3</sub> pH 9.6). A total of 50 µL of mixture per well was used to coat Maxisorp 96 well-plates (Thermo Scientific, 430431) for 1 hour at 37°C. After each incubation, plates were washed 3 times with phosphate-buffered saline (PBS)/0.05% Tween 20. Then plates were blocked with 100 µL/well PBS/1% bovine serum albumin (BSA) for 1 hour at 37°C. Samples containing bsAbs (from 0.1 µg/mL to 10 µg/mL) and 1% normal human serum (NHS) were mixed in Roswell Park Memorial Institute medium (RPMI) 1640 (Gibco, 22409015) and preincubated on ice water. After washing, 50 µL/well samples were added to the plates and incubated 1 hour at 37°C. C5b-9 was detected by mouse anti-human C5b-9 (Dako, M0777, 1:333 dilution) and horseradish peroxidase-labelled goat anti-mouse Ig (Dako, P0447, 1:2000 dilution), which were both diluted in PTB buffer (PBS/1% BSA/.05% Tween20) and incubated 45 minutes at 37°C. Plates were developed by incubating with 50 µL/well 2,2'-Azino-bis(3-ethylbenzothiazoline-6-sulfonic acid) (ABTS, Sigma-Aldrich, A1888) containing 1:2000 diluted H<sub>2</sub>O<sub>2</sub> and read at 415 nm using a microplate reader (Multiskan FC Microplate Photometer, Thermo Fisher).

For the complement activation ELISA in which complement was activated by RA patient sera, plates were coated with 10 µg/mL CarP-FCS. After blocking, RA patient sera (1:50 dilution) were diluted in PTB-ethylenediaminetetraacetic acid (EDTA) (PTB buffer + 10 mM EDTA) and added to the plates, after incubation at 4°C overnight, plates were washed with PBS/0.05% Tween 20. Then, 3% NHS was diluted in RPMI 1640 and added to the plate, 50 µL/well. After a 1-hour incubation, C5b-9 was detected as previously described.

For the complement inhibition ELISA in which complement was activated by RA patient sera, plates were coated with 10  $\mu\text{g/mL}$  CarP-FCS. After blocking, RA patient sera (1:50 dilution in the final mixture) were mixed with bsAbs (from 0.1  $\mu\text{g/mL}$  to 10  $\mu\text{g/mL}$ ) in PTB-EDTA. Then 50  $\mu\text{L}$ /well mixture was added to the plate and incubated at 4°C overnight. Plates were washed the day after, then 3% NHS were diluted in RPMI 1640 and added to the wells, then incubated 1 hour at 37°C. C5b-9 was detected as previously described.

For the complement inhibition ELISA in which complement was activated by wild type ACPA (wt ACPA, 3F3) [16], 10  $\mu\text{g/mL}$  streptavidin (Invitrogen, 434301) and 10  $\mu\text{g/mL}$  CarP-FCS were coated simultaneously overnight at 4°C, 10  $\mu\text{g/mL}$  citrulline-containing CCP2 peptide (biotin labelled, produced in the peptide lab in the Leiden University Medical Center [LUMC]) was added after wash. After 1 hour incubation and 1 hour blocking, 10  $\mu\text{g/mL}$  wt ACPA was added to the plate. Then, 1% NHS (final dilution) and bsAbs were mixed in RPMI 1640 and added to the plate for 1 hour incubation. C5b-9 was detected as previously described.

### Bispecificity ELISA

Maxisorp 96 well-plates were coated with 10  $\mu\text{g/mL}$  CarP-FCS, after blocking with PBS/1% BSA, parental antibodies and bispecific antibodies were diluted and transferred to the wells. After incubation, 10  $\mu\text{g/mL}$  factor H (FH) (CompTech, A137) or C4b-binding protein (C4BP) (CompTech, A109) were added to the plates. Goat anti-human FH (Quidel, A312, 1:1000 dilution) or rabbit anti-human C4BP (kindly provided by Anna M. Blom, Malmö, Sweden, 1:2000 dilution) were used for detection. Corresponding secondary antibodies were added after incubation and ABTS was used as described before.

### Mass spectrometry

To assess bsAbs yield and quality, the parental mAbs and bsAbs were analysed at the intact protein level using nano-reverse phase liquid chromatography (nano-RP-LC) coupled to an Impact QTOF mass spectrometer (Bruker Daltonics). For the analysis, an UltiMate 3000 nanoRSLC system (Thermo Fisher Scientific) with a C4 trap column (5  $\times$  0.3 mm i.d., Acclaim PepMap; Thermo Fisher Scientific) and a diphenyl reversed phase column (150  $\times$  0.1 mm i.d, Halo Bioclass, Advanced Material Technology, Wilmington, DE, USA) were used. The antibodies were diluted in water to a concentration of 1  $\mu\text{g}/\mu\text{L}$  prior injection. The injection volume was set to 0.4  $\mu\text{L}$ , resulting in an injected amount of 400 ng of antibody. Mobile phases consisted of water and 0.1% trifluoroacetic acid (TFA) for mobile phase A, and acetonitrile with 0.1% TFA for mobile phase B. The sample was first trapped onto the C4 trap column for 5 minutes at 30% B followed by an increase to 32% B in 1 minute. The separation was performed using a linear gradient of 12 minute to 50% B followed by an increase to 60% B in 2 minutes. The column was cleaned at 98% B for 5 minutes followed by reconditioning with 30% mobile phase B in the last 5 minutes of the 30-minute gradient. The mass spectrometer was operated in positive ionisation mode using an acetonitrile enriched dopant nitrogen gas for improved ionisation at a pressure of 0.2 bar. The capillary voltage was set to 900 V, a drying gas temperature of 220°C, and a flow of 3 L/min. An in-source collision-induced dissociation energy of 120 eV was used for in-source declustering. To further improve declustering, 5.0 and 7.0 eV were set for

the quadrupole and collision cell energy, respectively. The data were analysed using the maximum entropy algorithm in the data analysis software (Bruker). A baseline subtraction with a flatness of 0.4 points as well as a Gaussian smoothing with a width of 0.4 m/z and 2 cycles was applied to the deconvoluted data.

### Statistical methods

Statistical analysis was conducted using GraphPad Prism 10. Descriptive statistics are represented as mean  $\pm$  standard deviation. For comparisons between groups, data was assessed using one way analysis of variance. For paired data, paired t-test was used for analysis.

## RESULTS

### Production of bispecific antibodies

BsAbs were generated by using the clinically validated controlled Fab-arm exchange (cFAE) technology [17]. Combinations of different parental antibodies and the methods to make bsAbs are shown in Figure 1A. The anti-CarP mAb 4A10, generated in-house, was used to target carbamylated proteins. This antibody binds to a variety of carbamylated proteins but not to unmodified proteins or to citrullinated proteins (Fig 1B, Supplementary Fig). MABs OX24 (anti-FH) and 3B9D6 (anti-C4BP) were selected for generating bsAbs that recruit the endogenous circulating complement inhibitors FH and C4BP, respectively. Mab b12 (anti-HIV) against an irrelevant HIV-1 envelope protein, served as a negative control (Fig 1A). After producing these antibodies as parentals with the relevant cFAE mutations (F405L/K409R) and mutations in the Fc domain (L234A/L235A/P329G) that disable Fc-mediated effector functions [4], we performed cFAE and quality control of the bsAbs. We verified the binding to carbamylated proteins and observed that the bivalent parental anti-CarP antibody and all bsAbs with an anti-CarP arm effectively bound to carbamylated protein-coated plates (Fig 1B). As expected, the parental antibody bound more strongly than the bsAbs due to its ability to bind the carbamylated antigens bivalently. The control bsAbs that did not have an anti-CarP arm did not bind to the plates. Using nano-RP-LC and mass spectrometry, we confirmed efficient Fab-arm exchange for both bsAbs. The masses of the bsAbs showed an average between the masses of the parental Abs (Fig 1C). In the case of bsAb anti-CarP  $\times$  anti-FH, although the mass range of both monospecific Abs was very similar (ie, ranging from 146,300 to 147,400 Da for anti-CarP and from 146,100 to 146,600 Da for anti-FH), but still clear masses corresponding to the bsAbs were observed indicating efficient Fab-arm exchange. For bsAb anti-CarP  $\times$  anti-C4BP the masses of both parental mAbs were very different (eg, ranging from 146,300 to 147,400 Da for anti-CarP and from 149,100 to 150,200 for anti-C4BP), which resulted in a mass range of 147,400 to 148,500 for bsAbs which was clearly detected (Fig 1C right panel). For both bsAbs preparations only minor amounts of parental mAbs were observed proving a successfully generation of highly pure bsAbs. To summarise, these data all demonstrated correct formation of bispecific antibodies.

### Targeted complement inhibition by bsAbs

After making the bsAbs, we continued with their functional validation using ELISA. First, inhibitor recruitment was

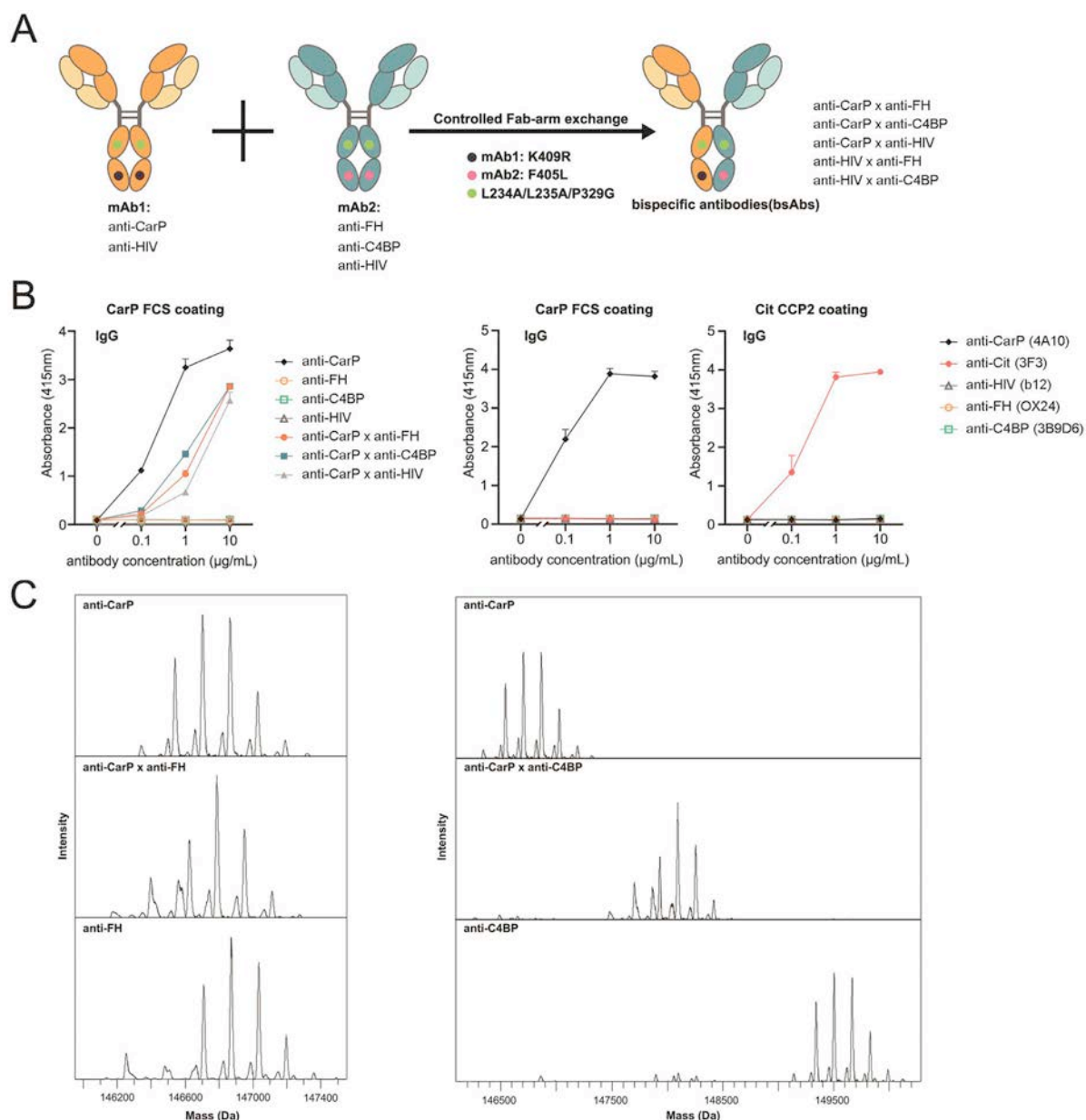


**Figure 1.** Generation and validation of anti-CarP-based bispecific antibodies. A, Schematic representation bsAbs production using controlled Fab-arm exchange. Parental monoclonal antibody (mAb) 1 and 2 carried K409R and F405L mutations, respectively. Both mAbs contained Fc-mediated effector function-attenuating mutations (LALAPG: L234A/L235A/P329G). Schematic was made using Biorender. B, Left panel shows antibody binding ELISA. Plates were coated with carbamylated protein, antibodies were added and detected with rabbit anti-Human IgG (Dako, P0214, 1:2000 dilution). A representative experiment is shown ( $n = 3$ ). B, Middle and right panel show antibody binding ELISA. Plates were coated with carbamylated proteins or citrulline-containing peptide 2 (cit CCP2) separately. Antibodies were added and detected with rabbit anti-Human IgG (Dako, P0214, 1:2000 dilution). A representative experiment is shown ( $n = 3$ ). C, Masses of parental antibodies and bispecific antibodies measured by mass spectrometry. bsAb, bispecific antibody; CarP, carbamylated protein; CCP2, citrulline-containing peptide 2; C4BP, C4b-binding protein; ELISA, enzyme-linked immunosorbent assay; Fab, fragment antigen-binding; Fc, fragment crystallizable; FH, factor H; IgG, immunoglobulin G; LALAPG, L234A/L235A/P329G; mAb, monoclonal antibody.

analysed. After adding antibodies to CarP-FCS-coated plates, purified FH or C4BP were added. Next, FH or C4BP antibodies were used to detect their presence. FH or C4BP were only captured by bsAbs containing both a carbamylated protein-binding arm and a FH or C4BP recruiting arm (Fig 2A). This confirmed formation of the correct bsAbs and their capacity to recruit inhibitors.

To determine whether the bsAbs could inhibit complement activation, we tested their complement inhibitory function in a double coating ELISA in which IgG and carbamylated proteins were coated simultaneously to the same surface. This allows

IgG-mediated complement activation and localises the ligand required for bsAb-mediated complement inhibition. In the absence of inhibitory antibodies, we observed a strong complement activation (Fig 2B). Addition of increasing amounts of either anti-CarP x anti-FH or anti-CarP x anti-C4BP bsAb showed dose-dependent complement inhibition, in contrast to the control bsAbs that did not inhibit complement activation (Fig 2B). Together, these data indicate that the anti-CarP based bsAbs are able to bind specifically, recruit the endogenous complement regulators, and successfully inhibit complement activation.

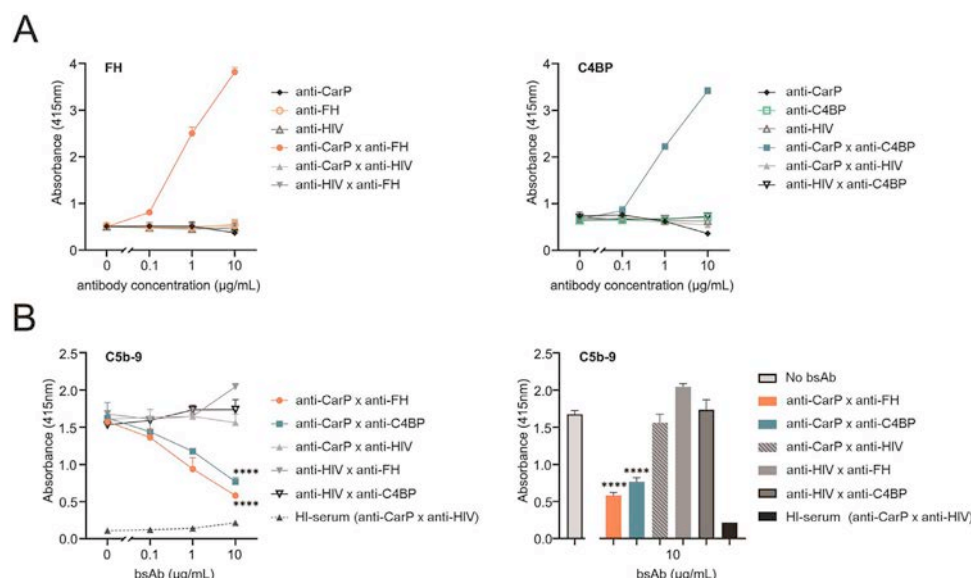


**Figure 2.** Recruitment of complement inhibitors and validation of functional impact by bispecific antibodies. A, ELISA to confirm bispecificity. Parental mAbs and bsAbs were added in a dose response to carbamylated protein-coated wells. The capacity to capture FH (left panel) or C4BP (right panel) by the bsAbs, but not the parental mAbs, is shown. Representative data of 3 replicate experiments shown. B, Complement inhibition ELISA for classical pathway mediated complement activation. As described in detail in the Methods section, plates were coated with a mix of IVIG and carbamylated proteins. The IgG triggers the classical pathway and the carbamylated proteins serves as the target for the bsAb. The anti-CarP bsAbs that recruit FH or C4BP both demonstrated significant complement inhibition, whereas the controls did not. Data are representative of 3 replicate experiments, one way ANOVA was used for statistical analysis, \*\*\*\* $P < .0001$ . HI-serum: heat inactivate serum. ANOVA, analysis of variance; bsAb, bispecific antibody; CarP, carbamylated protein; C4BP, C4b-binding protein; ELISA, enzyme-linked immunosorbent assay; FH, factor H; HI-serum, heat-inactivated serum; IgG, immunoglobulin G; IVIG, intravenous immunoglobulin; mAb, monoclonal antibody.

### BsAbs inhibit complement activation driven by autoantibodies from RA patient serum

To determine the complement inhibitory capacity of the bsAbs using a pathologically relevant conditions, we used a set of sera from RA patients. First, we analysed the capacity of the anti-CarP autoantibodies present in these RA sera to mediate complement activation on carbamylated protein-coated plates. We indeed showed that the anti-CarP-positive RA patient sera displayed substantial complement activation, confirming the capacity of patient-derived anti-CarP antibodies to mediate complement activation (Fig 3A, left, middle). In contrast, complement activation was not observed in sera of healthy controls or in heat-inactivated sera. A set of 15 anti-CarP-positive sera (red dots) were pooled and used to analyse the capacity of the bsAbs to inhibit patient-derived anti-CarP autoantibody-mediated complement activation. After addition of bsAbs, we observed strong inhibition by the anti-CarP × anti-FH bsAb and close-to-complete inhibition by the anti-CarP × anti-C4BP bsAb, whereas the control bsAb did not inhibit complement activation (Fig 3A, right). These findings were confirmed in a separate assay in which 15 individual patient sera were tested as well (Fig 3B).

As it is known that citrullination [4] and carbamylation [18] both take place in the inflamed joint, we determined if we could inhibit local complement activation induced by ACPA binding to citrullinated antigens with complement inhibitors recruited carbamylated antigens immobilised in the same well. Importantly, the used anti-CarP based bsAb does not crossreact with citrullinated proteins (Fig 2B). Interestingly, we found that both the FH- and the C4BP-recruiting anti-CarP bsAbs were able to inhibit the ACPA-driven complement activation (Fig 3C).

In conclusion, this study demonstrates that targeted complement inhibition can be achieved by bsAbs targeting endogenous complement inhibitors to post-translationally modified proteins,

providing first evidence and a strong rationale to perform *in vivo* studies to determine the efficacy of selective targeted complement inhibition.

## DISCUSSION

The presence of AMPA is an important feature of RA [19]. These AMPA may contribute to inflammation and tissue damage by activating cellular Fc receptors [20] or by activating complement [21]. Both ACPA and anti-CarP are present in the joint and can contribute to the pathological processes. In this study, we have employed one of the AMPA reactivities, anti-CarP, to target complement inhibition specifically to the sites where anti-CarP antibodies are triggering complement activation.

Here, we demonstrate a new format of a targeted complement inhibitor integrating anti-CarP into a bispecific antibody, together with anti-FH or anti-C4BP. Both bsAbs were able to achieve selective complement inhibition in a targeted way. They inhibited under conditions in which complement activation was induced by human IgG, as well as in the context of RA patient sera, where complement activation was triggered by anti-CarP autoantibodies of RA patients.

Carbamylated proteins and citrullinated proteins are both present in the inflamed joint. In our experiments, we showed that anti-CarP based bispecific complement inhibitors were also able to inhibit ACPA-driven complement activation *in vitro*. In these assays, both citrullinated and carbamylated proteins were coated in the same well, mimicking post-translationally modified protein mixtures occurring *in vivo*. These data indicate that complement inhibiting anti-CarP based bsAb may be used to target inflamed joints, where they might inhibit complement activation conceivably triggered by any complement activator (AMPA, RF, immune complexes).



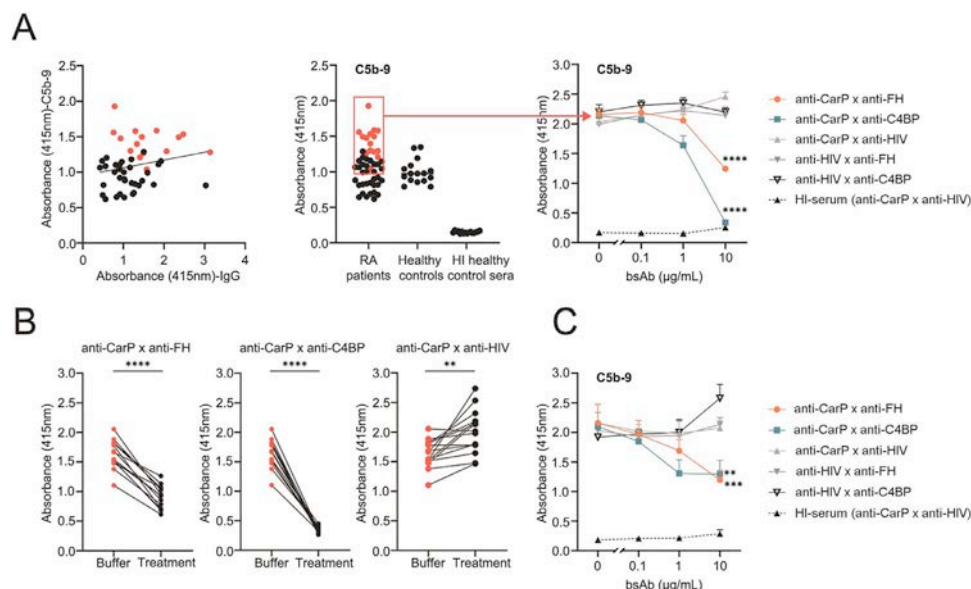


**Figure 3.** Anti-CarP bsAbs inhibit complement activation triggered by autoantibodies from RA patient serum. A, Left panel shows correlation between antibody binding to CarP-FCS (IgG detection, X axis) and its capacity to activate complement (C5b-9 detection, Y axis). Each dot represents one individual, sera indicated by the red dots were selected and pooled for the complement inhibition in the right panel. Middle panel shows comparison of complement activation on CarP-FCS triggered by sera of RA patients and healthy controls. Heat inactivate serum (HI-serum) was used to indicate background activation level. Right panel: Anti-CarP bsAbs demonstrated significant inhibition of complement activation driven by anti-CarP antibodies present in the pool of RA patient sera. Data are representative of 3 replicate experiments, one way ANOVA was used for statistical analysis, \*\*\*\* $P < .0001$ . B, Complement inhibition in individual RA patient sera. Paired t-test was used for statistical analysis. \*\*\*\* $P < .0001$ . \*\* $P < .01$ . C, Anti-CarP bsAbs showed significant inhibition of complement activated by wild type anti-citrullinated mAb 3F3 (wt ACPA), ie, data points at 0 μg/mL bsAb. Anti-CarP x anti-FH: \*\*\* $P < .001$ . Anti-CarP x anti-C4BP: \*\* $P < .01$ . One way ANOVA was used for statistical analysis. ACPA, anti-citrullinated protein antibody; ANOVA, analysis of variance; bsAb, bispecific antibody; CarP, carbamylated protein; FCS, fetal calf serum; C4BP, C4b-binding protein; FH, factor H; HI-serum, heat-inactivated serum; IgG, immunoglobulin G; mAb, monoclonal antibody; RA, rheumatoid arthritis; wt, wild type.

Most approved complement inhibitory drugs act systemically, eg, as with the exemplary C5 inhibitors eculizumab and ravulizumab [22] or the C1s inhibitor sutimlimab [23]. Systemic inhibition of the complement system increases the risk of infection, as is seen in the increased risk of invasive meningococcal disease during treatment with eculizumab [14], and as demonstrated by black box warnings on the drugs' packaging. Therefore, selective targeted complement inhibition might be a better way to achieve complement inhibition localised to specific pathogen sites while leaving the systemic complement system intact to fight infections. Antibodies were already investigated to modulate complement function as antibody-fusion proteins, like C3d targeted FH, which consists of monoclonal anti-C3d antibody with FH domains 1 to 5 fused at the Fc-tail [24]. Compared to our bispecifics, targeting C3d may have downsides. Although the C3d antibody may bind to specific locations where complement is activated, it may also do so on undesired surfaces, such as on pathogens like *Streptococcus pneumoniae* covered by C3 activation fragments [25]. Therefore, anti-C3d antibody may possibly protect pathogens from complement activation. Our bsAb in contrast targets to specific locations of the body where carbamylated proteins are present and anti-CarP accumulates, such as the inflamed joints. We therefore believe that our approach may have a lower infection risk profile.

We cannot exclude the possibility that at sites of bacterial infection some degree of tissue carbamylation may occur, but even in that setting we envision a more favourable safety profile of our bsAbs. Consequently, we eagerly await further results of the C3d-targeted complement inhibitors [26] and our tissue-targeted bispecific based inhibitors. Clearly these approaches have distinct mechanism, each with its unique

properties. Overall, we are convinced that selective local targeted complement inhibition will provide substantial improvements over conventional systemically acting complement inhibitors.

Our study has some limitations. These bsAbs were not evaluated *in vivo*, and the bsAb molecules to recruit FH or C4BP generated are both human specific and do not crossreact with the corresponding mouse FH and C4BP. We are currently generating surrogate antibodies against mouse FH to allow such *in vivo* experiments. The bsAbs utilise endogenously present inhibitors. Our previous work clearly indicated that the circulating concentrations of FH and C4BP are sufficient to allow the bsAbs to induce effective inhibition. However, future *in vivo* experiments will have to provide insight into the pharmacodynamics of the bsAbs and the regulators to be recruited.

The developed bsAbs will not specifically home to joints; they will home to locations where carbamylated proteins accumulate. Since we have previously shown [18] that in the inflamed joint there is extensive presence of such carbamylated proteins, we argue that it is plausible that the anti-CarP based bsAb will localise to the inflamed joint. *In vivo* experimentation will have to reveal if the antibodies do indeed home to the locations where carbamylated proteins are present.

In conclusion, our study describes a new strategy to perform local complement inhibition, which could be a new option for future clinical use in RA and other autoimmune diseases.

## CRediT authorship contribution statement

**Haiyu Wang:** Writing – review & editing, Visualization, Software, Funding acquisition, Data curation, Writing – original

draft, Validation, Methodology, Formal analysis. **Saskia Nugteren:** Formal analysis, Writing – review & editing, Data curation. **Rick J. Groenland:** Writing – original draft, Data curation, Investigation. **Stef van der Meulen:** Formal analysis, Writing – original draft, Data curation. **Hanneke Kapsenberg:** Writing – review & editing, Methodology. **Christoph Gstöttner:** Investigation, Writing – review & editing. **Elena Domínguez-Vega:** Writing – review & editing, Investigation. **Jan Piet van Hamburg:** Investigation, Writing – review & editing. **Sander W. Tas:** Writing – review & editing, Investigation. **Rene E.M. Toes:** Writing – review & editing, Supervision, Writing – original draft. **Paul W.H.I. Parren:** Writing – original draft, Writing – review & editing, Supervision. **Leendert A. Trouw:** Supervision, Conceptualization, Project administration.

## Acknowledgements

The authors acknowledge the kind technical support from Lisanne J.E. van Rooijen and Sofie Keijzer from the Amsterdam Medical Center, Amsterdam, the Netherlands.

## Funding

The authors would like to acknowledge the financial support from the Chinese Scholarship Council grant number 202006210040 awarded to HW.

## Competing interests

Leendert A. Trouw and Paul W.H.I. Parren are mentioned as inventors on a patent application on the use of bispecific antibody and uses thereof. The other authors do not have competing interests to report.

## Patient consent for publication

n.a.

## Ethics approval

This study was conducted in accordance with the Helsinki Declaration. The sera for the healthy controls were collected under biobank number B19.008. The sera of RA patients were originally collected as anonymised leftover material from routine diagnostics. The serum pool used as the source of complement active serum was obtained through the Leiden University Voluntary Donor Service with the permit number (LuVDS24.021) and was approved by the LUMC Toetsing Commissie Biobanken & Biomaterialen (TCBio). All samples arrived at our lab completely anonymised to protect donor identities.

## Provenance and peer review

Not commissioned, externally peer reviewed.

## Supplementary materials

Supplementary material associated with this article can be found in the online version at doi:10.1016/j.ard.2025.06.2130.

## Orcid

Haiyu Wang: <http://orcid.org/0000-0002-1764-4385>

Saskia Nugteren: <http://orcid.org/0009-0006-3709-1526>  
Rick J. Groenland: <http://orcid.org/0009-0006-3227-8260>  
Stef van der Meulen: <http://orcid.org/0000-0001-6496-603X>  
Hanneke Kapsenberg: <http://orcid.org/0009-0006-7119-2179>

Christoph Gstöttner: <http://orcid.org/0000-0003-4033-4024>  
Elena Domínguez-Vega: <http://orcid.org/0000-0002-6394-0783>

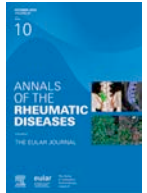
Jan Piet van Hamburg: <http://orcid.org/0000-0002-6760-4648>

Sander W. Tas: <http://orcid.org/0000-0002-8940-1788>  
Rene E.M. Toes: <http://orcid.org/0000-0002-9618-6414>  
Paul W.H.I. Parren: <http://orcid.org/0000-0002-4365-3859>  
Leendert A. Trouw: <http://orcid.org/0000-0001-5186-2290>

## REFERENCES

- [1] Guo Q, Wang Y, Xu D, Nossent J, Pavlos NJ, Xu J. Rheumatoid arthritis: pathological mechanisms and modern pharmacologic therapies. *Bone Res* 2018;6:15.
- [2] McInnes IB, Schett G. The pathogenesis of rheumatoid arthritis. *N Engl J Med* 2011;365(23):2205–19.
- [3] Dörner T, Egerer K, Feist E, Burmester GR. Rheumatoid factor revisited. *Curr Opin Rheumatol* 2004;16(3):246–53.
- [4] Klareskog L, Rönnelid J, Lundberg K, Padyukov L, Alfredsson L. Immunity to citrullinated proteins in rheumatoid arthritis. *Annu Rev Immunol* 2008;26:651–75.
- [5] Shi J, Knevel R, Suwannalai P, van der Linden MP, Janssen GM, van Veelen PA, et al. Autoantibodies recognizing carbamylated proteins are present in sera of patients with rheumatoid arthritis and predict joint damage. *Proc Natl Acad Sci U S A* 2011;108(42):17372–7.
- [6] Nielen MM, van Schaardenburg D, Reesink HW, van de Stadt RJ, van der Horst-Bruinsma IE, de Koning MHMT, et al. Specific autoantibodies precede the symptoms of rheumatoid arthritis: a study of serial measurements in blood donors. *Arthritis Rheum* 2004;50(2):380–6.
- [7] Gan RW, Trouw LA, Shi J, Toes REM, Huizinga TWJ, Demoruelle MK, et al. Anti-carbamylated protein antibodies are present prior to rheumatoid arthritis and are associated with its future diagnosis. *J Rheumatol* 2015;42(4):572–9.
- [8] Kempers AC, Nejadnik MR, Rombouts Y, Ioan-Facsinay A, van Oosterhout M, Jiskoot W, et al. Fc gamma receptor binding profile of anti-citrullinated protein antibodies in immune complexes suggests a role for FcγRI in the pathogenesis of synovial inflammation. *Clin Exp Rheumatol* 2018;36(2):284–93.
- [9] Trouw LA, Haisma EM, Levarht EW, van der Woude D, Ioan-Facsinay A, Daha MR, et al. Anti-cyclic citrullinated peptide antibodies from rheumatoid arthritis patients activate complement via both the classical and alternative pathways. *Arthritis Rheum* 2009;60(7):1923–31.
- [10] Daha NA, Banda NK, Roos A, Beurskens FJ, Bakker JM, Daha MR, et al. Complement activation by (auto-) antibodies. *Mol Immunol* 2011;48(14):1656–65.
- [11] Mullazehi M, Mathsson L, Lampa J, Rönnelid J. High anti-collagen type-II antibody levels and induction of proinflammatory cytokines by anti-collagen antibody-containing immune complexes in vitro characterise a distinct rheumatoid arthritis phenotype associated with acute inflammation at the time of disease onset. *Ann Rheum Dis* 2007;66(4):537–41.
- [12] Brodeur JP, Ruddy S, Schwartz LB, Moxley G. Synovial fluid levels of complement SC5b-9 and fragment Bb are elevated in patients with rheumatoid arthritis. *Arthritis Rheum* 1991;34(12):1531–7.
- [13] Perrin LH, Nydegger UE, Zubler RH, Lambert PH, Miescher PA. Correlation between levels of breakdown products of C3, C4, and properdin factor B in synovial fluids from patients with rheumatoid arthritis. *Arthritis Rheum* 1977;20(2):647–52.
- [14] McNamara LA, Topaz N, Wang X, Hariri S, Fox L, MacNeil JR. High risk for invasive meningococcal disease among patients receiving eculizumab (Soliris) despite receipt of meningococcal vaccine. *MMWR Morb Mortal Wkly Rep* 2017;66(27):734–7.
- [15] Wang H, van de Bovenkamp FS, Dijkstra DJ, Abendstein L, Borggreven NV, Pool J, et al. Targeted complement inhibition using bispecific antibodies that bind local antigens and endogenous complement regulators. *Front Immunol* 2024;15:1288597.
- [16] Kissel T, Reijm S, Slot LM, Cavallari M, Wortel CM, Vergroesen RD, et al. Antibodies and B cells recognising citrullinated proteins display a broad

- cross-reactivity towards other post-translational modifications. *Ann Rheum Dis* 2020;79(4):472–80.
- [17] Labrijn AF, Meesters JI, de Goeij BE, van den Bremer ET, Neijssen J, van Kampen MD, et al. Efficient generation of stable bispecific IgG1 by controlled Fab-arm exchange. *Proc Natl Acad Sci U S A* 2013;110(13):5145–50.
- [18] Verheul MK, Janssen GMC, de Ru A, Stoeken-Rijsbergen G, Levarht EWN, Kwekkeboom JC, et al. Mass-spectrometric identification of carbamylated proteins present in the joints of rheumatoid arthritis patients and controls. *Clin Exp Rheumatol* 2021;39(3):570–7.
- [19] Trouw LA, Rispens T, Toes REM. Beyond citrullination: other post-translational protein modifications in rheumatoid arthritis. *Nat Rev Rheumatol* 2017;13(6):331–9.
- [20] Anquetil F, Clavel C, Offer G, Serre G, Sebbag M. IgM and IgA rheumatoid factors purified from rheumatoid arthritis sera boost the Fc receptor- and complement-dependent effector functions of the disease-specific anti-citrullinated protein autoantibodies. *J Immunol* 2015;194(8):3664–74.
- [21] Dijkstra DJ, Joeloem Singh JV, Bajema IM, Trouw LA. Complement activation and regulation in rheumatic disease. *Semin Immunol* 2019;45:101339.
- [22] Rother RP, Rollins SA, Mojcić CF, Brodsky RA, Bell L. Discovery and development of the complement inhibitor eculizumab for the treatment of paroxysmal nocturnal hemoglobinuria. *Nat Biotechnol* 2007;25(11):1256–64.
- [23] Nikitin PA, Rose EL, Byun TS, Parry GC, Panicker S. C1s inhibition by BIVV009 (Sutimlimab) prevents complement-enhanced activation of autoimmune human B cells in vitro. *J Immunol* 2019;202(4):1200–9.
- [24] Liu F, Ryan ST, Fahnoe KC, Morgan JG, Cheung AE, Storek MJ, et al. C3d-targeted factor H inhibits tissue complement in disease models and reduces glomerular injury without affecting circulating complement. *Mol Ther* 2024;32(4):1061–79.
- [25] Gil E, Noursadeghi M, Brown JS. *Streptococcus pneumoniae* interactions with the complement system. *Front Cell Infect Microbiol* 2022 Jul 28;12:929483.
- [26] Liu F, Wawersik S, Tomlinson S, Thurman JM, Holers VM. Tissue-targeted regulators of complement for amelioration of human disease: rationale and novel therapeutic strategies. *J Immunol* 2025:vkaf053.



## Rheumatoid arthritis

Collagen-binding integrin  $\alpha 11\beta 1$  contributes to joint destruction in arthritic *hTNFtg* mice

Anna De Giuseppe<sup>1</sup>, Adrian Deichsel<sup>1</sup>, Alina Reese<sup>1</sup>, Simon Kleimann<sup>1</sup>, Deniz Wawersig<sup>1</sup>, Isabel Zeinert<sup>2</sup>, Kerstin K. Rauwolf<sup>1</sup>, Denise Beckmann<sup>1</sup>, Uwe Hansen<sup>1</sup>, Jordana Miranda de Souza Silva<sup>1</sup>, Annika Krause<sup>1</sup>, Beate Eckes<sup>2</sup>, Daniel Kronenberg<sup>1</sup>, Corinna Wehmeyer<sup>1</sup>, Berno Dankbar<sup>1</sup>, Ning Lu<sup>3</sup>, Donald Gullberg<sup>3</sup>, Thomas Pap<sup>1</sup>, Adelheid Korb-Pap<sup>1,\*</sup>

<sup>1</sup> Institute of Musculoskeletal Medicine, University Hospital Muenster, Muenster, Germany

<sup>2</sup> Translational Matrix Biology, Faculty of Medicine, University of Cologne, Cologne, Germany

<sup>3</sup> Department of Biomedicine, University of Bergen, Bergen, Norway

## ARTICLE INFO

Article history:  
Received 30 May 2025  
Accepted 10 July 2025

## ABSTRACT

**Objectives:** In rheumatoid arthritis (RA), fibroblast-like synoviocytes (FLS) acquire an aggressive, tumour-like phenotype characterised by increased adhesion to extracellular matrix, contributing to joint degradation. The collagen-binding integrin  $\alpha 11\beta 1$  is involved in similar processes in cancer-associated fibroblasts, but its role in RA and arthritic mice remains unclear.

**Methods:** Integrin  $\alpha 11$  expression was analysed in synovial tissue and FLS from RA and osteoarthritis patients and human tumour necrosis factor transgenic (*hTNFtg*) and wild-type mice supported by Accelerating Medicines Partnership Rheumatoid Arthritis and Pathobiology of Early Arthritis Cohort data. A novel 3-dimensional (3D) organoid coculture model and electron microscopy were used to analyse FLS invasion into cartilage explants, *Itga11*<sup>−/−</sup> were crossed with *hTNFtg* mice, and disease severity was evaluated using microcomputed tomography ( $\mu$ CT) and histology. Functional assays using FLS included cell morphology, adhesion, degradation, and matrix metalloproteinase expression and were complemented by osteoclast and coculture studies.

**Results:** In the context of RA, strong  $\alpha 11$  expression was detected in the synovium, particularly in sublining clusters of FLS within fibroid-type synovial tissue *in vivo* and at focal adhesions of arthritic FLS and at invasion sites within the 3D coculture model *in vitro*. Clinical scores,  $\mu$ CT imaging, and histomorphological analyses revealed significantly reduced cartilage degradation, bone erosions, and FLS attachment to cartilage in *Itga11*<sup>−/−</sup>*hTNFtg* compared to *hTNFtg* mice. *In vitro* studies revealed that  $\alpha 11$  deficiency led to a decreased receptor activator of nuclear factor kappa-B ligand/osteoprotegerin ratio along with reduced TNF $\alpha$ -induced proteolytic degradation activity, and signalling pathway activation.

**Conclusions:** Integrin  $\alpha 11$  levels are increased in RA, and its deficiency notably diminishes joint destruction in *hTNFtg* mice, emphasising its potential as promising therapeutic target.

\*Correspondence to Dr. Adelheid Korb-Pap, Institute of Musculoskeletal Medicine, University Hospital Muenster, Muenster, Germany.

E-mail address: [korba@uni-muenster.de](mailto:korba@uni-muenster.de) (A. Korb-Pap).

Handling editor Josef S. Smolen.

<https://doi.org/10.1016/j.ard.2025.07.011>



### WHAT IS ALREADY KNOWN ON THIS TOPIC

- Rheumatoid arthritis is characterised by the tumour-like transformation of fibroblast-like synoviocytes (FLS) that is accompanied by increased expression of adhesion molecules and progressive cartilage degradation, ultimately leading to irreversible joint damage. The role of the collagen-binding integrin  $\alpha 11\beta 1$ —primarily expressed on mesenchymal cells—remains poorly understood in this context and requires further investigation.

### WHAT THIS STUDY ADDS

- Integrin  $\alpha 11\beta 1$  expression is upregulated in the context of rheumatoid arthritis and can be attributed to specific sublining FLS populations. The loss of integrin  $\alpha 11\beta 1$  results in significantly reduced bone and cartilage destruction, reduced matrix metalloproteinase expression and reduced invasiveness of FLS along with altered signalling.

### HOW THIS STUDY MIGHT AFFECT RESEARCH, PRACTICE OR POLICY

- The study provides novel mechanistic insights into the role of integrin  $\alpha 11\beta 1$  in FLS pathology, encouraging further exploration of integrin  $\alpha 11\beta 1$  as a stromal target in rheumatoid arthritis.

## INTRODUCTION

Rheumatoid arthritis (RA) is a chronic systemic inflammatory disease with a high prevalence and socioeconomic burden affecting joints in a characteristic symmetrical pattern. If untreated, RA leads to massive irreversible destruction of articular structures such as cartilage and bone. It has been shown that, in addition to the influx of immune and inflammatory cells, fibroblast-like synoviocytes (FLS) can be attributed to a key role in the pathogenesis of RA, as these cells are known to contribute significantly to the development, progression, and chronic course of this disease [1]. A major feature of FLS in RA is their stable activation and transformation into an autonomously aggressive phenotype. This, among other features, leads to an increased expression of adhesion molecules, triggering further destruction of cartilage as these facilitate the binding of RA FLS to components of the extracellular matrix (ECM) [2,3].

In this context, different matrix adhesion receptors such as integrins and syndecans were shown to play important roles in the attachment of RA FLS to collagens [4–6]. One of the major receptors for fibrillary collagens the main structural protein making up cartilage and bone in joint tissue is integrin  $\alpha 11\beta 1$ . The gene *Itga11* encodes for the alpha subunit of integrin  $\alpha 11\beta 1$  and is 1 of 4 known integrins (besides  $\alpha 1\beta 1$ ,  $\alpha 2\beta 1$ , and  $\alpha 10\beta 1$ ) to bind to collagen [7,8]. First discovered in 1995, it has been shown to be expressed mainly on cells of mesenchymal origin, notably fibroblasts [9–11]. Integrin  $\alpha 11\beta 1$  was demonstrated to mediate not only cellular adhesion but also cell migration, collagen reorganisation and the expression of matrix-modifying enzymes [7,12,13]. In the tumour context, integrin  $\alpha 11\beta 1$  expressed in cancer-associated fibroblasts (CAFs) within the tumour stroma has been shown to positively influence tumour growth and metastatic potential and to negatively affect disease outcome [14–16].

Given the similarities between tumour cells and RA FLS, which amongst others are characterised by increased adhesion, migration, and invasion capacities, we hypothesised that  $\alpha 11\beta 1$  serves not only as a pivotal factor in CAFs across diverse cancer types but could also potentially exacerbate joint destruction severity in RA.

## METHODS

### Human synovial samples

The ethics committees of the Medical University of the University Hospital Muenster approved all studies with human samples. Samples of synovial tissues from subjects with RA or osteoarthritis (OA) (according to the 1987 revised American College of Rheumatology criteria for RA and OA [17]) were obtained as operational waste at joint replacement surgery.

### Isolation of human FLS

RA FLS and OA FLS were isolated by enzymatic digestion using collagenase type 4 (Worthington Biochemicals) and cultured in complete medium consisting of high-glucose Dulbecco's modified Eagle's medium Dulbecco's Modified Eagle Medium (DMEM) supplemented with 10% heat-inactivated fetal calf serum (FCS) Supreme (PAN-Biotech), 100 U/mL penicillin, and 10  $\mu$ g/mL streptomycin (PAA Laboratories) at 37°C and 5% CO<sub>2</sub>. Cells at passages 3 to 5 were used for all experiments.

### Animals

For the study, human tumour necrosis factor transgenic (*hTNFtg*) mice carrying the transgene from human tumour necrosis factor- $\alpha$  (strain Tg197; C57BL/6 genetic background) obtained from Alexander Fleming Biomedical Science Research Center (Vari, Greece) and mice deficient for integrin  $\alpha 11$  (*Itga11*<sup>-/-</sup>) were used [18,19]. Both mouse strains were interbred within the C57BL/6 genetic background. The genotype was confirmed by polymerase chain reaction (primer sequence, see [Supplementary Table](#)). Mice were scored every week up to the age of 12 weeks to evaluate arthritis symptoms. The evaluation was based on a scoring range from 0 (no symptoms) to 3 (severe symptoms), including grip strength, paw swelling, and weight [20]. All animal procedures were approved by the State Office for Nature, Environment and Consumer Affairs (Landesamt für Natur, Umwelt und Verbraucherschutz LANUV), Germany (reference numbers 8.87-51.05.2011.033, 84-02.04.2015. A511 and 2024-645-Grundantrag).

### Microcomputed tomographic analysis

The right hind paws from 12-week-old mice were dissected from the leg, and the skin and claws were removed and fixed overnight in 4% paraformaldehyde (PFA) at 4°C. Hind paws were transferred in phosphate buffered saline (PBS) and scanned with the SkyScan 1176 microcomputed tomography ( $\mu$ CT) scanner (Bruker) using the provided software (version 11.0.0.2) at 40 kV tube voltage, 0.6 mA using an aluminium filter (0.2 mm thick) and 0.5° rotation steps. Associated software was used for the reconstructions (NRecon, version 1.7.5.9), 3-dimensional (3D) visualisation (CTVox, version 3.3.0r1412) and analysis (Data Viewer, version 1.5.6.6 and CTAn, version 1.20.3.0). Analysis was performed at the tarsal bones 2 to 4. Firstly the 8-bit images were binarised, defining grey values from 40 to 200 as bone. The region of interest was determined visually by the bone borders. The bone volume (BV)/tissue volume (TV) is the ratio of defined BV to the region of interest.

### Isolation of FLS and bone marrow-derived macrophages from mice

Mice were sacrificed at week 12 for FLS isolation. The skin and nails of the hind paws were removed and larger ligaments

were dissected. Finally, the hind paws were dislocated and paws were digested with 1 mg/mL collagenase type 4 (Worthington Biochemicals) in DMEM for 1 hour at 37°C. After digestion, the cell suspension was centrifuged at 1500 rpm and room temperature (RT) for 5 minutes. The supernatant was discarded, and the pellet was resuspended in DMEM supplemented with 10% heat-inactivated FCS and 1% penicillin–streptomycin. Isolated fibroblasts were cultured at 37°C and 5% CO<sub>2</sub>, experiments were performed between passage 3 and 5. Additionally, bone marrow-derived macrophages (BMDMs) were isolated from 6-week-old mice. Femora and tibiae were removed, and the bone marrow was flushed out of the bone marrow cavity using Minimum Essential Medium ( $\alpha$ -MEM) containing 10% FCS. Osteoclast differentiation was achieved by culturing the cells in an  $\alpha$ -MEM medium supplemented with 10% FCS and 30 ng/mL Macrophage Colony-Stimulating Factor (M-CSF) (R&D) for 2 days followed by incubation in presence of 30 ng/mL M-CSF (R&D) and 50 ng/mL receptor activator of nuclear factor kappa-B ligand (RANKL) (R&D) with or without recombinant TNF $\alpha$  (R&D) until osteoclasts formed.

### Resorption assay

To measure the capacity of osteoclasts to dissolve bone minerals,  $6 \times 10^5$  BMDMs were directly seeded and differentiated in calcium phosphate-coated multiwell (48 well) plates (Hözl Biotech) following the same protocol as in the osteoclast assay. After the differentiation period, brightfield microscopy was used for resorption pit evaluation using Zen Pro Software (Zeiss).

### Osteoclast coculture assay

FLS ( $5 \times 10^3$  cells per well) were seeded in FLS medium (10% heat-inactivated FCS, 1% penicillin–streptomycin) in 96-well plates. The following day, the supernatant was removed, and  $1 \times 10^5$  green fluorescent protein (GFP)-positive wild-type BMDMs were added onto the fibroblast layer. Cocultures were maintained in  $\alpha$ -MEM supplemented with 10% FCS and 1  $\mu$ M prostaglandin E<sub>2</sub>, with or without recombinant TNF $\alpha$ . The medium was replaced every 3 days. After 7 days, cells were fixed and stained with 4',6-diamidino-2-phenylindole (DAPI) for visualisation and quantification.

### Gelatin zymography

Gelatin zymography was conducted to analyse MMP-2 and MMP-9 activity. Cell lysis was performed with radioimmunoprecipitation assay (RIPA) buffer. Proteins (30  $\mu$ g) were separated on a 10% sodium dodecyl sulphate-polyacrylamide gel containing 0.1% porcine gelatin (Merck). Following electrophoresis, proteases were refolded by incubating gels in a renaturation buffer (50 mM Tris-HCl, 5 mM CaCl<sub>2</sub>, pH 8.5) for 16 hours. Gels were stained with Coomassie Brilliant Blue, and lysis areas were quantified using Image Studio software (Li-Cor).

### Preparation of human and murine tissues for histology

Human samples from RA and OA patients as well as hind paws from 12-week-old mice were fixed in 4% PFA overnight at 4°C. Before paraffin embedding, murine samples were decalcified in 20% Na-EDTA (Sodium Ethylenediaminetetraacetate) (AppliChem) for 8 weeks. Paraffin-embedded human tissues and hind paws were cut into 5  $\mu$ m sections and transferred onto microscope slides.

### Immunohistochemistry staining

Sections of decalcified, paraffin-embedded hind paws and human synovial tissues were deparaffinated in xylene and rehydrated in decreasing concentrations of ethanol. Subsequently, sections were incubated in distilled water and washed in PBS. Endogenous peroxidase activity was blocked with a 30% hydrogen peroxide solution in methanol. For proteolytic induced epitope retrieval, the sections were pretreated with trypsin for 10 minutes at 37°C and blocked with 20% normal horse serum for 1 hour. Human tissues were stained with a sheep polyclonal antibody to integrin subunit  $\alpha$ 11 (R&D Systems, Minneapolis, Minnesota) and murine tissues with a rabbit polyclonal antibody to mouse  $\alpha$ 11 [10] or with a rabbit polyclonal antibody to MMP-14 (Invitrogen). Biotinylated anti-sheep IgG or anti-rabbit IgG (Vector Laboratories) were used as secondary antibodies. The staining was performed using the Vectastain ABC peroxidase kit and DAB (3,3'-Diaminobenzidine) substrate kit (Vector Laboratories). Counterstaining was conducted with Mayer's Hemalaun (Sigma-Aldrich). Sections were mounted with dibutylphthalate polystyrene xylene (Merck Millipore) for microscopy.

### Toluidine-blue and haematoxylin-eosin staining of paraffin sections

Paraffin sections were deparaffinated in xylene and rehydrated in decreasing concentrations of ethanol. Subsequently, sections were incubated in distilled water and stained with toluidine-blue (Sigma-Aldrich) or Mayer's Hemalaun (Sigma-Aldrich) and eosin Y (Sigma-Aldrich). Stained sections were dehydrated in increasing concentration of ethanol and incubated in xylene followed by mounting the slides with dibutylphthalate polystyrene xylene.

### Tartrate-resistant acid phosphatase staining

The tartrate-resistant acid phosphatase (TRAP) kit (Sigma-Aldrich) was used for osteoclast detection on paraffin sections of twelve-week-old hind paws using the TRAP kit following the manufacturer's instructions.

### Histomorphometry analysis

Toluidine-blue stained sections were used for analysing synovial inflammation, total cartilage area, cartilage damage, and attachment of FLS to the cartilage surface. The extent of destined cartilage due to proteoglycan loss and degradation was quantified relative to the total cartilage content and presented as percentage. Synovial inflammation area was evaluated by relating pannus tissue to total tissue area expressed as a percentage, furthermore, the length of the FLS attachment to the cartilage surface was evaluated. Quantification of the images was performed by using Zen Pro Software (Zeiss). The MMP-14-positive area was calculated by performing image deconvolution via ImageJ, version 2.1.0/1.53c.

### Cartilage attachment assay and transmission electron microscopy

As previously described [4,21], freshly isolated cartilage of the femoral heads of 4 to 6 weeks mice and isolated wild-type (wt) and *hTNFtg* FLS were cocultivated for 9 days in a 3D organoid model using Matrigel. Subsequently, transmission electron microscopy and immunogold staining techniques were employed for characterisation of adhesion and invasion sites of FLS. In brief, 3D

cell culture samples with small pieces of hip cartilage were fixed in 2% (v/v) formaldehyde and 0.25% (v/v) glutaraldehyde in 100 mM cacodylate buffer, pH 7.4, for 3 hours at 4 °C. Afterwards samples were rinsed in PBS, dehydrated in ethanol up to 70%, and embedded in LR White embedding medium (London Resin Company, UK) according to the manufacturer's instructions using ultraviolet light for polymerisation. Ultrathin sections were cut with an ultramicrotome and collected on copper grids. For immunogold electron microscopy, ultrathin sections were incubated with 100 mM glycine in PBS for 2 minutes, washed with PBS and blocked with 2% (w/v) Bovine Serum Albumin (BSA) and 1% normal goat serum (Aurion) in PBS. Afterwards, ultrathin sections were incubated for 1 hour at RT on drops of primary antibodies (polyclonal sheep anti-integrin  $\alpha 11$  antibodies; R&D, AF 6498) in PBS containing 1% (v/v) BSA-c (Aurion) and 0.025% (v/v) Tween 20. After washing with the same solution, ultrathin sections were incubated with secondary antibodies conjugated to 12 nm gold particles (Dianova). Controls were performed with secondary antibodies only. After washing with distilled water, ultrathin sections were negatively stained with 2% (w/v) uranyl acetate for 15 minutes. Electron micrographs were taken at 60 kV with a Philips EM-410 electron microscope using imaging plates (Ditabis).

### Western blot analyses

FLS were lysed in RIPA buffer. Protein concentrations were determined by a bichinonic acid protein assay kit (Thermo Fisher) according to the manufacturer's instructions. The protein extracts were resolved with dodecyl sulphate-polyacrylamide gel electrophoresis using a 12% separation gel. Proteins were transferred to a polyvinylidene difluoride membranes (GE Healthcare) in a Trans-Blot Turbo device (Bio-Rad). Anti-integrin  $\alpha 11$  antibodies were provided by Donald Gullberg, (Department of Biomedicine, University of Bergen, Norway), other antibodies such as anti-ILK (Abcam), anti-phospho-ERK, anti-total ERK, and glyceraldehyde 3-phosphate dehydrogenase (Cell Signaling) were commercially available. Secondary antibodies were conjugated with horseradish peroxidase (Dako). Images were quantified using the gel analysing tool ImageJ, version 2.1.0/1.53c.

### Immunofluorescence staining of human and mouse FLS

Cells were seeded onto sterile glass coverslips coated with bovine collagen coating solution (Cell Applications, Inc) for improved attachment. FLS were incubated in DMEM supplemented with 10% h-FCS at 37°C and 5% CO<sub>2</sub> overnight. Thereafter, cells were washed in PBS and fixed for 20 minutes in 4% PFA. Ammonium chloride (50 mM, 10 minutes at RT) was used to reduce the autofluorescence of the cells followed by permeabilisation with 0.1% Triton X-100. To block unspecific protein interactions, FLS were incubated with 10% normal horse serum (NHS) for 20 minutes at RT. Murine and human cells were stained with primary antibodies diluted in 0.1% NHS/PBS for 1 hour and with a secondary goat anti-rabbit or goat anti-mouse Alexa Fluor 488-labelled antibody (Life Technologies) diluted in 2% NHS/PBS for 30 minutes at RT. The cytoskeleton was visualised by rhodamine-phalloidin (Invitrogen), and nuclei were stained with DAPI (Invitrogen). Mowiol (Roth) was used as a mounting medium.

### Cell area measurement

Cell area of FLS was assessed after immunofluorescence staining for filamentous actin (F-actin) and paxillin. Glass coverslips

were coated with fibronectin (10 µg/mL, Roche) or collagen I (30 µg/mL, BD Bioscience), all diluted in PBS for 1 hour at 37°C. FLS were seeded at 20,000 cells per coverslip in serum-free DMEM (duplicate wells) for 6 hours. Cells were washed once with PBS, fixed with 4% PFA in PBS for 10 minutes, permeabilised with 0.2% Triton X100 in PBS for 10 minutes, and blocked with 5% BSA in PBS for 45 minutes. Mouse anti-paxillin antibody (BD Bioscience) was used as the primary antibody (in 1% BSA/PBS for 1 hour at RT). Alexa 568 conjugated anti-mouse antibody (Invitrogen) was used as a secondary antibody (in 1% BSA/PBS for 1 hour at RT). F-actin was stained with *DyLight*<sup>TM</sup> 488 Phalloidin (Cell Signaling), and nuclei were stained with DAPI (Sigma-Aldrich). Images were acquired by confocal microscopy with Leica TCS SP5 system and Leica TCS SP8 system using 63 × /1.4 to 0.6 NA oil immersion and HC PL APO CS2 63 × /1.4 oil immersion objective, respectively. Microscopes were controlled using LAS AF 3 and LAS X software (Leica Microsystems). Cell area was determined using the following macro for Fiji/Image J2 software [22].

### Adhesion assay

For the adhesion assay, FLS were seeded on pre-coated (collagen I at 5 µg/cm<sup>2</sup> and fibronectin at 1 µg/ml) 6-well plates (5 × 10<sup>5</sup> cells/well) in complete medium and incubated for 1 hour at 37°C and 5% CO<sub>2</sub>. Afterwards, the supernatant was aspirated, and the cells were trypsinised and centrifuged at 1500 rpm and RT for 5 minutes before counting.

### Degradation assay on fluorescein isothiocyanate-gelatine

A petri dish was covered with a damp tissue to create a humidity chamber and covered with parafilm. Gelatine-fluorescein Oregon Green 488 conjugate (Invitrogen) was mixed with a sucrose solution (1 g/mL in PBS) at a 59:1 ratio. Drops of this mixture were placed on the parafilm, covered with coverslips, and incubated for 15 minutes. Coverslips were then transferred to another humid chamber containing 0.5% glutaraldehyde solution drops on ice for 15 minutes. Next, coverslips were placed in a well plate, washed with PBS, and disinfected with ethanol for 15 minutes followed by 3 15-minutes incubation steps with culture medium at 37°C. FLS were seeded onto the pre-coated coverslips in complete medium and incubated for 16 hours at 37°C and 5% CO<sub>2</sub>. After incubation, cells were washed with PBS, fixed with 4% PFA for 15 minutes, and permeabilised with acetone at −20°C for 4 minutes. F-actin and nuclei were visualised with rhodamine-phalloidin (Invitrogen) and DAPI (Invitrogen).

### ELISA

FLS supernatants and lysates from a 24 or 48 hours incubation with or w/o recombinant TNF $\alpha$  at 37°C were collected to quantify MMP-3, MMP-9, RANKL, and osteoprotegerin (OPG) levels using commercially available Enzyme-Linked Immunosorbent Assay (ELISA) kits (R&D Systems, Minneapolis, Minnesota) were used following the manufacturer's protocols. Absorbance was measured using a microplate reader (SPARK 10M, Tecan).

### Statistical analysis

Bar graphs display all data points with SD or are presented as line graphs connecting data points with SEM. The software GraphPad Prism 10, version 10.4.1 was used for statistical analysis. A comparison of 2 different groups was performed using



one-way analysis of variance (ANOVA), whereas significant differences among more than 2 groups were assessed using two-way ANOVA. *P* values less than .05 were considered to be statistically significant.

## RESULTS

### *In inflammatory arthritis, synovial tissue exhibits increased integrin $\alpha 11$ levels*

To assess integrin  $\alpha 11$  levels in synovial tissue in the context of inflammatory arthritis, publicly available platforms such as the Accelerating Medicines Partnership Rheumatoid Arthritis phase II study or the Pathobiology of Early Arthritis Cohort were used [23,24]. These provided single-cell RNA sequencing and expression data in differently categorised synovial tissues, depending on parameters such as cell clusters and synovial cell architecture. The results showed increased integrin  $\alpha 11$  in CD34+, POSTN+, and DKK3+ sublining FLS cell clusters with a highly significant correlation to fibroid-type synovial tissue (Fig 1A, Supplementary Fig S1).

To verify and substantiate these data, immunohistochemical staining was performed on paraffin-embedded human synovial tissues obtained from RA patients as well as OA patients undergoing joint replacement surgery as a control. Tissue samples from RA patients displayed the characteristic formation of an invasive hypercellular pannus and a strong signal for integrin  $\alpha 11$ , particularly in sublining areas. In contrast, no pannus formation and lower intensity in the integrin  $\alpha 11$  immunostaining were observed in tissues from OA patients (Fig 1B, Supplementary Fig S2A), in line with the publicly available data. Subsequently, paraffin-embedded hind paws derived from wt and *hTNFtg* mice at the age of 12 weeks were stained for integrin  $\alpha 11$  to verify whether a staining pattern comparable to the human situation could be seen in an animal model of RA. Comparable to the staining pattern in human RA synovial tissues, *hTNFtg* mice showed a strong upregulation of  $\alpha 11$  expression in the pannus tissue whereas just a faint staining was detectable in wt sections (Fig 1B, Supplementary Fig S2A).

As integrin  $\alpha 11$  expression is predominantly restricted to mesenchymal cells and the pannus tissue mainly formed by FLS, FLS from RA and *hTNFtg* mice as well as their respective controls were analysed for their expression levels of  $\alpha 11$  and its cellular distribution. In line with prior *in vivo* findings from histological sections, RA FLS and *hTNFtg* FLS showed an increased expression of  $\alpha 11$  compared to the controls, and  $\alpha 11$  was found primarily at focal adhesion sites (Fig 1C). Western blot analyses were performed for further quantification. These analyses could confirm the previous observation. Specifically, both RA and *hTNFtg* FLS showed significant higher quantities of integrin  $\alpha 11$  compared to controls (Fig 1D).

Next, the direct interaction between FLS and articular cartilage was investigated to understand how the localisation of  $\alpha 11$  might be affected and whether there are differences between wt and *hTNFtg* FLS. In a modified 3D coculture assay, hip caps from wt animals were incorporated into 3D organoids formed by Matrigel-embedded FLS isolated from wt and *hTNFtg* mice [4,10]. These organoids were then cocultured for 9 days, after which they were prepared for electron microscopy analyses and immunogold staining using a specific anti-integrin  $\alpha 11$  antibody with secondary antibodies conjugated to gold particles. Quantifications demonstrated that in FLS-cartilage cocultures there were striking differences between the genotypes not only in the  $\alpha 11$  labelling intensity but also in its localisation. In *hTNFtg* FLS,

a significant higher number of particles was detectable, and most strikingly these were found in areas with direct contact to the cartilage ECM and at invading sites. Interestingly, a few particles were also discovered directly within the ECM itself, located beneath the invading sites, suggesting the existence of further FLS cell extensions which were not captured in these images. In contrast, very few particles were found in wt FLS with no prominent localisation, and no invasion into the cartilage was detectable (Fig 1E).

### **Itga11*<sup>-/-</sup>*hTNFtg* mice display an alleviated arthritic phenotype in comparison to *hTNFtg* mice*

To investigate the impact of integrin  $\alpha 11$  deficiency on the course and severity of RA, *Itga11*<sup>-/-</sup> mice were crossed with *hTNFtg* mice, a well-established mouse model that exhibits joint destructions similar to human RA.

Mice of all resulting genotypes were scored weekly by 2 independent observers assessing paw swelling and loss of grip strength. As expected, wt and *Itga11*<sup>-/-</sup> mice displayed no symptoms of inflammatory arthritis. In contrast, both *Itga11*<sup>-/-</sup>*hTNFtg* and *hTNFtg* mice displayed an onset of symptoms at approximately 5 weeks of age with increasing disease severity over time, as previously described [18]. Although *Itga11*<sup>-/-</sup>*hTNFtg* mice displayed an alleviated phenotype with attenuated loss of grip strength and reduced paw swelling during the disease course, these differences were no longer detectable at 12 weeks of age (Fig 2A) [6].

The mice were then sacrificed and  $\mu$ CT analyses of hind paws were analysed qualitatively and quantitatively and significant less bone erosions were observed in hind paws from *Itga11*<sup>-/-</sup>*hTNFtg* in comparison to *hTNFtg* mice. In detail, quantification of residual BV and TV revealed significant differences in the BV/TV ratio in *Itga11*<sup>-/-</sup>*hTNFtg* compared to *hTNFtg* mice (+6.98% vs *hTNFtg*, Fig 2B), indicating less bone erosion. Histomorphological evaluations of paraffin-embedded sections of these mice were performed using haematoxylin and eosin and toluidine-blue staining, supplemented by visualisation of TRAP-positive cells (Fig 2C). Although no significant differences between *Itga11*<sup>-/-</sup>*hTNFtg* and *hTNFtg* were found in the inflammation area, *Itga11*<sup>-/-</sup>*hTNFtg* mice showed less joint destruction, and cartilage damage compared to *hTNFtg* mice. Specifically, the quantification of cartilage destruction parameters in toluidine-blue staining revealed a larger total cartilage area in *Itga11*<sup>-/-</sup>*hTNFtg* mice (+1.31% vs. *hTNFtg*, Fig 2D) and a less destained cartilage area (-19.35 % vs *hTNFtg*, Fig 2D) indicative of reduced proteoglycan loss and cartilage damage. Furthermore, a significant reduction in the length of synovial attachment to cartilage surface was evaluated in *Itga11*<sup>-/-</sup>*hTNFtg* mice (-392  $\mu$ m vs *hTNFtg*, Fig 2D). Analyses of TRAP-positive osteoclasts revealed significantly less numbers in *Itga11*<sup>-/-</sup>*hTNFtg* mice (-44.7 % vs *hTNFtg*, Fig 2D). Under inflammatory conditions, FLS act as key producers of RANKL, promoting osteoclastogenesis. In our study, analysis of RANKL and its antagonist OPG revealed a significantly reduced RANKL/OPG ratio in *Itga11*<sup>-/-</sup> compared to wt FLS after TNF $\alpha$  stimulation (-65.2% vs wt FLS) (Fig 2E). To further characterise the effects of  $\alpha 11$  deficiency on osteoclast differentiation and resorption capacities, functional assays were performed without showing any significant differences between the genotypes (Fig 2F). Based on the RANKL data, we also performed cocultures of GFP-positive BMDMs and wt and *Itga11*<sup>-/-</sup> FLS, but no significant differences were detectable after TNF $\alpha$  stimulation although a slight decrease was observed (Fig 2G).



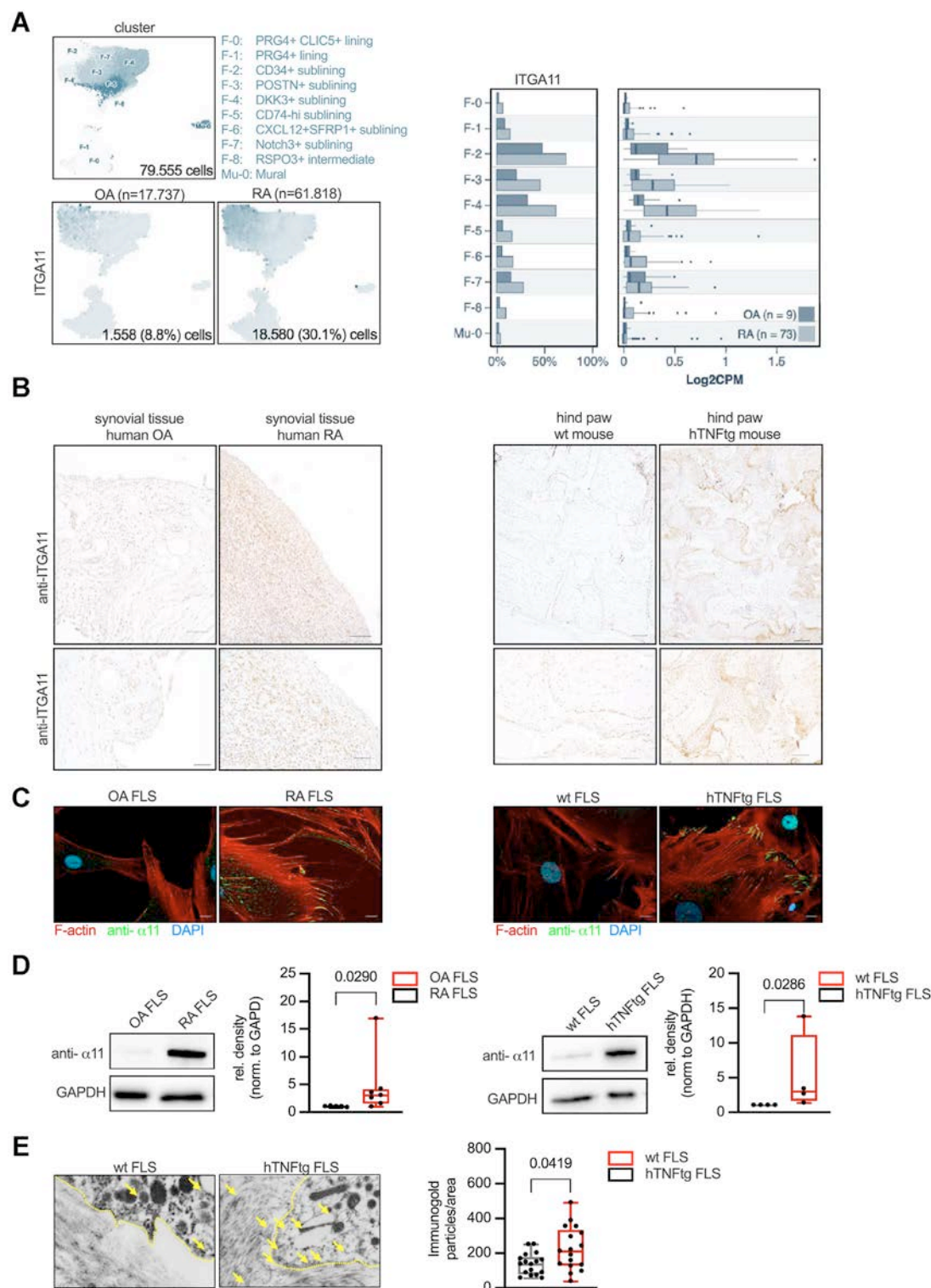


**Figure 1.** Expression of  $\alpha 11$  in inflammatory arthritis. (A) scRNAseq correlation of *Itga11* expression and specific FLS cluster within the synovial tissue of RA and OA patients using data of AMPRA phase II study. (B) Immunohistochemistry staining against  $\alpha 11$  visualised by DAB of human tissue from OA and RA patients (n = 3) and murine tissue from wt and *hTNFtg* mice (n = 4) (human tissue: large image scale bar 100  $\mu$ m; small image scale bar 50  $\mu$ m, murine tissue: large image scale bar 200  $\mu$ m; small image scale bar 100  $\mu$ m). (C) Immunofluorescence of human and murine FLS using specific antibodies against  $\alpha 11$  (green), F-actin was visualised by rhodamine-phalloidin (red) and nuclei by DAPI (blue) (scale bars = 10  $\mu$ m) (human FLS n = 3, murine FLS n > 5). (D) Western blot analyses of  $\alpha 11$  expression in FLS normalised to GAPDH (n  $\geq$  4). (E) Immunogold-labelling of  $\alpha 11$  in 3D organoids of wt and *hTNFtg* FLS cocultivated with cartilage hip caps derived from murine femoral heads, particle size 12 nm ( $P < .05$  determined by two-tailed Mann–Whitney U test, wt and *hTNFtg* FLS organoids n = 2, >8 sections each, bar graphs display all data points with SD).  $\alpha 11$ , alpha 11 integrin; AMPRA, Accelerating Medicines Partnership Rheumatoid Arthritis; DAB, 3,3'-diaminobenzidine; DAPI, 4',6-diamidino-2-phenylindole; F-actin, filamentous actin; FLS, fibroblast-like synoviocyte; GAPDH, glyceraldehyde 3-phosphate dehydrogenase; *hTNFtg*, human tumour necrosis factor transgenic; *Itga11*, integrin alpha 11; OA, osteoarthritis; RA, rheumatoid arthritis; scRNAseq, single-cell RNA sequencing; 3D, 3-dimensional; wt, wild-type.

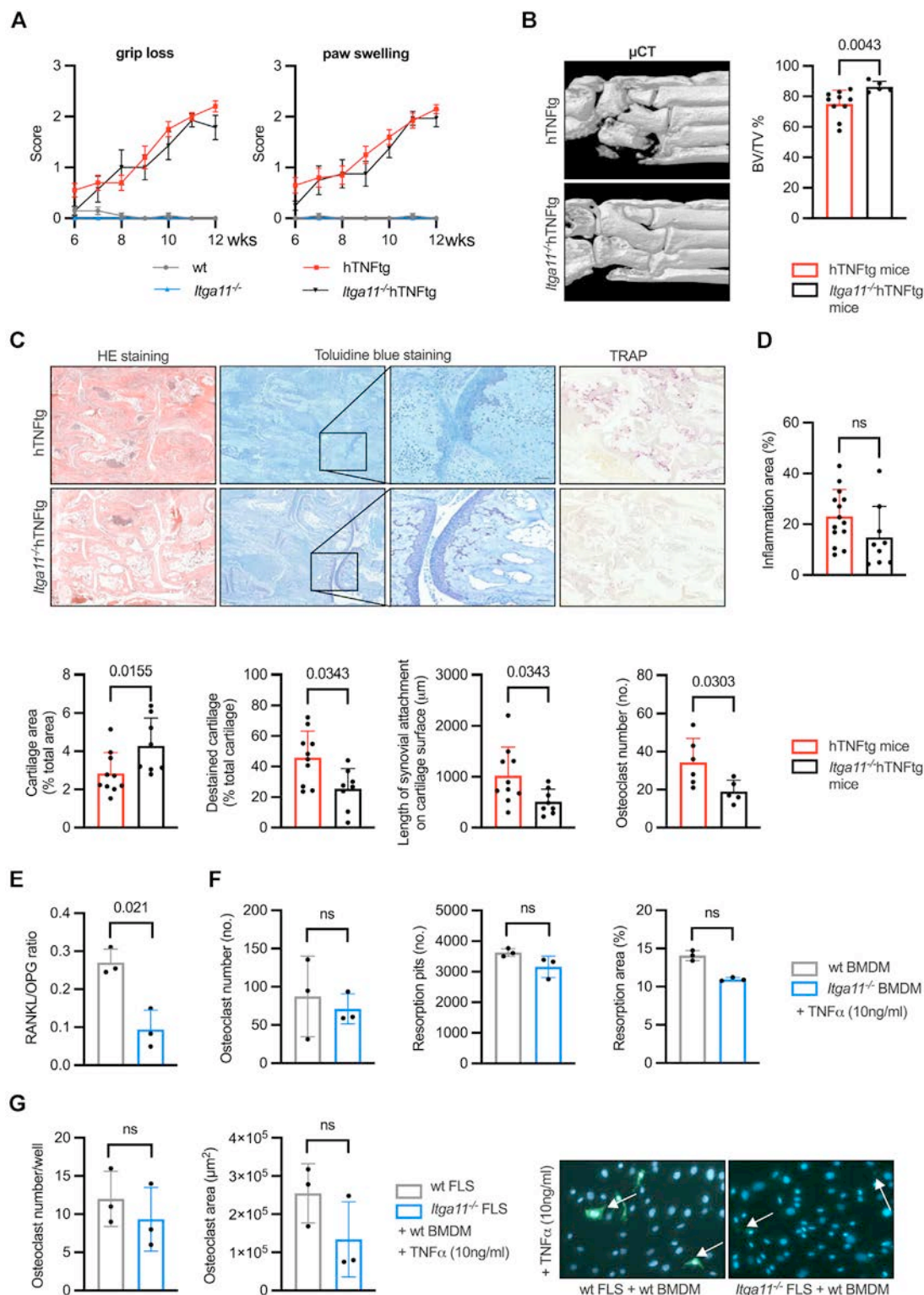


**Figure 2.** Effects of *Itga11* deficiency in *hTNFtg* mice. (A) Clinical scoring of grip strength and paw swelling as parameters for inflammatory arthritis were assessed weekly ( $n = 7$ ) as previously described [6]. *Itga11*<sup>-/-</sup>*hTNFtg* mice displayed reduced severity of symptoms in comparison to *hTNFtg* mice from weeks 9 to 12 (data are represented as means  $\pm$  SEM). (B)  $\mu$ CT imaging of hind paws showed significantly less bone destruction in *Itga11*<sup>-/-</sup>*hTNFtg* in comparison to *hTNFtg* mice at 12 weeks and quantification revealed higher residual bone volume ( $+6.98\%$  vs. *hTNFtg*,  $n \geq 5$ ,  $P < .01$ , two-tailed Mann–Whitney U test; bar graphs display all data points with SD). (C) H&E and Toluidine-blue staining as well as detection of TRAP-positive cells were performed in paraffin-embedded hind paws to visualise pathomorphological changes (scale bars: 200  $\mu$ m and 100  $\mu$ m). (D) Quantifications of Toluidine-blue staining and TRAP-positive cells in sections from *Itga11*<sup>-/-</sup>*hTNFtg* mice revealed significantly more cartilage area ( $+1.31\%$ ), less destained cartilage area ( $-19.36\%$ ), reduction in length of synovial attachment to cartilage surface ( $-392.1 \mu$ m) and decreased osteoclast numbers ( $-44.7\%$ ) compared to *hTNFtg* animals. No significant differences were found in the inflammation area ( $n \geq 7$ ,  $P < .05$ , two-tailed Mann–Whitney U test; bar graphs display all data points with SD). (E) Evaluation of RANK/OPG ratio, with significant decrease in *Itga11*<sup>-/-</sup> compared to wt FLS following TNF $\alpha$  stimulation (10 ng/mL) ( $-65.2\%$ ). (F) Functional osteoclast differentiation and resorption assays analysing osteoclast numbers, resorption pit numbers and resorption area ( $n = 3$ , n.s.). (G) Coculture assays of GFP-positive OC precursors and FLS after TNF $\alpha$  stimulation (10 ng/mL) ( $n = 3$ , n.s.). FLS, fibroblast-like synoviocyte; GFP, green fluorescent protein; H&E, hematoxylin and eosin; *hTNFtg*, human tumour necrosis factor transgenic; *Itga11*<sup>-/-</sup>, integrin alpha 11 knockout;  $\mu$ CT, microcomputed tomography; n.s., not significant; OC, osteoclast; OPG, osteoprotegerin; RANK, receptor activator of nuclear factor kappa-B; TNF $\alpha$ , tumour necrosis factor alpha; TRAP, tartrate-resistant acid phosphatase; wt, wild-type.

## Differences in cell morphology and functionality induced by *Itga11* deficiency

Due to the markedly attenuated arthritic phenotype linked to integrin  $\alpha 11$  deficiency, particularly concerning cartilage damage and FLS attachment, investigations were conducted to ascertain whether the absence of integrin  $\alpha 11$  affects the morphology of FLS or their adhesion ability. This involved conducting cell area measurements and adhesion assays on specific matrices. For this purpose, fibronectin and collagen I were chosen as different culture dish coatings to analyse the effects of integrin  $\alpha 11$  deficiency. A significant increase in cell size was observed in *hTNFtg* FLS compared to wt FLS, regardless of the coating used (fibronectin: +76% vs wt FLS; collagen I: +88.5% vs wt FLS). Additionally, these differences were also evident between *Itga11*<sup>-/-</sup>*hTNFtg* compared to *hTNFtg* FLS (fibronectin: +29.2% vs *hTNFtg* FLS; collagen I: 48.9% vs *hTNFtg* FLS). In contrast, no significant differences were detectable between *Itga11*<sup>-/-</sup> and wt FLS on either coating (Fig 3A and Supplementary Fig S3).

Adhesion assays using fibronectin and collagen I revealed no significant differences in adhesion properties between the genotypes or the coatings. However, coating with collagen I resulted in lower adhesion rates compared to those on fibronectin across all genotypes (Fig 3B).

The capability of *hTNFtg* FLS to secrete gelatinolytic enzymes in comparison to *Itga11*<sup>-/-</sup>*hTNFtg* was investigated by a degradation assay. For this purpose, FLS were incubated for 16 hours on gelatine labelled with a fluorophore. Afterwards, the degraded area, visualised by dark regions lacking light emission due to missing fluorophores, was quantified. The FLS expressing integrin  $\alpha 11$  exhibited an increased proteolytic activity resulting in a larger degraded lysis area compared to the respective integrin  $\alpha 11$  deficient counterpart (Fig 3C). Intriguingly, *Itga11*<sup>-/-</sup>*hTNFtg* FLS presented a significantly less pronounced breakdown of the gelatine compared to *hTNFtg* FLS (-21.18% vs *hTNFtg*). To determine whether the capacity in degrading gelatine of the *Itga11*<sup>-/-</sup>*hTNFtg* was reduced by a decrease in protease expression or secretion further experiments were performed. The concentration of MMP-9 was comparable in the supernatants of *hTNFtg* and *Itga11*<sup>-/-</sup>*hTNFtg* FLS (Fig 3C). Additionally, we performed zymography and found a TNF $\alpha$ -dependent increase in the levels of MMP-2 and MMP-9, albeit with no significant differences between the genotypes (Fig 3E). In contrast, the results of the MMP-3 ELISA showed a significant reduction in MMP-3 secretion in *Itga11*<sup>-/-</sup>*hTNFtg* FLS when compared to *hTNFtg* FLS (Fig 3D). Moreover, levels of membrane-bound MMP-14 were significantly higher in the area of pannus tissue of *hTNFtg* hind paws but not in *Itga11*<sup>-/-</sup>*hTNFtg* animals (Fig 3F, Supplementary Fig S2B). Subsequently, we analysed signalling pathways involved in integrin-mediated MMP regulation by stimulating FLS with TNF $\alpha$  over a defined time period. This analysis revealed a lack of ILK expression and ERK phosphorylation in *Itga11*<sup>-/-</sup> FLS, whereas expression levels in unstimulated controls were comparable to those in wild-type FLS (Fig 3G).

## DISCUSSION

Cells of mesenchymal origin have been shown to express integrin  $\alpha 11/\beta 1$ , including different types of fibroblasts [13,19]. Concerning CAFs, integrin  $\alpha 11/\beta 1$  has been related to their migration towards collagen and its remodelling in various tumour entities [25]. Several studies could also show that integrin  $\alpha 11/\beta 1$  expression might be linked to type 1 interferons, which are known to be involved in RA FLS transformation into

the characteristic aggressive phenotype triggering further joint inflammation and destruction [26–30].

Several studies illustrated the role of other integrins in RA FLS associated with increased matrix binding, migration, proliferation, and cartilage destruction [5,6,31]. However, not all aspects of the functional role of integrin  $\alpha 11/\beta 1$  in RA have been understood. Although there is evidence that collagen citrullination negatively influences FLS adhesion by decreasing the binding of integrin  $\alpha 11/\beta 1$  to arginine-containing motifs and potentially altering intracellular signalling in RA pathogenesis [32], analyses of integrin  $\alpha 11/\beta 1$  deficiency on joint destruction and disease progression have not been performed before.

Our study describes the effects of integrin  $\alpha 11$  subunit deficiency and joint destruction in patients with RA and the *hTNFtg* mouse model. We could show that  $\alpha 11$  was upregulated in both synovial tissues obtained from human RA patients as well as from *hTNFtg* mice compared to non-inflammatory controls such as OA patients and wt mice. In human RA samples, integrin  $\alpha 11$  was mainly located at the synovial sublining layer as shown by immunohistochemistry. Interestingly, this was also observed in mice, but in addition, distinct clusters of integrin  $\alpha 11$  were found in areas of pannus tissue adjacent to cartilage and bone at joint destruction sites. Immunofluorescence studies and Western blot analyses confirmed the elevated levels of integrin  $\alpha 11$  in human and murine FLS under arthritic conditions suggesting an inflammation-induced upregulation of  $\alpha 11$  in FLS. Supporting a role for integrin  $\alpha 11$  in FLS-mediated cartilage destruction, the subcellular expression pattern showed an integrin  $\alpha 11$  localisation primarily at sites of focal adhesion and cellular invasion visualised using electron microscopy. This was also demonstrated in our newly established *in vitro* 3D organoid coculture model, in which wt and *hTNFtg* FLS were embedded in Matrigel followed by insertion of murine femoral head cartilage explants in order to ensure interactions between the FLS and ECM components over a period of several days. Interestingly, only in *hTNFtg* FLS cellular protrusions deeply invading the cartilage were detectable by transmission electron microscopy. In addition, integrin  $\alpha 11$  could be located in clusters at these invasion sites whereas in wt FLS this expression pattern was completely absent.

In our *in vivo* studies, knockout of *Itga11* in the *hTNFtg* background resulted in the alleviation of the inflammatory arthritic phenotype as shown by clinical scoring,  $\mu$ CT imaging, and histological staining. Less cartilage destruction was observed in histomorphometric analyses of *Itga11*<sup>-/-</sup>*hTNFtg* mice in comparison to *hTNFtg* animals. In detail, higher residual cartilage area, reduced articular cartilage destaining, a surrogate for proteoglycan loss, were found in *Itga11*<sup>-/-</sup>*hTNFtg* mice. Additionally, significantly less synovial attachment to cartilage was found in these mice. Attachment of RA FLS to cartilage is a long-known hallmark feature in the induction of invasive cartilage destruction [4,33,34]. Similarly, the absence of the collagen-binding integrin  $\alpha 2/\beta 1$  in antigen-induced arthritis and *hTNFtg* mice, was shown to reduce the attachment of FLS to cartilage and overall cartilage destruction, providing an interesting functional link to the data obtained from the 3D coculture model [6].

Of note, *Itga11*<sup>-/-</sup>*hTNFtg* mice also displayed an increased BV/TV ratio in the hind paws, suggesting less bone resorption confirmed by histologic data and quantifications with reduced TRAP-positive cells compared to *hTNFtg* samples (Fig 2C,D). Under inflammatory conditions, FLS contribute indirectly to bone erosions [32], by mediating osteoclastogenesis through RANKL expression and activation of the RANK pathway [35,36], that is diminished by *Itga11* deficiency. Osteoclast



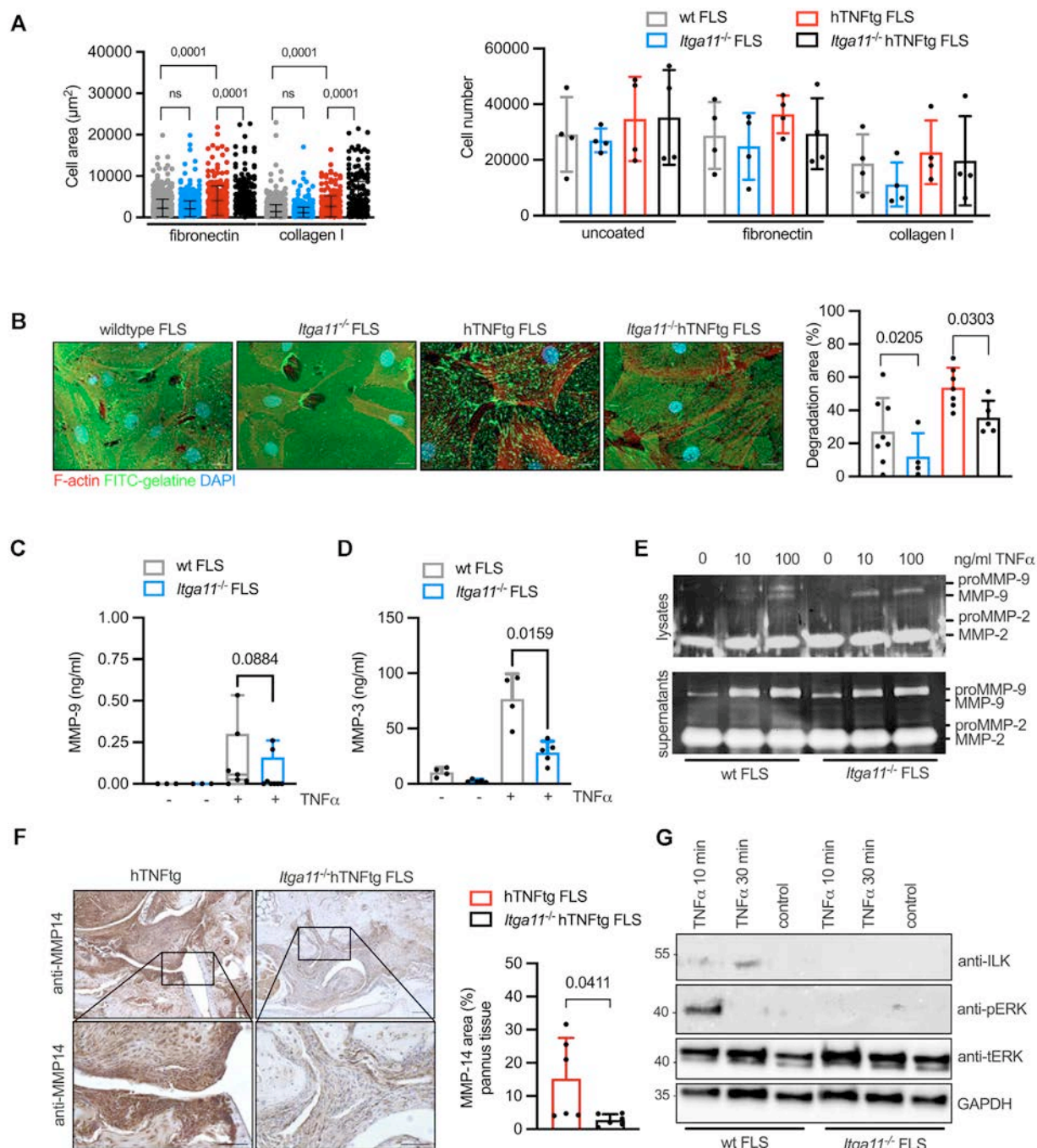


**Figure 3.** Arthritic FLS lacking *Itga11* show increased cell size and reduced degradation capacity. (A) Manhattan plot showing the cell size of FLS ( $n \geq 160$  cells pooled from at least 3 animals per genotype,  $P < .05$ , Two-way ANOVA). (B) Bar graphs of adherent cells after one hour of incubation on fibronectin (FN) and collagen I (COL I) ( $n = 4$ ,  $P > .05$ , two-way ANOVA; bar graphs display all data points with SD). (C) Degradation assay after 16-hour incubation of FLS on FITC-gelatin (green) visualised by rhodamine-phalloidin (red) for F-actin and DAPI (blue) for nuclei. Analysis of black areas corresponding to gelatin breakdown displays significant differences within the correlated genotypes ( $n \geq 4$ ,  $P < .05$ , two-tailed Mann–Whitney U test, bar graphs display all data points with SD, scale bar = 20  $\mu\text{m}$ ). (D) ELISA of MMP-9 secretion of hTNFtg and *Itga11*<sup>-/-</sup> hTNFtg FLS after 48 hours of incubation time ( $n \geq 4$ ,  $P < .05$ , two-tailed Mann–Whitney U test, bar graphs display all data points with SD). (E) ELISA of MMP-3 secretion of hTNFtg and *Itga11*<sup>-/-</sup> hTNFtg FLS after 48 hours of incubation time ( $n \geq 4$ ,  $P < .05$ , two-tailed Mann–Whitney U test, bar graphs display all data points with SD). (F) Zymography of supernatants and lysates of wt and *Itga11*<sup>-/-</sup> FLS following incubation with increasing concentrations of TNF $\alpha$  showing MMP-2 and MMP-9 levels and pro-forms, respectively ( $n = 2$ ). (G) Immunohistochemistry staining of MMP-14 from murine hind paws displayed less pronounced MMP-14 expression within the pannus tissue of *Itga11*<sup>-/-</sup> hTNFtg (-10.25%) compared to hTNFtg ( $n = 6$ ,  $P < .05$ , two-tailed Mann–Whitney U test, scale bar = 100  $\mu\text{m}$ , bar graphs display all data points with SD). (H) Signalling pathway activation analyses in wt and *Itga11*<sup>-/-</sup> FLS after 10 and 30 min TNF $\alpha$  stimulation (10 ng/mL) by WB using antibodies against ILK, pERK, tERK, and GAPDH. ANOVA, analysis of variance; COL I, collagen type I; DAPI, 4',6-diamidino-2-phenylindole; ELISA, enzyme-linked immunosorbent assay; F-actin, filamentous actin; FITC, fluorescein isothiocyanate; FLS, fibroblast-like synoviocyte; GAPDH, glyceraldehyde 3-phosphate dehydrogenase; hTNFtg, human tumor necrosis factor transgenic; ILK, integrin-linked kinase; *Itga11*<sup>-/-</sup>, integrin alpha 11 knockout; MMP, matrix metalloproteinase; pERK, phosphorylated extracellular signal-regulated kinase; tERK, total extracellular signal-regulated kinase; TNF $\alpha$ , tumor necrosis factor alpha; WB, Western blot; wt, wild-type.



differentiation and resorption assays revealed no significant differences between the genotypes following TNF $\alpha$  stimulation, confirming that the loss of  $\alpha$ 11 expression in the monocytic lineage does not affect osteoclastogenesis per se. However, coculture of *Itga11*-deficient FLS with BMDMs resulted in a slight reduction in osteoclast numbers and osteoclast area, warranting further investigation into a potential indirect, FLS-mediated role of integrin  $\alpha$ 11 in these processes. The significance of this interaction is underscored by research indicating that *Itga11* deletion from bone marrow stromal cells impairs osteogenesis in mice and humans [37].

Our *in vitro* analyses demonstrate that in particular in the inflammatory background, as is present in *hTNFtg* FLS, a lack of integrin  $\alpha$ 11 contributes significantly to the cell size and morphology. Furthermore, *Itga11*<sup>-/-</sup>*hTNFtg* FLS displayed a decreased ability to degrade gelatine after 16 hours of incubation compared to *hTNFtg* FLS implying that *hTNFtg* FLS lacking *Itga11* are less invasive. We have investigated the expression of several members of the MMP family of matrix degrading enzymes based on their involvement in distinct but partially overlapping signalling pathways and pathological processes relevant to RA. The reduced production of the MMP-3 and membrane-bound MMP-14 in *Itga11*<sup>-/-</sup>*hTNFtg* mice could be a further explanation for the diminished proteolytic activity and at the same time point relevant for mechanisms such as invadopodia formation and signalling pathways, particularly the ERK pathway.

These results align with findings in published reports regarding the functional effects of integrin  $\alpha$ 11 $\beta$ 1 beyond the context of RA [10,38,39]. In analogy to other collagen-binding integrins, integrin  $\alpha$ 11 $\beta$ 1 was found to mediate fibroblast adhesion, cell migration and collagen reorganisation as well as contraction and cell survival on collagen matrices leading to reduced proliferation and reduced adhesion of the cells to collagen in its absence. In summary, the available literature suggests that integrin  $\alpha$ 11 $\beta$ 1 mediates cell survival, adhesion to matrix, migration, and matrix remodelling in fibroblasts, which are all essential characteristics for joint destruction mediated by RA FLS in RA.

Integrins were previously proposed as a viable target for the treatment of RA [40,41]. This study shows that  $\alpha$ 11 $\beta$ 1 plays a role in RA and that its deficiency leads to a partial reduction of hallmark features of RA. Further studies into the precise molecular mechanisms of how  $\alpha$ 11 is regulated and how  $\alpha$ 11-mediated FLS interactions with components of the ECM contribute to and persist in the aggressive phenotype of RA FLS are required to evaluate the potential of integrin  $\alpha$ 11 $\beta$ 1 as a therapeutic target.

## CONCLUSION

The results of this study suggest that the collagen-binding integrin  $\alpha$ 11 $\beta$ 1 is upregulated in the context of RA and plays a role in adhesion and migration of fibroblasts on collagen and triggers cartilage degradation. The absence of  $\alpha$ 11 in the *hTNFtg* mouse model leads to an alleviated arthritis phenotype, marked by reduced bone erosion and cartilage destruction, making the molecule a potentially interesting target for future therapeutical intervention studies.

## Competing interests

All authors declare no competing interests.

## Acknowledgements

We thank George Kollias for providing us with *hTNFtg* mice and Amelie Franke and Nina Große-Coosmann for their zymography expertise.

## Contributors

ADG contributed, participated in all experiments, performed *in vitro* assays, and wrote the manuscript. AD evaluated histomorphological changes of murine sections and helped with the manuscript. AR performed *in vitro* assays and WB. SK performed osteoclast differentiation and resorption assays. DW performed and evaluated osteoclast cocultures. IZ analysed cell morphology analyses. KR performed *in vitro* assays. DB contributed to the experimental design. UH performed the transmission electron microscopy experiments. JMDSS carried out cocultures of cartilage hip caps and FLS. AK performed *in vitro* assays and WB. BE and DK contributed to the experimental design and performed zymography. CW participated in data interpretation. BD contributed to experimental design. NL supported with ICC and WB. DG made substantial contributions to data interpretation. TP and AK-P participated in all data analyses, directed the project, and revised the manuscript.

## Funding

This work was supported by the German Research Council (DFG) FOR2722 (BE: project ID 407239409 and TP/AKP: project ID 384170921) and the Norwegian Cancer Society grant (DG: KF-223052 and Nasjonalföreningen for folkehelsen project 16216).

## Patient consent for publication

Not applicable.

## Ethics approval

The ethics committees of the University Hospital Muenster approved all studies with human samples. All animal procedures were approved by the State Office for Nature, Environment and Consumer Affairs (Landesamt für Natur, Umwelt und Verbraucherschutz LANUV), Germany (reference numbers 8.87-51.05.2011.033, 84-02.04.2015.A511 and 2024-645-Grundantrag).

## Provenance and peer review

Not commissioned; externally peer reviewed.

## Supplementary materials

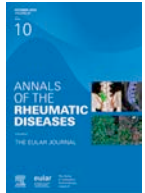
Supplementary material associated with this article can be found in the online version at [doi:10.1016/j.ard.2025.07.011](https://doi.org/10.1016/j.ard.2025.07.011).

## Orcid

Adelheid Korb-Pap: <http://orcid.org/0000-0002-0106-903X>

## REFERENCES

- [1] Lefèvre S, Knedla A, Tennie C, Kampmann A, Wunrau C, Dinser R, et al. Synovial fibroblasts spread rheumatoid arthritis to unaffected joints. *Nat Med* 2009;15(12):1414–20 Dec.
- [2] Fassbender HG, Simmling-Annefeld M. The potential aggressiveness of synovial tissue in rheumatoid arthritis. *J Pathol* 1983;139(3):399–406.
- [3] Mousavi MJ, Karami J, Aslani S, Tahmasebi MN, Vaziri AS, Jamshidi A, et al. Transformation of fibroblast-like synoviocytes in rheumatoid arthritis; from a friend to foe. *Auto Immun Highlights* 2021;12(1):3. Feb 5.
- [4] Korb-Pap A, Stratis A, Mühlenberg K, Niederreiter B, Hayer S, Echtermeyer F, et al. Early structural changes in cartilage and bone are required for the attachment and invasion of inflamed synovial tissue during destructive inflammatory arthritis. *Ann Rheum Dis* 2012;71(6):1004–11 Jun.
- [5] Rinaldi N, Schwarz-Eywill M, Weis D, Leppelmann-Jansen P, Lukoschek M, Keilholz U, et al. Increased expression of integrins on fibroblast-like synoviocytes from rheumatoid arthritis in vitro correlates with enhanced binding to extracellular matrix proteins. *Ann Rheum Dis* 1997;56(1):45–51 Jan 1.
- [6] Peters MA, Wendholt D, Strietholt S, Frank S, Pundt N, Korb-Pap A, et al. The loss of  $\alpha 2\beta 1$  integrin suppresses joint inflammation and cartilage destruction in mouse models of rheumatoid arthritis. *Arthritis Rheum* 2012;64(5):1359–68 May.
- [7] Tiger CF, Fougereuse F, Grundström G, Velling T, Gullberg D.  $\alpha 11\beta 1$  integrin is a receptor for interstitial collagens involved in cell migration and collagen reorganization on mesenchymal nonmuscle cells. *Dev Biol* 2001;237(1):116–29 Sep.
- [8] Zhang WM, Kämpylä J, Puranen JS, Knight CG, Tiger CF, Pentikäinen OT, et al.  $\alpha 11\beta 1$  integrin recognizes the GFOGER sequence in interstitial collagens. *J Biol Chem [Internet]* 2003;278(9):7270–7 Feb.
- [9] Gullberg D, Velling T, Sjöberg G, Sejersen T. Up-regulation of a novel integrin  $\alpha$ -chain ( $\alpha$ mt) on human fetal myotubes. *Dev Dyn* 1995;204(1):57–65 Sep.
- [10] Popova SN, Rodriguez-Sánchez B, Lidén A, Betsholtz C, Van Den Bos T, Gullberg D. The mesenchymal  $\alpha 11\beta 1$  integrin attenuates PDGF-BB-stimulated chemotaxis of embryonic fibroblasts on collagens. *Dev Biol* 2004;270(2):427–42 Jun 15.
- [11] Kaltz N, Ringe J, Holzwarth C, Charbord P, Niemeyer M, Jacobs VR, et al. Novel markers of mesenchymal stem cells defined by genome-wide gene expression analysis of stromal cells from different sources. *Exp Cell Res* 2010;316(16):2609–17 Oct 1.
- [12] Schulz JN, Zeltz C, Sørensen IW, Barczyk M, Carracedo S, Hallinger R, et al. Reduced granulation tissue and wound strength in the absence of  $\alpha 11\beta 1$  integrin. *J Invest Dermatol* 2015;135(5):1435–44 May.
- [13] Barczyk MM, Lu N, Popova SN, Bolstad AI, Gullberg D.  $\alpha 11\beta 1$  integrin-mediated MMP-13-dependent collagen lattice contraction by fibroblasts: evidence for integrin-coordinated collagen proteolysis. *J Cell Physiol* 2013;228(5):1108–19 May.
- [14] Navab R, Strumpf D, To C, Pasko E, Kim KS, Park CJ, et al. Integrin  $\alpha 11\beta 1$  regulates cancer stromal stiffness and promotes tumorigenicity and metastasis in non-small cell lung cancer. *Oncogene* 2016;35(15):1899–908 Apr 14.
- [15] Zeltz C, Kusche-Gullberg M, Heljasvaara R, Gullberg D. Novel roles for cooperating collagen receptor families in fibrotic niches. *Curr Opin Cell Biol* 2023;85:102273.
- [16] Zheng H, An M, Luo Y, Diao X, Zhong W, Pang M, et al. PDGFR $\alpha$  + ITGA11 + fibroblasts foster early-stage cancer lymphovascular invasion and lymphatic metastasis via ITGA11-SELE interplay. *Cancer Cell* 2024;42(4):682–700.e12.
- [17] Arnett FC, Edworthy SM, Bloch DA, Mcshane DJ, Fries JF, Cooper NS, et al. The American Rheumatism Association 1987 revised criteria for the classification of rheumatoid arthritis. *Arthritis Rheum* 1988;31(3):315–24.
- [18] Keffer J, Probert L, Cazlaris H, Georgopoulos S, Kaslaris E, Kioussis D, et al. Transgenic mice expressing human tumour necrosis factor: a predictive genetic model of arthritis. *EMBO J* 1991;10(13):4025–31 Dec.
- [19] Popova SN, Barczyk M, Tiger CF, Beertsen W, Zigrino P, Aszodi A, et al.  $\alpha 11\beta 1$  integrin-dependent regulation of periodontal ligament function in the erupting mouse incisor. *Mol Cell Biol* 2007;27(12):4306–16 Jun 1.
- [20] Redlich K, Hayer S, Ricci R, David JP, Tohidast-Akrad M, Kollias G, et al. Osteoclasts are essential for TNF- $\alpha$ -mediated joint destruction. *J Clin Invest* 2002;110(10):1419–27 Nov.
- [21] Beckmann D, Römer-Hillmann A, Krause A, Hansen U, Wehmeyer C, Intemann J, et al. Lasp1 regulates adherens junction dynamics and fibroblast transformation in destructive arthritis. *Nat Commun* 2021;12(1):3624. Jun 15.
- [22] Schindelin J, Arganda-Carreras I, Frise E, Kaynig V, Longair M, Pietzsch T, et al. Fiji: an open-source platform for biological-image analysis. *Nat Methods* 2012;9(7):676–82 Jul.
- [23] Zhang F, Jonsson AH, Nathan A, Millard N, Curtis M, Xiao Q, et al. Deconstruction of rheumatoid arthritis synovium defines inflammatory subtypes. *Nature* 2023;623(7987):616–24 Nov.
- [24] Lewis MJ, Barnes MR, Blighe K, Goldmann K, Rana S, Hackney JA, et al. Molecular portraits of early rheumatoid arthritis identify clinical and treatment response phenotypes. *Cell Rep* 2019;28(9) Aug 272455-70.e5.
- [25] Zeltz C, Alam J, Liu H, Erusappan PM, Hoschuetzky H, Molven A, et al.  $\alpha 11\beta 1$  integrin is induced in a subset of cancer-associated fibroblasts in desmoplastic tumor stroma and mediates in vitro cell migration. *Cancers* 2019;11(6):765. Jun 1.
- [26] Leomil Coelho LF, Mota BEF, Sales PCM, Marques JT, de Oliveira JG, Bonjardim CA, et al. Integrin  $\alpha 11$  is a novel type I interferon stimulated gene. *Cytokine* 2006;33(6):352–61 Mar 21.
- [27] Muskardin TLW, Niewold TB. Type I interferon in rheumatic diseases. *Nat Rev Rheumatol* 2018;14(4):214–28 Mar 21.
- [28] Bira Y, Tani K, Nishioka Y, Miyata J, Sato K, Hayashi A, et al. Transforming growth factor  $\beta$  stimulates rheumatoid synovial fibroblasts via the type II receptor. *Mod Rheumatol* 2005;15(2):108–13.
- [29] Lu N, Carracedo S, Ranta J, Heuchel R, Soininen R, Gullberg D. The human  $\alpha 11$  integrin promoter drives fibroblast-restricted expression in vivo and is regulated by TGF- $\beta 1$  in a Smad- and Sp1-dependent manner. *Matrix Biol* 2010;29(3):166–76 Apr.
- [30] Sipilä K, Haag S, Denessiouk K, Kämpylä J, Peters EC, Deneszyuk A, et al. Citrullination of collagen II affects integrin-mediated cell adhesion in a receptor-specific manner. *FASEB J* 2014;28:3758–68.
- [31] Lowin T, Straub RH. Integrins and their ligands in rheumatoid arthritis. *Arthritis Res Ther* 2011;13(5):244.
- [32] Zeltz C, Gullberg D. Post-translational modifications of integrin ligands as pathogenic mechanisms in disease. *Matrix Biol* 2014;40:5–9 Nov 1.
- [33] Müller-Ladner U, Kriegsmann J, Franklin BN, Matsumoto S, Geiler T, Gay RE, et al. Synovial fibroblasts of patients with rheumatoid arthritis attach to and invade normal human cartilage when engrafted into SCID mice. *Am J Pathol* 1996;149(5):1607–15 Nov.
- [34] Zeinert I, Schmidt L, Baar T, Gatto G, De Giuseppe A, Korb-Pap A, et al. Matrix-mediated activation of murine fibroblast-like synoviocytes. *Exp Cell Res* 2025;445(1):114408 Feb 1.
- [35] Tanaka S. Regulation of bone destruction in rheumatoid arthritis through RANKL-RANK pathways. *World J Orthop* 2013;4(1):1–6 Jan 18.
- [36] Takayanagi H, Oda H, Yamamoto S, Kawaguchi H, Tanaka S, Nishikawa T, et al. A new mechanism of bone destruction in rheumatoid arthritis: synovial fibroblasts induce osteoclastogenesis. *Biochem Biophys Res Commun* 1997;240(2):279–86 Nov 17.
- [37] Shen B, Vardy K, Hughes P, Tasdogan A, Zhao Z, Yue R, et al. Integrin  $\alpha 11$  is an osteoclast receptor and is required for the maintenance of adult skeletal bone mass. *eLife* 2019;8:e42274 Jan 11.
- [38] Popov C, Radic T, Haasters F, Prall WC, Aszodi A, Gullberg D, et al. Integrins  $\alpha 2\beta 1$  and  $\alpha 11\beta 1$  regulate the survival of mesenchymal stem cells on collagen I. *Cell Death Dis* 2011;2(7):e186. Jul 28.
- [39] Erusappan P, Alam J, Lu N, Zeltz C, Gullberg D. Integrin  $\alpha 11$  cytoplasmic tail is required for FAK activation to initiate 3D cell invasion and ERK-mediated cell proliferation. *Sci Rep* 2019;9(1):15283 Oct 25.
- [40] Hamidi H, Pietilä M, Ivaska J. The complexity of integrins in cancer and new scopes for therapeutic targeting. *Br J Cancer* 2016;115(9):1017–23 Oct.
- [41] Wilder RL. Integrin  $\alpha V\beta 3$  as a target for treatment of rheumatoid arthritis and related rheumatic diseases. *Ann Rheum Dis* 2002;61(Supplement 2):ii96–9 Nov 1.



## Psoriatic arthritis

# Highly selective tyrosine kinase 2 inhibition with zasocitinib (TAK-279) improves outcomes in patients with active psoriatic arthritis: a randomised phase 2b study

Alan Kivitz<sup>1,a</sup>, Xenofon Baraliakos<sup>2,a</sup>, Elena Tomaselli Muensterman<sup>3,\*</sup>, Arthur Kavanaugh<sup>4</sup>, Désirée van der Heijde<sup>5</sup>, Piotr A Klimiuk<sup>6</sup>, Guillermo Valenzuela<sup>7</sup>, Eva Dokoupilova<sup>8</sup>, Gabrielle Poirier<sup>9</sup>, Bhaskar Srivastava<sup>9</sup>, Sue Dasen<sup>9</sup>, Xinyan Zhang<sup>9</sup>, Ting Hong<sup>3</sup>, Jingjing Chen<sup>3</sup>, Peter Pothula<sup>3</sup>, Haoling Holly Weng<sup>10</sup>, Mona Trivedi<sup>3</sup>, Apinya Lertratanakul<sup>3</sup>

<sup>1</sup> Altoona Center for Clinical Research, Duncansville, PA, USA

<sup>2</sup> Rheumazentrum Ruhrgebiet Herne, Ruhr-University Bochum, Germany

<sup>3</sup> Takeda Development Center Americas, Inc, Cambridge, MA, USA

<sup>4</sup> Division of Rheumatology, Autoimmunity and Inflammation, University of California San Diego Medical School, San Diego, CA, USA

<sup>5</sup> Leiden University Medical Center, Leiden, Netherlands

<sup>6</sup> Department of Rheumatology and Internal Diseases, Medical University of Białystok and Inter Clinic Piotr Adrian Klimiuk, Białystok, Poland

<sup>7</sup> Integral Rheumatology & Immunology Specialists, Plantation, FL, USA

<sup>8</sup> Department of Pharmaceutical Technology, Faculty of Pharmacy, Masaryk University, Brno, Czech Republic and MEDICAL PLUS, s.r.o., Uherské Hradiště, Czech Republic

<sup>9</sup> Nimbus Discovery, Inc, Boston, MA, USA

<sup>10</sup> HW MedAdvice LLC, San Diego, CA, USA

## ARTICLE INFO

## Article history:

Received 31 January 2025

Received in revised form 29 May 2025

Accepted 30 May 2025

## ABSTRACT

**Objectives:** To assess the efficacy, safety, and tolerability of the investigational, oral, allosteric, highly selective, and potent tyrosine kinase 2 inhibitor zasocitinib (TAK-279) in patients with active psoriatic arthritis (PsA).

**Methods:** In this phase 2b, randomised, multicentre, double-blind, placebo-controlled, multiple-dose study, patients (≥18 years, with PsA symptoms for ≥6 months) received 30 mg, 15 mg, or 5 mg zasocitinib or placebo (1:1:1:1) once daily for 12 weeks, with a 4-week safety follow-up. The primary endpoint was American College of Rheumatology (ACR)20 response at week 12. Secondary efficacy endpoints included ACR50 response, ACR70 response, Psoriasis Area and Severity Index (PASI) 75 response among those with ≥3% body surface area at baseline and minimal disease activity (MDA) at week 12.

\*Correspondence to Dr Elena Tomaselli Muensterman.

E-mail address: [elena.muensterman@takeda.com](mailto:elena.muensterman@takeda.com) (E.T. Muensterman).

Affiliations for Bhaskar Srivastava, Sue Dasen, Xinyan Zhang, Mona Trivedi and Apinya Lertratanakul are reported at the time of the study.

Handling editor Josef S Smolen

<sup>a</sup> Dr Alan Kivitz and Dr Xenofon Baraliakos are cofirst authors.

<https://doi.org/10.1016/j.ard.2025.05.023>

**Results:** Overall, 290 patients (mean [SD] age, 49.9 [11.6] years; 57.2% female) received treatment. At week 12, 30 mg or 15 mg zasocitinib treatment resulted in significantly higher ACR20 responses (54.2%;  $P = .002$  and 53.3%;  $P = .002$ , respectively) than placebo (29.2%). A numerically higher number of ACR50 responses were achieved at week 12 with 30 mg (26.4%; nominal  $P = .009$ ) or 15 mg (26.7%; nominal  $P = .005$ ) zasocitinib than placebo (9.7%). In addition, 30 mg zasocitinib demonstrated a numerically higher number of ACR70 responses (13.9% versus 5.6%, respectively; nominal  $P = .158$ ), PASI 75 responses (45.7% versus 15.4%, respectively; nominal  $P = .002$ ), and MDA (29.2% versus 12.5%, respectively; nominal  $P = .014$ ) at week 12 versus placebo. In this small study of limited duration, most adverse events were mild/moderate and were more frequently observed in the higher dose group. In this small sample size, no new safety signals or clear dose-dependent laboratory parameter changes were identified.

**Conclusions:** Here, 30 mg and 15 mg zasocitinib demonstrated efficacy across core domains in patients with active PsA with no new safety signals. These findings will be confirmed in ongoing larger studies of longer duration.

#### WHAT IS ALREADY KNOWN ON THIS TOPIC

- Tyrosine kinase 2 (TYK2) is a critical mediator of the proinflammatory pathways fundamental to the pathophysiology of some immune-mediated inflammatory diseases (IMiDs) including psoriatic arthritis (PsA).
- Zasocitinib (TAK-279) is an investigational, oral, allosteric, highly selective, and potent TYK2 inhibitor being developed for the treatment of IMiDs, including PsA and plaque psoriasis.

#### WHAT THIS STUDY ADDS

- This phase 2b study reports a significantly higher proportion of patients achieved an American College of Rheumatology 20 response at week 12 with once daily 30 mg or 15 mg zasocitinib than with placebo.
- Treatment with 30 mg or 15 mg zasocitinib resulted in a numerically higher number of patients achieving low disease activity or remission across multiple composite measures of disease activity versus placebo, as early as week 12.
- Zasocitinib (30 mg) demonstrated numerically greater efficacy versus placebo across all skin efficacy endpoints assessed, with rapid onset evident as early as week 2.
- The safety and laboratory parameter profile of zasocitinib was consistent with previous studies in patients with plaque psoriasis, supporting the high selectivity of zasocitinib for TYK2.

#### HOW THIS STUDY MIGHT AFFECT RESEARCH, PRACTICE, OR POLICY

- The efficacy and tolerability of zasocitinib in patients with active PsA demonstrated in this phase 2b study could propel further long-term comparative clinical trials, potentially leading to new oral therapeutic options for PsA with an improved benefit-risk profile.
- The rapid and meaningful clinical responses observed with zasocitinib suggest that it could become a valuable oral treatment in clinical practice for patients with PsA, providing more options for individualised patient care.

## INTRODUCTION

Psoriatic arthritis (PsA) is a chronic, systemic, immune-mediated inflammatory disease (IMiD) with diverse manifestations [1–3]. Patients with PsA have a high overall burden of disease and are more likely to develop comorbidities, including obesity, cardiovascular disease, and hypertension, than matched controls, and also have a high prevalence of anxiety and depression [4,5]. The Group for Research and Assessment of Psoriasis and Psoriatic Arthritis (GRAPPA), in conjunction with Outcome Measures in Rheumatology (OMERACT), has developed a core set of domains for PsA aiming to standardise outcome measurements in randomised clinical trials and longitudinal

observational studies [6]. The goals of PsA treatment are to ameliorate signs and symptoms across multiple domains of the disease, improve physical function, prevent structural damage, and enhance health-related quality of life (HRQoL) [4,7].

Despite current treatment options, some patients with PsA continue to experience a high disease burden because available treatments may not adequately address all core PsA domains, while also not providing acceptable long-term safety [5,8]. This highlights the need for more comprehensive treatment strategies in patients without adequate disease control or with tolerability issues with current treatments and ultimately improvement in the long-term outcomes and quality of life of these patients with PsA. Tyrosine kinase 2 (TYK2) is a critical mediator of the activation of proinflammatory pathways fundamental to the pathophysiology of some IMiDs, including interleukin (IL)-12, IL-23, and type I interferon signalling [9,10]. Loss-of-function variants in the TYK2 gene have protective effects against psoriasis and other IMiDs without detrimental effects [11]. Therefore, TYK2 inhibition is being investigated for the treatment of IMiDs including PsA and plaque psoriasis [9,10,12,13].

Zasocitinib (TAK-279) is an investigational, oral, allosteric, highly selective, and potent TYK2 inhibitor being developed for the treatment of IMiDs, including PsA and plaque psoriasis [14]. Zasocitinib was designed to maximise specific TYK2 inhibition and prevent inhibition of Janus kinase (JAK)1, JAK2, and JAK3 [14]. *In vitro* studies of zasocitinib have demonstrated selectivity for the TYK2 Janus homology (JH)2 domain over the JAK JH1 domain, without affecting JAK-mediated signalling [14,15].

The efficacy, safety, and tolerability of zasocitinib were assessed in patients with moderate-to-severe plaque psoriasis in a phase 2b study (ClinicalTrials.gov: NCT04999839) [16]. The study met its primary endpoint (Psoriasis Area and Severity Index [PASI] 75 at week 12) at doses  $\geq 5$  mg, with about one-third of patients in the highest dose group (30 mg) achieving PASI 100 (complete skin clearance) at week 12. Zasocitinib was generally well tolerated with no clear dose-related treatment-emergent adverse events (TEAEs) observed.

The aim of this phase 2b, randomised, clinical trial was to assess the efficacy, safety, and tolerability of zasocitinib in patients with active PsA.

## METHODS

### Study design

This was a phase 2b, randomised, multicentre, double-blind, placebo-controlled, multiple-dose study (NCT05153148) [17]. Patients with active PsA from 45 centres across the USA ( $n = 17$ ),



Poland (n = 18), Germany (n = 4), and the Czech Republic (n = 6) were enrolled. Patients were randomised 1:1:1:1 to receive orally administered 5 mg, 15 mg, or 30 mg zasocitinib or an identical placebo once daily for 12 weeks, with an additional 4-week follow-up period for safety monitoring (Supplementary Fig S1). Randomisation occurred at the day –7 visit, and patients were stratified according to region (USA/Germany, Czech Republic/Poland) and whether they had received prior treatment with biologic disease-modifying antirheumatic drugs (bDMARDs) or any other disease-modifying antirheumatic drugs (DMARDs) except for azathioprine, chloroquine, ciclosporin, hydroxychloroquine, leflunomide, methotrexate, and sulfasalazine.

### Patient involvement

Patients and/or the public were not involved in the design, conduction, reporting, or dissemination of this research.

### Patient population

Eligible patients were aged  $\geq 18$  years with active PsA and a history of PsA symptoms for  $\geq 6$  months before screening (screening occurred  $\leq 30$  days before day 1 of the study), had  $\geq 3$  tender and  $\geq 3$  swollen joints, and met the Classification Criteria for Psoriatic Arthritis (CASPAR) [3]. Additionally, eligible patients had active PsA despite previous therapy with nonsteroidal anti-inflammatory drugs; DMARDs including azathioprine, chloroquine, ciclosporin, hydroxychloroquine, leflunomide, methotrexate, and sulfasalazine, or tumour necrosis factor inhibitors (TNFis). Alternatively, eligible patients were intolerant to these treatments. There was no limit to number or class of prior bDMARD exposure (excluding those with lack of response after 12 weeks of treatment or adverse events [AEs]) or minimum high-sensitivity C-reactive protein (hsCRP) requirement at baseline.

Patients were excluded if they previously had a lack of response to any therapeutic agent targeting IL-12, IL-17, and/or IL-23 (and/or received 1 of these therapies  $\leq 6$  months before baseline [day 1]) or to more than 1 TNFi or had any other disease that might confound evaluation of the benefit of zasocitinib.

Full inclusion and exclusion criteria are reported in the Supplementary Material.

The intent-to-treat analysis set included all patients who were randomised. The full analysis set comprised all patients who were randomised and received at least 1 dose of the study drug. The safety analysis set included all patients who were randomised and received at least one dose of the study drug, with patients analysed based on the actual treatment they received.

### Endpoints

#### Efficacy

The primary efficacy endpoint was the proportion of patients achieving an American College of Rheumatology (ACR)20 response at week 12. Secondary efficacy endpoints at week 12 were the proportion of patients achieving ACR50 response; proportion of patients achieving ACR70 response; proportion of patients achieving PASI 75 response among those with  $\geq 3\%$  body surface area (BSA) psoriatic involvement at baseline; proportion of patients achieving a Physician Global Assessment of Psoriasis (PGA-PsO) score of 0 (clear) or 1 (almost clear) and a  $\geq 2$ -point improvement from baseline; change from baseline in Physician Global Assessment (PGA) score (investigator-assessed change from baseline in the patients' overall disease status using a visual analogue scale [VAS]: 0 indicated 'asymptomatic' and 100 indicated 'very severe

symptoms'); proportion of patients achieving minimal disease activity (MDA) (the patient met at least 5 of the following criteria: (1) tender joint count [TJC]  $\leq 1$ ; (2) swollen joint count [SJC]  $\leq 1$ ; (3) PASI score  $\leq 1$  or  $\leq 3\%$  BSA; (4) pain VAS  $\leq 15$ ; (5) Patient Global Assessment [PtGA], using VAS score  $\leq 20$ ; (6) Health Assessment Questionnaire Disability Index [HAQ-DI] score  $\leq 0.5$ ; and (7) tender enthesal points, using the Leeds Enthesitis Index  $\leq 1$ ); change from baseline in Disease Activity Index for Psoriatic Arthritis (DAPSA) score; change from baseline in pain VAS; change from baseline in TJC (TJC68); change from baseline in SJC (SJC66); change from baseline in dactylitis count among patients who had dactylitis at baseline; and change from baseline in Leeds Enthesitis Index among patients who had enthesitis at baseline. The proportion of patients achieving low disease activity (LDA; DAPSA  $> 4$  and  $\leq 14$ ) and remission (REM; DAPSA  $\leq 4$ ) was assessed *post hoc*.

Patient-reported secondary efficacy endpoints assessed at week 12 were change from baseline in PtGA (patients rated their PsA using a VAS score in which 0 indicated 'very good, no symptoms' and 100 indicated 'very poor, severe symptoms') and HAQ-DI. Change from baseline to week 12 in Psoriatic Arthritis Disease Activity Score (PASDAS) was assessed as an exploratory endpoint. Further exploratory endpoints are reported in the Supplementary Material.

Additional skin endpoints analyses included least-squares mean (LSM) change from baseline in PASI response and the proportion of patients achieving PASI 90 or PASI 100 responses (among those with baseline BSA  $\geq 3\%$ ).

#### Safety and tolerability

The severity of AEs was classified using Common Terminology Criteria for Adverse Events (CTCAE v5.0) and AEs were coded using Medical Dictionary for Regulatory Activities Version 26.0 or higher. Safety and tolerability endpoints comprised the incidence of TEAEs, treatment-emergent serious AEs, TEAEs of special interest (TEAESIs), and changes in vital signs, clinical laboratory parameters, and proportion of patients with clinically relevant electrocardiogram findings and physical examinations. TEAESIs included cytopenia (Grade  $\geq 2$ ), elevation of creatine kinase (Grade  $\geq 3$ ), major adverse cardiovascular events (MACEs), thromboembolic events, gastrointestinal perforation, malignancies, infections, AEs of abnormal liver function tests, and renal dysfunction. Liver function tests included Hy's Law, hepatobiliary investigations, liver-related investigations, signs and symptoms (including increase in liver enzymes), and drug-related hepatic disorders (CTCAE grades considered).

#### Statistical analysis

A sample size of 260 patients (65 patients per group) was determined to provide 83% power to detect an ACR20 response rate of 55% in each zasocitinib treatment group at a significance level of  $\alpha = 0.05$  using a 2-sided chi-square test, assuming a placebo response rate of 30%. The sample size was calculated in nQuery 8.7 (Dotmatics) using a pooled variance estimate for difference of proportions.

Patient demographics and baseline clinical characteristics were summarised using descriptive statistics. Comparisons of the primary and binary secondary endpoints between each treatment group and placebo were made using a 2-sided Mantel–Haenszel test stratified by the randomisation stratification factors.

A fixed-sequence hierarchical testing approach was applied to the primary endpoint at a 2-sided significance level of 0.05 in the following prespecified order: 30 mg, 15 mg, and 5 mg zasocitinib versus placebo. If one comparison was found not to be significant,

all subsequent comparisons of lower doses could not be claimed and *P* values were considered nominal. No multiplicity adjustment was planned for other efficacy endpoints in this study, and nominal *P* values are presented where appropriate.

Patients who discontinued the study drug, used a prohibited medication expected to influence PsA clinical outcomes or with missing data for binary endpoints at week 12 were imputed as nonresponders.

Subgroup analysis for the primary efficacy endpoint was conducted using the same framework as the primary efficacy analysis. Longitudinal continuous secondary efficacy endpoints were analysed using a mixed model for repeated measures, in which the change from baseline was the dependent variable. The following were the fixed effects: treatment group, visit, treatment-by-visit interaction, and randomisation stratification factors. Baseline score was included as a covariate.

An analysis of the safety endpoints in the safety analysis set was conducted using descriptive statistics.

# Ethics

This study was performed in accordance with ethical principles originating from the Declaration of Helsinki, which are consistent with Good Clinical Practice and applicable regulatory requirements. Patients provided written, informed consent before starting the study. The clinical study protocol (and amendments), investigator brochure, samples of informed consent forms, and other study-related documents were reviewed and approved by institutional review boards or independent ethics committees of all study sites.

# RESULTS

## Patients

The study was conducted from January 6, 2022 to June 2, 2023. In total, 387 patients were screened for eligibility, of



**Figure 1.** Patient disposition. <sup>a</sup>Patients who received ≥1 dose of study drug (randomised patients).

whom 305 were randomised to 1 of the 3 active treatment groups or placebo (intention-to-treat population), 290 received at least one dose of study treatment (full analysis set and safety analysis set populations), and 245 (84.5%) completed 12 weeks of treatment. Reasons for study discontinuation before receiving the first study drug dose are summarised in Figure 1.

Patient demographics and disease characteristics at baseline were generally similar across groups, except for a higher proportion of females in the 30 mg (59.7%) and 15 mg (61.3%) groups than in the 5 mg (56.3%) and placebo groups (51.4%) (Table 1, Supplementary Table S1). Lower mean TJC (14.0 vs 18.0–18.5) and SJC (8.5 vs 9.0–9.7) were observed in the

zasocitinib 30 mg group compared with the other groups (Table 1). The mean (SD) age of patients was 49.9 (11.6) years, and the patient population was predominantly White (95.2%), female (57.2%), and from Eastern Europe (76.9%). At baseline, 62.4% of patients were receiving azathioprine, chloroquine, ciclosporin, hydroxychloroquine, leflunomide, methotrexate, and/or sulfasalazine; 57.6% of patients were receiving methotrexate. Approximately one-third of patients had received previous treatment with bDMARDs at baseline (31.0–33.3%), and the patient population contained both bDMARD-inadequate responders (reasons for discontinuing bDMARDs before the study included lack of efficacy, safety, and other; 7.2% of patients

**Table 1**  
**Baseline demographics and disease characteristics (FAS)**

	Placebo (N = 72)	Zasocitinib 5 mg once daily (N = 71)	Zasocitinib 15 mg once daily (N = 75)	Zasocitinib 30 mg once daily (N = 72)	Total (N = 290)
<b>Demographics</b>					
Age, y, mean (SD)	49.7 (11.8)	48.3 (10.4)	52.5 (12.2)	49.0 (11.5)	49.9 (11.6)
Female, n (%)	37 (51.4)	40 (56.3)	46 (61.3)	43 (59.7)	166 (57.2)
Race, n (%)					
American Indian/Alaskan Native	0	1 (1.4)	0	0	1 (0.3)
Asian	0	0	2 (2.7)	0	2 (0.7)
Black/African American	1 (1.4)	1 (1.4)	2 (2.7)	3 (4.2)	7 (2.4)
Native Hawaiian/Other Pacific Islander	0	1 (1.4)	0	0	1 (0.3)
White	69 (95.8)	67 (94.4)	71 (94.7)	69 (95.8)	276 (95.2)
Unknown	2 (2.8)	0	0	0	2 (0.7)
Not available	0	2 (2.8)	0	0	2 (0.7)
BMI, kg/m <sup>2</sup> , mean (SD)	29.5 (6.9)	29.8 (8.2)	30.0 (7.9)	30.2 (6.6)	29.9 (7.4)
Baseline DMARD treatment, <sup>a</sup> n (%)	43 (59.7)	45 (63.4)	46 (61.3)	47 (65.3)	181 (62.4)
Baseline methotrexate treatment, <sup>b</sup> n (%)	38 (52.8)	44 (62.0)	43 (57.3)	42 (58.3)	167 (57.6)
Baseline sulfasalazine treatment, n (%)	5 (6.9)	2 (2.8)	3 (4.0)	6 (8.3)	16 (5.5)
Baseline hydroxychloroquine, <sup>c</sup> treatment, n (%)	0	0	1 (1.3)	0	1 (0.3)
Baseline leflunomide treatment, n (%)	1 (1.4)	0	0	0	1 (0.3)
Previous DMARD treatment, <sup>a</sup> n (%)	33 (45.8)	35 (49.3)	32 (42.7)	31 (43.1)	131 (45.2)
Previous bDMARD treatment, n (%)	24 (33.3)	22 (31.0)	24 (32.0)	23 (31.9)	93 (32.1)
Previous TNF inhibitor use, n (%)	16 (22.2)	17 (23.9)	16 (21.3)	11 (15.3)	60 (20.7)
<b>Disease characteristics</b>					
Disease duration, y, median (range)	4.0 (0.2–30.9)	4.0 (0.5–37.7)	5.1 (0.1–24.3)	4.3 (0.1–30.7)	4.2 (0.1–37.7)
TJC, mean (SD)	18.5 (14.7)	18.4 (15.2)	18.0 (12.8)	14.0 (9.4)	17.2 (13.3)
SJC, mean (SD)	9.0 (6.1)	9.7 (6.6)	9.7 (6.1)	8.5 (5.7)	9.2 (6.1)
PGA, <sup>d</sup> mean (SD)	59.9 (16.0)	59.6 (17.4)	62.0 (15.1)	57.6 (19.8)	59.8 (17.1)
PtGA, <sup>e</sup> mean (SD)	55.3 (22.7)	52.2 (19.8)	59.6 (19.4)	53.2 (20.6)	55.1 (20.7)
Pain VAS, <sup>f</sup> mean (SD)	53.6 (24.1)	48.2 (21.0)	58.3 (20.9)	49.8 (22.4)	52.5 (22.4)
HAQ-DI, mean (SD)	1.1 (0.6)	1.1 (0.6)	1.2 (0.6)	1.1 (0.6)	1.1 (0.6)
hsCRP, mg/L, mean (SD)	5.8 (9.1)	8.1 (15.2)	6.4 (11.5)	7.6 (12.3)	7.0 (12.2)
Psoriasis BSA ≥3%, n (%)	39 (54.2)	39 (54.9)	46 (61.3)	46 (63.9)	170 (58.6)
PASI in patients with ≥3% BSA, <sup>g</sup> mean (SD)	7.1 (7.0)	5.9 (4.6)	5.4 (3.9)	6.5 (6.2)	6.2 (5.5)
Dactylitis count ≥1, n (%)	17 (23.6)	16 (22.5)	14 (18.7)	17 (23.6)	64 (22.1)
Dactylitis count, <sup>h</sup> mean (SD)	1.8 (1.2)	4.1 (4.3)	2.1 (1.8)	2.8 (3.7)	2.7 (3.1)
Enthesitis (LEI ≥1), n (%)	36 (50.0)	36 (50.7)	40 (53.3)	35 (48.6)	147 (50.7)
LEI absolute values, <sup>i</sup> mean (SD)	2.5 (1.5)	2.5 (1.7)	2.5 (1.5)	2.3 (1.4)	2.5 (1.5)

bDMARD, biologic disease-modifying antirheumatic drug; BMI, body mass index; BSA, body surface area; DMARD, disease-modifying antirheumatic drug; FAS, full analysis set; HAQ-DI, Health Assessment Questionnaire Disability Index; hsCRP, high-sensitivity C-reactive protein; LEI, Leeds Enthesitis Index; PASI, Psoriasis Area and Severity Index; PGA, Physician Global Assessment; PtGA, Patient Global Assessment; SJC, swollen joint count; TJC, tender joint count; TNF, tumour necrosis factor; VAS, visual analogue scale.

BMI was calculated based on the collected weight and height values. Disease duration (years) was calculated as (date of day 1 visit - date of initial disease diagnosis + 1)/365.25. Mean (SD) values were based on nonmissing observations at baseline for continuous endpoints.

<sup>a</sup> DMARDs included azathioprine, chloroquine, ciclosporin, hydroxychloroquine, leflunomide, methotrexate, and sulfasalazine.

<sup>b</sup> Includes medications coded to methotrexate or methotrexate sodium.

<sup>c</sup> Includes medications coded to hydroxychloroquine or hydroxychloroquine phosphate.

<sup>d</sup> The investigator or qualified subinvestigator assessed the patients' overall disease status by considering the signs, symptoms, and function of all components of joint and skin affected at the time of the visit. This overall status was then rated using a VAS: 0 indicated 'very good, asymptomatic and no limitation of normal activities' and 100 indicated 'very poor, very severe symptoms that were intolerable and inability to carry out all normal activities'.

<sup>e</sup> Patients rated their assessment of their PsA using a VAS: 0 indicated 'very good, no symptoms' and 100 indicated 'very poor, severe symptoms'.

<sup>f</sup> Patients rated their assessment of their PsA pain using a VAS: 0 indicated 'no pain' and 100 indicated 'most severe pain'.

<sup>g</sup> Placebo: n = 38; zasocitinib 5 mg: n = 39; zasocitinib 15 mg: n = 46; zasocitinib 30 mg: n = 46; total: n = 169. One patient in the placebo group had a missing PASI score at baseline.

<sup>h</sup> In patients with dactylitis count ≥1.

<sup>i</sup> In patients with LEI score ≥1.

reported lack of efficacy as the reason for discontinuing TNFis) and bDMARD-exposed patients in each treatment group. Among enrolled patients with coexistent psoriasis, the mean (SD) PASI score in those with  $\geq 3\%$  BSA ( $n = 169$  [58.3%]) was 6.2 (5.5). At baseline, 45.9% of patients had elevated hsCRP ( $\geq 3.0$  mg/L).

### Efficacy outcomes

The primary endpoint of this study was met, with a significantly higher proportion of patients (95% CI) receiving 30 mg or 15 mg zasocitinib achieving ACR20 response at week 12 (54.2% [42.7, 65.7] and 53.3% [42.0, 64.6], respectively; both  $P = .002$ ) than those receiving placebo (29.2% [18.7, 39.7]) (Fig 2). The ACR20 response rate for the 5 mg zasocitinib group was 35.2% (24.1, 46.3;  $P = .446$ ) at week 12. The proportions of patients achieving an ACR20 response in the 30 mg and 15 mg zasocitinib groups increased from baseline to week 12 (Supplementary Fig S2). Generally, numerically higher LSM improvements were observed at week 12 for the 30 mg or 15 mg zasocitinib groups across most of the ACR subcomponents versus placebo (nominal  $P = .003$ –.675) (Supplementary Table S2).

Data for all secondary endpoints are presented in Supplementary Table S2. ACR50 response rate (95% CI) at week 12 was numerically higher in the 30 mg (26.4% [16.2, 36.6], nominal  $P = .009$ ) and 15 mg (26.7% [16.7, 36.7], nominal  $P = .005$ ) zasocitinib groups versus the placebo (9.7% [2.9, 16.6]) group (Fig 2). A numerically higher proportion of patients achieved an ACR70 response (95% CI) in the zasocitinib 30 mg (13.9% [5.9, 21.9], nominal  $P = .158$ ) and 15 mg (14.7% [6.7, 22.7], nominal  $P = .101$ ) groups compared with placebo (5.6% [1.5, 13.6]). In addition, patients in the 30 mg and 15 mg zasocitinib groups reported numerically higher LSM (SE) reductions from baseline

in PtGA scores of PsA at week 12 when compared with placebo (placebo:  $-11.1$  [2.9]; 30 mg:  $-19.8$  [2.9], nominal  $P = .030$ ; 15 mg:  $-20.2$  [2.9], nominal  $P = .021$ ; Supplementary Table S2). Across all zasocitinib-treated groups, a numerical reduction from baseline in PGA was observed compared with placebo (nominal  $P = .003$ –.016) (Supplementary Table S2). Results for efficacy endpoint response rates stratified by geographic region are presented in Supplementary Table S3. Numerical differences between regions were observed in patients receiving zasocitinib 30 mg or placebo, with the Eastern Europe subgroup demonstrating generally higher response rates than those in the USA/Germany subgroup. The ACR20 treatment response differences versus placebo for the 30 mg, 15 mg, or 5 mg zasocitinib groups were 21.7%, 17.2%, and 2.6%, respectively, in the Eastern Europe subgroup and 29.7%, 39.1%, and 12.6%, respectively, in the USA/Germany subgroup, highlighting considerable variability in placebo response across regions.

Treatment with zasocitinib led to improvements in multiple skin disease activity endpoints, with the greatest improvements observed at the highest dose of zasocitinib. A numerically higher reduction in the LSM (SE) PASI score from baseline was observed in the 30 mg zasocitinib group compared with the placebo group as early as week 2 ( $-1.7$  [0.4] vs  $-0.7$  [0.4], nominal  $P = .023$ ) and persisted through week 12 (Fig 3A). There were numerical improvements in PASI 75 response rate (95% CI) at week 12 for all zasocitinib groups compared with placebo (placebo: 15.4% [4.1, 26.7]; 30 mg: 45.7% [31.3, 60.0], nominal  $P = .002$ ; 15 mg: 28.3% [15.2, 41.3], nominal  $P = .101$ ; 5 mg: 25.6% [11.9, 39.3], nominal  $P = .186$ ; Fig 3B). Consistent with PASI 75, similar trends were observed with higher threshold efficacy endpoints such as PASI 90 and PASI 100 (among patients with  $\geq 3\%$  BSA). Compared with placebo, a numerically higher proportion of patients achieved PASI 90 (37.0% versus

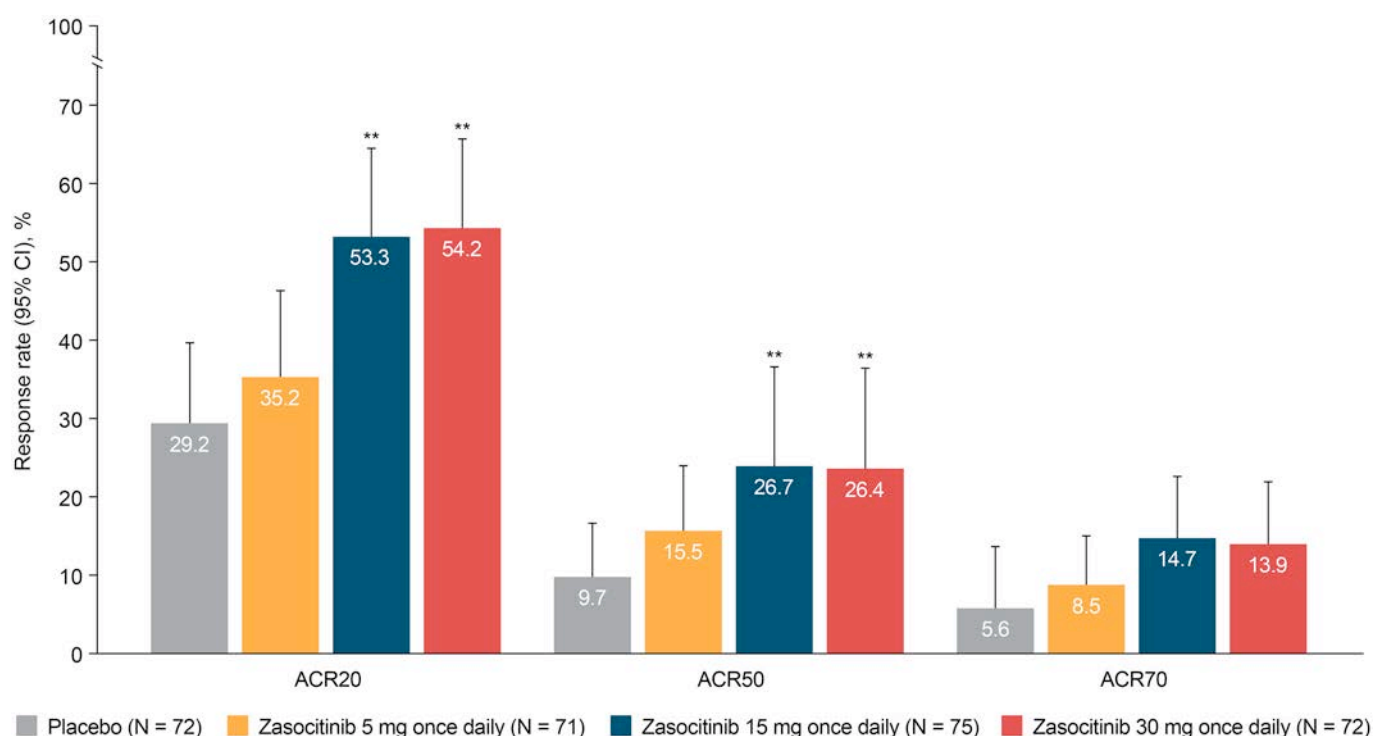


**Figure 2.** ACR20, ACR50, and ACR70 responses at week 12 (FAS).  $^{**}P \leq .01$ .  $P$  values for secondary endpoints (ACR50/70) are nominal. ACR20/50/70 are composite measures defined as improvements from baseline of  $\geq 20\%/50\%/70\%$  in both the number of tender joints and swollen joints and  $\geq 20\%/50\%/70\%$  improvement from baseline in 3 of the following 5 criteria: Patient Global Assessment of psoriatic arthritis, Physician Global Assessment of psoriatic arthritis, Patient Global Assessment of psoriatic arthritis pain, Health Assessment Questionnaire Disability Index, and high-sensitivity C-reactive protein. ACR, American College of Rheumatology; FAS, full analysis set.



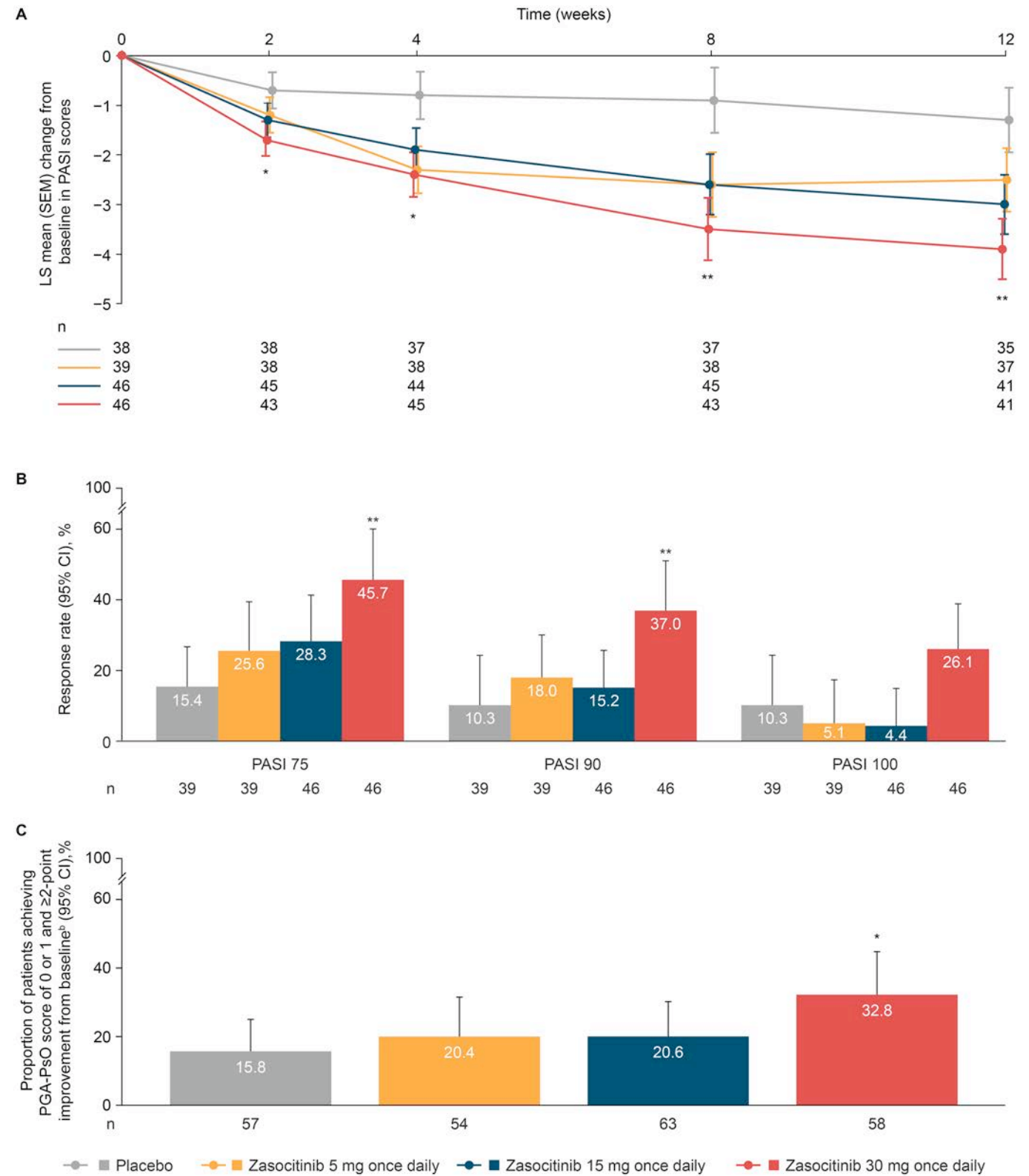


**Figure 3.** A, LS mean change from baseline to week 12 in PASI<sup>a</sup> scores. B, Week 12 PASI 75/90/100 response rates<sup>a</sup>. C, Patients achieving PGA-PsO score of 0 or 1 and ≥2-point improvement from baseline<sup>b</sup> (FAS). \* $P \leq .05$ ; \*\* $P \leq .01$ .  $P$  values for secondary endpoints are nominal. FAS included all randomised patients who received ≥1 dose of the study drug. Patients were included in the analysis as randomised. <sup>a</sup>In patients with ≥3% BSA involvement at baseline. <sup>b</sup>Among those with a PGA-PsO score ≥2 at baseline. BSA, body surface area; FAS, full analysis set; LS, least-squares; PASI, Psoriasis Area and Severity Index; PGA, Physician Global Assessment; PsO, psoriasis.

10.3%, nominal  $P = .0054$ ) and PASI 100 responses (26.1% versus 10.3%, nominal  $P = .0941$ ) at week 12 in the 30 mg zascotinib group (Fig 3B). Numerical improvements at week 12 were also observed in the proportions of patients (95% CI) achieving a PGA-PsO score of 0 or 1 and ≥2-point improvement from baseline in the 30 mg zascotinib group compared with placebo

(placebo: 15.8% [6.3, 25.3]; 30 mg: 32.8% [20.7, 44.8], nominal  $P = .034$ ; 15 mg: 20.6% [10.6, 30.6], nominal  $P = .466$ ; 5 mg: 20.4% [9.6, 31.1], nominal  $P = .540$ ; Fig 3C).

Treatment with zascotinib led to improvements in various composite outcomes and disease activity scores, such as MDA, DAPSA, and PASDAS. Numerically higher improvements in

MDA (95% CI) at week 12 were observed in patients treated with 30 mg or 15 mg zasocitinib than those treated with placebo (placebo: 12.5% [4.9, 20.1]; 30 mg: 29.2% [18.7, 39.7]; 15 mg: 28.0% [17.8, 38.2]; 5 mg: 18.3% [9.3, 27.3]; nominal  $P = .014$ ,  $P = .017$ , and  $P = .349$ , respectively, Fig 4A). Relative to placebo, the LS mean change from baseline in DAPSA score (SE) at week 12 was numerically higher in all zasocitinib-treated groups (placebo: −11.6 [1.9]; 30 mg: −16.8 [2.0]; 15 mg: −18.0 [1.9]; 5 mg, −15.3 [1.9]; nominal  $P = .056$ ,  $P = .018$ , and  $P = .167$ , respectively, Fig 4B). Numerically higher proportions of patients achieved LDA ( $4 < \text{DAPSA} \leq 14$  or  $1.9 < \text{PASDAS} < 3.2$ ) and REM ( $\text{DAPSA} \leq 4$  or  $\text{PASDAS} \leq 1.9$ ) at week 12 in the 30 mg and 15 mg zasocitinib groups than in the placebo group (Fig 4C,D).

### Safety outcomes

TEAEs occurred in 77.8%, 60.0%, 59.2%, and 54.2% of patients receiving zasocitinib 30 mg, 15 mg, 5 mg, or placebo, respectively. TEAEs leading to study treatment discontinuation occurred in 8.5% to 12.5% of patients in the zasocitinib treatment groups and 5.6% in the placebo group. The majority of TEAEs leading to study discontinuation were not considered related to the study drug, as assessed by the investigator. The most common TEAEs were nasopharyngitis (occurring in 9.7%, 9.3%, 8.5%, and 4.2% of patients receiving zasocitinib 30 mg, 15 mg, 5 mg, or placebo, respectively) and upper respiratory tract infections (occurring in 9.7%, 4.0%, 11.3%, and 2.8% of patients receiving zasocitinib 30 mg, 15 mg, 5 mg, or placebo, respectively) (Table 2). One patient in each of the placebo and 15 mg zasocitinib groups experienced a nondisseminated case of herpes zoster infection (Supplementary Table S4). Most TEAEs were Grade 1 or 2 in severity. In total, 22 (7.6%) patients reported at least one Grade 3 TEAE (placebo:  $n = 7$  [9.7%]; zasocitinib 30 mg:  $n = 3$  [4.2%]; 15 mg:  $n = 7$  [9.3%]; 5 mg:  $n = 5$  [7.0%]), and 1 patient in the 5 mg group had a Grade 4 coronary artery disease event that was considered unrelated to study treatment, as assessed by the investigator. A higher rate of transient, Grade 1 or 2 dermatological events was observed in the 30 mg and 15 mg zasocitinib groups than in the other groups. All dermatological events resolved within a mean of 34 days mostly without pharmacologic intervention, except for 1 patient who experienced a Grade 2 maculopapular rash considered related to the study drug, which resolved with medication. Acneiform dermatitis (Grade 2), related to the study drug, led to study discontinuation in one patient. No deaths were reported in the study.

In this small study of limited duration, no systemic opportunistic infection, MACES, thromboembolic event, gastrointestinal perforation, or malignancy TEAEs were observed in patients treated with zasocitinib (Supplementary Table S4). Rates of discontinuation due to TEAEs were numerically similar across study groups. One patient in each treatment group reported a treatment-related adverse event of special interest (AESI) that led to study drug discontinuation. Overall, serious infections were observed in 3 (1.0%) patients. These were observed in the 5 mg ( $n = 2$ ; cellulitis and respiratory tract infection) and 30 mg ( $n = 1$ ; pharyngitis) treatment groups, all of which resolved. According to the defined criteria in the study protocol, Grade  $\geq 2$  cytopenia and  $\geq 3$  elevations of creatine kinase were considered AESIs. Overall, 24 patients reported any cytopenia ( $n = 14$ ) or creatine kinase ( $n = 10$ ) related events. One patient in the placebo group reported both a leukopenia and lymphopenia event. Infrequent Grade  $\geq 3$  events of elevated creatine kinase (placebo:  $n = 1$ ; 5 mg:

$n = 2$ ; 15 mg:  $n = 3$ ; 30 mg:  $n = 0$ ) and Grade  $\geq 2$  cytopenia (placebo:  $n = 2$ ; 5 mg:  $n = 5$ ; 15 mg:  $n = 1$ ; 30 mg:  $n = 5$ ) were observed. Overall, 2 patients (one each in the 5 mg and 30 mg zasocitinib groups) with Grade  $\geq 2$  cytopenia reported clinical events with similar onset (lymphopenia and nasopharyngitis).

Laboratory parameters generally stayed within the normal range, with no clinically meaningful longitudinal changes observed across any groups and no clear dose-dependency in the zasocitinib groups. Shifts from baseline to postbaseline for haematology, lipid, and serum chemistry parameters were generally similar between all groups (Table 3). Over the study period, no notable differences in laboratory shifts and the frequency of Grade  $\geq 2$  changes between placebo and zasocitinib groups were observed (Supplementary Table S5). There were no clinically meaningful longitudinal changes throughout the 12-week study observed in haematology parameters (neutrophils, platelet counts, haemoglobin, lymphocytes), serum chemistry (creatinine kinase, alanine aminotransferase, aspartate aminotransferase, bilirubin, creatinine), and no clinically meaningful elevations in cholesterol or triglyceride levels were observed at week 12 (Fig 5, Supplementary Fig S3).

Evaluated vital signs included diastolic and systolic blood pressure, heart rate, temperature and body weight. No TEAEs related to these were reported.

### DISCUSSION

Zasocitinib is an investigational, oral, allosteric, highly selective, and potent TYK2 inhibitor in late-stage clinical development for the treatment of IMiDs. In this phase 2b trial of patients with active PsA, the primary endpoint (ACR20 response at week 12) was met in the 30 mg and 15 mg groups. Treatment with once daily 30 mg or 15 mg zasocitinib was associated with numerically greater improvements in musculoskeletal and skin signs and symptoms, as well as in patient-reported and physician-assessed outcomes, compared with placebo. Notably, the ACR20 response curve observed with 30 mg or 15 mg zasocitinib increased over 12 weeks; studies of a longer duration will help determine whether the ACR20 response will further increase with treatment with zasocitinib.

PsA prevalence is equal in male and female patients; however, female patients typically exhibit higher disease activity, greater disease burden, increased pain, and poorer physical function than male patients [18–21]. Additionally, female patients appear more likely than male patients to experience a poorer clinical response to bDMARDs (including IL-17 and IL-23 inhibitors) versus targeted synthetic DMARDs (tsDMARDs) [22]. This was an all-comers study design, and a greater proportion of patients in the 30 mg and 15 mg groups were female compared with the 5 mg and placebo groups. Treatment with 30 mg and 15 mg zasocitinib resulted in greater ACR20 responses than placebo, regardless of sex, supporting the hypothesis that female patients may exhibit improved outcomes versus bDMARD treatment with tsDMARD treatment like zasocitinib [23]; these findings would need to be validated in studies of a longer duration.

The patient population in this study was not selectively enriched for elevated hsCRP levels. As such, baseline mean hsCRP concentrations across the study groups were comparatively low compared with some hsCRP levels reported in other PsA clinical trials [24–26]. However, as hsCRP levels are not consistently elevated in active PsA, the hsCRP levels in this

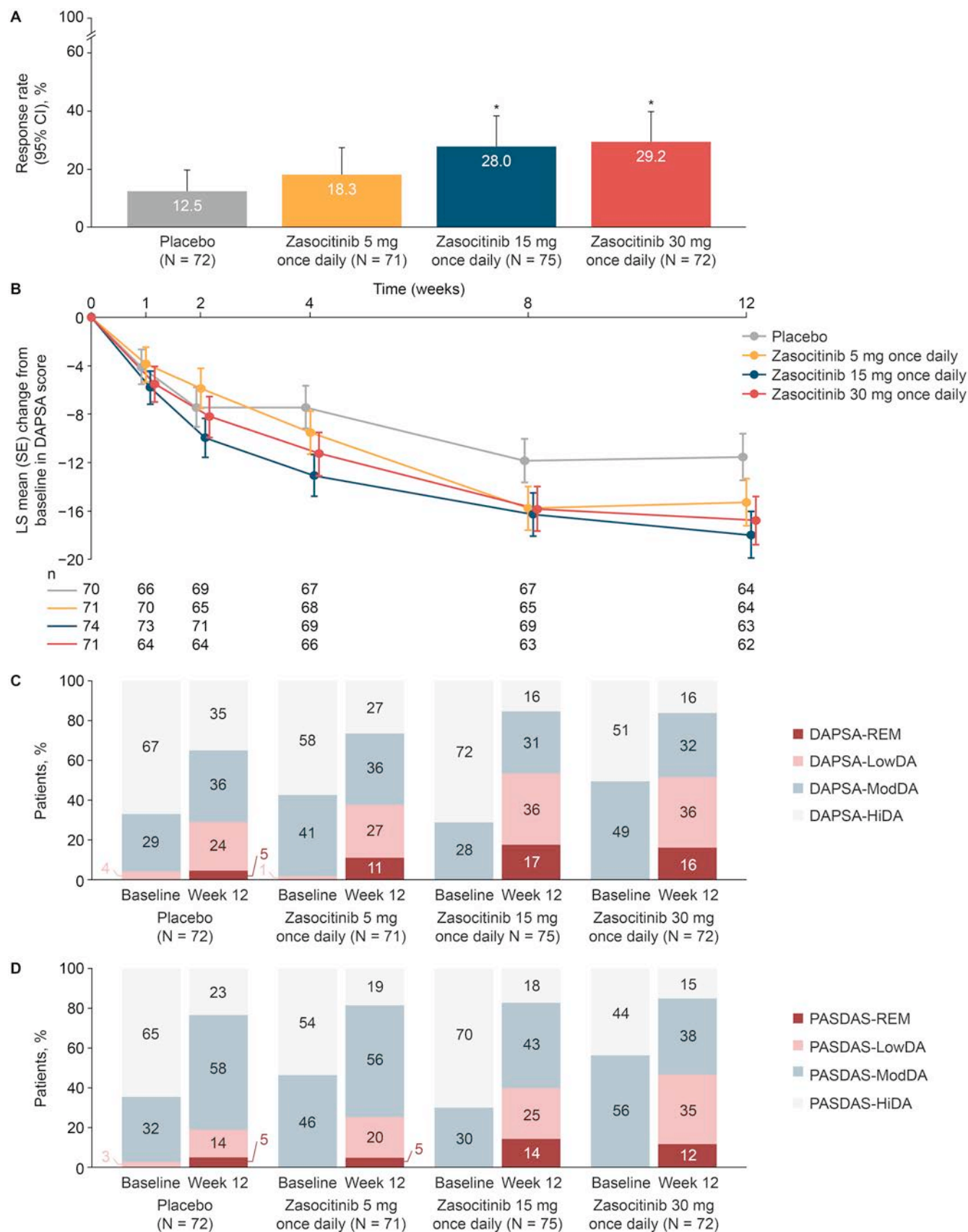


**Figure 4.** A, Proportion of patients achieving MDA. B, Change from baseline in DAPSA score. C, DAPSA state. D, PASDAS state at week 12 (FAS). \* $P \leq .05$ .  $P$  values in secondary endpoints are nominal. FAS included all randomised patients who received  $\geq 1$  dose of the study drug. Patients were included in the analysis as randomised. LDA =  $4 < \text{DAPSA} \leq 14$  or  $1.9 < \text{PASDAS} \leq 3.2$ ; REM =  $\text{DAPSA} \leq 4$  or  $\text{PASDAS} \leq 1.9$ . MDA is measured as the patient meeting  $\geq 5$  of the 7 criteria. The criteria are 1) tender joint count  $\leq 1$ ; 2) swollen joint count  $\leq 1$ ; 3) PASI score  $\leq 1$  or  $\leq 3\%$  BSA; 4) Patient Global Assessment of psoriatic arthritis pain, VAS  $\leq 15$ ; 5) Patient Global Assessment of psoriatic arthritis, VAS  $\leq 20$ ; 6) HAQ-DI score  $\leq 0.5$ ; 7) tender entheses points, using the LEI score  $\leq 1$ . DAPSA, Disease Activity in Psoriatic Arthritis; FAS, full analysis set; HiDA, high disease activity; LEI, Leeds Enthesitis Index; LowDA, low disease activity; LS, least squares; MDA, minimal disease activity; ModDA, moderate disease activity; PASDAS, Psoriatic Arthritis Disease Activity Score; PASI, Psoriasis Area and Severity Index; REM, remission; VAS, visual analogue scale.

**Table 2**  
**Number of patients with TEAEs, reported by treatment group (SAS)**

n (%) [#]	Placebo (N = 72)	Zasocitinib 5 mg once daily (N = 71)	Zasocitinib 15 mg once daily (N = 75)	Zasocitinib 30 mg once daily (N = 72)
Any TEAE	39 (54.2) [87]	42 (59.2) [88]	45 (60.0) [106]	56 (77.8) [135]
Drug-related TEAEs	11 (15.3) [13]	15 (21.1) [23]	20 (26.7) [49]	29 (40.3) [61]
TEAEs leading to study drug discontinuation	4 (5.6) [4]	6 (8.5) [6]	7 (9.3) [9]	9 (12.5) [11]
TEAEs leading to study discontinuation	1 (1.4) [1]	0	3 (4.0) [5]	5 (6.9) [5]
Serious TEAEs	4 (5.6) [4]	4 (5.6) [4]	3 (4.0) [3]	2 (2.8) [2]
Grade 3 or higher TEAE	7 (9.7) [8]	6 (8.5) [6]	7 (9.3) [9]	3 (4.2) [3]
TEAEs leading to death	0	0	0	0
TEAESI <sup>a</sup>	19 (26.4) [27]	33 (46.5) [43]	22 (29.3) [25]	38 (52.8) [50]
Serious infections	0	2 (2.8) [2]	0	1 (1.4) [1]
Most frequent TEAEs, n (%) <sup>b</sup>				
Nasopharyngitis	3 (4.2) [4]	6 (8.5) [6]	7 (9.3) [7]	7 (9.7) [7]
URTIs	2 (2.8) [3]	8 (11.3) [8]	3 (4.0) [4]	7 (9.7) [7]
Headache	3 (4.2) [3]	2 (2.8) [3]	6 (8.0) [6]	4 (5.6) [6]
Rash	0	3 (4.2) [4]	6 (8.0) [6]	4 (5.6) [4]
Blood CK increased <sup>c</sup>	3 (4.2) [3]	2 (2.8) [2]	4 (5.3) [4]	1 (1.4) [1]
Dermatitis acneiform	0	0	2 (2.7) [4]	6 (8.3) [7]
Psoriatic arthropathy	5 (6.9) [6]	0	2 (2.7) [2]	1 (1.4) [1]
Rash papular	0	1 (1.4) [1]	3 (4.0) [3]	4 (5.6) [4]
Aphthous ulcer	0	0	1 (1.3) [1]	6 (8.3) [7]
Dermatitis allergic	0	1 (1.4) [1]	1 (1.3) [1]	4 (5.6) [5]
Rash maculopapular	0	0	2 (2.7) [4]	4 (5.6) [5]
Any TEAEs related to cytopenia <sup>c</sup>				
Anaemia	0	0	0	3 (4.2) [4]
Leukopenia <sup>d</sup>	1 (1.4) [1]	1 (1.4) [1]	0	0
Lymphopenia <sup>d</sup>	2 (2.8) [2]	4 (5.6) [5]	1 (1.3) [2]	3 (4.2) [3]
Any rash-related TEAEs <sup>e</sup>	0	6 (8.5) [7]	11 (14.7) [13]	13 (18.1) [15]
Rash erythematous	0	2 (2.8) [2]	0	2 (2.8) [2]

AE, adverse event; CK, creatine kinase; CTCAE, Common Terminology Criteria for Adverse Events; MedDRA, Medical Dictionary for Regulatory Activities; SAS, safety analysis set; TEAE, treatment-emergent adverse event; TEAESI, treatment-emergent adverse event of special interest; URTI, upper respiratory tract infection.

AEs were coded using MedDRA Version 26.0 or higher. The SAS included all randomised patients who received  $\geq 1$  dose of the study drug. Patients were included in the analysis based on actual treatment received, regardless of the treatment group to which they were randomised.

[#] is the number of individual occurrences of the TEAE in that category.

<sup>a</sup> Patients with at least one TEAESI including laboratory TEAESIs.

<sup>b</sup> TEAEs occurring at  $>5\%$  in any treatment group, categorised by preferred term.

<sup>c</sup> According to the defined criteria in the study protocol, CTCAE Grade  $\geq 2$  cytopenia and  $\geq 3$  CK elevations are considered AESIs.

<sup>d</sup> One patient in the placebo group reported both a leukopenia and lymphopenia AE.

<sup>e</sup> Rash-related TEAEs included rash, rash papular, rash macropapular, and rash erythematous.

**Table 3**  
**Laboratory parameters: shift from baseline to postbaseline visits (SAS)**

	Placebo (N = 72)	Zasocitinib 5 mg once daily (N = 71)	Zasocitinib 15 mg once daily (N = 75)	Zasocitinib 30 mg once daily (N = 72)
Haematology: shift from normal to low values, n (%)				
Haemoglobin	10 (13.9)	9 (12.7)	10 (13.3)	10 (13.9)
Lymphocytes	7 (9.7)	8 (11.3)	3 (4.0)	6 (8.3)
Neutrophils	0 (0.0)	0 (0.0)	0 (0.0)	0 (0.0)
Platelets	1 (1.4)	3 (4.2)	0 (0.0)	1 (1.4)
Serum chemistry: shift from normal to high values, n (%)				
ALT	9 (12.5)	7 (9.9)	11 (14.7)	11 (15.3)
AST	6 (8.3)	3 (4.2)	10 (13.3)	9 (12.5)
CK	13 (18.1)	14 (19.7)	10 (13.3)	10 (13.9)
Creatinine	5 (6.9)	6 (8.5)	11 (14.7)	8 (11.1)
Lipids: shift from normal to high values, n (%)				
Cholesterol	8 (11.1)	7 (9.9)	11 (14.7)	8 (11.1)
LDL cholesterol	5 (6.9)	9 (12.7)	7 (9.3)	12 (16.7)
Triglycerides	5 (6.9)	3 (4.2)	6 (8.0)	5 (6.9)

ALT, alanine aminotransferase; AST, aspartate aminotransferase; CK, creatine kinase; LDL, low-density lipoprotein; SAS, safety analysis set.

Laboratory parameter values were categorised as low, normal, or high based on the reference range for each laboratory variable. Data represent laboratory parameter shifts in patients who had normal values at baseline. The lowest/highest postbaseline value for each laboratory parameter was used to determine whether patients had shifted from a normal to a low/high value.



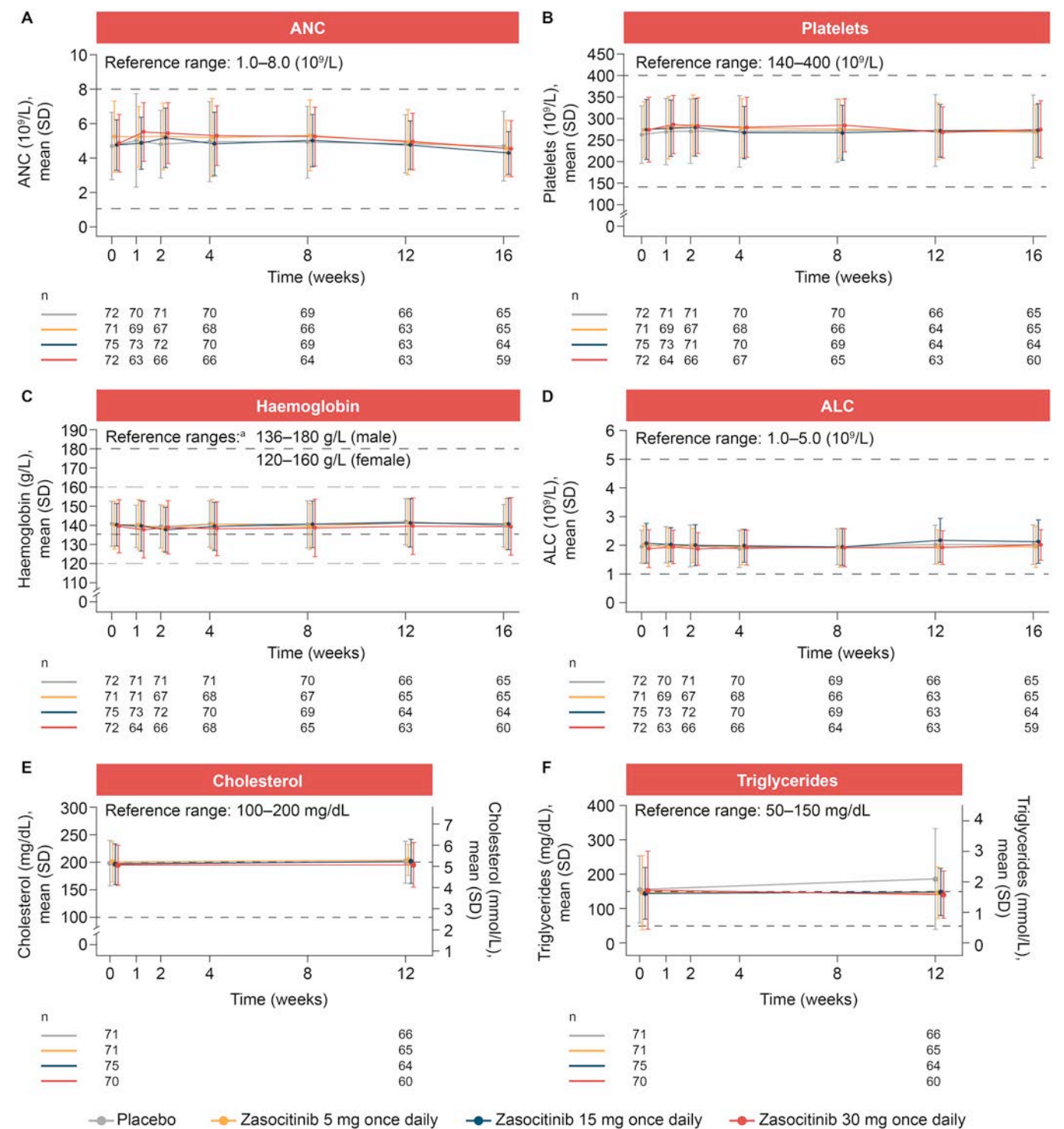


**Figure 5.** Key laboratory parameter changes over 16 weeks (SAS). A, Neutrophils. B, Platelets. C, Haemoglobin. D, Lymphocytes. E, Cholesterol. F, Triglycerides. Data are observed values from the safety analysis set and presented as mean  $\pm$  SD. Dashed lines represent upper and lower limits of the normal range for each parameter. <sup>a</sup>For graphs with 4 dashed lines, the black lines represent the male limits, and the grey lines represent the female limits. ALC, absolute lymphocyte count; ANC, absolute neutrophil count; SAS, safety analysis set.

study may be more reflective of a real-world PsA population [27].

Skin disease is one of the core domains of PsA [28,29], and it is estimated that as many as 82% of patients with PsA have coexisting psoriasis [30]. Patients with PsA and psoriasis exhibit worse physical function and higher disease activity scores, utilise more health care resources, and report greater impairment on HRQoL than those with PsA or psoriasis alone [31–35]. However, treatment with zasocitinib demonstrated early and

greater improvements versus placebo across skin efficacy end-points. Differences in PASI scores were observed between patients receiving zasocitinib 30 mg and placebo as early as week 2. At week 12, 26.1% of patients with skin involvement treated with 30 mg of zasocitinib experienced complete skin clearance (PASI 100), and 32.8% achieved clear or almost clear skin (PGA-PsO score of 0 or 1 with a  $\geq 2$ -point improvement from baseline). The skin activity response data from this study are consistent with those observed in the phase 2b study of

zasocitinib in moderate-to-severe plaque psoriasis, in which one-third of patients receiving 30 mg zasocitinib achieved complete skin clearance after 12 weeks of treatment [16].

Several guidelines for PsA treatment support LDA and REM as treat-to-target goals [4,7,36,37]. MDA is a PsA specific composite measure, and achievement is shown to correspond with quality of life and a level of symptoms that are acceptable to patients [37]. Treatment with 30 mg and 15 mg zasocitinib consistently ameliorated disease activity, assessed by achievement of MDA and improvement in DAPSA and PASDAS. By week 12, 30 mg or 15 mg zasocitinib treatment resulted in higher rates of patients achieving LDA or REM versus placebo across multiple disease activity composite instruments.

Zasocitinib was generally well tolerated at all doses, with a low proportion of patients discontinuing the study owing to TEAEs across all groups. However, the number of discontinuations was numerically higher in the zasocitinib groups than the placebo group. These findings were consistent with those observed in healthy volunteers and patients with plaque psoriasis [16,38]. In the present study, an increase in dermatological TEAEs was observed with increasing doses of zasocitinib. However, these were generally mild to moderate in severity and resolved within a mean duration of 34 days mostly without pharmacological intervention; only 1 event led to study drug discontinuation. Few serious infections were observed. MACEs, systemic opportunistic infections, thromboembolic events, and malignancies were not observed in any zasocitinib group; larger studies will be needed to confirm the safety profile of zasocitinib. Over the study period, zasocitinib did not result in any dose-dependent clinically meaningful changes in the laboratory parameters, and there were no notable differences in laboratory shifts or frequency of Grade  $\geq 2$  changes between placebo and treatment groups. No correlations between laboratory changes associated with JAK1, JAK2, and JAK3 inhibitors (eg, cytopenia, renal and liver enzyme elevations, and lipid elevations) and zasocitinib were observed, consistent with the high selectivity of zasocitinib for TYK2.

This study had some limitations, including a potential lack of statistical power and a lack of hierarchical testing approach for secondary and exploratory endpoints, owing to the small sample size. This was particularly evident for endpoints with impacts on domains only present in subsets of patients, such as dactylitis and enthesitis. Larger studies are required to further assess the effect of zasocitinib on these disease domains. As shown by the lack of a plateau observed in ACR20 response at week 12, longer studies are also required to determine the timing of the maximal response associated with zasocitinib treatment across various endpoints representing the core domains of the disease. Finally, patient recruitment focused on 4 countries, with the majority of patients being recruited from Eastern Europe. The numerical differences in ACR20 responses for the placebo group between regions in this study are not uncommon and have also been observed between other randomised, placebo-controlled PsA trials; such variability in response may be due to several factors including differences in csDMARD treatment, publication year, and number of study sites [39].

In conclusion, 30 mg and 15 mg zasocitinib demonstrated efficacy versus placebo across key PsA domains (musculoskeletal and skin activity), with the highest dose consistently providing numerically superior responses on skin activity measures. Safety results were consistent with data previously reported in patients with plaque psoriasis and healthy volunteers [16,38]. The lack of safety events associated with JAK1, JAK2, or JAK3 inhibition is reflective of the highly selective TYK2 inhibition of

zasocitinib. These results highlight the potential of zasocitinib as a new oral therapeutic option in patients with active PsA. Consequently, phase 3 studies are ongoing (NCT06671483 and NCT06671496) to explore its full potential and to confirm these preliminary results in larger, more diverse patient populations, aiming to improve management and outcomes for patients with PsA.

## Competing interests

A Kivitz has received consulting fees from Fresenius Kabi, Genzyme, Gilead, Grunenthal, GSK, Horizon, Janssen, Pfizer, Selecta Biosciences, SynAct Pharma, and Takeda; has received payments or fees for lectures, presentations, speakers bureaus, manuscript writing or educational events from AbbVie, Amgen, Eli Lilly, GSK, Pfizer, and UCB; has been part of a board or advisory board for ChemoCentryx, Horizon Therapeutics, Janssen, Novartis, Princeton Biopartners, and UCB; and has stock or stock options in Amgen, Gilead, GSK, Novartis, and Pfizer. XB has received research grants and been a consultant and member of advisory boards for AbbVie, Alfasigma, Amgen, Bristol Myers Squibb, Celltrion, Cestas, Eli Lilly, Galapagos, Janssen, Moonlake Immunotherapies, Novartis, Pfizer, Roche, Sandoz, Springer, STADA, Takeda, UCB, and Zuellig Pharma. Non-commercial disclosures: ASAS President and EULAR President-Elect. ETM, TH, JC, and PP are employees and equity holders of Takeda Development Center Americas, Inc. A Kavanaugh has received consulting fees from AbbVie, Amgen, Eli Lilly, Janssen, Novartis, Pfizer, Takeda, and UCB. DvdH has received consulting fees from AbbVie, Alfasigma, Argenx, Bristol Myers Squibb, Eli Lilly, Grey-Wolf Therapeutics, Janssen, Novartis, Pfizer, Takeda, and UCB Pharma and is an Associate Editor for *Annals of the Rheumatic Diseases*, an Editorial Board member for *The Journal of Rheumatology* and *RMD Open*, an advisor for the Assessment of Spondyloarthritis International Society, and Director of Imaging Rheumatology B.V. PAK has no potential conflicts of interest to disclose. GV has received grant/research support from Mallinckrodt Pharmaceuticals and has received consulting fees from, or been involved in, speakers bureaus for AbbVie, Alexion, Amgen, AstraZeneca, Bristol Myers Squibb, Boehringer Ingelheim, Celgene, Centocor, Eli Lilly, Esaote, Exagen, Genentech, Gilead, Global Health Living, Horizon Therapeutics, Image Analysis Group, Janssen, Mallinckrodt Pharmaceuticals, Merck, Novartis, Pfizer, Pharmacia, Radius, Regeneron, Sandoz, Sanofi, Takeda, and UCB. ED has received grant/research support from AbbVie, UCB Biopharma SPRL, Eli Lilly, Galapagos, Gilead, GSK, Hexal AG, Janssen, Nimbus Lakshmi, Inc, Novartis, Pfizer, Sanofi, and Samsung. GP is an employee and equity holder of Nimbus\*. BS, SD, and XZ were employees and equity holders of Nimbus\* at the time of the study. HHW is an employee of HW MedAdvice, LLC and received consultancy fees in relation to the conduct of this study. MT and AL were employees and equity holders of Takeda Development Center Americas, Inc, at the time of the study. \*Nimbus refers to the group of entities including Nimbus Therapeutics, LLC; Nimbus Discovery, Inc; and Nimbus Lakshmi, Inc. (NB: Nimbus Lakshmi, Inc was acquired by Takeda Pharmaceuticals in February 2023). A video abstract of this article can be found in the Supplementary Materials.

## CRediT authorship contribution statement

**Alan Kivitz:** Writing – review & editing, Visualization, Supervision, Resources, Investigation. **Xenofon Baraliakos:** Writing – review & editing, Supervision. **Elena Tomaselli**

**Muensterman:** Writing – review & editing, Writing – original draft, Formal analysis, Data curation. **Arthur Kavanaugh:** Writing – review & editing, Conceptualization. **Désirée van der Heijde:** Writing – review & editing, Methodology, Conceptualization. **Piotr A Klimiuk:** Writing – review & editing, Investigation, Data curation. **Guillermo Valenzuela:** Writing – review & editing, Investigation, Conceptualization. **Eva Dokoupilova:** Writing – review & editing, Investigation, Data curation. **Gabrielle Poirier:** Supervision, Project administration. **Bhaskar Srivastava:** Writing – review & editing, Supervision, Methodology, Investigation, Conceptualization. **Sue Dasen:** Writing – review & editing, Supervision, Methodology, Data curation, Conceptualization. **Xinyan Zhang:** Methodology, Formal analysis, Data curation, Conceptualization. **Ting Hong:** Writing – review & editing, Methodology, Formal analysis, Data curation. **Jingjing Chen:** Writing – review & editing, Methodology, Formal analysis, Data curation. **Peter Pothula:** Writing – review & editing, Writing – original draft, Formal analysis, Data curation. **Haoling Holly Weng:** Writing – review & editing, Supervision, Methodology, Formal analysis, Conceptualization. **Mona Trivedi:** Writing – review & editing, Writing – original draft, Visualization, Supervision. **Apinya Lertratana-kul:** Writing – review & editing, Writing – original draft, Visualization, Supervision.

## Acknowledgements

The authors would like to thank Bharani Guttikonda, Deepak Khambadakone, Lily Xu, and Michael Williams for their programming support during this study.

## Funding

This study was funded by Nimbus Discovery, Inc, and Takeda Development Center Americas, Inc. Nimbus refers to the group of entities including Nimbus Therapeutics, LLC; Nimbus Discovery, Inc; and Nimbus Lakshmi, Inc (NB: Nimbus Lakshmi, Inc was acquired by Takeda Pharmaceuticals in February 2023). Medical writing support was provided by Alexandra Smith, MSc, of Oxford PharmaGenesis, Oxford, UK, under the direction of the authors, and was funded by Takeda Development Center Americas, Inc. Technical and editing support for the author video was provided by Oxford PharmaGenesis, Oxford, UK, and was funded by Takeda Development Center Americas, Inc.

## Patient consent for publication

Not applicable.

## Ethics approval

This study was performed in accordance with ethical principles originating from the Declaration of Helsinki, which are consistent with Good Clinical Practice and applicable regulatory requirements. Patients provided written, informed consent before starting the study. The clinical study protocol (and amendments), investigator brochure, samples of informed consent forms and other study-related documents were reviewed and approved by institutional review boards or independent ethics committees of all study sites.

## Provenance and peer review

Not commissioned; externally peer reviewed.

## Data availability statement

The data sets, including the redacted study protocol, redacted statistical analysis plan, and individual participants' data supporting the results reported in this article, will be made available within 3 months from initial request to researchers who provide a methodologically sound proposal. The data will be provided after its deidentification, in compliance with applicable privacy laws, data protection, and requirements for consent and anonymisation.

## Previous publications

1. ACR Convergence (2023) American College of Rheumatology 2023 Annual Scientific Meeting. Kivitz A, et al. Efficacy and safety outcomes of TAK-279, a selective oral tyrosine kinase 2 (TYK2) inhibitor, from a randomized, double-blind, placebo-controlled phase 2b trial in patients with active psoriatic arthritis. Poster presentation: 10–15 November, 2023.
2. IDEOM Annual Meeting (2024) International Dermatology Outcome Measures Annual Meeting. Winkelman W, et al. Efficacy and safety outcomes of TAK-279, a selective oral tyrosine kinase 2 (TYK2) inhibitor, from a randomized, double-blind, placebo-controlled phase 2b trial in patients with active psoriatic arthritis. Poster presentation: 4–6 April, 2024.
3. JCR Meeting (2024) Japan College of Rheumatology Meeting. Tanaka N, et al. Phase 2b study of tyrosine kinase 2 (TYK2) inhibitor TAK-279 in psoriatic arthritis (PsA) patients. Poster presentation: 18–20 April, 2024.
4. EULAR Congress (2024) European Alliance of Associations for Rheumatology Congress. Kivitz A, et al. Efficacy and safety outcomes of TAK-279, a selective oral tyrosine kinase 2 (TYK2) inhibitor, from a randomized, double-blind, placebo-controlled phase 2b trial in patients with active psoriatic arthritis. Oral presentation: 12–15 June, 2024.
5. IFPA Conference (2024) International Federation of Psoriasis Associations Conference. Kivitz A, et al. Efficacy and safety of zasocitinib (TAK-279), a selective oral TYK2 inhibitor, in a randomized, placebo-controlled phase 2b trial in psoriatic arthritis. Poster presentation: and oral presentation: 27–29 June, 2024.
6. APLAR Congress (2024) Asia-Pacific League of Associations for Rheumatology Congress. Kivitz A, et al. Efficacy and safety of zasocitinib (TAK-279), a selective, oral TYK2 inhibitor: a randomized, placebo-controlled phase 2b trial in psoriatic arthritis. Oral presentation: 21–25 August, 2024.
7. EADV Congress (2024) European Academy of Dermatology and Venereology Congress. Gottlieb A, et al. Zasocitinib (TAK-279), a highly selective oral tyrosine kinase 2 (TYK2) inhibitor, elicits early skin responses and minimal disease activity in patients with active psoriatic arthritis: results from a randomized phase 2b study. Oral presentation: 25–28 September, 2024.
8. ACR Convergence (2024) American College of Rheumatology 2024 Annual Scientific Meeting. Kavanaugh A, et al. Assessment of laboratory parameter changes in a phase 2b trial of zasocitinib (TAK-279), an oral, selective TYK2 inhibitor, in patients with active psoriatic arthritis. Poster presentation: 14–19 November, 2024.
9. ACR Convergence (2024) American College of Rheumatology 2024 Annual Scientific Meeting. Gottlieb A, et al. Zasocitinib



(TAK-279), a highly selective oral tyrosine kinase 2 (TYK2) inhibitor, elicits early skin responses and minimal disease activity in patients with active psoriatic arthritis: results from a randomized phase 2b study. Poster presentation: 14–19 November, 2024.

10. ACR Convergence (2024) American College of Rheumatology 2024 Annual Scientific Meeting. Mease P, et al. Zascotinib (TAK-279), an oral, selective tyrosine kinase 2 inhibitor: additional improvements in disease activity and achievement of remission in patients with psoriatic arthritis enrolled in a phase 2b Trial. Oral presentation: 14–19 November, 2024.

## Supplementary materials

Supplementary material associated with this article can be found in the online version at doi:10.1016/j.ard.2025.05.023.

## Orcid

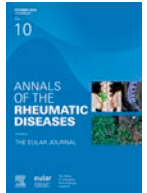
Alan Kivitz: <http://orcid.org/0000-0002-1045-1310>  
 Xenofon Baraliakos: <http://orcid.org/0000-0002-9475-9362>  
 Elena Tomaselli Muensterman: <http://orcid.org/0009-0007-8916-3680>  
 Arthur Kavanaugh: <http://orcid.org/0000-0001-6942-5830>  
 Désirée van der Heijde: <http://orcid.org/0000-0002-5781-158X>  
 Piotr A Klimiuk: <http://orcid.org/0000-0003-3457-6203>  
 Guillermo Valenzuela: <http://orcid.org/0000-0003-4283-9683>  
 Eva Dokoupilova: <http://orcid.org/0009-0003-9363-145X>  
 Bhaskar Srivastava: <http://orcid.org/0009-0000-9859-4203>  
 Sue Dasen: <http://orcid.org/0009-0000-8877-1384>  
 Xinyan Zhang: <http://orcid.org/0009-0001-6419-425X>  
 Ting Hong: <http://orcid.org/0009-0007-7464-3462>  
 Jingjing Chen: <http://orcid.org/0000-0003-4252-9255>  
 Peter Pothula: <http://orcid.org/0000-0002-0531-4127>  
 Haoling Holly Weng: <http://orcid.org/0009-0002-8484-3955>  
 Mona Trivedi: <http://orcid.org/0009-0000-4586-0619>  
 Apinya Lertratanakul: <http://orcid.org/0000-0003-0696-4129>

## REFERENCES

- Ogdie A, Coates LC, Gladman DD. Treatment guidelines in psoriatic arthritis. *Rheumatology (Oxford)* 2020;59:137–46.
- Ritchlin CT, Colbert RA, Gladman DD. Psoriatic arthritis. *N Engl J Med* 2017;376:957–70.
- Taylor W, Gladman D, Helliwell P, Marchesoni A, Mease P, Mielants H, et al. Classification criteria for psoriatic arthritis: development of new criteria from a large international study. *Arthritis Rheum* 2006;54:2665–73.
- Coates LC, Soriano ER, Corp N, Bertheussen H, Callis Duffin K, et al. Group for Research and Assessment of Psoriasis and Psoriatic Arthritis (GRAPPA): updated treatment recommendations for psoriatic arthritis 2021. *Nat Rev Rheumatol* 2022;18:465–79.
- FitzGerald O, Ogdie A, Chandran V, Coates LC, Kavanaugh A, Tillett W, et al. Psoriatic arthritis. *Nat Rev Dis Primers* 2021;7:59.
- Orbai AM, de Wit M, Mease P, Shea JA, Gossec L, Leung YY, et al. International patient and physician consensus on a psoriatic arthritis core outcome set for clinical trials. *Ann Rheum Dis* 2017;76:673–80.
- Gossec L, Kerschbaumer A, Ferreira RJO, Aletaha D, Baraliakos X, Bertheussen H, et al. EULAR recommendations for the management of psoriatic arthritis with pharmacological therapies: 2023 update. *Ann Rheum Dis* 2024;83:706–19.
- Mease PJ, Armstrong AW. Managing patients with psoriatic disease: the diagnosis and pharmacologic treatment of psoriatic arthritis in patients with psoriasis. *Drugs* 2014;74:423–41.
- Shang L, Cao J, Zhao S, Zhang J, He Y. TYK2 in immune responses and treatment of psoriasis. *J Inflamm Res* 2022;15:5373–85.
- Muromoto R, Oritani K, Matsuda T. Current understanding of the role of tyrosine kinase 2 signaling in immune responses. *World J Biol Chem* 2022;13:1–14.
- Dendrou CA, Cortes A, Shipman L, Evans HG, Attfield KE, Jostins L, et al. Resolving TYK2 locus genotype-to-phenotype differences in autoimmunity. *Sci Transl Med* 2016;8:363ra149.
- Gonciarz M, Pawlak-Buś K, Leszczyński P, Owczarek W. TYK2 as a therapeutic target in the treatment of autoimmune and inflammatory diseases. *Immunotherapy* 2021;13:1135–50.
- McElwee JJ, Garcet S, Li X, Ceuto I, Kunjraiva N, Rambhia D, et al. Analysis of histologic, molecular and clinical improvement in moderate-to-severe psoriasis: results from a phase 1b trial of the novel allosteric TYK2 inhibitor NDI-034858 [poster]. Presented at the American Academy of Dermatology; 25–29 March 2022.
- Leit S, Greenwood J, Carriero S, Mondal S, Abel R, Ashwell M, et al. Discovery of a potent and selective tyrosine kinase 2 inhibitor: TAK-279. *J Med Chem* 2023;66:10473–96.
- Mehrotra S, Sano Y, Halkowycz P, Wilson E, Durairaj C, Kong KF, et al. Pharmacological characterization of zascotinib (TAK-279): an oral, highly selective and potent allosteric TYK2 inhibitor. *J Invest Dermatol* 2025. doi: 10.1016/j.jid.2025.05.014.
- Armstrong AW, Gooderham M, Lynde C, Maari C, Forman S, Green L, et al. Tyrosine kinase 2 inhibition with zascotinib (TAK-279) in psoriasis: a randomized clinical trial. *JAMA Dermatol* 2024;160:1066–74.
- ClinicalTrials.gov. A study to evaluate the efficacy, safety, and tolerability of NDI-034858 in participants with active psoriatic arthritis [Internet]. 2024 [cited 2025 May]. Available from: <https://clinicaltrials.gov/study/NCT05153148>
- Lubrano E, Scryfallano S, Fatica M, Triggianese P, Conigliaro P, Perrotta FM, et al. Psoriatic arthritis in males and females: differences and similarities. *Rheumatol Ther* 2023;10:589–99.
- Passia E, Vis M, Coates LC, Soni A, Tchetverikov I, Gerards AH, et al. Sex-specific differences and how to handle them in early psoriatic arthritis. *Arthritis Res Ther* 2022;24:22.
- Coates LS, Mease C, Ogdie P, Nantel A, Lavie F, Sharaf F, et al. Sex-related differences in baseline patient and disease characteristics: post hoc analyses of three phase 3, randomized, double-blind, placebo-controlled studies in patients with active psoriatic arthritis [abstract]. *Arthritis Rheumatol* 2024;76.
- Eder L, Richette P, Coates LC, Azevedo VF, Cappelleri JC, Johnson EP, et al. Gender differences in perceptions of psoriatic arthritis disease impact, management, and physician interactions: results from a global patient survey. *Rheumatol Ther* 2024;11:1115–34.
- Eder L, Mylvaganam S, Pardo Pardo J, Petkovic J, Strand V, Mease P, et al. Sex-related differences in patient characteristics, and efficacy and safety of advanced therapies in randomised clinical trials in psoriatic arthritis: a systematic literature review and meta-analysis. *Lancet Rheumatol* 2023;5:e716–27.
- Eder L, Muensterman E, van der Heijde D, Kivitz A, Trivedi M, Hong T, et al. ABO403 influence of body weight, sex and prior biologic history on treatment outcomes associated with TAK-279, a highly selective oral tyrosine kinase 2 (TYK2) inhibitor, in a phase 2b randomized trial in patients with active psoriatic arthritis. *Ann Rheum Dis* 2024;83:1449.
- Mease PJ, Deodhar AA, van der Heijde D, Behrens F, Kivitz AJ, Neal J, et al. Efficacy and safety of selective TYK2 inhibitor, deucravacitinib, in a phase II trial in psoriatic arthritis. *Ann Rheum Dis* 2022;81:815–22.
- Mease PJ, Lertratanakul A, Anderson JK, Papp K, Van den Bosch F, Tsuji S, et al. Upadacitinib for psoriatic arthritis refractory to biologics: SELECT-PsA 2. *Ann Rheum Dis* 2021;80:312–20.
- Mease PJ, Gladman DD, Ritchlin CT, Ruderman EM, Steinfeld SD, Choy EH, et al. Adalimumab for the treatment of patients with moderately to severely active psoriatic arthritis: results of a double-blind, randomized, placebo-controlled trial. *Arthritis Rheum* 2005;52:3279–89.
- Houttekiet C, de Vlam K, Neerincx B, Lories R. Systematic review of the use of CRP in clinical trials for psoriatic arthritis: a concern for clinical practice? *RMD Open* 2022;8:e001756.
- Ogdie A, Weiss P. The epidemiology of psoriatic arthritis. *Rheum Dis Clin North Am* 2015;41:545–68.
- Gladman DD. Consensus exercise on domains in psoriatic arthritis. *Ann Rheum Dis* 2005;64(Suppl 2) ii13–4.
- Asgari MM, Wu JJ, Gelfand JM, Salman C, Curtis JR, Harrold LR, et al. Validity of diagnostic codes and prevalence of psoriasis and psoriatic arthritis in a managed care population, 1996–2009. *Pharmacoepidemiol Drug Saf* 2013;22:842–9.
- Houghton K, Patil D, Gomez B, Feldman SR. Correlation between change in Psoriasis Area and Severity Index and Dermatology Life Quality Index in



- patients with psoriasis: pooled analysis from four phase 3 clinical trials of secukinumab. *Dermatol Ther (Heidelb)* 2021;11:1373–84.
- [32] Walsh JA, Ogdie A, Michaud K, Peterson S, Holdsworth EA, Karyekar CS, et al. Impact of key manifestations of psoriatic arthritis on patient quality of life, functional status, and work productivity: findings from a real-world study in the United States and Europe. *Joint Bone Spine* 2023;90:105534.
- [33] Tillett W, Merola JF, Thaçi D, Holdsworth E, Booth N, Lobosco LS, et al. Disease characteristics and the burden of joint and skin involvement amongst people with psoriatic arthritis: a population survey. *Rheumatol Ther* 2020;7:617–37.
- [34] Duvetorp A, Østergaard M, Skov L, Seifert O, Tveit KS, Danielsen K, et al. Quality of life and contact with healthcare systems among patients with psoriasis and psoriatic arthritis: results from the NORdic PATient survey of Psoriasis and Psoriatic arthritis (NORPAPP). *Arch Dermatol Res* 2019;311:351–60.
- [35] de Vlam K, Merola JF, Birt JA, Sandoval DM, Lobosco S, Moon R, et al. Skin involvement in psoriatic arthritis worsens overall disease activity, patient-reported outcomes, and increases healthcare resource utilization: an observational, cross-sectional study. *Rheumatol Ther* 2018;5:423–36.
- [36] Gladman DD. Toward treating to target in psoriatic arthritis. *J Rheumatol Suppl* 2015;93:14–6.
- [37] Dures E, Shepperd S, Mukherjee S, Robson J, Vlaev I, Walsh N, et al. Treat-to-target in PsA: methods and necessity. *RMD Open* 2020;6:e001083.
- [38] Gangolli E, Carreiro S, Leit S, McElwee JJ, Dave N, Lombardi A, et al. Characterization of pharmacokinetics, pharmacodynamics, tolerability and clinical activity in Phase I studies of the novel allosteric tyrosine kinase 2 (TYK2) inhibitor NDI-034858 [poster]. In: Presented at the Society for Investigative Dermatology; 18–21 May 2022.
- [39] Erre GL, Mavridis D, Woodman RJ, Mangoni AA. Placebo response in psoriatic arthritis clinical trials: a systematic review and meta-analysis. *Rheumatology (Oxford)* 2022;61:1328–40.



## Systemic lupus erythematosus

## BCMA-targeted CAR T cell therapy can effectively induce disease remission in refractory lupus nephritis

Ziwei Hu<sup>1,a</sup>, Shaozhe Cai<sup>1,a</sup>, Yikai Yu<sup>1</sup>, Yu Chen<sup>1</sup>, Bei Wang<sup>1</sup>, Di Wang<sup>2</sup>, Rui Zeng<sup>3</sup>, Xiaofeng He<sup>3</sup>, Guifen Shen<sup>1</sup>, Fei Yu<sup>1</sup>, Zhipeng Zeng<sup>1</sup>, Yuxue Chen<sup>1</sup>, Xiaofang Luo<sup>1</sup>, Ziyun Zhang<sup>1</sup>, Peiling Zhang<sup>2</sup>, Hui Xiong<sup>1</sup>, Lin Bai<sup>1</sup>, Ping Ye<sup>1</sup>, Shengyan Lin<sup>1</sup>, Jishuai Zhang<sup>4,\*\*\*</sup>, Cong Ye<sup>1,\*</sup>, Chunrui Li<sup>2,\*\*</sup>, Lingli Dong<sup>1,\*</sup>

<sup>1</sup> Department of Rheumatology and Immunology, Tongji Hospital, Tongji Medical College, Huazhong University of Science and Technology, Wuhan, Hubei, China

<sup>2</sup> Department of Hematology, Tongji Hospital, Tongji Medical College, Huazhong University of Science and Technology, Wuhan, Hubei, China

<sup>3</sup> Department of Nephrology, Tongji Hospital, Tongji Medical College, Huazhong University of Science and Technology, Wuhan, Hubei, China

<sup>4</sup> Shenzhen Pregene Biopharma Company Ltd., Shenzhen, China

## ARTICLE INFO

## Article history:

Received 24 March 2025

Received in revised form 21 May 2025

Accepted 18 June 2025

## ABSTRACT

**Objectives:** This study aims to evaluate the safety and efficacy of anti-B cell maturation antigen (BCMA)-targeting chimeric antigen receptor (CAR) T cells in treating refractory lupus nephritis (LN). **Methods:** This is an open-label, single-arm clinical trial assessing anti-BCMA CAR T cells in treating refractory LN patients. CAR T cells were infused following lymphodepletion therapy with cyclophosphamide and fludarabine. Patients were regularly followed up, in which clinical assessments were performed and laboratory indices were collected. Repeated renal biopsies and single cell RNA sequencing in certain patients were performed to help evaluate the therapeutic efficacy. The primary endpoints were the safe dosage of single infusion and the occurrence of adverse events, while the secondary endpoints focused on the therapeutic efficacy (eg, changes of Systemic Lupus Erythematosus Disease Activity Index 2000 [SLEDAI-2000]).

**Results:** Seven biopsy-confirmed LN patients were enrolled in this study with a median follow-up of 9 months, whose peripheral B cells were effectively eliminated within the first month postinfusions and restored within 3 months except one patient. Hypogammaglobulinemia was frequently observed in this study. Only one case of grade 1 cytokine release syndrome was noted, and no immune effector cell-associated neurotoxicity syndrome or severe infection was reported. SLEDAI-2K scores decreased from a median of 18 (range 10–22) at baseline to 0 (range 0–4) at the last follow-up, and 5 out of 7 patients achieved definition of remission in systemic lupus erythematosus (DORIS) complete remission. Decreased deposition of immune complex, reduced clonal abundance, and alleviated proinflammatory status of peripheral lymphocytes were also observed in repeated renal biopsy and transcriptomic analyses.

\*Correspondence to Prof. Lingli Dong and Prof. Cong Ye, Department of Rheumatology and Immunology, Tongji Hospital, Tongji Medical College, Huazhong University of Science and Technology, Wuhan, Hubei, China. \*\*Correspondence to Prof. Chunrui Li, Department of Hematology, Tongji Hospital, Tongji Medical College, Huazhong University of Science and Technology, Wuhan, Hubei, China. \*\*\*Correspondence to Dr. Jishuai Zhang, Shenzhen Pregene Biopharma Company Ltd., Shenzhen, China.

E-mail addresses: [zhangjs@pregene.com](mailto:zhangjs@pregene.com) (J. Zhang), [yecong@tjh.tjmu.edu.cn](mailto:yecong@tjh.tjmu.edu.cn) (C. Ye), [cunrui5650@hust.edu.cn](mailto:cunrui5650@hust.edu.cn) (C. Li), [tjhdongll@163.com](mailto:tjhdongll@163.com) (L. Dong).

Handling editor Josef S. Smolen.

<sup>a</sup> These authors contributed equally.

<https://doi.org/10.1016/j.ard.2025.06.2128>

**Conclusions:** Anti-BCMA CAR T therapy can help LN patients inducing and maintaining disease remission status safely and effectively, which indicated the potential feasibility of the BCMA-only-targeting strategy in treating autoimmune diseases with abnormal humoral immune responses through CAR products.

#### WHAT IS ALREADY KNOWN ON THIS TOPIC

- Conventional treatments for refractory lupus nephritis (LN) often fall short of consistent effectiveness, with one-third of patients experiencing relapses, and the potential side effects posing significant challenges to medication adherence and management.
- CD19-targeting chimeric antigen receptor (CAR) T products (both CD19 and CD19-anti-B cell maturation antigen (BCMA) targeting) have demonstrated effectiveness in inducing complete remission in systemic lupus erythematosus, while the knowledge of potential therapeutic efficacy of BCMA-targeting strategy is still limited.

#### WHAT THIS STUDY ADDS

- Anti-BCMA only CAR T cell can treat LN patients safely and effectively, indicating its potential to be a feasible therapeutic strategy in treating autoimmune diseases with abnormal humoral immune responses.

#### HOW THIS STUDY MIGHT AFFECT RESEARCH, PRACTICE OR POLICY

This study indicates that anti-BCMA strategy is potentially effective for CAR T cell based therapy in treating refractory LN.

## INTRODUCTION

Lupus nephritis (LN), one of the most severe organ manifestations of systemic lupus erythematosus (SLE), occurs in 25% to 50% of patients with SLE [1,2]. LN remains a significant cause of morbidity and mortality in patients with SLE, with 5% to 30% of patients with LN potentially progressing to end-stage renal disease, which poses a life-threatening risk [3,4]. Conventional treatment for LN, including glucocorticoids and immunosuppressive agents, such as cyclophosphamide (CTX) and mycophenolate mofetil (MMF), are not uniformly effective, with approximately 35% of patients who initially respond to treatment experiencing a relapse [3].

The production of large amounts of pathogenic autoantibodies by antibody-secreting cells (ASCs) derived from autoreactive B cells, and the following formation of immune complexes either in situ or in circulation, are one of the fundamental contributors to SLE [2,5,6]. Most of the ASCs exhibit low or absent expression CD20 and are predominantly located in bone marrow or inflamed tissues; therefore, these ASCs may be refractory to anti-CD20-only biologics with limited deep tissue depleting capacity, which might be the reason of their poor therapeutic response in a part of patients [7–10].

In the past few years, anti-CD19 chimeric antigen receptor (CAR) T cell therapy has demonstrated effectiveness in deep tissue depletion of targeted cells, and in inducing complete clinical and serological remission in autoimmune diseases, including SLE [8,11–13]. Currently, no study has evaluated the efficacy of anti-B cell maturation antigen (BCMA)-only strategy in treating LN, which is a molecule expressed on the surface of ASCs (plasmablasts and plasma cells) and some memory B cells [14]. Therefore, in this study, we initiated a

single-arm study to evaluate the safety profiles and therapeutic efficacy of a novel BCMA-only targeting CAR T cell product in treating refractory LN.

## METHODS

### Study design and participants

This is an investigator-initiated, open-label, single-arm clinical trial. The main inclusion criteria for this study are as follows: (1) Participants aged 18 to 70 years; (2) A classification of SLE in accordance with the European League Against Rheumatism/American College of Rheumatology 2019 criteria [15]; (3) Patients with active LN, confirmed by renal biopsy, specifically classified as active, proliferative LN classes III to V, according to the 2003 International Society of Nephrology/Renal Pathology Society classification [16]; and (4) Failure to respond to multiple therapies including glucocorticoids combined with 2 or more immunosuppressants or biological agents (eg, mycophenolate mofetil, cyclosporin A, cyclophosphamide, rituximab, belimumab, and etc.). The main exclusion criteria for this study are as follows: (1) Pregnant or breastfeeding women; (2) Patients with severe extrarenal clinical manifestations such as lupus encephalopathy, pulmonary haemorrhage, lupus myocarditis, lupus enteritis, and lupus crisis; (3) Individuals with known allergies, hypersensitivity, intolerance, or contraindications to any components of BCMA CAR T cells or drugs that may be used in the study; (4) Subjects with a malignant tumour within the past 5 years; (5) Subjects that have received the following drug therapy within the prescribed time before apheresis: (a) Have received B cell depleting agents such as rituximab treatment within 24 weeks; (b) Have received treatment with biologics (such as belimumab, telitacicept, etc.) within 4 weeks or within 2 half-lives; (c) Have received treatment with immunosuppressants or similar therapies within 2 weeks or 5 half-lives; (d) If long-term use of systemic glucocorticoids is required within 2 weeks prior to apheresis and during the study period, the dosage of the hormone must not exceed 10 mg per day; (e) Have received plasma exchange or immunoadsorption therapy within the past 24 weeks, or intravenous immunoglobulin (IVIG) treatment within the past 4 weeks; (6) Having received or planning to receive live vaccines/attenuated live vaccines within 4 weeks prior to apheresis or during the study period; (7) Chronic and active hepatitis B (HBV, excluding cases where the hepatitis B core antibody is positive and HBV DNA test is below 500 IU/mL), hepatitis C, HIV infection, or syphilis infection; (8) Subjects with other conditions determined by the investigator to be unsuitable for lymphocyte clearance or cell infusion, or who are otherwise unsuitable for study participation. The detailed inclusion and exclusion criteria are provided in the study protocol (Supplementary Table S1).

### Outcome measures

The primary endpoint of this study focused on the safety profiles of anti-BCMA CAR T therapy. Adverse events (AEs) and severe AEs (SAEs) were assessed by investigators according to

Common Terminology Criteria for Adverse Events version 5.0. Hypogammaglobulinemia was recorded. Cytokine release syndrome (CRS) and immune effector cell-associated neurotoxicity syndrome (ICANS) were defined according to published criteria [17]. The secondary endpoints included the efficacy of LN, as evaluated by Systemic Lupus Erythematosus Disease Activity Index-2000 (SLEDAI-2K) score [18], physician global assessment (PGA) score [19], the functional assessment of chronic illness therapy fatigue (FACIT-F) score [20], and CAR expressions. Key exploratory outcomes included the levels of autoantibodies, renal function, immunoglobulins, and complements. Additional details are provided in the supplemental materials.

### CAR products, therapeutic procedure, and follow-ups

BCMA CAR T cells were produced for each patient individually (personalised therapy) by Shenzhen Pregene Biopharma Co., Ltd, of which the CAR construct is comprised of a humanised anti-BCMA single domain antibody, along with the CD8 $\alpha$  hinge and transmembrane domains, a 4-1BB costimulatory domain, and a CD3 $\zeta$  activation domain (Supplementary Fig S1).

Before CAR T cells were infused on day 0, patients received lymphodepleting chemotherapy (from day –5 to day –3) with fludarabine (25 mg/m<sup>2</sup>/d) and cyclophosphamide (300 mg/m<sup>2</sup>/d) after leukapheresis. All patients received a single dose CAR T cell ( $2.5 \times 10^6$  cells/kg or  $35 \times 10^6$  cells) infusion following scheduled lymphodepletion regimen, specifically, 300 mg/m<sup>2</sup>/day cyclophosphamide and 30 mg/m<sup>2</sup>/day fludarabine for 3 consecutive days (D-5 to D-3). During the whole procedure, the use of immunosuppressants and biologics were discontinued, and the dose of glucocorticoids was tapered to no more than 10 mg prednisone per day prior to the leukapheresis. The prednisone dosage was gradually reduced to 5 mg per day before the infusion and subsequently discontinued within 1 month following the infusion. Signs of CRS and ICANS were observed for at least 28 days after cell infusion. To prevent the potential infections, IVIG was administered prophylactically to patients exhibiting IgG reduction with infection risks (eg, recent viral outbreaks or household exposure). Several infection-preventing measures were applied, including strict laminar air flow isolation (during the first 14 days after infusion) and postdischarge hygiene education. In order to avoid potential nephrotoxicity exacerbation in LN patients, and balance the infection prevention with minimising additional renal injury, prophylactic antimicrobial treatment and renal protective agents were discontinued during the trial. However, we implemented a strict monitoring protocol: regular follow-up examinations were conducted, and anti-infective agents were initiated only upon confirmation of infection (clinical symptoms or microbiologically confirmed pathogens), with dose adjustments guided by renal function.

Patients were regularly followed up according to the protocol, with the longest follow-up duration extending to 12 months postinfusion, in which therapeutic efficacy was evaluated, and laboratory indices including titres of serum autoantibodies, levels of urine protein, serum cytokine (interleukin-6), immunoglobulins, complements, and composition of lymphocyte subsets were detected. The copies of CAR and levels of soluble BCMA (sBCMA) were also screened based on the schedule. Repeated renal biopsy was made in patient 2 at the sixth month.

### Detection of antibodies against certain pathogens

Vaccination antibody titres were examined via enzyme-linked immunosorbent assay (ELISA) method based on stored

(–80 °C) serum collected from participants at the corresponding follow-up. IgG antibodies against measles (cut-off: 0.17 OD<sub>450nm</sub>) (optical density (absorbance) measurement at a wavelength of 450 nanometers), mumps (cut-off: 0.15 OD<sub>450nm</sub>) and coronavirus disease (COVID)-19 (cut-off: 10 AU/mL) were analysed with kits from Beier (catalogue number: 60019,60082) and YHLO Biotech company (catalogue number: C86095G), separately. IgG antibodies against tetanus (cut-off: 0.09 OD<sub>450nm</sub>) were detected with kit from Etebio (catalogue number: ET-2019000). Antibodies against hepatitis B surface antigen (cut-off: 10 mIU/mL) were analysed using an ELISA from Abbott.

### Single cell RNA sequencing and statistical analyses

The single cell RNA sequencing (scRNA-Seq) of the peripheral T and B cells of patient 3 were performed and analysed primarily based on the procedures illustrated in our previous study [21]. Briefly, peripheral blood mononuclear cells of patient 3 before leukapheresis and at the third month after infusion were separated for fluorescence-activated cell sorting (CD3+ for T cells and CD19+ for B cells). The 10X Genomics platform was applied for scRNA-Seq library construction. Gene quantifications were realised with CellRanger software and further analysed primarily with R package Seurat and scRepertoire, and annotated based on known marker genes. Gene set variation analysis (GSVA) based on the Gene Ontology Biological Process database at single cell level were performed with the GSVA package. Paired comparisons of laboratory indices between 2 different time points were performed with paired Wilcoxon rank-sum test, and a *P* value <0.05 (2-sided) was regarded as statistic significant. Visualisation of individual clinical laboratory data, and their descriptive analyses were conducted with Prism software.

## RESULTS

### Patient characteristics

Seven patients (5 females and 2 males) with SLE were enrolled in this study, with a median age of 35 years (range 27–61), confirmed with LN via renal biopsy (median time before infusion: 1.5 months, ranging from 1 to 5). Specifically, 4 patients (patients 1, 3, 6, and 7) were classified as class IV, whereas the remaining 3 patients (patients 2, 4, and 5) were classified as class III + V, III, IV + V, separately. All patients had previously been exposed to several drugs, including glucocorticoid (7/7), C (5/7), MMF (6/7), CTX (4/7), cyclosporin A (4/7), tacrolimus (4/7), belimumab (2/7), and telitacicept (3/7). Additionally, 3 patients (patients 2, 3, and 7) have received plasma exchange treatment (Table 1, Fig 1A). Despite the repeated treatment of oral glucocorticoids and immunosuppressants or biologics previously, patients enrolled in this study continued to exhibit high disease activity, as indicated by a median SLEDAI-2K score of 18 (range 10–22).

### Therapeutic efficacy and safety profiles

After lymphodepletion, produced CAR T cells were infused on day 0 (Fig 1A). The dynamics of CAR copies and sBCMA levels were recorded in Figure 1B, which indicated a median 3 months duration of CAR T cells and realisation of the elimination of BCMA expressing cells within 60 days. All 7 patients demonstrated a significant decrease in their SLEDAI-2K scores (Fig 1C, Supplementary Table S2), of which the median values declined from 18 (ranging from 10 to 22) at baseline to 0



**Table 1**  
**Patient characteristics at baseline**

	Pat. 1	Pat. 2	Pat. 3	Pat. 4	Pat. 5	Pat. 6	Pat. 7
<b>Demographics</b>							
Sex	F	M	F	F	F	M	F
Age	61	33	44	38	27	35	37
Disease duration (y)	10	12	1	2	5	0.33	6
Follow-up (mo)	12	12	9	6	6	6	6
SLEDAI-2K	20	10	22	18	18	12	18
<b>Laboratory values (baseline)</b>							
Haemoglobin (g/L)	86	139	128	109	96	98	85
White blood cells ( $10^3$ N/ $\mu$ L)	8.58	5.31	12.6	6.96	5.1	5.9	7.05
Lymphocytes ( $10^3$ N/ $\mu$ L)	1.33	1.28	0.87	1.26	0.86	1.08	1.09
Platelets ( $10^3$ N/ $\mu$ L)	126	248	306	189	242	185	276
C3 (g/L)	0.41	0.9	0.46	0.64	0.45	0.83	0.42
ANA (titre)	1000	1000	320	1000	1000	100	320
Anti-dsDNA (IU/mL)	10.1	13.23	48.47	11.36	31.75	11.04	11.31
<b>Urine</b>							
Proteinuria (g/24 h)	1.24	1.10	12.22	1.95	1.14	7.28	7.0
Protein/creatinine ( $\mu$ g/mg)	1.95	0.50	3.36	0.96	0.72	8.25	4.81
RBC count (N/ $\mu$ L)	71.8	4	289.1	59.2	9.5	187	92
WBC count (N/ $\mu$ L)	0.6	1	795.6	87.7	63.8	21.1	93.6
Pathological tube type (N/ $\mu$ L)	0	0	5.5	0.1	5.5	0.1	5.5
Renal biopsy stage	IV	III + V	IV	III	IV + V	IV	IV
<b>Treatment</b>							
Glucocorticoid	+	+	+	+	+	+	+
Hydroxychloroquine	+	+	+	+	+	–	–
Mycophenolate Mofetil	+	+	+	+	+	+	–
Cyclophosphamide	+	+	–	–	–	+	+
Tacrolimus	–	+	+	–	+	–	+
Cyclosporin A	+	–	–	+	+	–	+
Belimumab	+	–	–	–	–	–	+
Telitacicept	–	–	+	+	–	+	–
PLEX	–	+	+	–	–	–	+

ANA, antinuclear antibody; anti-dsDNA, anti-double-stranded DNA antibody; C3, complement component 3; Pat, patients; PLEX, plasma exchange; RBC, red blood cell; SLEDAI-2K, Systemic Lupus Erythematosus Disease Activity Index 2000; WBC, white blood cell.

(ranging from 0 to 4) at the last follow-up. Significant decrease of PGA (from 2.5 at baseline, ranging from 2 to 3, to 0 at the last follow-up, ranging from 0 to 0.5) and elevation of FACIT (from 28 at baseline, ranging from 6 to 39, to 44 at the last follow-up, ranging from 32 to 50) median scores were also observed ([Supplementary Fig S2A](#)). Five patients satisfied the definition of remission in systemic lupus erythematosus (DORIS) complete remission (CR) criteria at the last follow-up, and all 7 patients met the Lupus Low Disease Activity State criteria 6 months post-infusion. Among these patients, patient 1 and patient 2 achieved drug-free remission at the second and first month, respectively, and maintained this state without recurrence until the 12th month postinfusion. Patient 5 also achieved drug-free remission in the second month and maintained it until the ninth month, while patient 4 and 6 both achieved DORIS CR at month 9. Significant disease improvements were observed in both patients 3 and 7. In these patients, serum albumin levels came back to normal at the sixth month, and urinary protein levels decreased from 12.21 g/24 h to 2.79 g/24 h at the ninth month and from 7.03 g/24 h to 2.39 g/24 h at the sixth month, respectively ([Fig 1C-E](#); [Supplementary Fig S3](#)). Levels of immunoglobulins (IgG, IgM, and IgA) and titres of autoantibodies (eg, anti-dsDNA, anti-Ro52, anti-SSA, and anti-U1-RNP) decreased rapidly and significantly in all 7 patients following CAR T cell infusion, accompanied with increase of complement levels throughout the follow-up period ([Fig 1D](#); [Supplementary Fig S2B](#)). A significantly lower total level of 24-hour urine protein and urine protein-to-creatinine ratio were also observed at sixth month after infusion, while limited changes in the estimated glomerular

filtration rate were detected ([Fig 1E](#)). Repeated renal biopsy of patient 2 further revealed significant reduction of immunocomplex deposition and improvements in the disease condition ([Fig 1F](#)).

For the safety profile of BCMA-targeting CAR T cell therapy ([Tables 2 and 3](#)), during the therapeutic process, no instances of ICANS or severe infections related to CAR T cell therapy were reported. Only one case of grade 1 CRS was observed. Fever ( $<38^{\circ}\text{C}$ ) lasting no more than 3 days was observed in 6 patients following cell infusion, whereas fever exceeding  $38^{\circ}\text{C}$  (no more than  $39.5^{\circ}\text{C}$ ) was noted only in 1 patient (patient 6). All instances of fever were effectively managed through physical cooling or the administration of non-steroidal anti-inflammatory drugs ([Supplementary Fig S3](#)). Haematological toxic effects (leukopenia and neutropenia) were noted in relation to lymphodepletion regimen, and were resolved within 4 weeks. Titres of vaccination antibodies were also examined ([Supplementary Fig S4](#)), which revealed that the majority of patients exhibited decreased pathogen-specific antibody (measles, mumps, tetanus, COVID-19, and HBV) levels following CAR T treatment. However, it is worth mentioning, that patient 3 experienced a COVID-19 infection near the third month follow-up, in which an elevated titre of anti-COVID-19 antibody compared with that at baseline was detected. Despite no severe infection occurred, hypogammaglobulinemia was observed in all 7 cases, for which IVIG supplementations were performed ([Supplementary Table S3](#)).

The dynamics of peripheral B cells after infusion may help explain the therapeutic effects and safety profiles of BCMA CAR T cells ([Fig 2A](#)). Peripheral B cells were totally depleted within

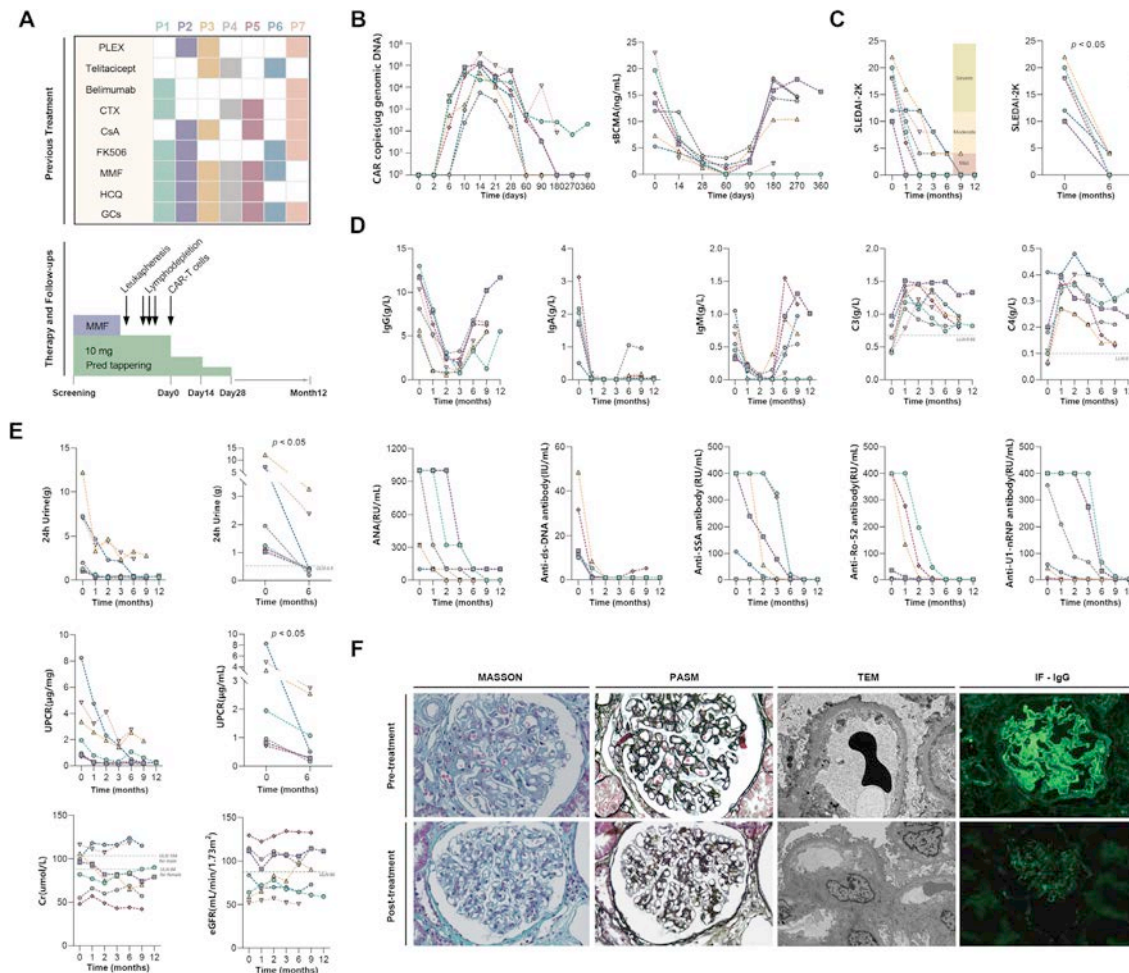


**Figure 1.** Therapeutic efficacy of BCMA CAR T therapy in treating refractory LN. A, Information of medication before screening, therapeutic process, and follow-up of enrolled patients. B, Dynamics of copy numbers of CAR gene, and levels of soluble BCMA. C, SLEDAI-2K. D, Levels of serum immunoglobulins, complement, and autoantibodies during the follow-ups. Note: The dashed line on plots of C3 and C4 indicated their lower limit of normal (LLN). E, Renal function: levels of 24-hour urine protein, UPCR, serum creatinine, and eGFR during the follow-ups. F, Representative histopathological images before and after CAR T cell infusion of patient 2. BCMA, anti-B cell maturation antigen; CAR T, chimeric antigen receptor T cell; C4, complement component 4; C3, complement component 3; eGFR, estimated glomerular filtration rate; LN, lupus nephritis; SLEDAI-2K, Systemic Lupus Erythematosus Disease Activity Index 2000; UPCR, urine protein-to-creatinine ratio.

the first month after infusion, and returned to normal levels within 3 months in 5 of 7 patients. In patient 7, level of B cells returned to normal at the sixth month postinfusion. Although B cells in patient 1 remained nearly undetectable at the 12th month after infusion, her drug-free remission state was maintained. An in-depth analysis of the reconstructed immune phenotyping of B cells in these 7 patients revealed that the majority of the reconstituted B cells are naive B cells (CD19+CD27-IgD+), comprising more than 90%. Nonswitched memory B cells (CD19+CD27+IgD+) gradually returned to normal levels within 2 to 3 months, and the number of switched memory B cells (CD19+CD27+IgD-) and plasmablasts (CD19+CD27+CD38high) also recovered gradually. scRNA-Seq was also applied to investigate the changes of immune receptor repertoire and functional phenotypes of lymphocytes after CAR T cell infusion in patient 3 sorted T and B cells before leukapheresis and at the third month postinfusion were sequenced, clustered, and annotated based on known markers (Fig 2B) [22–24]. Decreased ratios of memory B cells, CD8+ effector memory T cells (Tem), and CD4+ Tem were observed, whereas the ratios of other annotated cell types increased (Supplementary Fig S5A). Decreased clonal abundance and diversity in both B cell receptors (BCRs) and T cell receptors can be observed

(Fig 2C). V-gene usage and top clones also changed after infusion, particularly in the BCR (Fig 2D, Supplementary Fig S5B). The single cell GSVA analyses further revealed significant lower scores of Janus kinase activation, and monocyte chemotaxis processes in both B cells and CD4+ Tem cells at third month postinfusion, indicating a relative lower proinflammatory status of lymphocytes (Fig 2E). In addition, B cells and CD4+ Tem at the third month after infusion showed an increased antigen presentation process score and an increased B cell chemotaxis score, respectively. Significant decrease of signatures of response to interferon (IFN)- $\alpha$  and IFN- $\beta$  in B cells at the third month after infusion were also observed (Supplementary Fig S6).

## DISCUSSION

Although B cell-targeting biologics (eg, rituximab and belimumab) have been successfully applied in the treatment of LN, repeated therapies are needed, and not all patients respond well to them [25–27]. These may result from several limitations of biologics: the limited capacity of deep tissue penetration and/or the inability of targeting pathogenic auto-ASCs. BCMA is a molecule expressing on ASCs and some mature B cell subsets, indicating its potential to be the target of B cell depletion therapy.

Table 2  
Short-term safety of BCMA CAR T therapy in LN

Events	ALL <sup>a</sup>	Pat. 1	Pat. 2	Pat. 3	Pat. 4	Pat. 5	Pat. 6	Pat. 7
CRS (grade)	1	0	0	0	0	0	1	0
ICANS (grade)	0	0	0	0	0	0	0	0
TOC treatment (N)	0	0	0	0	0	0	0	0
GC treatment <sup>b</sup> (N)	0	0	0	0	0	0	0	0
Low IgG (N)	7	1	1	1	1	1	1	1
IgG substitution (N)	5	1	1	1	0	0	1	1

BCMA, anti-B cell maturation antigen; CAR T, chimeric antigen receptor T; CRS, cytokine release syndrome; GC, glucocorticoid; ICANS, immune effector cell-associated neurotoxicity syndrome; IgG, immunoglobulin G; IVIG, intravenous immunoglobulin; LN, lupus nephritis; N, number; Pat, patients; TOC, tocilizumab.

Among the 7 patients, only 1 case developed CRS (grade 1), and no ICANS was observed. Regarding therapeutic management, none of the patients received tocilizumab after CAR T cell infusion. All 7 patients exhibited serum IgG hypogammaglobulinemia (<8 g/L), and 5 patients received IgG substitution (IVIG).

<sup>a</sup> The total number of events that occurred among the 7 patients.  
<sup>b</sup> Glucocorticoid therapy was administered to control CRS. No glucocorticoid was used postinfusion to control CRS (as illustrated in Fig 1A, glucocorticoid was tapered to 5mg/day at the time of CAR T cell infusion, and subsequently discontinued within one month following the infusion).

Alexander et al [28] reported that teclistamab, a BCMA/CD3 bispecific antibody, induced rapid depletion of autoreactive B cells and plasma cells in refractory SLE, achieving complete clinical remission with normalised serological markers in a case study. This promising case highlights the potential efficacy of targeting BCMA in treating SLE. Additionally, Tur et al [8] demonstrated that CAR T cells exhibit enhanced tissue infiltration compared to rituximab, enabling elimination of B cells within secondary lymphoid tissues. Furthermore, Müller et al [29] recently reported a case of anti-CD19 CAR T-refractory idiopathic inflammatory myositis patient who responded to anti-BCMA CAR T therapy, further indicating the potential efficacy of anti-BCMA CAR T in autoimmune diseases. Effective treatment using a CD19/BCMA dual targeting strategy has been observed in SLE [30]. However, whether narrower-spectrum B cell depletion realised via a BCMA-only targeting strategy could also achieve comparable therapeutic efficacy is still unclear. Therefore, this study may not only offer a novel therapeutic paradigm for SLE, but also advance mechanistic insights into LN’s pathogenesis by

dissecting the differential roles of B cell subsets in disease progression.

Significant improvements in clinical symptoms and laboratory indicators were observed in all 7 patients with LN. Notably, 5 of these patients achieved drug-free CR, and 3 of them have maintained for more than 6 months. Furthermore, no obvious immune complex deposition was observed in the renal tissue of patient 2 at 6 months postinfusion. These findings indicate the preliminary clinical efficacy of BCMA CAR T therapy in the treatment of LN. Although clinical symptoms and laboratory indicators improved in all patients after CAR T treatment, the urine protein levels of 2 patients did not decrease below the upper limit of normal, which might be related to the potential irreversible damage existed before CAR T therapy. However, the specific cause and whether CAR T therapy should be applied at an earlier stage of the disease to avoid the potential irreversible tissue damage remain to be explored.

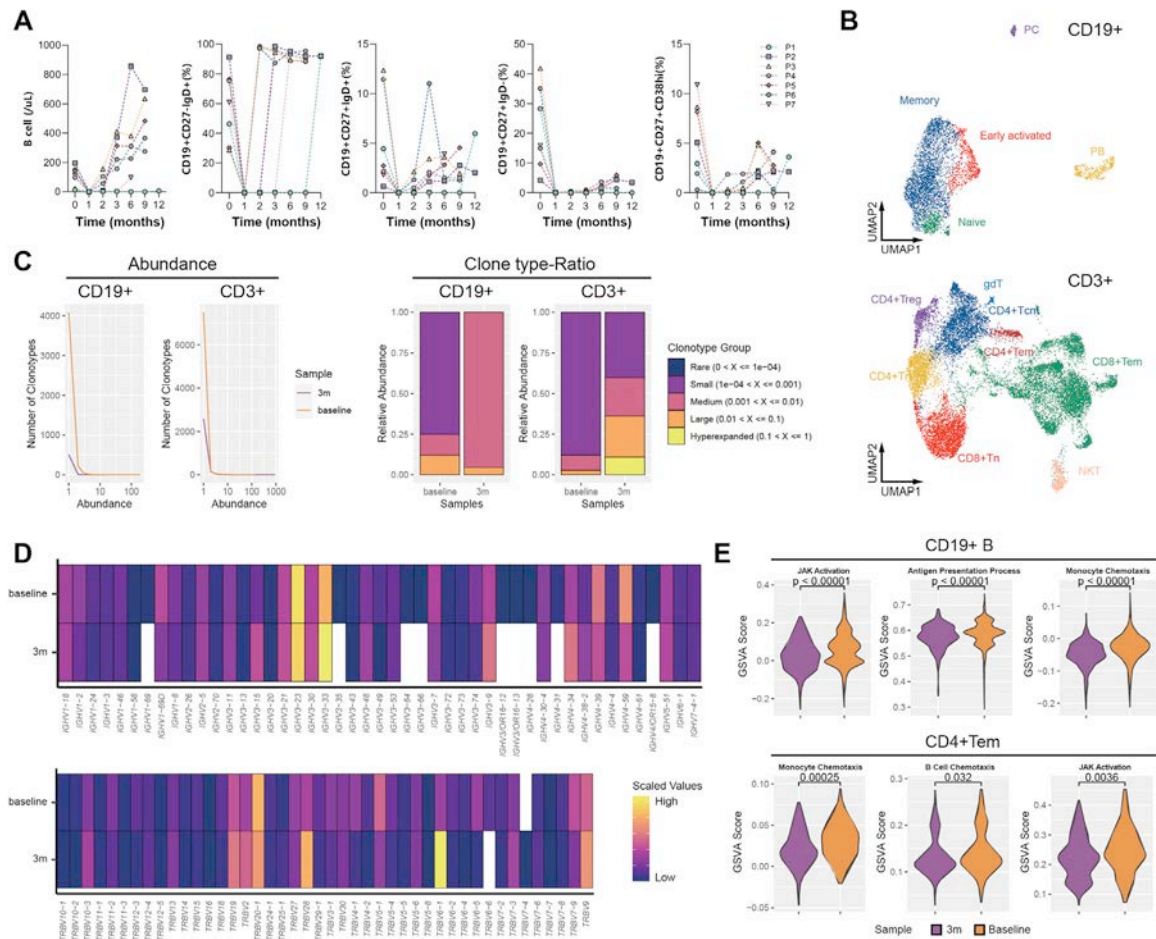
In addition to significant therapeutic efficacy, in our study, no SAEs related to CAR T cell therapy were reported throughout

Table 3  
Overall safety of BCMA CAR T therapy in LN

Adverse events	30 days post-CAR T infusion		>30 days post-CAR T infusion	
	Any grade (all patients)	Grade 3 or higher	Any grade (all patients)	Grade 3 or higher
AE haematologic				
Leukopenia	7 (100%)	6 (85.7%)	3 (42.9%)	1 (14.3%)
Neutropenia	6 (85.7%)	6 (85.7%)	3 (42.9%)	2 (28.6%)
Lymphocytopenia	7 (100%)	7 (100%)	3 (42.9%)	1 (14.3%)
Anaemia	7 (100%)	4 (57.1%)	7 (100%)	1 (14.3%)
AE infections				
COVID-19 infection	0 (0%)	0 (0%)	1 (14.3%)	0 (0%)
Herpes zoster virus infection	0 (0%)	0 (0%)	2 (28.6%)	0 (0%)
Oral herpes simplex virus infection	1 (14.3%)	0 (0%)	0 (0%)	0 (0%)
AE gastrointestinal				
Nausea/vomiting	5 (71.4%)	0 (0%)	0 (0%)	0 (0%)
Diarrhoea	1 (14.3%)	0 (0%)	1 (14.3%)	0 (0%)
AE others				
Fever	5 (71.4%)	0 (0%)	1 (14.3%)	0 (0%)
Hypotension	0 (0%)	0 (0%)	0 (0%)	0 (0%)
AST increased	2 (28.6%)	0 (0%)	2 (28.6%)	0 (0%)
ALT increased	3 (42.9%)	0 (0%)	2 (28.6%)	0 (0%)

AE, adverse event; ALT, alanine aminotransferase; AST, aspartate aminotransferase; BCMA, anti-B cell maturation antigen; CAR, chimeric antigen receptor; LN, lupus nephritis.





**Figure 2.** Features of peripheral lymphocytes during the BCMA CAR T therapy. A, Dynamics of B cells and B cell subsets during the follow-up. Note: Ratios of B cell subsets were derived from the cell number of subsets/number of CD19+ B cells. B, Annotated UMAP of the sequenced CD3+ and CD19+ cells sorted from the peripheral blood patient 3 before leukapheresis and 3 months after infusion. C, Abundances and composition of clones with different TCR and BCR sizes from different samples. D, The V-gene usage of BCR heavy chains (up) and TCR  $\beta$  chains (down). E, Single cell GSVA analyses based on GO BP database of all CD19+ B cells, and CD4+ effector memory T cells (Tem). BCMA, anti-B cell maturation antigen; BCR, B cell receptor; BP, biological process; CAR T, chimeric antigen receptor T cell; CD, cluster of differentiation; GO, gene ontology; GSVA, gene set variation analysis; TCR, T cell receptor; Tem, effector memory T cells; UMAP, uniform manifold approximation and projection.

the follow-up period. Cytopenia was one of the most prevalent AEs observed in our patients, typically occurring in the initial days postinfusion, possibly attributable to lymphodepletion therapy. Hypoimmunoglobulinemia was another common side effect observed in this study. Notably, Frerichs et al [31] reported that IgG supplementation ( $<4$  g/L) in teclistamab-treated myeloma patients significantly reduced infection rates, providing reference for postimmunosuppressive therapy management. There is no report on the IgG supplementation strategy after CAR T treatment for autoimmune diseases. In this trial, in order to prevent severe infections related to CAR T therapy, strict laminar airflow isolation was implemented from lymphodepletion initiation through day 14 postinfusion in all patients, complemented by postdischarge hygiene education. IVIG was prophylactically administered to patients exhibiting IgG reduction with concurrent infection risks/signs. Although several infection-related AEs, primarily involving herpes zoster virus, oral herpes simplex virus and COVID-19 infections, were still reported, none of these cases required hospitalisation. Remarkably, none of the patients developed ICANS, and only one case of grade 1 CRS was recorded, possibly due to the lower antigen burden in LN compared to multiple myeloma (MM). The number of plasma cells in LN patients is significantly less than that in

MM patients, as evidenced by the baseline levels of sBCMA in LN (median 13504.7 pg/mL) were markedly lower than those reported in MM patients (median  $>100000$  pg/mL) [32,33]. Overall, the AEs observed throughout the study were manageable, indicating that BCMA CAR T cell therapy is relatively safe.

Although CAR T cell therapy has offered a promising new direction for achieving drug-free remission in patients with autoimmune diseases, it is crucial to consider the long-term preservation of normal immune cells and to further reduce the risk of infection [34]. In our study, a continuous reduction of autoantibodies accompanied with increasing serum IgG and IgM levels and a relatively rapid recovery of the peripheral B cell pool were recorded in the majority of enrolled patients, which might be one of the potential reasons that no severe infection occurred during the study. The elevation in the anti-COVID-19 titre in patient 3 after infection at the third month postinfusion may also indicate the recovery of capacity of the humoral immune response within a relatively short period of time after anti-BCMA CAR T cell infusion.

This study has limitations. First, this study is an investigator-initiated, single-arm clinical trial with a small sample size. Research with larger sample sizes and longer follow-up periods is needed to further confirm the safety and efficacy of BCMA



CAR T cell therapy. Second, we did not explore the potential reasons for anti-BCMA CAR T cell persistence in LN patients. Peripheral CAR gene detection accompanied with the absence of B cell recovery and the low sBCMA levels was observed in 2 patients even 6 months after infusion, which potentially resulted from the long-term persistence or reactivation of functional CAR T cells. The persistence of CAR T cells was reported to have associations with the features of preinfusion CAR T products, in which CD4+ CAR T subsets exhibiting upregulated CD44/cytotoxic molecules (granzyme A and granulysin, *GZMA/GNLY*) and low L-selectin expression. This suggested that CAR T persistence may depend on autologous cell differentiation states, particularly CD4+ T cell subsets [35]. The functional persistence might be a key characteristic of durable clinical responses in leukaemias [36]. The precise reason and clinical indication of this persistence in SLE patients remain to be elucidated. Third, despite our prophylactic IgG supplementation strategy seemed to prevent patients from infections efficiently; however, the different immunology states among different diseases and patients necessitate further validation in large cohorts to determine optimal IgG supplementation strategies for certain conditions. In addition, it should also be mentioned that BCMA-only targeting may not be suitable for all refractory LN patients due to the complexity of LN's immunopathogenesis, and further studies focusing on the immune/molecular phenotypes and strategies for precise CAR selection for individual LN patient are recommended.

In summary, our data demonstrate that anti-BCMA CAR T cell therapy can deplete B cells in patients with LN, promote immune reconstitution, and induce drug-free remission safely and effectively, indicating the feasibility of BCMA-only-targeting strategies for treating autoimmune diseases with abnormal humoral immune responses using CAR products.

### CRedit authorship contribution statement

**Ziwei Hu:** Writing – original draft, Validation, Software, Project administration, Methodology, Investigation, Formal analysis, Data curation, Conceptualization. **Shaozhe Cai:** Writing – review & editing, Writing – original draft, Supervision, Software, Project administration, Methodology, Funding acquisition, Formal analysis, Data curation, Conceptualization. **Yikai Yu:** Resources, Project administration, Investigation. **Yu Chen:** Supervision, Resources, Investigation. **Bei Wang:** Supervision, Resources, Investigation. **Di Wang:** Supervision, Resources, Project administration, Investigation. **Rui Zeng:** Resources, Investigation. **Xiaofeng He:** Resources, Investigation. **Guifen Shen:** Resources, Investigation. **Fei Yu:** Resources, Project administration, Investigation. **Zhipeng Zeng:** Supervision, Resources. **Yuxue Chen:** Supervision, Resources. **Xiaofang Luo:** Supervision, Resources. **Ziyun Zhang:** Supervision, Project administration, Methodology. **Peiling Zhang:** Supervision, Resources, Methodology, Investigation. **Hui Xiong:** Validation, Resources, Methodology. **Lin Bai:** Validation, Methodology. **Ping Ye:** Resources, Methodology. **Shengyan Lin:** Validation, Methodology. **Jishuai Zhang:** Supervision, Resources, Project administration, Methodology, Investigation, Conceptualization. **Cong Ye:** Supervision, Resources, Project administration, Methodology, Investigation, Conceptualization. **Chunrui Li:** Writing – review & editing, Supervision, Resources, Project administration, Methodology, Investigation. **Lingli Dong:** Writing – review & editing, Supervision, Resources, Project administration, Methodology, Investigation, Funding acquisition, Conceptualization.

### Funding

This work was supported by the National Natural Science Foundation of China (Nos. 32450786, 82271847, and 32400583), Tongji Hospital Clinical Research Flagship Program Funding (2019CR206), and Tongji Hospital High-Quality Clinical Research Funding (2024TJCR008).

### Competing interests

Dr. JSZ is the employee of Shenzhen Pregene Biopharma Company Ltd., Shenzhen, China. All other authors declare no competing interests.

### Patient consent for publication

Consent obtained directly from patients.

### Ethics approval

This study was approved by the Institutional Review Board and Medical Ethics Committee of Tongji Medical College of Huazhong University of Science and Technology. Written informed consent was obtained from all patients prior to screening. The trial was registered at Clinical Trials.gov (NCT06277427 and NCT06497387).

### Provenance and peer review

Externally peer reviewed.

### Data availability statement

Data are available on reasonable request.

### Patient and public involvement

Patients and/or the public were not involved in the design, or conduct, or reporting, or dissemination plans of this research.

### Supplementary materials

Supplementary material associated with this article can be found in the online version at [doi:10.1016/j.ar.2025.06.2128](https://doi.org/10.1016/j.ar.2025.06.2128).

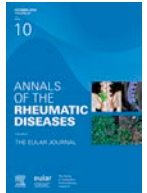
### Orcid

Lingli Dong: <http://orcid.org/0000-0003-2017-1125>

### REFERENCES

- [1] Hanly JG, O'Keeffe AG, Su L, Urowitz MB, Romero-Diaz J, Gordon C, et al. The frequency and outcome of lupus nephritis: results from an international inception cohort study. *Rheumatology (Oxford)* 2016;55(2):252–62.
- [2] Siegel CH, Sammaritano LR. Systemic lupus erythematosus: a review. *JAMA* 2024;331(17):1480–91.
- [3] Anders HJ, Saxena R, Zhao MH, Parodis I, Salmon JE, Mohan C. Lupus nephritis. *Nat Rev Dis Primers* 2020;6(1):7.
- [4] Mok CC, Teng YKO, Saxena R, Tanaka Y. Treatment of lupus nephritis: consensus, evidence and perspectives. *Nat Rev Rheumatol* 2023;19(4):227–38.
- [5] Hoi A, Igel T, Mok CC, Arnaud L. Systemic lupus erythematosus. *Lancet* 2024;403(10441):2326–38.
- [6] Crow MK. Pathogenesis of systemic lupus erythematosus: risks, mechanisms and therapeutic targets. *Ann Rheum Dis* 2023;82(8):999–1014.
- [7] Merrill JT, Neuwelt CM, Wallace DJ, Shanahan JC, Latinis KM, Oates JC, et al. Efficacy and safety of rituximab in moderately-to-severely active

- systemic lupus erythematosus: the randomized, double-blind, phase II/III systemic lupus erythematosus evaluation of rituximab trial. *Arthritis Rheum* 2010;62(1):222–33.
- [8] Tur C, Eckstein M, Velden J, Rauber S, Bergmann C, Auth J, et al. CD19-CAR T-cell therapy induces deep tissue depletion of B cells. *Ann Rheum Dis* 2025;84:106–14.
  - [9] Schett G, Mackensen A, Mougiakakos D. CAR T-cell therapy in autoimmune diseases. *Lancet* 2023;402(10416):2034–44.
  - [10] Mei HE, Wirries I, Frölich D, Brisslert M, Giesecke C, Grün JR, et al. A unique population of IgG-expressing plasma cells lacking CD19 is enriched in human bone marrow. *Blood* 2015;125(11):1739–48.
  - [11] Mackensen A, Müller F, Mougiakakos D, Böltz S, Wilhelm A, Aigner M, et al. Anti-CD19 CAR T cell therapy for refractory systemic lupus erythematosus. *Nat Med* 2022;28(10):2124–32.
  - [12] Mougiakakos D, Krönke G, Völkl S, Kretschmann S, Aigner M, Kharboulitli S, et al. CD19-targeted CAR T cells in refractory systemic lupus erythematosus. *N Engl J Med* 2021;385(6):567–9.
  - [13] Müller F, Taubmann J, Bucci L, Wilhelm A, Bergmann C, Völkl S, et al. CD19 CAR T-cell therapy in autoimmune disease - a case series with follow-up. *N Engl J Med* 2024;390(8):687–700.
  - [14] Hiepe F, Radbruch A. Plasma cells as an innovative target in autoimmune disease with renal manifestations. *Nat Rev Nephrol* 2016;12(4):232–40.
  - [15] Aringer M, Costenbader K, Daikh D, Brinks R, Mosca M, Ramsey-Goldman R, et al. 2019 European League Against Rheumatism/American College of Rheumatology classification criteria for systemic lupus erythematosus. *Ann Rheum Dis* 2019;78(9):1151–9.
  - [16] Weening JJ, D'Agati VD, Schwartz MM, Seshan SV, Alpers CE, Appel GB, et al. The classification of glomerulonephritis in systemic lupus erythematosus revisited. *Kidney Int* 2004;65(2):521–30.
  - [17] Lee DW, Santomaso BD, Locke FL, Ghobadi A, Turtle CJ, Brudno JN, et al. ASTCT consensus grading for cytokine release syndrome and neurologic toxicity associated with immune effector cells. *Biol Blood Marrow Transplant* 2019;25(4):625–38.
  - [18] Gladman DD, Ibañez D, Urowitz MB. Systemic lupus erythematosus disease activity index 2000. *J Rheumatol* 2002;29(2):288–91.
  - [19] Piga M, Chessa E, Morand EF, Ugarte-Gil MF, Tektonidou M, van Vollenhoven R, et al. Physician Global Assessment international standardisation consensus in systemic lupus erythematosus: the PISCOS study. *Lancet Rheumatol* 2022;4(6):e441–9.
  - [20] Yellen SB, Cella DF, Webster K, Blendowski C, Kaplan E. Measuring fatigue and other anemia-related symptoms with the Functional Assessment of Cancer Therapy (FACT) measurement system. *J Pain Symptom Manage* 1997;13(2):63–74.
  - [21] Cai S, Chen Y, Hu Z, Zhou T, Huang Y, Lin S, et al. The landscape of T and B lymphocytes interaction and synergistic effects of Th1 and Th2 type response in the involved tissue of IgG4-RD revealed by single cell transcriptome analysis. *J Autoimmun* 2022;133:102944.
  - [22] Quan F, Liang X, Cheng M, Yang H, Liu K, He S, et al. Annotation of cell types (ACT): a convenient web server for cell type annotation. *Genome Med* 2023;15(1):91.
  - [23] Sanz I, Wei C, Jenks SA, Cashman KS, Tipton C, Woodruff MC, et al. Challenges and opportunities for consistent classification of human B cell and plasma cell populations. *Front Immunol* 2019;10:2458.
  - [24] Cossarizza A, Chang HD, Radbruch A, Abirgani S, Addo R, Akdis M, et al. Guidelines for the use of flow cytometry and cell sorting in immunological studies (third edition). *Eur J Immunol* 2021;51(12):2708–3145.
  - [25] Shipa M, Embleton-Thirsk A, Parvaz M, Santos LR, Muller P, Chowdhury K, et al. Effectiveness of belimumab after rituximab in systemic lupus erythematosus: a randomized controlled trial. *Ann Intern Med* 2021;174(12):1647–57.
  - [26] Stohl W, Schwarting A, Okada M, Scheinberg M, Doria A, Hammer AE, et al. Efficacy and safety of subcutaneous belimumab in systemic lupus erythematosus: a fifty-two-week randomized, double-blind, placebo-controlled study. *Arthritis Rheumatol* 2017;69(5):1016–27.
  - [27] Ng KP, Cambridge G, Leandro MJ, Edwards JCW, Ehrenstein M, Isenberg DA. B cell depletion therapy in systemic lupus erythematosus: long-term follow-up and predictors of response. *Ann Rheum Dis* 2007;66(9):1259–62.
  - [28] Alexander T, Krönke J, Cheng Q, Keller U, Krönke G. Teclistamab-induced remission in refractory systemic lupus erythematosus. *N Engl J Med* 2024;391(9):864–6.
  - [29] Müller F, Wirsching A, Hagen M, Völkl S, Tur C, Raimondo MG, et al. BCMA CAR T cells in a patient with relapsing idiopathic inflammatory myositis after initial and repeat therapy with CD19 CAR T cells. *Nat Med* 2025;31:1793–7.
  - [30] Wang W, He S, Zhang W, Zhang H, DeStefano VM, Wada M, et al. BCMA-CD19 compound CAR T cells for systemic lupus erythematosus: a phase 1 open-label clinical trial. *Ann Rheum Dis* 2024;83(10):1304–14.
  - [31] Frerichs KA, Verkleij CPM, Mateos MV, Martin TG, Rodriguez C, Nooka A, et al. Teclistamab impairs humoral immunity in patients with heavily pre-treated myeloma: importance of immunoglobulin supplementation. *Blood Adv* 2024;8(1):194–206.
  - [32] Wang D, Wang J, Hu G, Wang W, Xiao Y, Cai H, et al. A phase 1 study of a novel fully human BCMA-targeting CAR (CT103A) in patients with relapsed/refractory multiple myeloma. *Blood* 2021;137(21):2890–901.
  - [33] Raju N, Berdeja J, Lin Y, Siegel D, Jagannath S, Madduri D, et al. Anti-BCMA CAR T-cell therapy bb2121 in relapsed or refractory multiple myeloma. *N Engl J Med* 2019;380(18):1726–37.
  - [34] Lungova K, Putman M. Barriers to CAR T-cell therapy in rheumatology. *Lancet Rheumatol* 2025;7:e212–6.
  - [35] Qin C, Zhang M, Mou DP, Zhou LQ, Dong MH, Huang L, et al. Single-cell analysis of anti-BCMA CAR T cell therapy in patients with central nervous system autoimmunity. *Sci Immunol* 2024;9(95):eadj9730.
  - [36] Porter DL, Hwang WT, Frey NV, Lacey SF, Shaw PA, Loren AW, et al. Chimeric antigen receptor T cells persist and induce sustained remissions in relapsed refractory chronic lymphocytic leukemia. *Sci Transl Med* 2015;7(303):303ra139.



## Systemic lupus erythematosus

# Frontoparietal functional connectivity is related to active disease and processing speed in adolescents with childhood-onset lupus

Diana Valdés Cabrera<sup>1,\*</sup>, Oscar Mwizerwa<sup>2</sup>, Busi Zapparoli<sup>1,3</sup>,  
Asha Jeyanathan<sup>2</sup>, Lawrence Ng<sup>2</sup>, Tala El Tal<sup>4</sup>, Birgit Ertl-Wagner<sup>5,6</sup>,  
Ann Yeh<sup>1,7</sup>, Helen Branson<sup>5,6</sup>, Adrienne Davis<sup>8</sup>, Linda Hiraki<sup>2,9</sup>,  
Deborah Levy<sup>2,9</sup>, Ashley Danguedan<sup>1,3</sup>, Andrea Knight<sup>1,2,9</sup>

<sup>1</sup> Neurosciences and Mental Health Program, SickKids Research Institute, The Hospital for Sick Children, Toronto, ON, Canada

<sup>2</sup> Department of Rheumatology, The Hospital for Sick Children, Toronto, ON, Canada

<sup>3</sup> Department of Psychology, The Hospital for Sick Children, Toronto, ON, Canada

<sup>4</sup> Dermatology/Rheumatology, Children's Hospital of Eastern Ontario, Ottawa, ON, Canada

<sup>5</sup> Department of Diagnostic & Interventional Radiology, The Hospital for Sick Children, Toronto, ON, Canada

<sup>6</sup> Department of Medical Imaging, University of Toronto, Toronto, ON, Canada

<sup>7</sup> Division of Neurology, Department of Pediatrics, University of Toronto, Toronto, ON, Canada

<sup>8</sup> Department of Emergency Medicine, The Hospital for Sick Children, Toronto, ON, Canada

<sup>9</sup> Temerty Faculty of Medicine, University of Toronto, Toronto, ON, Canada

## ARTICLE INFO

## Article history:

Received 10 March 2025

Received in revised form 30 May 2025

Accepted 19 June 2025

## ABSTRACT

**Objectives:** To evaluate brain functional connectivity (FC) with resting-state magnetic resonance imaging (rs-fMRI) in adolescents with childhood-onset systemic lupus erythematosus (cSLE) compared to healthy controls (HCs) and to evaluate associations among FC, disease characteristics, and cognitive performance.

**Methods:** Patients with cSLE aged 11 to 17 years, and age- and sex-matched HCs, underwent rs-fMRI at 3T and clinical (current and cumulative cSLE activity and glucocorticoid dose, anti-dsDNA positivity, nephritis diagnosis) and cognitive (attention, working memory, processing speed, inhibition) data collection. Group differences in FC between brain regions of interest (ROI) within/across resting-state networks as well as associations between FC and clinical and cognitive variables were evaluated with age-adjusted general linear models. Analyses were corrected for multiple comparisons with family-wise error (FWE) methods (threshold-free cluster enhancement  $P\text{-FWE} < .05$ , individual pairs of ROI connections  $P < .01$ ).

**Results:** Participants included 60 patients ( $14.9 \pm 1.84$  years, 52 females) with cSLE and 59 HCs. Patients had lower FC compared to HCs in frontoparietal connections that were exacerbated in subgroups with active cSLE features (all  $P\text{-FWE} \leq .049$ ). In cSLE patients, lower FC in frontocerebellar connections were associated with higher cumulative disease activity and glucocorticoid use ( $P\text{-FWE} \leq .018$ ). Positive associations were found between FC in frontoparietal–occipital connections and processing speed scores in cSLE patients ( $P\text{-FWE} = .010$ ) but not in HCs.

\*Correspondence to Dr. Diana Valdés Cabrera, Neurosciences and Mental Health, The Hospital for Sick Children, Toronto, ON, Canada.

E-mail address: [diana.valdescabrera@sickkids.ca](mailto:diana.valdescabrera@sickkids.ca) (D.V. Cabrera).

Handling editor Josef S. Smolen.

**Conclusions:** Adolescents with cSLE, compared to HCs, exhibited lower brain FC in frontoparietal regions of the dorsal attention and somatosensory regions, which was associated with greater disease activity. Higher FC in frontoparietal–occipital regions, critical for visual attention, was associated with better processing speed, which could be compensatory to disease effects.

### WHAT IS ALREADY KNOWN ON THIS TOPIC

- Diffuse neuropsychiatric manifestations, such as cognitive dysfunction, are prevalent in patients with systemic lupus erythematosus (SLE), yet clinical care is challenging due to the limited accuracy of clinical diagnostic tools.
- Resting-state functional magnetic resonance imaging (rs-fMRI), measuring the intrinsic functional organisation of the brain, has shown brain abnormalities in adults with SLE with and without clinical diagnosis of neuropsychiatric SLE.
- Rs-fMRI studies are needed in childhood-onset SLE (cSLE) to better understand the impact of cSLE on the developing brain.

### WHAT THIS STUDY ADDS

- The results of this rs-fMRI study examining brain function in adolescents diagnosed with cSLE indicate that regional functional brain abnormalities may occur early in the disease course.
- Higher disease activity and cumulative glucocorticoid doses could be drivers of abnormal brain function.
- Moreover, brain functional changes associate with performance in cognitive domains such as processing speed through visual pathways.

### HOW THIS STUDY MIGHT AFFECT RESEARCH, PRACTICE OR POLICY

- The study identifies frontoparietal brain regions as early indicators of atypical brain function and abnormal neurodevelopment in cSLE that might inform clinical radiological readings.
- Given that neurodevelopment in youth shapes functional brain organisation in adults, this study emphasises which brain regions could be targets of future neurocognitive training therapies in SLE.
- It also highlights the need for further neuroimaging research in children with cSLE, specifically of longitudinal studies evaluating brain function changes with disease evolution and treatment.

## INTRODUCTION

Neuropsychiatric manifestations are highly prevalent (over 50%) in patients with systemic lupus erythematosus (SLE), and they tend to be more severe when diagnosed in childhood-onset (cSLE) compared to adult-onset patients [1,2]. A wide range of symptoms have been described in association with neuropsychiatric SLE (NPSLE). Diffuse symptoms such as headaches and cognitive dysfunction (CD) are the most common but are difficult to definitively attribute to NPSLE as they are driven by multiple pathologic mechanisms [3]. Affected cognitive domains in SLE include attention, processing speed, and executive functioning (eg, working memory, inhibition) [4]. In children, NPSLE can occur in approximately 15% to 95% of cSLE patients [2], who may be at high risk for disease damage and persistent CD [5]. However, our clinical tools, including conventional magnetic resonance imaging (MRI) have limited accuracy for clinical NPSLE diagnosis, and its underlying mechanisms remain poorly understood.

Brain function in patients with SLE can be examined by measuring changes in the blood oxygen level-dependent (BOLD) signal, a proxy of regional neuronal activity, with functional MRI (fMRI). Temporal correlations between functionally connected regions, referred as functional connectivity (FC), can be measured with resting-state fMRI (rs-fMRI), and they can reveal the intrinsic functional organisation of the brain [6,7]. Furthermore, rs-fMRI is especially suitable for evaluating brain function in paediatric populations and in patients who may have difficulties following task instructions [8]. Functional brain abnormalities have been detected in a number of regions across large-scale networks in adult patients with and without clinical NPSLE. Some studies have yielded heterogeneous results (eg, hypo- and hyper-connectivity across frontoparietal and hippocampal regions in SLE patients versus controls) [9–12], and connections to the frontal cortex have been associated with disease characteristics, mostly to active/flaring status in SLE patients [12–15]. This heterogeneity could be related to differences in imaging and analytical protocols. Nevertheless, the reliability of rs-fMRI to study SLE populations is supported by a recent whole-brain rs-fMRI meta-analysis study spanning different types of rs-fMRI analyses that reported higher FC in the bilateral hippocampus and right superior temporal gyrus and lower FC in the left superior/inferior frontal and middle temporal gyrus, right cerebellum, and thalamus as common abnormalities in patients with SLE compared to healthy controls (HCs) [16]. Few studies have specifically evaluated FC related to cognitive performance in SLE and, again, their results are heterogeneous (eg, higher and lower FC within and across frontoparietal, and medial temporal cortical regions of the default mode and task-positive networks correlated with various cognitive functions) [9,10,17,18]. This may also suggest the co-occurrence of adaptive (ie, compensatory mechanisms including cortical reorganisation to partially limit cognitive/clinical deficits) and maladaptive (ie, detrimental changes to overall brain function, potentially leading to cognitive/clinical deficits) responses within networks, which might vary according to SLE patients' clinical characteristics, as it has been postulated in other neurological conditions [19]. Furthermore, modest sample sizes and not addressing medication effects have been indicated as common deficiencies in prior work [20].

Additionally, there is a paucity of rs-fMRI studies in cSLE populations and, to date, only 2 task-based fMRI studies have evaluated brain function in small cohorts of children with cSLE [21,22]. These 2 studies reported greater activation of regions involved in attention (insula and superior temporal gyrus), working memory (parietal inferior gyrus), language (somatosensory cortex), and visuoconstructional ability (occipital and frontal cortices) in response to task-based stimuli and undersuppressed activity in the hippocampus and medial prefrontal cortex at rest in patients with cSLE with and without CD compared to controls. Generally, children and adolescents with cSLE are early in the disease course, have fewer confounding disease effects, little presence of comorbid conditions, and could evolve into more aggressive disease phenotypes compared to adults. Hence, they are the ideal population to understand early brain functional changes in patients with SLE. The aims of our



study therefore were to (i) examine if there are brain FC differences in adolescents with cSLE and HCs; (ii) evaluate if FC is associated with disease characteristics and glucocorticoid treatment in cSLE; and (iii) evaluate if FC is associated with cognitive performance in patients and controls and if these associations differ between groups.

## METHODS

### *Study design and participants*

This cross-sectional study utilised baseline data from a prospective longitudinal study examining the effects of cSLE on the structure and function of the developing brain conducted at The Hospital for Sick Children in Toronto, Canada. Patients between 10 and 17 years of age were consecutively recruited from the outpatient lupus clinic and age- and sex-matched HCs were recruited via advertising. Inclusion criteria for patients with cSLE included meeting 1997 American College of Rheumatology (ACR), System Lupus International Collaborating Clinics (SLICC), or 2019 European League Against Rheumatism/ACR SLE classification criteria [23–25]. Exclusion criteria for patients and HCs were a history of head trauma, current psychotropic medication use, and major hearing/vision problems or English language barriers that preclude the completion of cognitive assessments. Additional exclusion criteria for HCs were chronic illness, major neuropsychiatric conditions that significantly affect cognition, and glucocorticoid use. The study was approved by the institutional Research Ethics Board, and all participants and their parents provided written informed consent and/or assent as appropriate.

### *Study measures*

#### *Demographic and clinical variables*

Collected demographic variables were age, biological sex, self-reported ethnic or cultural origins, and level of education (eg, sixth grade is equivalent to 6 years of education). Data collection on ethnicity and Indigenous identity was categorised as Black, East Asian, Indigenous, Latin American, Middle Eastern, South Asian, Southeast Asian, White, or another ethnicity-based category, including multiple categories, in agreement with Canadian Institute for Health Information standards [26]. cSLE-related data included the following: SLE Disease Activity Index 2000 (SLEDAI-2K) collected most proximal to MRI scan date (within 2 months prior or following MRI scan date) with active disease defined as SLEDAI-2K  $\geq 4$ ; adjusted mean SLEDAI-2K (AMS), which is a cumulative measure of disease activity calculated as the area under the curve of SLEDAI-2K over time for the past 2 years or since cSLE diagnosis [27], whichever is shortest; presence of disease damage defined as SLICC/ACR Damage Index  $> 0$ ; disease duration (from diagnosis date to MRI scan date); presence of anti-dsDNA antibodies (positive  $> 35$  IU/mL from blood test most proximal to MRI scan date, range values of 9.8–666.9 IU/mL); proportion of patients with lupus nephritis (biopsy-proven or clinician diagnosis when biopsy unavailable); clinical NPSLE diagnosis (NPSLE manifestations requiring diagnostic work-up, eg, psychiatric consultation and/or neuroimaging, requiring specific treatment and demonstrating treatment response), and documented NPSLE concern (suspected NPSLE requiring diagnostic work-up, but subsequently not given clinical NPSLE diagnosis with specific treatment and documented response); current and cumulative glucocorticoid doses

(prednisone equivalent dose in milligrams); and other current treatments.

### *Cognitive assessments*

The following cognitive domains were assessed for all participants: visual attention, working memory, processing speed, and inhibition. Visual attention, specifically inattentiveness, was evaluated with the combined detectability, omissions, and commissions T-scores from the Conners Continuous Performance Test Third Edition (higher scores mean higher inattentiveness) [28]. Auditory working memory was assessed with the combined digit-span and letter-number sequencing scaled scores from either the Wechsler Intelligence Scale for Children Fifth Edition or the Wechsler Adult Intelligence Scale Fourth Edition, and lower scores indicate worse working memory [29]. The Delis–Kaplan Executive Function System-Color-Word Interference (DKEFS-CWI) test, specifically the naming/reading combined scaled score was utilised as a proxy for processing speed, because deficits in processing speed have been reported as significant contributors to decreased performance on these tasks [30,31]. Inhibition was evaluated with the DKEFS-CWI inhibition and inhibition/cognitive flexibility contrast scaled scores (minus naming/reading scores) [31,32]. For the DKEFS-CWI test, lower scores indicated worse performance.

### *MRI acquisition, preprocessing, and analysis*

Brain MRI was performed on a 3T Siemens Prisma Fit scanner with a 32-channel head coil and included whole-brain rs-fMRI, high-resolution T1-weighted anatomical, and dual-echo gradient-recall echo MRIs. Technical parameters for these acquisitions are described in the Supplementary Material (Acquisition Parameters). Anatomical and functional MRIs were preprocessed with the integrative software pipeline fMRIPrep, and all subsequent analyses were carried out with CONN 22.a in MatLabR2022. For further details on MRI preprocessing, see the Supplementary Material (fMRI Preprocessing-Technical Details) [33–35]. Voxel-wise group independent component analysis (ICA) was performed with G1 FastICA and GICA3 back-projection algorithm [36]. The total number of independent components was chosen in agreement with prior work [9]; components that spatially overlapped with CONN resting-state networks were selected with a template-matching procedure and visually inspected [37]. Group maps of selected components were thresholded to  $z = 3.29$  ( $P < .001$ ) and converted into network ROIs. Then, ROI-to-ROI FC matrices were calculated for all participants.

### *Statistical analyses*

Demographics were compared between groups using independent samples t-tests, chi-square test, or Mann–Whitney  $U$  tests, and cognitive variables were compared with analyses of covariance (ANCOVA) adjusted for education levels. ROI-to-ROI FC differences between patients and HCs and between patient subgroups classified according to features of ‘active’ disease and HCs were evaluated with age-adjusted general linear models. Post hoc sensitivity analysis was performed by removing patients with a clinical NPSLE diagnosis and NPSLE symptoms of concern and rerunning the main group analysis. Associations between FC and disease duration, current and cumulative disease activity scores, and glucocorticoid doses as well as their interactions were evaluated in the full cSLE group. Associations between FC and cognitive performance were evaluated in each group with age- and education-adjusted regression models and

Table  
Demographics and clinical characteristics for cSLE and healthy control groups

Demographic variable, median (IQR)	cSLE (n = 60)	HC (n = 59)
Age (y)	16 (13-16)	15 (14-16)
Biological female sex, n (%)	52 (86.7)	49 (83.1)
Ethnicity-based categories, n (%) <sup>a</sup>		
Black	8 (13.3)	4 (6.8)
East/South/Southeast Asian	12 (20) / 9 (15) / 8 (13.3)	5 (8.5) / 5 (8.5) / 2 (3.4)
Latin American	2 (3.3)	5 (8.5)
White	15 (25)	35 (59.3)
Other <sup>b</sup>	3 (5)	0
Multiple categories	3 (5)	3 (5.1)
Education level (y)	10 (9-12)	11 (9-12)
Disease characteristics, median (IQR)		
Duration (years since diagnosis)	0.93 (0.60-1.82)	-
SLEDAI-2K (current activity)	2.5 (0.75-5.25)	-
AMS (cumulative activity)	3.0 (1.48-7.03)	-
SDI (damage)	0 (0,0)	-
Anti-dsDNA positive, n (%)	35 (58.3)	-
Nephritis diagnosis, n (%)	23 (38.3)	-
NPSLE diagnosis, n (%)	2 (3.3)	-
Current glucocorticoid dose (mg)	0 (0,10)	-
Cumulative glucocorticoid dose (×10 <sup>3</sup> mg)	1.89 (0-6.03)	-
Immunosuppressant treatment, n (%)	Mycophenolate mofetil, 26 (43.3) Azathioprine, 3 (5.0) Methotrexate, 2 (3.3)	-
Cognitive assessments, median (IQR)		
CPT-3 (attention)	45 (41.1-52.7)	48 (44.2-56.5)
WISC/WAIS (auditory working memory)	10 (8-11.1)	10 (8.5-12.0)
DKEFS-CWI (processing speed) <sup>a</sup>	10.5 (8-12)	11 (10-12)
DKEFS-CWI (inhibition)	11 (9.75-12)	11(9-12)
DKEFS-CWI (inhibition/switching)	10 (9-12)	10 (9-12)

AMS, adjusted mean SLEDAI-2K; ANCOVA, analyses of covariance; cSLE, childhood-onset systemic lupus erythematosus; HC, healthy control; NPSLE, neuropsychiatric SLE; SDI, SLICC/ACR Damage Index; SLE, systemic lupus erythematosus; SLEDAI-2K, SLE Disease Activity Index 2000.  
Conners Continuous Performance Test Third Edition (CPT-3)—6 patients with cSLE and 4 HC had missing scores; Wechsler Intelligence Scale for Children Fifth Edition (WISC)/Wechsler Adult Intelligence Scale Fourth Edition (WAIS)—4 HC had missing scores; Delis—Kaplan Executive Function System—Color-Word Interference (DKEFS-CWI)—2 HC had missing scores.  
<sup>a</sup>  $P < .05$ , independent t-tests, ANCOVA, Mann–Whitney  $U$  tests, or chi-square tests.  
<sup>b</sup> ‘Other’ ethnicity-based category includes patients of Indigenous and Middle Eastern ethnicity.

compared between groups for those showing significant within-group associations. For each analysis, cluster-level inferences were calculated with family-wise error (FWE) threshold-free cluster enhancement (TFCE) nonparametric statistics (connection threshold  $P$ -few < .05, 10,000 permutations) [38]. Only pairs of ROI-to-ROI connections with  $P < .01$  were considered as part of significant clusters, given the number of group analyses performed (HCs versus patient group/subgroups) and variables of interest (5 clinical disease and 5 cognitive variables).

RESULTS

Group characteristics: demographic, clinical, and cognitive findings

Sixty adolescents with cSLE and 59 HCs aged 11 to 17 years were included in the study. Participant demographic information, cSLE disease characteristics, and cognitive scores for cSLE patients and HCs are reported in the Table. There were no differences in age, sex, and education level between the groups.  
For the cSLE group, 46 (77%) patients were diagnosed with cSLE less than 2 years prior to the assessment, 26 (43%) had current active disease, 23 (38%) had lupus nephritis, and 5 (8%) had disease damage. Only 2 patients had clinical NPSLE (patient #1: headaches, chorea/movement disorder, diplopia, and slurred speech; patient #2: severe anxiety, CD). Additionally, 15 cSLE patients (25%) had documented NPSLE concern, with headaches (11/15), mood disorders (7/15), anxiety disorders

(6/15), transient psychotic symptoms (5/15), and CD (5/15) as the most common symptoms, although no clinical diagnosis of NPSLE was made. All patients were taking hydroxychloroquine, and 31 (52%) were on immunosuppressant treatment, mainly mycophenolate mofetil (43%). In addition, 26 (43%) were on glucocorticoid treatment, while 16 (27%) were never exposed to glucocorticoids. All 23 patients with nephritis were exposed to glucocorticoids at some point during the disease course. In addition, 18 of them (78%) were currently prescribed glucocorticoids, and 22 of them (96%) were on immunosuppressant treatment.  
There were no group differences in most cognitive domains except for processing speed assessed with the combined colour-naming/word-reading scores from the DKEFS-CWI test, which were on average 9% lower in participants with cSLE compared to HCs (ANCOVA,  $F = 4.89$ ,  $P = .029$ ). The DKEFS-CWI combined measure of processing speed was mainly driven by the colour-naming scores (data not shown).

FC analysis across all participants

No participants were excluded for more than 20% of their BOLD timeseries volumes marked as outliers. Eleven networks (1 cerebellar, 2 default mode, 1 frontoparietal, 3 visual, 2 dorsal attention, 2 sensorimotor; Fig 1) were identified from 40 components decomposed with ICA (spatial similarity, correlation coefficient  $\geq 0.33$ ; spatial overlap, Dice coefficient  $\geq .30$ ), and their spatial maps were thresholded into 44 ROIs. The list of 44 ROIs,

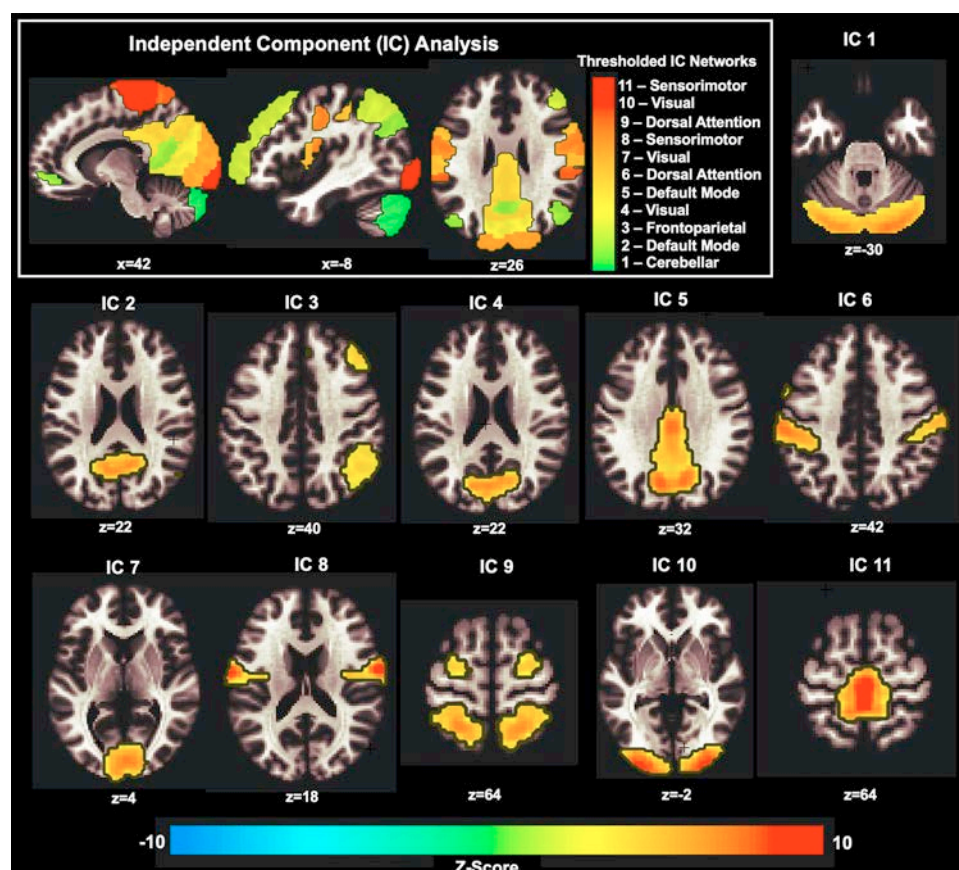


**Figure 1.** Eleven networks that spatially matched resting-state network templates were identified across all participants with independent component analysis (superimposed in sagittal and axial views—white box): cerebellar—IC 1; default mode—IC 2 and IC 6; frontoparietal—IC 3; visual—IC 4, IC 7, and IC 10; dorsal attention—IC 6 and IC 9; sensorimotor—IC 8 and IC 11. Group IC spatial maps (showed as axial cuts in MNI space) were thresholded and parcellations transformed into nodes/regions of interest (Z-score > 3.29,  $P < .001$ ). IC, independent component; MNI, Montreal Neurological Institute.

brain regions underlying their peak locations, peak coordinates, and sizes are summarised in the Supplementary Table. There were no significant associations between FC and age or level of education in the entire cohort nor in each group separately.

### FC differences between groups

From the connectome of 44 ROIs (Fig 2, top panel), a cluster of 5 connections between 5 superior frontoparietal ROIs (TFCE = 66.07,  $P$ -FWE = .0001) overlapping with the dorsal attention network differed between cSLE and HC groups (Fig 2, bottom panel). Lower FC in the bilateral superior parietal lobule and superior frontal and left precentral gyri was observed in cSLE patients when compared to HCs (Fig 3).

When patients were categorised into subgroups according to cSLE characteristics (current/cumulative ‘active’ cSLE—SLEDAI-2K/AMS  $\geq 4$  versus ‘nonactive’ cSLE, nephritis diagnosis versus not nephritis diagnosis, presence of anti-dsDNA antibodies versus absence of anti-dsDNA antibodies from blood test), subgroup differences compared to HCs were driven by those subgroups of patients displaying each of these features (current active cSLE status, Fig 4; nephritis diagnosis, Fig 5; presence of anti-dsDNA antibodies, TFCE = 54.62,  $P$ -FWE = .003, Supplementary Fig S1 top panel; cumulative active cSLE status, TFCE = 43.62,  $P$ -FWE = .019, Fig S1 bottom panel) and included consistent clusters of frontoparietal ROIs located within the dorsal attention network and that expanded to the sensorimotor network. For example, the subgroup of patients with current ‘active’ disease status exhibited lower FC between extensive superior

frontoparietal regions (eg, supplementary motor cortex, precentral gyrus, supramarginal gyrus, right insular cortex; Fig 4A, B) and the left cerebellum (Fig 4C) when compared to HCs; yet, these differences were not found between the subgroup of patients with current ‘nonactive’ cSLE status and HCs or between cSLE subgroups. The subgroup of patients with nephritis also displayed superior frontoparietal connections (eg, medial portion of the precentral gyrus) with lower FC when compared to HC (Fig 5); no differences were found between the subgroup of patients without a nephritis diagnosis and HCs or between cSLE subgroups. Post hoc sensitivity analysis revealed that FC differences were only moderately driven by patients with NPSLE diagnosis/concern as reflected by slightly decreased but statistically significant TFCE statistics (TFCE = 52.21,  $P$ -FWE = .007 in the modified cSLE group compared to HCs) and no low FC between the right superior frontal gyrus and left superior parietal lobule in the modified cSLE group compared to controls (Supplementary Fig S2). There were no significant differences between patients with and without NPSLE diagnosis/concern.

### FC associations with disease activity scores and glucocorticoid dose in cSLE

In patients with cSLE, higher cumulative disease activity (AMS) scores were negatively associated with lower FC within regions of the dorsal attention network, specifically in portions of the precentral and the superior frontal gyri (left side) and the right cerebellum VIIb (Fig 6, left panel). The effects of AMS on



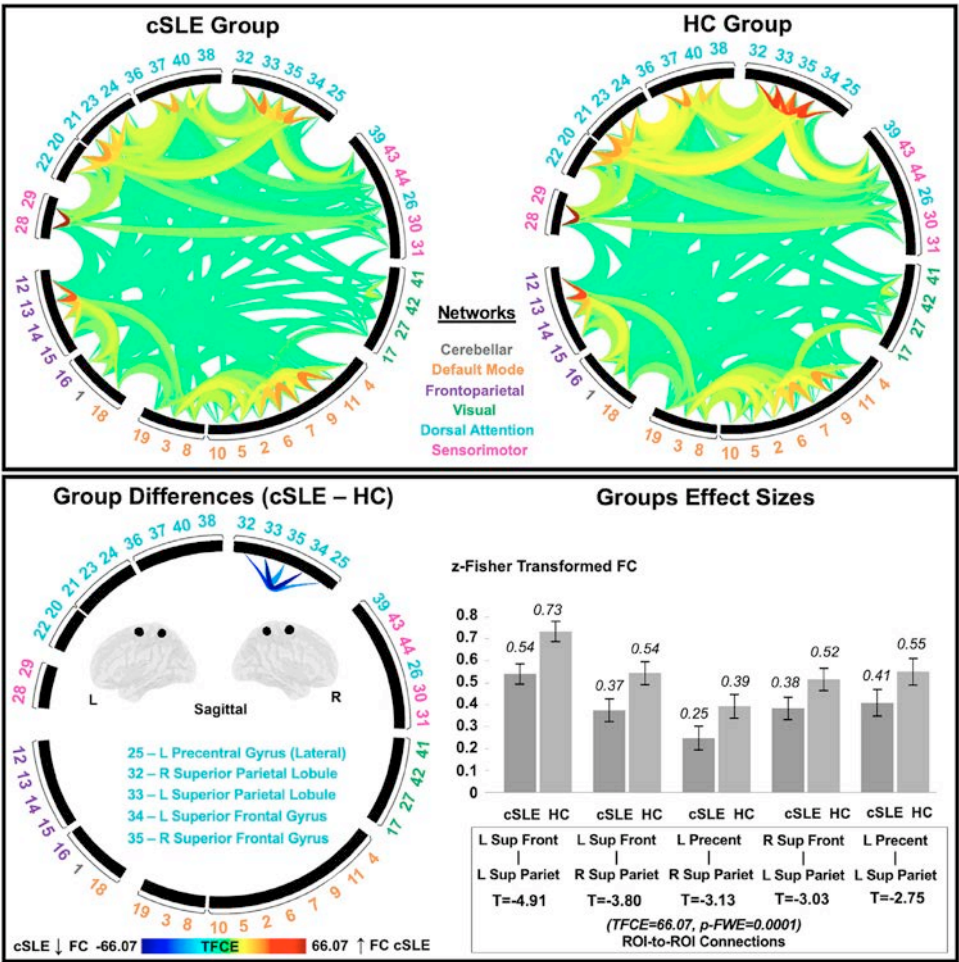


**Figure 2.** Lower functional connectivity within superior frontoparietal regions was observed in patients with cSLE when compared to HCs. Connections from 44 ROIs (connectome ring with numbered ROIs) in the cSLE and the HC groups (top panel) were compared with age-adjusted models. Lower FC (cSLE minus HC; bottom panel) was found between the bilateral superior frontal, parietal and the left precentral gyri in patients with cSLE when compared to HC. cSLE, childhood-onset systemic lupus erythematosus; FC, functional connectivity; FWE, family-wise error; HC, healthy control; ROI, region of interest; TFCE, threshold-free cluster enhancement.

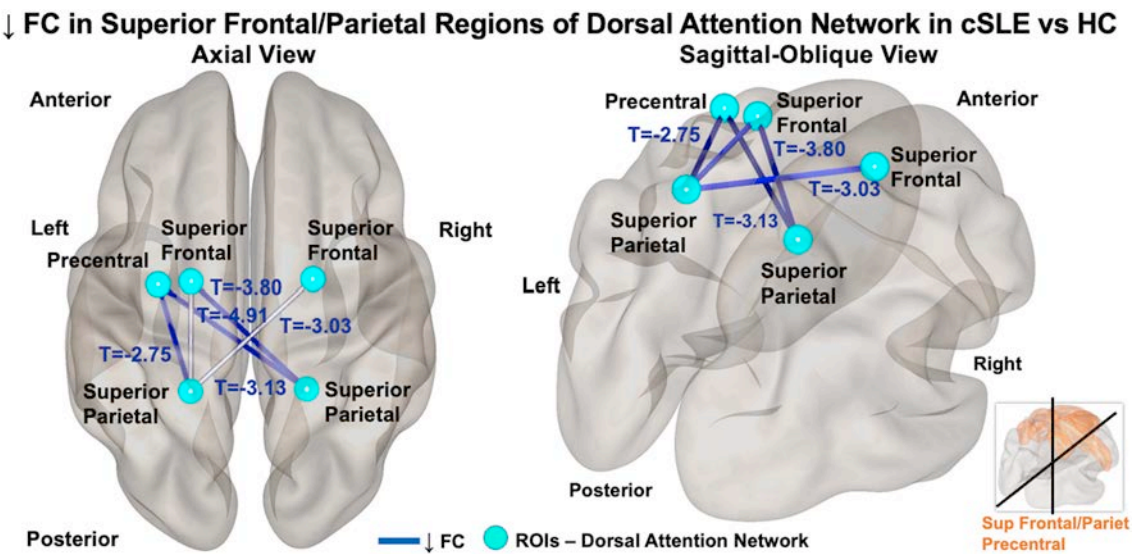


**Figure 3.** Lower functional connectivity was observed within superior frontoparietal regions of the dorsal attention network in patients with cSLE when compared to HCs (ROIs as spheres and lower FC as navy-blue lines). Brain structures that were consistently abnormal across all analyses were labelled as per Harvard-Oxford atlas and shown in orange in a thumbnail brain (lower right corner). cSLE, childhood-onset systemic lupus erythematosus; FC, functional connectivity; HC, healthy control; ROI, region of interest.



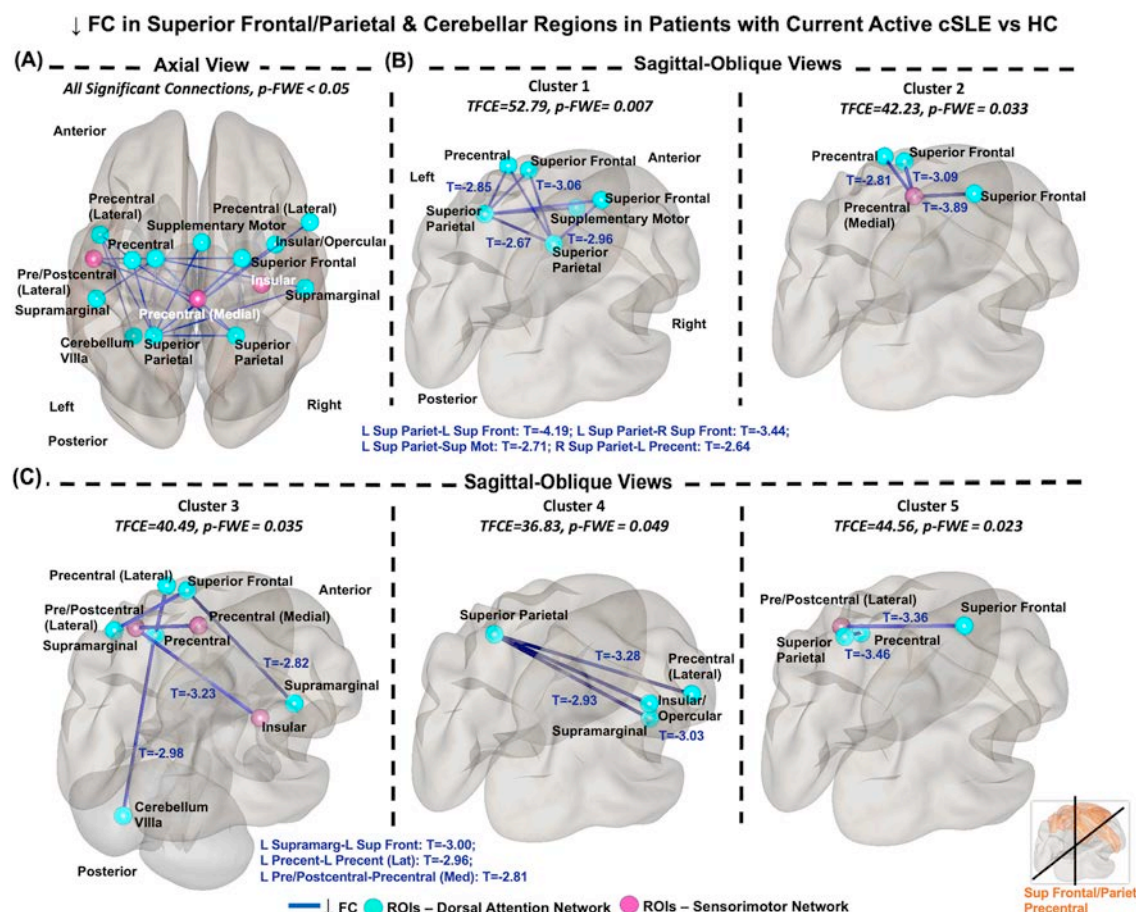


**Figure 4.** Lower functional connectivity (ROIs as spheres and lower FC as navy-blue lines; A) in 5 clusters spanning frontoparietal and cerebellar regions of the dorsal attention and sensorimotor networks (B, C) was observed in a subgroup of patients with current active cSLE status when compared to HCs. Brain structures that were consistently abnormal across all analyses were labelled as per the Harvard-Oxford atlas and shown in orange in a thumbnail brain (lower right corner). cSLE, childhood-onset systemic lupus erythematosus; FC, functional connectivity; FWE, family-wise error; HC, healthy control; ROI, region of interest; TFCE, threshold-free cluster enhancement.

FC remained significant, although slightly decreased, when the cumulative glucocorticoid dose was adjusted for ( $TFCE = 45.85$ ,  $P\text{-FWE} = .019$ ). Higher cumulative glucocorticoid dose was associated with lower FC between the lateral portion of the right precentral gyrus (dorsal attention network) and the left cerebellum VI (sensorimotor network; Fig 6, centre

panel). The effects of cumulative glucocorticoid dose on FC remained significant when the AMS score was adjusted for. Additionally, the strength of these effects increased to supplementary ROIs of the sensorimotor network, specifically in portions of bilateral pre/postcentral gyri and the insula (Fig 6, right panel). This highlights the unique although not completely

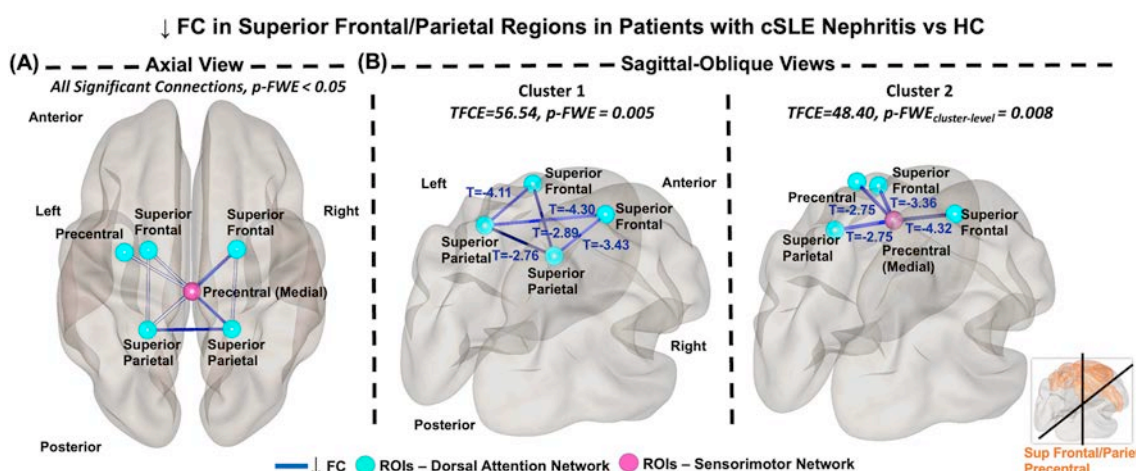


**Figure 5.** Lower functional connectivity (ROIs as spheres and lower FC as navy-blue lines; A) in 2 clusters spanning frontoparietal regions of the dorsal attention and sensorimotor networks (B) was observed in a subgroup of patients with nephritis when compared to HCs. Brain structures that were consistently abnormal across all analyses were labelled as per the Harvard-Oxford atlas and shown in orange in a thumbnail brain (lower right corner). cSLE, childhood-onset systemic lupus erythematosus; FC, functional connectivity; FWE, family-wise error; HC, healthy control; ROI, region of interest; TFCE, threshold-free cluster enhancement.

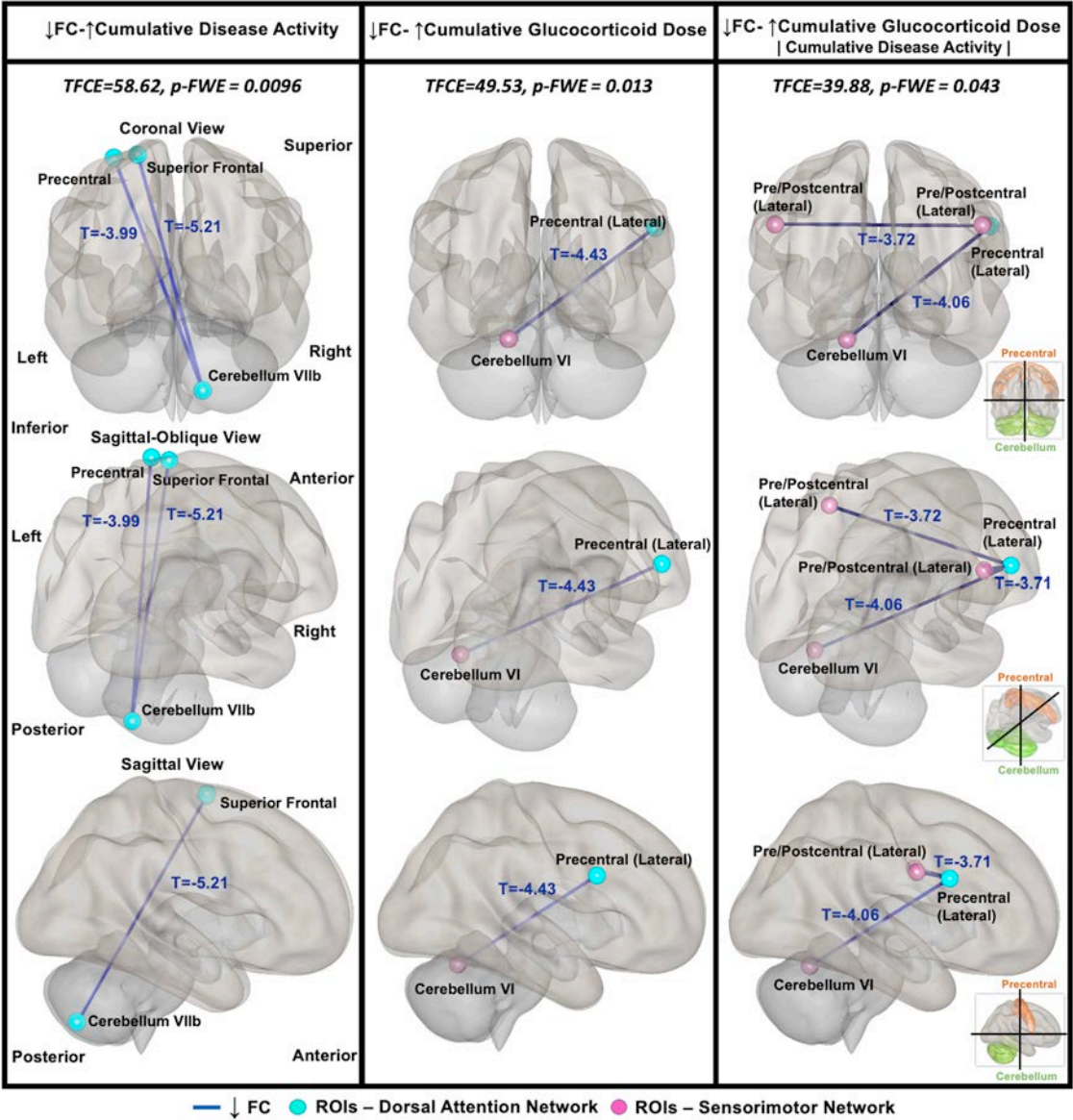


**Figure 6.** Lower functional connectivity (ROIs as spheres and negative associations with FC as navy-blue lines) between interhemispheric frontoparietal and cerebellar regions of the dorsal attention and sensorimotor networks was correlated with greater cumulative disease activity scores and glucocorticoid dose. Brain structures that were consistently abnormal across all analyses were labelled as per the Harvard-Oxford atlas and shown in orange in a thumbnail brain. FC, functional connectivity; FWE, family-wise error; ROI, region of interest; TFCE, threshold-free cluster enhancement.

independent contributions of the cumulative effects of disease activity and glucocorticoid dose on brain FC. There were no significant linear relationships between FC and disease duration, current disease activity (SLEDAI-2K) scores, or current glucocorticoid dose in the entire cSLE cohort.

*FC associations with cognitive performance in the cSLE and HC groups*

There was a positive association between FC and processing speed in a cluster of 4 connections within visual and sensorimotor networks. This cluster was comprised by the bilateral occipital pole, supracalcarine, right insular/opercular cortex, and the medial portion of the precentral gyrus (TFCE = 55.48,  $P$ -FWE = .010). Also, the effects of FC on processing speed scores between these ROIs in patients with cSLE strengthened after adjusting for the current glucocorticoid dose (Fig 7A). These associations were not found in the HC group. Moreover, correlations between weaker positive FC (and higher negative FC)

averaged across the 4 cluster connections and worse processing speed within the cSLE group appeared to be driven by patients with low scores, especially those with values 1.0 SD below the normative mean scaled score (DKEFS-CWI < 7.0; Fig 7B). No significant relationships between FC and other cognitive domains were found in the cSLE or HC groups.

**DISCUSSION**

This study contributes to the limited research on functional brain abnormalities in adolescents with cSLE. We identified brain regions that are part of established resting-state networks and found FC differences between cSLE patients and HCs that were driven by patient subgroups with active disease features. We also found linear associations among FC, cumulative disease activity, and glucocorticoid doses in cSLE patients. Furthermore, our findings indicated relationships between FC and cognitive performance, specifically with respect to processing speed in



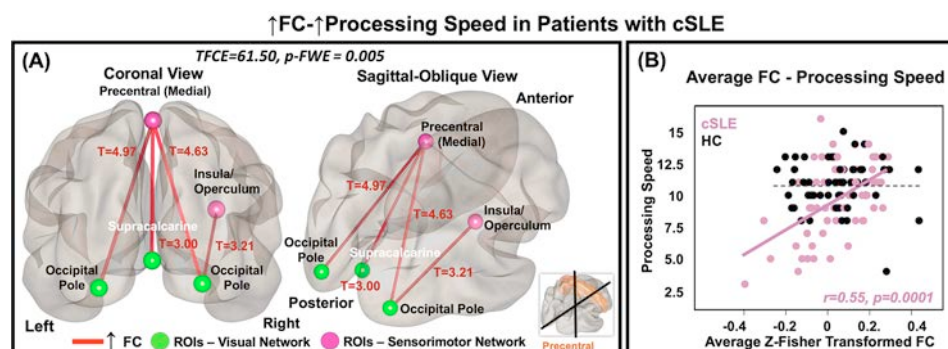


**Figure 7.** Higher functional connectivity (ROIs as spheres and positive associations with FC as red lines) between frontoparietal and occipital brain regions classified as part of visual and sensorimotor networks was correlated with greater (higher) processing speed scores in patients with cSLE (A). Participant's cluster FC values (averaged between all pairs of ROI connections) were displayed as a scatterplot against processing speed scores (B). Associations between FC and processing speed reported in the cSLE group were not observed in HCs. cSLE, childhood-onset systemic lupus erythematosus; FC, functional connectivity; FWE, family-wise error; HC, healthy control; ROI, region of interest; TFCE, threshold-free cluster enhancement.

cSLE. Our results therefore provide new insight into the impact of lupus on the functional organisation of the developing brain.

Less than 2 years had passed since the initial cSLE diagnosis in 77% of our patients, and the prevalence of clinical NPSLE (3%) and accumulated systemic organ disease damage (5%) in our cohort was low. Despite these mild clinical disease characteristics, our results revealed functional brain changes in cSLE patients when compared to controls. They suggest that pathological brain involvement may occur early in cSLE and often without a clinical NPSLE diagnosis. These group differences showed lower FC within superior frontoparietal regions, which are known for their role in visuospatial attention. Our results are in keeping with the results of a meta-analysis of 12 rs-fMRI studies that reported decreased brain activity in the superior frontal gyrus as part of a consistent pattern of functional abnormalities in adults with SLE [16]. Moreover, our results agree with other metrics of decreased brain activity, including lower degree centrality (DC) and fractional amplitude of low-frequency fluctuation, in the superior frontal and central gyri in non-NPSLE patients, and lower hemodynamic lag and DC in the superior parietal lobule in non-NPSLE/NPSLE patients [39–43]. Frontoparietal regions are vulnerable to inflammatory and immune-mediated injury in part due to their proximity to neuroimmune interfaces such as the blood–brain and the blood–cerebrospinal fluid barriers, their high levels of specific glutamate receptors and other synaptic proteins targeted by SLE autoantibodies, and their high metabolic demand. Furthermore, these regions, especially the prefrontal cortex, continue to develop through the adolescence, potentially making their functional connections more susceptible to immune-mediated processes during key neurodevelopmental stages [44]. Therefore, dysfunction in these frontoparietal areas might be a robust indicator of atypical brain function in cSLE.

In addition, FC differences across more extensive frontoparietal regions, including the supplementary motor cortex, and the cerebellum were found in groups of patients with features associated with active disease phenotypes when compared to the control group. Likewise, higher cumulative disease activity scores and cumulative glucocorticoid doses were negatively correlated with decreased long-range interhemispheric frontocerebellar FC. These results agree with 2 rs-fMRI studies that reported lower regional homogeneity, another indicator of functional activity, in the frontal and pre/postcentral gyri negatively correlated with higher SLEDAI scores in patients less than 2 years since SLE diagnosis and with glucocorticoid dose in non-NPSLE patients [12,15,39]. Thus, our results suggest that the

cumulative effects of lupus activity and flaring states over time combined with cumulative glucocorticoid exposure may negatively influence brain function in adolescents with cSLE ahead of a clinical NPSLE diagnosis and/or overt CD.

Our cSLE cohort displayed lower processing speed scores than controls. This was also the only domain where positive associations between visual-sensorimotor network FC and cognitive performance were found in cSLE but not in controls. It is noteworthy that several patients with decreased FC also had atypically low processing speed scores, suggesting a link between functional dysconnectivity across visual-motor networks and mild visual processing impairment in cSLE. No other SLE work has showed resting-state functional abnormalities across visual pathways associated with processing speed. Although, 1 rs-fMRI study reported opposite trends, specifically high FC within ‘task-negative’ (default mode) and between ‘task-negative’ and ‘task-positive’ (dorsal attention, visual) networks associated with low psychomotor speed and reaction time in SLE, and it was hypothesised that this might relate to suboptimal compensatory mechanisms in SLE patients [17]. Beyond SLE, 1 rs-fMRI study examined the effects of reading-training programs in older children and reported higher FC in visual-sensorimotor regions in children with reading difficulties versus typical readers before reading training and in visual-attention regions in both groups after reading training [45]. Additionally, a multimodal structural-functional MRI study in paediatric multiple sclerosis reported atrophy, diffusion abnormalities, and reduced FC in posterior parietal regions of adolescents with cognitive impairment when compared to those not impaired and HCs [46]. Given the crucial roles of occipital regions in visual pathways, associations between frontoparietal–occipital FC and processing speed may be an early compensatory mechanism employed by cSLE patients to achieve and sustain adequate cognitive performance [47].

It is noticeable that in our study, cSLE patients displayed regional FC patterns, specifically lower homotopic (connectivity between mirror regions across hemispheres) and heterotopic (mirrored connectivity between 2 different regions across hemispheres) FC when compared to controls and related to clinical variables. Two recent rs-fMRI studies reported abnormal homotopic connectivity in frontoparietal, temporal, and occipital regions of SLE patients compared to controls and associated with anxiety, attention, and abstraction in the SLE group [48,49]. This may be a consequence of early microstructural injury to commissural white matter (WM) fibres connecting equivalent cortical regions across hemispheres, specifically the

corpus callosum, as postulated in a structural MRI study in SLE patients and should be evaluated in future work [50].

There are some limitations to our study. First, we did not adjust for sex effects. We decided to not consider this variable as our study groups were matched by sex, and our cSLE cohort was imbalanced (87% of cSLE patients were females); therefore, the samples of certain subcategories were too small to make proper statistical inferences (eg, male cSLE patients). Nevertheless, we suggest considering biological sex when studying cohorts with a comparable number of female/male participants in each group. Second, the lack of an alternate disease group (eg, an additional control group diagnosed with a chronic autoimmune condition with a low risk of neuropsychiatric manifestations such as juvenile dermatomyositis) to test if, within these type of rheumatic disorders, abnormal brain FC is specific to cSLE. Third, we limited our analysis to static FC. Other rs-fMRI studies have combined FC with graph theory-based metrics and/or utilised dynamic analyses that allow to investigate specific timepoints/windows of the BOLD signal timeseries [11,14,42]. We performed several statistical tests; therefore, we limited our analysis to one metric of rs-fMRI activity to accomplish multiple comparisons without underpowering our analyses. Future work might include dynamic FC analyses and methods that might focus on FC between reciprocal voxels/regions across hemispheres such as voxel-mirrored homotopic connectivity. Future longitudinal work in larger cohorts could also help to distinguish between beneficial and nonbeneficial neuroplastic changes in cSLE with disease variability and to understand glucocorticoid effects with disease activity through time.

In conclusion, our study found lower FC in frontoparietal areas of adolescents with cSLE when compared to controls. These FC differences were stronger in patients with active disease features and higher disease activity scores. Moreover, increased FC between occipital and precentral regions was associated with better processing speed in patients with cSLE but not in controls. Taken together, these findings suggest that in adolescents with cSLE, brain functional abnormalities may occur early in the disease process, are influenced by cSLE activity, and can affect cognitive performance.

## Competing interests

All authors declare they have no competing interests.

## CRediT authorship contribution statement

**Diana Valdés Cabrera:** Writing – review & editing, Visualization, Software, Investigation, Writing – original draft, Validation, Methodology, Formal analysis, Conceptualization, Data curation. **Oscar Mwizerwa:** Validation, Investigation, Writing – review & editing, Methodology, Conceptualization. **Busi Zapparo:** Writing – review & editing, Methodology, Conceptualization, Validation, Investigation. **Asha Jeyanathan:** Project administration, Writing – review & editing, Data curation. **Lawrence Ng:** Writing – review & editing, Data curation, Project administration. **Tala El Tal:** Writing – review & editing, Methodology, Validation, Conceptualization. **Birgit Ertl-Wagner:** Validation, Writing – review & editing, Methodology. **Ann Yeh:** Writing – review & editing, Methodology, Validation. **Helen Branson:** Validation, Writing – review & editing, Methodology. **Adrienne Davis:** Writing – review & editing, Methodology, Validation. **Linda Hiraki:** Validation, Writing – review & editing, Methodology. **Deborah Levy:** Writing – review & editing, Methodology, Validation. **Ashley Danguécan:** Writing

– review & editing, Methodology, Validation, Investigation. **Andrea Knight:** Writing – review & editing, Validation, Methodology, Funding acquisition, Writing – original draft, Resources, Investigation, Conceptualization.

## Funding

This work was supported by Lupus Research Alliance [Novel Research Grant No. 481569, Empowering Lupus Research Career Development Award No. 935840] and US Department of Defense [Lupus Research Program Impact Award No. W81XWH-20-1-0560] grants (AK).

## Patient consent for publication

All participants and their parents provided written informed consent and/or assent for publication.

## Ethics approval

The study was performed in compliance with the World Medical Association Declaration of Helsinki and approved by the Hospital for Sick Children Research Ethics Board REB numbers 1000063027 (approval date July Fourth 2019, renewal date June 10th 2025) and 1000071306 (approval date February Fourth 2021, renewal date January 6th 2025).

## Provenance and peer review

Not commissioned; externally peer reviewed.

## Supplementary materials

Supplementary material associated with this article can be found in the online version at doi:10.1016/j.ard.2025.06.2129.

## Orcid

Diana Valdés Cabrera: <http://orcid.org/0000-0001-9374-5279>

Andrea Knight: <http://orcid.org/0000-0003-4278-9049>

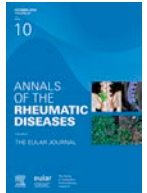
## REFERENCES

- [1] Hanly JG, Urowitz MB, Gordon C, Bae SC, Romero-Diaz J, Sanchez-Guerrero J, et al. Neuropsychiatric events in systemic lupus erythematosus: a longitudinal analysis of outcomes in an international inception cohort using a multi-state model approach. *Ann Rheum Dis* 2020;79(3):356–62. doi: 10.1136/annrheumdis-2019-216150.
- [2] Natoli V, Charras A, Hahn G, Hedrich CM. Neuropsychiatric involvement in juvenile-onset systemic lupus erythematosus (JSLE). *Mol Cell Pediatr* 2023;10(1):5. doi: 10.1186/s40348-023-00161-7.
- [3] Schwartz N, Stock AD, Putterman C. Neuropsychiatric lupus: new mechanistic insights and future treatment directions. *Nat Rev Rheumatol* 2019;15(3):137–52. doi: 10.1038/s41584-018-0156-8.
- [4] Seet D, Allameen NA, Tay SH, Cho J, Mak A. Cognitive dysfunction in systemic lupus erythematosus: immunopathology, clinical manifestations, neuroimaging and management. *Rheumatol Ther* 2021;8(2):651–79. doi: 10.1007/s40744-021-00312-0.
- [5] Lim LSH, Lefebvre A, Benseler S, Silverman ED. Longterm outcomes and damage accrual in patients with childhood systemic lupus erythematosus with psychosis and severe cognitive dysfunction. *J Rheumatol* 2013;40(4):513–9. doi: 10.3899/jrheum.121096.
- [6] Fox MD, Greicius M. Clinical applications of resting state functional connectivity. *Front Syst Neurosci* 2010;4:19. doi: 10.3389/fnsys.2010.00019.
- [7] Uddin LQ, Castellanos FX, Menon V. Resting state functional brain connectivity in child and adolescent psychiatry: where are we now? *Neuropsychopharmacology* 2024;50:196–200. doi: 10.1038/s41386-024-01888-1.



- [8] Lv H, Wang Z, Tong E, Williams LM, Zaharchuk G, Zeineh M, et al. Resting-state functional MRI: everything that nonexperts have always wanted to know. *AJNR Am J Neuroradiol* 2018;39(8):1390–9. doi: [10.3174/ajnr.A5527](https://doi.org/10.3174/ajnr.A5527).
- [9] Bonacchi R, Rocca MA, Ramirez GA, Bozzolo EP, Canti V, Preziosa P, et al. Resting state network functional connectivity abnormalities in systemic lupus erythematosus: correlations with neuropsychiatric impairment. *Mol Psychiatry* 2021;26(7):3634–45. doi: [10.1038/s41380-020-00907-z](https://doi.org/10.1038/s41380-020-00907-z).
- [10] Pentari A, Simos N, Tzarakis G, Kagiialis A, Bertsias G, Kavroulakis E, et al. Altered hippocampal connectivity dynamics predicts memory performance in neuropsychiatric lupus: a resting-state fMRI study using cross-recurrence quantification analysis. *Lupus Sci Med* 2023;10(2):e000920. doi: [10.1136/lupus-2023-000920](https://doi.org/10.1136/lupus-2023-000920).
- [11] Cao ZY, Wang N, Jia JT, Zhang HY, Shang SA, Hu JJ, et al. Abnormal topological organization in systemic lupus erythematosus: a resting-state functional magnetic resonance imaging analysis. *Brain Imaging Behav* 2021;15(1):14–24. doi: [10.1007/s11682-019-00228-y](https://doi.org/10.1007/s11682-019-00228-y).
- [12] Barracough M, McKie S, Parker B, Elliott R, Bruce IN. The effects of disease activity, inflammation, depression and cognitive fatigue on resting state fMRI in systemic lupus erythematosus. *Rheumatology (Oxford)* 2022;61(SI):SI39–47. doi: [10.1093/rheumatology/keab734](https://doi.org/10.1093/rheumatology/keab734).
- [13] Hou J, Lin Y, Zhang W, Song L, Wu W, Wang J, et al. Abnormalities of frontal-parietal resting-state functional connectivity are related to disease activity in patients with systemic lupus erythematosus. *PLoS One* 2013;8(9):e74530. doi: [10.1371/journal.pone.0074530](https://doi.org/10.1371/journal.pone.0074530).
- [14] Tan X, Liu X, Han K, Zhao L, Niu M, Yao Q, et al. Disrupted resting-state brain functional network properties in non-neuropsychiatric systemic lupus erythematosus patients. *Lupus* 2023;32(4):538–48. doi: [10.1177/09612033231160725](https://doi.org/10.1177/09612033231160725).
- [15] Liu S, Cheng Y, Xie Z, Lai A, Lv Z, Zhao Y, et al. A conscious resting state fMRI study in SLE patients without major neuropsychiatric manifestations. *Front Psychiatry* 2018;9:677. doi: [10.3389/fpsy.2018.00677](https://doi.org/10.3389/fpsy.2018.00677).
- [16] Wang L, Han K, Huang Q, Hu W, Mo J, Wang J, et al. Systemic lupus erythematosus-related brain abnormalities in the default mode network and the limbic system: a resting-state fMRI meta-analysis. *J Affect Disord* 2024;355:190–9. doi: [10.1016/j.jad.2024.03.121](https://doi.org/10.1016/j.jad.2024.03.121).
- [17] Nystedt J, Mannfolk P, Jönsen A, Nilsson P, Strandberg TO, Sundgren PC. Functional connectivity changes in core resting state networks are associated with cognitive performance in systemic lupus erythematosus. *J Comp Neurol* 2019;527(11):1837–56. doi: [10.1002/cne.24656](https://doi.org/10.1002/cne.24656).
- [18] Ma Y, Tie N, Ni S, Ma X, Qiao P. Correlation between the changes of brain amplitude of low-frequency fluctuation and cognitive impairment in patients with neuropsychiatric lupus. *Lupus* 2024;33(3):255–65. doi: [10.1177/09612033241228783](https://doi.org/10.1177/09612033241228783).
- [19] Valsasina P, Hidalgo de la Cruz M, Filippi M, Rocca MA. Characterizing rapid fluctuations of resting state functional connectivity in demyelinating, neurodegenerative, and psychiatric conditions: from static to time-varying analysis. *Front Neurosci* 2019;13:618. doi: [10.3389/fnins.2019.00618](https://doi.org/10.3389/fnins.2019.00618).
- [20] Mikdashi JA. Altered functional neuronal activity in neuropsychiatric lupus: a systematic review of the fMRI investigations. *Semin Arthritis Rheum* 2016;45(4):455–62. doi: [10.1016/j.semarthrit.2015.08.002](https://doi.org/10.1016/j.semarthrit.2015.08.002).
- [21] DiFrancesco MW, Holland SK, Ris MD, Adler CM, Nelson S, DelBello MP, et al. Functional magnetic resonance imaging assessment of cognitive function in childhood-onset systemic lupus erythematosus: a pilot study. *Arthritis Rheum* 2007;56(12):4151–63. doi: [10.1002/art.23132](https://doi.org/10.1002/art.23132).
- [22] DiFrancesco MW, Gitelman MW, Klein-Gitelman MS, Sagcal-Gironella ACP, Zelko F, Beebe D, et al. Functional neuronal network activity differs with cognitive dysfunction in childhood-onset systemic lupus erythematosus. *Arthritis Res Ther* 2013;15(2):R40. doi: [10.1186/ar4197](https://doi.org/10.1186/ar4197).
- [23] Hochberg MC. Updating the American College of Rheumatology revised criteria for the classification of systemic lupus erythematosus. *Arthritis Rheum* 1997;40(9):1725. doi: [10.1002/art.1780400928](https://doi.org/10.1002/art.1780400928).
- [24] Petri M, Orbai AM, Alarcón GS, Gordon C, Merrill JT, Fortin PR, et al. Derivation and validation of the systemic lupus international collaborating clinics classification criteria for systemic lupus erythematosus. *Arthritis Rheum* 2012;64(8):2677–86. doi: [10.1002/art.34473](https://doi.org/10.1002/art.34473).
- [25] Aringer M, Costenbader K, Daikh D, Brinks R, Mosca M, Ramsey-Goldman R, et al. 2019 European League Against Rheumatism/American College of Rheumatology Classification criteria for systemic lupus erythematosus. *Arthritis Rheumatol* 2019;71(9):1400–12. doi: [10.1002/art.40930](https://doi.org/10.1002/art.40930).
- [26] Canadian Institute for Health Information. Guidance on the use of standards for race-based and indigenous identity data collection and health reporting in Canada. Ottawa ON: CIHI; 2022. ISBN 978-1-77479-120-2. <https://www.cihi.ca/en/race-based-and-indigenous-identity-data#:~:text=Featured%20resources-,Guidance%20on%20the%20Use%20of%20Standards%20for%20Race%2DBased%20and,appropriate%20Use%20of%20the%20data>. Accessed April 14, 2025.
- [27] Ibañez D, Urowitz MB, Gladman DD. Summarizing disease features over time: I. Adjusted mean SLEDAI derivation and application to an index of disease activity in lupus. *J Rheumatol* 2003;30(9):1977–82.
- [28] Kao GS, Thomas HM. Test review: C. Keith Connors Connors 3rd edition Toronto, Ontario, Canada: Multi-Health Systems, 2008. *J Psychoeduc Assess* 2010;28(6):598–602.
- [29] Wilson AC. Cognitive profile in autism and ADHD: a meta-analysis of performance on the WAIS-IV and WISC-V. *Arch Clin Neuropsychol* 2024;39(4):498–515. doi: [10.1093/arclin/acad073](https://doi.org/10.1093/arclin/acad073).
- [30] Genova HM, DeLuca J, Chiaravalloti N, Wylie G. The relationship between executive functioning, processing speed, and white matter integrity in multiple sclerosis. *J Clin Exp Neuropsychol* 2013;35(6):631–41. doi: [10.1080/13803395.2013.806649](https://doi.org/10.1080/13803395.2013.806649).
- [31] Cichocki A, Kirsch A, Nicholson L. A - 38 Impact of working memory and processing speed on executive function performances in youth with attention-deficit/hyperactivity disorder and learning disorder. *Arch Clin Neuropsychol* 2024;39(7):973. doi: [10.1093/arclin/acad067.052](https://doi.org/10.1093/arclin/acad067.052).
- [32] Homack S, Lee D, Riccio CA. Test review: Delis-Kaplan executive function system. *J Clin Exp Neuropsychol* 2005;27(5):599–609. doi: [10.1080/13803390490918444](https://doi.org/10.1080/13803390490918444).
- [33] Power JD, Barnes KA, Snyder AZ, Schlaggar BL, Petersen SE. Spurious but systematic correlations in functional connectivity MRI networks arise from subject motion. *Neuroimage* 2012;59(3):2142–54. doi: [10.1016/j.neuroimage.2011.10.018](https://doi.org/10.1016/j.neuroimage.2011.10.018).
- [34] Satterthwaite TD, Elliott MA, Gerraty RT, Ruparel K, Loughead J, Calkins ME, et al. An improved framework for confound regression and filtering for control of motion artifact in the preprocessing of resting-state functional connectivity data. *Neuroimage* 2013;64(1):240–56. doi: [10.1016/j.neuroimage.2012.08.052](https://doi.org/10.1016/j.neuroimage.2012.08.052).
- [35] Behzadi Y, Restom K, Liu J, Liu TT. A component based noise correction method (CompCor) for BOLD and perfusion based fMRI. *Neuroimage* 2007;37(1):90–101. doi: [10.1016/j.neuroimage.2007.04.042](https://doi.org/10.1016/j.neuroimage.2007.04.042).
- [36] Calhoun VD, Adali T, Pearlson GD, Pekar JJ. A method for making group inferences from functional MRI data using independent component analysis. *Hum Brain Mapp* 2001;14(3):140–51. doi: [10.1002/hbm.1048](https://doi.org/10.1002/hbm.1048).
- [37] Nieto-Castanon A. Handbook of functional connectivity magnetic resonance imaging methods in CONN. Hilbert Press; 2020. ISBN: 978-0-578-64400-4. doi: [10.56441/hilbertpress.2207.6598](https://doi.org/10.56441/hilbertpress.2207.6598).
- [38] Smith SM, Nichols TE. Threshold-free cluster enhancement: addressing problems of smoothing, threshold dependence and localisation in cluster inference. *Neuroimage* 2009;44(1):83–98. doi: [10.1016/j.neuroimage.2008.03.061](https://doi.org/10.1016/j.neuroimage.2008.03.061).
- [39] Chen L, Sun J, Wang Q, Hu L, Zhang Y, Ma H, et al. Altered temporal dynamics of brain activity in multiple-frequency bands in non-neuropsychiatric systemic lupus erythematosus patients with inactive disease. *Neuropsychiatr Dis Treat* 2021;17:1385–95. doi: [10.2147/NDT.S292302](https://doi.org/10.2147/NDT.S292302).
- [40] Li X, Zhang P, Zhou W, Li Y, Sun Z, Chen J, et al. Altered degree centrality in patients with non-neuropsychiatric systemic lupus erythematosus: a resting-state fMRI study. *J Investig Med* 2022;70(8):1746–52. doi: [10.1136/jim-2021-001941](https://doi.org/10.1136/jim-2021-001941).
- [41] Piao S, Wang R, Qin H, Hu B, Du J, Wu H, et al. Alterations of spontaneous brain activity in systemic lupus erythematosus patients without neuropsychiatric symptoms: a resting-functional MRI study. *Lupus* 2021;30(11):1781–9. doi: [10.1177/09612033211033984](https://doi.org/10.1177/09612033211033984).
- [42] Papadaki E, Simos NJ, Kavroulakis E, Bertsias G, Antypa D, Fanouriakis A, et al. Converging evidence of impaired brain function in systemic lupus erythematosus: changes in perfusion dynamics and intrinsic functional connectivity. *Neuroradiology* 2022;64(8):1593–604. doi: [10.1007/s00234-022-02924-x](https://doi.org/10.1007/s00234-022-02924-x).
- [43] Wang Y, Jiang M, Huang L, Meng X, Li S, Pang X, et al. Altered functional brain network in systemic lupus erythematosus patients without overt neuropsychiatric symptoms based on resting-state functional magnetic resonance imaging and multivariate pattern analysis. *Front Neurol* 2021;12:690979. doi: [10.3389/fneur.2021.690979](https://doi.org/10.3389/fneur.2021.690979).
- [44] Sydnor VJ, Larsen B, Bassett DS, Alexander-Bloch A, Fair DA, Liston C, et al. Neurodevelopment of the association cortices: patterns, mechanisms, and implications for psychopathology. *Neuron* 2021;109(18):2820–46. doi: [10.1016/j.neuron.2021.06.016](https://doi.org/10.1016/j.neuron.2021.06.016).
- [45] Horowitz-Kraus T, DiFrancesco M, Kay B, Wang Y, Holland SK. Increased resting-state functional connectivity of visual- and cognitive-control brain networks after training in children with reading difficulties. *Neuroimage Clin* 2015;8:619–30. doi: [10.1016/j.nicl.2015.06.010](https://doi.org/10.1016/j.nicl.2015.06.010).
- [46] Rocca MA, Absinta M, Amato MP, Moiola L, Ghezzi A, Veggioni P, et al. Posterior brain damage and cognitive impairment in pediatric multiple sclerosis. *Neurology* 2014;82(15):1314–21.
- [47] Küchenhoff S, Sorg C, Schneider SC, Kohl O, Müller HJ, Napiórkowski N, et al. Visual processing speed is linked to functional connectivity between

- right frontoparietal and visual networks. *Eur J Neurosci* 2021;53(10):3362–77. doi: [10.1111/ejn.15206](https://doi.org/10.1111/ejn.15206).
- [48] Wang YL, Jiang ML, Huang LX, Meng X, Li S, Pang XQ, et al. Disrupted resting-state interhemispheric functional connectivity in systemic lupus erythematosus patients with and without neuropsychiatric lupus. *Neuroradiology* 2022;64(1):129–40. doi: [10.1007/s00234-021-02750-7](https://doi.org/10.1007/s00234-021-02750-7).
- [49] Ni S, An N, Li C, Ma Y, Qiao P, Ma X. Altered structural and functional homotopic connectivity associated with cognitive changes in SLE. *Lupus Sci Med* 2024;11(2):e001307. doi: [10.1136/lupus-2024-001307](https://doi.org/10.1136/lupus-2024-001307).
- [50] Nystedt J, Nilsson M, Jönsen A, Nilsson P, Bengtsson A, Lilja A, et al. Altered white matter microstructure in lupus patients: a diffusion tensor imaging study. *Arthritis Res Ther* 2018;20(1):21. doi: [10.1186/s13075-018-1516-0](https://doi.org/10.1186/s13075-018-1516-0).



## Myositis

## HLA loci heterozygosity modulates genetic risk in idiopathic inflammatory myopathies

Gang Chen<sup>1</sup>, Catherine Zhu<sup>2</sup>, Hector Chinoy<sup>3,4,5</sup>, Christopher I. Amos<sup>2,6,7</sup>, Andrew P. Morris<sup>3,4</sup>, Janine A. Lamb<sup>1,\*</sup>, International Myositis Assessment & Clinical Studies Group (IMACS) Myositis Genetics Scientific Interest Group (MYOGEN)

<sup>1</sup> Epidemiology and Public Health Group, School of Health Sciences, The University of Manchester, Manchester, UK

<sup>2</sup> Institute for Clinical and Translational Research, Baylor College of Medicine, Houston, TX, USA

<sup>3</sup> Centre for Musculoskeletal Research, Faculty of Biology, Medicine and Health, The University of Manchester, Manchester, UK

<sup>4</sup> NIHR Manchester Biomedical Research Centre, Manchester University NHS Foundation Trust, Manchester Academic Health Science Centre, Manchester, UK

<sup>5</sup> Department of Rheumatology, Salford Royal Hospital, Northern Care Alliance NHS Foundation Trust, Manchester Academic Health Science Centre, Salford, UK

<sup>6</sup> Epidemiology and Population Sciences, Department of Medicine, Baylor College of Medicine, Houston, TX, USA

<sup>7</sup> Dan L Duncan Comprehensive Cancer Center, Baylor College of Medicine, Houston, TX, USA

## ARTICLE INFO

## Article history:

Received 27 February 2025

Received in revised form 17 June 2025

Accepted 2 July 2025

## ABSTRACT

**Objectives:** Idiopathic inflammatory myopathies (IIMs) are rare autoimmune disorders. Genetic association studies have highlighted the role of human leukocyte antigen (HLA) polymorphisms in IIM. We aimed to characterise the nonadditive effects (dominance and interaction) of HLA alleles on IIM risk.

**Methods:** This study included a total of 3206 IIM cases and 11,697 controls of European ancestry. HLA alleles were imputed using a multiethnicity HLA reference panel. Logistic regressions were conducted to estimate the nonadditive effects of HLA alleles. Clinical subgroup analysis, calculation of phenotypic variance explained, and stepwise conditional analyses were conducted to further characterise these effects.

**Results:** We identified significant nonadditive effects in 5 HLA genes, particularly in the core alleles of ancestral haplotype 8.1 (8.1 AH), including *HLA-B\*08:01* ( $P = 3.93 \times 10^{-13}$ ), *HLA-C\*07:01* ( $P = 3.14 \times 10^{-8}$ ), *HLA-DQA1\*05:01* ( $P = 3.03 \times 10^{-9}$ ), *HLA-DQB1\*02:01* ( $P = 3.53 \times 10^{-23}$ ), and *HLA-DRB1\*03:01* ( $P = 8.47 \times 10^{-21}$ ). Notable risk difference between heterozygotes and homozygotes was observed in IIM, such as *HLA-DRB1\*03:01* (homozygote odds ratio [OR], 2.17; heterozygote OR, 3.13). In the interaction model, *HLA-DQA1* and *HLA-DRB1* showed specific significant allelic interactions. The nonadditive effect model explained a larger proportion of phenotypic variance than the model with additive effects alone. Conditional analysis indicated the independent nonadditive effect of *HLA-DRB1\*03:01* in 8.1 AH and amino acid residue Arg-74 in *HLA-DRB1*.

**Conclusions:** This study identified significant nonadditive effects within the HLA region of IIM. A genetic risk model including nonadditive effects could provide more accurate individual risk estimates. These findings highlight a complex role of HLA heterozygosity in the development of IIM and support further research into HLA nonadditive effects with clinical relevance.

\*Correspondence to Dr Janine A. Lamb.

E-mail address: [janine.lamb@manchester.ac.uk](mailto:janine.lamb@manchester.ac.uk) (J.A. Lamb).

Andrew P. Morris and Janine A. Lamb contributed equally to this work.

Handling editor Josef S. Smolen.

### WHAT IS ALREADY KNOWN ON THIS TOPIC

- Previous studies have identified multiple human leukocyte antigen (HLA) alleles significantly associated with the risk of idiopathic inflammatory myopathies (IIMs).
- HLA heterozygotes carry expanded antigen response repertoires, increasing the risk of autoimmunity.

### WHAT THIS STUDY ADDS

- This study characterised distinct risk patterns in the HLA and non-HLA regions associated with IIM.
- We identified significant nonadditive effects (dominance and interaction) within the HLA region.
- The nonadditive effect model explained a larger proportion of phenotypic variance than the model with additive effects alone.
- Conditional analysis identified independent HLA alleles and amino acid residues with nonadditive effects.

### HOW THIS STUDY MIGHT AFFECT RESEARCH, PRACTICE OR POLICY

- Nonadditive effects in the HLA region highlight the potential impact of HLA heterozygosity on IIM pathogenesis and support further research into its clinical relevance.
- A genetic risk model incorporating nonadditive effects could provide more accurate individual risk estimates.

## INTRODUCTION

Idiopathic inflammatory myopathies (IIMs) are a group of rare autoimmune disorders primarily characterised by muscle weakness and inflammation [1]. Clinically, IIM can be classified into dermatomyositis (DM), juvenile DM (JDM), polymyositis (PM), and inclusion body myositis (IBM) [2,3]. Each IIM subgroup has its own unique symptoms and recommended treatment. Myositis-specific autoantibodies (MSAs) can serve as a further tool to classify IIM cases [3,4]. The association of serological markers with clinical outcomes implicates their complicated role in abnormal autoimmune activation and persistence [1,3,5]. The most common MSAs, anti-Jo1 autoantibodies, are detected in nearly 30% of adult IIM patients in Europe [6].

In the past decade, the International Myositis Genetics Consortium (MYOGEN) aggregated the largest collection of IIM genome-wide association studies (GWAS) comprising individuals of European ancestry [7,8]. The GWAS identified the human leukocyte antigen (HLA) region as the locus with the strongest IIM association signal, pinpointing the elevated genetic risk of the HLA 8.1 ancestral haplotype (8.1 AH) [7,8]. HLA variants have long been linked to autoimmune conditions due to their unique role in presenting internal peptides and external antigens [9,10]. The later MYOGEN investigation of MSAs confirmed their association with specific HLA alleles [11]. However, it remains unclear how HLA polymorphisms affect the antigen-presenting process, the subsequent autoimmune response, and antibody production.

Elucidation of the HLA allele risk pattern may shed light on immunogenetic mechanisms. The additive genetic model assumes that each allele contributes independently, and the log-risk of disease accumulates in a linear manner [12]. Additive effects have been widely observed in non-HLA variants, although not in the HLA region [13–15]. Widespread nonadditive effects, including dominance and interaction, were identified within the HLA region in 4 autoimmune conditions, including rheumatoid arthritis, type 1 diabetes, psoriasis, and

celiac disease [13]. An early study of familial IIM suggests that homozygosity of the *HLA-DQA1* locus is a unique genetic risk factor that is not observed in sporadic cases [16]. Recent MYOGEN studies also observed a lower risk in *HLA-DRB1\*03:01* and *HLA-DRB1\*01:01* homozygotes with IBM, implying potential deviations from additivity [17]. The deviation in heterozygote risk could derive from the expanded antigen-presenting repertoire, as 2 HLA alleles function divergently [9,18].

Here, we systematically examined the nonadditive risk of HLA alleles of IIM and their subtypes to more accurately reflect individual risk. Conditional analysis of the 8.1 AH and amino acids further clarified independent signals with nonadditive effects.

## METHODS

### Study population

This study used 2 IIM cohorts established by MYOGEN. Before deduplication, the ImmunoChip and GWAS Illumina array cohorts consisted of 2688 and 1710 IIM cases of European ancestry, respectively. After removing duplicated or highly related samples between the 2 cohorts, 2589 cases and 7482 controls in the ImmunoChip dataset and 617 cases and 4215 controls in the GWAS Illumina array dataset were retained. Control samples were obtained from geographically matched consortia. The IIM subtypes included PM, DM, JDM, IBM, and anti-Jo1. The dataset in this study is consistent with the recent MYOGEN meta-analysis [19], with the addition of IBM cases. More details on the clinical and serological classification criteria can be found in previous MYOGEN studies [7,8,19].

### Genotyping, quality control, and imputation

Genotyping of the MYOGEN cohorts was conducted at the University of Manchester, UK and the Feinstein Institute, US. Standard quality control was then applied, and highly related and duplicated samples between the 2 cohorts were excluded. HLA alleles were imputed using the multiethnicity HLA reference panel on the Michigan Imputation Server [20]. Genome-wide imputation was performed using the Trans-Omics for Precision Medicine reference panel [21]. Details regarding genotyping, quality control, and imputation are available in previous meta-analyses [19]. In the nonadditive effect analysis, we further compared imputed HLA allele frequencies in cohort controls with those in the European population and reviewed the correlation between imputation quality and *P* value significance to avoid imputation artefacts [20].

### Homozygote and heterozygote risk

To compare the risk patterns of HLA and non-HLA variants, we calculated the odds ratios (ORs) for heterozygous and homozygous carriers against noncarriers. The HLA alleles in this study have at least 10 homozygous cases of IIM or the tested subtype. Non-HLA single-nucleotide polymorphisms (SNPs) were selected based on the *P* value in the MYOGEN fixed-effects meta-analysis ( $P < 5 \times 10^{-6}$ ) [19]. The OR and CI calculations were performed using the ‘epitools’ package [22] in R (R Foundation for Statistical Computing). The heterozygote proportions were calculated using Plink 1.9 [23] and visualised as De Finetti diagrams.



### Nonadditive effect analysis

The classical HLA class I and II genes (*HLA-A*, *-B*, *-C*, *-DRB1*, *-DQA1*, *-DQB1*, *-DPA1*, and *-DPB1*) were included in the nonadditive association tests, with only alleles meeting the criterion of 10 homozygotes in the cases included. The statistical framework we used is similar to previous studies on nonadditive effects [13,24,25]. Briefly, logistic regression was used to construct the case-control allele risk model. The nonadditive terms capture both dominance and intralocus interaction effects between the 2 alleles at a single HLA locus. After including nonadditive terms, the likelihood ratio test was employed to assess model fit improvement. In all models, 5 principal components (PCs; derived from the genetic relationship matrix using Plink) and sex (biological characteristics) were included as covariates [23]. The analysis details and model formulae are available in the [Supplementary Methods](#). In the omnibus gene model, the most common allele was designated as the reference. Noncarriers were used as the reference group for effect size estimation of individual alleles. Statistical significance levels were corrected using the Bonferroni method. We primarily applied the statistical test to the ImmunoChip cohort, with the GWAS array cohort serving as an independent validation. HLA alleles were imputed and represented in 2 formats: allele dosages, representing the expected allele copy number (ranging from 0 to 2) based on posterior imputation probabilities, and best-guess genotypes, defined as the most probable genotype at each locus. Initial analyses employed best-guess genotypes in both cohorts, while dosage data were used for validation.

### Conditional analysis

Linkage disequilibrium (LD), as measured by  $r^2$ , was calculated in the ImmunoChip cohort controls using Plink 1.9 [23]. Forward stepwise conditioning analysis was conducted in 8.1 AH and *HLA-DRB1*. The amino acid sequences of *HLA-DRB1* alleles were obtained from the International Immunogenetics Information System HLA database [26]. In the analysis, the model started with only covariates (5 PCs and sex). We subsequently added the additive term and nonadditive dominance variable to the model and reported their significance in model fitness improvement. After the inclusion of both additive and dominance terms, the alleles' contribution to model fit improvement was compared to select which allele was to be added to the model in the next conditioning. The model details are available in the [Supplementary Methods](#). This process was repeated to identify independent significant alleles until none met a Bonferroni corrected significance threshold ( $P < .05$ ).

### Calculation of phenotypic variance explained

The liability threshold model was used to calculate the proportion of phenotypic variance explained by a specific HLA locus [13,27]. The model posits that the underlying distribution of genetic factors contributes to an individual's liability to develop the disease. An individual will manifest the disease when their liability exceeds a certain threshold. The explained phenotypic variance was calculated by measuring differences among genotype liability distributions [27].

The prevalence of IIM was set at 0.01% [5]. The OR of HLA allele combinations approximates the relative risk (RR) in the population. The RR of specific allele combination groups were calculated using effect sizes from the additive model, nonadditive dominance model, and nonadditive interaction model. Rare

alleles were aggregated into the complementary allele group. Using these genetic RRs, we constructed  $n$  distributions (each with a different mean) for  $n$  allele combinations. After determining the penetrance of each combination and calculating the variance among mean liabilities, we quantified the proportion of variance in liability attributed to the specific HLA locus by  $V_{exp} = \frac{V_{between}}{V_{within} + V_{between}} = \frac{V_{between}}{1 + V_{between}}$ .  $V_{exp}$  is the proportion of variance in liability explained by the specific HLA locus.  $V_{between}$  is the variance between genotype-specific liability distributions.  $V_{within}$  is the variance within genotype-specific liability distributions.

## RESULTS

### HLA region shows evidence of nonadditive effects in IIM

The cohort characteristics and imputation quality are provided in [Supplementary Tables S1](#) and [S2](#). For the IIM analysis, 36 common HLA alleles were determined based on the criterion of a minimum of 10 homozygous cases ([Supplementary Table S3](#)). We calculated the ORs and 95% CIs of common HLA alleles for homozygotes and heterozygotes vs noncarriers to observe the risk pattern of the variants in IIM ([Supplementary Table S4](#)). In the HLA region, 5 alleles, all part of the 8.1 AH, including *HLA-B\*08:01*, *HLA-C\*07:01*, *HLA-DQA1\*05:01*, *HLA-DQB1\*02:01*, and *HLA-DRB1\*03:01*, showed deviations from log-OR additivity ([Fig 1A](#) and [Supplementary Table S4](#)). However, non-HLA variants did not show similar additivity deviations ([Fig 1B](#)). The elevation of heterozygote ORs was also observed in the GWAS array dataset ([Supplementary Table S4](#)

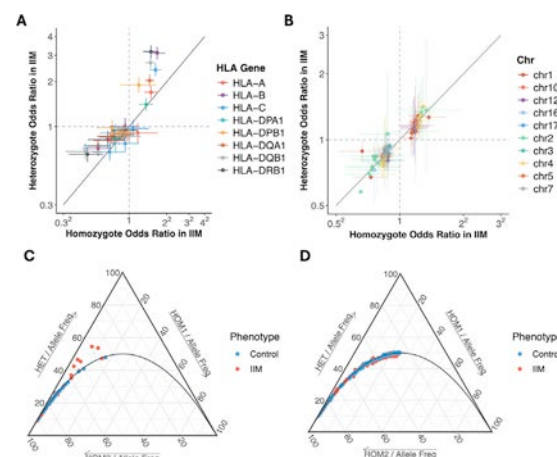


**Figure 1.** Human leukocyte antigen (HLA) and non-HLA variant risk patterns in idiopathic inflammatory myopathies (IIMs). (A) Comparison of odds ratios (ORs) for common high-resolution HLA allele heterozygotes and homozygotes in the ImmunoChip cohort. The allele noncarriers served as the reference group, with a risk set to 1. The solid line represents the expected relationship under the additive assumption. Error bars indicate 95% CIs. (B) Comparison of ORs for non-HLA variants in the ImmunoChip dataset ( $P$  value  $< 5 \times 10^{-6}$  in previous meta-analysis). The OR calculation and visualisation used here are the same as those of HLA alleles. The SNP noncarriers served as the reference group, with a risk set to 1. (C) De Finetti diagrams of common high-resolution HLA alleles in the ImmunoChip cohort cases and controls. Dots represent observed frequencies of homozygotes and heterozygotes, while the solid line shows the expected proportion of heterozygotes under the Hardy-Weinberg equilibrium. (D) De Finetti diagrams of non-HLA variants in the ImmunoChip dataset ( $P$  value  $< 5 \times 10^{-6}$  in the previous meta-analysis). Chr, chromosome; HET, individuals carrying one copy of the HLA allele (heterozygous); HOM1, individuals carrying two copies of the allele (homozygous); HOM2, individuals carrying no copies of the allele (non-carriers).

and [Supplementary Fig S1A](#)). The departure from Hardy-Weinberg equilibrium (HWE) in IIM cases could be another indicator of nonadditive effects. We calculated the homozygote proportions of HLA alleles and non-HLA variants in cases and controls. Only HLA alleles in IIM cases showed significant HWE deviation ([Fig 1C,D](#) and [Supplementary Fig S1B](#)).

### Five HLA alleles show a significant nonadditive effect in IIM

We used logistic regression to test whether the inclusion of the dominance term improves risk model fit. The dominance term represents potential dominant, recessive, or heterozygote advantage/disadvantage effects. The multiallelic HLA locus omnibus nonadditive test identified significant improvement in risk model fit for 5 HLA genes (*HLA-B*:  $P = 1.01 \times 10^{-11}$ ; *HLA-C*:  $P = 1.93 \times 10^{-6}$ ; *HLA-DQA1*:  $P = 1.50 \times 10^{-8}$ ; *HLA-DQB1*:  $P = 1.40 \times 10^{-21}$ ; *HLA-DRB1*:  $P = 1.10 \times 10^{-19}$ ). Excluding individuals without 2 imputed dosage alleles or using complement alleles yielded similar omnibus test results ([Supplementary Table S5](#)). Subsequent tests of each specific allele revealed that 5 alleles of these HLA genes showed significant nonadditive effects: *HLA-B\*08:01*, *HLA-C\*07:01*, *HLA-DQA1\*05:01*, *HLA-DQB1\*02:01*, and *HLA-DRB1\*03:01* ([Table](#)). After adjusting for sex and population structure in the logistic model, heterozygotes carrying these alleles showed elevated risk of IIM. The most significant nonadditive effect was *HLA-DRB1\*03:01*, where the heterozygote risk (OR, 3.13; 95% CI, 2.84-3.46) was higher than the homozygote risk (OR, 2.17; 95% CI, 1.62-2.91), suggesting a potential overdominance effect. The validation analysis of imputed allele dosages in the ImmunoChip dataset produced results consistent with the best-guess approach ([Supplementary Table S6](#)). We also validated the 5 significant HLA alleles in the MYOGEN GWAS array cohort. Their nonadditive effect  $P$  values remained significant for all previously significant HLA alleles in the ImmunoChip dataset except *HLA-DQA1\*05:01*, despite the smaller sample size and different subtype composition ([Supplementary Table S7](#)).

Using the effect sizes of both additive and nonadditive models, we calculated the RR of different genotypes and estimated the explained phenotypic variance on the liability scale. The 5 HLA genes (*HLA-B*, *HLA-C*, *HLA-DQA1*, *HLA-DQB1*, and *HLA-DRB1*) accounted for a larger proportion of heritability compared with other HLA genes ([Supplementary Table S8](#)). The inclusion of nonadditive effects further increased their proportion of phenotypic variance explained, consistent with the improvement in model fit. For example, the genetic risk of *HLA-DRB1* in the purely additive model explained 1.38% of phenotypic variance (6.28% of heritability). Including nonadditive effects added an additional 0.35% to the phenotypic variance (1.58% of heritability). For *HLA-B*, *HLA-C*, *HLA-DQA1*, and *HLA-DQB1*, the nonadditive model improved phenotypic variance by 0.21%, 0.18%, 0.25%, and 0.49%, respectively.

### Nonadditive effects of sex stratification and IIM subtypes

The sex-stratified HLA dosage-based nonadditive effects remained significant, as observed in the main analysis ([Supplementary Table S9](#)). Males showed higher additive ORs for all 5 HLA alleles, while females exhibited a potentially stronger additivity deviation between heterozygote and homozygote ORs. In females, the heterozygote effect of *HLA-DRB1\*03:01* (OR, 2.95; 95% CI, 2.61-3.34) was larger than the homozygote effect (OR, 1.56; 95% CI, 1.06-2.28), which was not seen within the male group ([Supplementary Table S9](#)).

Nonadditive models of IIM subtypes demonstrated a better fit compared with purely additive models ([Supplementary Table S10](#)). Except for *HLA-C\*07:01* in DM, the nonadditive effects of the 5 HLA alleles (*HLA-B\*08:01*, *HLA-C\*07:01*, *HLA-DQA1\*05:01*, *HLA-DQB1\*02:01*, and *HLA-DRB1\*03:01*) in IIM remained significant in the DM, PM, IBM, and anti-Jo1 subtypes. Only *HLA-C\*07:01* (nonadditive  $P = 6.15 \times 10^{-3}$ ) reached the significance threshold for JDM, while *HLA-DQA1\*05:01* and *HLA-DQB1\*02:01* did not meet the significance level after multiple testing correction. *HLA-B\*08:01* and *HLA-DRB1\*03:01* were not tested for JDM due to low homozygote numbers.

**Table**  
Additive and nonadditive effect sizes of HLA alleles in IIM

HLA allele	Additive model			Nonadditive model (dominance)				
	P value	OR	95% CI	P value	Homozygote effect		Heterozygote effect	
					OR	95% CI	OR	95% CI
<i>HLA-B*07:02</i>	$7.75 \times 10^{-12}$	0.69	0.62-0.77	$9.58 \times 10^{-2}$	0.32	0.18-0.54	0.72	0.64-0.81
<b><i>HLA-B*08:01</i></b>	<b><math>7.84 \times 10^{-97}</math></b>	<b>2.59</b>	<b>2.37-2.83</b>	<b><math>3.93 \times 10^{-13}</math></b>	<b>2.76</b>	<b>2.04-3.73</b>	<b>3.09</b>	<b>2.79-3.42</b>
<i>HLA-C*03:04</i>	$4.85 \times 10^{-8}$	0.71	0.62-0.80	$6.98 \times 10^{-1}$	0.54	0.30-0.96	0.70	0.61-0.80
<i>HLA-C*06:02</i>	$1.20 \times 10^{-4}$	0.79	0.70-0.89	$2.97 \times 10^{-1}$	0.81	0.47-1.39	0.77	0.67-0.88
<b><i>HLA-C*07:01</i></b>	<b><math>2.00 \times 10^{-64}</math></b>	<b>2.00</b>	<b>1.85-2.17</b>	<b><math>3.14 \times 10^{-8}</math></b>	<b>2.62</b>	<b>2.07-3.32</b>	<b>2.33</b>	<b>2.12-2.57</b>
<i>HLA-C*07:02</i>	$3.97 \times 10^{-11}$	0.71	0.64-0.79	$3.69 \times 10^{-2}$	0.32	0.19-0.52	0.75	0.67-0.84
<i>HLA-DQA1*01:02</i>	$8.80 \times 10^{-18}$	0.68	0.63-0.75	$3.07 \times 10^{-3}$	0.31	0.22-0.44	0.74	0.67-0.82
<i>HLA-DQA1*02:01</i>	$7.04 \times 10^{-5}$	0.81	0.72-0.90	$1.97 \times 10^{-1}$	0.48	0.29-0.81	0.83	0.74-0.94
<b><i>HLA-DQA1*05:01</i></b>	<b><math>2.27 \times 10^{-39}</math></b>	<b>1.62</b>	<b>1.50-1.74</b>	<b><math>3.03 \times 10^{-9}</math></b>	<b>1.99</b>	<b>1.68-2.36</b>	<b>1.96</b>	<b>1.78-2.17</b>
<b><i>HLA-DQB1*02:01</i></b>	<b><math>1.21 \times 10^{-64}</math></b>	<b>1.92</b>	<b>1.78-2.07</b>	<b><math>3.53 \times 10^{-23}</math></b>	<b>2.04</b>	<b>1.67-2.49</b>	<b>2.60</b>	<b>2.36-2.86</b>
<i>HLA-DQB1*03:01</i>	$1.46 \times 10^{-5}$	0.83	0.76-0.90	$7.58 \times 10^{-1}$	0.69	0.53-0.90	0.82	0.74-0.91
<i>HLA-DQB1*06:02</i>	$2.22 \times 10^{-16}$	0.64	0.57-0.71	$7.09 \times 10^{-3}$	0.19	0.10-0.37	0.68	0.60-0.77
<b><i>HLA-DRB1*03:01</i></b>	<b><math>7.51 \times 10^{-96}</math></b>	<b>2.49</b>	<b>2.28-2.71</b>	<b><math>8.47 \times 10^{-21}</math></b>	<b>2.17</b>	<b>1.62-2.91</b>	<b>3.13</b>	<b>2.84-3.46</b>
<i>HLA-DRB1*07:01</i>	$6.62 \times 10^{-5}$	0.80	0.72-0.90	$3.46 \times 10^{-1}$	0.52	0.32-0.86	0.82	0.73-0.93
<i>HLA-DRB1*15:01</i>	$8.63 \times 10^{-19}$	0.62	0.55-0.69	$2.44 \times 10^{-2}$	0.21	0.11-0.39	0.65	0.58-0.73

HLA, human leukocyte antigen; IIM, idiopathic inflammatory myopathy; OR, odds ratio.

The  $P$  values reflect the significance levels of the model fit improvement when additive and nonadditive terms were subsequently included in the baseline model with only covariates. The ORs and 95% CIs are displayed for both the additive and nonadditive models. The noncarriers of the respective alleles were used as the reference group, with their risk set to 1. Heterozygous and homozygous genotype ORs were also calculated using the nonadditive model. HLA alleles with significant nonadditive model  $P$  values are marked in bold.

Nonadditive effects of HLA-DQA1 and HLA-DRB1 on specific allelic combinations

Nonadditive effects may result from heterozygous interactions between different alleles within the HLA locus rather than simple allele dominance. We constructed a nonadditive risk model incorporating allelic interactions and tested whether this model showed an improved fit compared with the dominance model. Among the 5 nonadditive HLA loci, *HLA-DQA1* ( $P = 8.58 \times 10^{-7}$ ) and *HLA-DRB1* ( $P = 1.59 \times 10^{-7}$ ) demonstrated improved model fit when the dominance term was replaced by the allelic interaction term (Supplementary Table S11). The additional phenotypic variance explained by *HLA-DQA1* (0.22%) and *HLA-DRB1* (0.22%) using allelic interaction effect sizes further confirmed the model improvement (Supplementary Table S6). In contrast, the phenotypic variance explained by *HLA-B*, *HLA-C*, and *HLA-DQB1* remained largely unchanged.

The effect sizes of allelic interactions within *HLA-DQA1* and *HLA-DRB1* were tested (Fig 2). *HLA-DQA1*\*05:01 and *HLA-DRB1*\*03:01 were identified with significant nonadditive dominance effects. In the allelic interaction model, *HLA-DQA1*\*01:02-*HLA-DQA1*\*05:01 (OR, 1.89;  $P = 2.6 \times 10^{-8}$ ), *HLA-DRB1*\*03:01-*HLA-DRB1*\*01:01 (OR, 2.56;  $P = 1.08 \times$

$10^{-7}$ ), and *HLA-DRB1*\*03:01-*HLA-DRB1*\*15:01 (OR, 3.11;  $P = 1.47 \times 10^{-8}$ ) significantly increased the genotype risk. *HLA-DRB1*\*03:01 also interacted with ‘other alleles’ (OR, 2.33;  $P = 2.1 \times 10^{-19}$ ), which included rare and nonclassical HLA alleles that could not be tested independently in the model. Other HLA allelic interactions did not meet the significance level after adjustment. Notably, the genotype risks of *HLA-DRB1*\*03:01-*HLA-DRB1*\*01:01 (OR, 2.01; 95% CI, 1.42–2.85), *HLA-DRB1*\*03:01-*HLA-DRB1*\*15:01 (OR, 1.25; 95% CI, 0.88–1.76), and *HLA-DRB1*\*03:01-*Others* (OR, 1.58; 95% CI, 1.17–2.14) exceeded the risk of the *HLA-DRB1*\*03:01 homozygotes reference group (Supplementary Table S12).

Independent nonadditive effect of HLA-DRB1\*03:01 and HLA-DQB1\*02:01 on 8.1 AH

As the core alleles of the HLA 8.1 AH, the LD between *HLA-B*\*08:01, *HLA-C*\*07:01, *HLA-DQA1*\*05:01, *HLA-DQB1*\*02:01, and *HLA-DRB1*\*03:01 was assessed (Fig 3A). *HLA-B*\*08:01 and *HLA-C*\*07:01, *HLA-DQB1*\*02:01 and *HLA-DRB1*\*03:01, and *HLA-B*\*08:01 and *HLA-DRB1*\*03:01 showed moderate LD ( $r^2 > 0.5$ ). We used the *HLA-B*\*08:01-*HLA-DRB1*\*03:01 as a proxy haplotype for 8.1 AH, which exhibited strong significance in both additive and nonadditive effects (Fig 3B).

A

	<i>HLA-DQA1</i>	*others	*01:01	*01:02	*02:01	*03:01	*05:01
<i>HLA-DQA1</i>	Additive OR	0.68 (0.53 - 0.88)	0.79 (0.66 - 0.94)	0.5 (0.41 - 0.60)	0.6 (0.46 - 0.79)	0.86 (0.74 - 1.01)	1(ref)
*05:01	1.00 (ref)	1.61 (1.19 - 2.17)	1.36 (1.09 - 1.70)	1.89 (1.51 - 2.36)	1.15 (0.84 - 1.59)	1.12 (0.91 - 1.38)	-
*03:01	0.86 (0.74 - 1.01)	0.84 (0.56 - 1.24)	0.70 (0.51 - 0.96)	0.97 (0.71 - 1.32)	1.54 (1.07 - 2.22)	-	0.279
*02:01	0.6 (0.46 - 0.79)	1.26 (0.78 - 2.06)	1.23 (0.82 - 1.83)	1.48 (0.99 - 2.20)	-	0.020	0.380
*01:02	0.5 (0.41 - 0.60)	1.52 (1.02 - 2.24)	0.74 (0.52 - 1.06)	-	0.056	0.840	2.60×10 <sup>-8</sup>
*01:01	0.79 (0.66 - 0.94)	1.08 (0.72 - 1.61)	-	0.104	0.314	0.025	0.006
*others	0.68 (0.53 - 0.88)	-	0.717	0.037	0.347	0.371	0.002

B

	<i>HLA-DRB1</i>	*others	*01:01	*04:01	*07:01	*15:01	*03:01
<i>HLA-DRB1</i>	Additive OR	0.68 (0.58 - 0.79)	0.79 (0.59 - 1.04)	0.6 (0.42 - 0.87)	0.61 (0.46 - 0.82)	0.4 (0.29 - 0.56)	1 (ref)
*03:01	1 (ref)	2.33 (1.94 - 2.80)	2.56 (1.81 - 3.61)	1.89 (1.21 - 2.97)	1.47 (1.01 - 2.13)	3.11 (2.10 - 4.61)	-
*15:01	0.4 (0.29 - 0.56)	1.38 (0.96 - 1.97)	0.62 (0.32 - 1.18)	1.64 (0.91 - 2.94)	1.55 (0.92 - 2.62)	-	1.47×10 <sup>-8</sup>
*07:01	0.61 (0.46 - 0.82)	1.38 (1.03 - 1.86)	1.12 (0.69 - 1.81)	1.54 (0.88 - 2.71)	-	0.103	0.043
*04:01	0.6 (0.42 - 0.87)	1.47 (1.00 - 2.18)	0.5 (0.25 - 0.98)	-	0.129	0.099	0.005
*01:01	0.79 (0.59 - 1.04)	0.97 (0.71 - 1.31)	-	0.043	0.647	0.145	1.08×10 <sup>-7</sup>
*others	0.68 (0.58 - 0.79)	-	0.822	0.052	0.032	0.081	2.10×10 <sup>-19</sup>

**Figure 2.** Nonadditive interaction effect of *HLA-DQA1* and *HLA-DRB1* combinations in idiopathic inflammatory myopathies. (A, B) Logistic regression model with an interaction term in the *HLA-DQA1* and *HLA-DRB1* regions. Common alleles and others (rare alleles aggregated) were included in the model. The additive odds ratio (OR) of human leukocyte antigen (HLA) alleles represents individual risk without interaction with others. Interaction ORs and their 95% CIs are presented in the upper triangle; corresponding *P* values are shown in the lower triangle (red colour indicates a significant interaction). The *HLA-DQA1*\*05:01 and *HLA-DRB1*\*03:01 were used as the reference (ref) allele, with a risk set to 1.



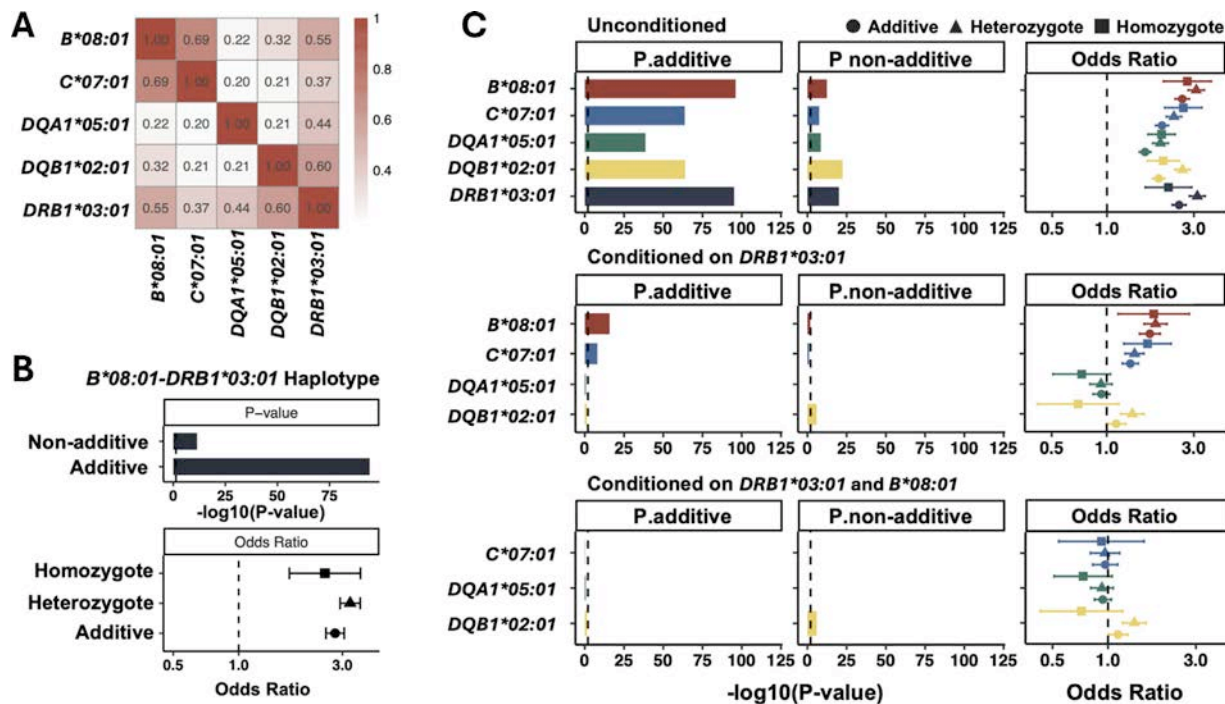


**Figure 3.** Additive and nonadditive effects of the 8.1 ancestral haplotype (8.1 AH). (A) Linkage structure of core alleles within the 8.1 AH. (B) *P* values and effect sizes of the additive and nonadditive effect tests for the 8.1 AH proxy (*HLA-B\*08:01-HLA-DRB1\*03:01*). The additive and nonadditive bars correspond to the model fit improvement test after including the additive and nonadditive term of *HLA-B\*08:01-HLA-DRB1\*03:01*. The odds ratios and 95% CIs for the additive model, heterozygotes, and homozygotes are reported relative to noncarriers of the haplotype. (C) Conditional analyses of the 8.1 AH alleles using both additive and nonadditive effects. P.additive and P.nonadditive indicate the significance level of the alleles at each round of conditioning. Conditioning alleles were selected based on the model fit improvement *P* value after including both additive and nonadditive terms. The dotted lines represent the Bonferroni-corrected significance threshold ( $P < .05$ ). Odds ratios and CIs for the additive model, heterozygotes, and homozygotes at each step are shown in the third column. The 3 rows of the plot show allele significance and effect with no allele conditioning, conditioned on *HLA-DRB1\*03:01*, and conditioned on both *HLA-DRB1\*03:01* and *HLA-B\*08:01*.

The conditional analysis further differentiated the independent additive and nonadditive effects within the 8.1 AH alleles (Supplementary Table S13). All 5 alleles showed significant additive and nonadditive effects when no alleles were conditioned. *HLA-DRB1\*03:01* was identified as having the strongest joint genetic effect (Fig 3C). After conditioning on *HLA-DRB1\*03:01*, *HLA-B\*08:01* and *HLA-C\*07:01* remained significant for additive effects, although no nonadditive effects persisted. *HLA-DQB1\*02:01* was the only allele showing a nonadditive effect after conditioning on *HLA-DRB1\*03:01*. After *HLA-B\*08:01* was added to the conditioned allele list, the additive effect of *HLA-C\*07:01* was no longer significant, but the nonadditive effect of *HLA-DQB1\*02:01* remained.

#### Independent nonadditive effect of Arg-74 on *HLA-DRB1*

The LD between *HLA-DRB1\*03:01* amino acids was evaluated (Supplementary Fig S2). The residues 26:tyrosine (26:Y), 71:lysine (71:K), 73:glycine (73:G), 74:arginine (74:R), and 77:asparagine (77:N) formed a tightly linked block in *HLA-DRB1*, which also showed a strong additive and nonadditive effect in the IIM risk model (Fig 4A and Supplementary Table S14). After conditioning on 74:R, the genetic effect of the remaining amino acids was largely decreased (Fig 4B and Supplementary Table S14).

## DISCUSSION

In this study, we observed a different risk pattern among several HLA alleles compared with non-HLA variants. We systematically investigated HLA nonadditive effects in IIM and its

subtypes, revealing allele dominance and allelic interaction effects.

Previous studies have established that HLA polymorphisms are strongly associated with autoimmune diseases [9]. Many association studies and meta-analyses of IIM have also identified significant signals in the HLA region [7,19,28–35]. These strong associations are rooted in the unique and indispensable role of HLA proteins in antigen presentation during the immune process [9,36]. Recent studies hypothesised that 2 different alleles at an HLA locus may expand the antigen-binding repertoire and increase the risk of presenting autoantigens, potentially leading to a greater heterozygote risk than expected [9,18]. Deviation from additivity of HLA alleles has been reported in several autoimmune conditions in European and Asian ancestry populations [13,14,25]. The divergence of risk patterns between HLA and non-HLA regions in IIM suggests that considering the impact of nonadditive effects is important when conducting association analyses in rare autoimmune diseases such as IIM. Selecting an appropriate risk model can increase statistical power and more precisely attribute risk to variants [37].

The nonadditive model showed a significant improvement in model fit compared with the additive model for the 8.1 AH IIM risk alleles *HLA-B\*08:01*, *HLA-C\*07:01*, *HLA-DQA1\*05:01*, *HLA-DQB1\*02:01*, and *HLA-DRB1\*03:01*. The 5 HLA alleles with nonadditive effects also contributed the strongest additive effect in IIM. Their nonadditive effect reflects allele dominance, with the heterozygote having a greater risk than expected. The nonadditive effect directions are more diverse in other autoimmune diseases. In the analysis by Lenz et al [13], 12 out of 14 nonadditive effect alleles had positive dominance components, but some HLA alleles exhibited a recessive effect. Interestingly,



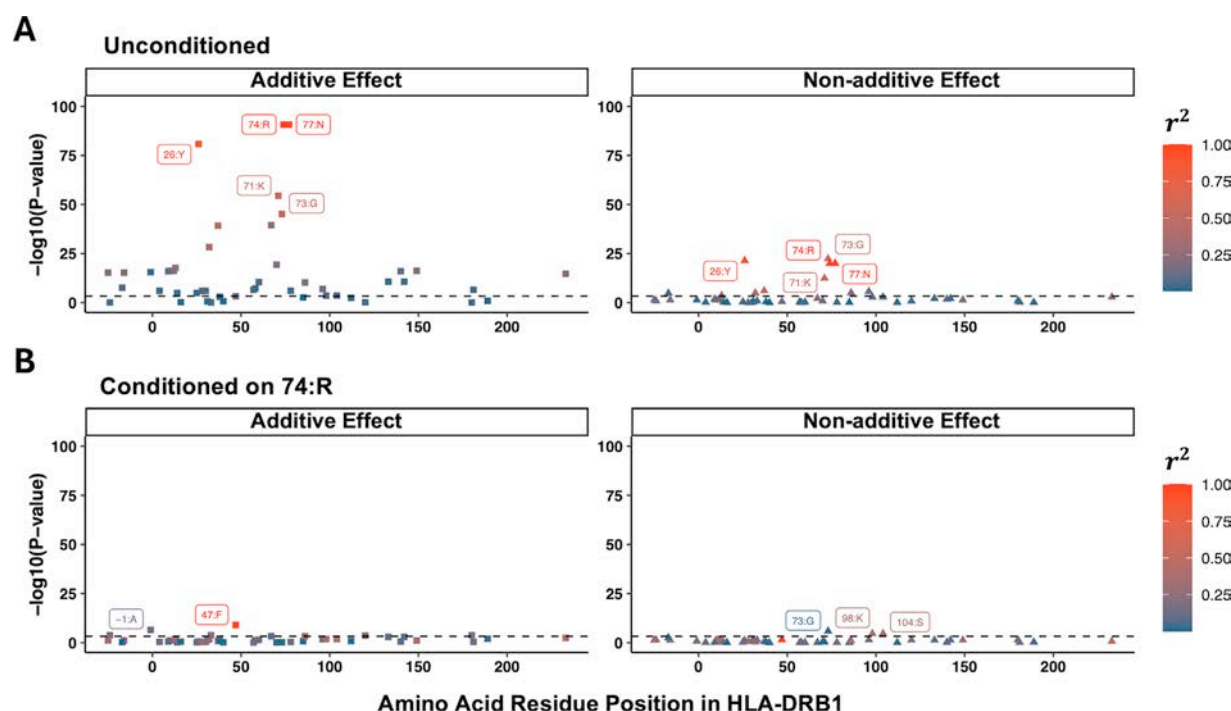


**Figure 4.** Stepwise conditional analyses of amino acid residues in *HLA-DRB1\*03:01*. (A) Unconditioned. (B) Conditioned on 74:arginine (74:R). The conditioning residues were selected based on their combined additive and nonadditive effects. The ‘additive effect’ and ‘nonadditive effect’ panel displays the significance levels of amino acids in each round of conditioning. The dotted lines indicate the Bonferroni-corrected significance threshold ( $P < .05$ ). The top amino acids with the strongest significance are labelled. Colours represent the linkage disequilibrium ( $r^2$ ) between the marked residues and the residue with the strongest significance. 71:K, 71:lysine; 77:N, 77:asparagine; 73:G, 73:glycine; 26:Y, 26:tyrosine; -1:A, -1:alanine; 47:F, 47:phenylalanine; 98:K, 98:lysine; 104:S, 104:serine.

some studies have reported that homozygous genotypes are at increased risk of infectious diseases or cancer, which manifests the ‘heterozygote advantage’ of certain variants in preventing the acquisition of these diseases [38–40]. It is reasonable to speculate that the divergence in HLA allele antigen-binding affinity leads to an expanded antigen-presenting repertoire in heterozygotes, increasing the risk of autoimmunity but potentially preventing infections or cancer. However, the mechanism could be more complex for specific autoimmune conditions. For example, the nonadditive effect in ulcerative colitis suggests that HLA homozygosity might impair the ability to appropriately control colonic microbiota [41]. Some studies suggest that homozygosity is associated with antibody production, indicating that the immune response may be more intense in homozygotes [42]. This hypothesis needs further experimental validation in IIM.

In the subtype analysis, several HLA alleles did not meet the minimum homozygote number required for the nonadditive test, including *HLA-DRB1\*03:01* and *DRB1\*01:01* in IBM. Previous IBM studies reported a low risk associated with their homozygous genotype [17]. Although their nonadditive effect could not be tested, the significance of the correlated *HLA-DQA1\*05:01* suggests a potential deviation from additivity in *HLA-DRB1*, which is consistent with the previously identified high frequency of *HLA-DRB1* heterozygotes in cases [17]. The nonadditive effect of *HLA-DRB1* should be validated in a larger cohort. The subtypes DM, PM, IBM, and Jo-1 showed similar nonadditive effect results to IIM, except for *HLA-C\*07:01* in DM, which did not reach the significance level. Additionally, *HLA-DQA1\*01:02* in PM showed a nonadditive effect with recessive protection against IIM. This allele has previously been reported to have a protective effect in IIM, DM, and IBM, but it did not

show a significant nonadditive effect in DM and was not tested in IBM in our analysis. In JDM, only *HLA-C\*07:01* exhibited a nonadditive effect, and the additive effects of other alleles were smaller than those of other subtypes. This may stem from the heterogeneity of JDM cases or from divergent immune genetic mechanisms. It is noteworthy that the Jo-1 autoantibody subtype showed the strongest significance in both additive and non-additive effects compared with other clinical subtypes, despite having a relatively small sample size. This finding supports the hypothesis of greater homogeneity in autoantibody classification in IIM. Anti-Jo1 is the most common autoantibody in the antisynthetase antibody family, which defines the antisynthetase syndrome subtype of IIM [4,33]. Unfortunately, there was insufficient data on other autoantibodies to assess their nonadditive effects in this study. Other subtypes, such as immune-mediated necrotising myopathies (IMNM), amyopathic DM, and overlap myositis, could be the subject of future investigation. In the sex-stratified analysis, we validated the significant nonadditive effect in males and females separately. The potential difference in their nonadditive effects requires a larger external cohort for validation.

In the allelic interaction model, we identified a significant nonadditive effect of specific allele combinations within the HLA gene. In *HLA-DQA1*, the interaction effect of *DQA1\*01:02* and *DQA1\*05:01* increased the risk of IIM. A recent IBM analysis reported that carrying *DQA1\*01:02* negates the risk associated with *DRB1\*03:01* [43]. The interaction effect between *HLA-DRB1* and *HLA-DQA1* alleles would require a larger cohort to validate these findings. For *HLA-DRB1*, we also identified an interaction effect of *DRB1\*03:01-DRB1\*01:01* and *DRB1\*03:01-DRB1\*15:01*. Their heterogeneous genotype risks were higher than those of *DRB1\*03:01* homozygotes, suggesting a potential

overdominance effect. The *DRB1\*03:01-DRB1\*01:01* interaction has also been associated with a nonadditive increased risk in rheumatoid arthritis [13].

The analysis of phenotypic variance explained validated the better fit of the nonadditive model. For example, the single locus of *HLA-DRB1* accounted for a proportion of 8.8% in known IIM heritability [44], with an additional 2.6% of heritability compared with the additive models. It is noteworthy that the phenotypic variance of other HLA genes may arise from a single causal HLA gene, such as *HLA-DRB1*, due to strong LD between HLA genes. It remains a challenge to calculate the exact contribution of each HLA gene or its combined effects. In addition, multiple rare variants were aggregated into a single complementary allele in our analysis. Their genotype variance was considered as within-genotype variance instead of between-genotype variance, which will lead to an underestimation of phenotypic variance explained.

The 5 HLA alleles with a nonadditive effect are known as the core alleles of the 8.1 AH [45]. The 8.1 AH has been associated with multiple autoimmune diseases, including myositis, myasthenia gravis, celiac disease, and Sjögren's syndrome [45]. The haplotype's nonadditive effect has been partly documented in type 1 diabetes (*HLA-DRB1\*03:01-HLA-DQA1\*05:01-HLA-DQB1\*02:01*) and celiac disease (*HLA-DQA1\*05:01-HLA-DQB1\*02:01*) [13]. Their nonadditive effect with a positive dominant component in risk is similar to our findings in IIM. However, the nonadditivity of 8.1 AH risk remains unclear for some related autoimmune diseases like myasthenia gravis. Investigation of the nonadditivity pattern of 8.1 AH across multiple autoimmune diseases may offer insights into the immune genetic mechanisms involved. Given the strong LD between alleles of the 8.1 AH, we investigated the independent nonadditive effect signal within this haplotype. *HLA-DRB1\*03:01* showed strong significance for both additive and nonadditive effects. It is notable that *HLA-DQB1\*02:01* exhibited a stronger nonadditive effect when no other alleles were conditioned, and it remained significant even after conditioning on *HLA-DRB1\*03:01* and *HLA-B\*08:01*, suggesting an independent, although weak, nonadditive effect. Further amino acid conditional analysis identified 74:R and 77:N as the top residues in *HLA-DRB1*. These residues, located in the antigen-binding groove, have been reported to be associated with multiple autoimmune diseases [46]. HLA protein structure analysis indicated that the replacement of alanine or glycine with positively charged arginine alters the pocket structure and promotes efficient autoantigen presentation to CD4<sup>+</sup> T cells [43,46].

A limitation of conditional analysis is that major histocompatibility complex (MHC) class III genes were not included to clarify their potential nonadditive effects. These genes may represent an additional mechanism contributing to the nonadditive genetic risk of IIM. The *C4A* null allele and the *TNF-α-308 G>A* polymorphism, both of which are in LD with the HLA 8.1 AH, have been implicated in various autoimmune diseases and the presence of autoantibodies [47–49]. A recent study indicated that *C4A* deficiency independently increases the risk of DM and JDM, *HLA-DRB1\*03* is a prominent risk factor for IBM, and both factors independently and interactively increase the risk of PM [47]. In contrast, the effect of the *TNF-α* allele is not independent of *HLA-B\*08* in adult IIM [50]. Given their strong LD with HLA 8.1 AH, these MHC class III alleles may show similar nonadditive genetic patterns in IIM susceptibility, although this requires further investigation.

Beyond the HLA region, numerous immune-related genes contribute to IIM autoimmunity and are associated with disease

severity [1]. Increasing evidence highlights the importance of interferons (IFNs) in perpetuating inflammation in IIM. Clinical research reveals a correlation between IFN scores and IIM severity, with distinct patterns observed among different subtypes [51]. Type I IFN-associated genes are predominant in DM, whereas type II IFN signatures are more characteristic of IBM and anti-synthetase syndrome (ASyS) [51]. Despite differences in IFN signatures among IIM subtypes, the nonadditive patterns of the HLA 8.1 AH across these subtypes remain consistent. A study of Sjögren's syndrome reported that the *DRB1\*03:01-DQA1\*05:01-DQB1\*02:01* haplotype is associated with IFN-α levels [52]. It remains uncertain whether this association extends to IIM and how HLA heterozygosity affects the severity and chronicity of autoimmunity in the progression of IIM.

This study is limited to the nonadditive effect of HLA alleles on IIM susceptibility. Further research is needed to clarify the nonadditive effects of MHC class III alleles and clinical phenotypes in IIM. Another limitation of our study is the relatively small number of IIM cases, particularly for specific IIM subtypes. The classification of IIM does not include recently defined subtypes, such as ASyS, IMNM, and other autoantibody-defined subtypes. Additionally, our findings on the nonadditive effects of IIM in individuals of European ancestry require further investigation in more diverse population groups.

In summary, this is the first study to focus on the nonadditive effects in IIM using the largest cohort to date. The divergence between HLA and non-HLA risk models and the nonadditive effects of HLA molecule residues support further mechanistic investigation into HLA antigen presentation in immune responses. Our nonadditive risk model could also provide more precise individual risk estimation and warrants exploration of its clinical relevance.

## Competing interests

All authors declare they have no competing interests.

## CRedit authorship contribution statement

**Gang Chen:** Writing – review & editing, Writing – original draft, Visualization, Validation, Software, Project administration, Methodology, Investigation, Formal analysis, Data curation, Conceptualization. **Catherine Zhu:** Data curation. **Hector Chinoy:** Writing – review & editing, Supervision. **Christopher I. Amos:** Data curation. **Andrew P. Morris:** Writing – review & editing, Supervision, Software, Project administration, Methodology, Conceptualization. **Janine A. Lamb:** Writing – review & editing, Supervision, Resources, Project administration, Methodology, Funding acquisition, Data curation, Conceptualization.

## Acknowledgements

We extend our sincere gratitude to the patients who participated in the cohort, as well as the physicians and nurses for their essential role in sample collection and data acquisition. Additionally, we acknowledge the Lisa Riders and other MYOGEN members for their invaluable support in data management, project approval, and manuscript review.

## Contributors

JAL, APM, and GC designed the study. MYOGEN contributed to cohort establishment, data management, and project approval. CZ provided imputed data for the MYOGEN cohorts. GC performed the analyses and drafted the manuscript. All authors participated in the result interpretation and manuscript revision.

## Funding

Supported by the Association Francaise Contre Les Myopathies (AFM); European Union Sixth Framework Programme (project AutoCure; LSH-018661); European Science Foundation (ESF) in the framework of the Research Networking Programme European Myositis Network (EUMYONET); European Reference Network for Rare Neuromuscular Diseases (ERN EURO-NMD); The Swedish Research Council and grants provided by the Stockholm County Council (ALF project), the Swedish Rheumatism Association, King Gustaf V 80 year Foundation; the intramural research program of the National Institute of Environmental Health Sciences (NIEHS), the National Institutes of Health (NIH) (Project ZIA ES101074); Myositis UK; Arthritis Research UK (awards 18474, 21593, 21552 and 20380); Medical Research Council (MR/N003322/1); The Cure JM Foundation; the Wellcome Trust (awards 085860 and 105610); the Henry Smith Charity UK; Action Medical UK; the Remission Charity; BMA Dorris Hillier Grant 2012 and the Bath Institute of Rheumatic Diseases; Prinses Beatrix Spierfonds (W.OR12–15); the Research Fund of Region Zealand, Denmark; the Ministry of Health, Czech Republic (Project for Conceptual Development of Research Organization grant 00023728); National Institute for Health Research (NIHR) Biomedical Research Centres (BRC) at Great Ormond Street Hospital (GOSH), Manchester and University College London Hospitals. The contributions of the NIH author(s) were made as part of their official duties as NIH federal employees, are in compliance with agency policy requirements, and are considered Works of the United States Government. However, the findings and conclusions presented in this paper are those of the author(s) and do not necessarily reflect the views of the NIH or the U.S. Department of Health and Human Services.

## Patient consent for publication

Not applicable.

## Ethics approval

Written informed consent was obtained from all patients with approval from research ethics committees of institutional review boards at each participating centre.

## Provenance and peer review

Not commissioned; externally peer reviewed.

## Supplementary materials

Supplementary material associated with this article can be found in the online version at doi:10.1016/j.ard.2025.07.002.

## Orcid

Gang Chen: <http://orcid.org/0000-0002-7440-5030>

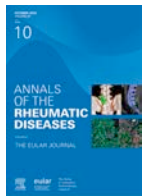
Janine A. Lamb: <http://orcid.org/0000-0002-7248-0539>

## REFERENCES

- [1] Lundberg IE, Fujimoto M, Vencovsky J, Aggarwal R, Holmqvist M, Christopher-Stine L, et al. Idiopathic inflammatory myopathies. *Nat Rev Dis Primers* 2021;7(1):87.
- [2] Lundberg IE, Tjärnlund A, Bottai M, Werth VP, Pilkington C, Visser M, et al. 2017 European League Against Rheumatism/American College of Rheumatology classification criteria for adult and juvenile idiopathic inflammatory myopathies and their major subgroups. *Ann Rheum Dis* 2017;76(12):1955–64.
- [3] Lundberg IE, de Visser M, Werth VP. Classification of myositis. *Nat Rev Rheumatol* 2018;14(5):269–78.
- [4] Espinosa-Ortega F, Lodin K, Dastmalchi M, Vencovsky J, Diederichsen LP, Shinjo SK, et al. Autoantibodies and damage in patients with idiopathic inflammatory myopathies: a longitudinal multicenter study from the MYO-NET international network. *Semin Arthritis Rheum* 2024;68:152529.
- [5] Khoo T, Lilleker JB, Thong BY, Leclair V, Lamb JA, Chinoy H. Epidemiology of the idiopathic inflammatory myopathies. *Nat Rev Rheumatol* 2023;19(11):695–712.
- [6] Galindo-Feria AS, Horuluoglu B, Lundberg IE. Anti-Jo1 autoantibodies, from clinic to the bench. *Rheumatol Autoimmun* 2022;2(2):57–68.
- [7] Rothwell S, Cooper RG, Lundberg IE, Miller FW, Gregersen PK, Bowes J, et al. Dense genotyping of immune-related loci in idiopathic inflammatory myopathies confirms HLA alleles as the strongest genetic risk factor and suggests different genetic background for major clinical subgroups. *Ann Rheum Dis* 2016;75(8):1558–66.
- [8] Miller FW, Chen W, O'Hanlon TP, Cooper RG, Vencovsky J, Rider LG, et al. Genome-wide association study identifies HLA 8.1 ancestral haplotype alleles as major genetic risk factors for myositis phenotypes. *Genes Immun* 2015;16(7):470–80.
- [9] Dendrou CA, Petersen J, Rossjohn J, Fugger L. HLA variation and disease. *Nat Rev Immunol* 2018;18(5):325–39.
- [10] Busch R, Kollnberger S, Mellins ED. HLA associations in inflammatory arthritis: emerging mechanisms and clinical implications. *Nat Rev Rheumatol* 2019;15(6):364–81.
- [11] Rothwell S, Chinoy H, Lamb JA, Miller FW, Rider LG, Wedderburn LR, et al. Focused HLA analysis in Caucasians with myositis identifies significant associations with autoantibody subgroups. *Ann Rheum Dis* 2019;78(7):996–1002.
- [12] Duenk P, Calus MPL, Wientjes YCJ, Bijma P. Benefits of dominance over additive models for the estimation of average effects in the presence of dominance. *G3 (Bethesda)* 2017;7(10):3405–14.
- [13] Lenz TL, Deutsch AJ, Han B, Hu X, Okada Y, Eyre S, et al. Widespread non-additive and interaction effects within HLA loci modulate the risk of autoimmune diseases. *Nat Genet* 2015;47(9):1085–90.
- [14] Raychaudhuri S, Sandor C, Stahl EA, Freudenberg J, Lee HS, Jia X, et al. Five amino acids in three HLA proteins explain most of the association between MHC and seropositive rheumatoid arthritis. *Nat Genet* 2012;44(3):291–6.
- [15] Hu X, Deutsch AJ, Lenz TL, Onengut-Gumuscu S, Han B, Chen WM, et al. Additive and interaction effects at three amino acid positions in HLA-DQ and HLA-DR molecules drive type 1 diabetes risk. *Nat Genet* 2015;47(8):898–905.
- [16] Rider LG, Gurley RC, Pandey JP, Garcia de la Torre I, Kalovidouris AE, O'Hanlon TP, et al. Clinical, serologic, and immunogenetic features of familial idiopathic inflammatory myopathy. *Arthritis Rheum* 1998;41(4):710–9.
- [17] Rothwell S, Cooper RG, Lundberg IE, Gregersen PK, Hanna MG, Machado PM, et al. Immune-array analysis in sporadic inclusion body myositis reveals HLA-DRB1 amino acid heterogeneity across the myositis spectrum. *Arthritis Rheumatol* 2017;69(5):1090–9.
- [18] Ishigaki K, Lagattuta KA, Luo Y, James EA, Buckner JH, Raychaudhuri S. HLA autoimmune risk alleles restrict the hypervariable region of T cell receptors. *Nat Genet* 2022;54(4):393–402.
- [19] Zhu C, Han Y, Byun J, et al. Genetic architecture of idiopathic inflammatory myopathies from meta-analyses. *Arthritis Rheumatol* 2025;77(6):750–64.
- [20] Luo Y, Kanai M, Choi W, Li X, Sakaue S, Yamamoto K, et al. A high-resolution HLA reference panel capturing global population diversity enables multi-ancestry fine-mapping in HIV host response. *Nat Genet* 2021;53(10):1504–16.
- [21] Das S, Forer L, Schönherr S, Sidore C, Locke AE, Kwong A, et al. Next-generation genotype imputation service and methods. *Nat Genet* 2016;48(10):1284–7.
- [22] Aragon T., (2020). *epitools: Epidemiology Tools*. R package version 0.5-10.1. Available at: <https://CRAN.R-project.org/package=epitools>.

- [23] Purcell S, Neale B, Todd-Brown K, Thomas L, Ferreira MA, Bender D, et al. PLINK: a tool set for whole-genome association and population-based linkage analyses. *Am J Hum Genet* 2007;81(3):559–75.
- [24] Sakaue S, Gurajala S, Curtis M, Luo Y, Choi W, Ishigaki K, et al. Tutorial: a statistical genetics guide to identifying HLA alleles driving complex disease. *Nat Protoc* 2023;18(9):2625–41.
- [25] Terao C, Okada Y, Ikari K, Kochi Y, Suzuki A, Ohmura K, et al. Genetic landscape of interactive effects of HLA-DRB1 alleles on susceptibility to ACPA (+) rheumatoid arthritis and ACPA levels in Japanese population. *J Med Genet* 2017;54(12):853–8.
- [26] Robinson J, Barker DJ, Marsh SGE. 25 years of the IPD-IMGT/HLA Database. *HLA* 2024;103(6):e15549.
- [27] So HC, Gui AH, Cherny SS, Sham PC. Evaluating the heritability explained by known susceptibility variants: a survey of ten complex diseases. *Genet Epidemiol* 2011;35(5):310–7.
- [28] Leclair V, Galindo-Feria AS, Rothwell S, Kryšufková O, Zargar SS, Mann H, et al. Distinct HLA associations with autoantibody-defined subgroups in idiopathic inflammatory myopathies. *EBioMedicine* 2023;96:104804.
- [29] Oyama M, Ohnuki Y, Uruha A, Saito Y, Nishimori Y, Suzuki S, et al. Association between HLA alleles and autoantibodies in dermatomyositis defined by sarcoplasmic expression of myxovirus resistance protein A. *J Rheumatol* 2023;50(9):1159–64.
- [30] Kishi T, Rider LG, Pak K, Barillas-Arias L, Henrickson M, McCarthy PL, et al. Association of anti-3-hydroxy-3-methylglutaryl-coenzyme A reductase autoantibodies with DRB1\*07:01 and severe myositis in juvenile myositis patients. *Arthritis Care Res (Hoboken)* 2017;69(7):1088–94.
- [31] Ohnuki Y, Suzuki S, Uruha A, Oyama M, Suzuki S, Kulski JK, et al. Association of immune-mediated necrotizing myopathy with HLA polymorphisms. *HLA*. 2023;101(5):449–57.
- [32] Deakin CT, Bowes J, Rider LG, Miller FW, Pachman LM, Sanner H, et al. Association with HLA-DRbeta1 position 37 distinguishes juvenile dermatomyositis from adult-onset myositis. *Hum Mol Genet* 2022;31(14):2471–81.
- [33] Remuzgo-Martínez S, Atienza-Mateo B, Ocejó-Vinyals JG, Pulito-Cueto V, Prieto-Peña D, Genre F, et al. HLA association with the susceptibility to anti-synthetase syndrome. *Joint Bone Spine* 2021;88(3):105115.
- [34] Chen Z, Wang Y, Kuwana M, Xu X, Hu W, Feng X, et al. HLA-DRB1 alleles as genetic risk factors for the development of anti-MDA5 antibodies in patients with dermatomyositis. *J Rheumatol* 2017;44(9):1389–93.
- [35] Johnson C, Schiffenbauer AI, Miller FW, Perin J, Danoff SK, Diwadkar AR, et al. Human leukocyte antigen alleles associated with interstitial lung disease in North Americans with idiopathic inflammatory myopathy. *Am J Respir Crit Care Med* 2023;207(5):619–22.
- [36] Lamb JA. The genetics of autoimmune myositis. *Front Immunol* 2022;13:886290.
- [37] Uffelmann E, Huang QQ, Munung NS, de Vries J, Okada Y, Martin AR, et al. Genome-wide association studies. *Nat Rev Methods Primers* 2021;1(1):59.
- [38] Liu Z, Huang CJ, Huang YH, Pan MH, Lee MH, Yu KJ, et al. HLA zygosity increases risk of hepatitis B virus-associated hepatocellular carcinoma. *J Infect Dis* 2021;224(10):1796–805.
- [39] Roark CL, Ho BE, Aubrey MT, Anobile C, Israeli S, Phang TL, et al. HLA homozygosity is associated with non-Hodgkin lymphoma. *Hum Immunol* 2022;83(10):730–5.
- [40] Garcia-Marquez MA, Thelen M, Bauer E, Maas L, Wennhold K, Lehmann J, et al. Germline homozygosity and allelic imbalance of HLA-I are common in esophagogastric adenocarcinoma and impair the repertoire of immunogenic peptides. *J Immunother Cancer* 2024;12(4):e007268.
- [41] Goyette P, Boucher G, Mallon D, Ellinghaus E, Jostins I, Huang H, et al. High-density mapping of the MHC identifies a shared role for HLA-DRB1\*01:03 in inflammatory bowel diseases and heterozygous advantage in ulcerative colitis. *Nat Genet* 2015;47(2):172–9.
- [42] Loeffler-Wirth H, Lehmann C, Lachmann N, Doxiadis I. Homozygosity in any HLA locus is a risk factor for specific antibody production: the taboo concept 2.0. *Front Immunol* 2024;15:1384823.
- [43] Slater N, Sooda A, McLeish E, Beer K, Brusch A, Shakya R, et al. High-resolution HLA genotyping in inclusion body myositis refines 8.1 ancestral haplotype association to DRB1\*03:01:01 and highlights pathogenic role of arginine-74 of DRbeta1 chain. *J Autoimmun* 2024;142:103150.
- [44] Che WI, Westerlind H, Lundberg IE, Hellgren K, Kuja-Halkola R, Holmqvist M. Familial aggregation and heritability: a nationwide family-based study of idiopathic inflammatory myopathies. *Ann Rheum Dis* 2021;80(11):1461–6.
- [45] Gambino CM, Aiello A, Accardi G, Caruso C, Candore G. Autoimmune diseases and 8.1 ancestral haplotype: an update. *HLA* 2018;92(3):137–43.
- [46] Ban Y, Davies TF, Greenberg DA, Concepcion ES, Osman R, Oashi T, et al. Arginine at position 74 of the HLA-DR beta1 chain is associated with Graves' disease. *Genes Immun* 2004;5(3):203–8.
- [47] Zhou D, King EH, Rothwell S, Krystufkova O, Notarnicola A, Coss S, et al. Low copy numbers of complement C4 and C4A deficiency are risk factors for myositis, its subgroups and autoantibodies. *Ann Rheum Dis* 2023;82(2):235–45.
- [48] Lintner KE, Patwardhan A, Rider LG, Abdul-Aziz R, Wu YL, Lundström E, et al. Gene copy-number variations (CNVs) of complement C4 and C4A deficiency in genetic risk and pathogenesis of juvenile dermatomyositis. *Ann Rheum Dis* 2016;75(9):1599–606.
- [49] Lundtoft C, Pucholt P, Martin M, Bianchi M, Lundström E, Eloranta ML, et al. Complement C4 copy number variation is linked to SSA/Ro and SSB/La autoantibodies in systemic inflammatory autoimmune diseases. *Arthritis Rheumatol* 2022;74(8):1440–50.
- [50] Chinoy H, Salway F, John S, Fertig N, Tait BD, Oddis CV, et al. Tumour necrosis factor-alpha single nucleotide polymorphisms are not independent of HLA class I in UK Caucasians with adult onset idiopathic inflammatory myopathies. *Rheumatology (Oxford)* 2007;46(9):1411–6.
- [51] Gasparotto M, Franco C, Zanatta E, Ghirardello A, Zen M, Iaccarino L, et al. The interferon in idiopathic inflammatory myopathies: different signatures and new therapeutic perspectives. A literature review. *Autoimmun Rev* 2023;22(6):103334.
- [52] Trutschel D, Bost P, Mariette X, Bondet V, Llibre A, Posseme C, et al. Variability of primary Sjogren's syndrome is driven by interferon-alpha and interferon-alpha blood levels are associated with the class II HLA-DQ locus. *Arthritis Rheumatol* 2022;74(12):1991–2002.





## Myositis

# Spatial transcriptomic analysis of muscle biopsy from patients with treatment-naïve juvenile dermatomyositis reveals mitochondrial abnormalities despite disease-related interferon-driven signature

Aris E. Syntakas<sup>1,2,3</sup>, Melissa Kartawinata<sup>1,2,3</sup>, Nia M.L. Evans<sup>1,2,3</sup>,  
Huong D. Nguyen<sup>1,2</sup>, Charalampia Papadopoulou<sup>2,4</sup>,  
Muthana Al Obaidi<sup>2,4</sup>, Clarissa Pilkington<sup>2,4</sup>, Yvonne Glackin<sup>2,4</sup>,  
Christopher B. Mahony<sup>5</sup>, Adam P. Croft<sup>5,6</sup>, Simon Eaton<sup>2,7</sup>,  
Mario Cortina-Borja<sup>2,8</sup>, Olumide Ogunbiyi<sup>9</sup>, Ashirwad Merve<sup>9</sup>,  
Lucy R. Wedderburn<sup>1,2,3,4</sup>, Meredyth G. Ll Wilkinson<sup>1,2,3,\*</sup>, on behalf of the  
JDCBS

<sup>1</sup> Infection, Immunity and Inflammation Research and Teaching Department, UCL Great Ormond Street Institute of Child Health, London, UK

<sup>2</sup> National Institute for Health and Care Research (NIHR) Biomedical Research Centre at Great Ormond Street Hospital, London, UK

<sup>3</sup> Centre for Adolescent Rheumatology Versus Arthritis at UCL, UCL Hospital and Great Ormond Street Hospital, London, UK

<sup>4</sup> Department of Rheumatology, Great Ormond Street Hospital for Children NHS Foundation Trust London, London, UK

<sup>5</sup> Department of Inflammation and Ageing, School of Infection, Inflammation and Immunology, College of Medicine and Health, University of Birmingham, Birmingham, UK

<sup>6</sup> NIHR Birmingham Biomedical Research Centre, Birmingham, UK

<sup>7</sup> Developmental Biology and Cancer Research & Teaching Department, UCL Great Ormond Street Institute of Child Health, London, UK

<sup>8</sup> Population Policy and Practice Research & Teaching Department, UCL Great Ormond Street Institute of Child Health, London, UK

<sup>9</sup> Department of Histopathology, Great Ormond Street Hospital for Children NHS Foundation Trust, London, UK

## ARTICLE INFO

## Article history:

Received 5 February 2025

Received in revised form 14 July 2025

Accepted 15 July 2025

## ABSTRACT

**Objectives:** This study aimed to investigate the spatial transcriptomic landscape of muscle tissue from patients with treatment-naïve juvenile dermatomyositis (JDM) in comparison to healthy paediatric muscle tissue.

**Methods:** Muscle biopsies from 3 patients with JDM and 3 age-matched controls were analysed using the Nanostring GeoMx Digital Spatial Profiler. Regions of interest were selected based on muscle fibres without immune cells, immune cell infiltration and CD68+ macrophage enrichment. Differential gene expression, pathway analysis and pathways clustering analysis were conducted. Key findings were validated in 19 cases of JDM using immunohistochemistry and chemical stains, and a bulk RNAseq dataset of 4 cases of JDM.

\*Correspondence to Dr Meredyth G Ll Wilkinson, UCL GOS Institute of Child Health, and Great Ormond Street Hospital NHS Trust, University College London, London, UK.

E-mail address: [meredyth.wilkinson.14@ucl.ac.uk](mailto:meredyth.wilkinson.14@ucl.ac.uk) (M.G.L. Wilkinson).

Lucy R Wedderburn and Meredyth G Ll Wilkinson are joint senior authors.

Handling editor Josef S. Smolen.

<https://doi.org/10.1016/j.ard.2025.07.015>

**Results:** JDM muscle tissues exhibited significant interferon pathway activation and mitochondrial dysfunction compared to controls. A 15-gene interferon signature was significantly elevated in JDM muscle and macrophage-enriched regions, correlating with clinical weakness. In contrast, mitochondrial dysregulation, characterised by downregulated respiratory chain pathways, was present regardless of interferon activity or muscle strength. The interferon-driven and mitochondrial signatures were replicated in an independent RNAseq dataset from JDM muscle; the lack of association between interferon signature and mitochondrial dysregulation was validated in 19 cases by conventional staining methods. Clustering analysis revealed distinct transcriptomic profiles between JDM and control tissues, as well as between patients with JDM with varying clinical phenotypes.

**Conclusions:** This study highlights mitochondrial dysfunction as a consistent pathological feature in JDM muscle, which may be independent of interferon-driven inflammation. These findings highlight the potential for mitochondrial-targeted therapies in JDM management and emphasise the need for further studies to explore their therapeutic value.

#### WHAT IS ALREADY KNOWN ON THIS TOPIC

- Juvenile dermatomyositis (JDM) involves interferon (IFN)-driven inflammation and immune-mediated muscle damage.
- Mitochondrial abnormalities in blood immune cells persist despite treatment and contribute to disease pathology.

#### WHAT THIS STUDY ADDS

- Mitochondrial dysfunction is present in both muscle fibres and tissue-infiltrating immune cells within JDM muscle.
- These abnormalities are detectable even in clinically less severe muscle weakness.
- Degree of mitochondrial abnormality at transcript and protein level may be independent of the strength of IFN-driven signal.
- Mitochondrial dysregulation detected at the transcriptional level correlates with abnormal transcription of muscle (sarcomere) and the subcellular peroxisome organelle.

#### HOW THIS STUDY MIGHT AFFECT RESEARCH, PRACTICE OR POLICY

- Targeting mitochondrial dysfunction could enhance treatment outcomes for JDM, especially in patients whose disease is refractory to current therapies.
- Insights from this study support the development of stratification tools to detect aspects of pathology which are not tightly correlated with IFN-driven pathology.

## INTRODUCTION

Idiopathic inflammatory myopathies of childhood, of which the most common is juvenile dermatomyositis (JDM), are severe paediatric autoimmune conditions characterised by chronic inflammation of muscle, skin and in some cases major organs. A clear understanding of pathogenic mechanisms at the sites of tissue damage is lacking, and there is a significant unmet need for more targeted treatments [1,2]. We have previously detailed transcriptional changes detectable in blood immune cells in JDM [3]. We identified that blood CD14<sup>+</sup> monocytes from patients with active disease have severe mitochondrial dysfunction. Furthermore, we showed that alterations in mitochondrial biology and morphology in monocytes led to accumulation of oxidised mitochondrial DNA, which was able to trigger interferon (IFN)-signalling pathways. Interestingly, while the well-characterised IFN-driven signature detectable at diagnosis was reduced on treatment, we observed that mitochondrial abnormalities detected in peripheral blood monocytes persisted despite treatment.

Our previous studies on JDM muscle tissue obtained before treatment showed that proinflammatory, CD68<sup>+</sup> tissue

macrophages are frequently detectable [4,5] and that CD68<sup>+</sup> cell infiltration correlates with weakness [6]. Macrophage infiltration may be throughout the endomysium, or in perivascular clusters, where they are frequently colocalised with infiltrating T cells [5,6]. Abnormal macrophage polarisation has been implicated in perpetuating inflammation and tissue damage in myopathies [7–9]. A recent study in a myositis animal model suggests a self-perpetuating loop between mitochondrial dysfunction and inflammation [10].

To start to define at tissue level the complex interactions between immune and muscle cells in JDM-affected muscle tissue, we employed spatial transcriptomics. This method enables *in-situ* gene expression analysis while preserving critical tissue architecture, allowing precise localisation of cell types and their potential involvement in the pathogenic processes associated with myositis [11]. We employed the Nanostring GeoMx Digital Spatial Profiler (DSP) to interrogate the transcriptome of muscle tissue sections from patients with JDM and age-matched healthy controls. GeoMx facilitates the staining, selection and sequencing of specific spatial niches within the tissue known as regions of interest (ROIs) [12]. We opted to focus initially on CD68<sup>+</sup>-enriched areas in the analysis of inflammatory infiltrate.

We confirm that JDM muscle tissue exhibits significant upregulation of IFN pathways and dysregulation of mitochondrial pathways, particularly affecting the electron transport chain. By comparing tissue areas, we show that muscle weakness correlates with increased IFN signalling in both muscle- and CD68<sup>+</sup>-cell-derived transcriptome. Importantly, mitochondrial abnormalities were clearly demonstrated even in muscle with only moderate clinical weakness, and these were detected in both muscle fibres as well as in the CD68<sup>+</sup> infiltrate. We replicated our findings in another cohort, analysing bulk RNAseq data, and validated the lack of correlation between IFN-driven changes and mitochondrial abnormality at protein level in a larger cohort. We believe that our study is the first to provide spatial transcriptional insights into JDM pathogenesis, and will facilitate significant steps towards the delineation of the contributions of immune and muscle cells, to JDM pathology. Our results suggest that mitochondrial abnormalities, which we previously defined in blood cells, are also present in both muscle and infiltrating monocyte/macrophages in JDM even before significant clinical weakness is apparent.

## METHODS

All methods are provided in supplementary information.

**Table**  
**Demographics and clinical characteristics of patients with JDM and controls included in the study**

Characteristic	Value					
	JDM1	JDM2	JDM3	HC1	HC2	HC3
Sample ID						
Age at sample (y)	5.83	3.58	4.75	6.28	10.02	4.81
Sex	F	F	F	M	M	F
Disease duration at time of biopsy, months	1.05	5.91	3.28	NA	NA	NA
Myositis-specific antibody	TIF1- $\gamma$	TIF1- $\gamma$	Negative	NA	NA	NA
Disease activity at time of biopsy:						
Physician global assessment score, PGA (0.0–10.0 cm)	8.0	7.8	6.3	NA	NA	NA
CMAS (0–52)	30	12	52	NA	NA	NA
MMT8 (0–80)	44	42	78	NA	NA	NA
CK, U/L	2611	125	131	NA	NA	NA
sDAS <sup>a</sup>	4	3	5	NA	NA	NA
Muscle biopsy score data <sup>b</sup>						
Inflammatory domain (0–12)	7	8	7	NA	NA	NA
Muscle-fibre domain (0–10)	8	7	7	NA	NA	NA
Vascular domain (0–3)	2	1	1	NA	NA	NA
Connective tissue domain (0–2)	1	2	1	NA	NA	NA
Total biopsy score (0–27)	18	18	16	NA	NA	NA
Histopathology visual analogue score (0.0–10.0)	7.0	8.0	7.0	NA	NA	NA

CMAS, childhood myositis assessment scale; DAS, disease activity score; ID, identification; JDM, juvenile dermatomyositis; MMT8, manual muscle testing of 8 muscles; NA, not applicable; PGA, physician global assessment; sDAS, skin disease activity score.

<sup>a</sup> Skin disease activity score, or modified skin DAS as defined in Lam et al [13].

<sup>b</sup> Data generated using validated JDM muscle biopsy score tool from Varsani et al [6].

RESULTS

Patients and controls

Clinical and demographic features of the 3 patients with JDM and controls analysed by transcriptome profiling are shown in Table [6,13]. Of note, 2 of the patients were significantly weak at the time of biopsy as assessed by the Childhood Myositis Assessment Scale (CMAS) and Manual Muscle Testing of 8 muscles (MMT8) while the third was less weak but had more severe skin disease activity. Two patients with JDM tested positive for TIF1 $\gamma$ , while the third patient was negative for myositis-specific autoantibodies (MSAs). For histological analysis, a total of 19 cases were included: the 3 transcriptome-profiled patients, along with an additional 16 JDM cases (Supplementary Table S1).

Selection of ROIs for analysis of areas with or without leukocyte infiltration in JDM muscle biopsies

To determine the dominant pathways that are altered in the muscle of patients with JDM compared to healthy muscle and to test whether mitochondrial pathways are altered in muscle tissue early in JDM, we used spatial transcriptome analysis. Imaging of quadriceps muscle biopsy sections from all 6 cases was

performed on the Nanostring GeoMx scanning platform. Immunofluorescence staining was performed to enable selection of ROIs for sequencing using a nuclear marker and morphology markers laminin, CD45, and CD68, for identification of muscle fibres, leukocytes, and macrophages, respectively. For focused transcriptome analysis of infiltrating macrophages, segmentation was used, as described [12]. Figure 1A shows control muscle tissue, where no significant immune cell infiltration or inflammation is observed; Figure 1B shows JDM muscle ROI without immune cells, while Figure 1C reveals an area with substantial inflammatory infiltration (CD45+), which was not observed in the control samples. Figure 1D shows an area with infiltrating CD68+ cells within JDM muscle with Figure 1E further illustrating the ‘segmented’ view of CD68+ cells, allowing for transcriptomic profiling of this specific cell type. Thus, we selected 3 different ROI types for sequencing analysis: muscle-fibre, muscle with immune cell infiltration, and CD68-enriched, generating a total of 28 ROIs. The breakdown of the ROIs selected is shown in Supplementary Table S2.

Histological analysis of the muscle biopsy sections is presented in Supplementary Figure S1. All 3 control cases were found to have no significant pathology or inflammation, with no infiltration by CD3+ or CD68+ immune cells, confirmed by a senior histopathologist (AM) [6,14]. None of the 3 control cases had a genetic abnormality in known mitochondrial-related diseases. A representative hematoxylin and eosin (H&E)-stained section from a control case is shown in Supplementary Figure S1A. Active inflammation in a representative JDM case is demonstrated by H&E staining (Supplementary Fig S1B), CD3 (Supplementary Fig S1C), CD68 (Supplementary Fig S1D), and CD20 staining (Supplementary Fig S1E). These classical signs of JDM muscle inflammation are reflected in the biopsy scores (inflammatory domain) [6] (Table).

Principal component analysis confirms distinct transcriptomic differences between ROI types and JDM vs control tissues

Initial data quality checks were performed on the Nanostring platform, assessing tissue and sequencing quality, as well as the performance of negative control probes. None of the 28 ROIs or control probes were flagged as unsuitable for analysis. Further quality control and normalisation techniques were applied to address technical variation across data generated from ROIs. Relative log expression plots were used to visualise effects of normalisation: Supplementary Figure S2A shows unnormalised data, with Supplementary Figure S2B displaying log counts per million normalised data. This normalisation method, integrated into the voom function of the limma-voom pipeline [15], effectively centred the median expression levels of all ROIs around zero. This indicates successful removal of unwanted technical variation, enhancing comparability across samples.

We employed principal component analysis (PCA) to assess variance within the dataset, between patients, and between types of ROIs (Supplementary Fig S2C and D). Initial PCA analysis by patient revealed that all data from patients with JDM (22 ROIs) clustered into 2 clusters, with clear separation of patients with JDM from control samples (Supplementary Fig S2C). When data were labelled by ROI type, the 2 distinct clusters of data from JDM biopsies were clarified by cell type. As expected, CD68+ -selected ROIs (JDM samples only) formed a separate cluster (Supplementary Fig S2D blue symbols). Interestingly, JDM muscle-only (Supplementary Fig S2D red symbols) and JDM muscle plus-immune ROIs (Supplementary Fig S2D yellow symbols) clustered together (Supplementary Fig S2D). Note that



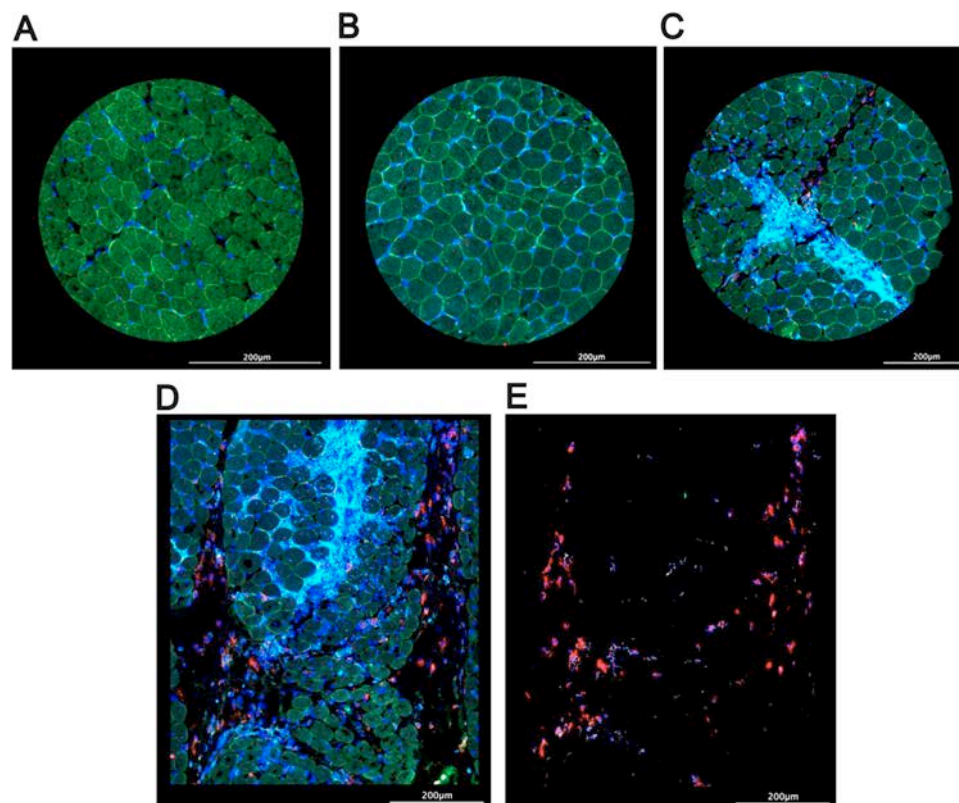


**Figure 1.** Immunofluorescent imaging of the muscle biopsy regions of interest (ROIs). (A–E) Representative fluorescent images of ROI types selected for sequence analysis and associated staining markers: (A) control muscle; (B) JDM muscle ROI with no infiltrating immune cells; (C) JDM muscle enriched with immune cells (CD45 + ); (D) CD68 + macrophage-enriched region. (E) Segmented CD68 + cells in the same region shown in (D). Staining antibodies: laminin (green), DNA nuclear stain (blue), CD68 (red), and CD45 (cyan), indicating muscle fibres, nuclei, macrophages, and leukocytes, respectively. (B–E) are derived from patient JDM3. JDM, juvenile dermatomyositis.

segmentation was not performed on CD45 + cells. Again, control muscle ROIs ([Supplementary Fig S2D pink symbols](#)) clustered away from all JDM data.

#### *Differential gene expression analysis confirms a high IFN-driven signature and demonstrates abnormal mitochondrial gene signature in JDM muscle compared to control muscle*

To investigate differences in the gene expression profiles of JDM muscle compared to control muscle, the data from muscle-only ROIs were initially used in the limma-voom differential gene expression (DGE) analysis pipeline. The analysis revealed 448 genes that were significantly differentially expressed in JDM muscle ( $|\text{Log}_2\text{FC}| \geq 0.58$  and adjusted  $P$  value  $\leq .05$ , using the Benjamini-Hochberg procedure for multiple testing correction), of which 336 genes were identified as upregulated and 112 as downregulated in JDM muscle compared to control samples ([Fig 2A](#)). Pathway enrichment using over-representation analysis (ORA) on significantly differentially expressed genes (DEGs) was used to identify dysregulated pathways in JDM muscle. The gene ontology (GO) cellular component (CC) gene sets were initially used to identify differentially expressed pathways. The GO CC annotations detail the subcellular structures and complexes involved, making this appropriate for highlighting mitochondrial functional pathways. Conversely, the GO biological process (BP) gene sets were then used to capture dynamic biological activities and signalling processes, such as immune response mechanisms, which are central to JDM. The first ORA (GO CC) indicated 101 significantly differentially expressed pathways in JDM muscle compared to controls (adjusted  $P$  value

$\leq .05$ , Benjamini-Hochberg procedure) while the second (GO BP) gave 310 significant pathways.

To simplify the interpretation of these numerous, often overlapping pathways, Advanced Pathway Enrichment Analysis Representation (aPEAR) cluster network analysis was performed [16], resulting in the construction of plots that visually organise and group related pathways into coherent clusters, for each of the 2 GO gene sets that were used. The GO CC network highlighted several clusters of mitochondria-related pathways, including clusters such as the ‘respiratory chain complex’, the ‘mitochondrial proton-transporting adenosine triphosphate (ATP) synthase complex’, and the ‘mitochondrial respiratory chain complex III’ ([Fig 2B](#)). Interestingly, pathways related to endoplasmic reticulum (ER) to Golgi protein transport were also differentially expressed in JDM muscle ([Fig 2B](#)). The GO BP network highlighted clusters of IFN and immune-related pathways, with the most prominent clusters being ‘interferon-mediated signalling pathway’, ‘pattern recognition receptor signalling pathway’, and ‘T cell mediated immunity’. In addition, several clusters related to muscle development and function were noted, including ‘muscle cell development’ and ‘regulation of muscle contraction’ ([Fig 2C](#)).

We were intrigued that a cluster of pathways annotated as ‘T cell immunity’ was enriched in JDM muscle-only regions ([Fig 2C](#)). Scrutiny of pathways that generated this annotation revealed 22 pathways ascribed to T cells and 85 others labelled as antigen processing, regulation of immunity, major histocompatibility complex (MHC), or other immune cells ([Supplementary Table S3](#)). Across these pathways, the top DE genes were HLA (human leukocyte antigen, the human MHC) genes or those involved in MHC processing such as *TAP2* ([Supplementary Table](#)



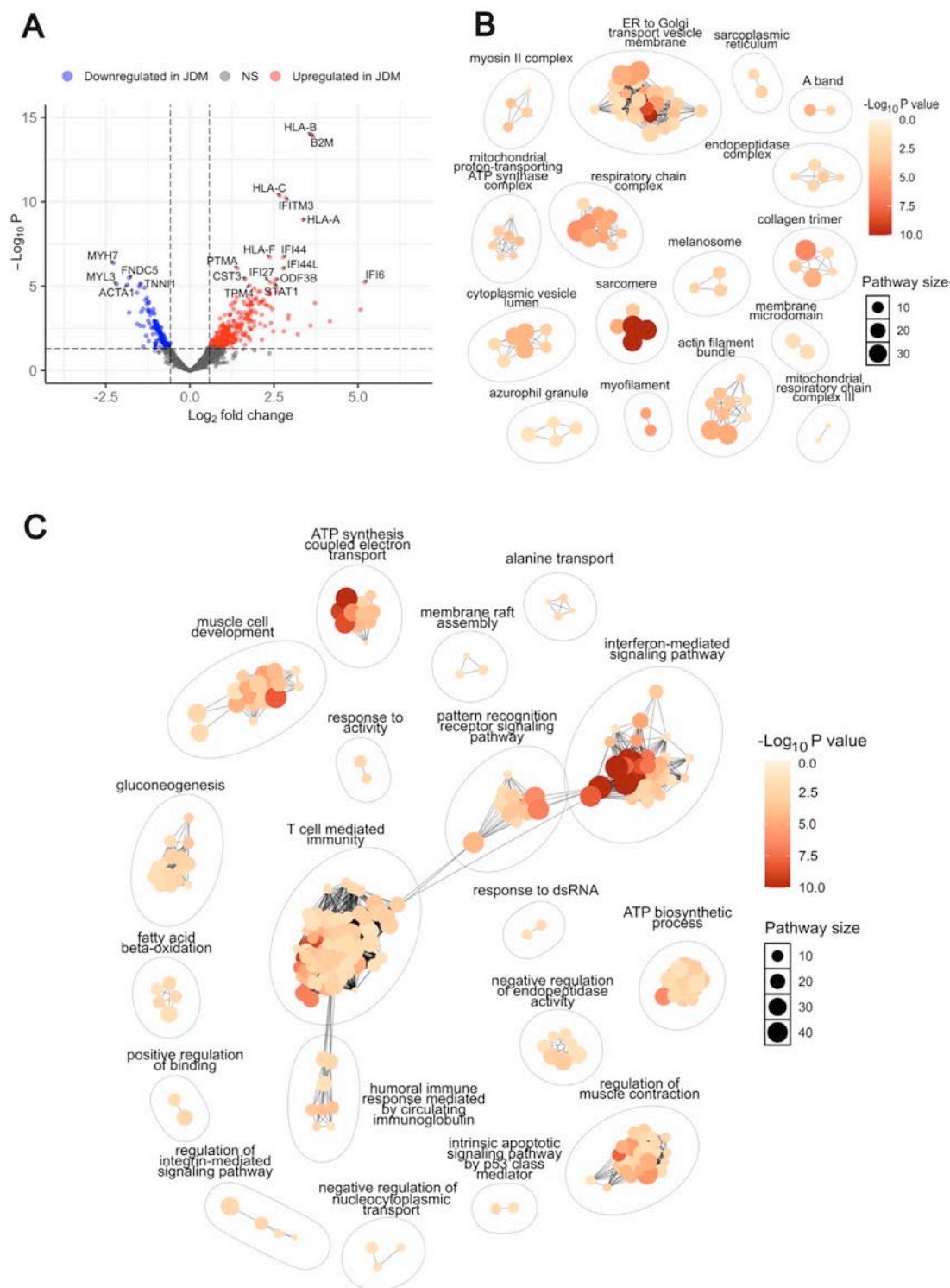


**Figure 2.** Differential gene expression analysis demonstrates a high interferon-driven signature and abnormal mitochondrial gene signature in JDM compared to control muscle. (A) Volcano plot illustrating differentially expressed genes (DEGs) between JDM and control muscle ROIs. Genes with an adjusted  $P$  value  $\leq 0.05$  and  $|\log_2 FC| \geq 0.58$  are considered statistically significant ( $n = 448$ ). Red points represent significantly upregulated genes, and blue significantly downregulated genes. The 20 genes with the smallest adjusted  $P$  values were annotated. (B) Network cluster plot of enriched gene ontology cellular component (CC) pathways among the 448 DEGs, generated using the aPEAR R package. Each cluster represents groups of similar cellular components, derived from gene ontology terms. Pathways with an adjusted  $P$  value  $\leq 0.05$  (Benjamini-Hochberg procedure) were included in the clustering and network analysis. (C) Network cluster plot of enriched gene ontology biological process (BP) pathways among the 448 DEGs, generated using the aPEAR R package. Each cluster represents groups of related BPs, highlighting functional pathways involved in JDM. Pathways with an adjusted  $P$  value  $\leq 0.05$  (Benjamini-Hochberg procedure) were included in this clustering and network analysis. For (B) and (C), larger dots represent pathways associated with a higher number of significant genes (shown in key, pathway size). Dot colour intensity corresponds to significance, with deeper red shades indicating smaller  $P$  values (shown in colour bar, adjusted  $P$  value). aPEAR, advanced pathway enrichment analysis representation; FC, fold change; JDM, juvenile dermatomyositis; NS, not significant; ROI, regions of interest.

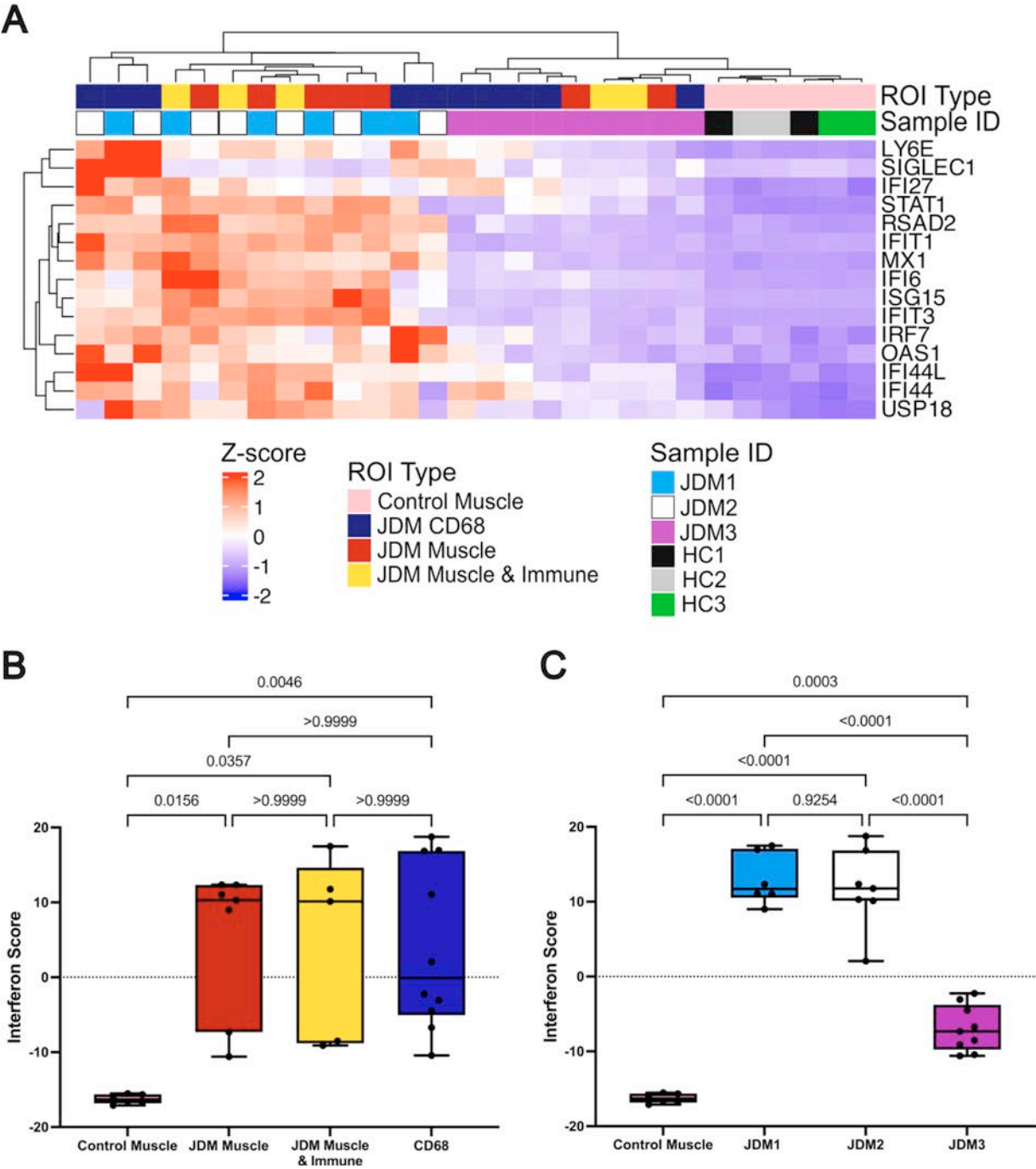


**Figure 3.** Interferon-driven signature is elevated across each cell type analysed in JDM tissue. (A) Heatmap showing the normalised, scaled expression levels of the 15-gene interferon score across the ROIs. Distinct ROI types (top row) are allocated colours pink, blue, red and yellow as shown; individual patients (second row sample ID) are allocated colours as shown. Unsupervised clustering groups the ROIs into 3 distinct clusters: one including ROIs patient JDM1 (light blue ID) and JDM2 (white bordered ID), a second cluster for patient JDM3 (purple ID), and a third for control ROIs (black, grey and green IDs). The coloured scaled bar red to blue highlights the Z-score ranges, with red indicating a positive Z-score and blue indicating a negative Z-score. (B, C) Boxplots showing the 15-gene interferon score, calculated as the sum of Z-scores for the 15 ISGs, compared across: (B) different ROI types and (C) individual patients and controls. For (B), statistical differences between the groups were assessed using the Kruskal-Wallis test, followed by post hoc pairwise comparisons using Dunn’s test. For (C), statistical differences were assessed using one-way ANOVA, followed by post hoc pairwise comparisons using Tukey’s HSD test. ANOVA, analysis of variance; HSD, honestly significant difference; ID, identification; ISG, interferon-stimulated gene; JDM, juvenile dermatomyositis; ROI, regions of interest.

S4). It is well established that both muscle and endothelium in adult and juvenile idiopathic inflammatory myopathy (IIM) express high levels of HLA class I and II proteins which can be independent of inflammatory infiltrates [17–20]. Therefore, we ascribe this result to the expression of *HLA* genes (driven by IFN) in muscle fibres or endothelium.

To determine whether differentially expressed pathways were upregulated or downregulated in JDM against controls,

gene set enrichment analysis was performed using the Fast Gene Set Enrichment Analysis (fgSEA) method [21]. This analysis provides complementary insights by considering the entire ranked gene list, identifying pathways with subtle but coordinated expression changes. Using fgSEA, 79 and 269 significant pathways (adjusted *P* value ≤.05, Benjamini-Hochberg procedure) were identified with the GO CC and GO BP gene sets, respectively, many of which overlapped with the ORA results.

Full lists of the significant pathways identified via fGSEA and their associated fold changes and clusters can be found in [Supplementary Tables S5 \(GO CC\) and S6 \(GO BP\)](#).

Clustering of the 79 pathways (GO CC) using aPEAR validated the previous results, with the generated network plots reinforcing involvement of ER to Golgi transport pathways (upregulated) and mitochondrial-related pathways (downregulated, [Supplementary Fig S3A and Table S5](#)). In contrast, clustering of the 269 GO BP pathways highlighted the significant upregulation of IFN signalling pathways, which fall under the cluster of ‘regulation of response to external stimulus’ ([Supplementary Fig S3B and Table S6](#)). [Supplementary Figure S3C](#) shows the 15 most downregulated and 15 most upregulated pathways from both GO CC and GO BP analyses, visualised by comparing normalised enrichment scores.

### *IFN-driven signature is elevated across tissue cell types analysed in patients with JDM*

We next used our previously validated 15-gene IFN-stimulated gene signature [3] to visualise variations in the expression patterns of IFN-stimulated genes across the different ROIs, from patients and controls [22]. All 15 of these genes are associated with both type I and type II IFN signalling as annotated in the Interferome database [23]. Heatmap visualisation of normalised, scaled expression levels across ROIs revealed distinct patterns of IFN-stimulated gene (ISG) expression between patients, with unsupervised clustering of ROIs primarily by patient. One patient with JDM (JDM3) exhibited lower ISG expression compared to the other 2 patients with JDM ([Fig 3A](#)). Notably, this patient was less weak at the time of biopsy than patients JDM1 and JDM2 ([Table](#)).

Quantification of the 15-gene ISG score (IFN score) demonstrated significant elevation in all ROI types from JDM tissues compared to controls. However, pairwise comparisons using Dunn’s multiple comparisons test revealed no statistically significant differences between different ROI types within the JDM group, indicating a consistent IFN activation signature across muscle cells, immune-infiltrated regions, and CD68+ macrophage-enriched regions ([Fig 3B](#)). Analysis of IFN score values by ROI confirmed that all 3 patients had significantly higher IFN scores than controls, but that the IFN score of JDM3 was significantly lower than scores of JDM1 or JDM2 ([Fig 3C](#)).

### *Mitochondrial dysfunction is consistent across all patients with JDM*

To further analyse mitochondrial involvement within JDM muscle tissue, the 448 DEGs identified in JDM muscle ROIs compared to controls ([Fig 2A](#)) were further examined based on their associated GO terms. Of these 448 genes, 75 were annotated with the GO term ‘mitochondrion’. This list was carefully curated, removing known ISGs, including 5 which were part of our IFN score, and other genes which are not specific to mitochondrial function, or only interact with mitochondria under specific conditions (see [Supplementary Methods](#)). Unsupervised clustering of the 41 remaining genes revealed clusters by ROI type (and therefore cell type), rather than by patient, suggesting that mitochondrial gene expression patterns are shaped by cell type and disease state, but were largely consistent across patients ([Fig 4A](#)). Genes included in analysis shown in [Figure 4](#) are listed in [Supplementary Table S7](#). Quantification of the mitochondrial gene score using these 41 genes demonstrated significant differences between all JDM ROIs and controls ([Fig 4B](#)).

Pairwise comparisons (Tukey’s multiple comparisons test) revealed that among the JDM patient data, CD68+ macrophage regions exhibited significantly distinct mitochondrial scores compared to both JDM muscle (adjusted  $P < .0001$ ) and control muscle ROIs (adjusted  $P < .0001$ ) indicating cell-specific variation in mitochondrial gene expression patterns ([Fig 4B](#)), unlike the uniformity across cell types seen in IFN dysregulation in JDM ([Fig 3B](#)). No statistically significant difference was observed between the muscle and muscle+immune cell JDM mitochondrial scores ([Fig 4B](#), adjusted  $P = .1438$ ). Analysis of the 41-gene score across patients confirmed that each patient had a highly significant altered mitochondrial score compared to controls, but there were no significant differences in mitochondrial scores between patients ([Fig 4C](#)). Together, these results suggested that while the degree of IFN-driven pathology varied between cases, the mitochondrial abnormality was observed consistently across these 3 cases.

To validate these findings in an independent cohort, fGSEA analysis was performed using a publicly available RNAseq dataset, comparing 4 JDM with 5 control muscle biopsies [24]. As these data were bulk RNAseq, analysis was performed at the whole-biopsy level but not for specific regions or cell types within each biopsy. Analysis confirmed upregulation of IFN-driven and immune activation pathways, and downregulation of mitochondrial pathways (including oxidative phosphorylation, respiratory electron transport chain, ATP synthesis coupled electron transport), [Supplementary Figure S4A](#). This dataset also enabled transcriptome-wide quantification, including mitochondrial-encoded gene transcripts not captured by the GeoMx whole transcriptome atlas. Of the 37 mitochondrial-encoded genes, 20 were significantly (adjusted  $P$  value  $< .05$ ,  $|\text{Log2FC}| \geq 0.58$ ) downregulated in JDM muscle compared to controls ([Supplementary Fig S4B](#)), and this was consistent across all cases ([Supplementary Fig S4C](#)). Furthermore, 10 of the 41 mitochondrial score genes were significantly and consistently downregulated in JDM in the replication cohort ([Supplementary Fig S4D, E](#)), while 13 genes of the 15-gene IFN score were significantly upregulated in this cohort ([Supplementary Fig S4F](#)). Again, we observed clear patient heterogeneity in levels of IFN-driven gene expression ([Supplementary Fig S4G](#)).

### *Relationship between IFN-driven and mitochondrial abnormalities in JDM muscle*

Given our intriguing finding of a lack of correlation between IFN and mitochondrial pathological gene expression, we investigated this at the protein level using conventional immunohistochemistry and chemical stains in a larger cohort ( $n = 19$ ), including 16 further UK Juvenile Dermatomyositis Cohort Biomarker Study & Repository (JDCBS) JDM cases and the index 3 JDM cases, all treatment naive. Sections were stained and scored for IFN-driven MxA protein expression ([Fig 5A–D](#)) and mitochondrial abnormality ([Fig 5E–J](#)) (see [Supplementary Methods](#)). JDM cases exhibited a range of mitochondrial deficiency severity (6 severe, 10 mild, and 3 none) and IFN-driven MxA protein expression. However, there was no correlation between these 2 features ([Fig 5K](#),  $P = .657$ ). In contrast, the level of MxA protein upregulation on muscle fibres correlated with clinical weakness measured by MMT8 (adjusted  $P = .0369$ , Benjamini-Hochberg procedure) and CMAS (adjusted  $P = .0084$ ), replicating our previous findings in 103 cases [25].

The histological feature of perifascicular atrophy (PFA) is well recognised in dermatomyositis and has been shown to correlate with COX deficiency and mitochondrial abnormalities in



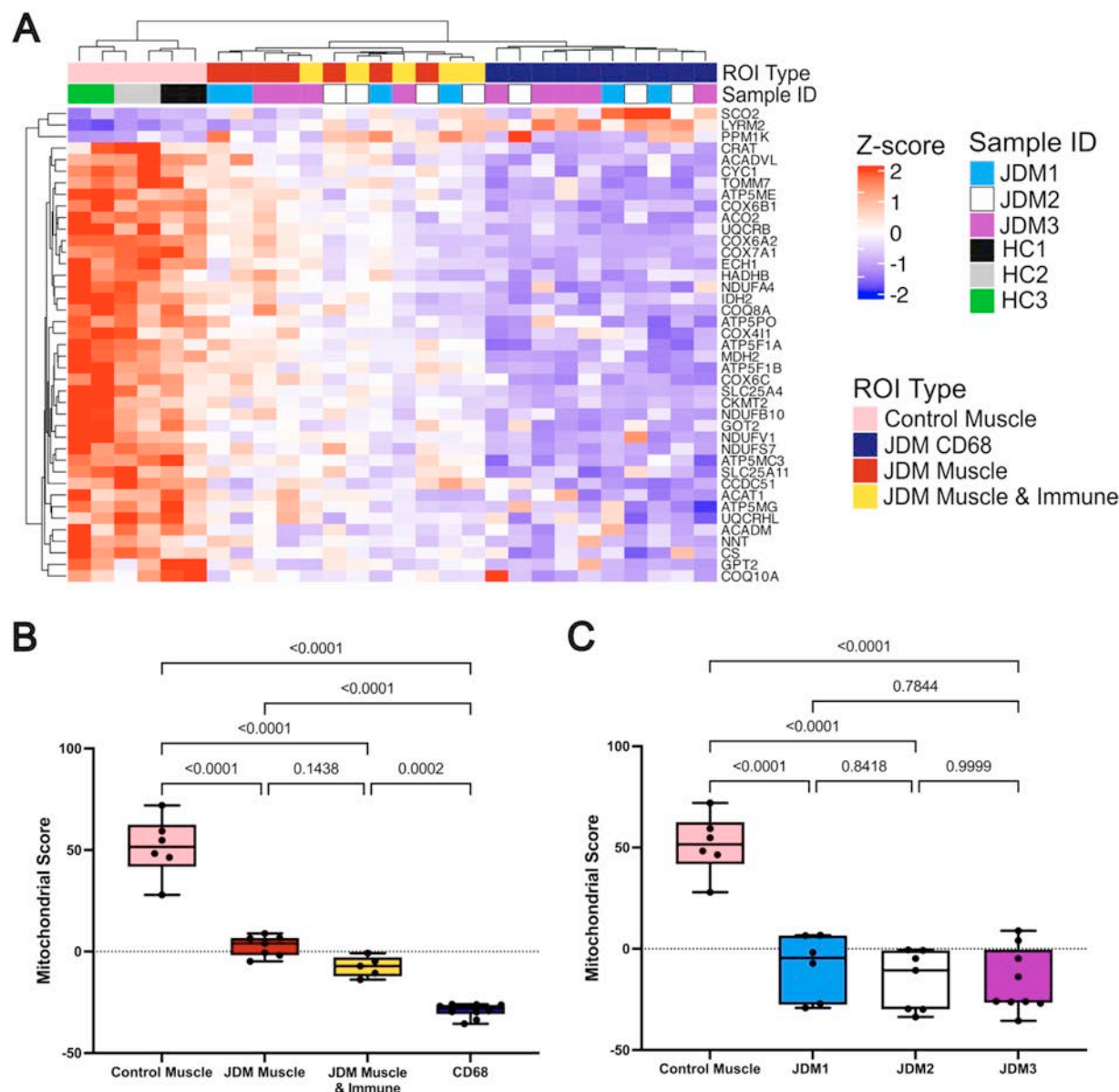


**Figure 4.** Abnormal mitochondrial signature is consistent across all patients with JDM but distinct between cell types. (A) Heatmap showing the normalised, scaled expression levels of the 41-gene mitochondrial score differentially expressed in JDM muscle against control ROIs. Distinct ROI types (top row) are allocated colours pink, blue, red and yellow as shown; individual patients (second row sample ID) are allocated colours as shown. All ROI types are included in the heatmap analysis. Unsupervised clustering groups the ROIs into 3 distinct clusters: one including JDM muscle ROIs and muscle + immune cell ROIs, a second for CD68+ ROIs, and a third for control muscle ROIs. The coloured scaled bar highlights the Z-score ranges, with red indicating a positive Z-score and blue indicating a negative Z-score. (B, C) Boxplots of 41-gene mitochondrial scores, calculated as the sum of Z-scores for the 41 mitochondrial genes, compared across: (B) different ROI types and (C) individual patients and controls. For (B) and (C), statistical differences were assessed using one-way ANOVA, followed by post hoc pairwise comparisons using Tukey's HSD test. ANOVA, analysis of variance; HSD, honestly significant difference; ID, identification; JDM, juvenile dermatomyositis; ROI, regions of interest.

JDM and adult DM [26]. We tested whether PFA within the ROIs analysed by GeoMx was associated with mitochondrial abnormality. All 3 JDM cases demonstrated evidence of PFA. Of the 22 ROIs, 18 contained the edge of a fascicle allowing analysis for PFA (Supplementary Fig S5A). PFA was present in 55% (10/18) of these ROI including regions from all 3 cases. In this small sample, no correlation was observed between PFA and mitochondrial abnormality, assessed in the 8 muscle/muscle + immune ROIs (Supplementary Fig S5B). However, this result may relate to small sample size, the fact that GeoMx does not measure expression of mitochondrial-encoded genes, or that each ROI covers areas with PFA and others without, while GeoMx generates a bulk-like average 41-gene mitochondrial score for the whole ROI.

To define other biological pathways associated with mitochondrial dysfunction, 2 complementary approaches were performed. First, for each pathway cluster shown in Supplementary Figure S3A, B, the most commonly shared genes within each cluster were used to generate cluster-specific expression scores. In the second approach, fGSEA was run using MSigDB Hallmark gene sets, and scores calculated from the leading-edge genes of each pathway (see Supplementary Methods). Across both methods, lower mitochondrial gene expression was consistently associated with reduced activity in metabolic pathways, including oxidative phosphorylation, fatty acid metabolism, glycolysis and genes involved in reactive oxygen species response as expected (Fig 6A, B). In addition, decreased expression of peroxisome-related genes and downregulation of sarcomere organisation



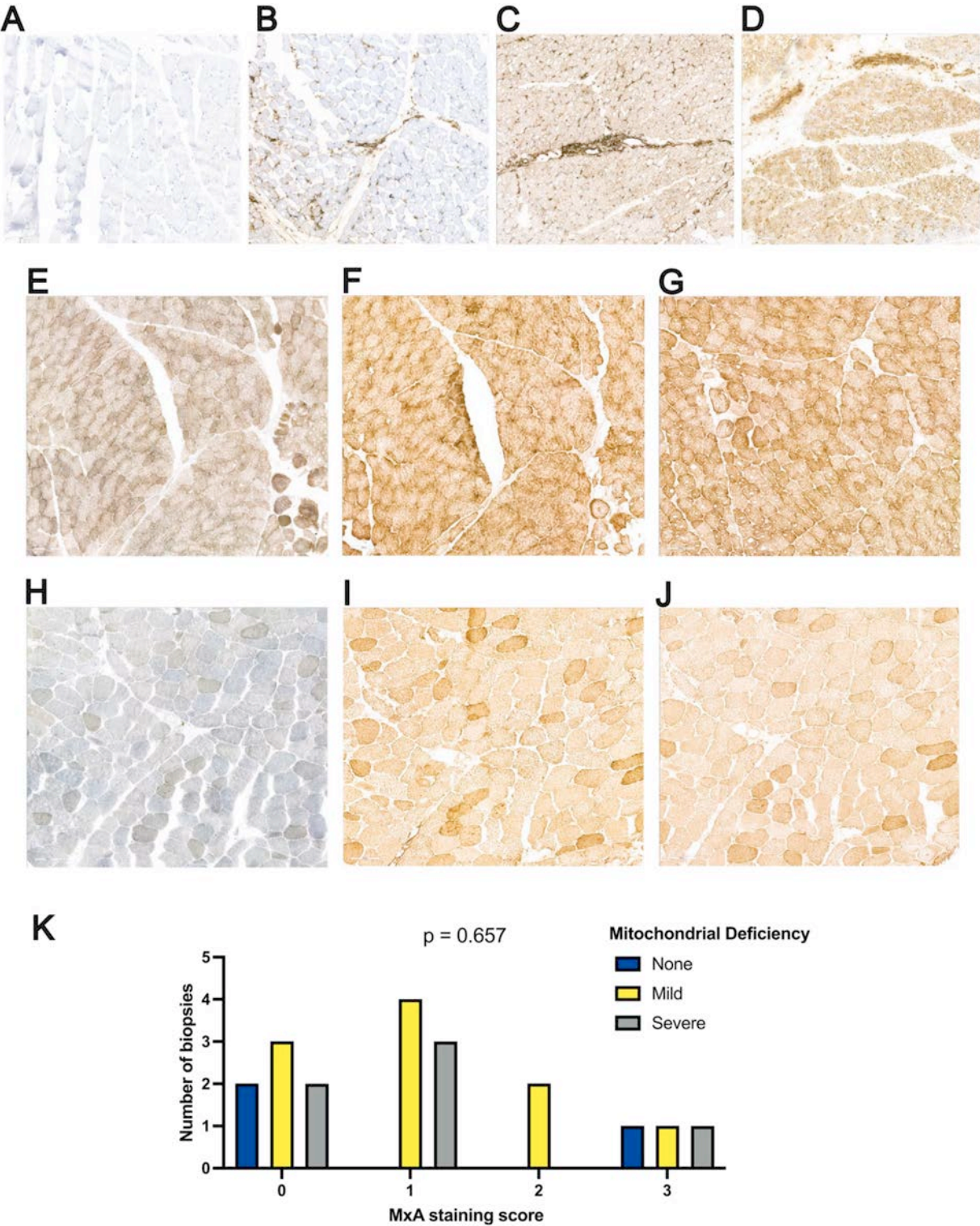


**Figure 5.** Lack of association between interferon dysregulation and mitochondrial deficiency assessed at protein level in an independent JDM cohort. (A-D) Representative immunohistochemical staining for myxovirus-resistance protein A (MxA), used to assess interferon-driven protein expression in muscle fibres. Scoring was performed using a 4-point scale: 0 = no staining (A), 1 = weak (B), 2 = moderate (C), and 3 = strong (D). (E-J) Representative staining for mitochondrial deficiency, assessed using combined COX–SDH histochemistry and supported by immunohistochemistry for MTCO1 (complex IV) and NDUF8 (complex I). Cases were categorised as having no (0), mild (1), or severe (2) mitochondrial deficiency. (E-G) Representative staining from a JDM biopsy with mild mitochondrial deficiency: (E) COX–SDH staining, (F) MTCO1, and (G) NDUF8. (H-J) Representative staining from a JDM biopsy with severe mitochondrial deficiency: (H) COX–SDH, (I) MTCO1, and (J) NDUF8. (K) Summary bar plot of 19 JDM muscle biopsies, showing the distribution of mitochondrial deficiency scores (0 = none, 1 = mild, 2 = severe) across each level of interferon activity (MxA score 0–3). Bar colours indicate the level of mitochondrial deficiency (none, mild, severe) as shown. Statistical analysis was performed using the *U*-statistic permutation test. JDM, juvenile dermatomyositis.

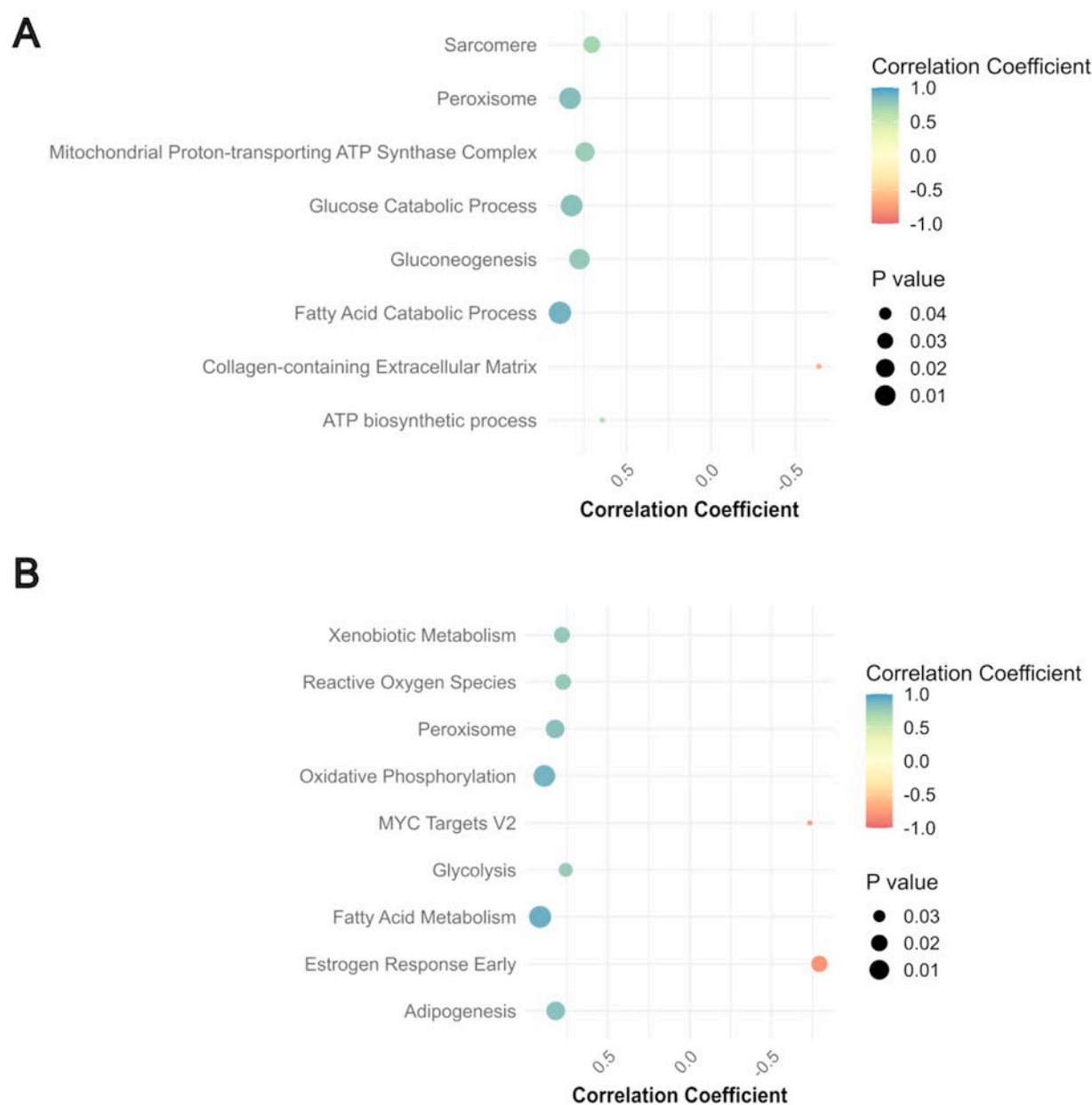


**Figure 6.** Pathway-level transcriptional signatures associated with mitochondrial dysfunction in JDM muscle. Dot plots show the significant correlation between the mitochondrial gene score and pathway-specific expression scores across muscle regions of interest (ROIs) from JDM biopsies (adjusted  $P \leq .05$ , Benjamini-Hochberg procedure). The mitochondrial gene score was calculated per ROI based on z-scores of 41 curated mitochondrial genes, using the mean and SD from control muscle as a reference. (A) Correlation with GO-based pathway clusters, derived from fGSEA of JDM ROIs compared to controls. For each cluster, a core gene signature was defined by selecting genes that appeared in the leading edge of  $\geq 75\%$  of constituent pathways. (B) Correlation with significantly enriched MSigDB Hallmark pathways (adjusted  $P \leq .05$ , Benjamini-Hochberg procedure) identified through gene set enrichment analysis of JDM vs control muscle. For both (A) and (B), each dot represents a single pathway or cluster. Dot size reflects the strength of the correlation ( $r$  coefficient), and dot colour indicates the statistical significance of the correlation, with deeper red shades corresponding to smaller adjusted  $P$  values. The colour scale bar reflects the adjusted  $P$  value. GO, gene ontology; JDM, juvenile dermatomyositis.

were observed to be correlated with more severe mitochondrial abnormalities.

*Transcriptomic differences between distinct regions of affected muscle and between patients*

Since we observed differences in IFN-driven signature between cases, we tested for other transcriptomic differences across patients, comparing patient JDM3 with JDM1 and JDM2. Initially, muscle and muscle-immune ROIs were combined to increase statistical power. Analysis comparing JDM3 vs JDM1 + JDM2 revealed 176 DEGs between groups (100 upregulated, 76 downregulated genes in patients JDM1 + JDM2,

Supplementary Fig S6A). Pathway analysis indicated 208 enriched GO BP pathways; cluster network analysis highlighted IFN and immune-related pathway clusters, including ‘positive regulation of type I interferon production’ (confirming our 15-gene IFN score result, Fig 3), ‘antigen processing and presentation via MHC Class I via ER pathways’, and ‘antibacterial humoral response’ (Supplementary Fig S6B). In this comparison between patients, mitochondrial pathways were not differentially expressed, confirming earlier results suggesting consistent mitochondrial abnormalities in all cases. Separate DGE analysis performed between the CD68+ cell ROIs of patient JDM3 against those of patients JDM1 + JDM2 revealed 63 DEGs (43 upregulated, 20 downregulated in JDM1 + JDM2,

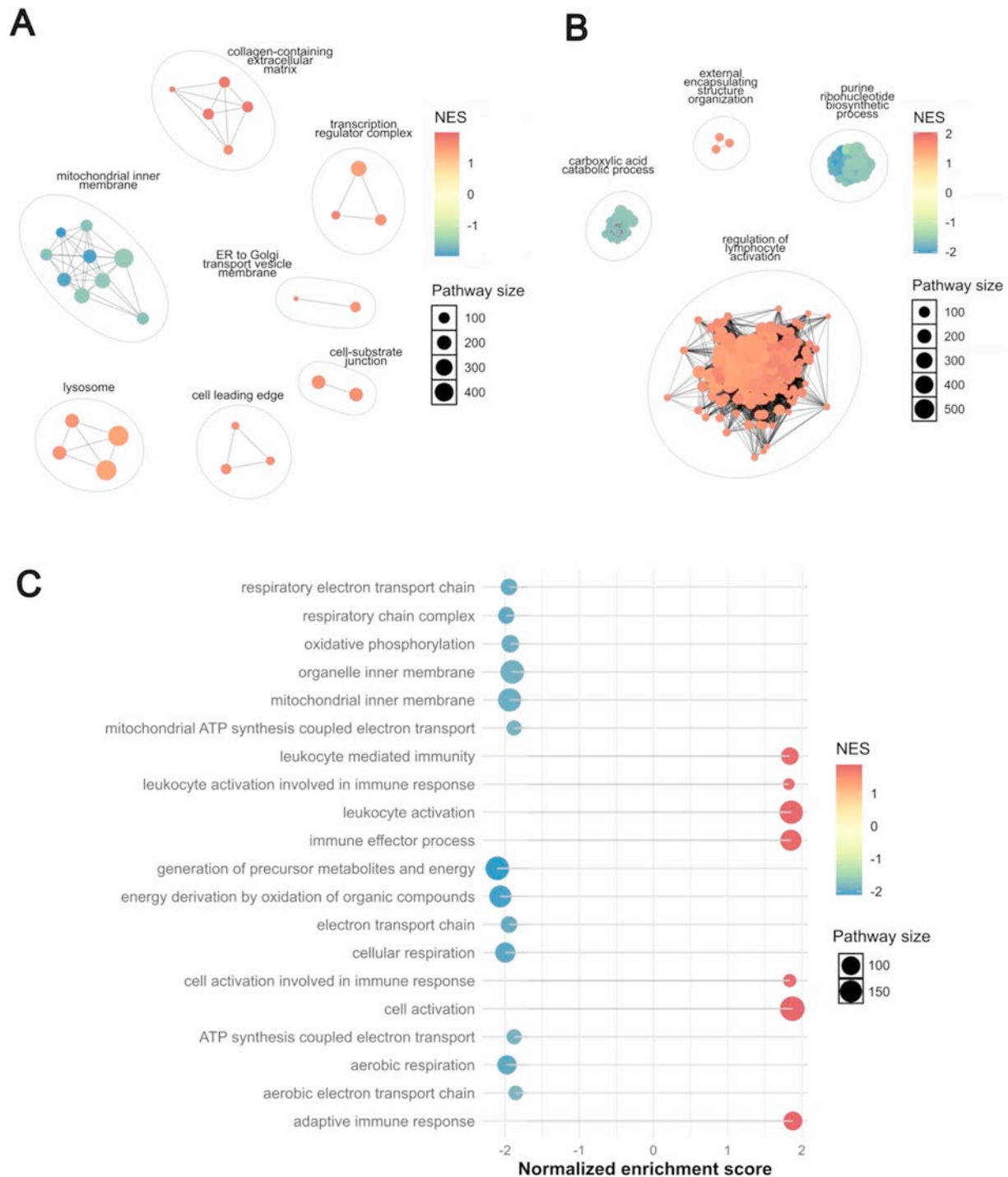


**Figure 7.** Gene set enrichment analysis reveals increased immune pathways and decreased mitochondrial functional pathways in JDM immune cell-rich muscle regions compared to JDM muscle-only regions. (A, B) Cluster plots of enriched gene ontology pathways, based on fGSEA performed on all genes for each comparison ranked by *P* value and fold change. (A) Plot of enriched GO cellular component pathways. (B) Plot of enriched GO biological process pathways. (C) Dot plot of the 20 GO BP and CC pathways with the highest absolute normalised enrichment score (NES). In panels (A–C), larger dots represent pathways associated with a higher number of genes (shown in key, pathway size), and the dot colour reflects the NES, with blue indicating negative NES and red indicating positive (shown in colour bar, NES). BP, biological process; CC, cellular component; GO, gene ontology; JDM, juvenile dermatomyositis.

Supplementary Fig S7A). Within this analysis, 148 GO BP pathways were significantly enriched, with the most prominent cluster being ‘negative regulation of viral genome replication’ (Fig 7B), indicating that expression of ISGs in muscle-infiltrating CD68+ cells also differed between the patients with JDM. We also conducted DGE analysis for each ROI type comparing JDM1 + JDM3 vs JDM2, and JDM2 + JDM3 vs JDM1. Those comparisons did not reveal meaningful differences, yielding between 0 and 4 DEGs only (data not shown).

Finally, we explored transcriptional patterns in muscle-immune ROI (which had dense infiltrates of CD45+ immune cells, including CD3+/CD68+/CD20+ cells), compared to muscle-fibre only regions. Initial DGE analysis using the limma-voom pipeline suggested no significant DEGs between these ROI groups, based on the same fold change and adjusted *P* value criteria (data not shown). However, fGSEA analysis revealed 28 significant pathways in the GO CC gene set and 317 significant pathways in the GO BP gene set (Fig 7A, B,



respectively). These pathway-level findings suggested that immune-infiltrated muscle regions exhibited further downregulation of mitochondrial and metabolic pathways, alongside increased expression of immune-related and leukocyte activation pathways (Fig 7C). While not captured at the significant DEG level, these transcriptional differences are consistent with the expected biological impact of immune infiltration. These significant pathways are found in [Supplementary Tables S8](#) (GO CC) and [S9](#) (GO BP).

## DISCUSSION

Our previous work and that of others studying affected muscle in JDM, a key target tissue of pathology, has demonstrated upregulated expression of IFN-driven gene and protein expression. In muscle fibres, this includes overexpression of class I MHC protein (also known as HLA class I) [6,20,27], and myxovirus-resistance protein A [25]. Expression of IFN-driven proteins is variable between cases, but typically correlates with the degree of weakness [25]. Many studies have confirmed a strong IFN-driven transcriptional signature in both muscle and blood of both adult and paediatric patients with IIM [3,28–31]. Therapies which target IFN or IFN signalling are increasingly being tested in myositis [32].

Our previous gene expression analysis of peripheral blood lineage-sorted immune cells from patients with JDM revealed not only this known IFN-driven signature, but also a signature of mitochondrial dysfunction, most marked in blood monocytes [3] which was confirmed at the functional level and found to persist, and was not restored to normal by treatment, despite clear reduction in expression of ISGs on treatment. Furthermore, we showed that mitochondrial DNA was abnormally released in patient monocytes and could drive production of IFN and downstream ISGs, an effect that was mediated via C-GAS-STING and TLR9 pathways.

To date, the majority of transcriptional studies published using muscle tissue of patients with IIM have used bulk RNA sequencing. In these datasets, it is challenging to understand or define the role of different cells, or to identify how specific tissue microniches contribute to pathology. In this study, we have for the first time used spatial transcriptomic methods to analyse muscle tissue from children with JDM obtained at diagnosis before starting treatment compared to age-matched healthy muscle. Thus, our data are not confounded by the effects of medication. We used Nanostring GeoMx DSP to generate transcriptional data of 3 specific region types within the muscle. This allowed comparison of regions within the disease tissue including those where infiltrating immune cells are scarce, or not detected, in regions of dense clusters of inflammatory cells, and in regions where CD68+ infiltrating macrophages were predominant. Our data confirm successful use of this platform for analysis using historical cryopreserved muscle tissue.

Initial analysis of JDM compared to control tissue confirmed high expression of IFN-stimulated genes in all regions analysed. Furthermore, strong upregulation of pathways related to protein transport through the ER and Golgi, and ER stress, was observed, aligning well with our previous studies in human muscle and a transgenic mouse myositis model [4,33,34]. We also demonstrate that, as previously observed in blood monocytes, in the JDM tissue itself, muscle fibres have a highly dysregulated mitochondrial signature. Dysregulated pathways included those related to mitochondrial function, respiratory chain, and mitochondrial proton transport: their expression was downregulated in muscle. In addition, the signal for mitochondrial and

respiratory chain-related genes was distinct in CD68-enriched regions. By analysing RNAseq data from a second JDM cohort, we validated our results for these nuclear-encoded mitochondrial genes and additionally showed downregulation of mitochondrial-encoded genes. We investigated the relationship of the signatures to clinical activity as assessed by muscle weakness. We observed a correlation between IFN signature and weakness, whereby 1 patient who was minimally weak (MMT8 score 78) had lower expression of IFN-induced signature than the 2 patients who were significantly weak (MMT8 scores 44 and 42). Interestingly, this was different for the mitochondrial signature detected in tissue, which was independent of the IFN signature. The downregulation of mitochondrial pathways was consistently observed for the index 3 patients, regardless of muscle strength, and across the 3 patients this result showed minimal variance for the 41-gene mitochondrial score we defined. We extended these findings in 19 cases at protein level, and replicated the observation of no correlation between level of IFN-driven protein expression with mitochondrial abnormality. A recent study suggested that IFN $\gamma$  itself leads to mitochondrial dysfunction and oxidative stress in both a mouse model and patients with adult IIM [10]. In contrast, our previous work in JDM monocytes suggested that circulating oxidised mitochondrial DNA itself may activate IFN pathways. The current study suggests that mitochondrial dysfunction can be equally prominent in patients with either low or high IFN score at both RNA and protein level, implying that IFN-independent drivers of mitochondrial dysfunction exist. If so, blocking of IFN by new therapeutic agents may not adequately control all aspects of disease pathology. Supporting this, recent evidence in Inclusion Body Myositis (IBM) and Polymyositis (PM) suggests that mitochondrial-encoded gene mutations lead to inflammation and immune cell infiltration, activating the cGAS/STING pathway, in the absence of IFN [35]. In a model of Parkinson's disease (PD) and patients with PD, mitochondrial DNA damage triggers neuron pathology, which is, remarkably, exacerbated in the IFN-deficient mouse [36]. Collectively, these findings suggest that the intersection between mitochondrial biology and IFN is bidirectional and complex, and that pathologies driven by altered mitochondrial DNA and function can act independently of IFN. Our demonstration that mitochondrial dysfunction correlates with altered function of the peroxisome, an organelle key to metabolic pathways which communicates with mitochondria, may reveal further potential novel treatment targets [37].

Our analysis of JDM muscle compared to healthy muscle also revealed other dysregulated pathways associated with disease, including ER to Golgi transport, sarcomere and T cell activation. We attribute this to the highly upregulated HLA class I and II DEGs which are known to be upregulated in muscle fibres themselves in JDM.

Direct comparison of muscle-only to muscle + immune regions revealed pronounced downregulation of mitochondrial and metabolic pathways, alongside increased expression of immune-related pathways, in immune-infiltrated regions. This indicates that relative mitochondrial abnormalities differ between cell types in inflamed tissue, and concurs with evidence that the mitochondrial transcriptome differs across tissue types [38]. To precisely dissect specific tissue niches and cell interactions in JDM, future single-cell spatial analyses will provide a more precise understanding of cell-specific contributions and define cell-cell interactions in JDM muscle tissue. Single-cell spatial analysis of JDM muscle is underway to allow us to distinguish these issues.

This study has several limitations. The initial sample size ( $n = 3$  in each group) was small which limited our ability to



detect gene expression differences with a small effect size, which may still be important to pathology: therefore, our findings should be interpreted with caution, especially when comparing 2 patients to one other. In addition, the 3 initial JDM and 3 control cases are not perfectly matched for sex or age, and in this group size it was not possible to adjust for these variables. Thus, despite close clustering of the control case data in both PCA and gene score analyses, larger studies are needed to assess the effect of these variables on muscle transcription in myositis.

Despite this, key significant differences between patients and controls were replicated in a second cohort and our findings were validated at protein level in a larger cohort. Our previous analysis of 103 JDM muscle biopsies showed significant histological heterogeneity across cases which varied in part by MSA status [25]. The current study was not powered to analyse for association between specific MSA status and transcriptional differences. A larger cohort will therefore be essential to capture the full variance in patient phenotype, MSA status, clinical severity, and pathology, to provide a robust understanding of JDM-associated gene expression changes. Furthermore, analysis of tissue-infiltrating CD68+ macrophages lacked a control comparison group due to the absence of CD68+ cells in normal muscle tissue limiting our ability to identify the unique transcriptomic signature of infiltrating macrophages against healthy macrophages.

This study represents the first application of spatial transcriptomics to muscle biopsies from a patient with JDM using the GeoMx technology, unveiling critical insights into mitochondrial and immune dysregulation at the tissue level. Importantly, we have defined parallel gene expression patterns in both the muscle and macrophage-rich regions of JDM muscle, as previously identified in blood monocytes. Together, these data suggest that mitochondrial dysfunction is present across tissues and, that within the muscle itself, this signal is readily detectable in both CD68+ infiltrating cells and muscle fibres. Our results also indicate that this mitochondrial dysfunction is uncoupled from the characteristic IFN-driven signature. Given that almost 50% of patients with JDM are not well-controlled on standard first-line treatments [2], which are currently focused on the suppression of immune pathways, our demonstration that mitochondrial dysfunction is present in the muscle of the majority of cases of JDM in this study has important implications. First, adjunctive therapies that target the mitochondrial pathology could be tested in combination with current treatments. Second, this signature may be readily tested and used to drive treatment choices in the future. Future work to define whether the mitochondrial signature in tissue correlates with that in blood will be important for the design of stratification tools in trials of novel agents targeting the mitochondrial abnormality.

Our findings advance the understanding of JDM pathogenesis and lay the groundwork for future research into the use of therapies which specifically target mitochondrial dysfunction and immune-mediated damage.

## Competing interests

LRW reports financial support was provided by Versus Arthritis, UK Research and Innovation Medical Research Council, National Institute for Health and Care Research, Myositis UK, Great Ormond Street Hospital Children's Charity, and Cure JM Foundation. MGLW reports financial support was provided by Versus Arthritis, National Institute for Health and Care Research, Connect Immune Partnership, Myositis UK, and Great

Ormond Street Hospital Children's Charity. APC reports financial support was provided by The Kennedy Trust for Rheumatology Research. LRW reports a relationship with Pfizer Inc that includes: consulting or advisory, funding grants, and speaking and lecture fees. LRW reports a relationship with Cabaletta Bio Inc that includes: consulting or advisory. LRW reports a relationship with Eli Lilly and Company that includes: funding grants. The other authors declare they have no competing interests.

## CRedit authorship contribution statement

**Aris E. Syntakas:** Writing – original draft, Visualization, Software, Methodology, Investigation, Formal analysis, Data curation. **Melissa Kartawinata:** Writing – review & editing, Methodology, Data curation. **Nia M.L. Evans:** Writing – review & editing, Methodology, Data curation. **Huong D. Nguyen:** Writing – review & editing, Methodology, Data curation. **Charalampia Papadopoulou:** Writing – review & editing, Data curation. **Muthana Al Obaidi:** Writing – review & editing, Data curation. **Clarissa Pilkington:** Writing – review & editing, Data curation. **Yvonne Glackin:** Writing – review & editing, Data curation. **Christopher B. Mahony:** Writing – review & editing, Formal analysis. **Adam P. Croft:** Writing – review & editing, Formal analysis. **Simon Eaton:** Writing – review & editing, Formal analysis. **Mario Cortina-Borja:** Writing – review & editing, Methodology, Data curation. **Olumide Ogunbiyi:** Writing – review & editing, Visualization, Software, Investigation. **Ashirwad Merve:** Writing – review & editing, Visualization, Software, Investigation. **Lucy R. Wedderburn:** Writing – review & editing, Writing – original draft, Supervision, Resources, Project administration, Methodology, Funding acquisition, Formal analysis, Conceptualization. **Meredith G. Li Wilkinson:** Writing – review & editing, Writing – original draft, Supervision, Resources, Project administration, Methodology, Funding acquisition, Formal analysis, Conceptualization.

## Patient and public involvement and engagement

Patients and carers were involved at every stage of this research, including study conception, design, delivery, and analysis, through our partnership stakeholder group, the JDCBS PPIE group. The study was discussed at our annual JDCBS study day and also at the UK JDM Family Day, where families, patients, and parents provided input. All patients and families who are part of the study across the UK hear about updates via a regular newsletter as well as on our dedicated website.

## Acknowledgements

We thank all of the families, patients, parents, and carers who contributed to the study and allowed us to use samples and data for this work. We are very grateful to Mr Dario Cancemi for excellent study management, to the clinical team who assist with data collection, to Dr Lizzy Rosser for critical review and to the BRAIN Bank UK for access to control cases. We are grateful to the members of the JDCBS research group (JDRG) and who are listed in the supplementary materials. We thank the team at Nanostring for valuable guidance, the GOSH histopathology team including Abigail White and Mwaka Mshanga, and Darren Chambers, Department of Neuropathology, UCL Queen Square Institute of Neurology for chemical stains. We thank Mr J A McBride for advice on colour figures.

The data presented in this manuscript have not been published previously. However, some of the data were submitted as

an abstract for the European Alliance of Associations for Rheumatology (EULAR) 2025 congress.

## Contributors

AES contributed to data curation, led the development of the formal analysis and methodology pipeline, visualisation, and drafting of the original manuscript. MK, HDN, NMLE and MC-B contributed to data curation and methodology development. APC, CBM and SE contributed to analysis. ChP, MAO, ClP and YG contributed to data collection and curation. AM and OO were responsible for histopathology analysis. LRW and MGLW conceptualised the study, acquired funding and coled analysis, methodology development, project supervision. LRW, MGLW and MK contributed to both original drafting and editing of the manuscript. All authors reviewed and approved the final manuscript for submission.

## Funding

This study was supported by generous grants from **Versus Arthritis** (Career Development fellowship to MGLW ref 23202, and PhD studentship to AS, ref 23202, Centre grant ref 21593 to LRW), Myositis UK, Great Ormond Street Children's Charity (W1143, and W1183), NIHR Biomedical Research Centre at GOSH (fellowship to MW ref 18IR33) and the Connect Immune Partnership (ref 22936). The work was also supported by grants from the Medical Research Council (MR/N003322/1 and MR/R013926/1), and Cure JM. APC is funded by a Kennedy Trust for Rheumatology Research Senior Fellowship KENN 19 20 06.

## Patient consent for publication

Not applicable, consent provided through recruitment to ethical approved study.

## Ethics approval

This study involves human participants; the study was fully approved by the North-East Yorkshire Research Ethics Committee (MREC 01/3/022). All participants gave fully informed consent (or had parental fully informed consent), and age-appropriate assent, in accordance with the declaration of Helsinki.

## Provenance and peer review

Not commissioned; externally peer reviewed.

## Data availability statement

The data that support the findings of this study are available from the corresponding authors on reasonable request. Script used in analyses is openly available in GitHub (<https://github.com/WedderburnLab/GeoMx-pipeline>).

## Supplementary materials

Supplementary material associated with this article can be found in the online version at doi:10.1016/j.ard.2025.07.015.

## Orcid

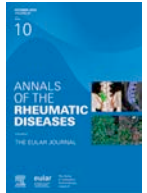
Aris E. Syntakas: <http://orcid.org/0009-0004-6225-9373>  
Melissa Kartawinata: <http://orcid.org/0000-0002-9432-393X>

Nia M.L. Evans: <http://orcid.org/0009-0004-9922-8896>  
Huong D. Nguyen: <http://orcid.org/0000-0003-1524-8028>  
Charalampia Papadopoulou: <http://orcid.org/0000-0002-1237-0557>  
Muthana Al Obaidi: <http://orcid.org/0000-0002-2144-3682>  
Clarissa Pilkington: <http://orcid.org/0000-0003-2289-2428>  
Christopher B. Mahony: <http://orcid.org/0000-0003-4487-2540>  
Adam P. Croft: <http://orcid.org/0000-0002-9487-0511>  
Simon Eaton: <http://orcid.org/0000-0003-0892-9204>  
Mario Cortina-Borja: <http://orcid.org/0000-0003-0627-2624>  
Olumide Ogunbiyi: <http://orcid.org/0000-0001-5208-5526>  
Ashirwad Merve: <http://orcid.org/0000-0001-9715-1849>  
Lucy R. Wedderburn: <http://orcid.org/0000-0002-7495-1429>  
Meredith G. Li Wilkinson: <http://orcid.org/0000-0002-7972-8066>

## REFERENCES

- [1] Kim H. Updates on interferon in juvenile dermatomyositis: pathogenesis and therapy. *Curr Opin Rheumatol* 2021;33(5):371–7. doi: 10.1097/BOR.0000000000000816.
- [2] Papadopoulou C, Chew C, Wilkinson MGL, McCann L, Wedderburn LR. Juvenile idiopathic inflammatory myositis: an update on pathophysiology and clinical care. *Nat Rev Rheumatol* 2023;19(6):343–62. doi: 10.1038/s41584-023-00967-9.
- [3] Wilkinson MGL, Moulding D, McDonnell TCR, Orford M, Wincup C, Ting JYJ, et al. Role of CD14+ monocyte-derived oxidised mitochondrial DNA in the inflammatory interferon type 1 signature in juvenile dermatomyositis. *Ann Rheum Dis* 2023;82(5):658–69. doi: 10.1136/ard-2022-223469.
- [4] Nistala K, Varsani H, Wittkowski H, Vogl T, Krol P, Shah V, et al. Myeloid related protein induces muscle derived inflammatory mediators in juvenile dermatomyositis. *Arthritis Res Ther* 2013;15(5):R131. doi: 10.1186/ar4311.
- [5] Yasin SA, Schutz PW, Deakin CT, Sag E, Varsani H, Simou S, et al. Histological heterogeneity in a large clinical cohort of juvenile idiopathic inflammatory myopathy: analysis by myositis autoantibody and pathological features. *Neuropathol Appl Neurobiol* 2019;45(5):495–512. doi: 10.1111/nan.12528.
- [6] Varsani H, Charman SC, Li CK, Marie SKN, Amato AA, Banwell B, et al. Validation of a score tool for measurement of histological severity in juvenile dermatomyositis and association with clinical severity of disease. *Ann Rheum Dis* 2015;74(1):204–10. doi: 10.1136/annrheumdis-2013-203396.
- [7] Arnold L, Henry A, Poron F, Baba-Amer Y, van Rooijen N, Plonquet A, et al. Inflammatory monocytes recruited after skeletal muscle injury switch into antiinflammatory macrophages to support myogenesis. *J Exp Med* 2007;204(5):1057–69. doi: 10.1084/jem.20070075.
- [8] Hernandez-Torres F, Matias-Valiente L, Alzas-Gomez V, Aranega AE. Macrophages in the context of muscle regeneration and duchenne muscular dystrophy. *Int J Mol Sci* 2024;25(19):10393.
- [9] Li Z, Liu H, Xie Q, Yin G. Macrophage involvement in idiopathic inflammatory myopathy: pathogenic mechanisms and therapeutic prospects. *J Inflamm (Lond)* 2024;21(1):48. doi: 10.1186/s12950-024-00422-w.
- [10] Abad C, Pinal-Fernandez I, Guillou C, Bourdenet G, Drouot L, Cosette P, et al. IFN $\gamma$  causes mitochondrial dysfunction and oxidative stress in myositis. *Nat Commun* 2024;15(1):5403. doi: 10.1038/s41467-024-49460-1.
- [11] Piñeiro AJ, Houser AE, Ji AL. Research techniques made simple: spatial transcriptomics. *J Invest Dermatol* 2022;142(4):993–1001.e1. doi: 10.1016/j.jid.2021.12.014.
- [12] Böning S, Schneider F, Huber AK, Langhoff D, Lin H, Kaczorowski A, et al. Region of interest localization, tissue storage time, and antibody binding density—a technical note on the GeoMx® Digital Spatial Profiler. *Immunoanal Technol* 2024;23:100727. doi: 10.1016/j.iotech.2024.100727.
- [13] Lam CG, Manhiot C, Pullenayegum EM, Feldman BM. Efficacy of intravenous Ig therapy in juvenile dermatomyositis. *Ann Rheum Dis* 2011;70(12):2089–94. doi: 10.1136/ard.2011.153718.
- [14] Varsani H, Newton KR, Li CK, Harding B, Holton JL, Wedderburn LR. Quantification of normal range of inflammatory changes in morphologically normal pediatric muscle. *Muscle Nerve* 2008;37(2):259–61. doi: 10.1002/mus.20898.
- [15] Law CW, Chen Y, Shi W, Smyth GK. voom: precision weights unlock linear model analysis tools for RNA-seq read counts. *Genome Biol* 2014;15(2):R29. doi: 10.1186/gb-2014-15-2-r29.

- [16] Kersevičiute I, Gordevicius J. aPEAR: an R package for autonomous visualization of pathway enrichment networks. *Bioinformatics* 2023;39(11):btad672. doi: [10.1093/bioinformatics/btad672](https://doi.org/10.1093/bioinformatics/btad672).
- [17] Emslie-Smith AM, Arahata K, Engel AG. Major histocompatibility complex class I antigen expression, immunolocalization of interferon subtypes, and T cell-mediated cytotoxicity in myopathies. *Hum Pathol* 1989;20(3):224–31. doi: [10.1016/0046-8177\(89\)90128-7](https://doi.org/10.1016/0046-8177(89)90128-7).
- [18] Englund P, Lindroos E, Nennesmo I, Klareskog L, Lundberg IE. Skeletal muscle fibers express major histocompatibility complex class II antigens independently of inflammatory infiltrates in inflammatory myopathies. *Am J Pathol* 2001;159(4):1263–73. doi: [10.1016/S0002-9440\(10\)62513-8](https://doi.org/10.1016/S0002-9440(10)62513-8).
- [19] Englund P, Nennesmo I, Klareskog L, Lundberg IE. Interleukin-1alpha expression in capillaries and major histocompatibility complex class I expression in type II muscle fibers from polymyositis and dermatomyositis patients: important pathogenic features independent of inflammatory cell clusters in muscle tissue. *Arthritis Rheum* 2002;46(4):1044–55. doi: [10.1002/art.10140](https://doi.org/10.1002/art.10140).
- [20] Li CK, Varsani H, Holton JL, Gao B, Woo P, Wedderburn LR, et al. MHC class I overexpression on muscles in early juvenile dermatomyositis. *J Rheumatol* 2004;31(3):605–9.
- [21] Korotkevich G, Sukhov V, Budin N, Shpak B, Artyomov MN, Sergushichev A. Fast gene set enrichment analysis. *bioRxiv* 2021:060012. doi: [10.1101/060012](https://doi.org/10.1101/060012).
- [22] Gu Z, Eils R, Schlesner M. Complex heatmaps reveal patterns and correlations in multidimensional genomic data. *Bioinformatics* 2016;32(18):2847–9. doi: [10.1093/bioinformatics/btw313](https://doi.org/10.1093/bioinformatics/btw313).
- [23] Rusinova I, Forster S, Yu S, Kannan A, Masse M, Cumming H, et al. INTERFEROME v2.0: an updated database of annotated interferon-regulated genes. *Nucleic Acids Res* 2013;41:D1040–6 (Database issue). doi: [10.1093/nar/gks1215](https://doi.org/10.1093/nar/gks1215).
- [24] Roberson EDO, Mesa RA, Morgan GA, Cao L, Marin W, Pachman LM. Transcriptomes of peripheral blood mononuclear cells from juvenile dermatomyositis patients show elevated inflammation even when clinically inactive. *Sci Rep* 2022;12(1):275. doi: [10.1038/s41598-021-04302-8](https://doi.org/10.1038/s41598-021-04302-8).
- [25] Soponkanaporn S, Deakin CT, Schutz PW, Marshall LR, Yasin SA, Johnson CM, et al. Expression of myxovirus-resistance protein A: a possible marker of muscle disease activity and autoantibody specificities in juvenile dermatomyositis. *Neuropathol Appl Neurobiol* 2019;45(4):410–20. doi: [10.1111/nan.12498](https://doi.org/10.1111/nan.12498).
- [26] Hedberg-Oldfors C, Lindgren U, Visuttijai K, Löf D, Roos S, Thomsen C, et al. Respiratory chain dysfunction in perifascicular muscle fibres in patients with dermatomyositis is associated with mitochondrial DNA depletion. *Neuropathol Appl Neurobiol* 2022;48(7):e12841. doi: [10.1111/nan.12841](https://doi.org/10.1111/nan.12841).
- [27] Wedderburn LR, Varsani H, Li CK, Newton KR, Amato AA, Banwell B, et al. International consensus on a proposed score system for muscle biopsy evaluation in patients with juvenile dermatomyositis: a tool for potential use in clinical trials. *Arthritis Rheum* 2007;57(7):1192–201. doi: [10.1002/art.23012](https://doi.org/10.1002/art.23012).
- [28] Pinal-Fernandez I, Casal-Dominguez M, Derfoul A, Pak K, Plotz P, Miller FW, et al. Identification of distinctive interferon gene signatures in different types of myositis. *Neurology* 2019;93(12):e1193–204. doi: [10.1212/WNL.00000000000008128](https://doi.org/10.1212/WNL.00000000000008128).
- [29] Corman VM, Preusse C, Melchert J, Melchert J, Benveniste O, Koll R, et al. Deep RNA sequencing of muscle tissue reveals absence of viral signatures in dermatomyositis. *Free Neuropathol* 2024;5:1. doi: [10.17879/freeneuropathology-2024-5149](https://doi.org/10.17879/freeneuropathology-2024-5149).
- [30] Bilgic H, Ytterberg SR, Amin S, McNallan KT, Wilson JC, Koeuth T, et al. Interleukin-6 and type I interferon-regulated genes and chemokines mark disease activity in dermatomyositis. *Arthritis Rheum* 2009;60(11):3436–46. doi: [10.1002/art.24936](https://doi.org/10.1002/art.24936).
- [31] Baechler EC, Bauer JW, Slaterry CA, Ortmann WA, Espe KJ, Novitzke J, et al. An interferon signature in the peripheral blood of dermatomyositis patients is associated with disease activity. *Mol Med* 2007;13(1-2):59–68. doi: [10.2119/2006-00085.Baechler](https://doi.org/10.2119/2006-00085.Baechler).
- [32] Li Wilkinson MG, Deakin CT, Papadopoulou C, Eleftheriou D, Wedderburn LR. JAK inhibitors: a potential treatment for JDM in the context of the role of interferon-driven pathology. *Pediatr Rheumatol Online J* 2021;19(1):146. doi: [10.1186/s12969-021-00637-8](https://doi.org/10.1186/s12969-021-00637-8).
- [33] Rayavarapu S, Coley W, Nagaraju K. Endoplasmic reticulum stress in skeletal muscle homeostasis and disease. *Curr Rheumatol Rep* 2012;14(3):238–43. doi: [10.1007/s11926-012-0247-5](https://doi.org/10.1007/s11926-012-0247-5).
- [34] Li CK, Knopp P, Moncrieffe H, Singh B, Shah S, Nagaraju K, et al. Overexpression of MHC class I heavy chain protein in young skeletal muscle leads to severe myositis: implications for juvenile myositis. *Am J Pathol* 2009;175(3):1030–40. doi: [10.2353/ajpath.2009.090196](https://doi.org/10.2353/ajpath.2009.090196).
- [35] Kleefeld F, Cross E, Lagos D, Walli S, Schoser B, Hentschel A, et al. Mitochondrial damage is associated with an early immune response in inclusion body myositis. *Brain* 2025:awaf118. doi: [10.1093/brain/awaf118](https://doi.org/10.1093/brain/awaf118).
- [36] Tresse E, Marturia-Navarro J, Sew WQG, Cisuella-Serra M, Jaber E, Riera-Ponsati L, et al. Mitochondrial DNA damage triggers spread of Parkinson's disease-like pathology. *Mol Psychiatry* 2023;28(11):4902–14. doi: [10.1038/s41380-023-02251-4](https://doi.org/10.1038/s41380-023-02251-4).
- [37] Picca A, Faltg J, Auwerx J, Ferrucci L, D'Amico D. Mitophagy in human health, ageing and disease. *Nat Metab* 2023;5(12):2047–61. doi: [10.1038/s42255-023-00930-8](https://doi.org/10.1038/s42255-023-00930-8).
- [38] Ali AT, Boehme L, Carbajosa G, Seitan VC, Small KS, Hodgkinson A. Nuclear genetic regulation of the human mitochondrial transcriptome. *Elife* 2019;8:e41927. doi: [10.7554/eLife.41927](https://doi.org/10.7554/eLife.41927).



## Systemic Sclerosis

# Antimitochondrial antibodies in systemic sclerosis target enteric neurons and are associated with GI dysmotility

Zsuzsanna H. McMahan<sup>1</sup>, Srinivas N. Puttapaka<sup>2</sup>, Livia Casciola-Rosen<sup>3</sup>, Timothy Kaniecki<sup>3</sup>, Laura Gutierrez-Alamillo<sup>3</sup>, Su Hong Ming<sup>2</sup>, Philippa Seika<sup>2</sup>, Subhash Kulkarni<sup>2,4,5,\*</sup>

<sup>1</sup> Division of Rheumatology, UTHealth Houston, Houston, TX, USA

<sup>2</sup> Department of Medicine, Division of Gastroenterology, Beth Israel Deaconess Medical Center, Boston, MA, USA

<sup>3</sup> Division of Rheumatology, Johns Hopkins University, Baltimore, MD, USA

<sup>4</sup> Division of Medical Sciences, Harvard Medical School, Boston, MA, USA

<sup>5</sup> Program in Neuroscience, Harvard Medical School, Boston, MA, USA

## ARTICLE INFO

## Article history:

Received 27 November 2024

Received in revised form 3 June 2025

Accepted 5 June 2025

## ABSTRACT

**Objectives:** Most patients with systemic sclerosis (SSc) experience gastrointestinal (GI) dysmotility. The enteric nervous system (ENS) regulates GI motility, and its dysfunction causes dysmotility. A subset of SSc patients harbour antimitochondrial M2 autoantibodies (AM<sub>2</sub>A). Here, we investigate whether M2 is expressed by specific ENS cells, and if AM<sub>2</sub>A are associated with GI dysmotility in SSc patients.

**Methods:** Sera from 154 well-characterised patients with SSc were screened for AM<sub>2</sub>A by enzyme-linked immunosorbent assay. Clinical features and GI transit data were compared between AM<sub>2</sub>A-positive and AM<sub>2</sub>A-negative patients. Hepatocellular carcinoma cell line 2 (HepG2) cells were cultured with these sera and costained with AM<sub>2</sub>A.

**Results:** Nineteen of 147 patients (12.9%) were AM<sub>2</sub>A-positive. AM<sub>2</sub>A positivity was significantly associated with slower transit in the oesophagus ( $\beta$  −14.4, 95%CI, −26.2, −2.6) and stomach ( $\beta$  −7.9, 95% CI, −14.1, −1.6). Immunostaining demonstrated pan-mitochondrial antigens TOM-20 and M2 enrichment in human ENS neurons, specifically in mesoderm-derived enteric neurons (MENS). Autoantibodies in SSc sera penetrated live adult murine MENS and HepG2 cells when adult murine longitudinal muscle containing myenteric plexus tissue and HepG2 cells were cultured in the presence of SSc sera. Upon penetrating live cells, AM<sub>2</sub>A localised to mitochondria, and immunoprecipitation demonstrated binding to the M2 antigen. Seahorse assays show that penetration of HepG2 cells with SSc-AM<sub>2</sub>A altered cellular respiration suggesting that penetrating AM<sub>2</sub>A is pathogenic.

**Conclusions:** AM<sub>2</sub>A in SSc patients are associated with slower GI transit. SSc autoantibodies penetrate live cells *in vitro*, and SSc-AM<sub>2</sub>A penetrates live cells to target the mitochondrial M2 antigen and cause functional deficits. Because a subset of enteric neurons (MENS) is enriched in mitochondria, which are similarly penetrated by SSc-AM<sub>2</sub>A *in vitro*, the presence of GI dysmotility in SSc patients harbouring AM<sub>2</sub>A suggests that SSc-AM<sub>2</sub>A may penetrate MENS *in vivo*, driving ENS and GI dysfunction. Further studies are warranted to test how AM<sub>2</sub>A alter ENS functions *in vivo* to contribute to GI dysmotility in SSc.

\*Correspondence to Dr. Subhash Kulkarni, Department of Medicine, Division of Gastroenterology, Beth Israel Deaconess Medical Center, 3 Blackfan Street, Center for Life Sciences 608, Boston, MA 02115, USA.

E-mail address: [skulkar1@bidmc.harvard.edu](mailto:skulkar1@bidmc.harvard.edu) (S. Kulkarni).

Handling editor: Josef S. Smolen.

<https://doi.org/10.1016/j.ard.2025.06.2119>

0003-4967/Published by Elsevier B.V. on behalf of European Alliance of Associations for Rheumatology (EULAR).



### WHAT IS ALREADY KNOWN ON THIS TOPIC

- A subset of SSc patients have antimitochondrial M2 autoantibodies (AM<sub>2</sub>A). Whether AM<sub>2</sub>A inform the presence or severity of GI dysfunction in SSc is unknown.

### WHAT THIS STUDY ADDS

- AM<sub>2</sub>A in SSc patients are associated with slower upper GI transit.
- Mitochondria are enriched in a recently identified mesoderm-derived lineage of enteric neurons (MENS), which play a major role in GI motility. This suggests that MENS may be more mitochondrial-dependent than other cell types and thus more susceptible to mitochondrial dysfunction. This may contribute to dysmotility in AM<sub>2</sub>A-positive SSc patients.
- SSc-AM<sub>2</sub>A penetrate live MENS and human cell lines to target the M2 antigen, causing functional deficits in cellular respiration.

### HOW THIS STUDY MIGHT AFFECT RESEARCH, PRACTICE OR POLICY

- AM<sub>2</sub>A in SSc patients may penetrate MENS *in vivo*, driving enteric nervous system dysfunction and subsequent GI dysmotility
- This potentially novel mechanism in SSc-GI disease could inform our current approach to diagnosing and managing these patients.

## INTRODUCTION

Systemic sclerosis (SSc) is a chronic and progressive autoimmune disease characterised by vascular abnormalities and degenerative and fibrotic changes in the skin, joints, and internal organs. Among these, gastrointestinal (GI) involvement is the most common, affecting over 80% of patients [1]. GI dysfunction in SSc, primarily due to impaired motility, is strongly associated with worse outcomes [1–3]. Our previous work has characterised the extent and severity of GI dysmotility in SSc patients and identified novel intracellular autoantigens in those with significant GI involvement (SSc-GI) [3–13]. These findings suggest that the full spectrum of autoantigens associated with SSc-GI remains undefined, which limits our understanding of the serological diversity among SSc-GI patients and how this diversity contributes to the heterogeneous clinical manifestations of SSc-GI disease. Identifying these autoantibodies may also reveal key biological pathways relevant to different SSc-GI subsets.

Among the autoantibodies present in SSc patient sera, antimitochondrial antibodies (AMA), specifically targeting the mitochondrial M2 antigen, are found in 8% to 15% of patients [14,15]. Fregeau et al [16] determined that all AMA in limited SSc/CREST syndrome (calcinosis, Raynaud's, esophageal dysmotility, sclerodactyly, telangiectasia) patients were immunoreactive against the M2 antigen, which is designated as AM<sub>2</sub>A. Antibodies against AM<sub>2</sub>A are an important diagnostic marker for primary biliary cholangitis (PBC), a condition in which patients also experience oesophageal dysmotility [17]. Notably, although antibodies against AM<sub>2</sub>A are found in a significant subset of SSc patients and are associated with GI dysfunction in PBC patients, the association between GI dysfunction and AM<sub>2</sub>A prevalence in patients with SSc is not yet defined.

AMA (specifically AM<sub>2</sub>A) are thought to arise either from primary disease-driven cellular damage that results in the exocytosis of mitochondrial antigens or disease-driving autoantibodies that impair mitochondrial function [18,19]. In either scenario, mitochondrial dysfunction is associated with the presence of

AMA. Mitochondrial disorders (MID), arising from genetic abnormalities in mitochondria, are associated with severe GI dysfunction. This often manifests as poor appetite, gastroesophageal reflux disease (GERD), dysphagia, vomiting, gastroparesis, constipation, GI pseudo-obstruction, and diarrhoea [20,21]. The presence of severe GI dysfunction in MID, whose manifestations mirror SSc-GI dysfunction, and the presence of AMA in SSc patients raises questions about the prevalence of AMA/AM<sub>2</sub>A in SSc patients with significant GI dysfunction and whether AM<sub>2</sub>A levels associated with GI severity in SSc patients.

This study assessed the AM<sub>2</sub>A status in a cohort of SSc patients with well-characterised GI dysfunction. We found that AM<sub>2</sub>A are present in ~13% of patients with SSc and GI disease and that these antibodies are associated with slower GI transit. We also determined that mitochondria are enriched in a recently identified mesoderm-derived lineage of enteric neurons (MENS), which play a major role in GI motility. This suggests that MENS may be more mitochondrial-dependent and thus more susceptible to mitochondrial dysfunction than other cell types. Using immunofluorescence-based and immunoprecipitation-based approaches, we demonstrate that these antibodies are internalised, and navigate to and bind mitochondria—and specifically mitochondrial M2 antigen—providing an opportunity for AM<sub>2</sub>A to impact function. These findings provide intriguing new insights into the potential aetiology of GI dysfunction in patients with SSc-GI disease.

## METHODS

### Patient cohorts

The Gastrointestinal Assessment Protocol (GAP) cohort is a prospectively enrolled National Institutes of Health (NIH)—sponsored GI cohort of well-characterised patients with SSc from the Johns Hopkins Scleroderma Center. It includes a subset of the Johns Hopkins Scleroderma Center Research Registry. Patients were consecutively recruited during routine clinical visits from July 2016 to April 2022 if they met either the 2013 American College of Rheumatology (ACR)/EULAR criteria for SSc or had at least 3 of the 5 features of CREST syndrome (calcinosis, Raynaud Phenomenon, oesophageal dysfunction, sclerodactyly, telangiectasias). During routine clinical visits, the treating physician (rheumatologist or gastroenterologist) screened for significant symptoms of GI dysfunction. Such symptoms included refractory gastroesophageal reflux disease, early satiety, nausea/vomiting, unintentional weight loss, distension, bloating, diarrhoea, and/or constipation. Patients with significant upper GI disease or lower and upper GI dysfunction symptoms who agreed to complete a whole gut transit study were included.

The Johns Hopkins Institutional Review Board approved all human patient protocols, and all individuals signed written informed consent. Paraffin sections of the adult small intestinal full-thickness gut from deidentified human tissues were obtained from the Department of Pathology at Beth Israel Deaconess Medical Center, and the Institutional Review Board approved using the deidentified human tissues.

### Clinical phenotyping of SSc

Demographic characteristics included age, sex, and race based on the standard data collection practice in the Johns Hopkins Scleroderma Center Research Registry. Clinical data such as

disease duration, smoking status, SSc subtype, presence (yes/no) of telangiectasia, calcinosis, arthralgia, synovitis, and tendon friction rubs were documented by the physician at the patient's first clinical encounter and longitudinally at 6-month intervals during routine clinical follow-up. Disease duration was defined as the interval between the first non-Raynaud symptom and the whole gut transit study (WGT). SSc subtype (diffuse or limited cutaneous disease) was determined based on the extent of skin involvement. GI, cardiac, muscle, and lung involvement and severity were also captured at baseline, and at the maximum severity, measures were captured longitudinally using Medsger Severity Scores [22]. Specifically, the modified Medsger GI severity score includes 5 categories: (a) score 0 = normal (no GI symptoms), (b) score 1 = requiring gastroesophageal reflux disease (GERD) medications (including H<sub>2</sub> blocker or proton-pump inhibitor), (c) score 2 = high-dose GERD medications or antibiotics for bacterial overgrowth, (d) score 3 = episodes of pseudo-obstruction or malabsorption syndrome, and (e) score 4 = severe GI dysmotility requiring enteral or total parenteral nutrition. Sicca symptoms were defined as the presence of any of the following: dry eyes for > 3 months, the sensation of sand or gravel in the eyes, the use of artificial tears 3 times daily, dry mouth for > 3 months, swollen salivary glands, and/or the requirement of liquids to swallow due to dry mouth. The presence of overlap PBC was identified through a retrospective chart review of the cohort. Participants were classified as having overlap PBC if they possessed a persistently elevated serum alkaline phosphatase with subsequent imaging and/or pathology consistent with this diagnosis. Participants without a persistently elevated alkaline phosphatase or a workup that revealed an alternative hepatobiliary pathology were classified as not having overlap PBC disease [23].

### Whole gut transit scintigraphy

All participants underwent WGT scintigraphy. Patients fasted the night before the study and were told to avoid promotility agents, antibiotics, opiates, benzodiazepines, and stool softeners 3 days before the study. Per protocol, patients ingested a standard amount of radiolabeled In-111 water to evaluate oesophageal and liquid gastric emptying and a radiolabeled Tc-99m egg meal to evaluate solid gastric emptying. A gamma camera was used to capture anterior and posterior images of the GI tract at predetermined time points (one-half hour, 1 hour, 2 hours, 4 hours, 6 hours, 24 hours, 48 hours, and 72 hours) to assess transit throughout the entire GI tract [24].

### Assessment of AM<sub>2</sub>A by enzyme-linked immunosorbent assay

155 serum samples from SSc-GI patients were screened for AM<sub>2</sub>A using the INOVA Quanta Lite M2 EP (MIT3) enzyme-linked immunosorbent assay kit from INOVA-WERFEN (Cat. No. 704540). Per the manufacturer's recommendations, results were interpreted as negative for < 20 units, equivocal for 20.1–24.9 units, and positive for > 25 units.

### Animal experiments

Tissues were derived from euthanised Wnt1-cre:tdTomato that were housed and then euthanised at the Beth Israel Deaconess Medical Center (BIDMC) animal colony under approved protocol from the BIDMC Animal Care and Use Committee.

### Uptake of SSc autoantibodies and immunostaining of HepG2 cells

Hepatocellular carcinoma cell line 2 (HepG2) cells were grown to 70% confluence on sterile four-chamber slides in DMEM/high glucose (Life Technologies) supplemented with 10% fetal bovine serum (FBS) (Life Technologies) at 37 °C and 5% CO<sub>2</sub>. The cells in 2 chambers were cultured without human serum, whereas cells in the other 2 chambers were cultured overnight with AM<sub>2</sub>A-positive and AM<sub>2</sub>A-negative SSc sera diluted 1:50 (AM<sub>2</sub>A-positive: FW-2530 and AM<sub>2</sub>A-negative: FW-2340). The culture medium was then removed, and the cells were washed, followed by fixation in ice-cold 4% paraformaldehyde (10 minutes), permeabilisation, and blocking (performed together for 30 minutes at room temperature with blocking permeabilizing buffer (BPB) comprising 5% goat serum (Life Technologies), 0.1% Triton X100 (Sigma), in phosphate-buffered saline [PBS]). The cells were then washed and incubated with antibodies against the M2 antigen (pyruvate dehydrogenase complex E2 [PDC-E2] protein encoded by the *Dlat* gene, Proteintech Cat. 13426-1-AP, 1:500 dilution for 1 hour at room temperature). The cells were subsequently counterstained with secondary antibodies antihuman 647 and antirabbit 488 (Life Technologies, 1:500 dilution for 1 hour at room temperature). Nuclei were stained with 4',6-diamidino-2-phenylindole (DAPI), and imaging was performed using Olympus confocal microscopy. Tissues were imaged under a × 40 oil-immersion objective lens, with laser settings selected to ensure no overlap between fluorophores. Images were analysed using the Fiji ImageJ software.

### Uptake of SSc-AM<sub>2</sub>A autoantibodies in adult small intestinal myenteric neurons

Freshly peeled and isolated adult small intestinal longitudinal muscle containing myenteric plexus (LM-MP) tissues from a male Wnt1-cre:tdTomato neural crest-specific lineage fate mapping mouse was used for this experiment. LM-MP tissues were incubated with FW-2530 SSc patient serum containing AM<sub>2</sub>A for 24 hours. Postincubation tissues were washed in sterile PBS and then fixed with freshly prepared ice-cold 4% paraformaldehyde (PFA) for 5 to 10 minutes. After washing off the 4% PFA solution, the tissues were blocked and permeabilised with BPB for 1 hour at room temperature. Next, the tissues were immunostained overnight at 16 °C with commercially available anti-M2 (Proteintech, 1:500) antibody. After washing away the primary antibody, the tissues were incubated with antihuman 647 and antirabbit 488 secondary antibodies for 1 hour at room temperature. The tissues were then washed with sterile PBS, nuclei were labelled with DAPI, and imaging was performed using a Leica Stellaris 5 confocal microscope and analysed using Fiji ImageJ software.

### Immunofluorescence staining of adult small intestinal murine LM-MP layer

Freshly peeled and isolated ileal longitudinal muscle-myenteric plexus (LM-MP) tissues from an adult male Wnt1-cre:tdTomato neural crest-specific lineage fate mapping mouse, which we have previously used to label all neural crest derivatives in the GI tract with the red fluorescent reporter tdTomato, were isolated as described [25]. Within 30 minutes of isolation, the LM-MP tissues were fixed with freshly prepared ice-cold 4% paraformaldehyde (PFA) for 5 to 10 minutes. After washing off the 4% PFA solution, the tissues were blocked and permeabilised with BPB for 30 minutes at room temperature. Next, the tissues were immunostained overnight at 16 °C either with (a)

paraneoplastic disease patient-derived antineuronal nuclear antibody type 1 (ANNA1) antisera with demonstrated and validated specific anti-Hu immunoreactivity (1:1000), and with commercial anti-TOM20 antibody (1:500), or with (b) ANNA1 antisera (1:1000) and commercially available anti-M2 (PDC-E2/*Dlat*, Proteintech, 1:500) antibody. Secondary immunostaining was performed for 1 hour at room temperature using antihuman 647 (cyan) and antirabbit 488 (green) secondary antibodies (both 1:500). Nuclei were stained with DAPI, and imaging was performed and analysed as described above.

### Immunoprecipitation and Western blot

HepG2 cells were grown (6W dish,  $0.5 \times 10^6$  cells/well) in DMEM/high glucose supplemented with 10% FBS and 1% antibiotic solution (Invitrogen). Cells were treated with FW-2530 SSc patient serum containing AM<sub>2</sub>A (1:500 dilution) for 24 hours at 37 °C and 5% CO<sub>2</sub>. After treatment, cells were lysed by sonication in an IP lysis buffer (Invitrogen, Cat. No. 87787), and samples were centrifuged at 14,000 g for 30 minutes. The resulting supernatant was collected, and the total protein was quantified using the bicinchoninic acid (BCA) kit (Pierce). A set of total protein lysate was kept aside to be used subsequently for positive control (called PC Lysate), whereas 500 µg of total protein lysate was incubated with 50 µL of Protein G Dynabeads (Invitrogen) overnight at 4 °C. Beads were then collected after centrifugation at 1000 g for 3 minutes and washed with lysis buffer 3 times. To elute the protein complex, beads were boiled with 50 µL reducing sample buffer for 10 minutes. This set of IgG-bound immunoprecipitated proteins was called IP.

Protein samples from both IP and PC Lysate were separated using sodium dodecyl sulfate–polyacrylamide gel electrophoresis (SDS–PAGE) with a 12% resolving and a 4% stacking gel. Proteins were separated by electrophoresis at constant voltage (100 V) in a running buffer and then transferred to a preactivated polyvinylidene difluoride membrane with constant voltage (90 V) at 4 °C for 90 minutes in a transfer buffer (0.1 M Tris base, 0.1 M glycine, 20% methanol). The membrane was blocked with 2.5% (w/v) bovine serum albumin (BSA) for 1 hour. Primary antibodies for PDC-E2/*Dlat* (Proteintech, 1:1000) and beta-actin (mouse monoclonal, MP Biochemicals, 1:5000) were added directly to the blocking solution and incubated overnight at 4 °C. The membrane was washed thrice for 5 minutes each with TBST buffer and incubated with IRDye-800 conjugated antirabbit and IRDye-680 conjugated antimouse secondary antibodies (Licor) in 2.5% BSA in Tris-buffered saline with Tween 20 (TBST) buffer for 90 minutes on a shaker at room temperature. After incubation, the membrane was washed thrice for 5 minutes each with TBST buffer. The membrane was developed using the Licor Odyssey M imager system.

### Immunofluorescence staining of adult small intestinal human tissue specimens

Formalin-fixed paraffin-embedded tissue sections of full-thickness adult human small intestine were obtained from a non-SSc patient with no known motility disease or dysfunction. Sections were immunostained with ANNA1 antisera (1:1000) and commercially available anti-M2 antibody (1:500, Proteintech). Briefly, the tissue sections were baked (60 °C for 10 minutes) and then blocked and permeabilised with 5% horse serum and 0.5% Triton X-100 in PBS for 1 hour. The tissues were washed and then immunostained with primary antibodies overnight at 16 °C. Counterstaining was performed with

antihuman 647 (cyan) and antirabbit 488 (green) secondary antibodies (both 1:500) for 1 hour at room temperature. After washing, the sections were mounted with a prolong antifade mounting medium. Nuclei were counterstained with DAPI, and imaging was performed and analysed as described above.

### Seahorse assay for determining functional effects of penetrating SSc-AM<sub>2</sub>A

A day prior to the assay, HepG2 cells were seeded on the rat collagen-coated XFe24 cell culture plates at 40,000 cells/well in DMEM culture medium containing 10% FBS either FW-2530 SSc patient serum containing AM<sub>2</sub>A or with serum from a healthy donor without any gastrointestinal motility or autoimmune condition (1:500 dilution). The cells were incubated at 37 °C, 5% CO<sub>2</sub> for 24 hours. The XFe24 cartridge plate was hydrated using 1 mL/well of calibrant and kept overnight at 37 °C in a nontissue culture incubator. On the day of the assay, cells in the culture plate were washed with freshly prepared assay media (XF Base DMEM medium, supplemented with 25 mM glucose, 1 mM pyruvate, and 2 mM glutaMAX, and adjusted to pH 7.4). Cells were incubated in 675 µL assay media in a nontissue culture incubator at 37 °C for 60 minutes prior to the experiment. Meanwhile, the mitochondrial stressors oligomycin A (50 µg, 10 ×), carbonyl cyanide-p-trifluoromethoxyphenylhydrazone (FCCP, 50 µg, 10 ×), and the mixture of rotenone/antimycin A (50 µg, 10 × each) were loaded in ports A, B, and C of the cartridge plate, respectively. At the start of each experiment, 3 initial baseline Oxygen consumption rate (OCR) measurements were recorded. After injection of mitochondrial stressors further 4 measurements of OCR were recorded. Each measure followed a 3-minute mixing, a 2-minute wait, and a 3-minute reading time. At the end of the experiment, cells were lysed using radioimmunoprecipitation assay buffer, and the protein content was measured by BCA assay (Thermo Fisher Scientific). The recordings were normalised to the total cellular protein content in each well.

### Statistical analysis

Clinical and demographic features were compared between AM<sub>2</sub>A-positive and AM<sub>2</sub>A-negative patients using chi-square or Fisher's exact tests, Student's *t* tests, or Mann-Whitney Wilcoxon tests according to the type and distribution of the data. Spearman correlation was used to assess the correlation between 2 continuous variables. Regression models were used to determine whether AM<sub>2</sub>A were associated with GI transit. Adjusted multivariable models were developed and adjusted for potential confounders. STATA15 (STATA Corporation) and GraphPad Prism were used for statistical analyses. A *P* value of < 0.05 was considered statistically significant.

## RESULTS

### AM<sub>2</sub>A are present in an SSc cohort enriched for GI disease

The SSc cohort studied (GAP) is enriched for patients with GI dysfunction. It is an NIH-funded cohort that was developed to study GI manifestations in SSc [7]. Among patients in this cohort, we determined that 12.9% (19/147) were AM<sub>2</sub>A-positive (> 25 units). Of these, none was scored as Medsger severity group 0 ('normal' GI function). Compared with patients in the cohort who were AM<sub>2</sub>A-negative, the antibody-positive patients were also less frequently classified as having mild GI severity (Medsger group 1; gastroesophageal reflux disease [GERD])



(16% versus 28%). However, more severe physician-determined upper GI disease (Medsger 2; GERD with high doses of medications required or small bowel dilation on radiographs) was seen among AM<sub>2</sub>A-positive compared with AM<sub>2</sub>A-negative patients (73% versus 52%). AM<sub>2</sub>A positivity was less frequent among patients with Medsger group 3 (malabsorption or intestinal pseudo-obstruction) (11% versus 13%) and was observed in none of the 7 patients in Medsger group 4 (requiring total parenteral nutrition [TPN]). No demographic or extraintestinal clinical features differed significantly between AM<sub>2</sub>A-positive and AM<sub>2</sub>A-negative patients (see [Supplementary Table S1](#)). Among the patients who were AM<sub>2</sub>A-positive, 15.8% (3/19) had documented PBC; there was one patient who was classified as having unknown PBC disease status due to lack of documented hepatobiliary evaluation in the setting of a persistently elevated serum alkaline phosphatase.

#### *AM<sub>2</sub>A-positive SSc patients have slower oesophageal and gastric transit*

We then sought to determine whether AM<sub>2</sub>A positivity in SSc is associated with GI transit. Using data acquired from scintigraphy-based WGT studies, we determined that AM<sub>2</sub>A-positive patients were significantly more likely to have slower median oesophageal percent emptying at 10 seconds than antibody-negative patients (69% [39, 84] versus 82% [68, 90];  $P = 0.03$ ). Furthermore, higher levels of AM<sub>2</sub>A correlated with worse oesophageal transit ( $\rho = -0.27$ ;  $P < 0.01$ ). Univariate

regression analyses demonstrated an inverse relationship between AM<sub>2</sub>A levels and percent emptying of the oesophagus at 10 seconds ( $\beta = -0.31$ ; 95% CI,  $-0.49, -0.13$ ;  $P < 0.01$ ) and percent emptying of solids in the stomach at 4 hours ( $\beta = -0.11$ ; 95% CI,  $-0.20, -0.01$ ;  $P = 0.04$ ). Interestingly, there were no associations between AM<sub>2</sub>A levels/positivity and transit in the small bowel and colon. The above associations remained statistically significant, even after adjusting for age, race, and disease duration.

#### *Specific neurons in the gut wall are enriched in mitochondria and the M2 antigen*

Intestinal motility is regulated by neurons and glial cells of the enteric nervous system (ENS), which are housed within the gut wall [26]. GI dysmotility in SSc patients and the positive association between delayed GI transit and higher AM<sub>2</sub>A levels suggest that ENS dysfunction may correlate with dysfunctional mitochondria. To examine the presence of the M2 antigen (PDC-E2 protein) in neurons of the human ENS, we immunostained sections of full-thickness small intestinal tissue obtained from a patient without SSc and any known GI motility disorder. This was performed with a commercially available anti-M2/PDC-E2 antibody and with the ANNA1 antiserum (from a patient with paraneoplastic disease and validated to contain antibodies specifically against the neuronal Hu proteins). We observed that compared to other cells in the gut wall, a subset of human enteric neurons in the myenteric ganglia showed a robust enrichment of M2 antigen ([Fig 1](#)).

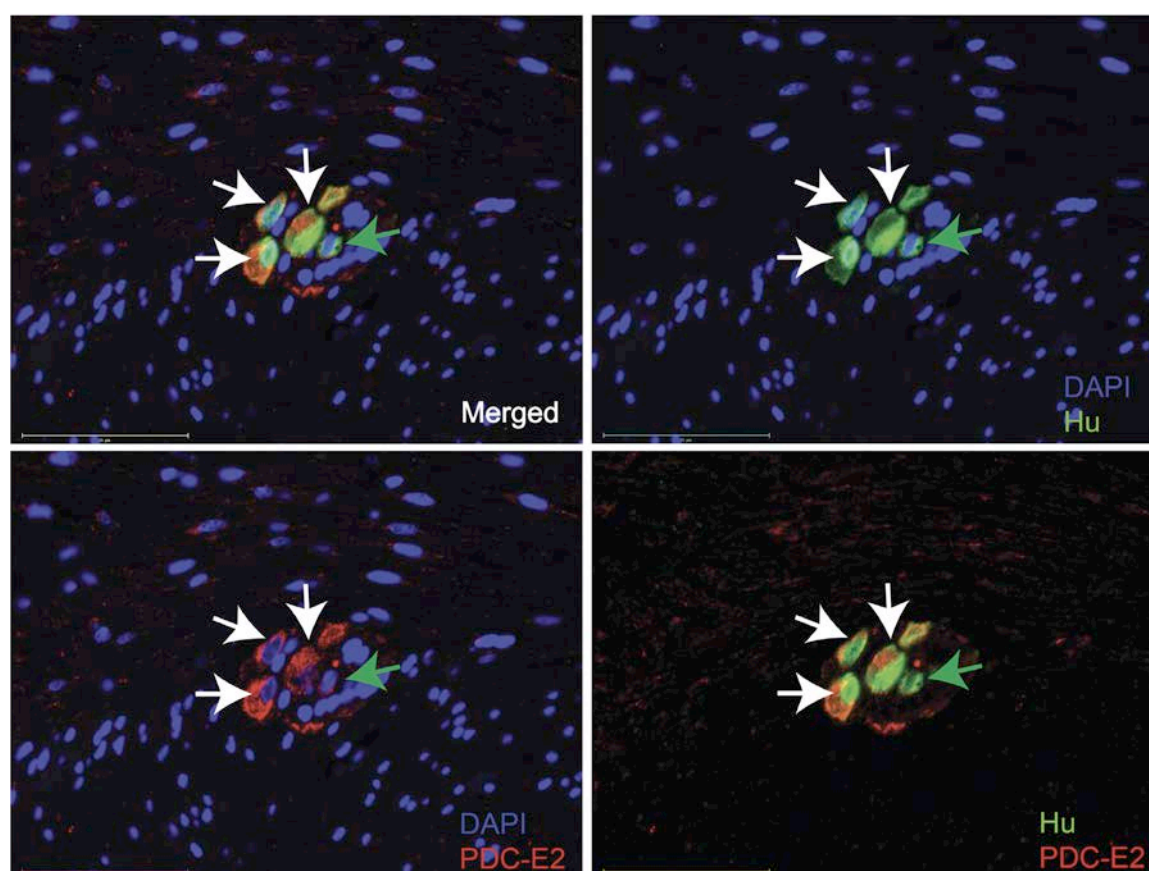


**Figure 1.** A subset of human small intestinal myenteric neurons is enriched in M2/PDC-E2 antigen. Immunostaining of a section of an adult human small intestinal tissue with ANNA1 antisera containing antibodies against Hu (green) and antibodies against M2 antigen (PDC-E2; red) shows that a subset of enteric neurons (white arrows) is enriched in the PDC-E2 protein, whereas other neurons are not (green arrow). The representative image also shows that other cells of the gut wall are not similarly enriched in the PDC-E2 protein. Nuclei are labelled with DAPI (blue). Scale bar = 75 mm. ANNA1, antineuronal nuclear antibody type 1; M2, mitochondrial antigen; PDC-E2, pyruvate dehydrogenase complex.



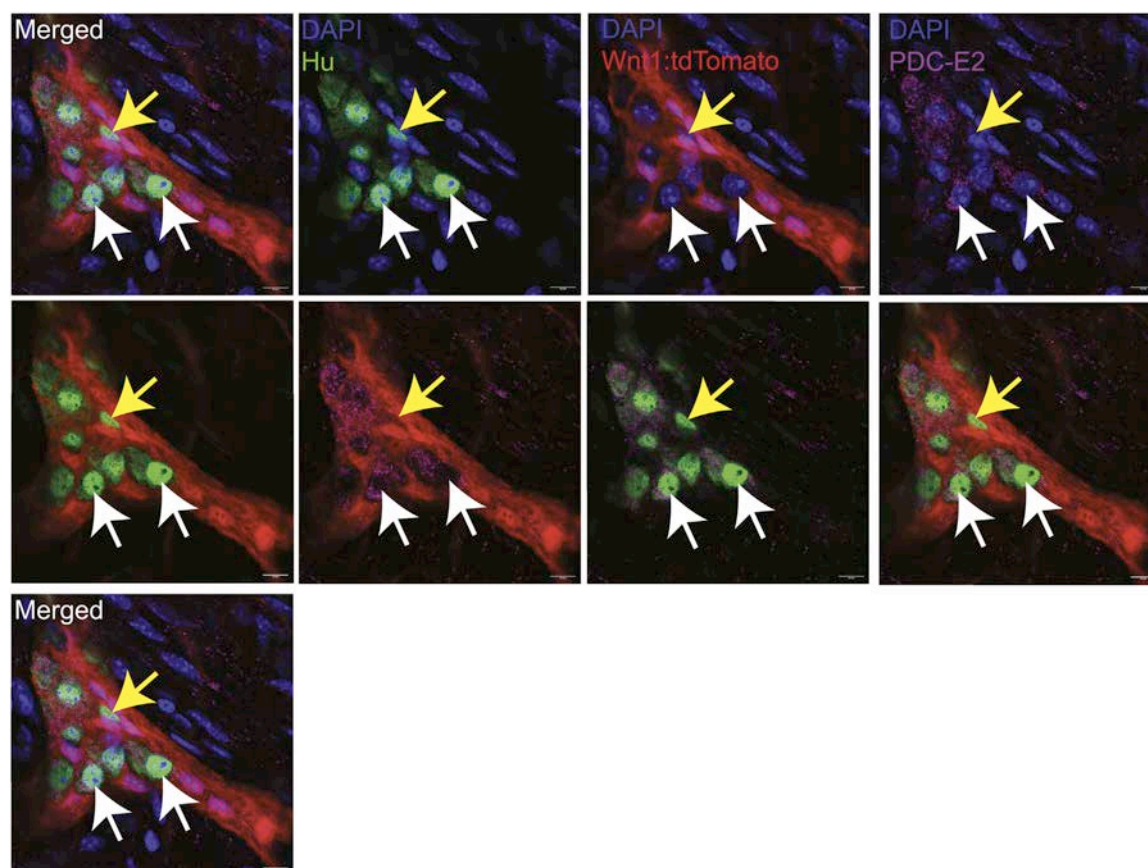


**Figure 2.** Mesoderm-derived enteric neurons (MENs) are enriched in M2/PDC-E2 antigen. Immunostaining of adult murine small intestinal longitudinal muscle-myenteric plexus (LM-MP) tissue with ANNA1 antisera containing antibodies against Hu (green) and antibodies against M2 antigen (PDC-E2; cyan). LM-MP is derived from an adult neural crest lineage-specific mouse Wnt1-cre:tdTomato, where tdTomato (red) labels neural crest-derived cells. The representative image shows that tdTomato<sup>+</sup> Hu<sup>+</sup> neurons (MENs, white arrows) are enriched in PDC-E2, while the neural crest-derived neurons (NENs, yellow arrow) are not. Nuclei are labelled with DAPI (blue). Scale bar = 10 mm. ANNA1, antineuronal nuclear antibody type 1; DAPI, 4',6-diamidino-2-phenylindole LM-MP, longitudinal muscle-myenteric plexus; M2, mitochondrial antigen; MENs, mesoderm-derived enteric neurons; NENs, neural crest-derived neurons; PDC-E2, pyruvate dehydrogenase complex.

We recently showed that the adult mammalian ENS comprises neurons of 2 developmental lineages: the canonical lineage of neural crest-derived enteric neurons (NENs) and postnatal-born MENs. These 2 subsets of ENS cells are molecularly distinct and contain significantly different neurochemical codes [25]. Whether NENs and MENs differ in their abundance of mitochondria and M2 antigen, thus making one of the neuronal lineages more significant in the pathophysiology of SSc patients with AM<sub>2</sub>A, is unknown. To address this, we immunolabeled adult murine small intestinal longitudinal muscle containing myenteric plexus (LM-MP) tissue from the neural crest lineage fate mapping mouse model Wnt1-cre:tdTomato with neuron-specific ANNA1 antiserum and with anti-M2/PDC-E2 or pan-mitochondrial anti-TOM-20 antibodies. We observed that both M2 and TOM-20 immunoreactivity are highly enriched in the tdTomato-MENs compared with other tdTomato<sup>+</sup> ENS cell populations in the myenteric plexus tissue that are derived from the neural crest (Figs 2 and 3). These data show that in addition to the M2 antigen, mitochondria are enriched within the ENS cells compared with the rest of the gut wall tissue. Furthermore, within the ENS, a subset of MENs (not the neural crest-derived cells) was enriched in mitochondria.

### SSc autoantibodies penetrate viable murine MENs and localise to their target antigens

The presence of AM<sub>2</sub>A and the enrichment of M2 antigen in MENs suggest that MENs may be impacted in AM<sub>2</sub>A-positive SSc patients with GI dysmotility. It is currently unknown whether AM<sub>2</sub>A is generated due to MEN cell death and whether it regulates MEN function. Prior reports have postulated that autoantibodies against intracellular antigens may penetrate live viable cells [27]. Here, we tested whether AM<sub>2</sub>A penetrates viable adult murine MENs in peeled preparations of small intestinal LM-MP cultured *ex vivo*. We found that AM<sub>2</sub>A penetrated viable MENs and that their subcellular localisation also showed the presence of immunostaining with a commercially available anti-M2 antibody (Fig 4). This suggests that upon penetration of viable cells, AM<sub>2</sub>A is localised to the mitochondria of MENs.

### SSc autoantibodies penetrate viable human cells and bind to their target antigen

Because the presence of MENs in the postnatal ENS is a very recent discovery [25], optimal conditions supporting their viability in culture have not yet been established. Thus, it is plausible

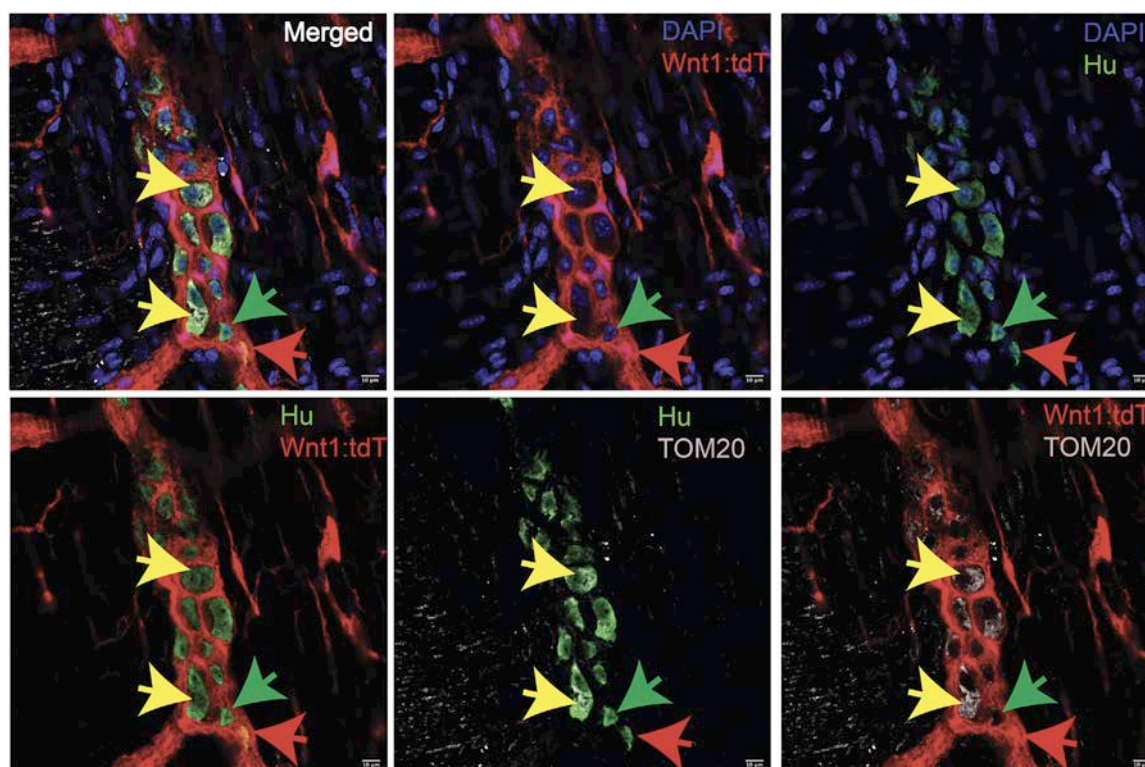


**Figure 3.** A subset of mesoderm-derived enteric neurons (MENs) are enriched in mitochondria. Immunostaining of adult murine small intestinal longitudinal muscle-myenteric plexus (LM-MP) tissue with ANNA1 antisera containing antibodies against Hu (green) and antibodies against the pan-mitochondrial antigen TOM20 (cyan). LM-MP is derived from an adult neural crest lineage-specific mouse *Wnt1-cre:tdTomato*, where tdTomato (red) labels neural crest-derived cells. The representative image shows that tdTomato<sup>−</sup> Hu<sup>+</sup> neurons (MENs, yellow arrows) are enriched in TOM20, whereas the neural crest-derived neurons (NENs, red arrow) and a subset of MENs (green arrow) are not. Nuclei are labelled with DAPI (blue). Scale bar = 10 mm. ANNA1, antineuronal nuclear antibody type 1; DAPI, 4',6-diamidino-2-phenylindole; LM-MP, longitudinal muscle-myenteric plexus; MENs, mesoderm-derived enteric neurons; NENs, neural crest-derived neurons; PDC-E2, pyruvate dehydrogenase complex; TOM20, pan-mitochondrial antigen.

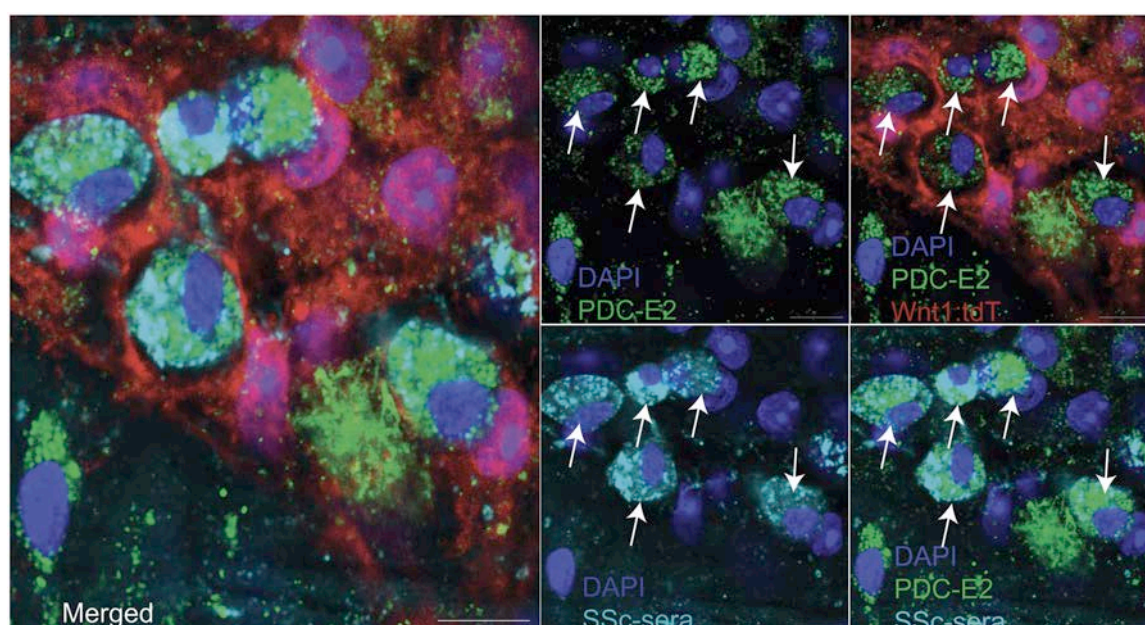


**Figure 4.** SSc-AM<sub>2</sub>A penetrate viable MENs *ex vivo*. Adult murine small intestinal LM-MP tissues from the *Wnt1-cre:tdTomato* lineage fate mapping mouse when cultured with SSc patient sera containing AM<sub>2</sub>A (FW-2530; annotated in figure as *SSc sera*) and immunostained with commercially available anti-DLAT antibodies post-culture show that tdTomato-negative mesoderm-derived enteric neurons (MENs) in the myenteric ganglia show presence of SSc autoantibodies (AM<sub>2</sub>A; cyan) within their soma which colocalises with the presence of DLAT (green) immunostaining (white arrows). Nuclei are labelled with DAPI (blue). Scale bar = 10 mm. AM<sub>2</sub>A, antimitochondrial M2 autoantibodies; ANNA1, antineuronal nuclear antibody type 1; DAPI, 4',6-diamidino-2-phenylindole; DLAT, dihydrolipoamide acetyltransferase; LM-MP, longitudinal muscle-myenteric plexus; MENs, mesoderm-derived enteric neurons; NENs, neural crest-derived neurons; PDC-E2, pyruvate dehydrogenase complex; SSc, systemic sclerosis; TOM20, pan-mitochondrial antigen.



that suboptimal culture conditions and the nature of peeled tissues may create conditions for the uptake of AM<sub>2</sub>A in MENs that do not reflect antibody penetrance in healthy viable cells. To test whether AM<sub>2</sub>A can similarly penetrate cells whose culture conditions have been optimised and are not primary cells that suffer from isolation-driven artefacts, we used cultured hepatocyte HepG2 cells, a cell line of GI origin that has been used to study mitochondrial biology [28], to test the ability of SSc autoantibodies to penetrate healthy human cells. By culturing HepG2 without patient sera, and then with 2 different SSc sera (with and without AM<sub>2</sub>A), we found that autoantibodies from both SSc sera gained access to the intracellular compartments of live viable HepG2 cells. However, only autoantibodies from the AM<sub>2</sub>A-positive

serum colocalised with the M2/PDC-E2 antigen (detected with a commercially available anti-M2 antibody). In a total of 7 wells, where we observed a total of 221,409 cells, we found that an average of  $18.77 \pm 0.67\%$  of all DAPI-labelled HepG2 cells showed the presence of intracellular antibodies when cultured with AM<sub>2</sub>A-positive serum overnight. In contrast, autoantibodies from the AM<sub>2</sub>A-negative patient did not label the cellular compartment containing the M2 antigen (Fig 5).

To determine whether AM<sub>2</sub>A localise specifically to mitochondria by binding the M2 antigen, we incubated HepG2 cells with AM<sub>2</sub>A-positive sera for 24 hours. The cells were then lysed, and human IgG-bound proteins were isolated using standard immunoprecipitation techniques. Western blots were performed

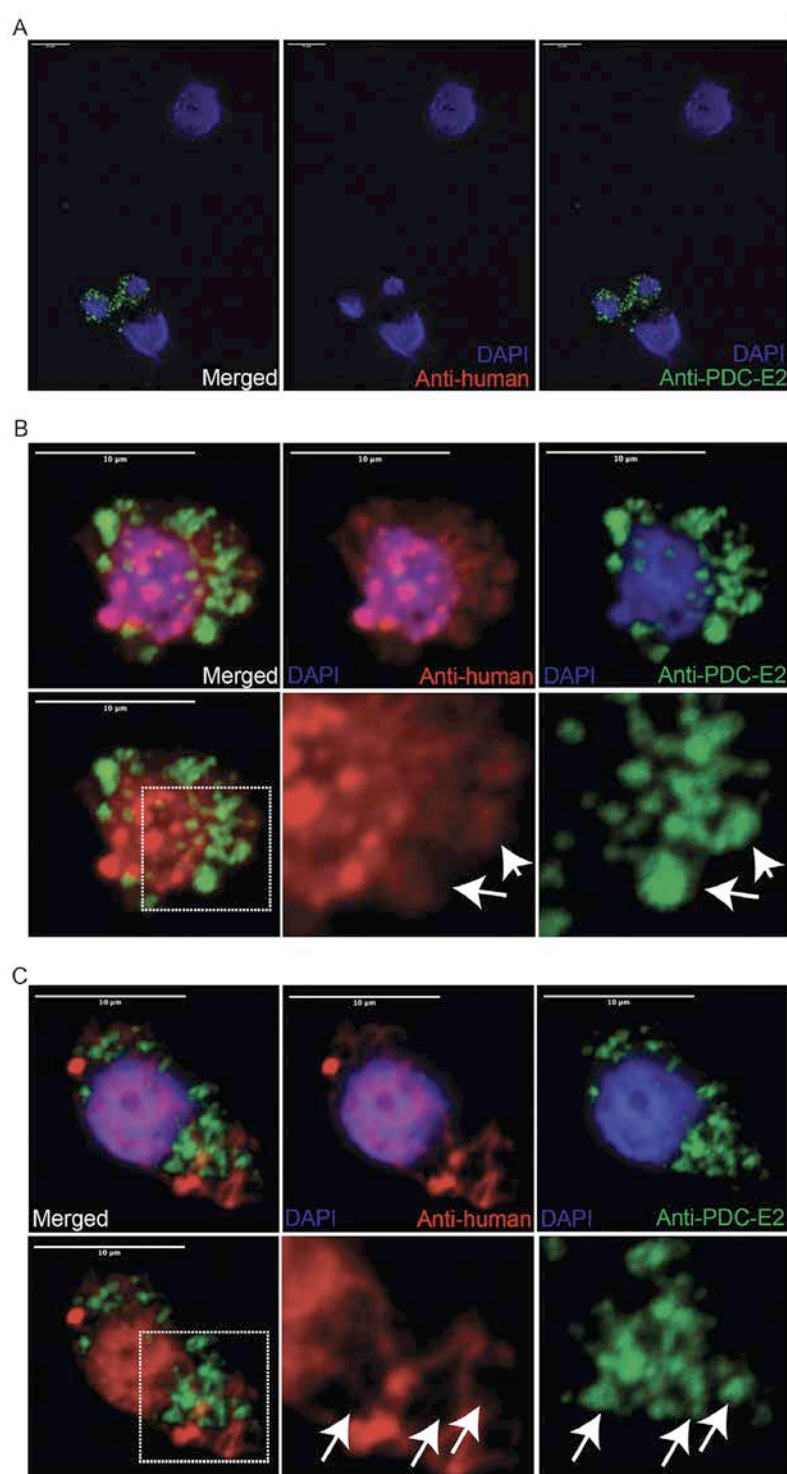


**Figure 5.** SSc autoantibodies penetrate viable cells and engage intracellular targets upon uptake. HepG2 cells when cultured with and without SSc antisera (red) can be used to test intracellular uptake. Live HepG2 cells cultured (A) without SSc antisera, and with (B) AM<sub>2</sub>A<sup>+</sup> SSc antisera (patient FW-2530), and (C) AM<sub>2</sub>A<sup>-</sup> SSc antisera (patient FW-2340), were subsequently fixed and immunostained with commercially available anti-M2/PDC-E2 antibody (green) and with antihuman secondary antibodies to detect patient sera, and imaged to observe that SSc autoantibodies were present within cells cultured with SSc patient antisera. The presence of patient-derived autoantibodies in cells, detected by antihuman secondary secondary antibody, is denoted as Antihuman. Furthermore, AM<sub>2</sub>A<sup>+</sup> antisera was detected in PDC-E2-expressing mitochondria (B, white arrow), but the AM<sub>2</sub>A<sup>-</sup> antisera labelled cellular compartments other than the PDC-E2-expressing mitochondria (C, white arrows). Nuclei are labelled with DAPI (blue). Scale bar = 10 μm. AM<sub>2</sub>A, antimitochondrial M2 autoantibodies; HepG2, hepatocellular carcinoma cell line 2; M2, mitochondrial antigen; PDC-E2, pyruvate dehydrogenase complex; SSc, systemic sclerosis.

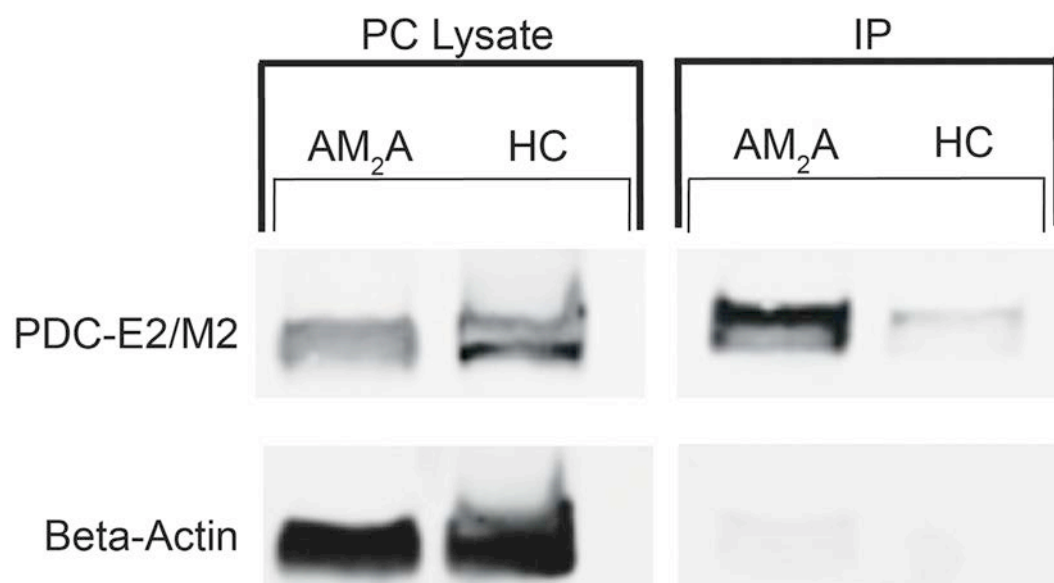


**Figure 6.** Western blot analyses show that cell-penetrating AM<sub>2</sub>A binds to the M2 antigen. Western blot analyses with antibodies against PDC-E2/M2 and against beta-actin of 2 fractions of proteins isolated from HepG2 cells, *PC Lysate* fraction—derived from lysate of HepG2 cells that were cultured either with SSc-AM<sub>2</sub>A patient sera or with non-SSc patient sera (HC)—and *IP* fraction—derived from immunoprecipitated fraction of lysate of HepG2 cells that were cultured either with SSc-AM<sub>2</sub>A patient sera or with non-SSc patient sera (HC). Although the *PC Lysate* fraction of both HC and SSc-AM<sub>2</sub>A cultured cells show the presence of PDC-E2/M2 and beta-actin proteins, the *IP* fraction of only the SSc-AM<sub>2</sub>A cultured cells but not of the HC cultured cells show the presence of PDC-E2/M2 protein. The *IP* fraction of neither the HC nor the SSc-AM<sub>2</sub>A cultured cells show the presence of beta-actin protein. This data show that SSc-AM<sub>2</sub>A specifically binds the PDC-E2/M2 protein. AM<sub>2</sub>A, antimitochondrial M2 autoantibodies; HepG2, hepatocellular carcinoma cell line 2; PDC-E2, pyruvate dehydrogenase complex; SSc, systemic sclerosis.

on total cell lysates (positive control) and on the immunoprecipitated (IP) fraction using commercial antibodies against the M2 antigen and beta-actin. The IP fraction contained the M2 antigen (PDC-E2) but not beta-actin, whereas the positive control lysate showed both proteins (Fig 6). These results indicate that AM<sub>2</sub>A from SSc patient sera penetrate viable cells, localise to mitochondria, and specifically bind their target antigen.

### Penetrating AM<sub>2</sub>A causes functional changes to cellular respiration

Seahorse assays help assess changes in cellular metabolism. Using the seahorse-mitostress assay, we assessed how exposure to penetrating AM<sub>2</sub>A in SSc patient sera alters mitochondrial respiration when compared to cells that were exposed to sera from healthy controls (HC). Oxygen consumption rate of cells exposed to SSc-AM<sub>2</sub>A is observably different from those exposed to HC sera (Fig 7A). By performing analyses of the individual parameters, we observe that AM<sub>2</sub>A-exposed cells show significantly elevated rates of nonmitochondrial oxygen consumption (Fig 7B), a near significant increase in proton leak (Fig 7C), and a strong tendency of decreased coupling efficiency (Fig 7D), but no other changes in basal respiratory rate, maximal respiration, spare respiratory capacity, and adenosine triphosphate (ATP) production (Fig 7E-H). These data support the fact that AM<sub>2</sub>A penetrate cells and target the mitochondrial M2 antigen (PDC-E2), a key enzyme in converting pyruvate to acetyl-CoA. Furthermore, the marked increase in nonmitochondrial oxygen consumption, despite preserved ATP production, suggests that AM<sub>2</sub>A functionally disrupt cellular respiration.

## DISCUSSION

Our study is the first to define AM<sub>2</sub>A in a subset of SSc patients with well-characterised GI dysfunction and to identify a

correlation between AM<sub>2</sub>A levels and GI transit in patients with SSc. Our findings highlight a previously unappreciated link between immune responses targeted towards a specific neuron lineage in the ENS and the presence of GI disease. In addition, we show that SSc autoantibodies against mitochondrial and other antigens can penetrate viable cells to *home in* to their target antigens and that these interactions are functional and impact cellular respiration. This study was performed on a large cohort of SSc patients with well-defined GI symptoms and objectively measured WGT. We found that a significant proportion (~13%) of SSc patients with GI dysfunction harbour autoantibodies against one defined mitochondrial antigen (M2). We also established that higher levels of AM<sub>2</sub>A are associated with slower oesophageal and gastric transit in SSc patients. Using an immunostaining approach, we showed that the M2 antigen and mitochondria are enriched in enteric neurons, specifically in the recently discovered lineage of MENs, relative to surrounding cell types within the ENS or the gut wall.

Prior studies have reported AMA and specifically AM<sub>2</sub>A in SSc patients [14,16], but the relevance of AM<sub>2</sub>A to GI dysfunction in SSc has not been described. Hoppner et al., in their SSc cohort with known cardiovascular dysfunction, estimated the prevalence of AM<sub>2</sub>A to be ~10% [29]. In our cohort of SSc patients with well-characterised GI dysfunction, a similar proportion (~13%) of patients were anti-M2 antibody-positive. However, it is unclear whether the antibody titers differed between the Hoppner cohort and ours. This is important, as it was the AM<sub>2</sub>A levels that correlated with worse GI transit (ascertained by the percent emptying of the oesophagus at 10 seconds and the percent emptying of the stomach at 4 hours), suggesting a disease-associated correlation between AM<sub>2</sub>A levels and the severity of GI dysfunction.

The M2 antigen contains 2 components, the E2 subunit of the PDC-E2 and the E2 subunit of the Branched Chain 2-Oxo Acid Dehydrogenase Complex (BCOADC-E2) [30]. Using



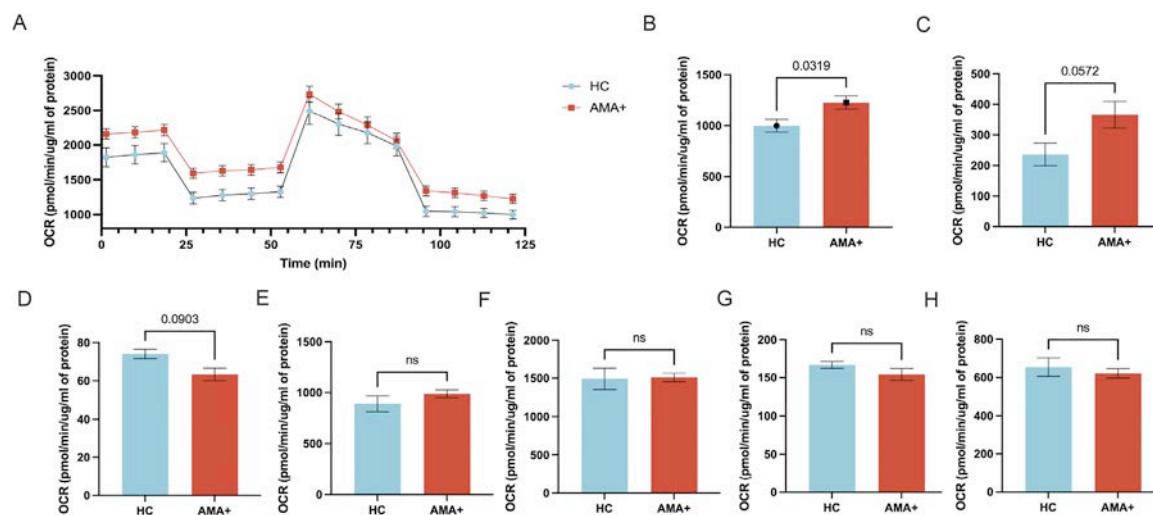


**Figure 7.** Seahorse analyses show that SSc-AM<sub>2</sub>A effect changes to cellular respiration. A, Using MitoStress Seahorse assay, oxygen consumption rate (OCR) of HepG2 cells cultured with or without SSc-AM<sub>2</sub>A show observable differences. Standard OCR calculations show that nonmitochondrial respiration rate is significantly elevated in SSc-AM<sub>2</sub>A-exposed cells than controls (B), proton leak shows a strong tendency for increase in SSc-AM<sub>2</sub>A-exposed cells than controls (C), and coupling efficiency (in percentage) shows a tendency for decrease in SSc-AM<sub>2</sub>A-exposed cells than controls (D). Panels E-H shows that other aspects of cellular respiration basal respiration rate, maximal respiration rate, ATP production, and spare respiratory capacity are not impacted after exposure for the given time to SSc-AM<sub>2</sub>A. AM<sub>2</sub>A, antimitochondrial M2 autoantibodies; ATP, adenosine triphosphate; OCR, oxygen consumption rate; SSc, systemic sclerosis.

commercially available antibodies against one of the M2 antigens (PDC-E2) as well as against a pan-mitochondrial marker (TOM20), we showed that the M2 antigen and mitochondria are abundant in murine and human ENS cells and are enriched in the lineage of MENs. We previously identified the lineage of MENs distinct from NENs. Enrichment of mitochondria and M2 antigens in neurons of this lineage suggests that the dysmotility observed in the AM<sub>2</sub>A-positive SSc-GI patients negatively impacts this lineage of neurons. The significant impact of AM<sub>2</sub>A on altering cellular respiration of HepG2 cells suggests that similar mechanisms would drive shifts *in vivo* in the metabolism of cells enriched in mitochondria, such as MENs. Clarifying how altered cellular metabolism in MENs contributes to AM<sub>2</sub>A-mediated pathogenesis of GI dysmotility will require dedicated mechanistic studies using animal models.

In contrast to prior reports suggesting an association between AMAs—particularly the AM<sub>2</sub>A subtype—and features of limited cutaneous systemic sclerosis (lcSSc), such as anticentromere antibody (ACA) positivity [14], our study did not identify a similar relationship. The earlier study, which reported AMA positivity exclusively among patients with limited disease, involved a small cohort ( $n = 61$ ), with only 4 AMA-positive cases, and may have been subject to selection bias. In our broader cohort, AM<sub>2</sub>A were not significantly associated with any specific cutaneous or serologic SSc subtype, including ACA positivity. Rather, they appear to be more closely linked to gastrointestinal (GI) manifestations, both within SSc and in other autoimmune conditions such as PBC.

Although ACA and AMA have both been associated with autoimmune liver disease [31], prior studies suggest potential cross-reactivity between target antigens, which may underlie the co-occurrence of these antibodies in patients with PBC. Our findings support the emerging hypothesis that AM<sub>2</sub>A may reflect a GI-predominant autoimmune phenotype, rather than a specific SSc clinical subtype.

Of note, we observed that higher AM<sub>2</sub>A levels correlated with worse oesophageal transit, supporting their relevance to GI involvement. Although ACA positivity has traditionally been associated with oesophageal complications in SSc, more recent

data challenge this assumption. For example, absent contractility—the most severe form of oesophageal dysfunction—is predominantly seen in patients with diffuse cutaneous disease and is rarely observed in ACA-positive individuals [32]. Instead, ACA-positive patients are more likely to exhibit ineffective oesophageal motility, a milder dysfunction. Furthermore, oesophageal dysmotility detected by scintigraphy has been shown to correlate with absent contractility on manometry. These findings suggest that ACA is not typically associated with severe oesophageal dysmotility, and our data raise the possibility that AM<sub>2</sub>A may identify a subset of patients at higher risk for more severe oesophageal dysfunction.

Our study has several key strengths. First, we demonstrate that AM<sub>2</sub>A—autoantibodies capable of penetrating viable cells and altering cellular respiration—are present in a significant proportion of SSc patients and inversely correlate with GI transit. We also show that ENS neurons, particularly enriched in mitochondria and mitochondrial antigens, may be especially vulnerable to mitochondrial-targeting autoantibodies like AM<sub>2</sub>A. Notably, our findings further reveal that this enrichment is specific to a subset of ENS neurons—those we recently identified as MENs—highlighting MENs as the lineage most reliant on mitochondrial function. These results suggest that mitochondrial dysfunction driven by AM<sub>2</sub>A predominantly affects MENs, contributing to GI dysmotility in SSc.

Our study has several limitations. The patient cohort was relatively small and included a few individuals with intestinal dysmotility, making it difficult to assess the broader relevance of AM<sub>2</sub>A to small bowel dysfunction. Additionally, MEN culture conditions are suboptimal, and culturing LM-MP tissue likely alters cellular metabolism in MENs and NENs, as suggested by PDC-E2 immunolabeling in a subset of cultured Wnt1-cre:tdTomato<sup>+</sup> NENs. Moreover, the *in vivo* effects of AM<sub>2</sub>A on gut physiology remain unaddressed. Future studies using model systems are needed to determine whether AM<sub>2</sub>A directly contributes to GI dysfunction.

Importantly, our finding that SSc autoantibodies can penetrate live cells, transit intracellularly, and bind their cognate antigens—thereby exerting functional effects—is noteworthy.

This raises the intriguing possibility that such autoantibodies may disrupt organelle function and cellular behaviour, ultimately impairing tissue and organ function. A recent lupus study similarly demonstrated the pathogenic potential of cell-penetrating autoantibodies [33]. Our findings underscore the need to study GI dysmotility across different GI organs in well-characterised AM<sub>2</sub>A-positive SSc patients. Such research will provide valuable insights into the role of AM<sub>2</sub>A in the pathophysiology of GI dysmotility in SSc and other autoimmune diseases.

## Competing interests

ZM received financial support from Rheumatology Research Foundation, Scleroderma Research Foundation, and NIH/NIAMS and received consulting fees from Boehringer Ingelheim, Allogene, and Aera Therapeutics. ZM received support for attending meetings and/or travel from ACR Convergence, Scleroderma Research Foundation, and InScar Meeting, and is Co-Chair of Committee of Finance for the ACR. PS received grant from DFG Walter Benjamin Fellowship. SK received funding from DIACOMP Pilot funding from Augusta University and grant from Harvard Digestive Disease Core. All other authors report no conflicts of interest.

## CRediT authorship contribution statement

**Zsuzsanna H. McMahan:** Writing – review & editing, Writing – original draft, Visualization, Validation, Supervision, Resources, Project administration, Methodology, Investigation, Funding acquisition, Formal analysis, Data curation, Conceptualization. **Srinivas N. Puttapaka:** Writing – review & editing, Investigation, Data curation. **Livia Casciola-Rosen:** Writing – review & editing, Methodology, Investigation, Data curation. **Timothy Kaniecki:** Writing – review & editing, Resources, Investigation, Data curation. **Laura Gutierrez-Alamillo:** Writing – review & editing, Validation, Methodology, Investigation, Data curation. **Su Hong Ming:** Writing – review & editing, Methodology, Formal analysis, Data curation. **Philippa Seika:** Writing – review & editing, Methodology, Investigation, Formal analysis, Data curation. **Subhash Kulkarni:** Writing – review & editing, Writing – original draft, Visualization, Validation, Supervision, Software, Resources, Project administration, Methodology, Investigation, Formal analysis, Data curation, Conceptualization.

## Acknowledgements

We would like to acknowledge the contribution of the JHU scleroderma center, physicians, support staff, and patients.

## Funding

This work was supported by funding from NIAMS R01 AR081382-01A1 (ZM), the Rheumatology Research Foundation and Scleroderma Research Foundation (ZM), NIA R01AG066768, DIACOMP pilot funding, and pilot and feasibility grant from Harvard Digestive Disease Core (all three to SK), R01 AR073208 (LCR), and the Donald B. and Dorothy L. Stabler Foundation. The Rheumatic Diseases Research Core Center, where the ELISA assays were performed, is supported by NIH P30-AR070254.

## Patient consent for publication

Patient consent to participate was obtained from all living patients.

## Ethics approval

The Johns Hopkins Institutional Review Board approved all human patient protocols, and all individuals signed written informed consent. Paraffin sections of the adult small intestinal full-thickness gut from deidentified human tissues were obtained from the Department of Pathology at Beth Israel Deaconess Medical Center, and the Institutional Review Board approved using the deidentified human tissues.

## Provenance and peer review

Submitted; External peer review.

## Supplementary materials

Supplementary material associated with this article can be found in the online version at [doi:10.1016/j.ar.2025.06.2119](https://doi.org/10.1016/j.ar.2025.06.2119).

## Orcid

Zsuzsanna H. McMahan: <http://orcid.org/0000-0001-6461-8940>

Timothy Kaniecki: <http://orcid.org/0000-0002-4244-8917>

Philippa Seika: <http://orcid.org/0000-0001-6760-0770>

Subhash Kulkarni: <http://orcid.org/0000-0002-2298-0623>

## REFERENCES

- [1] Kaniecki T, Hughes M, McMahan Z. Managing gastrointestinal manifestations in systemic sclerosis, a mechanistic approach. *Expert Rev Clin Immunol* 2024;20(6):603–22. doi: [10.1080/1744666X.2024.2320205](https://doi.org/10.1080/1744666X.2024.2320205).
- [2] McMahan ZH, Kulkarni S, Chen J, Chen JZ, Xavier RJ, Pasricha PJ, et al. Systemic sclerosis gastrointestinal dysmotility: risk factors, pathophysiology, diagnosis and management. *Nat Rev Rheumatol* 2023;19(3):166–81. doi: [10.1038/s41584-022-00900-6](https://doi.org/10.1038/s41584-022-00900-6).
- [3] Adler B, Hummers LK, Pasricha PJ, McMahan ZH. Gastroparesis in systemic sclerosis: a detailed analysis using whole-gut scintigraphy. *Rheumatology (Oxford)* 2022;61(11):4503–8. doi: [10.1093/rheumatology/keac074](https://doi.org/10.1093/rheumatology/keac074).
- [4] McMahan ZH, Paik JJ, Wigley FM, Hummers LK. Determining the risk factors and clinical features associated with severe gastrointestinal dysmotility in systemic sclerosis. *Arthritis Care Res (Hoboken)* 2018;70(9):1385–92. doi: [10.1002/acr.23479](https://doi.org/10.1002/acr.23479).
- [5] Adler BL, Russell JW, Hummers LK, McMahan ZH. Symptoms of autonomic dysfunction in systemic sclerosis assessed by the COMPASS-31 questionnaire. *J Rheumatol* 2018;45(8):1145–52. doi: [10.3899/jrheum.170868](https://doi.org/10.3899/jrheum.170868).
- [6] McMahan ZH, Domsic RT, Zhu L, Medsger TA, Casciola-Rosen L, Shah AA. Anti-RNPC-3 (U11/U12) antibodies in systemic sclerosis in patients with moderate-to-severe gastrointestinal dysmotility. *Arthritis Care Res (Hoboken)* 2019;71(9):1164–70. doi: [10.1002/acr.23763](https://doi.org/10.1002/acr.23763).
- [7] McMahan ZH, Tucker AE, Perin J, Volkmann ER, Kulkarni S, Ziessman HA, et al. Relationship between gastrointestinal transit, Medsger gastrointestinal severity, and University of California-Los Angeles Scleroderma Clinical Trial Consortium Gastrointestinal Tract 2.0 Symptoms in patients with systemic sclerosis. *Arthritis Care Res (Hoboken)* 2022;74(3):442–50. doi: [10.1002/acr.24488](https://doi.org/10.1002/acr.24488).
- [8] Kaniecki T, Abdi T, McMahan ZH. Clinical assessment of gastrointestinal involvement in patients with systemic sclerosis. *Med Res Arch* 2020;8(10):2252. doi: [10.18103/mra.v8i10.2252](https://doi.org/10.18103/mra.v8i10.2252).
- [9] Carlson DA, Prescott JE, Germond E, Brenner D, Carns M, Correia CS, et al. Heterogeneity of primary and secondary peristalsis in systemic sclerosis: a new model of “scleroderma esophagus. *Neurogastroenterol Motil* 2022;34(7):e14284. doi: [10.1111/nmo.14284](https://doi.org/10.1111/nmo.14284).

- [10] Cheah JX, Perin J, Volkmann ER, Hummers LK, Pasricha PJ, Wigley FM, et al. Slow colonic transit in systemic sclerosis: an objective assessment of risk factors and clinical phenotype. *Arthritis Care Res (Hoboken)* 2023;75(2):289–98. doi: [10.1002/acr.24767](#).
- [11] Bandini G, Alunno A, Ruaro B, Galetti I, Hughes M, McMahan ZH. Significant gastrointestinal unmet needs in patients with systemic sclerosis: insights from a large international patient survey. *Rheumatology (Oxford)* 2024;63(3) e92–e3. doi: [10.1093/rheumatology/kead486](#).
- [12] Hughes M, Allanore Y, Baron M, Del Galdo F, Denton CP, Frech T, et al. Proton pump inhibitors in systemic sclerosis: a reappraisal to optimise treatment of gastro-oesophageal reflux disease. *Lancet Rheumatol* 2022;4(11):e795–803. doi: [10.1016/s2665-9913\(22\)00183-7](#).
- [13] McMahan ZH, Kulkarni S, Andrade F, Perin J, Zhang C, Hooper JE, et al. Anti-gephyrin antibodies: a novel specificity in patients with systemic sclerosis and lower bowel dysfunction. *Arthritis Rheumatol* 2024;76(1):92–9. doi: [10.1002/art.42667](#).
- [14] Pope JE, Thompson A. Antimitochondrial antibodies and their significance in diffuse and limited scleroderma. *J Clin Rheumatol* 1999;5(4):206–9. doi: [10.1097/00124743-199908000-00005](#).
- [15] Assassi S, Fritzler MJ, Arnett FC, Norman GL, Shah KR, Gourh P, et al. Primary biliary cirrhosis (PBC), PBC autoantibodies, and hepatic parameter abnormalities in a large population of systemic sclerosis patients. *J Rheumatol* 2009;36(10):2250–6. doi: [10.3899/jrheum.090340](#).
- [16] Fregeau DR, Leung PS, Coppel RL, McNeillage LJ, Medsger Jr. TA, Gershwin ME. Autoantibodies to mitochondria in systemic sclerosis. Frequency and characterization using recombinant cloned autoantigen. *Arthritis Rheum* 1988;31(3):386–92. doi: [10.1002/art.1780310310](#).
- [17] Shuai Z, Wang J, Badamagunta M, Choi J, Yang G, et al. The fingerprint of antimitochondrial antibodies and the etiology of primary biliary cholangitis. *Hepatology* 2017;65(5):1670–82. doi: [10.1002/hep.29059](#).
- [18] Hutchison DM, Hosking AM, Hong EM, Grando SA. Mitochondrial autoantibodies and the role of apoptosis in *Pemphigus vulgaris*. *Antibodies (Basel)* 2022;11(3). doi: [10.3390/antib11030055](#).
- [19] Takahashi F, Sawada J, Minoshima A, Sakamoto N, Ono T, Akasaka K, et al. Antimitochondrial antibody-associated myopathy with slowly progressive cardiac dysfunction. *Intern Med* 2021;60(7):1035–41. doi: [10.2169/internal-medicine.5600-20](#).
- [20] Finsterer J, Frank M. Gastrointestinal manifestations of mitochondrial disorders: a systematic review. *Therap Adv Gastroenterol* 2017;10(1):142–54. doi: [10.1177/1756283x16666806](#).
- [21] Hom XB, Lavine JE. Gastrointestinal complications of mitochondrial disease. *Mitochondrion* 2004;4(5–6):601–7. doi: [10.1016/j.mito.2004.07.014](#).
- [22] Medsger Jr. TA, Silman AJ, Steen VD, Black CM, Akesson A, Bacon PA, et al. A disease severity scale for systemic sclerosis: development and testing. *J Rheumatol* 1999;26(10):2159–67.
- [23] Lindor KD, Bowlus CL, Boyer J, Levy C, Mayo M. Primary biliary cholangitis: 2018 practice guidance from the American Association for the Study of Liver Diseases. *Hepatology* 2019;69(1):394–419. doi: [10.1002/hep.30145](#).
- [24] Ziessman HA, Jeyasingam M, Khan AU, McMahan Z, Pasricha PJ. Experience with esophagogastrointestinal transit scintigraphy in the initial 229 patients: multiple regions of dysmotility are common. *J Nucl Med* 2021;62(1):115–22. doi: [10.2967/jnumed.120.243527](#).
- [25] Kulkarni S, Saha M, Slosberg J, Singh A, Nagaraj S, Becker L, et al. Age-associated changes in lineage composition of the enteric nervous system regulate gut health and disease. *eLife*. 2023;12:e88051. doi: [10.7554/eLife.88051](#).
- [26] Kulkarni S, Ganz J, Bayrer J, Becker L, Bogunovic M, Rao M. Advances in enteric neurobiology: the “brain” in the gut in health and disease. *J Neurosci* 2018;38(44):9346–54. doi: [10.1523/jneurosci.1663-18.2018](#).
- [27] Ruiz-Argüelles A, Rivadeneyra-Espinoza L, Alarcón-Segovia D. Antibody penetration into living cells: pathogenic, preventive and immuno-therapeutic implications. *Curr Pharm Des* 2003;9(23):1881–7. doi: [10.2174/1381612033454379](#).
- [28] Yang YL, Chuang YT, Huang YH. MicroRNA 29a alleviates mitochondrial stress in diet-induced NAFLD by inhibiting the MAVS pathway. *Eur J Pharmacol* 2024;982:176955. doi: [10.1016/j.ejphar.2024.176955](#).
- [29] Höppner J, Tabeling C, Casteleyn V, Kedor C, Windisch W, Burmester GR, et al. Comprehensive autoantibody profiles in systemic sclerosis: clinical cluster analysis. *Front Immunol* 2022;13:1045523. doi: [10.3389/fimmu.2022.1045523](#).
- [30] Miyakawa H, Kitazawa E, Fujikawa H, Kikuchi K, Abe K, Kawaguchi N, et al. Analysis of two major anti-M2 antibodies (anti-PDC-E2/anti-BCOADC-E2) in primary biliary cirrhosis: relationship to titers of immunofluorescent anti-mitochondrial antibody. *Hepatol Res* 2000;18(1):1–9. doi: [10.1016/s1386-6346\(99\)00079-0](#).
- [31] Favoino E, Grapsi E, Barbuti G, Liakouli V, Ruscitti P, Foti C, et al. Systemic sclerosis and primary biliary cholangitis share an antibody population with identical specificity. *Clin Exp Immunol* 2023;212(1):32–8. doi: [10.1093/cei/uxad012](#).
- [32] Salas AD, Yanek LR, Hummers LK, Shah AA, McMahan ZH. Abnormal esophageal scintigraphy associates with a distinct clinical phenotype in patients with systemic sclerosis. *ACR Open Rheumatol* 2025;7(1):e11796. doi: [10.1002/acr2.11796](#).
- [33] Chen X, Tang X, Xie Y, Cuffari BJ, Tang C, Cao F, et al. A lupus-derived autoantibody that binds to intracellular RNA activates cGAS-mediated tumor immunity and can deliver RNA into cells. *Sci Signal* 2025;18(879):eadk3320. doi: [10.1126/scisignal.adk3320](#).



## Vasculitis

# Mycophenolate mofetil plus methotrexate versus cyclophosphamide with sequential azathioprine for treatment of Takayasu arteritis

Xiaochuan Sun<sup>1</sup>, Jing Li<sup>2</sup>, Xinwang Duan<sup>3</sup>, Yahong Wang<sup>4</sup>, Yu Chen<sup>5</sup>, Ying Wang<sup>4</sup>, Liyun Zhang<sup>6</sup>, Dongyun Yao<sup>7</sup>, Jing Xue<sup>8</sup>, Zhenbiao Wu<sup>9</sup>, Yi Zhao<sup>10</sup>, Li Luo<sup>11</sup>, Hongfeng Zhang<sup>12</sup>, Xiuling Zhang<sup>3</sup>, Lili Pan<sup>13</sup>, Xiaofeng Zeng<sup>2</sup>, Mengtao Li<sup>2,\*\*\*</sup>, Peter A. Merkel<sup>14,\*\*</sup>, Xinpeng Tian<sup>2,\*</sup>

<sup>1</sup> Department of Internal Medicine, Peking Union Medical College Hospital, Beijing, China

<sup>2</sup> Department of Rheumatology and Clinical Immunology, Peking Union Medical College Hospital, Chinese Academy of Medical Sciences, Peking Union Medical College, National Clinical Research Center for Dermatologic and Immunologic Diseases (NCRC-DID), Ministry of Science & Technology, Key Laboratory of Rheumatology and Clinical Immunology, Ministry of Education, Beijing, China

<sup>3</sup> Department of Rheumatology, The Second Affiliated Hospital of Nanchang University, Nanchang, China

<sup>4</sup> Department of Ultrasound, State Key Laboratory of Complex Severe and Rare Diseases, Peking Union Medical College Hospital, Chinese Academy of Medical Sciences and Peking Union Medical College, Beijing, China

<sup>5</sup> Department of Radiology, State Key Laboratory of Complex Severe and Rare Diseases, Peking Union Medical College Hospital, Chinese Academy of Medical Sciences and Peking Union Medical College, Beijing, China

<sup>6</sup> Department of Rheumatology, Shanxi Bethune Hospital, Shanxi Academy of Medical Sciences, Tongji Shanxi Hospital, Taiyuan, China

<sup>7</sup> Department of Rheumatology, Jiaozuo People's Hospital, Jiaozuo, China

<sup>8</sup> Department of Rheumatology, The Second Affiliated Hospital of Zhejiang University School of Medicine, Hangzhou, China

<sup>9</sup> Department of Rheumatology and Immunology, Tangdu Hospital of Air Force Military Medical University, Xi'an, China

<sup>10</sup> Department of Rheumatology and Allergy, Xuanwu Hospital, Capital Medical University, Beijing, China

<sup>11</sup> Department of Rheumatology and Immunology, People Hospital of Xinjiang Uygur Autonomous Region, Urumchi, China

<sup>12</sup> Department of Rheumatology, The First Affiliated Hospital of Dalian Medical University, Dalian, China

<sup>13</sup> Departments of Rheumatology and Immunology, Beijing Anzhen Hospital, Capital Medical University, Beijing, China

<sup>14</sup> Division of Rheumatology, Department of Medicine, Division of Epidemiology, Department of Biostatistics, Epidemiology, and Informatics, University of Pennsylvania, Philadelphia, PA, USA

## ARTICLE INFO

## Article history:

Received 23 April 2025

Received in revised form 20 July 2025

Accepted 22 July 2025

## ABSTRACT

**Objectives:** Study the efficacy and safety of mycophenolate mofetil (MMF) combined with methotrexate (MTX) compared to cyclophosphamide (CYC) followed by azathioprine (AZA) to treat active Takayasu arteritis (TAK).

**Methods:** Adults with active TAK were randomised in a 2:1 ratio to receive oral MMF plus MTX or intravenous CYC followed by oral AZA. All subjects also received high-dose oral glucocorticoids with a predefined taper. The primary endpoint was overall response rate at week 52, defined as achieving a complete response (CR) or partial response (PR). Secondary endpoints included rates of CR and PR at weeks 28 and 52.

\*Correspondence to Dr. Xinpeng Tian. \*\*Correspondence to Dr. Peter A. Merkel. \*\*\*Correspondence to Dr. Mengtao Li.

E-mail addresses: [mengtao.li@cstar.org.cn](mailto:mengtao.li@cstar.org.cn) (M. Li), [pmerkel@upenn.edu](mailto:pmerkel@upenn.edu) (P.A. Merkel), [tianxp6@126.com](mailto:tianxp6@126.com) (X. Tian).

Xiaochuan Sun and Jing Li contributed equally to this study.

Handling editor Josef S. Smolen.

<https://doi.org/10.1016/j.ard.2025.07.018>



**Results:** A total of 111 patients with TAK were enrolled: 74 in the MMF + MTX group and 37 in the CYC/AZA group, with comparable baseline demographic and clinical features. The overall response rates at 28 and 52 weeks were 58.1% and 55.4% in the MMF + MTX group, respectively, higher than 32.4% at both time points in the CYC/AZA group ( $P = .011$  and  $.022$ ). CR and PR rates at 28 and 52 weeks were also higher in the MMF + MTX group. Relapse occurred in 4 patients in the MMF + MTX group and 2 in the CYC/AZA group. One serious adverse event, neutropenia with fever, occurred in 1 patient in the CYC/AZA group.

**Conclusions:** Treatment of active TAK with MMF + MTX has more favourable efficacy compared to CYC/AZA. These findings provide evidence to use the combination of MTX and MMF, 2 generally well-tolerated and inexpensive therapies, to treat TAK.

#### WHAT IS ALREADY KNOWN ON THIS TOPIC

- The management of Takayasu arteritis (TAK) remains challenging due to the scarcity of high-quality, large-scale clinical studies, particularly randomised clinical trials (RCTs).
- Cyclophosphamide (CYC) is commonly used to treat TAK but poses reproductive risks, which is particularly concerning given the predominance of TAK in women of childbearing age.
- Mycophenolate mofetil (MMF) and methotrexate (MTX) have emerged as potential alternatives, though currently supported only by observational data.

#### WHAT THIS STUDY ADDS

- The CommittedTA trial is an open-label, multicentre RCT evaluating the efficacy and safety of MMF combined with MTX versus CYC followed by azathioprine in adults with active TAK.
- This is only the second RCT investigating conventional disease-modifying antirheumatic drugs in TAK and the largest to date, enrolling 111 patients with this rare condition.
- The trial demonstrated that MMF plus MTX has superior efficacy in inducing and maintaining remission, along with a more favourable safety profile over 52 weeks of treatment.

#### HOW THIS STUDY MIGHT AFFECT RESEARCH, PRACTICE OR POLICY

- This study provides much-needed trial-level evidence and offers important clinical guidance for the management of TAK, particularly in resource-limited settings where access to biologics is limited.
- The findings support the use of MMF plus MTX, 2 well-tolerated and affordable therapies to treat TAK.
- The trial also supports limiting the use of CYC in TAK treatment, considering both its relatively lower efficacy and its known reproductive toxicity.

## INTRODUCTION

Takayasu arteritis (TAK) is a rare chronic systemic vasculitis of the aorta and its major branches. TAK predominantly affects young women and typically has an insidious onset, triggering systemic inflammation and arterial damage that can lead to irreversible organ damage and even life-threatening events [1]. Certain Asian regions, including China, bear a heavier disease burden of TAK compared to Western countries [2].

Managing TAK is challenging due to the scarcity of high-quality, large-scale clinical studies, particularly randomised clinical trials (RCTs) [3]. Current therapeutic approaches are primarily adapted from treatments for other autoimmune diseases, especially other forms of systemic vasculitis. Although glucocorticoids (GCs) are the mainstay of first-line treatment for TAK, additional immunosuppressive drugs are often added to the treatment regimen to both more effectively treat disease and to

allow for reduction of GCs [4–6], including both the so-called traditional disease-modifying antirheumatic drugs and targeted biologic agents.

In some countries, cyclophosphamide (CYC) is a commonly used agent for TAK, given its perceived efficacy as an immunosuppressive agent and its relatively low cost of administration compared to biologic drugs. To reduce the cumulative dose and toxicity of CYC, it is often replaced by azathioprine (AZA) once remission is achieved. However, given the significant adverse effects of CYC, including bone marrow suppression, infertility, and increased risk of malignancies, it is imperative to identify effective treatment regimens with at least comparable or improved efficacy and lower toxicity to treat patients with TAK [4].

Mycophenolate mofetil (MMF) and methotrexate (MTX) are promising alternative treatments to CYC due to their potent immunosuppressive effects, lack of impact on fertility, and suitability for long-term use. MMF has gradually replaced CYC in treating various severe rheumatic diseases, including systemic lupus erythematosus and systemic sclerosis. An observational study with a small sample size showed that MMF was effective in 80% of patients with active TAK with minimal adverse effects [7]. Similarly, the use of MTX to treat TAK is supported by several case series [8,9]. Combining immunosuppressive agents is a common approach to treating systemic inflammatory diseases, including rheumatoid arthritis, systemic lupus erythematosus, inflammatory bowel disease, and many others.

This clinical trial aimed to evaluate the efficacy and safety of GCs + MMF + MTX (experimental group) compared to GCs + CYC followed by GCs + AZA (control group) in treating active TAK.

## METHODS

### Trial design

This investigator-initiated, open-label, randomised controlled trial (the ‘CommittedTA’ trial) was conducted across 9 centres in China and registered on clinicaltrials.gov (NCT03096275). Patients with active TAK were recruited and randomised in a 2:1 ratio into the experimental (MMF + MTX) and active control (CYC/AZA) groups. The experimental group received MMF combined with MTX, while the control group received CYC followed by AZA. All subjects were followed for 52 weeks to evaluate the efficacy and safety of the treatments. MMF was supplied by Hunan Warrant Pharmaceutical, which had no role in the trial design, conduct, data analysis, or manuscript preparation. The trial was approved by the ethics committees at Peking Union Medical College Hospital and other participating sites. Written informed consent was obtained from each participant.

## Participants

Patients were eligible if they met the 1990 American College of Rheumatology (ACR) classification criteria for TAK [10], were at least 18 years old, and considered by the investigator to have active disease defined by at least 2 of the following 3 criteria: (1) one or more clinical manifestations of active disease; (2) one or more findings on imaging of progressive disease; or (3) elevated erythrocyte sedimentation rate (ESR) or C-reactive protein (CRP). Clinical criteria included constitutional symptoms such as fever, fatigue, and weight loss, musculoskeletal symptoms, vascular pain, neurological or visual symptoms, abdominal pain or angina, new or worsening limb claudication, loss of pulses, and worsening hypertension. Imaging criteria included new or worsening vascular stenosis or aneurysms detected by ultrasound, computed tomography angiography (CTA), or magnetic resonance angiography. Exclusion criteria involved prior use of MTX with dose reduction or discontinuation due to adverse events (AEs), discontinuation of MMF or CYC due to failed response or AEs, severe renal or liver disease, uncontrolled diabetes, hypertension, or heart failure, active infections, recent upper gastrointestinal bleeding, heterozygosity or homozygosity for the *TPMT* gene mutation, current or planned pregnancy during the trial period, severe coronary artery disease, or severe involvement of large head and neck vessels requiring urgent invasive procedures.

## Randomisation

Patients were randomly assigned in a 2:1 ratio to receive MMF combined with MTX or CYC followed by AZA without masking. The randomisation process was performed on the RheumCloud App supported by the Chinese Rheumatism Data Center [11].

## Interventions

All study subjects received high-dose GCs. Patients weighing less than 50 kg started prednisone 50 mg or equivalent dose of other GC daily, with a weekly reduction of 5 mg/d starting after 4 weeks, reaching 20 mg daily by week 12, followed by a weekly reduction of 2.5 mg/d until reaching 10 mg daily by week 16, the dose was maintained until week 52. Patients weighing 50 kg or more started prednisone 60 mg or equivalent dose of other GC daily, with a weekly reduction of 5 mg starting after 4 weeks, reaching 30 mg daily by week 8, followed by a weekly reduction of 2.5 mg/d until reaching 10 mg daily by week 16, the dose was maintained until week 52.

MMF was prescribed as 750 mg (body weight <50 kg) or 1000 mg (body weight ≥50 kg) twice daily, and MTX was given orally as 15 mg weekly. CYC was intravenously infused at 15 mg/kg (maximum dose of 1200 mg) every 2 weeks for the first 3 doses and then every 3 weeks, for a total of 10 infusions, followed by oral AZA 100 mg daily from weeks 28 to 52.

## Withdrawal

Patients were withdrawn from the study if they exhibited worsening ischaemia symptoms, new arterial lesions on imaging, or if ESR or CRP levels remained higher than twice the upper limit of normal after 6 months. Additionally, withdrawal occurred if patients required emergent surgery due to disease progression or demonstrated poor tolerance or noncompliance

with the study treatment. Other conditions warranting early withdrawal were determined by the investigators.

## Measurement and endpoints

Study visits occurred at baseline and weeks 4, 16, 28, 36, and 52 after the initiation of treatment. Demographic features, medical history, clinical symptoms, physical examinations, routine blood and urine tests, levels of CRP and ESR were obtained at baseline and each follow-up visit. Vascular Doppler ultrasonography was performed in all patients at baseline, week 28, and week 52. The mural thickness and lumen diameter of the accessible arteries (right and left carotid, vertebral, subclavian, axillary and renal arteries, mesenteric arteries, and descending and abdominal aorta) were measured. Cervical and aortic CTA were performed using a 64-slice or higher CT scanner in all patients at baseline and week 52. The scan range for cervical CTA extended from the aortic arch to the skull vertex, and for aortic CTA, from the thoracic inlet to the iliac bifurcation. Meglumine diatrizoate was injected via an antecubital vein at 4 to 5 mL/s: 50 mL for cervical CTA and 100 mL for aortic CTA, followed by a 30 to 40 mL saline flush, and scanning started when enhancement reached 100 to 150 HU. Pulmonary artery and coronary CTA were performed in patients presenting with symptoms indicative of potential involvement in these vascular territories; electrocardiogram gating was applied in coronary CTA. Vascular imaging was independently assessed in a standardised fashion at each participating centre by radiologists and ultrasonographers who specialise in vascular imaging.

The primary endpoint was the overall response rate at week 52. Secondary endpoints included response rates at weeks 28 and 52, relapse rates, and stability or improvement in imaging. Safety endpoints included the frequency of AEs. A complete response (CR) was defined as the complete resolution of signs and symptoms of active disease, normalisation of both ESR and CRP, no progression on imaging of involved arteries, and the dose of GC <15 mg daily. A partial response (PR) was defined as the same as CR except that ESR and CRP were not normal but were lower than twice the upper limit of normal or decreased by 50% compared to baseline. Overall response is the combination of CR and PR. If withdrawal from the study or switch to a different therapy occurred due to poor efficacy of the original treatment, the patient was assumed not to have achieved remission at subsequent follow-up assessments. A major relapse was defined as the recurrence of active disease, indicated by either clinical features of ischaemia or new-onset or progression of vessel dilation, stenosis, or occlusion. A minor relapse was defined as the recurrence of active disease, not fulfilling the criteria for a major relapse.

Severe AEs included death, life-threatening events, irreversible organ damage, hospitalisation, or prolongation of existing hospitalisation. Other adverse reactions were classified as mild AEs.

## Sample size

Sample size was calculated based on the hypothesis that an equivalence test for the overall remission rate at week 52 in 2 study arms. According to a previous study, the overall effective rate of therapy including MMF in treating TAK is 80% [6]. Due to lack of data regarding the efficacy of CYC for the treatment of TAK, the reported 52% response rate for treatment with CYC for proliferative nephritis was used to estimate the sample size calculation [12]. Comparable effectiveness of MMF + MTX versus CYC/AZA in treating TAK was assumed in this study. With a power of 90% and an alpha error of 5%, a minimum of 88

subjects in the MMF + MTX group and 44 subjects in the CYC/AZA group were required. After considering a potential dropout rate of 15%, the final sample size was 150 patients, including 100 in the experimental group and 50 in the control group.

### Statistical analysis

Efficacy analyses were performed on the intention-to-treat (ITT) and per-protocol (PP) populations. The ITT population included all randomised subjects, while the PP population included those without substantial protocol deviations, including premature discontinuation of study medicine for more than 1 month, taking any biologic drugs, or failure of tapering the dose of GCs to 10 mg daily at week 52. Patients who prematurely changed treatment due to inefficacy were included in the PP population as per their group assignment. Subgroup analyses on efficacy were performed based on prior use of MTX and distribution of vascular lesions, according to both Numano classification and a validated classification based on cluster analytics [13,14]. Safety profile assessment was performed in all subjects who received any study treatment and reported AEs.

Data are presented using descriptive statistics: normally distributed data are represented by the mean and SD and non-normally distributed data are expressed by the median and IQR. Categorical variables are represented by counts and percentages. The Shapiro-Wilk test was used to examine whether the variables were normally distributed. Chi-square test, t-test, or median test were used to identify differences in demographical or clinical characteristics at baseline between the intervention (MMF + MTX) and control (CYC/AZA) groups. Chi-square test was used to compare the effectiveness and safety profiles. All statistical analyses were performed using SPSS ver. 26 and Graphpad Prism ver. 9.5.

## RESULTS

### Patient population

Between February 2017 and September 2021, 130 patients with active TAK were screened for eligibility at 9 clinical centres. Of these, 111 patients were enrolled: 74 were randomly assigned to the MMF + MTX group, and 37 to the CYC/AZA group. Twelve patients were excluded based on the exclusion criteria: 6 for failure to respond to prior treatment with CYC, 1 for failure to respond to prior treatment with MMF, 4 due to the presence of the TMPT gene mutation, and 1 for severe coronary artery involvement requiring urgent invasive intervention. Seven patients declined to participate in this trial. After enrolment, all subjects were re-evaluated according to the 2022 ACR/European Alliance of Associations for Rheumatology (EULAR) classification criteria for TAK [15]. Only 2 patients in the MMF + MTX group and 1 patient in the CYC/AZA group did not meet the 2022 criteria, both due to a lack of clinical criteria for active disease. However, all 3 of these patients had new or worsening imaging lesions and elevated inflammatory markers, with other potential causes excluded; therefore, their diagnoses of TAK were confirmed, and they were included in the analysis. In the MMF + MTX group, 11 patients were excluded from the PP population at week 52, including 4 due to AEs, 2 due to loss of follow-up, and 5 for other reasons. In the CYC/AZA group, 8 patients were excluded from the PP population at week 52, 5 due to AEs, and 3 for other reasons (Fig 1).

The baseline characteristics of the patients were comparable between the 2 study arms (Table 1). Ninety-five (85.6%)

patients were women. The median age at recruitment and disease onset was 30.0 (26.0–33.0) and 27.0 (21.0–31.0) years, respectively, with a median disease duration of 1.4 (0.9–4.7) years. The median body weight was 55 kg and about one-fourth of the patients had a body weight less than 50 kg. Overall, 13 patients used MMF at a dose of 1.5 g daily due to their low body weights. Overall, 83 (74.8%) patients had relapsed, and 25.2% had new-onset disease. At baseline, 24 (21.6%) patients were currently using GCs, with a median dosage of 10 mg/d of prednisone or equivalent. Fourteen (12.6%) patients had previously used MTX and 2 (1.8%) patients had previously used biologic drugs: 1 with tocilizumab and 1 with a TNF inhibitor. The median baseline levels of serum CRP and ESR at baseline were 28.4 (10.5–59.1) mg/L and 46.5 (29.5–73.3) mm/h, respectively.

### Efficacy endpoints

The primary endpoint, achieving an overall response at week 52, occurred in 41 of 74 patients (55.4%) in the MMF + MTX group and 12 of 37 patients (32.4%) in the CYC/AZA group, with an odds ratio (OR) of 2.59 (95% CI: 1.13–5.92,  $P = .022$ ) (Table 2 and Fig 2). In the PP population, the overall response at week 52 was achieved by 37 of 63 patients (58.7%) in the MMF + MTX group and 12 of 29 patients (41.4%) in the CYC/AZA group, OR 2.02 (95% CI: 0.83–4.93,  $P = .121$ ).

With respect to secondary outcomes, CIs and  $P$  values were not adjusted for multiple comparisons. Both the CR and PR rates at week 52 were higher in the MMF + MTX group (41.9% and 13.5%, respectively) compared to the CYC/AZA group (29.7% and 2.7%, respectively), although these differences were not statistically significant. At week 28, 43 of 74 patients (58.1%) in the MMF + MTX group and 12 of 37 patients (32.4%) in the CYC/AZA group achieved an overall response, OR 2.89 (95% CI: 1.26–6.62,  $P = .011$ ). A significantly higher PR rate at week 28 was observed in the MMF + MTX group compared to the CYC/AZA group (21.6% versus 5.4%, OR = 4.83,  $P = .031$ ). The CR rate at week 28 was comparable between the 2 groups.

Although the conclusion regarding the primary endpoint was achieved, because the planned sample size was not reached, a post hoc power analysis was conducted for secondary endpoints. Specifically, for the differences in CR and PR at week 52, and CR at week 28 between the treatment groups, the estimated powers were 23.1%, 41.8%, and 16.1%, respectively, assuming a 2-sided alpha level of 0.05. Among those who achieved CR or PR at week 28 and week 52, all were maintained on 10 mg/d of prednisone or equivalent, a dosage aligned with the recommendations for maintenance of remission in TAK [4–6]. The PP analysis yielded similar results (Table 2). A subgroup analysis based on disease phase (new-onset versus relapsed) was performed. In both subgroups, patients treated with MMF + MTX achieved higher overall response rates compared to CYC/AZA (59.1% versus 33.3% in new-onset patients; 58.8% versus 32.3% in relapsed patients). Although these differences were not statistically significant due to limited sample sizes, the direction and magnitude of treatment effects were consistent with the primary analysis.

Among patients who achieved an overall response at week 28, 1 patient (2.3%) in the MMF + MTX group experienced a relapse at week 36, and 3 patients (7.0%) relapsed by week 52. All 4 patients had elevated inflammatory markers, and 2 developed new-onset arterial stenosis and thickening. Two of the relapses were minor, both occurring in treatment-naïve patients; one was managed by increasing GC to the last effective dose,

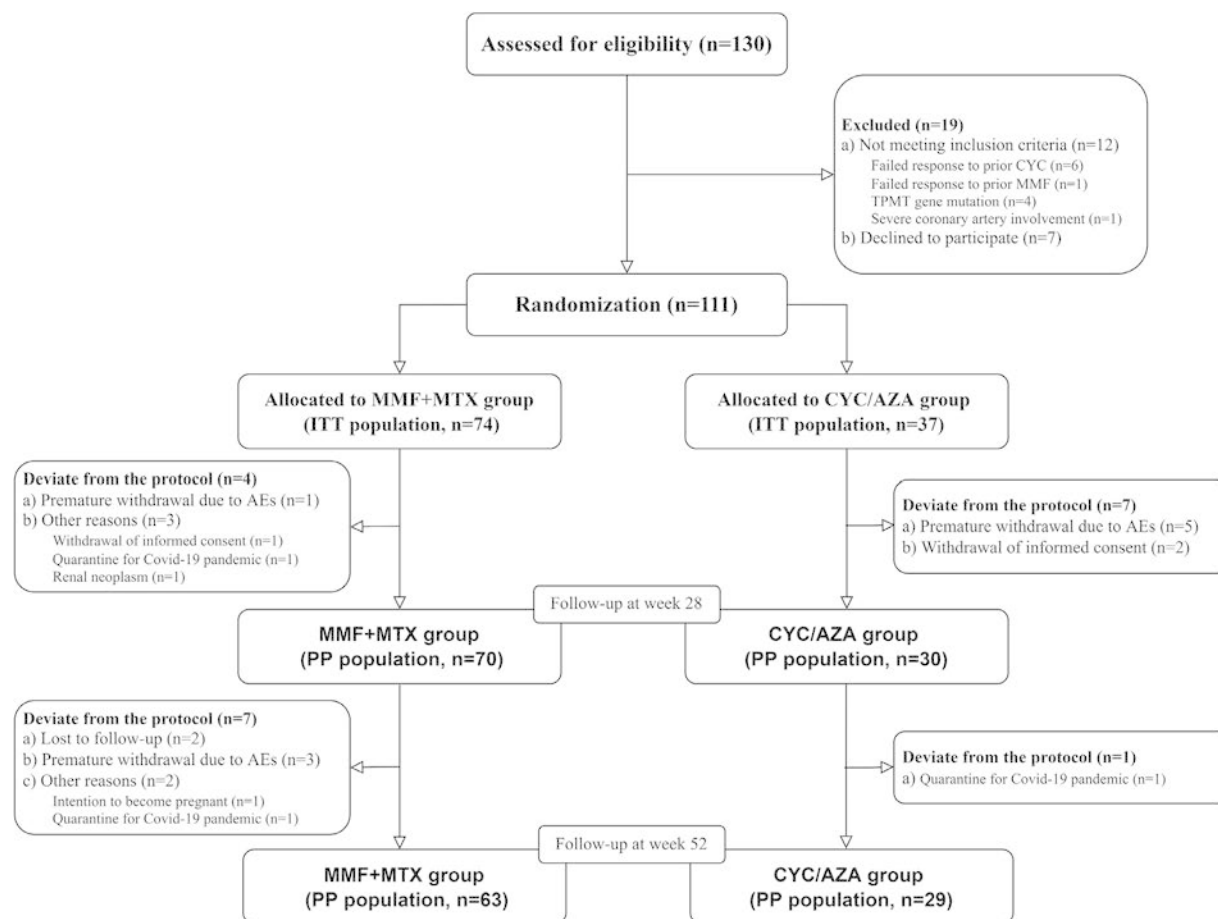


**Figure 1.** Enrolment and randomisation of patients. AE, adverse event; AZA, azathioprine; CYC, cyclophosphamide; ITT, intention-to-treat; MMF, mycophenolate mofetil; MTX, methotrexate; PP, per-protocol.

and the other by switching to a TNF inhibitor. The remaining 2 relapses were major and were managed with reinstitution of high-dose GC and a switch to alternative drugs. In the CYC/AZA group, 2 (16.7%) patients experienced major relapses at week 52. One patient had elevated inflammatory markers, and 2 patients showed progression on vessel thickening and stenosis. These relapses were managed with the reinstitution of high-dose GC and a switch to alternative drugs ([Supplementary Table S1](#)). The changes in white blood cell counts, lymphocyte counts, CRP, ESR, and rates of patients with stable or improved imaging findings at weeks 28 and 52 were similar between the MMF + MTX and CYC/AZA groups ([Fig 3](#) and [Supplementary Table S2](#)).

### Safety endpoints

AEs were reported in 29 of 74 patients (39.2%) in the MMF + MTX group and 18 of 37 patients (48.6%) in the CYC/AZA group,  $P = .342$ . The most common AEs included abnormal liver function tests, gastrointestinal discomfort, and infections ([Table 3](#)). Only 1 severe AE was documented in the CYC/AZA group in a patient who experienced neutropenia with fever and grade 4 thrombocytopenia after the initiation of AZA. This patient was immediately discontinued from the study treatment and supportive treatments were administered, including granulocyte colony-stimulating factor, thrombopoietin receptor agonist, and broad-spectrum antibiotics. The patient recovered without severe complications. All other AEs were mild.

Infections were observed in 8 (10.8%) patients in the MMF + MTX group and 2 (5.4%) patients in the CYC/AZA group over

the 52-week period,  $P = .491$ . One patient in the MMF + MTX group developed herpes zoster, while all other infections were upper respiratory tract infections. These infections were all mild and did not require intravenous antibiotics or hospitalisation. Bone marrow suppression and hair loss were reported only in the CYC/AZA group, in 4 (10.8%) patients and 3 (8.1%) patients, respectively. Four patients (10.8%) developed bone marrow suppression during treatment with AZA, including one severe case mentioned above. The other cases were mild and completely resolved after withdrawal of AZA, without complications such as infections or bleeding. Hair loss occurred in 3 patients (8.1%) during treatment of CYC and was mild and transient. Liver test abnormalities were more common in the MMF + MTX group, affecting 17 patients (23.0%). Four patients (5.4%) had alanine aminotransferase elevated 2 times the upper limit of normal and resulting in discontinuation of MTX. The remaining cases were mild and resolved without withdrawal of treatment regimens. Gastrointestinal discomfort was more frequently reported in the CYC/AZA group (6 patients, 16.2%) with all cases mild and the immunosuppressive treatments were not held or discontinued. The differences between groups in liver enzyme abnormalities and gastrointestinal discomfort were not statistically significant.

### DISCUSSION

TAK is a chronic, systemic large-vessel vasculitis characterised by remissions and relapses. Although most patients with TAK achieve disease remission with treatment with high-dose GCs; however, nearly half of such patients will experience a disease relapse or progression during tapering of GCs [16].



**Table 1**  
**Characteristics of the study patients at entry into the trial**

Characteristics	Mycophenolate mofetil + methotrexate (N = 74)	Cyclophosphamide followed by azathioprine (N = 37)	P value
Female sex, no. (%)	61 (82.4%)	34 (91.9%)	.181
Age at recruitment, median (IQR) (y)	29.5 (24.0-33.0)	32.0 (29.0-38.5)	.253
Age at disease onset, median (IQR) (y)	26.5 (19.8-30.3)	29.0 (25.0-32.5)	.122
Disease duration, median (IQR) (y)	1.3 (0.9-5.1)	1.6 (0.9-4.0)	.638
Body weight, median (IQR) (kg)	55.0 (50.0-66.3)	54.0 (50.0-62.5)	.637
BMI, median (IQR) (kg/m <sup>2</sup> )	20.7 (18.5-23.4)	20.3 (18.3-23.7)	.946
Numano classification, no. (%)			.313
I	10 (13.5%)	4 (11.1%)	
IIa	7 (9.5%)	8 (22.2%)	
IIb	8 (10.8%)	6 (16.7%)	
III	0 (0%)	0 (0%)	
IV	2 (2.7%)	1 (2.8%)	
V	47 (63.5%)	17 (47.2%)	
New classification, no. (%)			.695
Cluster 1	26 (35.1%)	10 (27.0%)	
Cluster 2	39 (52.7%)	21 (56.8%)	
Cluster 3	8 (10.8%)	5 (13.5%)	
Pulmonary artery involvement, no. (%)	8 (10.8%)	4 (10.8%)	1.000
Coronary artery involvement, no. (%)	1 (1.4%)	1 (2.7%)	1.000
Relapsed patients, no. (%)	52 (70.3%)	31 (83.8%)	.122
History of invasive intervention, no. (%)	12 (16.2%)	3 (8.1%)	.378
Current use of glucocorticoids, no. (%)	13 (17.8%)	11 (30.6%)	.146
Glucocorticoid dose, median (IQR), mg/d of prednisone or equivalent	10.0 (7.5-12.5)	10.0 (5.0-15.0)	.456
Prior use of methotrexate, no. (%)	7 (9.6%)	7 (19.4%)	.222
Prior use of a biologic agent, no. (%)	2 (2.7%)	0 (0.0%)	1.000
WBC, median (IQR) (10 <sup>9</sup> /L)	8.3 (6.5-9.4)	8.2 (6.7-10.9)	1.000
LYM, median (IQR) (10 <sup>9</sup> /L)	2.0 (1.5-2.3)	2.0 (1.6-2.5)	1.000
CRP, median (IQR) (mg/L)	27.8 (9.2-56.8)	30.6 (11.7-62.3)	.945
ESR, median (IQR) (mm/h)	45.5 (30.0-73.3)	47.0 (23.5-77.5)	.839

BMI, body mass index; CRP, C-reactive protein; ESR, erythrocyte sedimentation rate; LYM, lymphocyte count; WBC, white blood cell count.

**Table 2**  
**Response to treatment at 28 and 52 weeks by intention-to-treat and per-protocol analysis**

Intention-to-treat analysis		MMF+MTX (N = 74)	CYC/AZA (N = 37)	OR (95% CI)	P value
28 weeks	Overall response	43 (58.1%)	12 (32.4%)	2.89 (1.26-6.62)	0.011
	Complete response	27 (36.5%)	10 (27.0%)	1.55 (0.65-3.69)	0.395
	Partial response	16 (21.6%)	2 (5.4%)	4.83 (1.05-22.27)	0.031
52 weeks	Overall response	41 (55.4%)	12 (32.4%)	2.59 (1.13-5.92)	0.022
	Complete response	31 (41.9%)	11 (29.7%)	1.70 (0.73-3.96)	0.213
	Partial response	10 (13.5%)	1 (2.7%)	5.63 (0.69-45.74)	0.096
Per-protocol analysis		MMF+MTX (N = 63) *	CYC/AZA (N = 29) *	OR (95% CI)	P value
28 weeks	Overall response	43 (61.4%)	12 (40.0%)	2.39 (0.99-5.73)	0.048
	Complete response	27 (38.6%)	10 (33.3%)	1.26 (0.51-3.09)	0.619
	Partial response	16 (26.7%)	2 (6.7%)	5.09 (1.09-23.85)	0.027
52 weeks	Overall response	37 (58.7%)	12 (41.4%)	2.02 (0.83-4.93)	0.121
	Complete response	27 (42.9%)	11 (37.9%)	1.23 (0.50-3.02)	0.656
	Partial response	10 (15.9%)	1 (3.4%)	5.28 (0.64-43.40)	0.163

0.51248163264

Favors CYC/AZAFavors MMF+MTX

AZA, azathioprine; CYC, cyclophosphamide; MMF, mycophenolate mofetil; MTX, methotrexate; OR, odds ratio.  
\*In the per-protocol population at week 28, 70 patients in the MMF + MTX group and 30 patients in the CYC/AZA group were included.

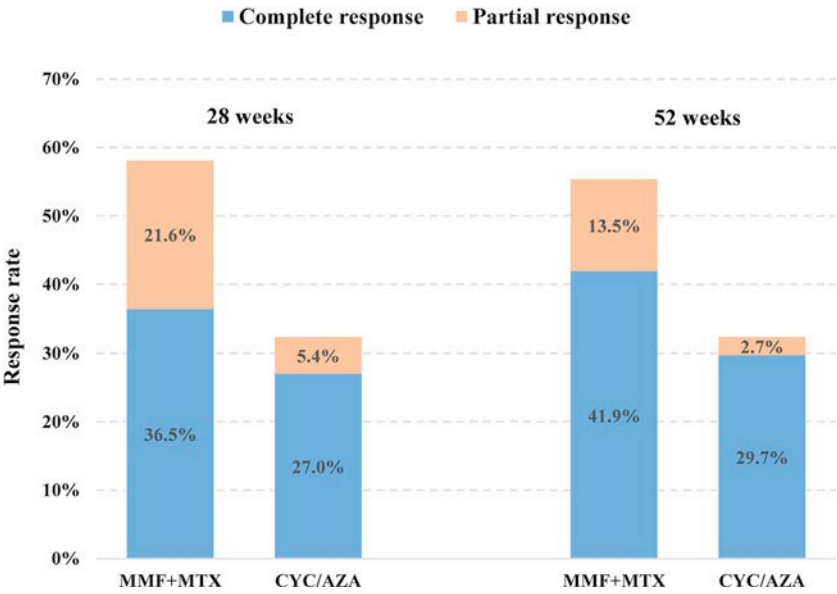


**Figure 2.** Response to treatment at 28 and 52 weeks by intention-to-treat analysis. AZA, azathioprine; CYC, cyclophosphamide; MMF, mycophenolate mofetil; MTX, methotrexate.

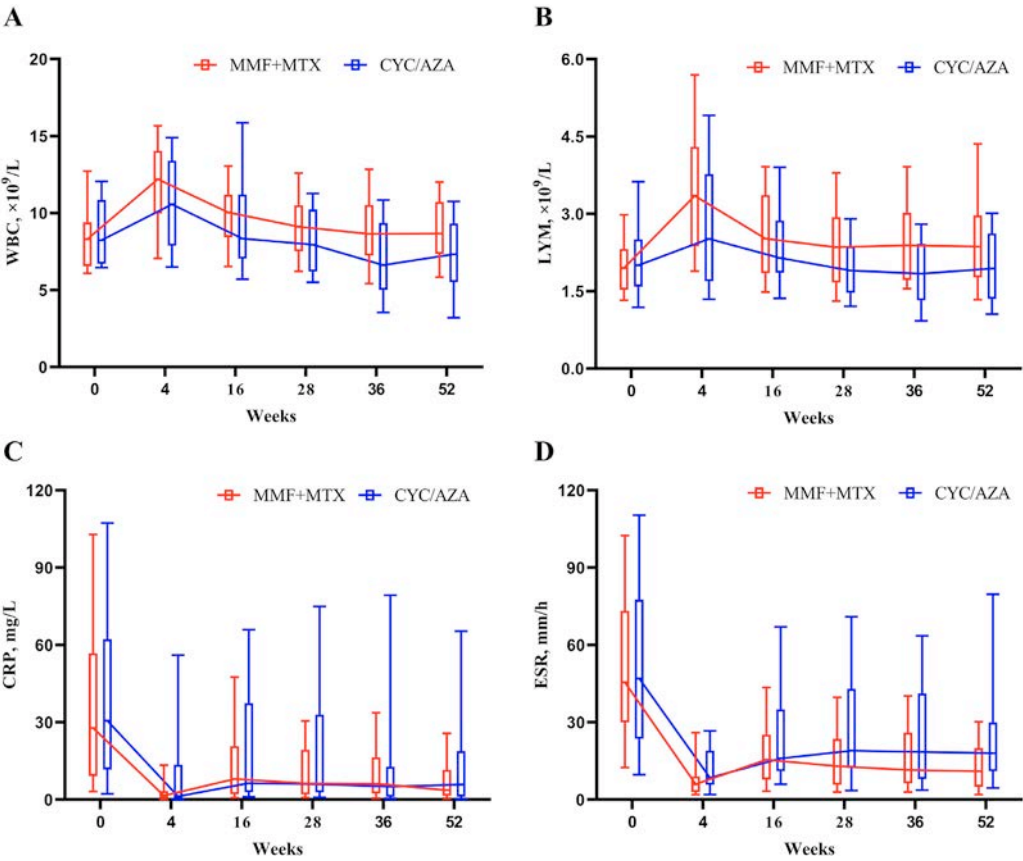


**Figure 3.** Changes in levels of (A) white blood cell counts (WBC), (B) lymphocyte counts (LYM), (C) C-reactive protein (CRP), and (D) erythrocyte sedimentation rate (ESR) during the 52-week follow-up of patients in the (i) mycophenolate mofetil combined with methotrexate (MMF + MTX) and (ii) cyclophosphamide followed by azathioprine (CYC/AZA) treatment groups. Horizontal lines and boxes show the median and the 25th-75th percentile range of distribution; whiskers represent 10th-90th percentile.

Therefore, early initiation of immunosuppressive agents in addition to GCs is suggested by both EULAR recommendations and ACR guidelines [4,5]. Despite the development of biological disease-modifying agents, conventional synthetic disease-modifying agents (csDMARDs) remain a mainstay of GC-sparing agents for TAK, especially in resource-limited areas. However, the choice of csDMARDs in the treatment of TAK is currently based on low-evidence data from observational studies with limited sample sizes or expert opinions, making these choices controversial [17]. This

RCT study compared the efficacy and safety of 2 regimens of csDMARDs to treat TAK: MMF + MTX versus CYC/AZA.

A prior questionnaire-based investigation indicated that CYC is commonly the first choice of csDMARDs for active TAK in China [18]. However, this preference is mainly based on experience with other systemic vasculitides, such as ANCA-associated vasculitis, and not high-quality evidence from RCTs for TAK. Previous Chinese cohort studies reported that the effectiveness rates of CYC were 74% to 82% for treating TAK [19,20].

**Table 3**  
**Adverse events during the trial**

Adverse events	Mycophenolate mofetil plus methotrexate (N = 74)	Cyclophosphamide followed by azathioprine (N = 37)	OR (95% CI)	P value
All adverse events	29 (39.2%)	18 (48.6%)	0.68 (0.31–1.51)	.342
Severe adverse events	0 (0%)	1 (2.7%) <sup>a</sup>	0.97 (0.92–1.03)	.333
Infection	8 (10.8%) <sup>b</sup>	2 (5.4%)	2.12 (0.43–10.54)	.491
Bone marrow suppression	0 (0%)	4 (10.8%)	0.89 (0.80–1.00)	.011
Abnormal liver function	17 (23.0%)	5 (13.5%)	1.91 (0.64–5.66)	.239
Gastrointestinal discomfort	7 (9.5%)	6 (16.2%)	0.54 (0.17–1.74)	.297
Hair loss	0 (0%)	3 (8.1%)	0.92 (0.84–1.01)	.035

OR, odds ratio.

<sup>a</sup> The patient experienced neutropenia with fever and grade 4 thrombocytopenia after the initiation of azathioprine. All other adverse events were mild.

<sup>b</sup> One patient in the mycophenolate mofetil + methotrexate group developed herpes zoster. All other infections in both groups were upper respiratory infections.

However, the current trial found that only one-third of patients responded well to treatment with CYC at 28 and 52 weeks. This discrepancy may be due to differences in patient selection as the previous studies included only treatment-naïve patients, whereas the majority of participants in the current trial had relapsed disease. Additionally, this trial adopted stricter criteria for remission and collected data in a protocolised prospective fashion. It is interesting that CYC is not as effective as expected in treating TAK despite being a potent immunosuppressive agent. CYC is also a drug to particularly avoid in treating TAK as most patients are females who present during their childbearing years.

MMF has shown promising efficacy for treating TAK in several studies. A meta-analysis of 2 cohort studies involving 31 patients demonstrated significant reductions in ESR, CRP, and GCs dose after treatment with MMF [21]. A prospective study of 30 Chinese patients with TAK found that MMF combined with GCs was effective in 80% of patients [7]. MTX is also commonly used to treat TAK, mainly supported by case series [8,9]. In a cohort study including 28 Chinese patients with initial-onset TAK, nearly 70% of patients achieved CR at 12 months with MTX at a dose of 10 to 15 mg weekly [22]. Similarly, the current trial used a lower dose of MTX (15 mg weekly) compared to the typical dose used in Caucasian populations (20–25 mg weekly) due to the low body weight and tolerability of the medication in Chinese patients. Additionally, it is important to recognise that in this study MTX was combined with MMF; when drugs are combined, it is common to reduce the dose of one or both agents.

The 2018 EULAR recommendations suggest both MMF and MTX as potential first-line csDMARDs for TAK. However, previous studies were mainly uncontrolled cohorts or retrospective case series with limited sample sizes. A recent RCT comparing MMF and MTX for the treatment of TAK found that both drugs were effective and well-tolerated, with a response rate of 71% for MMF and 64% for MTX [23]. Thus, evidence of the efficacy of these 2 medications or their combination for relapsed disease is lacking. In addition, the sample size of this prior study was small, and the duration of follow-up was short. The current trial provides the highest quality evidence to date of the effectiveness of MMF combined with MTX in treating TAK, with the largest sample size, and a randomised controlled design. The observed nearly 60% response rates at 28 and 52 weeks after treatment with MMF combined with MTX were significantly higher than those for treatment with CYC/AZA. Additionally, the relapse rate, particularly for major relapses, was also lower in the MMF + MTX group compared to the CYC/AZA group. However, given

the limited sample size and relatively short follow-up duration, these findings warrant validation in future studies. All together, these results strongly support the use of MMF and MTX as csDMARDs over CYC to induce and maintain remission in TAK.

In this trial, the side effects of MMF + MTX and CYC/AZA were generally well-tolerated, except for 1 case of severe bone marrow suppression linked to AZA, and consistent with the known toxicities of these drugs. The risk of infection was similar between the 2 groups, with all infections being mild and not requiring intravenous antibiotics or hospitalisation. Liver test abnormalities were common in both treatment groups at similar rates, and all patients' liver tests returned to normal after withdrawal of the study medications. Although not severe, bone marrow suppression, gastrointestinal discomfort, and hair loss were all more frequent in the CYC/AZA group.

This trial has several notable strengths. First, it is a randomised controlled trial with a large sample size for such a rare disease. The randomised design, together with the exclusion of biologic drugs and the implementation of a standardised GC tapering strategy, allowed for a more accurate comparison of the responses to MMF + MTX and CYC/AZA. Second, vascular ultrasound studies and CTA were performed regularly, enabling a comprehensive and objective assessment of disease activity. Third, despite the impact of the COVID-19 pandemic, the rates of loss to follow-up were quite low in both treatment arms, reducing potential selection bias. Lastly, the study adds to the limited pool of high-quality evidence regarding management of TAK and has strong clinical implications.

This study also has some limitations to consider. The sample size calculation was based on efficacy estimates from studies of lupus nephritis, which may not be directly transferable to studies of TAK. The efficacy of lupus nephritis was used as the reference for sample size calculation was due to the lack of data in patients with TAK; using the high estimates of efficacy in lupus nephritis to ensure a conservative sample size calculation by assuming a smaller treatment difference. This approach may have helped increase the power of this trial, but the evidence to support the sample size calculation is weak. Because the intended sample size was not reached, primarily due to the COVID-19 pandemic which made the access to nonemergent medical services difficult, the study period was extended to about 5 years. Nevertheless, the sample size was sufficient to compare the primary endpoints between the 2 study arms. Although the differences in some secondary endpoints did not reach statistical significance, this may be attributable to the insufficient statistical power caused by reduced sample size, suggesting that these negative findings should be interpreted with

caution. Future studies with larger sample sizes are warranted to validate these findings. Additionally, the follow-up period was 52 weeks, which is relatively short for a chronic disease prone to relapse, although this was similar or longer compared to prior trials in TAK [23–25]. The long-term efficacy of MMF + MTX in maintaining remission remains uncertain and should be investigated in future studies with longer follow-up periods. The majority of trial participants had relapsed disease, possibly partially explaining the low overall response rate, and highlighting the challenges in managing relapsing TAK. However, it is patients with more extensive and relapsing disease who are the most in need of treatment with extended courses of immunosuppressive drugs. The open-label design in this trial may have introduced bias in outcome assessment. To minimise this risk, all patients underwent standardised evaluations at every visit, including comprehensive physical examinations and laboratory tests for inflammation. Additionally, vascular ultrasound and CTA were repeated and interpreted by physicians who were blinded to treatment allocation. Importantly, disease activity assessment was based on a combination of objective indicators, such as clinical symptoms and signs, inflammatory biomarkers, and imaging findings, rather than subjective reports alone. These measures substantially reduce the potential bias caused by the open-label design. Vascular imaging was not centrally reviewed; however, standardised protocols were applied at each participating centre. Lastly, as the analyses of CR and PR were secondary and exploratory, and given that the 2 are mutually exclusive and related, the risk of type I error inflation is lower than testing multiple independent outcomes, although should always be considered a possibility.

In conclusion, this 52-week RCT comparing treatment of TAK with MMF + MTX versus CYC/AZA demonstrated that MMF + MTX has more favourable efficacy in inducing and maintaining remission and a superior safety profile. These results provide much-needed trial-level evidence for immunosuppressive treatments in TAK, including the use of drugs that are currently much less expensive than biologic agents, an important factor in many countries with high prevalences of TAK.

## Competing interests

PAM reports receiving funds for the following activities in the past 2 years: Consulting: AbbVie, Alpine, Amgen, ArGenx, AstraZeneca, Boehringer-Ingelheim, Bristol-Myers Squibb, CSL Behring, GlaxoSmithKline, iCell, Interius, Kinevant, Kyverna, Metagenomia, Neutrolis, Novartis, NS Pharma, Q32, Quell, Regeneron, Sanofi, Sparrow, Takeda, Vistara. Research support: AbbVie, Amgen, AstraZeneca, Boehringer-Ingelheim, Bristol-Myers Squibb, Eicos, Electra, GlaxoSmithKline, Neutrolis, Takeda. Stock options: Kyverna, Q32, Lifordi, Neutrolis, Sparrow. Royalties: UpToDate.

## Acknowledgements

We thank the patients who participated in the CommittedTA trial for the time and effort they have invested in the project. We also thank the investigators, study nurses, patient partners and medical staff at the study centres for their contribution to study. We thank Professor Yanhong Wang for her support in statistical analysis. We thank the Hunan Warrant Pharmaceutical for supplying mycophenolate mofetil to study subjects, as well as the funding sources. This work was previously presented as an oral presentation at the ACR Convergence 2024 and published as a conference abstract: Sun X, Li J, Duan X, Zhang L, Yao D, Xue J,

et al. Comparison of mycophenolate mofetil plus methotrexate versus cyclophosphamide with sequential azathioprine for active Takayasu's arteritis: an open-label, randomized-controlled trial [abstract]. *Arthritis Rheumatol*. 2024 [cited 2025 Apr 20];76(suppl 9). Available from: <https://acrabstracts.org/abstract/comparison-of-mycophenolate-mofetil-plus-methotrexate-versus-cyclophosphamide-with-sequential-azathioprine-for-active-takayasus-arteritis-an-open-label-randomized-controlled-trial/>.

## Contributors

XT, PAM, and ML designed the study and reviewed the manuscript. XT, JL, XD, LZ, DY, JX, ZW, YZ, LL, HZ, XZ, and LP recruited and enrolled participants and collected data. Yahong W, YC, and Ying W conducted the imaging tests. XS and JL collected, analysed and interpreted data, and wrote the report. XZ reviewed the manuscript. XT is guarantor and accepts full responsibility for the work and the conduct of the study, had access to the data and controlled the decision to publish.

## Funding

This study was supported by CAMS Innovation Fund for Medical Sciences (CIFMS) 2021-I2M-1-005, 2022-I2M-1-004, 2023-I2M-2-005), National High Level Hospital Clinical Research Funding (2022-PUMCH-B-013).

## Patient consent for publication

Written informed consent was obtained from each participant.

## Ethics approval

The trial was approved by the ethics committees at Peking Union Medical College Hospital and other participating sites.

## Provenance and peer review

Not commissioned; externally peer reviewed.

## Supplementary materials

Supplementary material associated with this article can be found in the online version at [doi:10.1016/j.ard.2025.07.018](https://doi.org/10.1016/j.ard.2025.07.018).

## Orcid

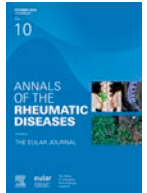
Xiaochuan Sun: <http://orcid.org/0000-0003-3697-6737>

## REFERENCES

- [1] Pugh D, Karabayas M, Basu N, Cid MC, Goel R, Goodyear CS, et al. Large-vessel vasculitis. *Nat Rev Dis Primers* 2022;7:93.
- [2] Danda D, Manikuppam P, Tian X, Harigai M. Advances in Takayasu arteritis: an Asia Pacific perspective. *Front Med (Lausanne)* 2022;9:952972.
- [3] Misra DP, Wakhlu A, Agarwal V, Danda D. Recent advances in the management of Takayasu arteritis. *Int J Rheum Dis* 2019;22(suppl 1):60–8.
- [4] Hellmich B, Agueda A, Monti S, Buttgeit F, de Boysson H, Brouwer E, et al. 2018 Update of the EULAR recommendations for the management of large vessel vasculitis. *Ann Rheum Dis* 2020;79(1):19–30.
- [5] Maz M, Chung SA, Abril A, Langford CA, Gorelik M, Guyatt G, et al. 2021 American College of Rheumatology/Vasculitis Foundation Guideline for the management of giant cell arteritis and Takayasu arteritis. *Arthritis Rheumatol* 2021;73(8):1349–65.



- [6] Tian X, Zeng X. Chinese guideline for the diagnosis and treatment of Takayasu's arteritis (2023). *Rheumatol Immunol Res* 2024;5(1):5–26.
- [7] Li J, Yang Y, Zhao J, Li M, Tian X, Zeng X. The efficacy of mycophenolate mofetil for the treatment of Chinese Takayasu's arteritis. *Sci Rep* 2016;6:38687.
- [8] Hoffman GS, Leavitt RY, Kerr GS, Rottem M, Sneller MC, Fauci AS. Treatment of glucocorticoid-resistant or relapsing Takayasu arteritis with methotrexate. *Arthritis Rheum* 1994;37(4):578–82.
- [9] Mevorach D, Leibowitz G, Brezis M, Raz E. Induction of remission in a patient with Takayasu's arteritis by low dose pulses of methotrexate. *Ann Rheum Dis* 1992;51(7):904–5.
- [10] Arend WP, Michel BA, Bloch DA, Hunder GG, Calabrese LH, Edworthy SM, et al. The American College of Rheumatology 1990 criteria for the classification of Takayasu arteritis. *Arthritis Rheum* 1990;33(8):1129–34.
- [11] Huang C, Zhao J, Tian X, Wang Q, Xu D, Li M, et al. RheumCloud app: a novel mobile application for the management of rheumatic diseases patients in China. *Rheumatol Immunol Res* 2022;3(4):184–9.
- [12] Ong LM, Hooi LS, Lim TO, Goh BL, Ahmad G, Ghazalli R, et al. Randomized controlled trial of pulse intravenous cyclophosphamide versus mycophenolate mofetil in the induction therapy of proliferative lupus nephritis. *Nephrology (Carlton)* 2005;10(5):504–10.
- [13] Hata A, Noda M, Moriawaki R, Numano F. Angiographic findings of Takayasu arteritis: new classification. *Int J Cardiol* 1996;54:S155–63.
- [14] Goel R, Gribbons KB, Carette S, Cuthbertson D, Hoffman GS, Joseph G, et al. Derivation of an angiographically based classification system in Takayasu's arteritis: an observational study from India and North America. *Rheumatology (Oxford)* 2020;59:1118–27.
- [15] Grayson PC, Ponte C, Suppiah R, Robson JC, Gribbons KB, Judge A, et al. 2022 American College of Rheumatology/EULAR classification criteria for Takayasu arteritis. *Ann Rheum Dis* 2022;81:1654–60.
- [16] Comarmond C, Biard L, Lambert M, Mekinian A, Ferfar Y, Kahn JE, et al. Long-term outcomes and prognostic factors of complications in Takayasu arteritis: a multicenter study of 318 patients. *Circulation* 2017;136(12):1114–22.
- [17] Regola F, Uzzo M, Toniati P, Trezzi B, Sinico RA, Franceschini F. Novel therapies in Takayasu arteritis. *Front Med (Lausanne)* 2021;8:14075.
- [18] Dai XM, Dong ZH, Chen S, Cheng YJ, Da ZY, Dai SM, et al. Chinese expert investigation on diagnosis and disease activity evaluation in Takayasu's arteritis. *Fudan Univ J Med Sci* 2017;44(2):127–33.
- [19] Dai X, Cui X, Sun Y, Ma L, Jiang L. Effectiveness and safety of leflunomide compared with cyclophosphamide as induction therapy in Takayasu's arteritis: an observational study. *Ther Adv Chronic Dis* 2020;11:2040622320922019.
- [20] Ying S, Xiaomeng C, Xiaomin D, Jiang L, Peng L, Lili M, et al. Efficacy and safety of leflunomide versus cyclophosphamide for initial-onset Takayasu arteritis: a prospective cohort study. *Ther Adv Musculoskelet Dis* 2020;12:1759720X20930114.
- [21] Dai D, Wang Y, Jin H, Mao Y, Sun H. The efficacy of mycophenolate mofetil in treating Takayasu arteritis: a systematic review and meta-analysis. *Rheumatol Int* 2017;37(7):1083–8.
- [22] Wu C, Sun Y, Cui X, Wu S, Ma L, Chen H, et al. Effectiveness and safety of methotrexate versus leflunomide in 12-month treatment for Takayasu arteritis. *Ther Adv Chronic Dis* 2020;11:2040622320975233.
- [23] Padiyar S, Danda D, Goel R, Joseph E, Nair AM, Joseph G, et al. Clinical and angiographic outcomes of mycophenolate versus methotrexate in South Asian patients of Takayasu arteritis: results from an open-label, outcome-assessor blinded randomized controlled trial. *Mod Rheumatol* 2023;34(1):175–81.
- [24] Nakaoka Y, Isobe M, Takei S, Tanaka Y, Ishii T, Yokota S, et al. Efficacy and safety of tocilizumab in patients with refractory Takayasu arteritis: results from a randomised, double-blind, placebo-controlled, phase 3 trial in Japan (the TAKT study). *Ann Rheum Dis* 2018;77(3):348–54.
- [25] Sun Y, Wu B, Zhang W, Ma L, Kong X, Chen H, et al. Comparison of the efficacy and safety of leflunomide versus placebo combined with basic prednisone therapy in patients with active disease phase of Takayasu arteritis: study protocol for a randomized, double-blinded controlled trial (Takayasu arteritis clinical trial in China: TACTIC). *Ther Adv Chronic Dis* 2023;14:20406223231158567.



## Osteoarthritis

# Chondrocalcinosis and incident knee osteoarthritis: findings from 2 large prospective cohorts with 20 years of follow-up

Yahong Wu<sup>1,2</sup>, Jean W. Liew<sup>3</sup>, Justin D. Boer<sup>4</sup>, Maggie Westerland<sup>3</sup>, Michael LaValley<sup>5</sup>, Trudy Voortman<sup>1,6</sup>, Sita Bierma-Zeinstra<sup>7,8</sup>, Edwin H.G. Oei<sup>4</sup>, Joyce B.J. van Meurs<sup>2,7</sup>, Tuhina Neogi<sup>3</sup>, Cindy G. Boer<sup>2,\*</sup>

<sup>1</sup> Department of Epidemiology, Erasmus MC University Medical Center, Rotterdam, The Netherlands

<sup>2</sup> Department of Internal Medicine, Erasmus MC University Medical Center, Rotterdam, The Netherlands

<sup>3</sup> Section of Rheumatology, Boston University Chobanian & Avedisian School of Medicine, Boston, MA, USA

<sup>4</sup> Department of Radiology & Nuclear Medicine, Erasmus MC University Medical Center, Rotterdam, The Netherlands

<sup>5</sup> Department of Biostatistics, Boston University School of Public Health, Boston, MA, USA

<sup>6</sup> Meta-Research Innovation Center at Stanford, Stanford University, Stanford, CA, USA

<sup>7</sup> Department of General Practice, Erasmus MC University Medical Center, Rotterdam, The Netherlands

<sup>8</sup> Department of Orthopedics & Sports Medicine, Erasmus MC University Medical Center, Rotterdam, The Netherlands

## ARTICLE INFO

## Article history:

Received 14 April 2025

Received in revised form 9 July 2025

Accepted 9 July 2025

## ABSTRACT

**Objectives:** Chondrocalcinosis, a radiographic feature of calcium crystal deposition, is frequently observed alongside osteoarthritis. Although cross-sectional studies suggest an association, it remains unclear whether chondrocalcinosis is a consequence or a contributing factor in osteoarthritis development. This study investigates its role as a potential risk factor for incident knee osteoarthritis and knee pain in 2 large longitudinal cohorts: the Rotterdam Study (RS) and the Multicenter Osteoarthritis Study (MOST).

**Methods:** This prospective cohort study analysed 20-year follow-up data from 3737 participants in RS and 7-year follow-up data from 2750 in MOST. We examined the association of baseline knee chondrocalcinosis with (1) incident radiographic knee osteoarthritis and (2) incident knee pain in participants with Kellgren and Lawrence grade (KLG) 0 or 1, including a subgroup restricted to KLG = 0. Logistic regression models were adjusted for age, sex, and body mass index, with results pooled using meta-analysis.

**Results:** Chondrocalcinosis was present in 5% of osteoarthritis-free participants at baseline. It was significantly associated with incident knee osteoarthritis in both cohorts (pooled odds ratio [OR]: 1.75, 95% CI: 1.35–2.27,  $P < .001$ ), with significance maintained in KLG = 0 participants (pooled OR: 1.77, 95% CI: 1.04–3.01,  $P = .035$ ). No consistent association with incident knee pain was observed.

**Conclusions:** Chondrocalcinosis was associated with an increased risk of incident knee osteoarthritis in 2 large cohorts. These findings suggest that chondrocalcinosis may contribute to osteoarthritis incidence and represent a distinct disease subgroup. Future research is needed to explore potential targeted prevention and treatment strategies.

\*Correspondence to Dr Cindy G. Boer, Department of Internal Medicine, Erasmus MC University Medical Center, Rotterdam, The Netherlands. E-mail address: (C.G. Boer).

E-mail address: [c.boer@erasmusmc.nl](mailto:c.boer@erasmusmc.nl) (C.G. Boer).

Yahong Wu, Jean W. Liew, and Justin D. Boer contributed equally.

Handling editor Josef S. Smolen.

<https://doi.org/10.1016/j.ard.2025.07.009>

### WHAT IS ALREADY KNOWN ON THIS TOPIC

- Knee chondrocalcinosis represents abnormal calcification deposition which can be detected on radiographs. The co-occurrence of chondrocalcinosis with late-stage osteoarthritis has been observed. However, it is unclear whether chondrocalcinosis is a consequence of osteoarthritis or if it could also initiate joint damage from calcium deposition, contributing to osteoarthritis pathology.

### WHAT THIS STUDY ADDS

- Using longitudinal data of 2 large independent cohorts, the Rotterdam Study (n = 3737) and Multicenter Osteoarthritis Study (n = 2750), we found that chondrocalcinosis is a risk factor for incident radiographic knee osteoarthritis, after consideration of important confounders.

### HOW THIS STUDY MIGHT AFFECT RESEARCH, PRACTICE OR POLICY

- Our results suggest that chondrocalcinosis is a risk factor for osteoarthritis and may highlight a possible specific subtype of osteoarthritis.

## INTRODUCTION

As the highest contributor to global disability, knee osteoarthritis is the most frequent joint disease in the elderly worldwide, affecting 15% of individuals aged 30 years and older [1]. It is a chronic degenerative disease of the whole joint, affecting multiple tissues within the joint, most notably the bone and cartilage [1]. The definitive clinical diagnosis of osteoarthritis is made by the combination of the presence of clinical symptoms, such as stiffness, pain, and swelling, alongside radiological findings, which primarily include joint space narrowing and osteophytosis [1]. However, another radiological feature has been reported to be correlated with osteoarthritis: chondrocalcinosis [2].

Chondrocalcinosis is defined as a cloudlike radiopacity in the knee's articular cartilage and meniscus on radiographs, reflecting abnormal calcium-based crystal deposition [3]. These depositions primarily consist of basic calcium phosphate (BCP) and calcium pyrophosphate (CPP) crystals [4]. Both BCP and CPP crystals are common in end-stage knee osteoarthritis [5–8] and have been associated with disease severity [8,9]. Due to this well-observed coexistence of chondrocalcinosis and knee osteoarthritis, chondrocalcinosis is commonly considered a manifestation of osteoarthritis pathology [8,10]. However, this perspective fails to explain instances where chondrocalcinosis appears before other radiographic signs of osteoarthritis development [11]. This raises questions of whether chondrocalcinosis is a cause or merely a consequence of end-stage osteoarthritis [8,10].

Population studies have identified that 6.3% of individuals have chondrocalcinosis in joints unaffected by osteoarthritis [11]. These findings prompt the consideration of whether chondrocalcinosis may contribute to joint damage, rather than merely coexisting with osteoarthritis. Mechanistically, chondrocalcinosis is associated with the deposition of calcium-containing crystals, which have been shown to induce inflammation [12], stimulate matrix-degrading enzymes [12–14], and promote chondrocyte hypertrophy [8,15] and apoptosis [16]. These effects suggest a potential causal role for chondrocalcinosis in the joint degeneration and pain symptoms seen in osteoarthritis.

However, although previous studies have attempted to explore the link between chondrocalcinosis and osteoarthritis, most were limited by small sample sizes and short follow-up time, and the findings remain inconclusive [17–19].

Given these limitations, we conducted a large-scale longitudinal study to determine whether chondrocalcinosis contributes to the development of osteoarthritis and knee pain. We analysed 20 years of follow-up data from 3737 participants in the Rotterdam Study (RS), a community-based prospective cohort in the Netherlands, and 7 years of follow-up data from 2750 participants in the Multicenter Osteoarthritis Study (MOST), a prospective cohort in the United States consisting of individuals at high risk for osteoarthritis.

## METHODS

### Study design and population

This longitudinal study used data from both the RS and the MOST, as illustrated in Figure 1. Detailed information about the RS has been reported previously [20]. Briefly, between 1990 and 1993, 7983 individuals aged 55 years and older who resided in the Ommoord district of Rotterdam, the Netherlands, for at least 1 year were included in the original RS cohort (RS-I). RS is a community-based cohort that includes participants regardless of osteoarthritis status. Participants underwent a home interview and visits to the research center for examinations. Those participants have been re-examined every 4 to 5 years since. The present analysis includes data from the baseline (RS-I-1), third (RS-I-3), fourth (RS-I-4), and fifth (RS-I-5) visits. The RS has been approved by the Medical Ethics Committee of Erasmus MC (registration number MEC 02.1015) and by the Dutch Ministry of Health, Welfare, and Sport (Population Screening Act WBO, license number 1071272-159521-27 PG).

MOST is a National Institutes of Health-funded, longitudinal study of community-dwelling adults. The original cohort consisted of adults aged 50 to 79 years who either had pre-existing knee osteoarthritis or were at high risk due to overweight status, knee symptoms, or a history of knee injury or surgery, as determined during a baseline telephone screening [21]. Participants were recruited from Birmingham, Alabama, and Iowa City, Iowa, USA. The study was approved by the institutional review boards at the University of Iowa, the University of Alabama at Birmingham, the University of California at San Francisco, and Boston University Medical Center. For this study, we included

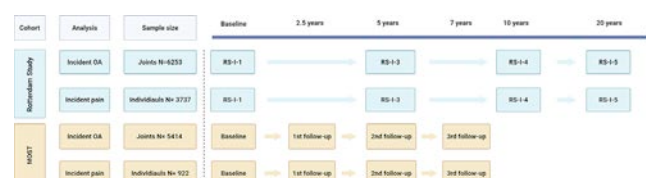


**Figure 1.** The design of the Rotterdam Study and the Multicenter Osteoarthritis Study. Overview of the Rotterdam Study (RS) and the Multicenter Osteoarthritis Study (MOST) data used for this study. For RS, RS-I-1 refers to the baseline measurement. RS-I-3, RS-I-4, and RS-I-5 refer to re-examinations of RS. In RS, a total of 6253 knees from 3301 participants were included for incident knee osteoarthritis analysis, and 3737 participants were included for incident knee pain analysis. For MOST, first, second, and third follow-ups represent the re-examinations at 30, 60, and 84 months after baseline measurement. In MOST, a total of 5414 knees from 2750 participants were included for incident knee osteoarthritis, and 922 participants were included for incident knee pain analysis. OA, osteoarthritis; RS-I, RS cohort.

participants’ baseline, 30-month, 5-year, and 7-year study visits with available radiographic and pain data.

*Patient and public involvement*

Patients and/or the public were not involved in the design, conduct, reporting, or dissemination plans of this research.

*Knee chondrocalcinosis*

In RS, the presence and severity of knee chondrocalcinosis were measured using the same knee radiographs as noted in previous studies [22], obtained in a weight-bearing anteroposterior position for both knee joints. The knee was extended with the patella in a central position. Radiographs were obtained at 70 kV with a focus of 1.8 m to a film distance of 120 cm on Fuji high-resolution G 35 × 43 cm film. Chondrocalcinosis was assessed in 2 ways: (1) its presence and (2) its severity. To quantify the severity of knee chondrocalcinosis, we developed a chondrocalcinosis severity score for radiograph assessment. For details about this severity score, see [Supplementary Text](#) and [Supplementary Figure](#). Briefly, this chondrocalcinosis severity score assessed the following 4 joint compartments: right medial femorotibial compartment, right lateral femorotibial compartment, left medial femorotibial compartment, and left femorotibial compartment. For each location, the radiographs were graded by a radiologist-in-training (JDB) based on the area of the joint space affected by chondrocalcinosis: grade 0, no chondrocalcinosis; grade 1, ≤20% chondrocalcinosis in the compartment space; grade 2, 20%–50% chondrocalcinosis in the compartment space; and grade 3, chondrocalcinosis >50% of the compartment space affected. By adding the score of compartments together, each knee had a sum score ranging from 0 to 6 (for knee-level analysis), and each participant had a sum score ranging from 0 to 12 (for individual-level analysis). The presence of chondrocalcinosis in a knee or an individual was defined if the sum score was ≥1. After developing the severity score, we assessed its reliability through intra- and inter-reader agreement and its validity by examining the known cross-sectional associations between knee chondrocalcinosis, age, and osteoarthritis. Further details are provided in [Supplementary Text](#).

In MOST, chondrocalcinosis was assessed from knee radiographs using weight-bearing, semi-flexed posteroanterior and lateral views obtained at baseline, following the MOST radiography protocol [23]. Chondrocalcinosis was scored as present or absent in the knee based on the presence of chondrocalcinosis in either view and categorised as present in the posteroanterior view’s medial or lateral tibiofemoral compartment.

Intraobserver reliability among 3 readers for radiographic chondrocalcinosis (2 rheumatologists and one radiologist with extensive experience) was good with a kappa of 0.79 to 0.91. Readers scored femorotibial compartments from the same individuals in a single session, with knowledge of the chronological order of their baseline and follow-up images. The chondrocalcinosis severity score was not measured in MOST.

*Incident radiographic knee osteoarthritis*

In both cohorts, knee osteoarthritis was determined previously based on the Kellgren and Lawrence grade (KLG) of the same radiographs used for the chondrocalcinosis scoring, evaluating the tibiofemoral compartment only [20,21,24]. Radiographic osteoarthritis was defined as KLG ≥ 2 or having a knee replacement at follow-up measurement(s) [24]. The inclusion criteria for the incident radiographic osteoarthritis analysis were having at least 2 measurements of knee osteoarthritis with no radiographic knee osteoarthritis at the first measurement. Incident radiographic knee osteoarthritis was defined as 1 knee having KLG < 2 at the first measurement and KLG ≥ 2 or a knee replacement at follow-up in that same knee. In the RS, incidence was assessed from baseline across 3 follow-up visits, with a mean follow-up duration of 10.4 years (range 2.5–19.9 years). In MOST, incidence was determined from baseline over a 7-year follow-up period ([Fig 1](#), [Table 1](#)).

*Incident knee pain*

In RS, knee pain data were collected using questionnaire-based home interviews. Participants were considered to report knee pain if they provided positive answers to the question, “Have you experienced pain in knee joints in the past month?” This question was not asked separately for the left and right knee. In MOST, the presence of knee pain was defined as a response of yes to the question, “During the past 30 days, have you had pain, aching, or stiffness in your knee on most days?” that was assessed during each in-person study visit. Participants with at least 2 measurements of knee pain and who did not report knee pain at their baseline visit were included in this analysis. The incidence of knee pain was assessed across 3 follow-up visits over 17.5 years in the RS and 3 follow-up visits over 7 years in the MOST cohort ([Fig 1](#), [Table 1](#)).

*Statistical analysis*

*Assessment of chondrocalcinosis progression in the RS*

To examine the progression of knee chondrocalcinosis, we analysed RS participants with at least 2 chondrocalcinosis

**Table 1**  
Baseline characteristics of the study population for the incident knee osteoarthritis analysis

General characteristics	Rotterdam Study			Multicenter Osteoarthritis Study		
	Total study population	Without knee CC	With knee CC	Total study population	Without knee CC	With knee CC
N	3301	3159 (95.7%)	142 (4.3%)	2750	2613 (95.0%)	137 (5.0%)
Age (SD)	65.43 (6.48)	65.25 (6.38)	69.37 (7.32)	62.4 (8.03)	62.1 (7.98)	67.6 (7.27)
Females, n (%)	1819 (55.1%)	1732 (54.8%)	87 (61.3%)	1645 (59.8%)	1570 (60.1%)	75 (54.7%)
BMI (SD)	26.12 (3.44)	26.10 (3.44)	26.57 (3.39)	30.6 (5.86)	30.7 (5.89)	29.3 (4.94)
Baseline KLG = 0, n (%)	2511 (76.1%)	2418 (76.5%)	93(65.5%)	1883 (68.5%)	1806 (69.1%)	74 (54.0%)
Outcomes						
Incident knee OA, n (%)	879 (26.6%)	817 (25.9%)	62 (43.7%)	1520 (55.3%)	1425 (54.5%)	95 (69.3%)
Follow-up time (SD)	10.44 (3.70)	10.49 (3.72)	9.48 (3.32)	7	7	7

BMI, body mass index; CC, chondrocalcinosis; KLG, Kellgren–Lawrence Grade; OA, osteoarthritis.  
Variables are expressed in mean and SD unless otherwise indicated. Age and follow-up time were expressed in years, and BMI was expressed in kg/m<sup>2</sup>.



severity assessments, including baseline (RS-I-1) and at least one follow-up visit (RS-I-3 or RS-I-4). Progression was determined by an increase in the chondrocalcinosis severity score (0–12), where 0 is no chondrocalcinosis,  $\geq 1$  is the presence of chondrocalcinosis, and 12 is severe chondrocalcinosis in both knees. Progression was defined as an increase (of 1 or more) in the chondrocalcinosis score compared to previous assessments, whereas regression was defined as a decrease of 1 or more in this score. Stability indicated no change in the score over time.

To explore the temporal relationship between chondrocalcinosis and osteoarthritis, we identified knees with available radiographic assessments for both conditions at 2 or more time-points across RS-I-1, RS-I-3, and RS-I-4. We classified knees that exhibited chondrocalcinosis in the absence of osteoarthritis (or vice versa) at the same visit and followed this over time to assess whether the other condition developed at subsequent visits.

### Longitudinal analysis of baseline chondrocalcinosis and incident knee osteoarthritis and pain

We examined the association between radiographic chondrocalcinosis and incident knee osteoarthritis in both cohorts using logistic regression, adjusting for age, sex, and body mass index (BMI). In the RS, the covariates age (years) and sex (male/female) were obtained through in-home and telephone interviews [20]. Height (cm) and weight (kg) were measured at the research center, and BMI ( $\text{kg}/\text{m}^2$ ) was calculated from these data. In MOST, age (years), sex (male/female), and BMI ( $\text{kg}/\text{m}^2$ ) were obtained from the baseline in-person study visits. The analysis was conducted at the knee level, and generalised estimating equations (GEEs) were used to account for the inclusion of 2 knees from the same individuals. For RS, we further examined the relationship between the severity of radiographic chondrocalcinosis measured by the chondrocalcinosis severity score and the outcome of incident knee osteoarthritis.

The association between the presence of radiographic chondrocalcinosis and incident knee pain was examined at the individual level using multivariable logistic regression in both RS and MOST. Model 1 was adjusted for age, sex, and BMI; Model 2 was additionally adjusted for baseline knee osteoarthritis status (yes/no). To address fluctuations in knee pain over time, we used a GEE model to account for repeated measures of pain and 2 knees within an individual. All knee pain measurements resulting from each available follow-up were included in the GEE model (Fig 1). For RS, we further examined the relationship between the severity of radiographic chondrocalcinosis measured by the sum of chondrocalcinosis severity scores and the outcome of incident knee pain.

Two predefined sensitivity analyses were performed to test the robustness of the results. First, we repeated both incident knee osteoarthritis and incident knee pain analyses restricted to knees with KLG = 0 at baseline to provide a more homogenous study population, as knees with KLG = 1 may represent early stages of development for knee osteoarthritis. Second, to address varying follow-up times, we conducted an interval-censored survival analysis using proportional hazards models by the ‘icenReg’ package in R [25], accounting for the duration of time between chondrocalcinosis and incident osteoarthritis. Bootstrapping was used to account for the clustering data structure of knees from the same individuals, as suggested and implemented by the ‘icenReg’ package [25].

For analyses available in both cohorts, we performed a meta-analysis using the inverse variance weighting method with a random-effects model using summary statistics from cohort-specific analysis results. This included incident knee osteoarthritis

and incident knee pain, each analysed in (1) the entire study population (KLG 0 or 1) and (2) a subset restricted to KLG = 0 only. Heterogeneity was assessed using Cochran’s Q test. All statistical analyses were performed using R version 4.4.0 [26]. Statistical significance was defined as  $P < .05$ .

## RESULTS

### Chondrocalcinosis was present in osteoarthritis-free individuals

To examine the longitudinal relationship between chondrocalcinosis and osteoarthritis, we analysed individuals without knee osteoarthritis at baseline from the RS ( $n = 3301$ ) and the MOST Study ( $n = 2750$ ; Table 1). The general characteristics are presented in Table 1. Knee chondrocalcinosis was seen in 4.3% to 5.0% (RS  $n = 145$ , MOST  $n = 137$ ) of osteoarthritis-free individuals ( $\text{KLG} \leq 1$ ) in both cohorts. This prevalence rate is slightly lower compared to prior reports, which found knee chondrocalcinosis in 5% to 15% of the general population [2,11,27]. In the RS, the mean chondrocalcinosis severity score was 3.1 (range 1–6) among knees with chondrocalcinosis. Within this osteoarthritis-free study population, 76.1% of RS ( $n = 2511$ ) and 68.5% of MOST ( $n = 1883$ ) participants did not have any signs of radiographic osteoarthritis at baseline ( $\text{KLG} = 0$ ).

### No regression of chondrocalcinosis over the years

In RS, knee chondrocalcinosis was assessed longitudinally at multiple time points, allowing us an opportunity to see its progression pattern (Fig 2). In every subsequent measured follow-up, we saw an increasing prevalence of chondrocalcinosis from baseline 5.0% (RS-1-1) to 9.1% (RS-1-3) and 11.3% (RS-I-4). Chondrocalcinosis is known to be more prevalent with increasing age, explaining the increased prevalence over time [2,27–30]. After a mean follow-up time of 7.8 years, nearly half of those knee compartments (197 out of 431) with chondrocalcinosis at baseline showed progression (higher chondrocalcinosis severity score), whereas the other half remained unchanged (234 out of 431). No cases of regression (ie, follow-up chondrocalcinosis severity score smaller than the previous visit) were identified. This longitudinal observation suggests that calcium deposition in the knee cartilage and meniscus does not diminish over time but can increase in severity.

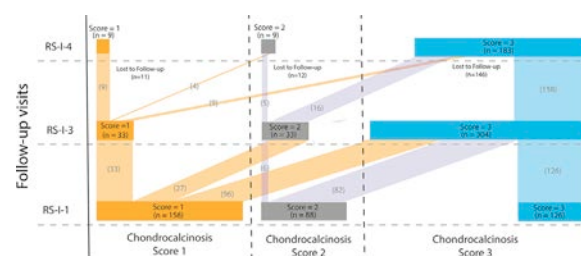


**Figure 2.** Sankey plot of chondrocalcinosis progression patterns. This Sankey plot illustrates how the severity of chondrocalcinosis in femorotibial compartments changed over a 10-year follow-up period in the Rotterdam Study. The score represents the chondrocalcinosis severity score, indicating the proportion of the femorotibial compartment area affected: 0 = no chondrocalcinosis, 1 =  $\leq 20\%$  of the compartment affected, 2 = 20%–50%, and 3 =  $> 50\%$ . RS-I-1 refers to the baseline visit; RS-I-3 and RS-I-4 represent subsequent re-examinations. As shown in the plot, chondrocalcinosis either worsened (an increase in severity score compared to the previous visit) or remained stable (no change in score). No regression (a decrease in severity score) was observed. RS-I, RS cohort.

Among 327 knees that showed chondrocalcinosis without coexisting osteoarthritis at the same visit and had available follow-up data, 18.7% (n = 61) subsequently developed osteoarthritis. Conversely, among 912 knees that presented with osteoarthritis in the absence of chondrocalcinosis at the same visit and had available follow-up data, 19.4% (n = 177) later developed chondrocalcinosis.

Chondrocalcinosis is associated with incident knee osteoarthritis

To determine if chondrocalcinosis is a risk factor for incident osteoarthritis, we conducted longitudinal analyses in individuals without baseline radiographic knee osteoarthritis (KLG ≤ 1). We observed that the presence of chondrocalcinosis at baseline was significantly associated with increased odds of incident radiographic knee osteoarthritis after adjusting for age, sex, and BMI, in both cohorts (RS: n = 6235 knees, incident osteoarthritis knees = 819 (13.1%), odds ratio [OR]: 1.63, 95% CI: 1.10-2.42, P = .01; MOST n = 5414 knees, incident osteoarthritis knees = 3069 (56.7%), OR: 1.85, 95% CI: 1.30-2.62, P < .001; Table 2). The meta-analysis of these results yielded a significant pooled OR of 1.75 (95% CI: 1.35-2.27; P < .001), with no evidence of heterogeneity (P = .22). It may be possible that our association between chondrocalcinosis and incident osteoarthritis was driven by knees with KLG = 1, as these may represent the early stages of osteoarthritis. Therefore, we ran a subgroup analysis to include only individuals at baseline without any radiographic signs of osteoarthritis (KLG = 0, n = 4428 knees for RS and 3102 knees for MOST, baseline characteristics in Supplementary Table S1). Here, we saw that the association between knee chondrocalcinosis presence and incident radiographic osteoarthritis was more prominent in RS (n = 4428 knees, incident osteoarthritis knees = 279 (6.3%), OR: 2.42, 95% CI: 1.29-4.55, P = .006, Table 2). In MOST, the OR was still positive but of a smaller magnitude, and the P value was not statistically significant (n = 3102 knees, incident osteoarthritis knees = 757 (24.4%), OR: 1.40, 95% CI: 0.87-2.26, P = .2, Table 2).

After meta-analysis, the pooled result was significant (pooled OR: 1.77; 95% CI: 1.04-3.01; P = .035; heterogeneity test P = .175). We also performed an interval-censored survival analysis to account for the varying follow-up times. Again, the association between knee chondrocalcinosis presence and incident radiographic osteoarthritis remained statistically significant (meta-analysis, hazard ratio: 1.26 (95% CI: 1.01-1.56, P = .039), Supplementary Table S2). These results suggest that chondrocalcinosis is not only a consequence of osteoarthritis pathology, but it could also be a causal factor in osteoarthritis pathology.

More severe chondrocalcinosis is associated with increased osteoarthritis incidence

In RS, the OR for chondrocalcinosis severity score and incident osteoarthritis is positive but is not statistically significant (RS: n = 6235 knees, incident osteoarthritis knee = 819 (13.1%), OR: 1.08, 95% CI: 0.97-1.21, P = .15, Table 2). When we restricted to include only individuals without any radiographic signs of posterior osteoarthritis at baseline (RS: KLG = 0, n = 4428 knees), we found that a higher chondrocalcinosis severity score was associated with increased odds of knee osteoarthritis in this subgroup (n = 4428 knees, incident osteoarthritis knees = 279 (6.3%), OR: 1.19, 95% CI: 1.01-1.40, P = .04, Table 2).

Table 2 Association between chondrocalcinosis and incident radiographic knee osteoarthritis

Study population	Chondrocalcinosis	Rotterdam Study				Multicenter Osteoarthritis Study				Meta-analysis <sup>a</sup>		
		Joins N	Incidence N (%)	OR (95% CI)	P value	Joins N	Incidence N (%)	OR (95% CI)	P value	OR (95% CI)	P value	Heterogeneity test P value
Baseline KLG = 0 or 1	Presence (0/1) <sup>b</sup>	6046	782 (12.9%)	Reference	-	5148	2880 (55.9%)	Reference	-	Reference	-	-
	Without CC	189	37 (23.1%)	1.63 (1.1-2.42)	.014	266	189 (71.1%)	1.85 (1.30-2.62)	<.001	1.75 (1.35-2.27)	<.001	.638
Baseline KLG = 0	With CC	6235	819 (13.1%)	1.08 (0.97-1.21)	.149	-	-	-	-	-	-	-
	Severity (0-6) <sup>c</sup>	4322	265 (6.1%)	Reference	-	2994	726 (24.2%)	Reference	-	Reference	-	-
	Presence (0/1) <sup>b</sup>	106	14 (13.2%)	2.42 (1.29-4.55)	.006	108	31 (28.7%)	1.40 (0.87-2.26)	.200	1.77 (1.04-3.01)	.035	.175
	Without CC	4428	279 (6.3%)	1.19 (1.01-1.40)	.042	-	-	-	-	-	-	-
	With CC	-	-	-	-	-	-	-	-	-	-	-
	Severity (0-6) <sup>c</sup>	-	-	-	-	-	-	-	-	-	-	-

KLG, Kellgren-Lawrence Grade; OR, odds ratio.

<sup>a</sup> The meta-analysis was conducted using the inverse variance method. Heterogeneity was assessed using Cochran's Q test and  $\tau^2$  (Tau-squared).

<sup>b</sup> The analysis was conducted at the knee level using a generalised estimating equation (GEE), adjusting for baseline age, body mass index, and sex. The results should be interpreted as the odds ratio for developing incident knee osteoarthritis when having chondrocalcinosis (yes vs no) at baseline.

<sup>c</sup> The sum of chondrocalcinosis severity score ranges from 0 to 6, with 0 representing no chondrocalcinosis and 6 representing severe chondrocalcinosis in the knee. The analysis is conducted at the knee level using a GEE, adjusting for baseline age, body mass index, and sex. The results should be interpreted as the odds ratio for developing incident knee osteoarthritis with a one-unit higher chondrocalcinosis severity score at baseline.

Chondrocalcinosis is associated with incident pain

The baseline characteristics of the study population for the incidence of knee pain were summarised in [Supplementary Table S3](#). Over the follow-up visits, the incidence rate of knee pain ranged from 24.7% to 34.0% in the RS and from 28.0% to 33.8% in MOST.

In RS, we observed that the baseline presence of chondrocalcinosis was associated with higher odds of incident knee pain (model 1,  $n = 3577$  individuals, incidence ranges from 24.7% to 30.3%, OR: 1.47, 95% CI: 1.12–1.93,  $P = .006$ ; [Table 3](#)). However, when adjusting for the presence of osteoarthritis at baseline, this association in RS loses significance (model 2, OR: 1.28, 95% CI: 0.97–1.69,  $P = .08$ ; [Table 3](#)). In contrast, greater severity of chondrocalcinosis was also found to be associated with higher odds of incident knee pain (model 1, OR: 1.08, 95% CI: 1.03–1.13,  $P = .003$ ; [Table 3](#)), even after adjusting for baseline osteoarthritis status (model 2, OR: 1.06, 95% CI: 1.01–1.12,  $P = .018$ ; [Table 3](#)). In the MOST cohort, we did not observe a statistically significant association between the presence of chondrocalcinosis and incident knee pain ( $n = 922$  individuals, incidence ranges from 28.0% to 33.8%, model 1: OR: 1.10, 95% CI: 0.76–1.58,  $P = .60$ , model 2: OR: 0.90, 95% CI: 0.64–1.27,  $P = .33$ ; [Table 3](#)). The pooled result from the meta-analysis also suggested that the presence of chondrocalcinosis was not significantly associated with incident knee pain (model 1: pooled OR: 1.31; 95% CI: 0.99–1.73;  $P = .06$ ; heterogeneity test  $P = .21$ ; model 2: pooled OR: 1.09, 95% CI: 0.77–1.54;  $P = .63$ ; heterogeneity test  $P = .12$ ). When we repeated these analyses in the subgroup with baseline KLG = 0 ( $n = 1943$  individuals for RS and 420 individuals for MOST, baseline characteristics in [Supplementary Table S4](#)), results from both cohort and meta-analysis were not significant ([Table 3](#)).

DISCUSSION

This study evaluated the relationship between chondrocalcinosis and the risk of developing knee osteoarthritis and knee pain using 2 large independent longitudinal cohorts. Our findings showed a strong association between the presence of chondrocalcinosis and an increased risk of incident knee osteoarthritis. We also observed that chondrocalcinosis severity tended to remain stable or worsen over time, further supporting its role in disease progression.

Our findings support the hypothesis that chondrocalcinosis contributes to osteoarthritis development rather than being merely a consequence of the disease. This hypothesis is strengthened by the observation that, when assessing the natural history of chondrocalcinosis in the RS, we observed that the chondrocalcinosis severity score of participants remained the same or increased compared to earlier visits. We did not observe decreasing amounts of chondrocalcinosis over time, indicating that crystal deposition in the cartilage or meniscus does not resolve itself. Moreover, a higher chondrocalcinosis severity score was associated with an increased incidence risk of knee osteoarthritis. Taken together, these findings suggest that crystal deposition may contribute to osteoarthritis progression [8,15,16], potentially leading to further crystal accumulation.

Our findings are consistent with a prior study in the Osteoarthritis Initiative (70 individuals with chondrocalcinosis, and 70 matched controls), which found chondrocalcinosis on baseline knee radiographs to be significantly associated with changes in MRI cartilage score [19]. Moreover, a prior study in MOST ( $n = 1673$ , 93 individuals with chondrocalcinosis), using

Table 3  
Association between chondrocalcinosis and incident knee pain

Study population	Chondrocalcinosis	Rotterdam Study			Multicenter Osteoarthritis Study			Meta-analysis <sup>a</sup>		
		Participants N	OR (95% CI)	P value	Participants N	OR (95% CI)	P value	OR (95% CI)	P value	Heterogeneity test P value
Baseline KLG = 0 or 1	Without CC	3556	Reference	-	876	Reference	-	Reference	-	-
	With CC	181	1.47 (1.12–1.93) <sup>c</sup>	.006	46	1.10 (0.76, 1.58)	.60	1.31 (0.99–1.73)	.061	.213
	Without CC	3737	1.28 (0.97, 1.69) <sup>d</sup>	.083	-	0.90 (0.64, 1.27)	.60	1.09 (0.77, 1.54)	.63	.117
	With CC	1884	1.08 (1.03–1.13) <sup>e</sup>	.003	-	-	-	-	-	-
Baseline KLG = 0	Without CC	1943	1.06 (1.01, 1.12)	.018	410	Reference	-	Reference	-	-
	With CC	59	1.22 (0.75–1.99) <sup>c</sup>	.420	10	0.74 (0.39, 1.43)	.40	1 (0.62–1.61)	.989	.228
	Without CC	1943	1.04 (0.96–1.13) <sup>d</sup>	.330	-	-	-	-	-	-

KLG, Kellgren-Lawrence Grade; OR, odds ratio.  
<sup>a</sup> The meta-analysis was conducted using the inverse variance method. Heterogeneity was assessed using Cochran's Q test and  $\tau^2$  (Tau-squared).  
<sup>b</sup> The analysis was conducted at the individual level using a generalised estimating equation (GEE). The results should be interpreted as the odds ratio for developing incident knee osteoarthritis when having chondrocalcinosis (yes vs no) at baseline.  
<sup>c</sup> Model 1 covariates: baseline age, body mass index, and sex.  
<sup>d</sup> Model 2 covariates: baseline age, body mass index, sex and baseline knee osteoarthritis status (yes/no).  
<sup>e</sup> The sum of chondrocalcinosis severity score ranges from 0 to 12, with 0 indicating no chondrocalcinosis in either knee, and 12 indicating severe chondrocalcinosis in both knees. The analysis is conducted in a logistic regression model with GEE. The results should be interpreted as the odds ratio for developing incident knee osteoarthritis with a one-unit higher chondrocalcinosis severity score at baseline.



computed tomography (CT)-detected intra-articular mineralisation as a measure of knee chondrocalcinosis [31], found the presence of intra-articular mineralisation increased the risk of cartilage damage on follow-up.

Our study did not find a significant association between the presence of chondrocalcinosis and incident knee pain in either the RS or MOST. In the RS, we did observe a significant association between presence of chondrocalcinosis and incident knee pain in model 1, but this association was no longer significant after adjusting for baseline knee osteoarthritis, suggesting that the observed effect may have been driven by pre-existing osteoarthritis rather than chondrocalcinosis itself. However, chondrocalcinosis severity in the RS remained significantly associated with incident knee pain even after adjustment of baseline knee osteoarthritis. Unfortunately, we could not replicate this finding in the MOST cohort due to the lack of chondrocalcinosis severity data. Nonetheless, a previous study in the MOST cohort using CT-detected chondrocalcinosis found that chondrocalcinosis was associated with a risk of having more frequent, persistent, and worsening knee pain over 2 years [32]. Further research is needed to better understand the relationship between chondrocalcinosis and knee pain.

Chondrocalcinosis may contribute to the risk of osteoarthritis through several possible mechanisms, one of which is inflammation. These deposited crystals could induce the production of inflammation markers (eg, IL-6 [12], PGE<sub>2</sub> [33,34]), matrix-degrading enzymes (eg, MMP13, MMP3 [12–14]), and induce chondrocyte hypertrophy [8,15] or chondrocyte death [16]. These effects not only damage the joint but also form a positive feedback loop to produce more calcium crystals [13]. Within our study population, only a small subset of knees with incident radiographic osteoarthritis had chondrocalcinosis at baseline (4.5% to 6.2%), indicating that chondrocalcinosis is not the only risk factor for osteoarthritis, which is in line with the heterogeneity of osteoarthritis pathology [35]. However, taking this study's results into account, it may also suggest that these individuals with chondrocalcinosis may represent a specific subgroup of patients, for which a treatment targeting chondrocalcinosis may present a viable strategy to prevent osteoarthritis.

The strengths of our study include using 2 independent cohorts with large sample sizes and prospectively collected data, where we replicate our findings in both cohorts. Further, we were also able to examine chondrocalcinosis severity using our semiquantitative score to assess the severity of radiographic chondrocalcinosis at the knee. Our findings align with 3 key principles from Bradford Hill's criteria for causality [36]: consistency, as the association between chondrocalcinosis and osteoarthritis was replicated in an independent cohort; temporality, as chondrocalcinosis preceded the onset of osteoarthritis; and biological gradient (dose–response relationship), as greater severity of chondrocalcinosis was associated with a higher risk of osteoarthritis. Together, these elements strengthen the argument that chondrocalcinosis may play a causal role in the development of osteoarthritis. However, there are still several limitations that should be acknowledged. First, our assessment of chondrocalcinosis severity relied on a semiquantitative scoring system, which may introduce some measurement errors compared to precise area-based quantification. Similarly, CT measures might also provide more accuracy in the presence of chondrocalcinosis over radiographs [37]. Second, we were not able to capture pain fluctuations that may occur between study visits, limiting our assessment of the second primary outcome of incident knee pain. Third, our study cohorts are subject to

survivor bias because we only have radiographs from participants who are healthy enough to come to the research centres during follow-up visits. Fourth, we were not able to determine whether chondrocalcinosis was due to BCP or CPP deposition based on radiographs [38]. We, therefore, cannot determine whether BCP and/or CPP crystals are a risk factor for osteoarthritis. Fifth, despite the large overall sample sizes in both cohorts, our results should still be read with caution because of the relatively small number of individuals with chondrocalcinosis who developed incident knee osteoarthritis or knee pain, which opens the possibility that some of the observed associations may be chance findings. Sixth, there are key differences in selection criteria between cohorts. Participants from MOST either had a high risk for (overweight, injury, or knee surgery history), or had pre-existing, knee radiographic osteoarthritis and complaints [21]. At the same time, the RS cohort consisted of general community residents older than 45 years without any other predefined selection criteria. Moreover, the presence of dominant risk factors for knee pain in MOST, such as obesity and prior knee injury, may have diminished the relative contribution of chondrocalcinosis, making its independent effect more challenging to identify. Lastly, like all observational studies, we cannot rule out any residual confounding.

In summary, our findings robustly demonstrate that radiographic knee chondrocalcinosis is associated with an increased risk of incident radiographic knee osteoarthritis. These results align with the known detrimental mechanisms through which calcium depositions contribute to osteoarthritis development. This suggests that chondrocalcinosis-related osteoarthritis may represent a distinct osteoarthritis subgroup. Future studies investigating the pathology of chondrocalcinosis could offer new insights into the prevention and treatment of osteoarthritis.

## Competing interests

CGGB reports financial support was provided by ReumaNederland. JBJvM reports financial support was provided by ReumaNederland. ML reports financial support was provided by National Institutes of Health. TV reports a relationship with Erasmus MC that includes: funding grants. TV reports a relationship with Erasmus University Rotterdam that includes: funding grants. TV reports a relationship with Delft University of Technology that includes: funding grants. Trudy Voortman reports a relationship with Dutch Heart Foundation that includes: funding grants. SB-Z reports a relationship with Erasmus MC that includes: employment and funding grants. ML reports a relationship with National Institutes of Health that includes: funding grants. SB-Z reports personal fees from Deputy Editor for Osteoarthritis Cartilage; consulting fees from Pfizer Infirst; healthcare grants or contracts: Independent Research Grants paid to the Institution from EU, Dutch Arthritis Association and ZonMw. The other authors declare they have no competing interests.

## Acknowledgements

The Rotterdam Study is funded by Erasmus Medical Center and Erasmus University, Rotterdam, Netherlands Organization for the Health Research and Development (ZonMw), the Research Institute for Diseases in the Elderly (RIDE), the Ministry of Education, Culture, and Science, the Ministry for Health, Welfare and Sports, the European Commission (DG XII) and the Municipality of Rotterdam. Joyce van Meurs and Cindy G. Boer are supported by ReumaNederland (Project number: LLP-34). Yahong Wu is supported by the China Scholarship Council



(CSC) Ph.D. fellowship for his Ph.D. study at Erasmus Medical Center, Rotterdam, the Netherlands. The authors are grateful to the study participants, the staff from the Rotterdam Study, and the participating general practitioners and pharmacists. The MOST Study was supported by NIA U01-AG-18820, U01-AG-18832, U01-AG-18947, U01-AG-19079, and NIAMS U19 AG076471. This work was supported by the NIAMS P30 AR072571. Dr. Neogi was supported by the NIAMS K24 AR070892. This work was presented orally in part at the Osteoarthritis Research Society International (OARSI) World Congress in April 2022 in Berlin, Germany and the OARSI World Congress in April 2024 in Vienna, Austria.

## Contributors

Yahong Wu: Conceptualization, Methodology, Investigation, Formal analysis, Writing - Original Draft, Writing - Review & Editing and Visualization. Jean W. Liew: Conceptualization, Methodology, and Writing - Review & Editing. Justin D. Boer: Investigation and Writing - Review & Editing. Maggie Westerland: Methodology, Formal Analysis and Writing - Review & Editing. Michael LaValley: Methodology and Writing - Review & Editing. Trudy Voortman: Writing - Review & Editing. Sita Bierma-Zeinstra: Writing - Review & Editing. Edwin H.G. Oei: Investigation and Writing - Review & Editing. Joyce B.J. van Meurs: Conceptualization, Methodology, Writing - Review & Editing, Supervision and Funding acquisition. Tuhina Neogi: Conceptualization, Methodology, Writing - Review & Editing and Funding acquisition. Cindy G. Boer: Conceptualization, Methodology, Writing - Review & Editing, Supervision and Funding acquisition.

## Funding

The Rotterdam Study is funded by Erasmus Medical Center and Erasmus University, Rotterdam, Netherlands Organization for the Health Research and Development (ZonMw), the Research Institute for Diseases in the Elderly (RIDE), the Ministry of Education, Culture, and Science, the Ministry for Health, Welfare and Sports, the European Commission (DG XII) and the Municipality of Rotterdam. Joyce van Meurs and Cindy G. Boer are supported by ReumaNederland (Project number: LLP-34). Yahong Wu is supported by the China Scholarship Council (CSC) Ph.D. fellowship for his Ph.D. study at Erasmus Medical Center, Rotterdam, the Netherlands. The MOST Study was supported by NIA U01-AG-18820, U01-AG-18832, U01-AG-18947, U01-AG-19079, and NIAMS U19 AG076471. This work was supported by the NIAMS P30 AR072571. Dr. Neogi was supported by the NIAMS K24 AR070892.

## Patient consent for publication

All participants in both the Rotterdam Study and the Multicenter Osteoarthritis Study (MOST) provided written informed consent.

## Ethics approval

The Rotterdam Study has been approved by the Medical Ethics Committee of Erasmus MC (registration number MEC 02.1015) and by the Dutch Ministry of Health, Welfare, and Sport (Population Screening Act WBO, license number 1071272-159521-27 PG). The Multicenter Osteoarthritis Study was approved by the institutional review boards at the

University of Iowa, the University of Alabama at Birmingham, the University of California, San Francisco, and Boston University Medical Center.

## Provenance and peer review

Not commissioned; externally peer reviewed.

## Data availability statement

The Rotterdam Study data are available upon reasonable request. All relevant data supporting the key findings of this study are available within the article and its supplementary data. Due to ethical and legal restrictions (GDPR), individual-level data from the Rotterdam Study cannot be made publicly available. Data are available upon request to the data manager of the Rotterdam Study, Frank van Rooij (f.vanrooij@erasmusmc.nl), and are subject to local rules and regulations. This includes submitting a proposal to the management team of RS, where upon approval, analysis needs to be done on a local server with protected access, complying with GDPR.

The Multicenter Osteoarthritis Study data are available in a public, open access repository. Data are available upon reasonable request.

## Declaration of generative AI and AI-assisted technologies in the writing process

During the preparation of this work, the authors used ChatGPT (OpenAI) and Grammarly to assist with grammar. After using these tools, the authors reviewed and edited the content as needed and took full responsibility for the content of the publication.

## Supplementary materials

Supplementary material associated with this article can be found in the online version at [doi:10.1016/j.ard.2025.07.009](https://doi.org/10.1016/j.ard.2025.07.009).

## Orcid

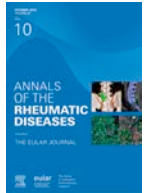
Yahong Wu: <http://orcid.org/0000-0001-5421-9022>

Cindy G. Boer: <http://orcid.org/0000-0003-4809-0044>

## REFERENCES

- [1] Kloppenburg M, Namane M, Osteoarthritis Cicuttini F. *Lancet* 2025;405 (10472):71–85.
- [2] Neame RL, Carr AJ, Muir K, Doherty M. UK community prevalence of knee chondrocalcinosis: evidence that correlation with osteoarthritis is through a shared association with osteophyte. *Ann Rheum Dis* 2003 Jun;62(6):513–8.
- [3] Rosenthal AK, Ryan LM. Calcium pyrophosphate deposition disease. *N Engl J Med* 2016 Jun 30;374(26):2575–84.
- [4] Halverson PB, McCarty DJ. Patterns of radiographic abnormalities associated with basic calcium phosphate and calcium pyrophosphate dihydrate crystal deposition in the knee. *Ann Rheum Dis* 1986 Jul;45(7):603–5.
- [5] Rosenthal AK. Crystals, inflammation, and osteoarthritis. *Curr Opin Rheumatol* 2011 Mar;23(2):170–3.
- [6] Viriyavejkul P, Wilairatana V, Tanavalee A, Jaovisidha K. Comparison of characteristics of patients with and without calcium pyrophosphate dihydrate crystal deposition disease who underwent total knee replacement surgery for osteoarthritis. *Osteoarthritis Cartilage* 2007 Feb;15(2):232–5.
- [7] Fuerst M, Niggemeyer O, Lammers L, Schäfer F, Lohmann C, Rütter W. Articular cartilage mineralization in osteoarthritis of the hip. *BMC Musculoskelet Disord* 2009;10:1–8.
- [8] Fuerst M, Bertrand J, Lammers L, Dreier R, Echtermeyer F, Nitschke Y, et al. Calcification of articular cartilage in human osteoarthritis. *Arthritis Rheum* 2009;10:166.

- [9] Mitsuyama H, Healey RM, Terkeltaub RA, Coutts RD, Amiel D. Calcification of human articular knee cartilage is primarily an effect of aging rather than osteoarthritis. *Osteoarthritis Cartilage* 2007;15(5):559–65.
- [10] Nguyen C, Bazin D, Daudon M, Chatron-Colliet A, Hannouche D, Bianchi A, et al. Revisiting spatial distribution and biochemical composition of calcium-containing crystals in human osteoarthritic articular cartilage. *Arthritis Res Ther* 2013;15:R103.
- [11] Han BK, Kim W, Niu J, Basnyat S, Barshay V, Gaughan JP, et al. Association of chondrocalcinosis in knee joints with pain and synovitis: data from the Osteoarthritis Initiative. *Arthritis Care Res (Hoboken)* 2017 Nov;69(11):1651–8.
- [12] Nasi S, So A, Combes C, Daudon M, Busso N. Interleukin-6 and chondrocyte mineralisation act in tandem to promote experimental osteoarthritis. *Ann Rheum Dis* 2016;75(7):1372–9.
- [13] McCarthy GM, Dunne A. Calcium crystal deposition diseases—beyond gout. *Nat Rev Rheumatol* 2018;14(10):592–602.
- [14] McCarthy GM, Westfall PR, Masuda I, Christopherson PA, Cheung HS, Mitchell PG. Basic calcium phosphate crystals activate human osteoarthritic synovial fibroblasts and induce matrix metalloproteinase-13 (collagenase-3) in adult porcine articular chondrocytes. *Ann Rheum Dis* 2001;60(4):399–406.
- [15] Rong J, Pool B, Zhu M, Munro J, Cornish J, McCarthy GM, et al. Basic calcium phosphate crystals induce osteoarthritis-associated changes in phenotype markers in primary human chondrocytes by a calcium/calmodulin kinase 2-dependent mechanism. *Calcif Tissue Int* 2019;104:331–43.
- [16] Stücker S, Bollmann M, Garbers C, Bertrand J. The role of calcium crystals and their effect on osteoarthritis pathogenesis. *Best Pract Res Clin Rheumatol* 2021;35(4):101722.
- [17] Neogi T, Nevitt M, Niu J, LaValley MP, Hunter DJ, Terkeltaub R, et al. Lack of association between chondrocalcinosis and increased risk of cartilage loss in knees with osteoarthritis: results of two prospective longitudinal magnetic resonance imaging studies. *Arthritis Rheum* 2006;54(6):1822–8.
- [18] Latourte A, Rat AC, Ngueyon Sime W, Ea HK, Bardin T, Mazières B, et al. Chondrocalcinosis of the knee and the risk of osteoarthritis progression: data from the Knee and Hip Osteoarthritis Long-term Assessment cohort. *Arthritis Rheumatol* 2020;72(5):726–32.
- [19] Foreman SC, Gersing AS, von Schacky CE, Joseph GB, Neumann J, Lane NE, et al. Chondrocalcinosis is associated with increased knee joint degeneration over 4 years: data from the Osteoarthritis Initiative. *Osteoarthritis Cartilage* 2020;28(2):201–7.
- [20] Ikram MA, Kieboom BCT, Brouwer WP, Brusselle G, Chaker L, Ghanbari M, et al. The Rotterdam Study. Design update and major findings between 2020 and 2024. *Eur J Epidemiol* 2024 Feb 7;39(2):183–206.
- [21] Segal NA, Nevitt MC, Gross KD, Hietpas J, Glass NA, Lewis CE, et al. The Multicenter Osteoarthritis Study: opportunities for rehabilitation research. *PM R* 2013 Aug;5(8):647–54.
- [22] Boer CG, Szilagyi I, Nguyen NL, Neogi T, Meulenbelt I, Ikram MA, et al. Vitamin K antagonist anticoagulant usage is associated with increased incidence and progression of osteoarthritis. *Ann Rheum Dis* 2021 May;80(5):598–604.
- [23] Sheehy L, Culham E, McLean L, Niu J, Lynch J, Segal NA, et al. Validity and sensitivity to change of three scales for the radiographic assessment of knee osteoarthritis using images from the Multicenter Osteoarthritis Study (MOST). *Osteoarthritis Cartilage* 2015 Sep;23(9):1491–8.
- [24] Kellgren JH, Lawrence JS. Radiological assessment of osteo-arthritis. *Ann Rheum Dis* 1957 Dec;16(4):494–502.
- [25] Anderson-Bergman C. icenReg: regression models for interval censored data in R. *J Stat Softw* 2017 Nov 13;81(12):1–23.
- [26] R Core Team. R: A Language and Environment for Statistical Computing. Vienna, Austria: R Foundation for Statistical Computing; 2025 <https://www.R-project.org/>.
- [27] Ramonda R, Musacchio E, Perissinotto E, Sartori L, Punzi L, Corti MC, et al. Prevalence of chondrocalcinosis in Italian subjects from northeastern Italy. The Pro.V.A. (PROgetto Veneto Anziani) study. *Clin Exp Rheumatol* 2009 Nov-Dec;27(6):981–4.
- [28] Ellman MH, Brown NL, Levin B. Prevalence of knee chondrocalcinosis in hospital and clinic patients aged 50 or older. *J Am Geriatr Soc* 1981 Apr;29(4):189–92.
- [29] Sanmartí R, Pañella D, Brancós MA, Canela J, Collado A, Brugués J. Prevalence of articular chondrocalcinosis in elderly subjects in a rural area of Catalonia. *Ann Rheum Dis* 1993 Jun;52(6):418–22.
- [30] Wilkins E, Dieppe P, Maddison P, Evison G. Osteoarthritis and articular chondrocalcinosis in the elderly. *Ann Rheum Dis* 1983 Jun;42(3):280–4.
- [31] Liew JW, Jarraya M, Guermazi A, Lynch J, Felson D, Nevitt M, et al. Intra-articular mineralization on computerized tomography of the knee and risk of cartilage damage: the Multicenter Osteoarthritis Study. *Arthritis Rheumatol* 2024;76(7):1054–61.
- [32] Liew JW, Jarraya M, Guermazi A, Lynch J, Wang N, Rabasa G, et al. Relation of intra-articular mineralization to knee pain in knee osteoarthritis: a longitudinal analysis in the MOST Study. *Arthritis Rheumatol* 2023;75(12):2161–8.
- [33] Kirsch T, Swoboda B, Nah HD. Activation of annexin II and V expression, terminal differentiation, mineralization and apoptosis in human osteoarthritic cartilage. *Osteoarthritis Cartilage* 2000;8(4):294–302.
- [34] Magne D, Bluteau G, Faucheu C, Palmer G, Vignes-Colombeix C, Pilet P, et al. Phosphate is a specific signal for ATDC5 chondrocyte maturation and apoptosis-associated mineralization: possible implication of apoptosis in the regulation of endochondral ossification. *J Bone Miner Res* 2003;18(8):1430–42.
- [35] Devez LA, Melo L, Yamato TP, Mills K, Ravi V, Hunter DJ. Knee osteoarthritis phenotypes and their relevance for outcomes: a systematic review. *Osteoarthritis Cartilage* 2017 Dec;25(12):1926–41.
- [36] Hill AB. The environment and disease: association or causation? *Proc R Soc Med* 1965 May;58(5):295–300.
- [37] Guermazi A, Jarraya M, Lynch JA, Felson DT, Clancy M, Nevitt M, et al. Reliability of a new scoring system for intraarticular mineralization of the knee: Boston University Calcium Knee Score (BUCKS). *Osteoarthritis Cartilage* 2020;28(6):802–10.
- [38] Stücker S, Kołowski F, Buchholz A, Lohmann CH, Bertrand J. High frequency of BCP, but less CPP crystal-mediated calcification in cartilage and synovial membrane of osteoarthritis patients. *Osteoarthritis Cartilage* 2024 May 11;32(12):1542–51.



## Letter

## In immune-mediated necrotising myopathy, anti-HMGCR antibodies inhibit HMGCR activity, leading to the sarcoplasmic accumulation of lipid droplets and myofibres necrosis

**Anti-3-hydroxy-3-methylglutaryl-coenzyme A reductase (HMGCR) antibodies are a biomarker of immune-mediated necrotising myopathy (IMNM), a subtype of inflammatory myopathies (IMs) characterised by weakness and myofibre necrosis whose mechanism is unknown [1]. It has recently been shown that anti-HMGCR antibodies are internalized into the myofibres of patients with IMNM [2]. Several observations indicate that this may result in disrupted HMGCR function and a subsequent myopathic effect: (i) anti-HMGCR antibodies target the HMGCR enzymatic active site [3]; (ii) both the statin inhibition of HMGCR [4] and mutations impairing its activity [4] lead to myofibre necrosis resembling IMNM [1]. However, no direct evidence of this hypothesis has been reported [2].**

In the present study, we investigated whether anti-HMGCR antibodies interfere with HMGCR activity and have a myopathic effect. Methods are presented in the Supplementary material.

To obtain polyclonal anti-HMGCR autoantibodies, the 6 peptides identified as the epitopes of anti-HMGCR antibodies [3] were synthesized and used to immunize a white New Zealand rabbit. Antibodies from a nonimmunized animal served as control. The serum was collected on day 56. Additionally, plasma samples from anti-HMGCR (n = 5) and anti-SRP (n = 2) patients with IMNM were obtained from plasmapheresis eluates performed for therapeutic purposes. Rabbit and human anti-HMGCR antibodies were purified by affinity chromatography. ELISA assays confirmed that purified anti-HMGCR antibodies and the related crude serum/plasma recognized the 6 epitopes (Supplementary Figure S1).

To test whether anti-HMGCR antibodies inhibit the function of their target, HMGCR enzymatic activity was assessed *in vitro* in the presence of anti-HMGCR, control antibodies and pravastatin. A dose-dependent inhibition of HMGCR activity was observed in the presence of anti-HMGCR (Fig 1A;

Supplementary Figure S2A). Rabbit anti-HMGCR 5 µg/mL and human anti-HMGCR 2 µg/mL had similar effects to that of pravastatin 0.5 µM (Fig 1A,B; Supplementary Figure S2A, B). IgG from the nonimmunized rabbit and plasma from anti-SRP patients did not affect HMGCR activity (Fig 1A,B; Supplementary Figure S2A, B).

The myopathic process underlying myofibre necrosis in anti-HMGCR IMNM is unknown. HMGCR knockout disrupts fatty acid beta-oxidation [5] that leads to muscle necrosis [5,6]. Lipid droplet accumulation, a marker of fatty acid beta-oxidation defect, and muscle necrosis have been observed in myofibres of statin myopathy patients [7]. Hence, to test whether anti-HMGCR internalization in myofibres [2] exerts a myopathic effect, human myotubes were electroporated with human-purified anti-HMGCR, control IgG or pravastatin. Antibody presence in the cytoplasm 4 days after electroporation was confirmed (Supplementary Figure S3). Human myotubes electroporated with purified anti-HMGCR and pravastatin, but not with control IgG, showed lipid droplet accumulation on Oil red-O staining and necrosis on haematoxylin and eosin as well as dystrophin stainings [8,9] (Fig 1C).

A recent study reported more frequent accumulation of lipid droplets in myofibres of anti-HMGCR patients compared with other IM subtypes [2]. However, information on patient selection, medications, co-morbidities, muscle biopsy site, assessment of lipid droplet accumulation and its extension were not reported. To test the validity of this pioneer finding, the internalization of anti-HMGCR antibodies into the myofibres of patients with IMNM was first confirmed (Supplementary Figure S4). Next, two blinded myopathologists scored (from 0 to 4) lipid droplet accumulation on oil red-O-stained cryosections of deltoid muscle prospectively sampled in 34 patients with IM (anti-HMGCR: n = 10; other IM n = 24) and 3 individuals with myalgia without neuromuscular disease (n = 3), whose characteristics are presented in Supplementary Table S1. None of the patients were taking immunomodulators or statins at the time of muscle biopsy. Lipid droplet accumulation score was ten-fold higher in anti-HMGCR patients with IMNM compared with patients with other IM and without neuromuscular disease ( $3.2 \pm 0.6$  vs  $0.3 \pm 0.5$ ; vs  $0.3 \pm 0.6$ , respectively;  $P = .0001$ ), and a score  $\geq 2$  was a hallmark of anti-HMGCR IMNM (Fig 1D,E). Additional studies will be required to determine HMGCR activity in the muscles of patients with anti-HMGCR IMNM.

Together, these data demonstrate that anti-HMGCR antibodies inhibit HMGCR activity, leading to the sarcoplasmic accumulation of lipid droplets and myofibre necrosis. These findings

MG and GQ equally contributed to the work.

Handling Editor: Josef Smolen.

<https://doi.org/10.1016/j.ard.2025.04.027>



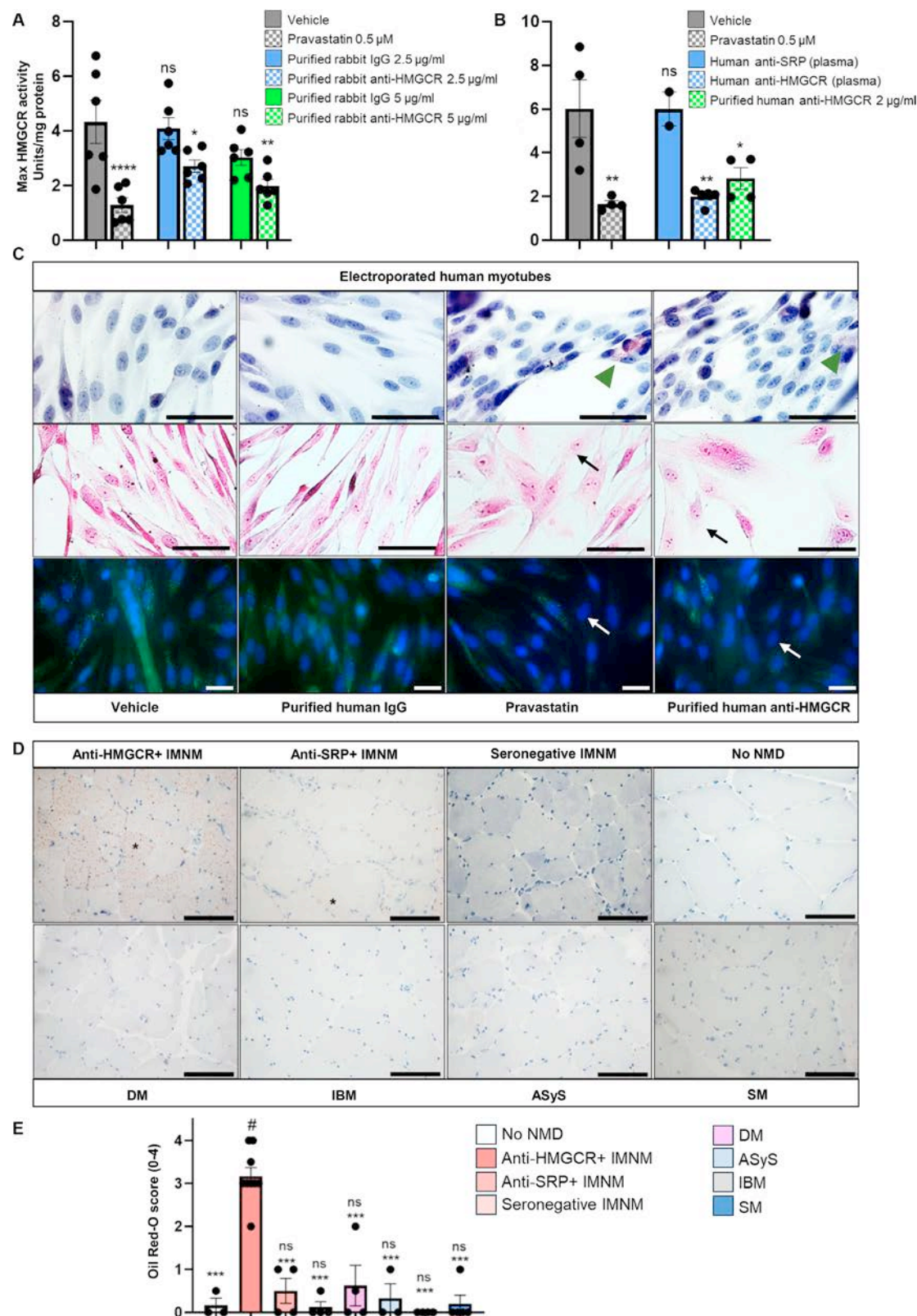


**Figure 1.** Anti-hydroxy-3-methylglutaryl CoA reductase (HMGCR) antibodies inhibit HMGCR activity leading to lipid droplet accumulation in myofibers. (A) Maximum (max) *in vitro* HMGCR activity in the presence of rabbit-purified polyclonal anti-HMGCR antibodies (5  $\mu$ g/mL and 2.5  $\mu$ g/mL), control antibodies (IgG, 5  $\mu$ g/mL and 2.5  $\mu$ g/mL) and pravastatin (0.5  $\mu$ M).  $n = 6$  for each condition; \* $P = .04$ , \*\* $P = .002$ , \*\*\*\* $P = .0001$ ; ns: not significant (vs vehicle). (B) Maximum *in vitro* HMGCR activity in the presence of plasma (1  $\mu$ L) and purified (2  $\mu$ g/mL) autoantibodies from patients with anti-HMGCR immune-mediated necrotizing myopathy (IMNM) ( $n = 5$ ), plasma (1  $\mu$ L) from patients with anti-signal recognition particle immune-mediated necrotizing myopathy (SRP IMNM) ( $n = 2$ ) and pravastatin (0.5  $\mu$ M,  $n = 4$ ). \* $P < .05$ , \*\* $P < .01$ , \*\*\* $P < .001$  (vs activity); # $P = .002$  (anti-HMGCR plasma vs anti-SRP plasma). (C) Representative images of human myotubes exposed for 4 days after electroporation to purified human anti-HMGCR antibodies (0.4 mg/mL) or human control antibodies (IgG, 1 mg/mL) or pravastatin (100  $\mu$ M): i) oil red-O staining: green arrowheads point to lipid droplets, scale bar: 50  $\mu$ m; ii) haematoxylin and eosin staining: black arrows point to necrotic myotubes characterized by a swollen and pale cytoplasm, loss of myonuclei staining, fusiform shape and sarcolemma. Scale bar: 50  $\mu$ m and iii) dystrophin staining (green fluorescence): white arrows point to necrotic myotubes characterized by a loss of dystrophin expression. Nuclei were counterstained with DAPI (blue



could have implications for both the diagnosis and treatment of IMNM.

## Competing interests

All authors declare they have no competing interests.

## CRedit authorship contribution statement

**Margherita Giannini:** Writing – review & editing, Writing – original draft, Visualization, Validation, Software, Resources, Project administration, Methodology, Investigation, Formal analysis, Data curation, Conceptualization. **Giulia Quiring:** Writing – review & editing, Writing – original draft, Visualization, Validation, Resources, Software, Methodology, Investigation, Formal analysis, Data curation. **Mustapha Oulad-Abdelghani:** Writing – review & editing, Methodology, Investigation, Formal analysis, Data curation. **Béatrice Lannes:** Writing – review & editing, Resources, Methodology, Investigation, Formal analysis, Data curation. **Yves Allenbach:** Writing – review & editing, Validation, Resources. **Olivier Benveniste:** Writing – review & editing, Validation, Resources, Conceptualization. **Olivier Boyer:** Writing – review & editing, Validation. **Aleksandra Nadaj Pakleza:** Writing – review & editing, Validation, Resources. **Bernard Geny:** Writing – review & editing, Supervision, Resources. **Alain Meyer:** Writing – review & editing, Writing – original draft, Visualization, Validation, Supervision, Resources, Project administration, Funding acquisition.

## Acknowledgements

We thank the CRBS imaging facility members (PIC-STRA, P. Kessler and I. Busnelli). We thank Mr Pierre Pothier for proof-reading.

## Funding

This research did not receive any specific grant from funding agencies in the public, commercial, or not-for-profit sectors.

## Ethics approval

This study was approved by the Committee for the Protection of Persons (Comité pour la Protection des Personnes) - Est (N°8181). Written informed consent was obtained from all participants.

## Data availability statement

Data will be shared upon request from any qualified investigator.

## Supplementary materials

Supplementary material associated with this article can be found in the online version at [doi:10.1016/j.ard.2025.04.027](https://doi.org/10.1016/j.ard.2025.04.027).

## REFERENCES

- [1] Allenbach Y, Mammen AL, Benveniste O, Stenzel W, Immune-Mediated Necrotizing Myopathies Working Group. 224th ENMC International Workshop:: Clinico-sero-pathological classification of immune-mediated necrotizing myopathies Zandvoort, The Netherlands, 14-16 October 2016. *Neuromuscul Disord* 2018;28(1):87–99.
- [2] Pinal-Fernandez I, Muñoz-Braceras S, Casal-Dominguez M, Pak K, Torres-Ruiz J, Musai J, et al. Pathological autoantibody internalisation in myositis. *Ann Rheum Dis* 2024;ard-2024-225773.
- [3] Musset L, Miyara M, Benveniste O, Charuel JL, Shikhman A, Boyer O, et al. Analysis of autoantibodies to 3-hydroxy-3-methylglutaryl-coenzyme A reductase using different technologies. *J Immunol Res* 2014;2014:405956.
- [4] Yoge Y, Shorer Z, Koifman A, Wormser O, Drabkin M, Halperin D, et al. Limb girdle muscular disease caused by *HMGCR* mutation and statin myopathy treatable with mevalonolactone. *Proc Natl Acad Sci* 2023;120(7):e2217831120.
- [5] Liepinsh E, Zvejniece L, Clemensson L, Ozola M, Vavers E, Cirule H, et al. Hydroxymethylglutaryl-CoA reductase activity is essential for mitochondrial  $\beta$ -oxidation of fatty acids to prevent lethal accumulation of long-chain acylcarnitines in the mouse liver. *Br J Pharmacol* 2024;181(16):2750–73.
- [6] Ribas GS, Vargas CR. Evidence that Oxidative Disbalance and Mitochondrial Dysfunction are Involved in the Pathophysiology of Fatty Acid Oxidation Disorders. *Cell Mol Neurobiol* 2022;42(3):521–32.
- [7] Phillips PS, Haas RH, Bannykh S, Hathaway S, Gray NL, Kimura BJ, et al. Statin-Associated Myopathy with Normal Creatine Kinase Levels. *Ann Intern Med* 2002;137(7):581.
- [8] Stenzel W, Preuße C, Allenbach Y, Pehl D, Junckerstorff R, Heppner FL, et al. Nuclear actin aggregation is a hallmark of anti-synthetase syndrome-induced dysimmune myopathy. *Neurology* 2015;84(13):1346–54.
- [9] Marmen MB, Orfi Z, Dort J, Proulx-Gauthier JP, Chrestian N, Dumont NA, et al. Decreased dystrophin expression and elevated dystrophin-targeting miRNAs in anti-HMGCR immune-mediated necrotizing myopathy. *Acta Neuropathol (Berl)* 2023;146(4):655–8.

Margherita Giannini\*

UR3072 Centre de Recherche en Biomédecine, Université de Strasbourg, Strasbourg, France  
Explorations fonctionnelles musculaires, Service de physiologie, Centre de référence des maladies autoimmunes rares, Hôpitaux Universitaires de Strasbourg, Strasbourg, France

Giulia Quiring

UR3072 Centre de Recherche en Biomédecine, Université de Strasbourg, Strasbourg, France

Mustapha Oulad-Abdelghani

Université de Strasbourg, CNRS, Inserm, IGBMC UMR 7104-UMR-S 1258, Illkirch, France

Béatrice Lannes

Département de Pathologie, Hôpitaux Universitaires de Strasbourg, Strasbourg, France

Yves Allenbach

Sorbonne Université, Assistance Publique Hôpitaux de Paris, National Reference Center for Inflammatory Myopathies, Pitié-Salpêtrière Hospital, Paris, France

Olivier Benveniste

Sorbonne Université, Assistance Publique Hôpitaux de Paris, National Reference Center for Inflammatory Myopathies, Pitié-Salpêtrière Hospital, Paris, France

fluorescence). Scale bar: 1 mm. N = 4 for each condition in each experiment. (D) Representative images of oil red-O-stained deltoid muscle cryosections of untreated patients with inflammatory myopathies (IM). Respective scores are anti-HMGCR IMNM: 4, anti-SRP IMNM: 1, seronegative IMNM: 0, dermatomyositis (DM): 0, inclusion body myositis (IBM): 0, antisynthetase syndrome (ASyS): 1, scleromyositis (SM): 0 and subjects with no neuromuscular disease (no NMD): 0. \* indicates fibres with lipid droplet accumulation (one example per image). Scale bar: 50  $\mu$ m. (E) Oil red-O staining score in deltoid muscle cryosections of patients with IM. Each dot represents a patient. Scores are expressed as mean  $\pm$  standard error of the mean. \*\*\* $P$  = .0001 compared with anti-HMGCR IMNM.  $P$  = .0001, ns: not significant compared with non-NMD patients.

Olivier Boyer

*University of Rouen Normandy, Inserm U1234, Department of Immunology and Biotherapies, Rouen University Hospital, Rouen, France*

Aleksandra Nadaj Pakleza

*Service de Neurologie, Centre de Référence des Maladies Neuromusculaires NEIdF, ERN EURO-NMD, Hôpitaux Universitaire de Strasbourg, Strasbourg, France*

Bernard Geny

*UR3072 Centre de Recherche en Biomédecine, Université de Strasbourg, Strasbourg, France*

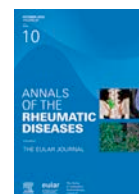
*Service de physiologie et Explorations fonctionnelles, Hôpitaux Universitaires de Strasbourg, Strasbourg, France*

Alain Meyer

*UR3072 Centre de Recherche en Biomédecine, Université de Strasbourg, Strasbourg, France*  
*Explorations fonctionnelles musculaires, Service de physiologie, Centre de référence des maladies autoimmunes rares, Hôpitaux Universitaires de Strasbourg, Strasbourg, France*

\*Correspondence to Dr Margherita Giannini.

E-mail address: [gianninim@unistra.fr](mailto:gianninim@unistra.fr) (M. Giannini).



## Correspondence

## Correspondence on 'Radiographic structural damage in axial spondyloarthritis: is there a preferred way to quantify progression over time? Comparison of blinded versus unblinded mSASSS scoring' by Protopopov et al.

Critics of the progress of medical science have argued that, over time, there exists an inverse relationship between the body of medical literature (sharply increasing) and the discovery of 'disruptive' novelties (sharply decreasing) [1]. It is another way of saying that the current literature is filled with duplication. This bold statement came to mind while reading the paper by Baraliakos et al [2], which compares blinded vs continuous scoring of progression on spinal radiographs in patients with axial spondyloarthritis (axSpA).

It is not that the article contains contentious or untrue material; rather, the opposite is true. However, there is at least 1 sentence in the paper that is demonstrably false, namely that this study is the first to compare spinal radiograph scoring in both a blinded and unblinded manner. Novelty is often the reason a publication is accepted in a high-impact journal, such as the Annals of the Rheumatic Diseases (ARD). The authors have amply cited our historic work in this field, for which we want to thank them graciously, but they have ignored our most important study, one that has also appeared in ARD [3]. Wanders et al [3] published their study with exactly the same study question already in 2004! Needless to say, they found the same as Baraliakos et al [2]. One may argue that this adds to the credibility of the communal results, but Baraliakos et al [2] seemed to be agnostic towards the work by Wanders et al [3] and missed the opportunity to learn from both studies in conjunction. Both studies differed slightly. While Baraliakos et al [2] used 5 readers, 2 of whom read with an 'open reading frame' (continuous) and 3 others scored blindly, Wanders et al [3] employed only 1 reader who applied both methods with some time in between. An expert in reading methodology would have advised that an appropriate study for methods comparison requires the same reader(s) scoring all radiographs in 2 tempi, once with blinded

and once with known time order, so that one could exclude reader-specific bias and attribute differences to reading order. One or multiple readers are irrelevant here and uninformative for this particular study question (even though the reader-specific error will be lower when the number of readers is higher).

The authors have cleverly waived responsibility for missing the paper by Wanders et al [3] by adding the words 'To our knowledge' (sic non). Should they want to use the argument of 'entire spectrum of axSpA' (Wanders et al [3] only included patients with radiographic axSpA (r-axSpA)) to claim novelty, we will cut the grass from under their feet by stipulating that 'entire spectrum of axSpA' is an irrelevant argument here. Comparing scoring methods for imaging is about applying ubiquitous measurement properties and goes beyond specific diseases. You may even apply these outside of rheumatology (eg, oncology trials), as has been done in the past. After 30 years of research into methods comparison, we appreciate how important the field has become in measuring progress in drug development and approval. We have also sadly learned that the topic is not tremendously popular among clinical and epidemiological scientists, and we have seen embarrassing examples of this in the rheumatological literature in the past. Field-specific researchers, field-specific reviewers, and journal editors apparently (and expectedly) can no longer oversee the entire realm of published evidence on a topic that requires specific methodological knowledge. This is disconcerting and is undoubtedly partly due to the surge in publications, as well as the 'publish or perish' mantra. On a more general note, scarce and valuable researcher time and funding could perhaps be better used to address really novel clinical and methodological research questions (after a thorough literature review). There are still many such questions left for further research. We acknowledge that 'novel' medical research may gain robustness by replication, especially when it comes to novel drugs, but when similar results in the niche of methods comparison were already amply presented in the past but are sadly missed in the present, it feels like a missed opportunity; it makes us modest and leaves us slightly unhappy.

Finally, we would like to refer the authors and readership to the more recent work by Sepriano et al [4], in which the concept of net progression is worked out in more detail (using axSpA as an example). Net progression, requiring paired reading, is a valuable extension of the principle that measurement error (the 'left tile' of the probability plots in Baraliakos et al [2]) should be taken into consideration when judging progression in observational studies in order to arrive at a fairer comparison.

To conclude on a positive note, we absolutely would have liked to give the authors of this work, who have all done seminal research in the clinical field of axSpA, the thrill of the scoop, but this means that nobody would have ever done it before.

Handling editor Josef S. Smolen.

<https://doi.org/10.1016/j.ard.2025.07.013>

Received 8 July 2025; Accepted 11 July 2025

## Funding

None.

## Competing interests

RL reports a relationship with AbbVie Inc that includes: consulting or advisory, funding grants, and speaking and lecture fees. RL reports a relationship with UCB Pharma SA that includes: consulting or advisory, funding grants, and speaking and lecture fees. RL reports a relationship with Janssen Pharmaceuticals Inc that includes: consulting or advisory, funding grants, and speaking and lecture fees. RL reports a relationship with Novartis that includes: consulting or advisory, funding grants, and speaking and lecture fees. RL reports a relationship with Alfasigma SpA that includes: consulting or advisory, funding grants, and speaking and lecture fees. RL reports a relationship with Annals of Rheumatic Diseases that includes: board membership. RL owns Joint Imaging BV. DvdH reports a relationship with Alfasigma SpA that includes: consulting or advisory. DvdH reports a relationship with AbbVie Inc that includes: consulting or advisory and speaking and lecture fees. DvdH reports a relationship with argenx BV that includes: consulting or advisory. DvdH reports a relationship with Bristol-Myers Squibb Company that includes: consulting or advisory. DvdH reports a relationship with Eli Lilly and Company that includes: consulting or advisory. DvdH reports a relationship with Gray-Wolf-therapeutics that includes: consulting or advisory. DvdH reports a relationship with Janssen Pharmaceuticals Inc that includes: consulting or advisory. DvdH reports a relationship with Novartis that includes: consulting or advisory. DvdH reports a relationship with Pfizer that includes: consulting or advisory. DvdH reports a relationship with Takeda Pharmaceutical Company Limited that includes: consulting or advisory. DvdH reports a relationship with UCB Pharma SA that includes: consulting or advisory. DvdH reports a relationship with Annals of Rheumatic Disease that includes: board membership. DvdH reports a relationship with The Journal of Rheumatology Publishing Co Ltd that includes: board membership. DvdH own Imaging Rheumatology BV.

## Patient consent for publication

Non applicable.

## Ethics approval

Non applicable.

## Provenance and peer review

Non applicable.

## Orcid

Robert B.M. Landewé: <http://orcid.org/0000-0002-0577-6620>

## REFERENCES

- [1] Park M, Leahey E, Funk RJ. Papers and patents are becoming less disruptive over time. *Nature* 2023;613(7942):138–44.
- [2] Baraliakos X, Protopopov M, Rodriguez VR, Torgutalp M, Dilbaryan A, Haibel H, et al. Radiographic structural damage in axial spondyloarthritis: is there a preferred way to quantify progression over time? Comparison of blinded versus unblinded mSASSScoring. *Ann Rheum Dis* 2025 in press. doi: [10.1016/j.ard.2025.03.017](https://doi.org/10.1016/j.ard.2025.03.017).
- [3] Wanders A, Landewé R, Spoorenberg A, de Vlam K, Mielants H, Dougados M, et al. Scoring of radiographic progression in randomised clinical trials in ankylosing spondylitis: a preference for paired reading order. *Ann Rheum Dis* 2004;63(12):1601–4.
- [4] Sepriano A, Ramiro S, Landewé R, Dougados M, van der Heijde D. Percentage of progressors in imaging: can we ignore regressors? *RMD Open* 2019;5(1): e000848. doi: [10.1136/rmdopen-2018-000848](https://doi.org/10.1136/rmdopen-2018-000848).

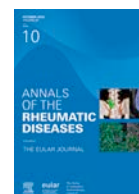
Robert B.M. Landewé <sup>1,\*</sup>, Desiree van der Heijde<sup>2</sup>

<sup>1</sup> Department of clinical immunology & rheumatology, Department of rheumatology, Academic Medical Center, University of Amsterdam, Amsterdam, The Netherlands

<sup>2</sup> Department of rheumatology, Leiden University Medical Center, Leiden, The Netherlands

\*Correspondence to Dr Robert B.M. Landewé, Academic Medical Center, University of Amsterdam, Amsterdam, The Netherlands  
E-mail address: [landewe@rlandewe.nl](mailto:landewe@rlandewe.nl) (R.B.M. Landewé).





## Response

## Response to the correspondence on “Radiographic structural damage in axial spondyloarthritis: is there a preferred way to quantify progression over time?”

Dear Editor,

We would like to thank Prof Landewé and Prof van der Heijde for their attention to our recently published analysis on the methodology of scoring radiographic spinal progression in axial spondyloarthritis (axSpA) [1]. We value open scientific discussion and welcome the opportunity to clarify issues in the context of our work. Constructive comments from experienced researchers, such as our Dutch colleagues, play an important role in improving scientific standards and collegial understanding. We do, however, feel that such conversations should always remain within the bounds of respectful scientific discourse. That said, we hope that this answer to their comments may help to bring the conversation back towards constructive scientific exchange.

Let us remind everyone that our manuscript underwent the customary rigorous blinded peer review process. We received detailed and thoughtful feedback from several reviewers. This input led to important methodological and statistical clarifications, including clarifications on the relevant literature that is discussed here.

The central concern raised by Profs Landewé and van der Heijde relates to the novelty of our study. We acknowledge the fact that Wanders et al [2] have published on the topic of blinded vs unblinded scoring of the modified Stoke Ankylosing Spondylitis Spinal Score (mSASSS) in the past. However, we felt that, although this work was an important contribution to the field at the time of its publication, it also needed confirmation from the methodological and other points of view. The fact that the article by Wanders et al [2] was not included in the reference list is simply explained by the inclusion of 2 subsequent publications from the same group [3,4], both of which explicitly addressed the results and implications of the original manuscript.

Our carefully worded statement, “To our knowledge, this is the first study to compare mSASSS reading in a blinded and unblinded manner in patients with the entire spectrum of

axSpA” is clearly justified, given that this refers to the whole spectrum of axSpA. Importantly, we have not claimed to have discovered a previously unknown phenomenon. Even though not much radiographic progression is expected to occur in non-radiographic (nr)-axSpA, it is important to look at the whole spectrum of the disease. Indeed, studies of nr-axSpA do assess radiographic progression [5]. Because structural changes are typically minimal in nr-axSpA, methodological challenges such as floor effects may increase uncertainty in the evaluation of progression as well as regression. These factors are known to affect the performance, sensitivity, and reliability of scoring systems like mSASSS. Finally, the validation of scoring approaches in early or nr-axSpA ensures their fit-for-purpose in clinical research and practice.

In addition, our study design was different: we systematically compared 2 reading strategies using multiple readers and a whole range of statistical analyses. Thus, our study employed multiple experienced readers for each imaging modality—3 unblinded and 2 blinded—allowing us to assess interreader variability, a key measure of reproducibility. This was not feasible in the single-reader design used by Wanders et al [2]. In fact, this methodology is no longer standard for scoring conventional radiographs in larger clinical trials.

Therefore, we do not agree with the commentary that additional readers are inconsequential for methodological comparisons. We respectfully suggest the opposite: the assessment of consistency across readers is essential to determine whether a method is appropriate for use in clinical trials.

In addition, we expanded the analytic framework beyond mean change scores. Our study includes shift analyses at the vertebral corner level, definitions of fast, moderate, and slow progression, and subgroup assessments. These complementary approaches provide greater granularity and practical insights relevant to trial design and endpoint selection.

Furthermore, we found that the study by Wanders et al [2] had other important methodological limitations. Specifically, as acknowledged by the authors in a related publication [3]: ‘the format of the radiographs was changed in some centres, which made it possible for the observer to identify the point in time’. This stresses the relevance of true time blinding and introduces potential expectation bias even in ‘blinded’ reads. In contrast, our use of the German Spondyloarthritis Inception cohort dataset did avoid such pitfalls, allowing for a robust and clean comparison between truly blinded and unblinded scoring.

The reference to the concept and utility of assessing net-progression is important, particularly in time-blinded scoring scenarios. In such settings, where readers are unaware of radiograph chronology, measurement error is typically assumed to be symmetrical: misclassification of progression and

regression occurs with roughly equal probability. Net-progression, by subtracting regressors from progressors, helps to reduce noise and isolate a more accurate signal of true structural change. However, in unblinded scoring, where chronology is known—as in our study—the symmetry breaks down. Readers are generally more inclined to detect and score progression rather than regression, reflecting the expectation that structural damage in the spine is typically irreversible. For this reason, we believe net-progression has less utility in the context of unblinded methodologies and is best suited to contexts in which error is more balanced.

Finally, we do believe that scientific inquiry, especially on methodological questions, always benefits from replication, particularly when performed under different conditions, with novel cohorts, and use of a more rigorous design. Thus, the presence of prior publications clearly does not argue against the need for more studies but rather invites them. Similar approaches have recently been applied, also by our Dutch colleagues, specifically in the context of spinal radiographic progression in axSpA, in which the role of the lower thoracic spine was investigated using more modern approaches [6,7]. These findings confirmed data published by our group more than a decade ago [8]. This is much appreciated and regarded as a valuable confirmation of previous results.

In conclusion, the results of our recently published study [1], though directionally consistent with Wanders et al [2], extend and refine those findings in several important ways. The sensitivity, specificity and reproducibility of assessing radiographic progression in axSpA will remain an important topic in clinical research. Whether conventional radiography will remain the gold standard is unclear at present.

Statistical thinking has led to many insights into the nature of truth. We are aware that one of the most important insights is that truth is impossible to pin down definitively. Thus, the truth is an unknown quantity that we can pursue, but never completely attain.

Finally, we believe that scientific discussions should always be respectful and in the spirit of the collaborative ethos that has characterised our scientific community in axSpA for the last decades.

## Competing interests

XB declares that he has received grants from Novartis; consultant fees from AbbVie, Alphasigma, Amgen, BMS, Cestas, Celltrion, Galapagos, Janssen, Lilly, Moonlake, Novartis, Pfizer, Roche, Sandoz, Springer, Stada, Takeda, UCB, and Zuellig; received speakers' honoraria from AbbVie, Alphasigma, Amgen, BMS, Cestas, Celltrion, Galapagos, Janssen, Lilly, Moonlake, Novartis, Pfizer, Roche, Sandoz, Springer, Stada, Takeda, UCB, and Zuellig; received support for attending meetings and/or travel from AbbVie, Alphasigma, Amgen, BMS, Cestas, Celltrion, Galapagos, Janssen, Lilly, Moonlake, Novartis, Pfizer, Roche, Sandoz, Springer, Stada, Takeda, UCB, and Zuellig; participated in advisory boards sponsored by AbbVie, Alphasigma, Amgen, BMS, Cestas, Celltrion, Galapagos, Janssen, Lilly, Moonlake, Novartis, Pfizer, Roche, Sandoz, Springer, Stada, Takeda, UCB, and Zuellig; and is an Editorial Board member of *Annals of Rheumatic Diseases*, ASAS President, and EULAR President-Elect. MP declares that he has received consulting fees from Janssen and Novartis and support for attending meetings and/or travel from Novartis, AbbVie, Janssen and UCB. JS declares that he has received speakers' honoraria from AbbVie, Merck, Novartis and UCB. DP declares that he has received grants from AbbVie, Eli

Lilly, MSD, Novartis and Pfizer; consulting fees from AbbVie, Biocad, Bristol Myers Squibb, Eli Lilly, Janssen, Moonlake, Novartis, Pfizer and UCB; speakers' honoraria from AbbVie, Canon, DKSH, Eli Lilly, Janssen, MSD, Medscape, Novartis, Peer-voice, Pfizer, and UCB; and is a member of the executive committee of ASAS and a member of the steering committee of GRAPPA. The other authors (JB and MR) declare they have no competing interests.

## CRedit authorship contribution statement

**Xenofon Baraliakos:** Writing – review & editing, Writing – original draft, Conceptualization. **Mikhail Protopopov:** Writing – review & editing, Writing – original draft, Conceptualization. **Joachim Sieper:** Writing – review & editing. **Juergen Braun:** Writing – review & editing. **Martin Rudwaleit:** Writing – review & editing. **Denis Poddubnyy:** Writing – review & editing, Writing – original draft, Conceptualization.

## Funding

None.

## Patient consent for publication

Does not apply.

## Ethics approval

Does not apply.

## Provenance and peer review

N/A

## Orcid

Xenofon Baraliakos: <http://orcid.org/0000-0002-9475-9362>  
Mikhail Protopopov: <http://orcid.org/0000-0003-4840-5069>  
Juergen Braun: <http://orcid.org/0000-0002-9156-5095>  
Martin Rudwaleit: <http://orcid.org/0000-0001-5445-548X>  
Denis Poddubnyy: <http://orcid.org/0000-0002-4537-6015>

## REFERENCES

- [1] Baraliakos X, Protopopov M, Rodriguez VR, Torgutalp M, Dilbaryan A, Haibel H, et al. Radiographic structural damage in axial spondyloarthritis: is there a preferred way to quantify progression over time? Comparison of blinded versus unblinded mSASSS scoring. *Ann Rheum Dis* 2025;84:1335–41.
- [2] Wanders A, Landewé R, Spoorenberg A, de Vlam K, Mielants H, Dougados M, et al. Scoring of radiographic progression in randomised clinical trials in ankylosing spondylitis: a preference for paired reading order. *Ann Rheum Dis* 2004;63(12):1601–4.
- [3] Wanders A, Landewé RBM, Spoorenberg A, Dougados M, van der Linden S, Mielants H, et al. What is the most appropriate radiologic scoring method for ankylosing spondylitis? A comparison of the available methods based on the Outcome Measures in Rheumatology Clinical Trials filter. *Arthritis Rheum* 2004;50(8):2622–32.
- [4] Wanders A, Landewé R, Dougados M, Mielants H, van der Linden S, van der Heijde D. Association between radiographic damage of the spine and spinal mobility for individual patients with ankylosing spondylitis: can assessment of spinal mobility be a proxy for radiographic evaluation? *Ann Rheum Dis* 2005;64(7):988–94.
- [5] van der Heijde D, Baraliakos X, Hermann KA, Landewé RBM, Machado PM, Maksymowych WP, et al. Limited radiographic progression and sustained reductions in MRI inflammation in patients with axial spondyloarthritis: 4-

- year imaging outcomes from the RAPID-axSpA phase III randomised trial. *Ann Rheum Dis* 2018;77(5):699–705.
- [6] de Hooze M, Marques ML, Ayan G, van Lunteren M, de Bruin L, Reijnierse M, et al. OP0308 Low-dose CT reveals syndesmophyte progression in axSpA, particularly in the thoracic spine: insights from the SPACE cohort covering early and established disease. *Ann Rheum Dis* 2025;84(suppl 1):246–7.
- [7] de Koning A, de Bruin F, van den Berg R, Ramiro S, Baraliakos X, Braun J, et al. Low-dose CT detects more progression of bone formation in comparison to conventional radiography in patients with ankylosing spondylitis: results from the SIAS cohort. *Ann Rheum Dis* 2018;77(2):293–9.
- [8] Baraliakos X, Listing J, Rudwaleit M, Sieper J, Braun J. Development of a radiographic scoring tool for ankylosing spondylitis only based on bone formation: addition of the thoracic spine improves sensitivity to change. *Arthritis Rheum* 2009;61(6):764–71.

Xenofon Baraliakos<sup>1,\*</sup>, Mikhail Protopopov<sup>2</sup>,  
Joachim Sieper<sup>2</sup>, Juergen Braun<sup>3</sup>, Martin Rudwaleit<sup>4</sup>,  
Denis Poddubnyy<sup>2,5</sup>

<sup>1</sup> *Rheumazentrum Ruhrgebiet Herne, Ruhr-University Bochum, Germany*

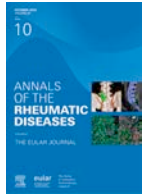
<sup>2</sup> *Department of Gastroenterology, Infectiology and Rheumatology (including Nutrition Medicine), Charité-Universitätsmedizin Berlin, Berlin, Germany*

<sup>3</sup> *Rheumatologisches Versorgungszentrum Steglitz, Berlin, Germany*

<sup>4</sup> *Klinikum Bielefeld Rosenhöhe, University Clinic for Internal Medicine and Rheumatology, Bielefeld, Germany*

<sup>5</sup> *Division of Rheumatology, University of Toronto and University Health Network, Toronto, ON, Canada*

**\*Correspondence to** Prof Xenofon Baraliakos, Rheumazentrum Ruhrgebiet Herne, Ruhr-University Bochum, Germany  
E-mail address: [baraliakos@me.com](mailto:baraliakos@me.com) (X. Baraliakos).



## Correspondence

## Correspondence on 'Pulmonary arterial hypertension in adults with Still's disease: another pulmonary manifestation associated with HLA-DRB1\*15'

Boucly et al [1] provide detailed descriptions of 16 cases of pulmonary arterial hypertension (PAH) confirmed by right heart catheterisation in adult patients with Still disease (SD), the largest such cohort reported to date. We would like to challenge their conclusion that PAH is related to difficult-to-treat SD and human leukocyte antigen (HLA)-DRB1\*15 status. Since this severe complication is associated with exposure to interleukin (IL)-1/IL-6 inhibitors (ie, drug-associated pulmonary hypertension), the data presented support promptly discontinuing the implicated medications according to expert guidance from the European Society of Cardiology and European Respiratory Society, cited by the authors [2]. Our original discovery of striking enrichment for HLA-DRB1\*15 haplotypes in SD was linked to scoring as drug reaction with eosinophilia and systemic symptoms (DRESS) by RegiSCAR [3], implicating these cytokine inhibitors. Those with HLA-DRB1\*15 haplotypes did not have severe SD compared to drug-tolerant controls before IL-1/IL-6-inhibition or, for those stopping these drugs, after avoiding these medications [4,5]. This includes enrichment of macrophage activation syndrome (MAS) only during IL-1/IL-6-inhibition, an inflammatory condition that is a DRESS-related risk [6]. Among the DRESS cases were cases of PAH, and the PAH+ cohort reported by Boucly et al [1] was similarly enriched for HLA-DRB1\*15. Additionally, during the reported disease course, these PAH+ cases had an increased incidence of MAS, marked eosinophilia, and clinical diagnosis of drug reaction implicating IL-1/IL-6 inhibitors, as demonstrated in our previous publications [4,5,7].

Diagnosis of drug-induced lung injury, which includes PAH, can be assessed by diagnostic criteria [8]. In the present study, 12 of 16 cases met 3 of these criteria: (i) identification of drug exposure (ie, treatment with IL-1/IL-6-inhibition); (ii) established drug-disease association [5]; and (iii) exclusion of other causes, which is the case considering PAH is not intrinsically associated with SD. In our work, these 3 criteria were met, as were the remaining 2 criteria: (iv) improvement (actually,

resolution) after drug discontinuation and (v) exacerbation of clinical manifestations after resuming drug administration (see below), which is generally not recommended [5].

Additionally, there is inherent danger in misattributing PAH as an HLA-associated SD risk and uncoupling PAH from the development of diffuse lung disease. The authors noted PAH without substantial parenchymal lung abnormalities. In our studies [4,5,7], PAH occurring during IL-1/IL-6-inhibition, with or without diffuse lung disease, was diagnosed by echocardiogram or right heart catheterisation and, if biopsy or autopsy tissue was available, tissue confirmation of pulmonary arterial vascular disease (Fig). Granular detail not reported in our studies are represented by 2 adult patients with SD. One with PAH diagnosed by right heart catheterisation was initially without computed tomography evidence of parenchymal disease. With continued IL-1 inhibition, progressive and extensive parenchymal lung disease developed prior to death. Another fatal case was a young adult, noted above as tragically having return of PAH after resolution off-drug with development of extensive parenchymal disease after drug reintroduction. These 2 fatal adult cases were found not to carry DRB1\*15. The former had recurrent MAS, and the latter never experienced MAS. Our recent report [5] includes 8 of 9 patients with PAH that resolved after abandoning IL-1/IL-6-inhibitors; 5 had stopped during MAS. None of the 8 patients with PAH who continued these drugs reported resolution. The instance of return of PAH after reintroduction of these drugs was not included, ie, a ninth example of resolution after stopping these drugs. Not considering drug association precludes the therapeutic option to stop the implicated class of drugs as expressly recommended [2] and may deprive a patient of a better outcome.

Recognising this severe, delayed drug reaction in the context of IL-1/IL-6 inhibition is difficult in the setting of SD as there is potential for significant postdrug withdrawal inflammation. Adding to the difficulty in recognising this condition, reaction features are asynchronous and discontinuous, typically noted within the first months of drug initiation, and these features may not reappear at the time of later recognition of PAH or other pulmonary complications [5,9]. Indeed, cases scored as DRESS that led to the striking HLA-DRB1\*15 link occurred in the typical time frame of a median of 2 to 8 weeks after drug initiation [4,5,10]. In the present SD-PAH paper, the latency from drug start to diagnosis of PAH was long, as noted previously [7], a time when persistence of scoring as DRESS was not characteristic in the published cohorts. In addition, MAS may be associated with SD, as well as with the adverse reactions to IL-1/IL-6 inhibition.

Handling editor Josef S. Smolen.

<https://doi.org/10.1016/j.ard.2025.06.2127>

Received 5 June 2025; Accepted 14 June 2025



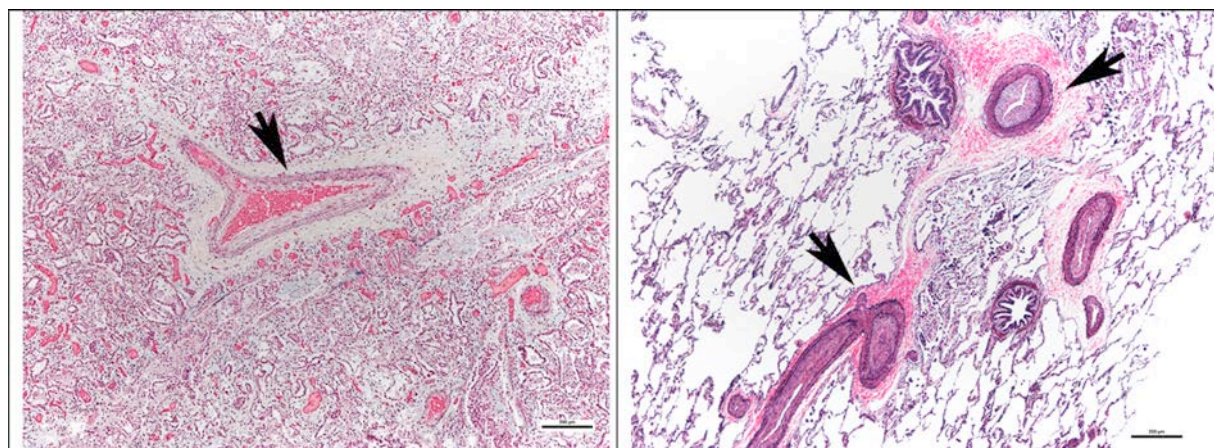


**Figure.** Severe pulmonary arterial pathology with and without diffuse lung disease. Examples of lung pathology during IL-1/IL-6 inhibition are shown. Each patient had been treated continuously for >1 year with  $\geq 1$  of the drugs and had scored as DReSS, implicating each cytokine inhibitor. Left panel: Hypertensive pulmonary arteriopathy with intimal fibrosis (arrow) is present within the postmortem lungs of a 2-year-old with sJIA, which also shows extensive endogenous lipoid pneumonia. Right panel: Severe occlusive pulmonary arteriopathy (arrows) in the lung biopsy of a 14-year-old with sJIA. (Movat pentachrome stain) DReSS, drug reaction with eosinophilia and systemic symptoms; IL, interleukin; sJIA, systemic juvenile idiopathic arthritis.

Given this overlap in DReSS and SD-related inflammation, it is not surprising that treatment of the related inflammation overlaps with treatments for each condition, including steroids in sufficient dose and consideration of cyclosporine or other immune suppressive medications [10]. In this report, attributing fatality to an SD flare without including the possible contribution or causality of this high-fatality drug-associated condition scoring as DReSS appears faulty.

We respectfully suggest that attention to drug-related PAH in 12 of the 16 patients reported is imperative. Given the population frequency of HLA-DRB1\*15 haplotypes is ~20% across ethnicities [11] and found to be drug reaction risk-related rather than SD severity-related, it aligns with the finding that PAH in SD was remarkably rare prior to the use of IL-1/IL-6 inhibitors and, as such, is at odds with the conclusion that PAH is intrinsic to SD and related to these alleles. With attention to possible postdrug withdrawal inflammation, discontinuation of IL-1/IL-6-inhibitors, regardless of onset age, is an approach to consider should PAH develop in SD during this treatment.

## Competing interests

VES has patent #US20240093299A1, issued to Stanford University, which covers anti-IL-1 and anti-IL-6 hypersensitivity and assaying for certain HLA allele. The other authors declare they have no competing interests.

## CRediT authorship contribution statement

**Vivian E. Saper:** Conceptualization, Writing – original draft, Writing – review & editing. **Ruud H. J. Versteegen:** Writing – review & editing. **Gail H. Deutsch:** Writing – review & editing.

## Funding

VES reports financial support was provided by Lucile Packard Foundation for Children's Health.

## Patient consent for publication

Not applicable.

## Ethics approval

Patient data were obtained in accordance with institutional review board requirements.

## Provenance and peer review

Not commissioned, externally peer reviewed.

## Data availability statement

Data from our prior publications are available upon reasonable request.

## Orcid

Vivian E. Saper: <http://orcid.org/0000-0001-9043-3229>

## REFERENCES

- [1] Boucly A, Mitrovic S, Carmagnat M, Savale L, Jaïs X, Taupin JL, et al. Pulmonary arterial hypertension in adults with Still's disease: another pulmonary manifestation associated with HLA-DRB1\*15. *Ann Rheum Dis* 2025.
- [2] Humbert M, Kovacs G, Hoeper MM, Badagliacca R, Berger RMF, Brida M, et al. 2022 ESC/ERS Guidelines for the diagnosis and treatment of pulmonary hypertension: developed by the task force for the diagnosis and treatment of pulmonary hypertension of the European Society of Cardiology (ESC) and the European Respiratory Society (ERS). Endorsed by the International Society for Heart and Lung Transplantation (ISHLT) and the European Reference Network on rare respiratory diseases (ERN-LUNG). *Eur Heart J* 2022;43(38):3618–731.
- [3] Kardaun SH, Sekula P, Valeyrie-Allanore L, Liss Y, Chu CY, Creamer D, et al. Drug reaction with eosinophilia and systemic symptoms (DRESS): an original multisystem adverse drug reaction. Results from the prospective RegiSCAR study. *Br J Dermatol* 2013;169(5):1071–80.
- [4] Saper VE, Ombrello MJ, Tremoulet AH, Montero-Martin G, Prahalad S, Canna S, et al. Severe delayed hypersensitivity reactions to IL-1 and IL-6 inhibitors link to common HLA-DRB1\*15 alleles. *Ann Rheum Dis* 2022;81(3):406–15.
- [5] Saper VE, Tian L, Versteegen RHJ, Conrad CK, Cidon M, Hopper RK, et al. Interleukin (IL)-1/IL-6-inhibitor-associated drug reaction with eosinophilia

- and systemic symptoms (DRESS) in systemic inflammatory illnesses. *J Allergy Clin Immunol Pract* 2024;12(11):2996–3013.
- [6] Yang JJ, Lei DK, Ravi V, Maloney NJ, Crew A, Worswick S. Overlap between hemophagocytic lymphohistiocytosis and drug reaction and eosinophilia with systemic symptoms: a review. *Int J Dermatol* 2020.
- [7] Saper VE, Chen G, Deutsch GH, Guillerman RP, Birgmeier J, Jagadeesh K, et al. Emergent high fatality lung disease in systemic juvenile arthritis. *Ann Rheum Dis* 2019;78(12):1722–31.
- [8] Kubo K, Azuma A, Kanazawa M, Kameda H, Kusumoto M, Genma A, et al. Consensus statement for the diagnosis and treatment of drug-induced lung injuries. *Respir Investig* 2013;51(4):260–77.
- [9] Taweessedt PT, Nordstrom CW, Stoeckel J, Dumic I. Pulmonary manifestations of drug reaction with eosinophilia and systemic symptoms (DRESS) syndrome: a systematic review. *Biomed Res Int* 2019;2019:7863815.
- [10] Hama N, Abe R, Gibson A, Phillips EJ. Drug-induced hypersensitivity syndrome (DIHS)/drug reaction with eosinophilia and systemic symptoms (DRESS): clinical features and pathogenesis. *J Allergy Clin Immunol Pract* 2022;10(5) 1155–67.e5.
- [11] Maiers M, Gragert L, Klitz W. High-resolution HLA alleles and haplotypes in the United States population. *Hum Immunol* 2007;68(9):779–88.

Vivian E. Saper <sup>1,\*</sup>, Ruud H. J. Versteegen<sup>2,3</sup>, Gail H. Deutsch<sup>4</sup>

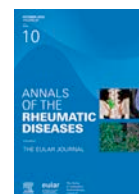
<sup>1</sup> Divisions of Human Gene Therapy, Allergy/Immunology, and Pediatric Rheumatology, Department of Pediatrics, Stanford University School of Medicine, Stanford, CA, USA

<sup>2</sup> Divisions of Rheumatology and Clinical Pharmacology/Toxicology, Department of Paediatrics, The Hospital for Sick Children, Toronto, ON, Canada

<sup>3</sup> Department of Paediatrics, University of Toronto, Toronto, ON, Canada

<sup>4</sup> Department of Laboratory Medicine and Pathology, Seattle Children's Hospital, Seattle, WA, USA

\*Correspondence to Dr Vivian E. Saper, Department of Pediatrics, Stanford University School of Medicine, Stanford, CA, USA.  
E-mail address: [vesaper@stanford.edu](mailto:vesaper@stanford.edu) (V.E. Saper).



## Response

## Response to correspondence on: Pulmonary arterial hypertension in adults with Still's disease: another pulmonary manifestation associated with HLA-DRB1\*15

We thank Saper et al [1] for their thoughtful correspondence, which allows us to clarify several major points and further enrich the scientific debate on the important issue of pulmonary involvement in Still's disease (SD).

Our study highlights that pulmonary arterial hypertension (PAH) may develop on the same background as other manifestations of SD-related pulmonary involvement, ie, in patients with macrophage activation syndrome, especially when recurrent, with eosinophilia, and carrying the HLA-DRB1\*15 allele [1,2]. It is crucial to differentiate PAH (group 1 of pulmonary hypertension [PH]), characterised by progressive remodelling of small pulmonary arteries, from PH associated with interstitial lung disease (PH-ILD), which falls under group 3 PH and results primarily from parenchymal lung involvement and hypoxic vasoconstriction [3]. In their important studies, Saper et al [4,5] estimated PH incidence at 30% at the time of ILD diagnosis but did not clearly distinguish PAH from other forms of PH. Indeed, in the absence of systematic invasive hemodynamic evaluation using right heart catheterisation, the reference standard for both confirming the diagnosis of PH and distinguishing between pre- and/or postcapillary mechanisms, the data should be interpreted with caution. It is equally important to note that Drug Reaction with Eosinophilia and Systemic Symptoms (DRESS) syndrome itself is not a recognised cause of PAH. PH in this setting typically results from acute respiratory distress, a frequent scenario in intensive care units, with a pathophysiology entirely distinct from that of PAH. The fact that PAH can be isolated in SD, ie, it can occur in the absence of major parenchymal involvement, has major implications (Fig) [2].

Drug reactions are frequently hypothesised in patients with SD and it is important to recall that a typical patient with SD could fulfil the criteria for “possible/probable” DRESS according to the RegiSCAR (European Registry of Severe Cutaneous Adverse Reactions) classification criteria set [6]. Saper et al [5] hypothesised that SD-related lung involvement could correspond to a DRESS. While we do not exclude that biologics may play a role in promoting the onset of pulmonary complications

in a subset of patients, the DRESS criteria are not fully specific and this hypothesis faces some conceptual hurdles [6]. Firstly, anakinra, canakinumab, and tocilizumab do not share any antigen-length peptides. The only excipient shared by these agents is polysorbate-80, a ubiquitous emulsifier used in numerous monoclonal antibodies and vaccines, making it an unlikely causative agent for DRESS [6]. Moreover, anakinra, canakinumab, and tocilizumab are used in diseases other than SD, such as rheumatoid arthritis, giant cell arteritis, and autoinflammatory diseases, without any similar manifestation being reported. Contrary to the statement suggested by Saper et al [1], the 2022 European Society of Cardiology (ESC) European Respiratory Society (ERS) guidelines do not recommend discontinuation of interleukin (IL)-1 or IL-6 inhibitors. These guidelines [3], along with the seventh World Symposium on PH [7], provide an extensive classification of drugs potentially associated with PAH. IL-1 and IL-6 inhibitors were not considered likely causative agents by expert consensus, despite years of clinical use. Additionally, most Human Leukocyte Antigen (HLA) associations with drug-induced hypersensitivity or DRESS are with major histocompatibility complex (MHC) class I alleles, whereas HLA-DRB1\*15 is part of the class II MHC system [6]. Finally, in our cohort, 25% of patients developed PAH although they had never been exposed to IL-1 or IL-6 inhibitors, yet exhibited highly inflammatory state, consistent with observations from other series [2,7,8].

DRESS or drug-induced hypersensitivity is not the only hypothesis to explain the development of SD lung disease. Bin-stadt and Nigrovic [6] have put forward an explanation to SD-related pulmonary involvement, the ‘Cytokine Plasticity Hypothesis’, which suggests that targeted therapies, such as IL-1 and IL-6 blockers, modulate the milieu in which T cells differentiate. This altered environment may foster a pathologic immune response triggered through exposure to common microbes, or to other exogenous or endogenous antigens, rather than to the drugs themselves [6]. According to this hypothesis, elevated IL-1 and IL-6 levels in SD lead to Th17 skewing in CD4+ Th and Treg cells. Blocking IL-1 or IL-6 converts these cells into interferon- $\gamma$ -producing Th1 cells and/or IL-4-producing Th2 cells, in particular CD4+ T cells recognising HLA-DRB1\*15:XX-presented antigens (exogenous or endogenous). Notably, such analogous transitions could occur in some patients even in the absence of IL-1 or IL-6R blockade.

IL-1 and IL-6R blocker withdrawal is probably not a relevant option since several patients got worse after discontinuation of targeted therapies. Instead, the alternative option is likely to add T-cell-directed immunosuppressive agents. Recently, an international group of paediatric and adult rheumatology experts established recommendations for the management of SD

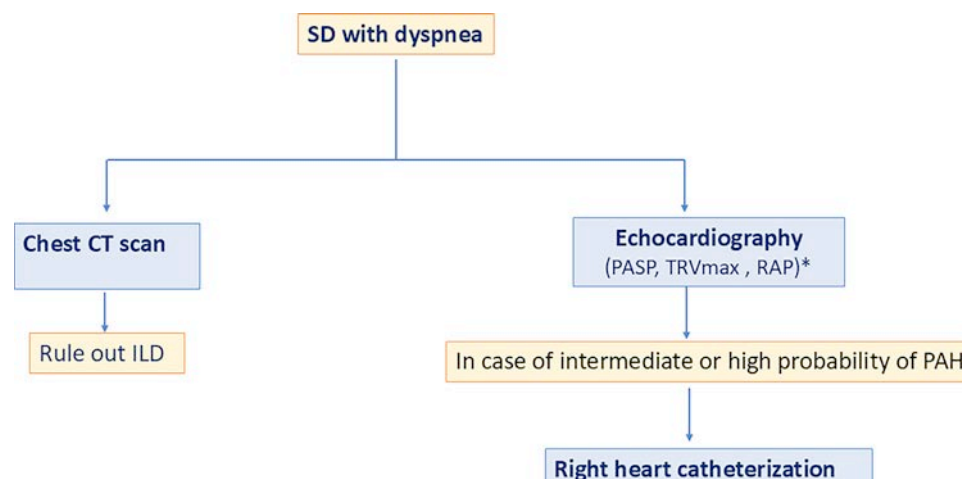


**Figure.** Algorithm for investigating dyspnoea in a patient with Still disease.

The fact that pulmonary arterial hypertension (PAH) can be isolated in Still disease (SD), ie, it can occur in the absence of major parenchymal involvement, should encourage physicians to screen for it using echocardiography in cases of unexplained dyspnoea, before confirmation by catheterisation in the case of intermediate or high probability of PAH. CT, computed tomography; ILD, interstitial lung disease; PAH, pulmonary arterial hypertension; PASP, pulmonary artery systolic pressure; RAP, qualitative assessment of right atrial pressure; SD, Still's disease; TRVmax, tricuspid regurgitation velocity.

under the auspices of the European Alliance of Associations for Rheumatology (EULAR) and the Paediatric Rheumatology European Society (PReS) [8]. The Task Force (TF) unanimously acknowledged that there is insufficient evidence to withhold first-line IL-1 or IL-6 inhibitors in patients with new onset SD and lung disease risk factors (recommendation 13). Additionally, given the potential involvement of T cells in lung disease pathogenesis, some TF experts felt that it is reasonable to initiate T cell-directed immunosuppression in patients at high risk for lung disease or developing lung disease. This is consistent with the fact that 7 patients in our PAH series showed improvement precisely by maintaining the IL-1 or IL-6 inhibition and increasing the treatment, ie, by adding an immunosuppressive treatment targeting T cells, such as ciclosporin, tacrolimus, or mycophenolate mofetil, an immunomodulator (leflunomide), or a Janus kinase (JAK) inhibitor [2]. The observation that our patients, as well as those reported in other series [9], demonstrated clinical improvement while continuing treatment with IL-1 or IL-6 inhibitors, provides a strong argument against DRESS as the underlying mechanism.

In conclusion, PAH and SD-related pulmonary involvement is a challenging and life-threatening complication in SD that deserves precise diagnosis and individualised management. A thorough evaluation, including right heart catheterisation and collaboration between SD and PH specialists, is essential to identify the underlying PH mechanism and guide therapy. Although the pathogenesis remains to be fully elucidated, current evidence and international guidelines do not support discontinuation of IL-1 or IL-6 inhibitors for SD patients who develop PAH [8].

## FUNDING

The authors did not receive funding for this study from any funding agency in the public, commercial, or not-for-profit sectors.

## Competing interests

None related to this work.

## CRedit authorship contribution statement

**Stéphane Mitrovic:** Conceptualization, Data curation, Formal analysis, Investigation, Project administration, Writing – original draft, Writing – review & editing. **Athénaïs Boucly:** Investigation, Visualization, Writing – review & editing. **Olivier Sitbon:** Visualization. **Bruno Fautrel:** Conceptualization, Data curation, Formal analysis, Investigation, Methodology, Supervision, Validation, Visualization, Writing – original draft, Writing – review & editing. **David Montani:** Conceptualization, Data curation, Formal analysis, Investigation, Methodology, Supervision, Validation, Visualization, Writing – review & editing.

## Patient consent for publication

Not applicable.

## Ethics approval

Not applicable.

## Provenance and peer review

Not commissioned; externally peer reviewed.

## Orcid

Stéphane Mitrovic: <http://orcid.org/0000-0001-5244-7881>  
 Athénaïs Boucly: <http://orcid.org/0000-0001-6246-5557>  
 Olivier Sitbon: <http://orcid.org/0000-0002-1942-1951>  
 Bruno Fautrel: <http://orcid.org/0000-0001-8845-4274>  
 David Montani: <http://orcid.org/0000-0002-9358-6922>

## REFERENCES

- [1] Saper VE, Verstegen RHJ, Deutsch GH. Correspondence re: Pulmonary arterial hypertension in adults with Still's disease: another pulmonary manifestation associated with HLA-DRB1\*15. *Ann Rheum Dis* 2025.
- [2] Boucly A, Mitrovic S, Carmagnat M, Savale L, Jaïs X, Taupin JL, et al. Pulmonary arterial hypertension in adults with Still's disease: another pulmonary



- manifestation associated with HLA-DRB1\*15. *Ann Rheum Dis* 2025 S0003-4967(25)00905-7.
- [3] Humbert M, Kovacs G, Hoepfer MM, Badagliacca R, Berger RMF, Brida M, et al. 2022 ESC/ERS Guidelines for the diagnosis and treatment of pulmonary hypertension. *Eur Respir J* 2023;61(1):2200879.
- [4] Saper VE, Chen G, Deutsch GH, Guillerman RP, Birgmeier J, Jagadeesh K, et al. Emergent high fatality lung disease in systemic juvenile arthritis. *Ann Rheum Dis* 2019;78(12):1722–31.
- [5] Saper VE, Ombrello MJ, Tremoulet AH, Montero-Martin G, Prahalad S, Canna S, et al. Severe delayed hypersensitivity reactions to IL-1 and IL-6 inhibitors link to common HLA-DRB1\*15 alleles. *Ann Rheum Dis* 2022;81(3):406–15.
- [6] Binstadt BA, Nigrovic PA. The conundrum of lung disease and drug hypersensitivity-like reactions in systemic juvenile idiopathic arthritis. *Arthritis Rheumatol* 2022;74(7):1122–31.
- [7] Kovacs G, Bartolome S, Denton CP, Gatzoulis MA, Gu S, Khanna D, et al. Definition, classification and diagnosis of pulmonary hypertension. *Eur Respir J* 2024;64(4):2401324.
- [8] Fautrel B, Mitrovic S, De Matteis A, Bindoli S, Antón J, Belot A, et al. EULAR/PRÉS recommendations for the diagnosis and management of Still's disease, comprising systemic juvenile idiopathic arthritis and adult-onset Still's disease. *Ann Rheum Dis* 2024;83(12):1614–27.
- [9] Schulert GS, Yasin S, Carey B, Chalk C, Do T, Schapiro AH, et al. Systemic juvenile idiopathic arthritis–associated lung disease: characterization and risk factors. *Arthritis Rheumatol* 2019;71(11):1943–54.

Stéphane Mitrovic 

*Department of Rheumatology, Sorbonne University–APHP (Assistance Publique–Hôpitaux de Paris), Pitié-Salpêtrière Hospital, Paris, France*

*CEREMAIA (Centre d'Etude et de Référence sur les Maladies AutoInflammatoires et les Amyloses), FAI<sup>2</sup>R (Filière de santé des maladies auto-immunes et auto-inflammatoires rares) Network, Paris, France*

*INSERM UMRS 959, Immunology-Immunopathology-Immunotherapy (i3), Sorbonne University, Paris, France*

Athénaïs Boucly , Olivier Sitbon 

*APHP, Hôpital Bicêtre, DMU Thorinno, Service de Pneumologie, Le Kremlin-Bicêtre, France*  
*Université Paris-Saclay, Faculté de Médecine, Le Kremlin-Bicêtre, France*  
*INSERM, UMR S\_999, Le Kremlin-Bicêtre, France*

Bruno Fautrel 

*Department of Rheumatology, Sorbonne University–APHP, Pitié-Salpêtrière Hospital, Paris, France*  
*CEREMAIA (Centre d'Etude et de Référence sur les Maladies AutoInflammatoires et les Amyloses), FAI<sup>2</sup>R (Filière de santé des maladies auto-immunes et auto-inflammatoires rares) Network, Paris, France*  
*INSERM UMR 1136, Pierre Louis Institute of Epidemiology and Public Health, Equipe PEPITES, Sorbonne University–APHP, Paris, France*

David Montani 

*APHP, Hôpital Bicêtre, DMU Thorinno, Service de Pneumologie, Le Kremlin-Bicêtre, France*  
*Université Paris-Saclay, Faculté de Médecine, Le Kremlin-Bicêtre, France*  
*INSERM, UMR S\_999, Le Kremlin-Bicêtre, France*

\* Correspondance to Dr Stéphane Mitrovic, Department of Rheumatology, Sorbonne University-APHP, Pitié-Salpêtrière Hospital, Paris, France.

E-mail address: [stephane.mitrovic@aphp.fr](mailto:stephane.mitrovic@aphp.fr) (S. Mitrovic).